

Neural networks dysfunction:
From resting-state electroencephalography
to dementia diagnosis

Alberto Jaramillo Jiménez

**Neural networks dysfunction:
From resting-state electroencephalography
to dementia diagnosis**

by

Alberto Jaramillo Jiménez

Thesis submitted in fulfilment of
the requirements for the degree of
PHILOSOPHIAE DOCTOR
(PhD)



Faculty of Health Sciences

2024

University of Stavanger
NO-4036 Stavanger
NORWAY
www.uis.no

©2024. Alberto Jaramillo Jiménez.

ISBN: [Click to enter ISBN.](#)

ISSN: [Click to enter ISSN.](#)

PhD: Thesis UiS No. [Click to enter PhD No.](#)

Acknowledgements

This thesis results from a joint effort of multiple researchers motivated by curiosity and an open science philosophy. My research journey has been a window to enhance my critical thinking, analytic, and methodological aspects towards robust, reproducible, interpretable, and applicable neuroscience. This Ph.D. would not be possible without the generous funding from Helse Vest Forskningsmidler 2021 (Project Number: F-12155), the research environment at Stavanger University Hospital – SESAM, the Faculty of Health Sciences at the University of Stavanger, and the support of the European – Dementia with Lewy Bodies consortium.

Becoming a health practitioner was motivated by my will to help people achieve their goals and life milestones without the stumble of diseases. Realising the deleterious impact of chronic diseases on patients and their relatives made me consider this a valuable field to contribute to. Among chronic conditions, mental health conditions received most of my attention as neuropsychiatric conditions can dilute the whole life of a patient, extending to the family nucleus and society. The entangled theories and hypotheses from philosophy, psychiatry, physiology, and neuroscience made me become a neuroscientist.

I started my journey in the early stages of medical school with the help of the Semillero de Investigación SINAPSIS at the Medical School of the University of Antioquia, Colombia. The Semillero is a research incubator group created by undergraduate students and directed to undergraduate students. This strategy engaged me in research networks, building the roots of my interest in neurophysiology and electrophysiology models as a correlate of brain-related activity, as well as data-science and statistical methods. Besides, my enrolment in the Grupo de Neurociencias de Antioquia - GNA (Neuroscience group of Antioquia) was crucial for me as it showcased the importance of translation medicine in neurodegenerative diseases. An endless number of technical and non-technical insights were acquired at GNA, working with the largest population worldwide with early-onset familial Alzheimer's Disease. I want to thank my colleagues and professors at GNA and the University of Antioquia, especially Drs Lucía Madrigal Zapata, Francisco Lopera Restrepo, David Aguillón Niño, and Carlos Andrés Tobón Quintero. I am also grateful to my patients at GNA, their caregivers, and relatives, who were keen to enroll in our research projects, even if our results might not benefit them immediately, but would help future generations. From the GNA team, I learned the significance of empathic care, as well as multiple perspectives on how to help people living with neurodegenerative diseases, extending the scope beyond laboratory and scientific publications.

As a casual encounter, I met Dr Miguel German Borda during a national conference in neurology in Colombia. His positive attitude allowed us to grow our research's networking and productivity. I had the opportunity to move to Norway thanks to the undeniable eagerness of Dr Dag Årsland, who supported my passion for electrophysiology and neuroscience by enrolling me in the research environment he grew at SESAM. I want to especially thank him for devoting himself to the field of dementia, serving me as the most exceptional example of collaborative efforts, promoting innovative approaches and encouraging early career researchers. Due to Prof. Årsland, I met my supervisory team, Drs Kolbjørn K. Brønnick, Laura Bonanni, and Ketil Oppedal. They have contributed to my knowledge with essential insights that invited me to always look towards a better approach to ease the limitations of current paradigms. In addition to my supervisory team, profound methodological discussions with Drs Claudio Babiloni, Pedro Antonio Valdes-Sosa, and the Global Brain Consortium resulted in the improvement of our methods, as well as long-lasting meetings with my co-authors Yorguin José Mantilla-Ramos, and Diego Alejandro Tovar-Rios to find the best analytic solutions.

Last but not least, I want to recognise my family's role in this pathway. My mother, Nora Alicia Jiménez Moreno, has always been proud of me and has done her best to support me in any potential difficulty, motivating me to succeed in my objectives. My life partner, Daniela Mejía Osorio, has made a tremendous effort to accompany me through this journey, always remembering her intention to give her greatest good for the greatest number of persons. I also want to thank my aunt Ana Isabel and my uncle Luis Octavio for their support throughout my life. They all made me realise the truth of William Blake's words: '*No bird soars too high if he soars with his own wings.*'

Abstract

This thesis proposes an integrative approach to analyse resting-state electroencephalography (rsEEG) signals in multi-centric studies, aiming to overcome methodological challenges towards the potential application of rsEEG as a diagnostic biomarker for various neurodegenerative disorders (NDDs). The primary objective was to evaluate the impact of combining rsEEG features from different conceptual families (i.e., spectral, complexity, connectivity) on the classification accuracy of different NDDs leading to dementia. First, differential patterns of rsEEG spectral, complexity, and connectivity features were identified at the group level in Alzheimer's Disease (AD), amnestic Mild Cognitive Impairment (MCI-AD), Parkinson's Disease (PD), Mild cognitive impairment in Lewy body diseases (MCI-LBD), Frontotemporal Dementia (FTD) and healthy controls (HC) in whom we explored potential age-related effects. Second, we compared the performance of various harmonisation pipelines in multicentric rsEEG datasets. Finally, we contrasted the classification performance (multi-class classification of NDD) between single-nature and multi-feature rsEEG analysis. The latter was achieved through automated machine learning (autoML).

Specific differences in epoch-to-epoch (frequency prevalence) and aperiodic parameterised spectral features, especially in the slow-theta, pre-alpha, and alpha bands, were identified as crucial contributors to distinguishing most NDDs from healthy controls. Complexity features revealed reduced complexity in AD patients. The combination of spectral and complexity features could provide a broader approximation to the neurophysiological alterations associated with NDDs by not focusing exclusively on slowed oscillatory activity and integrating other informative biomarkers of reduced complexity in the continuum of AD assessed through estimators of signal regularity and self-similarity (such as abnormal Hjorth parameters, increased Detrended Fluctuation Analysis exponent, and lower Fractal Dimensions).

Our results underscore the importance of addressing potential site-related variations in the rsEEG features extracted in multicentric studies. Our results indicated that the reComBat batch harmonisation significantly improved the classification performance (improving balanced accuracy by 29.6 % on average) by effectively re-centring and re-scaling the distribution of the rsEEG feature, mitigating batch effects related to site-specific variability. The best-performing autoML model utilised a combination of harmonised spectral and complexity features, demonstrating improved balanced accuracy (Bacc = 68.9%) compared to all evaluated models and an increased proportion of correctly classified individuals along the Alzheimer's disease (AD) continuum. Taken together, our findings suggest that statistical harmonisation of multi-feature rsEEG features with autoML modelling could provide a feasible and reproducible approach for pre-training accurate models for the identification of subjects with various types of NDDs, particularly those with clinical phenotypes of AD and MCI-AD.

List of Publications included in the thesis.

- Jaramillo-Jimenez, A., Suarez-Revelo, J. X., Ochoa-Gomez, J. F., Carmona Arroyave, J. A., Bocanegra, Y., Lopera, F., Buriticá, O., Pineda-Salazar, D. A., Moreno Gómez, L., Tobón Quintero, C. A., Borda, M. G., Bonanni, L., Ffytche, D. H., Brønnick, K., & Aarsland, D. (2021). Resting-state EEG alpha/theta ratio related to neuropsychological test performance in Parkinson's Disease. Clinical Neurophysiology, 132(3), 756–764. <https://doi.org/10.1016/j.clinph.2021.01.001>
- Jaramillo-Jimenez, A., Tovar-Rios, D. A., Mantilla-Ramos, Y.-J., Ochoa-Gomez, J.F., Bonanni, L., & Brønnick, K. (2023). ComBat models for harmonization of resting-state EEG features in multisite studies — manuscript in revision for publication (Clinical Neurophysiology – August 2023).
- Jaramillo-Jimenez, A., Mantilla-Ramos, Y.-J., Tovar-Rios, D. A., Ochoa-Gomez, J.-F., Oppedal, K., Aarsland, D., Brønnick, K., & Bonanni, L. (2023). Classifying Neurodegenerative Diseases from Resting-State EEG Signals Using Automated Machine Learning: A Multicenter Study — manuscript in preparation for submission.

List of Publications not included in the thesis.

- Jaramillo-Jimenez, A., Tovar-Rios, D. A., Ospina, J. A., Mantilla-Ramos, Y. J., Loaiza-López, D., Henao Isaza, V., Zapata Saldarriaga, L. M., Cadavid Castro, V., Suarez-Revelo, J. X., Bocanegra, Y., Lopera, F., Pineda-Salazar, D. A., Tobón Quintero, C. A., Ochoa-Gomez, J. F., Borda, M. G., Aarsland, D., Bonanni, L., & Brønnick, K. (2023). Spectral features of resting-state EEG in Parkinson's Disease: A multicenter study using functional data analysis. Clinical Neurophysiology : Official Journal of the International Federation of Clinical Neurophysiology, 151, 28–40. <https://doi.org/10.1016/J.CLINPH.2023.03.363>
- Jaramillo-Jimenez, A., Ying, Y., Ren, P., Xiao, Z., Zhang, Q., Wang, J., Rong, H., Borda, M. G., Bonanni, L., Aarsland, D., & Wu, D. (2022). Prodromal Dementia With Lewy Bodies and Recurrent Panic Attacks as the First Symptom: A Case Report. Frontiers in Neurology, 13, 587. <https://doi.org/10.3389/fneur.2022.839539>
- Kurbatskaya, A., Jaramillo-Jimenez, A., Fredy Ochoa-Gomez, J., Brønnick, K., & Fernandez-Quilez, A. (2023). Machine Learning-Based Detection of Parkinson's Disease From Resting-State EEG: A Multi-Center Study. ArXiv. <https://doi.org/10.48550/arXiv.2303.01389>
- Kurbatskaya, A., Jaramillo-Jimenez, A., Ochoa-Gomez, J. F., Brønnick, K., & Fernandez-Quilez, A. (2023). Assessing gender fairness in EEG-based machine learning detection of Parkinson's disease: A multi-center study. 1020–1024. <https://doi.org/10.23919/eusipco58844.2023.10289837>

List of Figures.

Figure 1. Estimated number of cases of all-type dementia across countries.

Figure 2. Evolution of conceptual approximation to neurodegenerative diseases (NDDs) from neurodegenerative syndromes to clinical phenotypes, neuropathological proteinopathies, and integrative biological frameworks considering individual and environmental risk factors.

Figure 3. Hallmarks of Neurodegenerative Diseases (NDDs) from an integrative biological framework.

Figure 4. Hallmarks of neurodegeneration in the most frequent types of neurodegenerative diseases (NDDs).

Figure 5. Protein aggregation/accumulation in Alzheimer's Disease (AD).

Figure 6. Protein aggregation/accumulation in Lewy Body Diseases (LBDs).

Figure 7. Pathophysiology of Frontotemporal Lobar Degeneration Spectrum.

Figure 8. Trajectories of successful, physiological, and abnormal ageing.

Figure 9. Theoretical models of Hormesis and Continuum in the context of Pathological Ageing and Neurodegenerative diseases (NDDs).

Figure 10. Neuronal origins of the resting-state electroencephalogram signals.

Figure 11. Oscillatory changes in the resting-state electroencephalogram (rsEEG) of patients with neurodegenerative diseases (NDDs).

Figure 12. Hypotheses on aperiodic (non-oscillatory) age-related changes in the resting-state electroencephalogram (rsEEG).

Figure 13. Changes in the resting-state EEG (rsEEG) rhythms and corresponding reductions in complexity.

Figure 14. Approximations to global complexity metrics in healthy subjects and neurodegenerative diseases (NDDs), exemplary cases.

Figure 15. Representation of changes in sensor space connectivity attributed to neurodegenerative diseases (NDDs).

Figure 16. Graphical abstract of the PhD project.

Figure 17. Demographical characteristics of the total sample for exploratory analyses ($n = 752$).

Figure 18. General organisation of the Brain Imaging Data Structure (BIDS).

Figure 19. Raw signals and derivatives organised in the Brain Imaging Data Structure (BIDS).

Figure 20. Illustration of the Fitting Oscillations and One-over-frequency (FOOOF) on rsEEG simulated data.

Figure 21. Demographic characteristics of the healthy controls subsample ($n = 374$) used to evaluate batch harmonisation.

Figure 22. Statistical harmonisation of resting-state electroencephalogram (rsEEG) spectral features extracted from multicentric data in a subsample of healthy subjects ($n = 374$).

Figure 23. Multilayer stacking implemented in the AutoGluon automated machine learning pipeline.

Figure 24. Group-level exploratory analysis of spectral features in the harmonised dataset ($n = 752$).

Figure 25. Group-level exploratory analysis of complexity features in the harmonised set ($n = 752$).

Figure 26. Group-level exploratory analysis of connectivity features in the harmonised set ($n = 752$).

Figure 27. Statistical harmonisation of the final dataset for automated Machine Learning (n = 507).

Figure 28. Summary of significant results in the exploratory analysis of harmonised data (n = 752) by feature type.

Figure 29. Most relevant rsEEG features for multiclass classification in the harmonised multi-feature final model (spectral + complexity + connectivity; n = 507).

Figure 30. Normalised confusion matrixes of unharmonised and harmonised spectral features and their combination with complexity and connectivity features.

Figure 31. Receiver Operator Characteristics (ROC) curves and confusion matrixes for best models tested with the harmonised spectral-only features and their combination with complexity and connectivity features.

List of Tables.

Table 1. Post Hoc Age comparisons by Neurodegenerative Diseases (NDDs) in the total sample (n = 752) - Exploratory analysis.

Table 2. Absolute and relative frequency of Neurodegenerative Diseases (NDDs) in the final set (n = 507) for automated machine-learning (autoML).

Table 3. Summary of model performance evaluation metrics (harmonised single-nature vs multi-features).

Table 4. Previously identified rsEEG features for AD and MCI-AD in a multiclass classification task.

Table of contents

| | |
|---|-----|
| AKNOWLEDGEMENTS | I |
| ABSTRACT | II |
| LIST OF PUBLICATIONS INCLUDED IN THE THESIS. | III |
| LIST OF PUBLICATIONS NOT INCLUDED IN THE THESIS. | III |
| LIST OF FIGURES..... | IV |
| LIST OF TABLES..... | IV |
| 1. INTRODUCTION | 1 |
| 1.1 DEMENTIA SYNDROME: DEFINITION AND RELEVANCE. | 2 |
| 1.2 EVOLUTION OF THE DEFINITION OF NEURODEGENERATION AND NEURODEGENERATIVE DISEASES (NDDs). | 4 |
| 1.2.1 <i>The spectrum of NDDs leading to dementia syndrome: an overview.</i> | 9 |
| 1.2.1.1 <i>Alzheimer's Disease.</i> | 9 |
| 1.2.1.2 <i>Lewy Body Diseases.</i> | 12 |
| 1.2.1.3 <i>Fronto-Temporal Lobar Degeneration (FTLD).</i> | 14 |
| 1.2.2 <i>Models of Hormesis and Continuum for Timely Detection and Prognosis of NDDs.</i> | 16 |
| 2. ELECTROENCEPHALOGRAM (EEG) IN NDDs..... | 20 |
| 2.1 ESSENTIAL CONCEPTS AND DEFINITIONS..... | 20 |
| 2.2 NEURAL MECHANISMS UNDERLYING THE NORMAL RESTING-STATE EEG (rsEEG). | 25 |
| 2.3 MECHANISTIC MODELS OF DISEASE: RSSEEG CORRELATES OF PATHOLOGICAL AND CLINICAL HALLMARKS OF NDDs. | 27 |
| 2.3.1 <i>Slowing-down of oscillations.</i> | 28 |
| 2.3.2 <i>Reduced complexity.</i> | 33 |
| 2.3.3 <i>Abnormal connectivity and synchronisation.</i> | 36 |
| 2.4 TOWARDS INTEGRATIVE MULTI-FEATURE MODELS IN rsEEG RESEARCH..... | 38 |
| 2.5 CURRENT CHALLENGES: WHY IS RSSEEG NOT INCLUDED IN MOST CRITERIA FOR NDDs LEADING TO DEMENTIA? | 39 |
| 2.5.1 <i>Challenges to reproducibility and validity of rsEEG findings.</i> | 40 |
| 2.5.2 <i>Small samples draw small conclusions: Harmonising and pooling multicentric data.</i> | 40 |
| 2.5.3 <i>Lack of uniform standardised preprocessing of rsEEG signals.</i> | 42 |
| 2.5.4 <i>Applicability of rsEEG in clinical settings</i> | 42 |
| 2.5.5 <i>Overcoming some of the challenges of rsEEG in NDDs diagnosis.</i> | 43 |
| 3. PH.D. PROJECT IN CONTEXT..... | 44 |
| 3.1 PHD PROJECT AIMS. | 46 |
| 4. METHODS..... | 47 |
| 4.1 DATASETS DESCRIPTION..... | 47 |
| 4.2 RSSEEG ACQUISITION AND PREPROCESSING..... | 51 |
| 4.2.1 <i>Brain Imaging Data Structure (BIDS) Standardisation.</i> | 51 |
| 4.2.2 <i>Preprocessing pipeline for rsEEG.</i> | 53 |
| 4.3 RSSEEG FEATURES..... | 54 |
| 4.3.1 <i>Spectral features.</i> | 54 |
| 4.3.2 <i>Complexity and Regularity Features.</i> | 55 |
| 4.3.3 <i>Connectivity features.</i> | 58 |
| 4.4 FEATURE HARMONISATION | 59 |
| 4.5 MULTICLASS CLASSIFICATION..... | 62 |
| 4.5.1 <i>Interpretability of model estimations.</i> | 64 |

| | |
|---|------------|
| 5. SUMMARY OF MAIN FINDINGS | 65 |
| 5.1 RS EEG PATTERNS IN SPECIFIC CLINICAL PHENOTYPES | 65 |
| 5.1.1 Spectral patterns. | 65 |
| 5.1.2 Complexity patterns. | 67 |
| 5.1.3 Global connectivity patterns. | 68 |
| 5.2 HARMONISATION OF RS EEG FEATURES IN MULTICENTER DATA..... | 69 |
| 5.3 COMBINED FEATURES OF THE RS EEG FOR DIAGNOSIS OF NDDs. | 70 |
| 6. DISCUSSION..... | 75 |
| 6.1 PARAMETERISATION OF OSCILLATORY ACTIVITY AND EPOCH-TO-EPOCH DESCRIPTORS HELP TO IDENTIFY SPECTRAL ABNORMALITIES IN NDDs..... | 75 |
| 6.2 REDUCED COMPLEXITY CHARACTERISES RS EEG SIGNALS OF AD PATIENTS..... | 78 |
| 6.3 HARMONISATION OF RS EEG FEATURES MITIGATES BATCH EFFECTS IN MULTICENTRIC STUDIES..... | 79 |
| 6.4 COMBINATION OF SPECTRAL AND COMPLEXITY ABNORMALITIES IN THE CLASSIFICATION OF NDDs. | 80 |
| 7. FUTURE PERSPECTIVES..... | 82 |
| 8. REFERENCES. | 83 |
| APPENDICES | 103 |
| PAPER 1 | |
| PAPER 2 | |
| PAPER 3 | |

1. Introduction.

In the words of Srinivasan and Nunez (Srinivasan and Nunez, 2012), the electroencephalogram (EEG) serves as a "*convenient, yet often opaque, window into the mind*". Technical and biological factors emerge as relevant challenges to tackle in EEG biomedical research; thus, robust signal processing and improved biological characterisation should be considered to explore brain-related correlates of health and disease from EEG signals. The rhythmic activity of EEG signals has led to an extended examination of EEG's oscillatory and non-oscillatory linear attributes (features). Still, signal complexity, synchronisation, and nonlinear dynamics could provide a more complete description and characterisation of EEG patterns.

Recent critical reviews have questioned the reproducibility of EEG markers of neurological and psychiatric diseases (Newson and Thiagarajan, 2019; Pavlov et al., 2021). Conflicting results in neuroscience research could potentially arise due to low statistical power and small sample size, as well as site-related aspects, including inter-rater variability in manual signal curation (preprocessing), differences in acquisition or analysis parameters and software, scanner/headset-related variability, etc. (Bigdely-Shamlo et al., 2020; M. Li et al., 2022). Given the associated costs, invasiveness, and lack of portability of standard neuroimaging methods, establishing reproducible EEG biomarkers for neurological diseases becomes crucial. As a case in point, a significant healthcare challenge is the increased number of individuals diagnosed with dementia due to neurodegenerative diseases (NDDs), reaching more than 50 million people in 2019 estimates (Nichols and Vos, 2021). A more dramatic perspective is stated for the predementia stages of neurodegeneration. Thus, most recent estimates suggest that people at risk of developing dementia due to NDDs could represent up to 315 million subjects (Gustavsson et al., 2023).

Considering the above problem, this research focuses on the analysis of resting-state EEG signals (rsEEG) to identify various types of NDDs leading to dementia. We propose an automatic method for signal preprocessing. Besides, we integrate multiple rsEEG features by capturing linear and nonlinear dynamics of the signal to detect abnormality patterns associated with specific types of NDDs. In order to avoid underpowered results, data from multicentric studies was pooled into a large single dataset, with subsequent control of potential site-specific differences. Finally, to provide reproducible and generalisable predictions across an extensive data collection, we applied automated machine learning models (autoML) for the classification of various NDDs.

Across the introductory chapters of the thesis, we will expand on five core elements of the research problem:

- A) Definition of Dementia syndrome and its epidemiological and social relevance.
- B) Evolution of the conceptualisation of NDDs and definition of the most frequent NDDs leading to dementia syndrome.
- C) Mechanistic models linking NDDs and pathological ageing trajectories with dementia syndrome.
- D) Potential of EEG biomarkers for NDDs and dementia syndrome.
- E) Methodological challenges in EEG biomarkers discovery and application.

Based on this theoretical framework, the research question and objectives will be contextualised. Then, a detailed description of the methods used in each analysis stage (from acquisition to automated classification of NDDs) will provide the reader with valuable information to evaluate and reproduce our procedures. To achieve the primary goal of this research, we will conclude this thesis by presenting a synthesis of our main findings with a critical discussion on current limitations and challenges that need to be addressed by future research.

1.1. Dementia syndrome: Definition and relevance.

Dementia syndrome is a common clinical outcome in most NDDs. Dementia is the result of a complex multifactorial process involving proteinopathies, vascular and mixed pathology that affects brain function and structure, leading to cognitive decline and neuropsychiatric symptoms that significantly interfere with the activities of daily living of an individual, causing dependency (Sachdev et al., 2014).

The definition of dementia syndrome was updated in the Fifth edition of the Diagnostic and Statistical Manual of Mental Disorders (DSM-5). The DSM-5 suggest a two-step approach by first identifying the dementia syndrome and then assessing potential causes to support the decision of the most probable aetiology. As an alternative to the term "dementia", authors of the DSM-5 have proposed the term "major neurocognitive disorder", considering that the former might elicit misconceptions of a prevalent condition only in older adults, not accounting for cases of young-onset dementia. Thus, "major neurocognitive disorder" is defined as:

- A) A significant and chronic decline in cognitive abilities (evident in one or more cognitive domains such as complex attention, executive function, learning and memory, language, perceptual-motor, or social cognition), with or without accompanying behavioural disturbances, such as mood changes or agitation.
- B) This decline is noticed by the individual, someone close to them, or a clinician and is documented as significantly reduced performance on neuropsychological tests.
- C) The magnitude of cognitive decline significantly impacts daily activities, such as handling finances or medications.
- D) Dementia does not occur solely during delirium and is not explained by other mental disorders.

Analogously, "minor neurocognitive disorder" has been proposed as an alternative to Mild Cognitive Impairment (MCI), where cognitive decline does not limit the appropriate performance of activities of daily living. Notwithstanding, adopting the proposed new terminology in the neuroscientific community may take a long time. Thus, in the DSM-5, the term "dementia" is still employed, given its prominent use in previous and current medical literature (American Psychiatric Association, 2013; Reisberg, 2006; Sachdev et al., 2014). Besides, under the cluster of three neurocognitive disorders proposed by the DSM-5 framework, delirium is also included. Unlike dementia, delirium is characterised by acute, transient, and often reversible abnormalities in awareness, behaviour, and cognition.

Apart from clarifications on terminology, dementia syndrome is a critical problem that demands necessary actions because of its epidemiological importance. Given the current worldwide demographic trends (i.e., decreased fertility rates and increased life expectancy), there are larger groups of people at the oldest ages than historically. It has been recognised that the risk of developing some NDDs leading to dementia increases with age, making it an epidemiological challenge nowadays. Worldwide forecasts estimate that, in 2050, the population with dementia will increase to 152.8 million (130.8–175.9), underscoring urgent needs for public health and society (Nichols and Vos, 2021). We capitalised on data from Nichols et al. (Nichols et al., 2022) to depict the 2019 and 2050 global estimations of all-type dementias and the expected increase in cases by country, **see Figure 1**.

The greatest absolute estimates could be observed in the most populated countries (**Figures 1A and B**). At the same time, the largest relative change in the number of cases might account for up to 300 % when not adjusted for age (**Figure 1C**), with a prominent rise in Low and middle-income countries (**Figure 1D**).

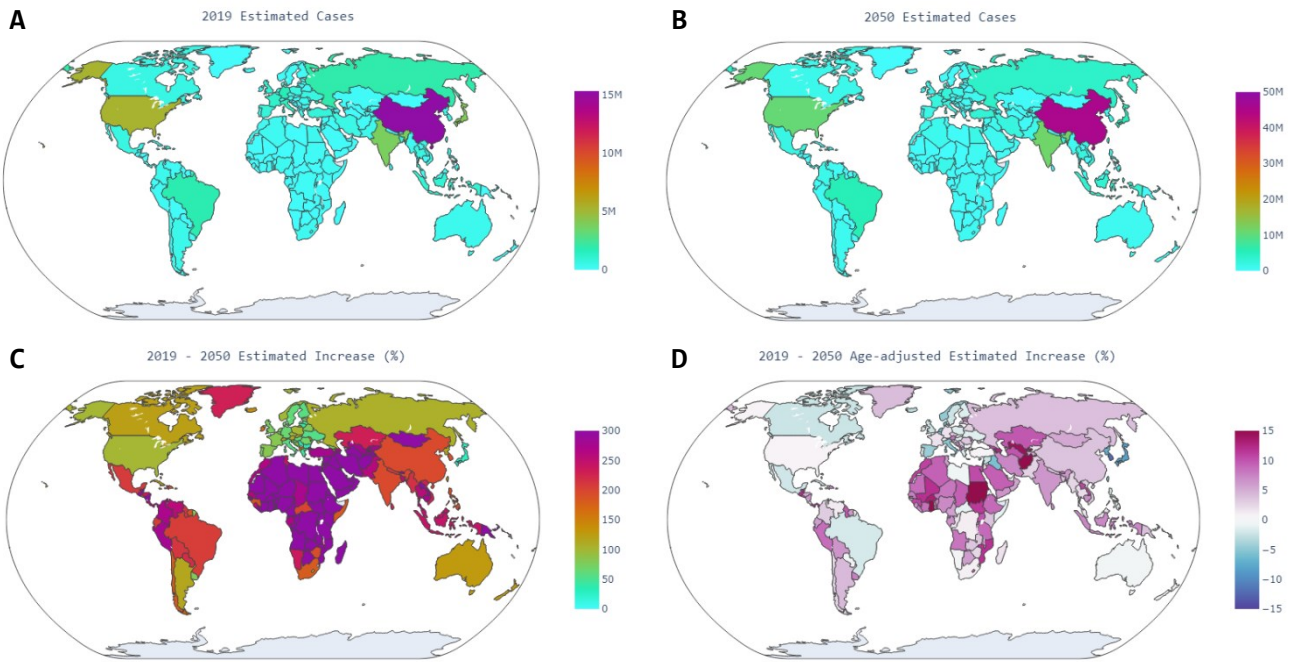


Figure 1. Estimated number of cases of all-type dementia across countries. Choropleth maps are used as follows: A) Represents the estimated absolute number of dementia cases by country in 2019. B) Illustrates the estimated absolute number of cases of all-type dementia expected for 2050. C) Displays the estimated relative increase in dementia cases from 2019 to 2050. D) Shows the age-adjusted estimated increase in those cases (negative values represent a reduction in the relative number of cases in each country). Data extracted from (Nichols et al., 2022).

Although dementia syndrome itself is not a direct cause of death, complications of severe dementia, such as bronchopneumonia, can lead to death. In 1990, dementia was ranked as the 20th leading cause of death worldwide (all-age mortality), but it reached the seventh position in 2019, with more than 1.6 million deaths linked to severe dementia syndrome. A close examination of these data also reveals an increase from the sixth leading cause of mortality to the fourth cause of mortality in those individuals over 70 years old (Nichols et al., 2021).

As noted earlier, multiple potential aetiologies can lead to different clinical subtypes of dementia syndrome according to the DSM-5 framework. Primary causes of dementia syndrome majorly comprise NDDs, but also vascular disease (e.g. stroke), HIV infection, substance/medication use disorder, and traumatic brain injury. Among NDDs, the most frequent cause of dementia syndrome is Alzheimer's Disease (AD). According to 2023 global estimates, 32 million people live with AD dementia, while prodromal (MCI) and preclinical stages of AD (at risk of MCI) represent 69 and 315 million cases, respectively (Gustavsson et al., 2023). Beyond AD, estimations on Dementia with Lewy Bodies (DLB) reach up to 5.5 million people (but underdiagnosis/misdiagnosis is often reported) (M. N. Sabbagh et al., 2023), while up to 80% of Parkinson's Disease (PD) patients may develop PD Dementia (PDD) 15 - 20 years after the onset of PD symptoms (Biundo et al., 2016). Dementia syndrome due to NDDs is not exclusive to individuals aged 65 or older. In 2021, estimates on young-onset dementia suggested a global prevalence of 3.9 million individuals aged 30 – 64. Remarkably, Frontotemporal Dementia (FTD) accounted for 1.2 – 1.7 million cases of young-onset dementia worldwide (Hendriks et al., 2021).

Beyond the epidemiological challenges discussed above, signs and symptoms of NDDs and dementia have repercussions in psychological, social and economic dimensions, often implying detrimental consequences for patients and their relatives. A large population-based study conducted in Denmark evidenced that loss of productivity, lower income, and increased social and health-related vulnerability were present in patients before dementia diagnosis and continued across the course of the disease (Frahm-Falkenberg et al., 2016). Patients might require assistance with activities of daily living such as transporting, eating, dressing, bathing, and toileting, resulting in loss of independence, increased social costs, and reduced quality of life (Maresova et al., 2020). Also, a two-fold risk of job loss in those with young-onset NDDs has been reported (Sakata and Okumura, 2017). Consistently, family members taking care of patients with NDDs and dementia are exposed to a higher burden, lower relationship satisfaction, increased risk of mental health disorders, and reduced quality of life due to disruptive symptoms of NDDs (Cheng, 2017; Klietz, 2022).

Negative impacts of dementia extend to the patient's family/caregivers but also to the healthcare system, accounting for one of the most expensive spendings compared to other chronic diseases. Notably, a recent report on health-related spending in 144 health conditions showed that dementias represented the highest spending in Norway, with more than 10 % of the total expenditures (Kinge et al., 2023). On the global panorama, the projected economic burden of dementia care might represent a four-fold increase by 2050. The authors found convergent results in country-wise analysis, reporting an inequitable economic impact of dementia in low and middle-income countries (Nandi et al., 2022).

Despite the crucial relevance of dementia, several factors hinder the early and accurate identification of its underlying causes and the role of ageing in the development of this syndrome. The following sections will review the definition of neurodegeneration and NDDs to account for the causes of dementia syndrome. Then, mechanistic models accounting for age-related effects in NDDs and their importance for the timely identification of dementia syndrome will be reviewed.

1.2. Evolution of the definition of Neurodegeneration and Neurodegenerative diseases (NDDs).

While etymology suggests loss of structure or function (degeneration) in nerve cells (neuro), a literal definition of neurodegeneration does not precisely describe the broad spectrum of NDDs. The term NDDs refers to a group of heterogeneous diseases primarily affecting specific neurons, leading to chronic dysfunction and loss of structure in particular organisation systems such as columns of the brain cortex, basal ganglia, etc. Thus, common clinical manifestations of the individual diseases clustered under the umbrella of NDDs are remarkably overlapping and may include motor or cognitive impairment, as well as behavioural and neuropsychiatric symptoms that lead, in most cases, to dementia syndrome. Unlike secondary causes of neural loss (neoplasm, hypoxia, metabolic defects, or toxins), the aetiology of NDDs remains unknown in most cases, given the interplay of multiple factors (Przedborski et al., 2003).

Before the early 20th century, there were few publications in the medical literature with the word "neurodegeneration" as part of the title. In fact, in the report of "*An unusual illness of the cerebral cortex*" by Dr Alöis Alzheimer in 1907, the word "degeneration" was only used to provide a general macroscopic inspection of the brain of a patient with early-onset AD, as follows: "*The post-mortem showed an evenly atrophic brain without macroscopic focal degeneration*" (Alzheimer, 1907; Stelzmann et al., 1995; Stoddart, 1913). Neither was it used in 1817 by Dr James Parkinson in his early clinical description of the "shaking palsy" or "paralysis agitans",

subsequently named PD by Dr Jean-Martin Charcot in 1868 (Goetz, 2011; Parkinson, 2002). Until the late 1960s, the term neurodegeneration was not broadly used to describe clinical aspects of different NDDs such as AD, PD, DLB, or Frontal-temporal Dementia (FTD) (Jennekens, 2014). Instead, these initial conceptualisations of NDDs favoured its understanding as neurological syndromes with prominent cognitive, motor, or behavioural alterations, with incipient emphasis on macroscopic pathological findings, **see Figure 2**.

Before 2000, the research paradigm refined earlier conceptualisation of NDDs by differentiating more detailed clinical phenotypes and their underlying neuroanatomical abnormalities. Although more clinical phenotypes were defined, the boundaries between some phenotypes were still blurry due to overlapping symptoms and neuroanatomical abnormalities, **see Figure 2**. Consequently, diagnostic approximations based on clinical phenotypes indirectly represented "where" the lesions might be localised instead of "what" was the aetiology behind a particular clinical phenotype; the emergence of neuropathology shed light on the latter question (Allegri, 2020).

As determining the aetiology of clinical phenotypes became the predominant paradigm, the abnormal deposition of misfolded proteins in cortical or subcortical brain structures (i.e., proteinopathy) was identified as a shared pathophysiological phenomenon across NDDs, **see Figure 2**. Hence, amyloid beta protein ($A\beta$), tau protein (tau), alpha-synuclein (α -syn), Fused-in Sarcoma protein (FUS), and TAR DNA-binding protein 43 (TDP-43) were initially recognised as principal signatures of individual diseases (clinical phenotypes) grouped as NDDs (Allegri, 2020). Thus, by the end of the 20th century, the definition and adoption of clinical diagnostic criteria for AD required the presence of specific neuropathological findings in post-mortem brain tissue to confirm the clinical diagnosis. These criteria considered the level of uncertainty in the diagnosis: a "possible" and "probable" diagnosis of AD resulted from clinical signs and symptoms (i.e., clinical phenotypes), whereas AD-related pathology in brain tissue yielded a "definitive" diagnosis (Blacker et al., 1994; McKhann et al., 1984).

The abovementioned efforts on determining specific underlying (and definitive) pathophysiological hallmarks for each clinical phenotype revealed, on the contrary, a pronounced overlapping across separated clinical entities. Therefore, the accumulation/aggregation of a single protein was observed across multiple clinical phenotypes. Similarly, individual clinical phenotypes could reflect the accumulation/aggregation of multiple proteins, **see Figure 2**. Briefly, post-mortem characterisation of AD brains identified abnormal plaques of misfolded $A\beta$ in the brain cortex and neurovascular units, as well as neurofibrillary tangles produced by aggregated residues of phosphorylated tau protein (p-tau). Besides, from the first extensive description of PD and atypical Parkinsonian syndromes, it took close to one hundred years to determine the brain pathology underlying individuals with PD. It was in 1912 when Dr Fritz Heinrich Lewy described basal-ganglia inclusions in the substantia nigra of PD patients, known today as Lewy bodies. However, in the 1970s, autopsies of patients with early cognitive decline (from the onset of Parkinsonian motor symptoms) elucidated the overlapping in pathological profiles of AD and the mentioned PD individuals. Consistently, the reports by Dr. Kenji Kosaka between 1976 and 1978 supported that Lewy bodies were not exclusively found in the substantia nigra of the basal ganglia but also diffusely across the cortex. These case reports in individuals with Lewy bodies also detected Alzheimer's $A\beta$ pathology, proposing the term Lewy Body Diseases to group PD and the so-called "Lewy body variant of Alzheimer's disease", re-defined in 1995 as "Dementia with Lewy Bodies". Nevertheless, determining the composition of Lewy Bodies was not possible until 1997, when α -syn aggregates were identified as its most prominent constituent (Kosaka, 2014).

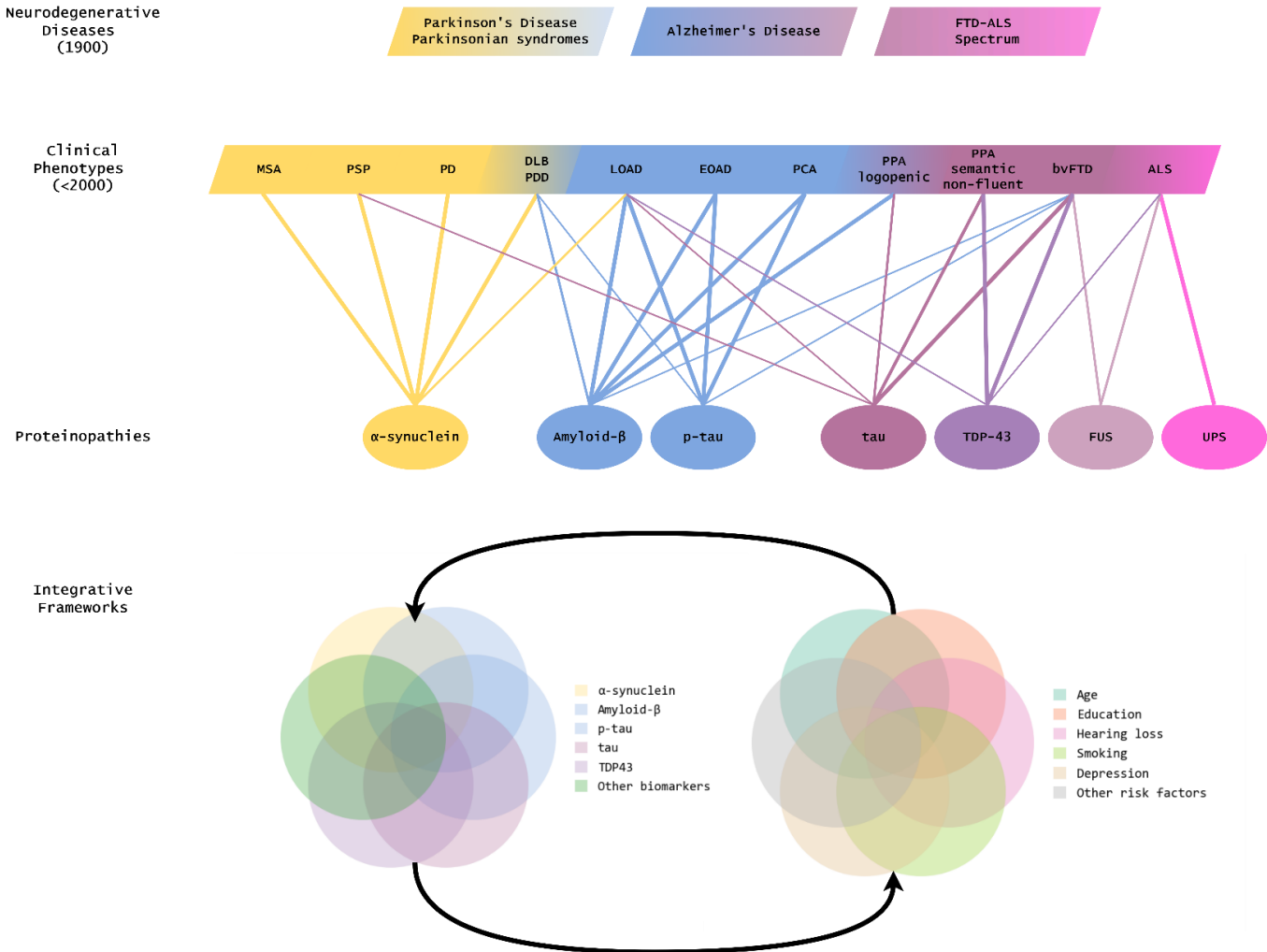


Figure 2. Evolution of conceptual approximation to neurodegenerative diseases (NDDs) from neurodegenerative syndromes to clinical phenotypes, neuropathological proteinopathies, and integrative biological frameworks considering individual and environmental risk factors. On top is the definition of the three most frequent neurological syndromes, subsequently described clinical phenotypes. Gradients represent overlapping across clinical phenotypes. Neuropathological characterisation of the proteins involved in each clinical phenotype is depicted in the Proteinopathies section of the plot. Lines illustrate a given protein's strong or weak contribution to a particular clinical phenotype. Clinical phenotypes with more than one line imply multiple pathological protein accumulation/aggregation contributions. Finally, integrative frameworks combine proteinopathies, other biological hallmarks of neurodegeneration, and the effect of individual and environmental risk factors. The figure was adapted from (Allegra, 2020).

Analogously, Dr Arnold Pick reported a case series of individuals with pre-senile cognitive disturbances and eminent personality changes with focal symptoms such as aphasia and apraxia. In this regard, the clinical patterns were explained by the circumscribed focal atrophy of the frontal and temporal lobes, as proposed by Pick in his original descriptions. Still, late histological findings made by Dr Alzheimer highlighted the presence of argyrophilic neuronal inclusions of tau protein (called Pick bodies). However, controversies about Pick disease appeared around the 1930s, with patients expressing different phenotypes than the classical description. Some exhibited motor neuron disease in addition to the behavioural and cognitive symptoms, as well as a prominent Pick pathology in not-expected brain regions (cortico-basal and extrapyramidal structures). Thus, diseases causing primarily atrophy of the frontal and temporal lobes with or

without Pick bodies were clustered in 1998 as Fronto-Temporal Lobar Degeneration (FTLD). This umbrella is characterised by tau, FUS, or TDP-43 pathology, covering very distinct clinical phenotypes of aphasias (i.e., fluent, nonfluent, and logopenic variants of Primary Progressive Aphasia), the behavioural variant of FTD (with apathetic or disinhibited phenotypes), as well as prominently motor neuron diseases such as ALS (Kertesz, 2007).

Clinical phenotypes may also lie under oversimplified binary classifications: typical versus atypical symptoms, young (or early) versus late-onset, sporadic versus familial, and gradual versus rapid progression. It has been recognised that 'canonical' or 'typical' clinical phenotypes are formulated in a pragmatic attempt to homogenise diagnostic criteria and clinical research cohorts, but individual trajectories of signs and symptoms of a single clinical phenotype vary across patients. The continued adoption of clinical phenotypes for diagnosis is supported as the 'typical' signs and symptoms of a given 'typical' clinical phenotype primarily correlate with its expected pathological hallmarks (aetiology). Thus, as supported by the DSM-5, characterising classical clinical phenotypes in patients with dementia could provide an additional level of certainty in diagnosis, prognosis, and management decisions in clinical practice. Despite this, it has been observed that the coexistence of multiple proteinopathies increases with age, resulting in overlapping symptoms that cross the boundaries of classical clinical phenotypes (Elahi and Miller, 2017; Jellinger and Attems, 2008). Beyond clinical applicability, the knowledge gaps in clinic-pathological characterisation have also promoted research advances on in-vivo biomarkers of NDDs, which are particularly helpful in identifying atypical cases and early events presented in the preclinical stages of the disease (Elahi and Miller, 2017).

In line with the above, in the 21st century, the increasing number of reports and improved analytic approaches extended the corpus of evidence showing overlapping clinical and neuropathological features across NDDs, pointing out that NDDs result from complex biological phenomena involving individual and environmental risk factors that trigger cellular changes leading to neural cell death (Livingston et al., 2020). A critical perspective was raised about potential oversimplification made by definitions focused on proteinopathy, favouring the identification of multiple potential biomarkers (apart from proteinopathies) that might reflect the process of neurodegeneration (Gauthier et al., 2018). The latter argues for integrative models where the interplay of multiple biological abnormalities (not only protein accumulation/aggregation) is responsible for the broad and heterogeneous manifestations of NDDs, see **Figures 2 and 3**.

To overcome the problem of simplified and fixed definitions across different types of NDDs, Wilson et al. recognised subject-specific differences in the strength of the links between the primary drivers of neurodegeneration, as depicted in **Figure 3**. Thus, rather than exclusively stating specific disease patterns at the group level, Wilson's framework accounts for inter-subject variability across patients with the same disease, enabling personalised diagnostics, stratification, and treatment (Wilson et al., 2023) with an elegant synthesis of the literature, proposing eight biological hallmarks of NDDs:

- Abnormal protein accumulation/aggregation
- Synaptic and neuronal network dysfunction
- Aberrant proteostasis
- Cytoskeletal abnormalities
- Altered energy homeostasis
- DNA and RNA defects
- Inflammation
- Neuronal cell death

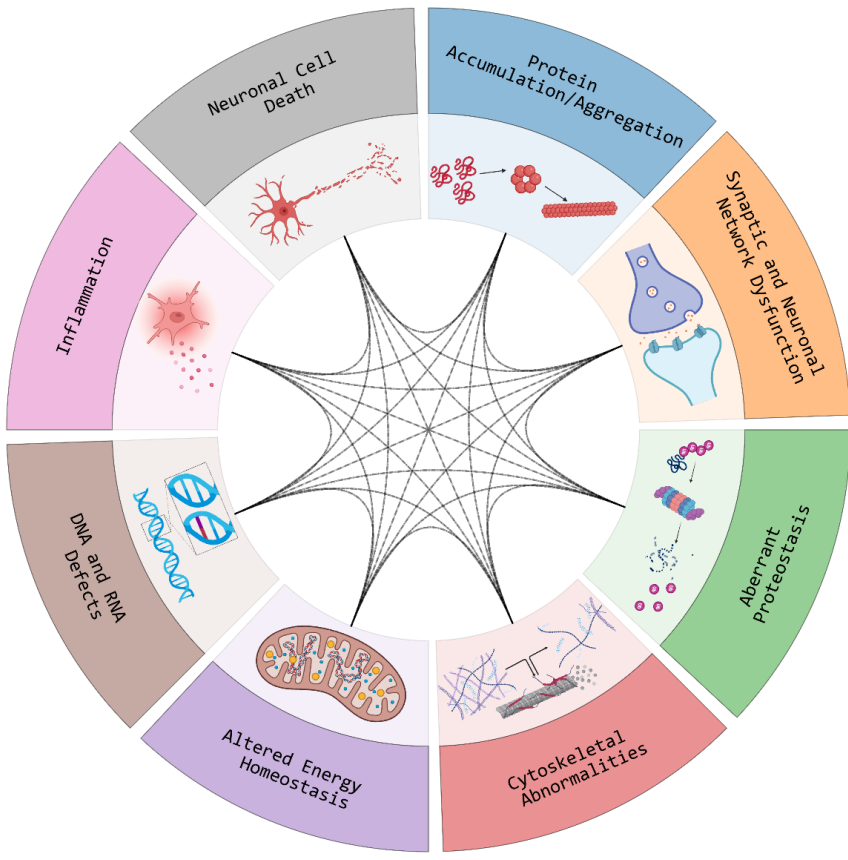


Figure 3. Hallmarks of Neurodegenerative Diseases (NDDs) from an integrative biological framework. Each sector of the circle depicts a particular aspect involved in the process of neurodegeneration. The associations between hallmarks vary among specific NDDs, representing potentially overlapping or more distinct patterns of abnormality, as illustrated by inner dashed lines. The figure was created with BioRender.com and adapted from (Wilson et al., 2023).

Although common to all types of NDDs, these determinants do not contribute to the same extent to the clinical phenotype, and their varying significance in distinct disorders appears to be influenced by a combination of genetic and environmental factors, as well as the strength of the abnormalities in a particular determinant, complex inter-relationships between determinants, specific neuronal populations, brain regions, or cell types that are affected.

Beyond a common framework for NDDs presented in **Figure 3**, Wilson et al. formulated "primary" disease pathway contributors for the most frequent types of NDDs. Thus, protein accumulation/aggregation, synaptic dysfunction, and inflammation are considered crucial contributors to AD. Also, although protein accumulation/aggregation are determinants of PD and DLB, the authors recognise aberrant proteostasis and altered energy homeostasis as relevant hallmarks in the spectrum of Lewy Body diseases (LBDs). In the spectrum of FTD and ALS, protein accumulation/aggregation with synaptic dysfunction and DNA and RNA defects are prominent hallmarks, see **Figure 4**.

The authors also recognise neuronal cell death as the endpoint of the cascade of neurodegeneration, stating that it is produced by synergistic or additive effects among individual disease hallmarks (Wilson et al., 2023). The combined effect of the abovementioned biological hallmarks, in addition to the susceptibility of a given individual, determines the clinical and

pathological phenotype expressed by this particular person and potential multi-targeted intervention alternatives (Wilson et al., 2023).

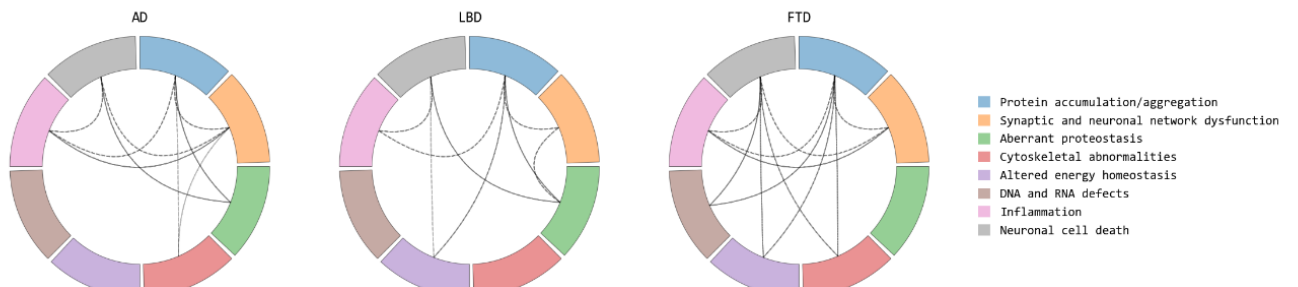


Figure 4. Hallmarks of neurodegeneration in the most frequent types of neurodegenerative diseases (NDDs). Circles illustrate patterns of abnormality in the three most frequent types of NDDs: Alzheimer's Disease (AD), Lewy Body Dementia (LBDs), and Frontal-temporal Dementia (FTD). Each sector of the circle depicts a particular hallmark of neurodegeneration. The associations between hallmarks vary among specific NDDs, representing potentially overlapping or more distinct patterns of abnormality, as illustrated by inner links in each circle. The figure was adapted from (Wilson et al., 2023).

1.2.1. The spectrum of NDDs leading to dementia syndrome: an overview.

These subsections will expand on the epidemiological aspects, typical biological hallmarks and clinical presentations of the most frequent NDDs leading to dementia syndrome, as well as overlapping between biomarkers of these diseases.

1.2.1.1. Alzheimer's Disease.

AD represents 60 - 75% of dementia cases (Abubakar et al., 2022). Two-thirds of patients clinically diagnosed with AD are women. The analysis of a Swedish population registry of older adult twins showed that the annual incidence rate of any dementia was comparable between male and female patients up to 85 years; from this age, women exhibited a significantly higher incidence rate. Similarly, the annual incidence rate of AD showed comparable results up to 80 years, followed by increased incidence in women (Beam et al., 2018). Observations have also suggested potential associations between augmented tau pathology susceptibility and loss of ovarian function, as well as delayed hormone therapy in post-menopausal women (Coughlan et al., 2023). Although age is not a direct cause of AD, increased age has been identified as a relevant risk factor for AD in individuals aged above 60 years (Rasmussen et al., 2018). For sporadic AD, the mean age at dementia onset has been estimated by large prospective cohorts at 80 years (Rujeedawa et al., 2021). Low education and cardiovascular and metabolic risk factors have been identified as potentially modifiable determinants of AD (Livingston et al., 2020). Most AD cases are sporadic, but a higher risk of AD has been found in individuals carrying the Apolipoprotein E (APOE) epsilon 4 allele. Nevertheless, up to 5% correspond to familial AD forms caused by monogenic genetic variations in the amyloid precursor protein (APP) or the presenilin -PSEN 1 and PSEN2 - genes affecting the APP cleavage. Familial AD presents as a young-onset dementia syndrome with an estimated mean age at onset ranging between 40 and 60 years, depending on the affected gene (Rujeedawa et al., 2021).

From the clinical standpoint, cognitive decline with pronounced anterograde amnesia (affecting short-term episodic memory) is one of the core clinical hallmarks of the disease. Cognitive decline in the continuum of AD extends to other neurocognitive functions than memory, including executive function, visuospatial function, and language (McDonald, 2017; Porsteinsson et al., 2021). Robust evidence concludes that neuropsychiatric symptoms in AD accompany cognitive decline in most patients (Nowrangi et al., 2015). Neuropsychiatric symptoms can fluctuate over time and vary in terms of frequency or severity across the course of AD (Vik-Mo et al., 2018). Consistent findings in large cohorts have shown that depression, apathy, agitation, and aggression are prevalent in AD (Lyketsos et al., 2002). When the presence of functional decline due to cognitive impairment is evident, the progression of dementia syndrome in AD ranges from mild to severe stages. Mild stages of dementia might only interfere with instrumental activities of daily living, such as keeping appointments, using telephone and digital devices, or paying bills. The moderate stage implies difficulties in dressing, cooking, and bathing, while patients with severe dementia experience limitations in walking and eating (Forchetti, 2005). There are existing validated diagnostic criteria for AD (Blacker et al., 1994; Jack et al., 2016; McKhann et al., 2011) and predementia phases characterised by an asymptomatic stage with biomarker abnormalities and subsequent progression to MCI syndrome affecting single or multiple cognitive domains (Albert et al., 2011; Petersen et al., 2013; Sperling et al., 2011).

The process of protein aggregation and subsequent accumulation in cortical regions antecedes the onset of clinical symptoms of dementia, prodromal dementia (MCI) and preclinical (asymptomatic) stages in the AD continuum. Under normal conditions, APP is a constitutive membrane protein cleaved majorly by α -secretase, see **Figure 5A**. By contrast, familial monogenic forms of AD are characterised by APP mutations and mutations in the presenilin component of the cleavage enzyme (PSEN1 or PSEN2) that promote cleavage by β or γ -secretase, respectively. The latter generates self-aggregating A β monomers that form oligomers in both intracellular and extracellular spaces. Extracellular A β toxic oligomers subsequently aggregate in fibrils and amyloid plaques, see **Figure 5B**. In sporadic AD, reduced clearance of A β protein is caused by the presence of APOE epsilon-4 alleles and inhibitory effects on γ -secretase (Sun et al., 2023). Early amyloid toxicity leads to further synaptic dysfunction (synaptic loss) mediated by hyperexcitability and excitotoxicity before neural death, where the decreased neural function is reflected by hypometabolism in imaging studies like positron emission tomography (PET). Glial inflammation, defects in DNA damage processing, altered mitochondrial function, and aberrant proteostasis in lysosomal and autophagic function have also been evidenced. On the other hand, tau protein stabilises microtubules in the cytoskeleton under normal conditions. In AD, hyperphosphorylated tau (p-tau) aggregates in oligomers and intracellular neurofibrillary tangles, causing loss of microtubule stability, synaptic dysfunction, neurotoxicity, and cytoskeletal abnormalities such as altered axonal transport, see **Figure 5C** (Querfurth and LaFerla, 2010; Wilson et al., 2023).

The accumulation of A β and p-tau pathology typically exhibits specific patterns. A β accumulation involves the hippocampus, entorhinal cortex, precuneus, medial orbitofrontal, and posterior cingulate cortex, diencephalic nuclei, striatum, cholinergic nuclei, brainstem and cerebellum (Palmqvist et al., 2017; Thal et al., 2002). The accumulation of p-tau follows four subtypes: the trans-entorhinal and limbic-predominant, as well as the medial temporal lobe-sparing, are the most predominant variants, whereas posterior and lateral temporal are less frequently observed. These patterns seem to be related to age of onset, disease severity, and atypical clinical symptoms, as shown by the conclusions driven by data from the AD Neuroimaging Initiative (ADNI) (Vogel et al., 2021).

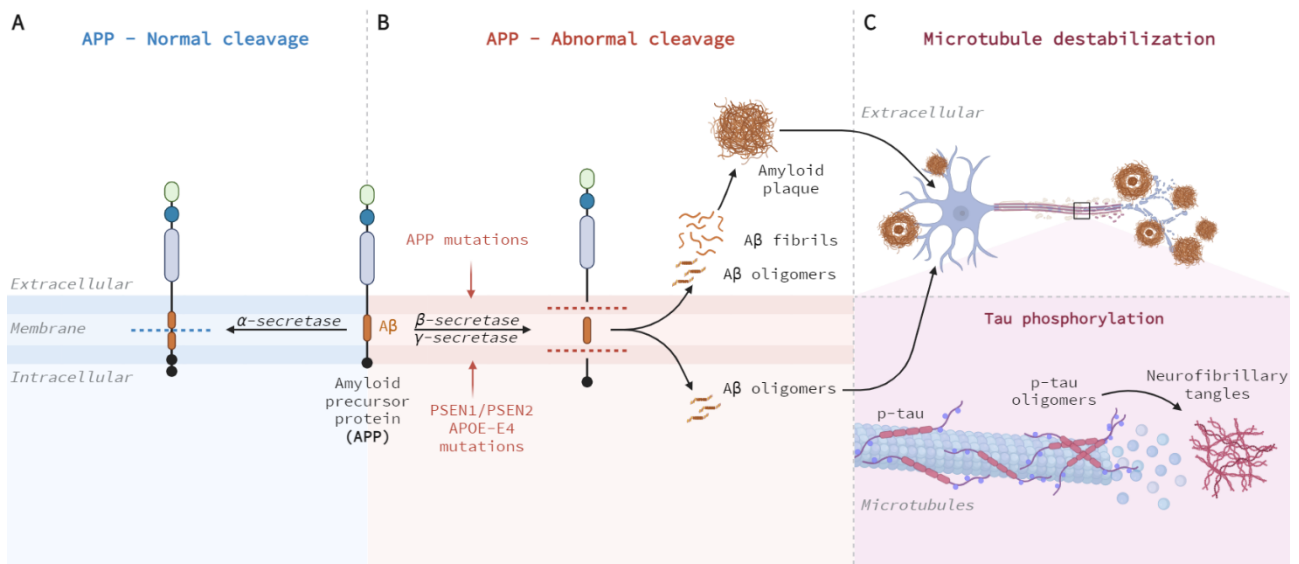


Figure 5. Protein aggregation/accumulation in Alzheimer's Disease (AD). **A)** Shows the normal cleavage of amyloid precursor protein (APP) in the brain cell membrane. APP is processed by α -secretase. **B)** Illustrates the abnormal cleavage of APP by β and γ -secretase. Mutations on the APP gene modulate the activity of β -secretase. In contrast, mutations in presenilin (PSEN1 and PSEN2) genes or the presence of apolipoprotein E epsilon 4 allele (APOE-E4) cause abnormal activity of γ -secretase. The peptidic fragments of A β are aggregated in the intracellular and extracellular space as A β oligomers. Extracellular oligomers aggregate in fibrils and amyloid plaques. **C)** Represents the phosphorylation of tau (p-tau) in the microtubules of the cytoskeleton. The destabilisation of microtubules is driven by p-tau aggregation. The figure was created with BioRender.com and adapted from (Querfurth and LaFerla, 2010).

The identification of pathological signatures of AD in the preclinical stages of the disease has promoted biomarker research and precision medicine. The definition of AD has been refined to include optimal indicative biomarkers that quantify A β , p-tau, and neuronal cell death (neurodegeneration) mainly through functional imaging, cerebrospinal fluid (CSF) and genetic techniques. To be considered optimal, the discriminatory properties of these biomarkers should offer sensitivity and specificity above 80%. Other characteristics of the ideal biomarker may include high accuracy, good predictive capabilities, robustness, simplicity, and non-expensiveness (Khoury and Ghossoub, 2019). CSF and genetic panels or functional imaging biomarkers like PET with radiotracers for A β or p-tau accumulation are limited in clinical practice, are not simple, and might be less affordable than other methods (Turner et al., 2020).

1.2.1.2. Lewy Body Diseases.

The spectrum of LBDs encompasses cognitively spared individuals with PD, PD with MCI and PDD, as well as DLB with and without co-existing AD pathology. DLB accounts for 4.2 to 20% of dementia diagnoses (Armstrong and MJ, 2019). PDD mean prevalence has been estimated at 31.4 % of PD individuals (Xu et al., 2016), and global cases of incident PD are estimated at 9.4 million (Maserejian et al., 2020). Altogether, clinical syndromes under the LBDs umbrella represent the second most frequent cause of neurodegeneration and neurodegenerative dementia (Donaghy and McKeith, 2014; Mhyre et al., 2012). As in AD, age is the primary risk factor for LBDs, with 60 years as the mean age at onset for PD and > 70 years for PDD and DLB. Thus, the age of onset seems to be comparable between AD, DLB and PDD (Mouton et al., 2018). In addition, up to one-third of patients with a de-novo diagnosis of PD exhibit MCI, and PDD is cumulatively developed after twenty years in around 80% of individuals with PD (Aarsland et al., 2021, 2017). On the other hand, a gender-related predominance of males (male/female ratio = 4/1) has been reported in LBDs, but multiple cohorts have observed variable results. A population-based cross-sectional study in France analysed a larger sample of PD (n = 8744), PDD (n = 3198), and DLB (n = 10309), describing a slight predominance of men with DLB before the age of 75. Conversely, the percentage of women with DLB was greater in those over 75 years. Similarly, among AD cases (n=135664), women were predominant. By contrast, PD and PDD were slightly more common in men, but this observation did not achieve statistical significance, suggesting comparable male/female ratios (Mouton et al., 2018).

In PD, PD-MCI, PDD, and DLB, the abnormal aggregation and accumulation of intraneuronal α -syn is a distinctive aspect of neuropathology. Besides, α -syn aggregates can also accumulate in oligodendroglia, as in the case of patients with Multiple Systems Atrophy (MSA). Thus, hypotheses suggest that those diseases leading to increased intracellular α -syn aggregates can be considered part of the same disease spectrum. These ideas were supported based on similar therapeutic management and shared clinic-pathological and genetic features among diseases (Jellinger and Korczyn, 2018). Nonetheless, novel critical perspectives have emphasised the reduced prevalence of "pure" α -syn pathology. Such perspective highlights a notable presence of double and triple pathology (α -syn combined with A β , tau, TDP-43, etc.), also referred to as "overlap syndrome", as well as prominent vascular abnormalities (Menšíková et al., 2022). As a case in point, up to half of the DLB patients exhibit co-existing A β pathology across the course of the disease, and 10 % present with neurofibrillary tangles of p-tau (Nedelska et al., 2019). Besides, up to 60 % of patients with sporadic AD may exhibit Lewy Bodies co-pathology (Chatterjee et al., 2021).

The protein aggregation process in LBDs is mediated by α -syn, a presynaptic protein regulating vesicle transport. The phosphorylation of α -syn in healthy subjects is minimal (< 4%) when compared to early cases with LBDs (> 90%). Phosphorylated α -syn correlates with the severity of the disease, can be induced by A β pathology, and facilitates α -syn aggregation in toxic oligomers, fibrils, and subsequently, Lewy bodies and neurites. Intermediate α -syn aggregates catalyse the production of more oligomeric forms. Despite Lewy bodies and neurites are the core neuropathological finding in LBDs, α -syn oligomers can also produce neural cell death before the formation of Lewy bodies (Menšíková et al., 2022). Once aggregated, Lewy bodies can spread from neuron to neuron in a prion-like way, see **Figure 6A**.

Hypothetical models state that the accumulation of Lewy pathology can start in different parts of the nervous system, potentially determining the expression of a given clinical phenotype. Thus, early ideas proposed that PD might reflect a pattern of brainstem-predominant Lewy pathology with caudal-rostral propagation. At the same time, DLB might exhibit a limbic-centered profile (causing more pronounced cognitive impairment)(Toledo et al., 2016). Empirical observations have not supported the latter hypothesis. A recent revision of earlier models showed promising

findings when including the global burden of Lewy pathology and the early or late development of Lewy pathology. Briefly, as autonomic dysfunction and rapid-eye-movement sleep behaviour disorder are known risk factors for dementia in LBDs (PDD and DLB), caudal-rostral accumulation with body-first Lewy pathology (i.e., in the peripheral nervous system) seems to be responsible for a faster progression to dementia. By contrast, those patients with brain-first Lewy pathology (limbic/amygdala-centred), without rapid-eye-movement sleep behaviour disorder, and prominent dopaminergic deficits without sympathetic denervation (i.e., spared autonomic nervous system) tend to exhibit a typical clinical PD with slow progression to dementia, see **Figure 6B** (Borghammer et al., 2021).

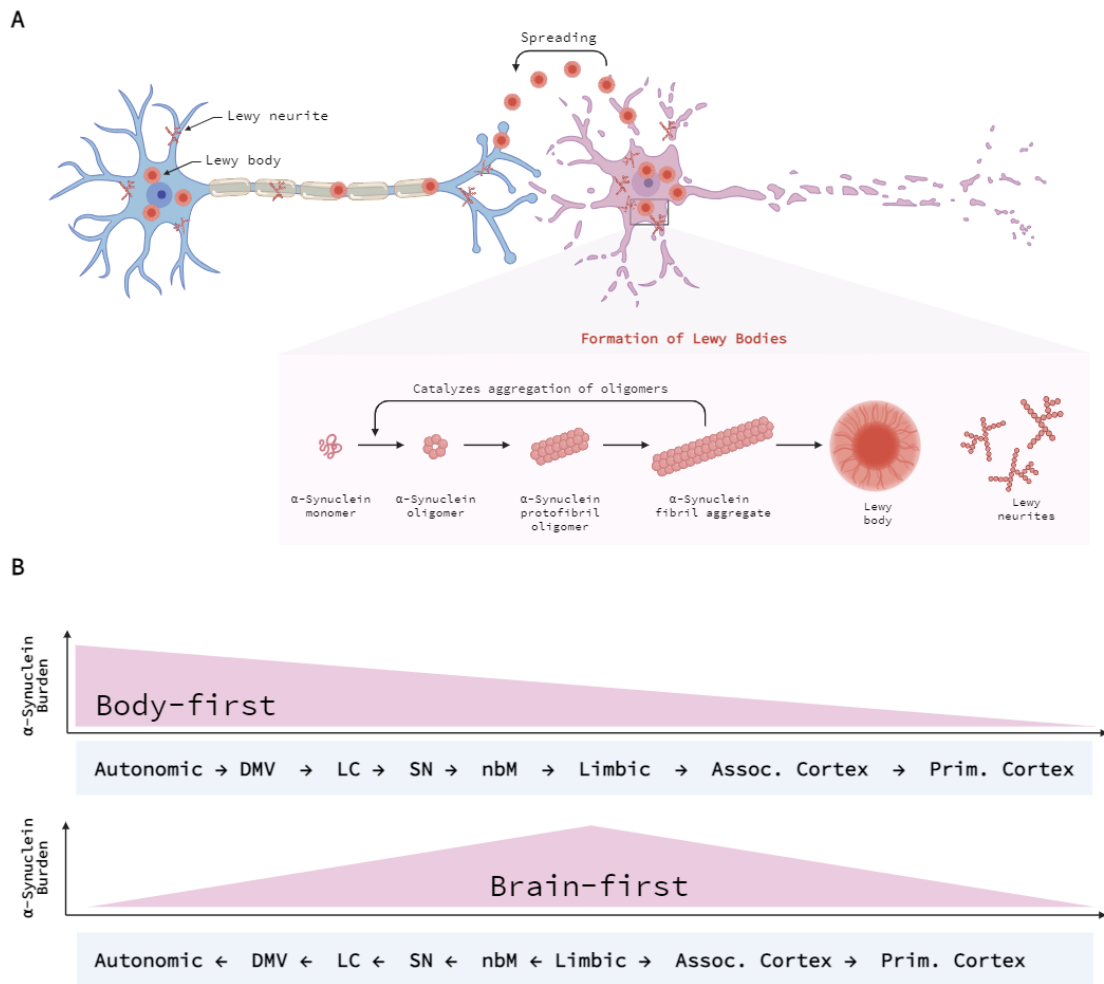


Figure 6. Protein aggregation/accumulation in Lewy Body Diseases (LBDs). **A)** Depicts the formation of intracellular Lewy bodies and Lewy neurites from α -synuclein monomers. Lewy bodies spread through adjacent neurons. **B)** Illustrates the accumulation (burden) of α -synuclein aggregates in LBDs. In the top figure, the accumulation described in the body-first case (with a faster progression to dementia) is presented. In body-first cases, a gradient burden of α -synuclein is observed from the autonomic nervous system, the dorsal motor nucleus of the vagus nerve (DMV), the locus coeruleus (LC), substantia nigra (SN), toward the nucleus basalis of Meynert (nbM), limbic, associative (Assoc.), and primary (Prim.) cortices. By contrast, brain-first cases (typically with slower progression to dementia) present with a limbic-centric elevation in the burden of α -synuclein pathology. The figure was created with BioRender.com.

Pathological discrimination between DLB and PDD is complex, and the distinction is often made from the clinical standpoint. Thus, PDD is defined as a progressive and significant multi-domain cognitive decline leading to dementia in the context of established PD. Conversely, dementia in DLB occurs first, and Parkinsonian symptoms appear later within the first year of dementia onset (following the so-called "one-year rule"). Remarkably, almost 25 % of DLB patients never exhibit parkinsonian motor symptoms (Menšíková et al., 2022). Other clinical core features of DLB include fluctuating cognition (variations in arousal and attention), recurrent visual hallucinations, and rapid-eye-movement sleep-behaviour disorder (Armstrong and MJ, 2019).

The identification of early biomarkers of DLB and PDD and predementia stages of LBDs has been promoted by international consensus (McKeith et al., 2020). The definition of probable DLB includes indicative biomarkers from imaging modalities and polysomnographic studies. Supportive biomarkers, including rsEEG, should be investigated in multiple cohorts, and their underlying methods should be improved to achieve optimal sensitivity and specificity (Armstrong, 2021).

1.2.1.3. Fronto-Temporal Lobar Degeneration (FTLD).

This cluster is defined prominently by the anatomical location of neurodegenerative pathology in the frontal and temporal lobes. Clinical phenotypes in FTLD could also exhibit various symptoms affecting executive function, complex attention, social cognition, and language, as in FTD. Besides, motor neuron disease and Parkinsonian syndromes have been included in the cluster of FTLD, with phenotypes like the nonfluent and semantic variants of Primary Progressive Aphasia (APP), extrapyramidal tauopathies such as corticobasal syndrome and progressive supranuclear palsy, as well as FTD associated with motor neuron diseases like Amyotrophic Lateral Sclerosis (ALS) (Finger, 2016).

In a recent European multicentric cohort, the behavioural variant FTD was the most frequently observed phenotype, representing 40–50 % of all FTLD cases. Language phenotypes of Primary progressive aphasia (PPA) were estimated at approximately 30 % and ALS at around 5 % (Logroscino et al., 2023). FTD is considered the second most frequent cause of young-onset neurodegenerative dementias (before 65 years old). Thus, FTD might account for 2.7 % of all dementia cases and up to 10.2% in young-onset cases (subjects below 65 years). Almost 60 % of FTD cases have a dementia onset age between 45 – 60 years, and up to 40 % are associated with familial inheritance. Genetic variants in at least eight different genes have been reported in half of FTD patients with familial aggregation and up to 6 % of FTD cases without a family history of dementia (Hogan et al., 2016).

FTLD is mainly associated with three types of protein aggregates (tau, TDP-43, and FUS) accumulated in different brain regions affecting specific subpopulations of neurons. Tau aggregates are observed in familial cases of FTD with mutations in the microtubule-associated protein tau (MAPT) protein-coding gene, as well as in the sporadic behavioural-variant FTD, nonfluent PPA, corticobasal syndrome and progressive supranuclear palsy (Finger, 2016). In healthy subjects, tau is prominently found in axons (contributing to microtubule stability). At the same time, TDP-43 and FUS proteins are mainly present inside the nucleus (in stress granules participating in RNA metabolism and nuclear clearance) and the cytoplasm (facilitating axonal mRNA and mitochondrial transport and cellular stress response) (Granatiero and Manfredi, 2019; Hock and Polymenidou, 2016a), **see Figure 7A**. Prominent tau and TDP-43 pathology account for up to 90 % of FTD cases with neuropathological confirmation, whereas FUS inclusions are the pathological hallmark in the remaining cases. The reduction of microtubule-binding affinity (often associated with MAPT mutations) triggers aggregation and phosphorylation of tau and

subsequent microtubule destabilisation, **see Figure 7B**. After tauopathies, ubiquitinopathies represent the majority of tau-negative cases, comprising FTD-TDP-43 and FTD-FUS (De Boer et al., 2021). In FTD-TDP-43 phosphorylation, ubiquitination and other mechanisms promote nuclear aggregation of TDP-43. TDP-43 aggregates in the nucleus are subsequently mislocalised to the cytoplasm. In the axons, TDP-43 condensate aggregates interfere with transporting mRNA and mitochondria, resulting in reduced translation of proteins, **see Figure 7C**. Similarly, FUS aggregates via ubiquitination in severe cases of sporadic FTD and is associated with earlier onset and rapid progression (Finger, 2016). FTD-FUS is linked to marked glial inflammatory activation and mitochondrial dysfunction, nucleocytoplasmic mislocalisation, and RNA sequestration in FUS aggregates, **see Figure 7D** (Hock and Polymenidou, 2016a).

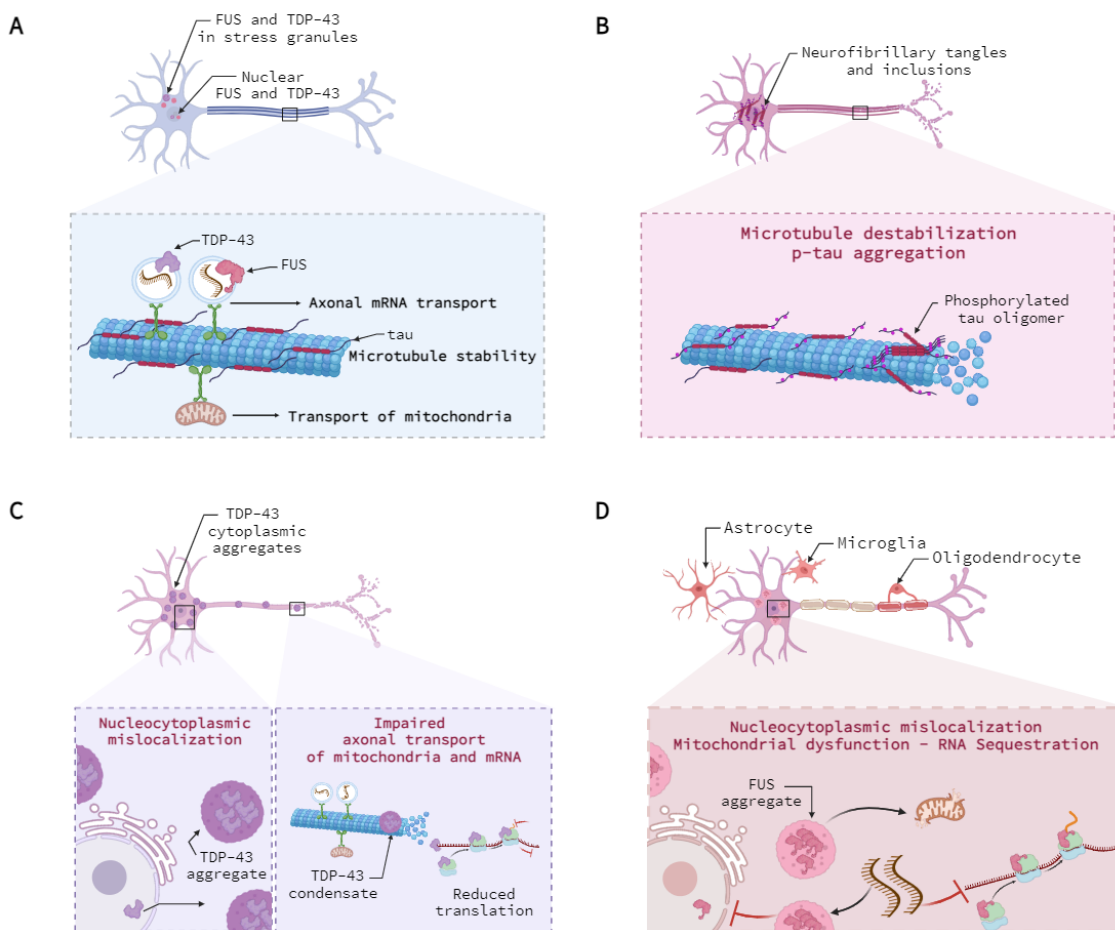


Figure 7. Pathophysiology of Frontotemporal Lobar Degeneration Spectrum. **A)** Healthy neurons with cytoplasmic stress granules and nuclear Fused in Sarcoma (FUS) and TAR DNA-binding Protein 43 (TDP-43). In the axons, the role of tau in microtubule stability. Mitochondrial transport, TDP-43 and FUS axonal mRNA transport are depicted. **B)** FTD-tau is characterised by phosphorylated tau accumulation (tau inclusions) and microtubule destabilisation. **C)** FTD-TDP-43 exhibits TDP-43 aggregates mislocalised from the nucleus to the cytoplasm. On the axons, TDP-43 condensates interfere with mRNA transport. **D)** FTD-FUS presents glial activation, nucleocytoplasmic mislocalisation, inhibited protein translation, and mitochondrial damage. The figure was created with BioRender.com and adapted from (Hock and Polymenidou, 2016b).

Biomarkers for FTD often aim to differentiate the patients from AD or healthy controls. However, up to 54% of patients with typical behavioural-variant FTD symptoms may also exhibit neuropathological findings consistent with AD co-pathology, whereas 11% have coexistent FTD and Lewy Body (Perry et al., 2017). Similarly, a large study performed in-vivo quantification of A β in patients with clinical diagnosis of primary progressive aphasia (PPA), demonstrating AD co-pathology present in 86 % of patients with the logopenic variant of PPA, 20 % in the nonfluent variant, and 16 % in the semantic variant of PPA (Bergeron et al., 2018). Validated biomarkers are based on genetic screening for the most common mutations in TDP-43, MAPT, and progranulin genes. Other valid biomarkers of FTD are obtained with structural or functional neuroimaging, as well as A β and p-tau pathology in cerebrospinal fluid. Novel imaging, fluid and rsEEG biomarkers have shown promising results in FTD across multiple populations (Duran-Aniotz et al., 2021; Meeter et al., 2017).

1.2.2. Models of Hormesis and Continuum for Timely Detection and Prognosis of NDDs.

The set of biological hallmarks of NDDs leading to dementia syndrome can be modified by individual modifiable and non-modifiable risk factors as outlined in the current integrative frameworks. This section will expand on mechanistic models proposed to explain how individual factors (such as age, education, and depression, among other risk factors) could interplay with the multiple biological hallmarks of NDDs to modify the clinical trajectories towards dementia syndrome.

Dementia syndrome is a common clinical outcome in most NDDs, and age has been considered a relevant non-modifiable factor for NDDs and dementia. However, NDDs and dementia syndrome are not present in all individuals at an advanced age, although it has been recognised that many cognitive abilities exhibit decline associated with "normal" physiological ageing. For example, age-related reduction in processing speed, complex attention tasks (divided and selected attention), working memory, visual-constructional skills, and executive functions like mental flexibility and inhibitory control have been reported as part of physiological ageing (Harada et al., 2013). Along with these expected cognitive changes associated with age, hypotheses have been formulated to explain the trajectories of individuals who exhibit faster cognitive decline or more severe cognitive deficits, such as those with NDDs, see **Figure 8**.

The model of inflammaging was proposed to explain age-related chronic diseases. Recognising that cellular and biological changes during "normal" physiological ageing are, to some extent, resembling changes in age-related diseases such as NDDs and dementia, Franceschi et al. suggested that physiological and pathological ageing are part of the same continuum process. However, the variability in the trajectories of decline is modulated by the balance between reserve and cumulative dose of stressors (Franceschi et al., 2018b, 2018a). The first step in the inflammaging process requires endogenous and exogenous proinflammatory stimuli (antenatal and postnatal, related to infections, diet, unhealthy habits, vaccinations), driving a limited inflammatory response, which might modulate other biological hallmarks of neurodegeneration. This inflammatory response should be specific to the stimuli and is necessary for survival until middle age. However, a sustained and cumulative inflammatory response induces long-lasting augmentation of the inflammatory tone. Consequently, this aberrant proinflammatory state accelerates the rate of physiological ageing, leading to increased inflammation in a feedback loop (Franceschi et al., 2018b). Conversely to accelerated ageing, individuals with "successful" ageing

manifest greater longevity and relative stability in their trajectories of cognitive functioning, see **Figure 8**.

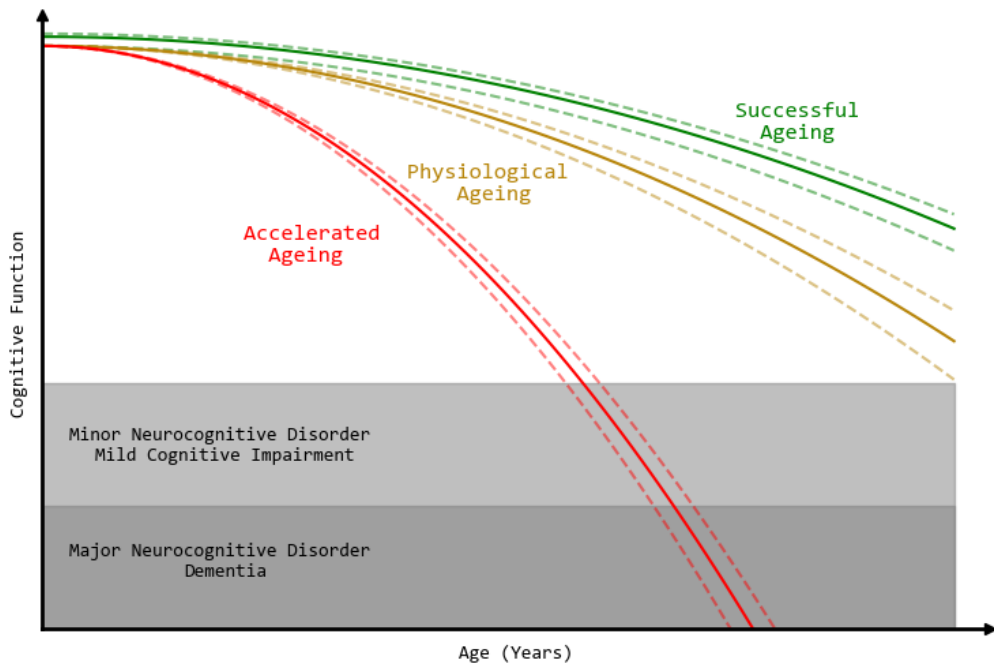


Figure 8. Trajectories of successful, physiological, and abnormal ageing. Curves represent the difference in the rate of age-related decline in cognitive function and cognitive domains. Green lines exemplify trajectories of successful ageing. Yellow lines illustrate physiological ageing. Red lines depict accelerated pathological ageing. Dashed lines indicate a variable rate of decline. On the bottom, shaded grey areas delimit the threshold of cognitive abnormalities leading to mild cognitive impairment (light grey) and dementia syndrome (dark grey). Note that the trajectories of cognitive decline in successful and physiological ageing do not cross the threshold of mild cognitive impairment and dementia. Observe that increased cognitive reserve is illustrated in some trajectories of the successful ageing subgroup exhibiting higher cognitive function at baseline. The figure was adapted from (Franceschi et al., 2018a).

This modulation in ageing trajectories due to environmental and individual risk factors due to inflammaging has multiple commonalities with the evolutionary concept of hormesis, which describes how biological systems adapt to low-moderate environmental or self-imposed challenges, leading to enhancements in their functionality and the ability to withstand more substantial challenges. On the other hand, high cumulative doses of stressors (biological or environmental) lead to deleterious effects (Calabrese and Mattson, 2017). From an evolutive perspective, challenging environments elicit adaptive responses conferring protective factors to the organisms. Conversely, sustained and chronic environmental and cellular stressors might result in the opposite outcome, namely deleterious effects and less preservation. This type of dynamic response can be considered a hormetic-like process. The concept of hormesis in neuroscience has been incorporated by Calabrese, who defined it as a biphasic dose-response, with low stressor doses giving rise to stimulation of a system/individual and high stressor doses causing inhibition (Calabrese, 2008).

The trade-off between protective and risk factors linked to age-related diseases and accelerated ageing can also be considered a stressor. Thus, this positive or negative risk balance has been linked to age-related NDDs such as AD. Capitalising on extensive evidence, risk factors for developing dementia were identified in early, middle, and late life. Among these risk factors,

some were potentially modifiable, such as low educational level in early life, midlife hearing loss, traumatic brain injury, hypertension, alcohol use, obesity, as well as late-life smoking, depression, social isolation, diabetes, sedentarism, and air pollution (Livingston et al., 2020). In addition to these modifiable risk factors, several non-modifiable individual risk factors can be present, including high oxidative stress, inflammation, synaptic dysfunction, abnormal proteostasis, genetic risk factors, and shortening of telomeres (Franceschi et al., 2018a).

Inflammaging also describes a chronic and sustained age-related increase of proinflammatory cytokines (stressors), with reduced production of anti-inflammatory substances (Franceschi et al., 2018b; Santoro et al., 2020). When the dose of the stressors is low and not chronic over time, adaptive responses to inflammation can be elicited, surpassing the deleterious effects of the stressors and leading to successful ageing. In centenarians, increased proinflammatory cytokines are counterbalanced by large amounts of anti-inflammatory molecules (Collino et al., 2013). By contrast, a high dose of stressors (chronic over time) is involved in accelerated ageing and age-related diseases like NDDs, diabetes, and cancer, among other geriatric syndromes (Franceschi et al., 2018a). The latter is illustrated in **Figure 9A**.

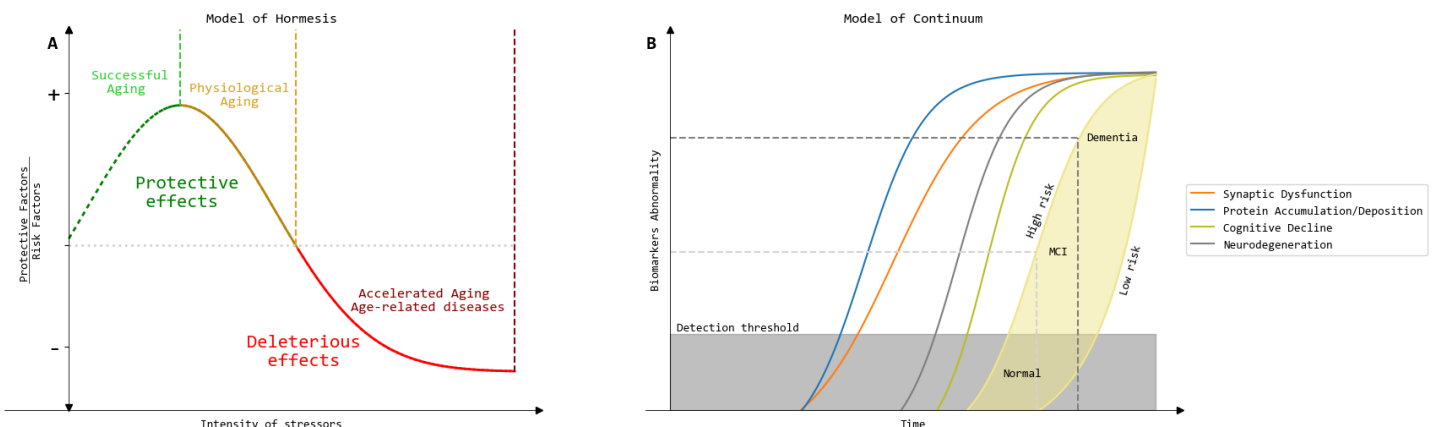


Figure 9. Theoretical models of Hormesis and Continuum in the context of Pathological Ageing and Neurodegenerative diseases (NDDs). **A)** Illustrates the model of hormetic responses to dose/intensity of stressors (horizontal axis). Protective or deleterious effects depend on the ratio between protective and risk factors (vertical axis). The horizontal dashed line separates those individuals with accelerated ageing or presenting age-related diseases (red lines) from those with successful ageing (green lines) and physiological ageing (golden lines). Successful ageing (dashed green lines) exhibits a low intensity of stressors and high protective factors, showing positive adaptive responses. Similarly, physiological ageing is the product of greater protective factors, but the increased intensity of stressors ameliorates the positive effects of adaptive response, causing subtle non-pathological changes. **B)** The model of Continuum shows biomarker abnormalities over time, from early stages to dementia. Individuals likely to develop NDDs will exhibit minimal biomarker abnormalities with relatively preserved cognition (grey region) until the detection threshold is crossed and early clinical abnormalities are observed. An increase in the level of biomarker abnormalities will result in mild cognitive impairment (MCI) and subsequent dementia. Risk factors mediate the degree of cognitive impairment (yellow region). Thus, progression from normal to MCI and dementia is faster and earlier in those with higher risk factors. Adapted from (Aisen et al., 2017; Franceschi et al., 2018b, 2018a; Iturria-Medina et al., 2016).

As we have highlighted, neuroinflammation and neurodegeneration can also result from inflammaging. A meta-analysis identified increased inflammation in AD patients (Swardfager et al., 2010). The activity of specific proinflammatory cytokines can also be associated with the continuum of events preceding the clinical onset of dementia in AD, including synaptic dysfunction, protein aggregation and accumulation, and energy balance. The latter favours a bridge between the hormesis model in age-related diseases and the continuum model in NDDs (Franceschi et al., 2018a). Thus, inflammaging and individual risk factors could trigger abnormalities in biological hallmarks of neurodegeneration, accelerating cognitive and functional decline. Longitudinal tracking of these events across the stages of dementia and predementia phases of NDDs allowed the formulation of the continuum model. The continuum model posits that abnormal biomarkers of the hallmarks of neurodegeneration characterise preclinical and prodromal stages of NDDs. This model was initially developed for sporadic late-onset AD (Aisen et al., 2017; Jack et al., 2013). Data-driven confirmation of this model has shown the prominent role of vascular and synaptic dysfunction in the early stages of AD and protein accumulation/aggregation (Iturria-Medina et al., 2016).

Similarly, hypothetical models in DLB, PDD, and PD have pointed out these hallmarks of neurodegeneration (Donaghy and McKeith, 2014). Additional models for the continuum of cognitive decline and catecholaminergic loss have also been proposed for PD (Aarsland et al., 2021, 2017; Vermeiren et al., 2020). The efforts on tracking α -syn-related diseases have recently resulted in a novel integrated staging system for research accounting for the presence of pathological neural α -syn (in vivo), evidence of dopaminergic neuronal dysfunction, and genetic risk factors in preclinical stages of PDD and DLB (Simuni et al., 2024). All these models recognise the presence of age-related biomarker abnormalities occurring in successful and physiological ageing. The magnitude of these abnormalities (stressors) is not always above the detection threshold and does not manifest as cognitive decline. On the other hand, when greater and chronic stressors (i.e., biomarker abnormalities) are present, the clinical syndromes of MCI and dementia can be observed. When comparing patients with similar biomarker abnormalities, the individual trade-off between risk and protective factors would mediate the velocity of progression of cognitive and functional decline, see **Figure 9B**.

Once the deleterious effects are established (i.e. poor adaptive response and increased biomarker abnormalities in NDDs), compensatory mechanisms can emerge to provide resilience to the insult. These compensatory mechanisms have been reported not only at the cellular level but also at the mesoscale (Hampel et al., 2019). For example, vulnerable brain regions in preclinical AD (e.g., the hippocampus) exhibit decoupling with other areas within the default-mode network. As a consequence, coupling between other areas (e.g. precuneus, middle and posterior cingulate cortices) is observed until the MCI stage, where the compensatory effects of precuneus are lost. The authors also showed that AD pathology was correlated with these compensatory effects (Skouras et al., 2019). Meta-analysis results have also supported this hypothesis, showing hyperconnectivity in preclinical AD to compensate for functional and structural abnormalities, followed by hypoconnectivity of brain networks in the dementia phase of AD (Jacobs et al., 2013). The latter argument solidifies the bridge between the continuum model and the hormesis model in NDDs, where increased stressors and risk factors lead to insufficient adaptive responses (augmenting biomarker abnormalities); subsequently, compensation mechanisms can be elicited, triggering a cascade of abnormalities in other biomarkers. The latter is supported by the high correlation in the degree of abnormalities across multiple biomarkers of neurodegeneration from the molecular to the body scale (Hampel et al., 2019).

The hypothesis of a hormetic-like response to individual stressors through the ageing continuum highlights the importance of early detection in individuals at risk of dementia (i.e., with

pathological ageing in preclinical and MCI stages) for timely detection and prognosis, which can ultimately lead to more effective strategies for managing NDDs and dementia syndrome.

In light of the reviewed evidence, tracking synaptic dysfunction biomarkers in NDDs could offer several potential advantages over focusing solely on protein accumulation/aggregation biomarkers. Synaptic dysfunction often occurs in the early stages of NDDs (hypothetically triggered by oligomeric protein aggregation and chronic inflammation, among other stressors), even before significant protein accumulation can be demonstrated using imaging techniques. (Al-Qazzaz et al., 2014; Colom-Cadena et al., 2020a; Law et al., 2020; Querfurth and LaFerla, 2010; Wilson et al., 2023). Notably, the rsEEG holds promise as it can reflect the synaptic dysfunction of brain networks in the early stages of the continuum through dementia syndrome. Although the exact mechanism causing the synaptic dysfunction is not directly reflected in rsEEG abnormalities, this high sensitivity might be advantageous when tracking overlapped protein accumulation and complex interactions between biological hallmarks and risk factors exposed throughout the introductory sections of the thesis.

2. Electroencephalogram (EEG) in NDDs.

2.1. Essential concepts and definitions.

"Wonderful as are the laws and phenomena of electricity when made evident to us in inorganic or dead matter, their interest can bear scarcely any comparison with that which attaches to the same force when connected with the nervous system and with life."
Faraday, 1839

Some technical definitions should be explored beforehand to warrant a proper understanding of the rsEEG correlates of neurodegeneration and some potential limitations regarding their interpretability.

In the early XIX century, Dr. Luigi Galvani proposed the concept of "animal electricity" based on his observations of a contractile response obtained after applying frictional energy to the nerve-muscle joint of frogs. Later advances in the physiology of muscular contraction confirmed the reports of Galvani. The second half of the XIX century was a relevant historical period for electrophysiology due to the shift in the scientific community's focus from muscle to the brain's electricity. Despite remarkable contributions in neuroanatomy made before 1840, brain physiology was poorly understood until the effects of electricity on brain activity were incorporated. Thus, the renowned Prof. Michael Faraday made notable contributions by reporting a "disruptive discharge" that allows electric eels to produce light and heat from electricity as a result of increased polar tension. The ideas of Faraday inspired the British scientist Robert Bentley Todd, who rejected early misconceptions about infectious and vascular aetiological aspects of epilepsy, attributing it to the "disruptive discharge" generated by neural microscopic structures (note that neurons were not even described at that time).

Further evidence favouring the idea of electromagnetic properties of the brain was an experimental characterisation of the motor cortex conducted in 1870 by Eduard Hitzig and Gustav Fritsch. They induced motor responses when stimulating the motor cortex (earlier hypothesised by John Hughlings Jackson) with an electric current generated from a battery. Similarly, in 1875, Richard Caton empirically supported these descriptions of electrical currents in the brain cortex and subcortical structures by recording these currents in monkeys and rabbits with a galvanometer (Reynolds, 2004).

Galvanometers are instruments designed to measure small electric currents and consist of a copper coil attached to a needle used to sense the current. Earlier galvanometers also had an

integrated pen to represent the electric current as a trace in a paper rolling below the device. However, the scale of EEG signals is very small (microVolts) and often requires amplification over 10,000 times. In line with that, galvanometers were used mainly in exposed brain tissue but did not succeed in capturing brain currents in scalp recordings. It was not until 1926-1929 when Prof. Hans Berger was able to record and publish the first oscillatory traces on the human scalp acquired with a Siemens double-coil galvanometer and a modified version of the Edelmann string galvanometer (Berger, 1929; Collura, 1993).

For a detailed review of the history of EEG amplifiers, sensors and acquisition technologies in Europe and America, the reader is referred to the article published by (Collura, 1993).

Apart from technological challenges in the acquisition methods, the seminal publications of Dr Berger posited several questions regarding stimuli-related changes in EEG, EEG variations associated with mental processing, and reduced arousal/vigilance (such as sleep or anaesthesia). Notably, in subsequent works, Berger observed the oscillatory nature of brain rhythms in the EEG traces, distinguishing two main rhythmic patterns:

- "Large amplitude, First-order waves" oscillating in frequencies between 8-11 Hz
- "Small amplitude, Second-order waves" oscillating in frequencies between 20 - 125 Hz

Berger further termed the above oscillatory patterns alpha and beta waves, respectively (Berger, 1936). His particular interest in alpha waves led him to crucial conclusions that remain valid:

- Alpha waves were pronounced while individuals maintained their eyes closed.
- Alpha waves were present across multiple electrode positions in the scalp.
- Alpha waves were abolished by eyes opening.

This dynamic response of alpha rhythms to the opening of the eyes was later termed alpha reactivity, alpha-blocking, or Berger effect. Berger also posited the emergence of second-order waves during tasks involving mental effort (Berger, 1929; Berger, 1936; Kropotov, 2016). Abnormal patterns related to multiple neuropsychiatric conditions and brain lesions were also reported in the reports of Dr Berger(Haas, 2003).

Reproducibility of Berger's findings was first achieved in Europe by Drs Edgar Adrian and Bryan Matthews in Cambridge, United Kingdom. In their conclusions, the authors expanded on Berger's observations, suggesting that alpha rhythms could represent a correlate of "resting state" in a particular brain region (Kropotov, 2016). Contemporarily, there was an increasing interest in studying EEG in North America, resulting in the creation of multiple labs. Thus, Berger's findings were also confirmed by the lab of Dr. Herbert Jasper in Rhode Island, USA, followed by Drs. Frederick and Erna Gibbs in collaboration with Hallowell Davis's lab in Boston, Massachusetts. Meanwhile, in New York, the variation of EEG patterns across sleep stages was reported in the work of Dr Alfred Loomis's team (Collura, 1993; Kropotov, 2016).

Due to the digitalisation of EEG recordings, quantitative EEG became state-of-the-art in EEG research and clinical praxis, demanding the application of methods and theories used in the field of signal processing. Thus, the characterisation of EEG patterns using computational methods (quantitative EEG) as well as advances in electrophysiology lead to models about potential generators or "sources" of alpha rhythms elicited by the resting-state involving the participation of the thalamus as "pacemaker", as well as occipital and parietal generators. Also, quantitative EEG methods facilitated the identification of age-related changes in the alpha rhythms described in healthy and pathological conditions, particularly in dementia, where the alpha rhythms in posterior electrodes exhibited a reduction in the oscillatory frequency below the 7.5 Hz threshold (Kropotov, 2016).

We propose a short glossary of terms as an introduction to specific EEG terminology used across the thesis.

Electric fields and potentials: Given the intrinsic properties and organisation of the brain, as well as the chemical and ionic mediators of the synapse, electric and magnetic fields are generated by the nervous system. Briefly, individual cellular generators of brain activity produce electric currents. The electric potentials that result from superimposing the electric currents of a given brain tissue are called post-synaptic potentials. Electric fields appear because of the difference between the post-synaptic potentials across brain tissue volumes. The EEG is intended to reflect post-synaptic potentials by capturing the voltage difference in the electric potential between an electrode of interest and a reference electrode placed in the scalp. Therefore, with a high temporal resolution, the EEG signal represents the summation of cortical columns' inhibitory and excitatory post-synaptic potential (particularly pyramidal neurons) over time(Buzsáki et al., 2012).

Cortical layers: The brain cortex reflects both a laminar and columnar organisation. The neocortex constitutes the majority of the grey matter in the brain; despite differences in thickness, cell organisation and composition of the layers, the neocortex has a laminar organisation arranged in six layers of neurons (cortical layers). Thus, layer I is the most superficial and layer VI is the deepest layer of the cortex. The constitutive neurons of the cortex can be classified as A) projection neurons (also termed principal neurons) and B) local inter-neurons. Projection neurons in layers III to VI have excitatory activity and a pyramidal soma. By contrast, local inter-neurons represent one-fifth to one-fourth of all cortical neurons, are located across all cortical layers, and have mainly an inhibitory activity (Grimbert and Faugeras, 2006; Lopes Da Silva, 2010).

Cortical columns: Besides laminar organisation, cortical neurons that share a common function often extend their axons and dendrites vertically, crossing from the superficial to deeper layers beside the white matter. As a case in point, excitatory subcortical neurons in the thalamus extend their projections towards layer IV of the cortex (connecting with excitatory spiny stellate neurons). Thalamocortical information is then shared and modulated perpendicularly from inner to outer structures of the cortex. With this in mind, the hypothesis of cortical columns as functional and anatomical units of the cortex emerged. Across this thesis, we will consider cortical columns as tightly connected populations of excitatory/inhibitory neurons with synchronous activity that can produce EEG-like patterns. We will follow Jansen's model of cortical columns based on earlier works from Lopes da Silva. Similarly, it will be considered that non-adjacent columns can exhibit synchronised activity in multiple dynamic states due to tangential connections between columns (Grimbert and Faugeras, 2006; Lopes Da Silva, 2010).

Volume Conduction effects: As EEG signals are recorded from the scalp, it is relevant to consider the folding of the brain cortex. Gyri and sulci result from cortex folding, changing the orientation of the neurons with respect to acquisition electrodes. Thus, cortical columns at the top of the gyri tend to be perpendicularly (radially) oriented to the skull. In contrast, columns in the sulci tend to exhibit a tangential orientation with respect to the electrodes on the scalp's surface. EEG signals mainly represent radial columnar electric fields but can also capture tangential columnar generators. Therefore, the recorded EEG activity does not correspond to the cortical sources (or generators) in the brain regions below the EEG sensors in a 1:1 relation. Differences in the conductivity of tissues, including the scalp, skull bone, cerebrospinal fluid, meninges, and brain, also explain why EEG signals acquired from scalp electrodes are not able

to exhibit an accurate spatial representation of their distant cortical sources. Volume conduction effects arise when conducting the radial and tangential electric fields from sources through a medium (volume, tissues) that separates the source from the EEG sensors (electrodes), distorting the spatial correspondence (Buzsáki et al., 2012; Lopes Da Silva, 2010).

Channels: EEG channels commonly refer to the sensors (electrodes) that capture EEG activity. The number of EEG channels might vary from single-channel EEG to 256 channels. Some research environments often use EEG arrays with 64 or more channels (high-density EEG), allowing subsequent analyses to approximate the potential cortical sources with less spatial distortion. However, low-density EEG arrays with 19-25 channels are frequently used in clinical practice. EEG channels can be attached to caps or manually applied over the scalp, disposed of following standard positions. The most commonly used conventions are the International 10-20 System (for low-density EEG recordings) and its 10-10 and 10-05 equivalents (for high-density EEG recordings) (Seeck et al., 2017).

Sensor space: Refers to signals acquired by the EEG channels distributed across the scalp, representing voltage changes over time. As noted earlier, signals in the sensor space are prone to volume conduction effects(Seeck et al., 2017). Derivative descriptors (features) can be extracted from the EEG in the sensor and source spaces.

Source space: Refers to the approximated EEG signals projected in a spatial template of the brain cortex. In order to solve the inverse problem (i.e., estimating the generators of the observed signal without recording them directly), the EEG signals in the sensor space can be analysed using algorithms that project these signals into a brain space. The rationale of this method is that EEG signals in sensor space can be considered linear transformations of the original signals produced by the cortical sources (Seeck et al., 2017).

Artefacts: EEG signals represent not only brain-related electrical potentials from cortical columns; the non-brain contributors of the EEG signal are considered artefacts generating noise. EEG artefacts can be classified as biological and non-biological. Blinks and eye movements also elicit rotating electrical fields projecting in the scalp, with strong enough voltage amplitude to affect the EEG signals generated by cortical columns. Also, electromyographic activity (EMG) and electrocardiographic activity (EKG) contribute to the summed voltage captured by EEG channels, creating biological non-brain artefacts. Nonetheless, non-biological noise generators in the EEG signal might include the 50-60 Hz oscillations of electrical lines and fixtures operating on alternating current. The impedance (resistance to the conductance) between a given EEG channel and the skin might introduce artefacts. The electrical fields of the abovementioned non-brain artefacts are mixed instantaneously, although the underlying cortical sources might be independent, and its activity coupling is not instantaneous. In line with the above, algorithmic methods to remove artefacts have emerged as state-of-the-art in quantitative EEG analysis and will be detailed in further chapters (Pion-Tonachini et al., 2019).

Time domain: Refers to the EEG signal analysis without any transformation; EEG as a function of voltage changes over time. The visual analysis of EEG voltage patterns as a function of time allowed the differentiation of rhythmic oscillatory activity and abnormal patterns in conditions

such as epilepsy. Acquisition of EEG signals in the time domain permits sampling voltage variations at small timescales. Time domain analysis is also used in quantitative methods to study event-related and stimuli-evoked activity, facilitating experimental control and intervention through experimental designs consisting of repeated stimuli presentation to elicit behavioural (active or passive) and brain-related responses (Keil et al., 2022).

Epochs: On visual qualitative analysis, EEG signals are often chunked into equal duration time segments called epochs. In the quantitative setting, the definition of epochs corresponds to specific time windows obtained from the original signal in the time domain. Still, epochs can be overlapped or time-locked concerning a particular event. The length of the epochs might also vary according to the methods used to process the signal (Keil et al., 2022).

Frequency domain: Analysis of EEG as dynamic brain rhythms supports using frequency domain analysis. Thus, quantitative methods underlying frequency domain analysis are based on the assumption that EEG signals result from a weighted sum of multiple oscillatory elementary rhythms (mathematically represented as functions, called basis functions). As sinusoidal functions repeat a cyclic temporal pattern, they can be measured in terms of frequency, indicating the number of complete cycles at a given temporal scale. One full cycle each second is equivalent to an oscillatory behaviour at 1 Hertz (Hz), while ten complete cycles per second describe an oscillatory activity at 10 Hz. Among the constitutive sinusoids of a given EEG signal, some oscillations contribute more to the recorded signal than others. Mathematically, the weights of each sinusoidal rhythm will denote the amplitude spectrum, the squared amplitude spectrum is referred to as the power spectrum, and the power spectrum over frequency will represent the power spectral density. Frequency domain analysis can be performed using other basis functions than sinusoids, sliding windows across epochs, and overlapping methods to obtain a greater frequency resolution with lower variance on the power spectral density (Babadi and Brown, 2014; Keil et al., 2022; Vallat and Walker, 2021).

Spectral analysis: Involves extracting derivative metrics from the frequency domain to be used as EEG features. As frequency domain analyses represent power spectral density (y-axis) as a function of frequencies (x-axis), multiple descriptors can be assessed as follows:

- **Relative and Absolute band powers:** Constitutes the areas under the power spectrum curve for a given frequency range or band. Canonical fixed bands are defined for clinical applications of EEG.
- **Peak Frequency or Center Frequency:** Frequency with a peak of power. Peak frequency often can reflect the peak of the highest power peak; in this scenario, it is termed Dominant Frequency.
- **Dominant Frequency Variability:** Reflects the variability in Hz of the Dominant Frequency across epochs.
- **Peak Bandwidth:** Difference between the upper and lower frequencies where the power peak lies over.
- **Frequency Prevalence:** Prevalence of peak frequency for a given frequency band.
- **Oscillatory and aperiodic parameters:** Epoching allows the analysis of EEG in small chunks of data that might be easier to approximate to oscillatory basis functions. EEG signal is also constituted by non-oscillatory (aperiodic) components, evident in the power spectral density as a one-over-frequency decay below the peaks of oscillatory activity.

Recent quantitative methods focus on estimating both the oscillatory and aperiodic parameters. Oscillatory features obtained from spectral analysis have been mentioned. Besides, aperiodic parameters have been conceptualised as A) the intercept of the 1/frequency slope at the lowest frequency acquired and B) the slope of the aperiodic component of the power spectrum (Donoghue et al., 2020b; Keil et al., 2022).

Stationary signals: A signal is classified as stationary if its frequency or spectral information does not vary over time. Biosignals are, by nature, nonstationary, nonlinear, and noisy, and EEG is not an exemption from this rule of thumb. Several facts support this observation, including the variable sensory input or mental tasks, but also from the variability of inherent metastable states across neural processing units originating EEG signals (distinct coupling between multiple sources with particular temporal and spatial activation patterns). Nonstationarities in EEG can represent relevant correlates of both pathological and physiological states (Klonowski, 2009).

Nonlinear complexity measures: Given the nonstationary behaviour of EEG signals, nonlinear methods taken from fractal theory, information theory, and complex systems theory have been used as derivative features of the EEG. These features encompass an umbrella of descriptors that capitalise on the scale-free nature of the signal and provide information about the regularity or complexity of the movement based on nonlinear approximations (Klonowski, 2009).

Connectivity: As a correlate of interaction between multiple neural sources, the connectivity of a signal represents the interdependence between two EEG signals acquired at different locations in terms of the signals in both the time domain and the frequency domain. Also, connectivity can be classified as directed or undirected; the former estimates potential relationships between signals and the direction of the spatiotemporal influence of one signal over the other (accounting for potential statistical causation). By contrast, undirected connectivity relies not on directionality but only on the interdependences between two signals. Similarly, the term 'synchronisation' has been considered to denote collective behaviour across rsEEG activity in sensors or sources (Bastos and Schoffelen, 2016).

2.2. Neural mechanisms underlying the normal resting-state EEG (rsEEG).

The acquisition of rsEEG activity starts with placing EEG channels directly over the scalp. Electrodes can be arranged in EEG caps following the positions of the international 10-20, 10-10, or 10-05 systems (**see Figure 10A**). EEG activity reflects differences in the electric fields sensed by two channels, one electrode of interest and another electrode used as a reference. In research environments, a single electrode is often used as the reference electrode (monopolar montage) to be compared with each channel of interest distributed across the scalp. These electrodes frequently require a conductive gel to reduce the impedance (resistance to electrical conductivity) between the cortex and scalp. In addition to increased impedance, volume conduction effects arise from the effects of the skin, connective tissue, aponeurosis, loose areolar tissue, periosteum, cranium, dura mater, subdural space, arachnoid mater, subdural space, cerebrospinal fluid, and pia mater (**see Figure 10B**).

Contrastingly to event-related and evoked activity, resting-state conditions are task-free, favouring the acquisition of EEG signals in patients with difficulties following complex instructions. Using rsEEG in clinical research aims to assess vigilance and arousal

neurophysiological systems in both static and dynamic conditions (Babiloni et al., 2020a). Thus, three potential conditions involving the arousal and alertness systems:

- Keeping low vigilance with the eyes closed for several minutes (5-15 mins).
- Repeated alternation between lower and higher vigilance, from the eyes closed to open eyes condition (1 min each).
- Steady maintenance of low vigilance in eyes closed (3-5 mins) and high vigilance in the eyes open condition (3-5 mins).

When EEG is acquired in quiet wakefulness, alpha oscillations emerge as the predominant rhythm, more evident with closed eyes. The origins of alpha rhythm have been discussed in detailed classical reviews on clinical neurophysiology. It has been hypothesised that the thalamic nuclei have a prominent role as a 'pacemaker' of alpha activity through thalamocortical loops. Thus, cells in the nucleus reticularis and the thalamic relay nucleus project to the cortex. At least two pathways can be identified in the thalamocortical circuits: the 'Core' pathway and the 'Matrix' pathway. The core populations in the thalamus are connected to the granular layers of the cortex (mainly pyramidal cells in layers 3-5), and the matrix populations in the thalamus are connected to the supragranular layers (layers 1 to 3), see **Figure 10C**. Cholinergic and aminergic presynaptic afferents to the cortex produce conformational changes in T-type calcium channels in the thalamus (**Figures 10C and 10D**), exhibit synchronous tonic firing spikes that subsequently elicit postsynaptic potentials and electric currents in pyramidal neurons in layers 4 and 5, leading to cortico-cortical and thalamo-cortical interactions (**Figure 10E**) (Bhattacharya et al., 2021; Llinás et al., 1999; Müller et al., 2020; Vanneste et al., 2018).

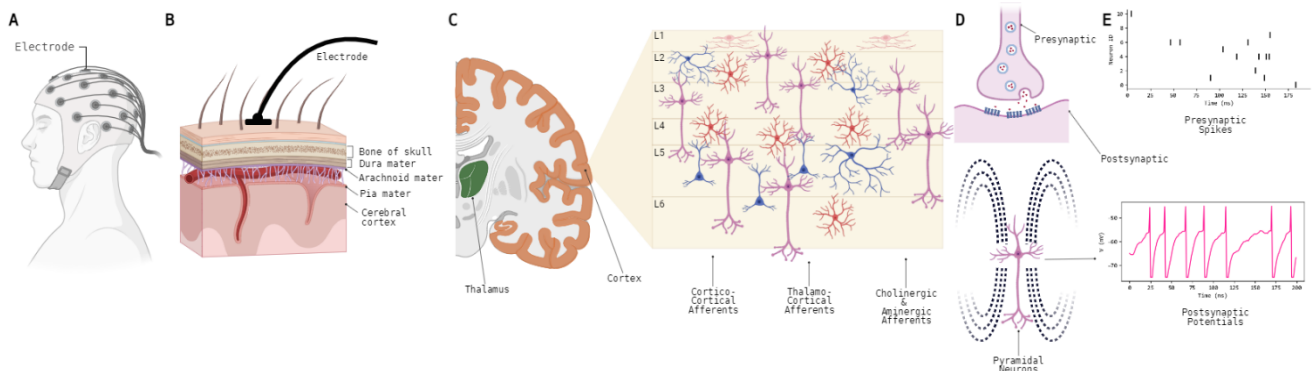


Figure 10. Neuronal origins of the resting-state electroencephalogram signals. **A)** Represents the cap with electrodes placed across the scalp according to the 10-20, 10-10, or 10-05 international system. **B)** Shows the volumes (i.e., tissues) that interfere with the electrical activity elicited in the cerebral cortex and the recording electrodes applied on the scalp. **C)** Depicts the macroscopic anatomy of thalamocortical structures, as well as afferents to the brain cortex's pyramidal neurons (pink) and inhibitory interneurons (blue), comodulated by stellate cells (red). **D)** Illustration of chemical synapses (top) eliciting depolarisation of pyramidal neurons generating an electric current. **E)** Representation of the coupling of presynaptic spikes (top) resulting in prolonged postsynaptic potentials (bottom), ultimately captured by the EEG. The figure was created with BioRender.com and adapted from (Portillo-Lara et al., 2021).

Despite classical descriptions of a pronounced thalamic orchestration of cortical rhythms, one recent experimental design using intracranial EEG probed the prominence of anteroposterior short-range supragranular cortico-cortical interactions that lead to top-down modulation of thalamic rhythms (Halgren et al., 2019). The participation of the cortical cholinergic and aminergic neuromodulatory inputs might shed light on this. A recent publication used

information theory metrics to examine arousal systems in simulated computational models and data from anaesthesia patients. The authors support how the thalamic matrix could originate this supragranular cortico-cortical communication to respond to shiftings between high information transmission (more diverse dynamics – in wakefulness state) vs high information storage (more predictable dynamics - under propofol) (Müller et al., 2023). The latter findings are consistent with the Activation/Information/Modulation (AIM) model of sleep. In this model, Activation refers to the variation from unconsciousness to consciousness; Modulation denotes the influence of cholinergic and monoaminergic neuromodulation to be “connected” or “disconnected” in the processing of Information (internal or external). Thus, noradrenergic input in the ascending arousal system seems to elicit a connected bursting state, while the cholinergic nucleus basalis of Meynert could be linked to a disconnected bursting state (Munn et al., 2023). The integrity of the cholinergic nucleus basalis of Meynert has been positively related to rsEEG alpha reactivity to the opening of the eyes, and age-related vascular lesions were associated with lower reactivity (Wan et al., 2019).

In addition, cortical oscillatory activity can further regulate the local neural firing and favour long-range network interactions via top-down modulation of EEG generators. Classical works have demonstrated a positive modulation of the activity of local neural subpopulations by low-frequency cortical rhythms (delta and theta band). Conversely, intermediate-frequency rhythms (alpha and beta), prominent in resting wakefulness, have been linked to inhibitory modulation of non-relevant neural activity (Klimesch, 1999; Klimesch et al., 2007; Ranasinghe et al., 2022).

Taking into account the integration of different molecular, structural and functional contributors involved in the generation of the EEG signal, its value for clinical research has been remarked as a promising biomarker of health and disease (Babiloni et al., 2020a). The following section will present the role of rsEEG as a promising biomarker of synaptic dysfunction and its association with pathological (protein accumulation/aggregation) and structural (neural cell death) biomarkers of NDDs.

2.3. Mechanistic models of Disease: RsEEG correlates of pathological and clinical hallmarks of NDDs.

In physiological ageing, translational studies have supported the hypothesis of an age-related synaptic failure even in the absence of prominent protein aggregation/accumulation. Resilience and compensatory mechanisms triggered by synaptic dysfunction are thought to favour spared cognition (Hampel et al., 2019). On the other hand, neural cell death in NDDs is preceded by early molecular and cellular events affecting chemical and electrical synapses (synaptopathy). Thus, conceptualising NDDs as synaptopathies has potentiated the integration of multiple findings toward theoretical mechanisms (Tyebji and Hannan, 2017).

The synaptic dysfunction model proposes an imbalance between excitatory and inhibitory activity in the neurons mediated by protein aggregation/accumulation and oxidative stress, among other hallmarks of neurodegeneration (Tönnies and Trushina, 2017; Tyebji and Hannan, 2017). This synaptic dysfunction results in impaired function at the synaptic scale, extending to the network scale in the cortico-cortical and cortico-thalamo-cortical circuits (Moretti et al., 2004). As electrochemical synapses are essential for rsEEG generation, this technique has increasingly gained traction as a promising biomarker of synaptic dysfunction in NDDs and dementia (Al-Qazzaz et al., 2014; Babiloni et al., 2020a; Colom-Cadena et al., 2020a). Multimodal approaches combining molecular, imaging, and electrophysiology techniques have shed light on robust potential mechanistic models of EEG changes observed in NDDs.

Neural Mass Models (NMMs) are mathematical approximations applied to electrophysiological brain signals aimed at modelling the dynamics of excitatory and inhibitory neuronal balance. In AD patients, NMMs in magnetoencephalographic data have supported the hypothesis of AD as a synaptopathy. In one cohort study, increased A β accumulation has been associated with aberrant inhibitory function in frontoparietal local neural ensembles. In addition, increased low-frequency power was observed with a high accumulation of A β (Ranasinghe et al., 2022). Low-frequency rhythms can positively modulate the firing of local neural generators of EEG signals, acting as a positive oscillatory modulator (Klimesch et al., 2007). Therefore, aberrant inhibitory function and high delta-theta oscillations (related to A β accumulation) promote network hyperactivation, which is characteristic of predementia stages like MCI (Ranasinghe et al., 2022). The latter has also been supported by models of epilepsy, where slow waves precede epileptiform activity due to the loss of perisomatic inhibitory synapses (Maestú et al., 2021).

On the other hand, high tau accumulation was related to aberrant excitatory function in the temporal lobe and precuneus, and increased tau accumulation was negatively associated with the power in intermediate-frequency rhythms like alpha (Ranasinghe et al., 2022). In normal conditions, intermediate-frequency rhythms act as negative oscillatory modulators, inhibiting irrelevant activity generators (firings in the absence of stimulus) to regulate network dynamics (Klimesch et al., 2007). With this in mind, the abnormal firing of excitatory populations seems to be mediated by the tau-related alpha power reduction, leading to ulterior network hypoactivity in AD (Ranasinghe et al., 2022).

Since EEG could reflect synaptic dysfunction, multiple quantitative descriptors of the rsEEG have been investigated to assess potential differences related to NDDs. The following sections will expand on the most robust and frequently reported rsEEG abnormalities in the neurodegeneration and dementia continuum.

2.3.1. Slowing-down of oscillations.

The spectral activity of the EEG displays two notorious components: the oscillatory and the aperiodic parts. The aperiodic activity (non-oscillatory, scale-free, or “arhythmic”) follows a quasi-linear decrease in power as frequency increases, noted as 1/frequency χ . The value of χ determines the slope of the 1/f activity, with higher values determining a steeper slope (Donoghue et al., 2020b; He et al., 2019). On the other hand, oscillatory “rhythmic” activity is superimposed on top of the 1/f aperiodic part. Alpha rhythm represents the most notable contributor to the oscillatory part of the spectrum (Waschke et al., 2021).

Oscillatory changes in NDDs have received the most attention in clinical research (Gerster et al., 2022). Abnormalities in rsEEG rhythms could involve frequency shifting from the alpha band ($\sim 8 - 12$ Hz) to low frequencies, with increased power in delta and theta bands and power reductions in higher frequency bands (like alpha, beta, and gamma) (Vanneste et al., 2018). A graphical representation of the rsEEG oscillatory abnormalities in NDDs is presented in **Figure 11**.

Since aperiodic power is more elevated in low-frequency bands and reduced in high-frequency bands, correcting for aperiodic activity seems mandatory to analyse rsEEG changes associated with NDDs (Bailey and Hoy, 2021). However, the research community has not widely implemented the parameterisation of the rsEEG spectrum into aperiodic and periodic components until the last decade, when standardized methods were robustly examined on simulated and real-life data (Wen and Liu, 2016).

In this classical paradigm of studying spectrum in clinical neurophysiology, researchers compute the spectrum to represent oscillations and brain rhythms, ignoring the contribution of subjacent aperiodic activity. Critiques were raised when simulated changes in the aperiodic component led to imprecise estimations of power and frequency descriptors of the spectrum in the canonical frequency bands (delta, theta, alpha, and beta) (Donoghue et al., 2020b; He, 2014). In line with this, separating the oscillatory spectrum and 1/f aperiodic activity is recommended to improve research methods on rsEEG in NDDs (Bailey and Hoy, 2021). Thus, it will provide more accurate descriptors of oscillatory activity and parameters for the aperiodic component as potential confounders or potential variables of interest.

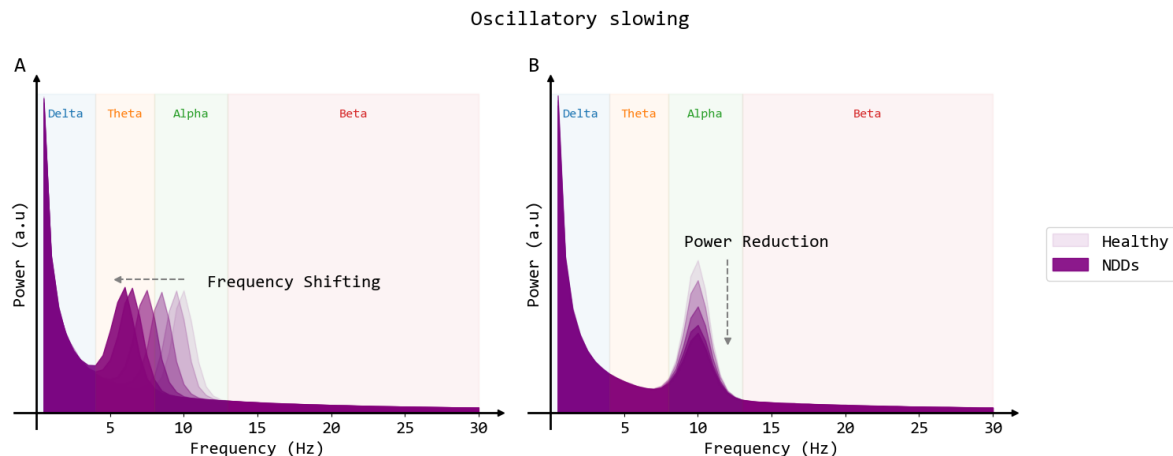


Figure 11. Oscillatory changes in the resting-state electroencephalogram (rsEEG) of patients with neurodegenerative diseases (NDDs). **A)** Represents the shifting to the left of the alpha peak frequency assessed in the power spectral density of the rsEEG signal. Healthy subjects exhibit posterior alpha peak frequency within the canonical alpha band (8-13 Hz), while patients with NDDs exhibit a peak frequency shifting towards lower frequencies within the theta and delta. **B)** Depicts power reductions in the alpha peak observed in the rsEEG power spectral density. Adapted from (Donoghue et al., 2020b; Kopčanová et al., 2023; Schumacher et al., 2020b).

Convergent evidence using rsEEG has supported that pronounced power reduction in high-frequency bands (alpha and beta) and the increase in power in low-frequency bands (delta and theta) are characteristic of the continuum of AD, with mild changes in the MCI stage (Babiloni et al., 2004; Benwell et al., 2020; Brueggen et al., 2017; Huang et al., 2000; Meghdadi et al., 2021; Neto et al., 2015). The abovementioned pattern exceeded physiological age-related changes in rsEEG and was associated with increased genetic risk (APOE epsilon 4 allele) and cognitive performance (Babiloni et al., 2011). CSF A β has also been related to increased power in low-frequencies, while reduced alpha and beta power have been associated with CSF tau pathology in AD and MCI (Smailovic et al., 2018; Smailovic and Jelic, 2019). The posterior-anterior gradient of alpha sources also seems to be shifted to an anterior-posterior topography across AD progression (Babiloni et al., 2004; Babiloni et al., 2011; Huang et al., 2000). Descriptors of power relationships between two frequency bands, so-called “band power ratios”, were also used to quantify this phenomenon, with the theta-to-alpha and alpha 3/alpha2 power ratios reflecting most MCI and AD abnormalities (Bennys et al., 2001; Moretti et al., 2013; Moretti, 2015; Özbek et al., 2021; Schmidt et al., 2013). In addition, some findings using classical methods (1/f uncorrected) supported the idea that the AD continuum shows a progressive reduction of the individual alpha frequency peak correlated with disease progression and memory

performance (Angelakis et al., 2004; López-Sanz et al., 2016; Neto et al., 2015; Peraza et al., 2018).

Recent multicentric evidence corrected for 1/f aperiodic activity. Multicentric cross-sectional data from AD and healthy subjects supports previous observations of power reductions in alpha and beta bands (Kopčanová et al., 2023). However, increased power in theta and delta bands was not replicated when correcting for 1/f activity. Despite this, three independent cross-sectional studies conducted on different AD and MCI samples have found reduced alpha power and increased theta power across the AD continuum (Azami et al., 2023; Chu et al., 2023; Wang et al., 2023). Complementarily, longitudinal quantitative rsEEG analysis on sensor space supports posterior alpha peak frequency reductions related to progression from the MCI stage ($A\beta$ positive) to AD dementia. Also, theta power in temporal and posterior channels increases over time (and posterior beta power slightly decreases) in those progressing to dementia. Unfortunately, the longitudinal assessment did not include healthy controls (Scheijbeler et al., 2023). Finally, results from simulation models have provided robust evidence against the use of power band ratios in NDDs as these descriptors could conflate underlying spectral changes; instead, the parameterization of descriptors of aperiodic and oscillatory parts of the spectrum is suggested (Donoghue et al., 2020a).

As noted, spectral analysis of the rsEEG is part of the current supportive criteria of DLB and is recommended for prodromal DLB (i.e., MCI-LBD) (McKeith et al., 2020, 2017). Specifically, posterior channels reflect power reductions in the alpha band with increased power in the fast-theta (so-called “pre-alpha” band). Frequency shifting towards the pre-alpha band (and lower frequencies) is characteristic of DLB, typically exhibiting peak frequencies below 8 Hz. This reduction in the posterior dominant frequency could happen with or without increased variability (>1.5 Hz) of the peak frequency across rsEEG epochs. (Bonanni et al., 2008; Bonanni et al., 2015; Bonanni et al., 2016). Evidence has been published supporting an anterior-posterior gradient of frequency shifting (towards pre-alpha) as well as the presence of frontal pre-alpha dominant frequency in those DLB patients without posterior shifting (Franciotti et al., 2020). The increased variability of the dominant frequency has also been associated with cognitive fluctuations in DLB, but increased variability compared to AD and controls was not reproduced (Peraza et al., 2018; Stylianou et al., 2018). A recent systematic review summarized most rsEEG findings in DLB. The authors found that, compared to AD, the rsEEG in DLB exhibits more power spectrum abnormalities (i.e. greater power reduction in high-frequency with a more pronounced increase in low-frequency power), also reflected in abnormal band power ratios. The most consistent finding is the reduction of the posterior dominant frequency in DLB (even more reduced in PDD). However, some spectral descriptors fail to show consistency or were not assessed in all the included studies, such as frontal intermittent rhythmic delta activity, dominant frequency variability, anteriorization of alpha peak frequency, and frequency prevalence, among others (Chatzikonstantinou et al., 2021). Compared to healthy subjects and MCI-AD, a reduced dominant frequency, increased pre-alpha power, and reduced alpha and beta power could differentiate the MCI stage of DLB (Bonanni et al., 2015; Schumacher et al., 2020a). To the best of our knowledge, only one publication has corrected for the 1/f aperiodic parameters of the power spectrum when studying DLB cases. The authors compared healthy controls to patients with DLB, PD, and amnestic MCI. In agreement with classical methods, the oscillatory component of the rsEEG followed a pattern of greater theta power in DLB, followed by PD, amnestic MCI and HC. It was noted that the power increase corresponds to the shifting of the alpha peak frequency towards the pre-alpha band. Also, significantly higher alpha power was found in PD compared to DLB, and lower beta power separated amnestic MCI and DLB (Rosenblum et al., 2023).

The continuum of PD to PDD has also been investigated, although few studies have directly compared healthy controls and patients with PD, PD-MCI, and PDD (Caviness et al., 2007, 2016a; Fonseca et al., 2009). The decline in dominant frequency (< 8 Hz) is observed toward the PDD stage with correspondent changes in power. Thus, in PD-MCI, theta power increases and alpha is reduced, while PDD patients exhibit much greater theta and delta power with more decreased alpha power (also reflected in alpha/theta power ratio) (Bonanni et al., 2008; Cozac et al., 2016; Massa et al., 2020; Rea et al., 2021; Zimmermann et al., 2015). Systematic reviews convergently support this trend (Geraedts et al., 2018; Peterson, 2020). Most recently, source space analysis in longitudinal rsEEG recordings pointed out potential patterns of 5-year global cognitive decline in PD, characterized by high delta and low beta power in the somatomotor network, with low alpha power in the default mode and frontotemporal networks (Yassine et al., 2023). Finally, the reproducibility of PD-related changes after correction for 1/f aperiodic activity has been examined in rsEEG. In a 5-year longitudinal study, PD patients with minor hallucinations who exhibited higher frontal theta power had lower performance on cognitive tests for frontal-subcortical functions. A similar trend in cognitive performance was observed for PD patients with lower alpha peak frequency on central and temporal electrodes. PD with minor hallucinations and increased theta power at baseline predicted future (5-year) cognitive decline in frontal-subcortical functions (Bernasconi et al., 2023; Rosenblum et al., 2023).

In FTLD, fewer rsEEG abnormalities have been reported compared to other types of dementia (Julin et al., 1995; Lindau et al., 2003; Yener et al., 1996). However, contradictory findings in the oscillatory rsEEG patterns have been found using canonical frequency bands (Nardone et al., 2018). The most consistent finding across reports is the alpha and beta power reduction with diffuse theta increase in FTD (particularly the behavioural variant) (Caso et al., 2012; Nishida et al., 2011). The latter has been particularly examined through power ratios (such as the alpha/theta and theta/beta1) as well as ratios between spectrum in temporal and frontal channels (Chang and Chang, 2023; Garn et al., 2017; Lindau et al., 2003). The correction for 1/f has recently been examined in FTD. The authors reproduced early results showing an evident reduction in the oscillatory alpha and beta power in FTD patients (comparable to AD). However, statistically significant findings of increased oscillatory theta power were not observed (Wang et al., 2023).

As reviewed, recent works investigating oscillatory rsEEG abnormalities in NDDs have examined potential bias created by 1/f activity in the power spectrum. Beyond controlling for the potential conflation of spectral descriptors, the separation of aperiodic activity in the rsEEG allows the quantification of two aperiodic descriptors, as follows: The aperiodic slope (so-called aperiodic exponent) and the aperiodic intercept (so-called offset). A recent multi-centric rsEEG study reproduced early age-related effects over the aperiodic component of the rsEEG spectrum. Briefly, aperiodic parameters decrease as age increases, with older adults reflecting a reduced slope (i.e. flatter spectrum) and offset (Merkin et al., 2023). Potential hypotheses tracking neural substrates of these aperiodic differences have been proposed based on computational models and empirical observations, suggesting that lower aperiodic slopes in older adults might result from abnormal excitation/inhibition balance (Gao et al., 2017; Merkin et al., 2023) as well as increased neural noise causing less synchronous spiking activity of neuronal populations (Voytek and Knight, 2015). On the other hand, age-related reductions in aperiodic offset seem to be linked with the rate of neural spiking (Donoghue et al., 2020b; Hill et al., 2022; Merkin et al., 2021; Merkin et al., 2023; Voytek and Knight, 2015). A graphical representation of hypothetical models underlying age-related changes in the rsEEG aperiodic activity is presented in **Figure 12**.

Some of the reported findings in NDDs on the aperiodic component of the rsEEG can be summarized as follows. Significant aperiodic abnormalities were not observed in a multicentric cohort of AD subjects (Kopčanová et al., 2023). However, AD patients from a cross-sectional study had increased exponent and offset in posterior channels (Wang et al., 2023). In PD subjects,

aperiodic exponent and offset are increased (compared to healthy controls), and antiparkinsonian medication did not modify these effects (McKeown et al., 2023). Consistently, cross-sectional findings reported that PD and DLB patients were characterized by an increased (steeper) slope compared to amnestic MCI patients and healthy older adults (Rosenblum et al., 2023). However, future cognitive decline in PD was not predicted by early changes in the aperiodic component of the rsEEG (Bernasconi et al., 2023). Altogether, 1/f changes in LBDs have been attributed to an increased spiking rate of subthalamic neurons (leading to higher offsets) and increased basal ganglia inhibition due to hypodopaminergic states (leading to steeper slopes) interfering with dynamic network communication across oscillatory and non-oscillatory neuronal generators (McKeown et al., 2023; Rosenblum et al., 2023; Voytek and Knight, 2015). In FTD, aperiodic parameters were comparable to healthy controls, but decreased offset and slopes in temporal and frontal channels were observed when compared to AD cases (Wang et al., 2023).

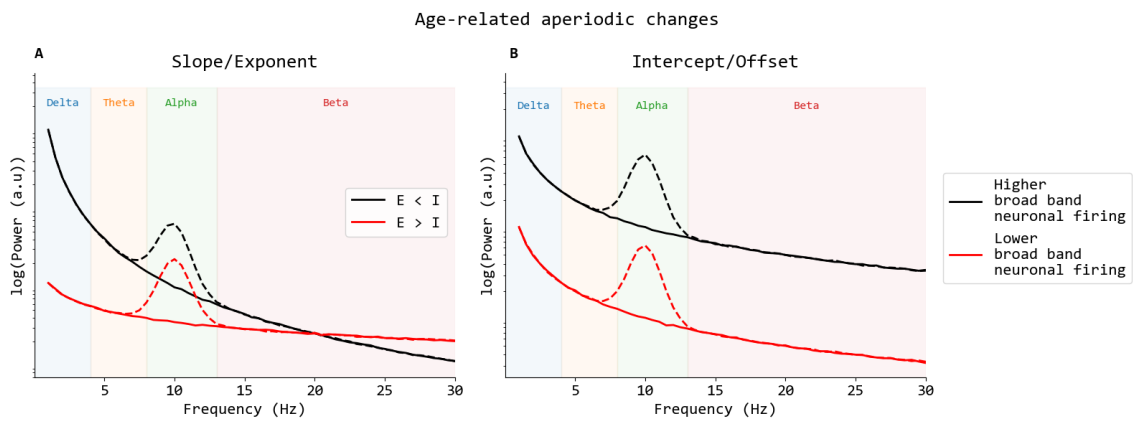


Figure 12. Hypotheses on aperiodic (non-oscillatory) age-related changes in the resting-state electroencephalogram (rsEEG). Aperiodic components of the rsEEG are represented with continuous lines, while oscillatory activity is depicted with dashed lines. **A)** Represents age-related changes in the aperiodic exponent, which is the slope of the one over frequency (1/f) aperiodic activity of rsEEG. Older adults exhibit a lower aperiodic slope/exponent, showing a flatter aperiodic component (continuous red line). Aperiodic flattening might reflect more excitatory (E) than inhibitory (I) activity on neural generators of the rsEEG. **B)** Depicts age-related changes in the aperiodic offset, which is the intercept of the 1/f aperiodic activity of rsEEG. Older adults exhibit a lower intercept, which seems to be related to a lower broadband neural firing produced by phenomena like neural and synaptic loss or brain atrophy. Adapted from (Donoghue et al., 2020b; Kopčanová et al., 2023; Merkin et al., 2023).

Despite the abovementioned observations, recent critiques have been stated supporting that the potential age-related differences in aperiodic activity might be partly attributed to non-cortical origins, showing clear associations with age-related aperiodic changes in magnetoencephalography and signals of cardiac activity (electrocardiogram). The electrocardiographic contributions to the aperiodic activity seem attenuated by artefact rejection methods based on independent component analysis. However, cardiac sources of electrical activity might still affect aperiodic parameters in rsEEG, and further efforts are needed to shed light on this issue (Schmidt et al., 2023).

2.3.2. Reduced complexity.

Studying biological systems has also proved complex interactions between individual subsystems and the richness of information transference and storage from/to the environment. Neurophysiological signals may represent a correlate of the integrity of underlying specialised information processing units. Non-linear dynamics and scale-free properties of neural systems allow mathematical descriptors from information theory to approximate the complexity of the rsEEG signals in healthy ageing and age-related diseases such as NDDs (Averna et al., 2023; Sun et al., 2020). Thus, complexity can be evaluated by estimators of the predictability, self-similarity, and regularity of the signals at multiple scales. These non-linear descriptors can complement the spectral analysis of rsEEG to provide valuable information used to characterise NDDs (Averna et al., 2023). Despite the potential of non-linear estimators of rsEEG complexity, its robust application to clinical settings has not been achieved due to a lack of standardised methods across researchers. Therefore, future research is needed to optimise and automatise the extraction of complexity descriptors (Babiloni et al., 2020a).

According to the entropic brain hypothesis, more regular firing patterns result from less complex systems, and more random and dynamic neural activity would represent a more complex system (Pappalettera et al., 2023). Thus, physiological and pathological brain states could be represented through the system's complexity reflected in the rsEEG signals. A graphical representation of changes in complexity metrics attributed to differences in brain states and brain diseases (NDDs) is presented in **Figures 13 and 14**.

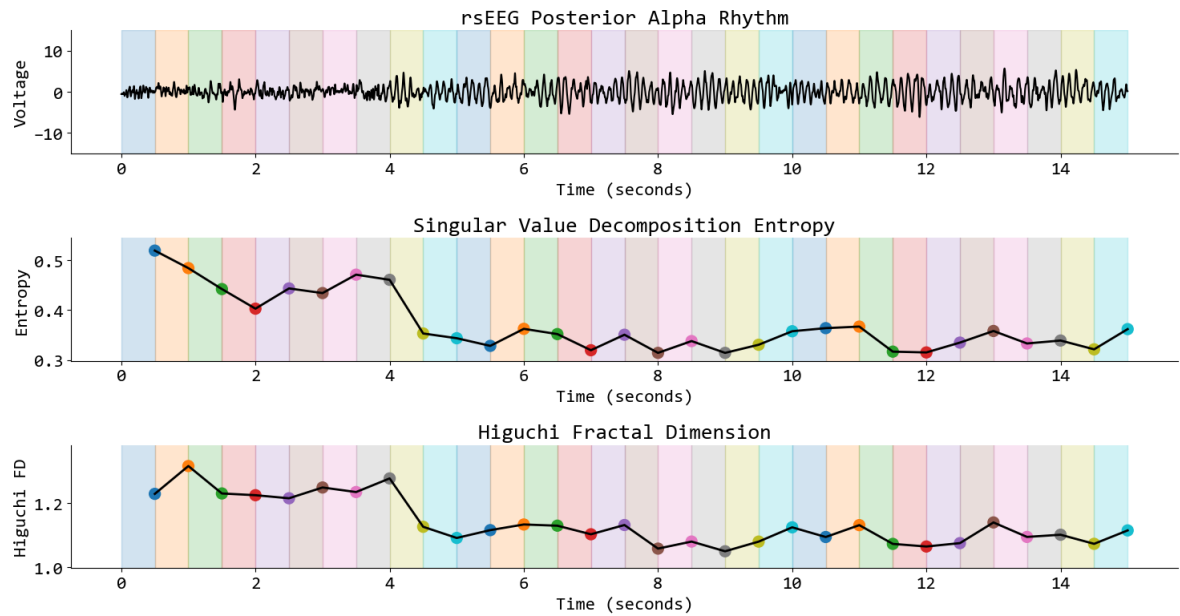


Figure 13. Changes in the resting-state EEG (rsEEG) rhythms and corresponding reductions in complexity. The top subplot illustrates rsEEG rhythms acquired in a posterior channel. RsEEG signal is depicted in the time domain (voltage as a function of time). The onset of a regular alpha rhythm is observed at time = 4 seconds. The middle subplot shows the entropy associated with each rsEEG signal segment. Thus, the initial rsEEG signal is segmented into non-overlapping windows (colour blocks). For each window, the entropy is calculated (colour dots). Note the trend towards reduced singular value decomposition entropy when the regular alpha rhythm starts (the olive green dot at time = 4 seconds). Similarly, the bottom subplot shows the fractal dimension of the rsEEG. Note the reduction at the onset of the regular alpha rhythm (the olive green dot at time = 4 seconds).

As we have pointed out, multiple derivative metrics can be obtained to assess signal complexity. Entropy-derived metrics capture the lack of regularity (repetitive patterns) of the rsEEG by approximating the magnitude of uncertainty over the time series (temporal dimension of signals) (Lau et al., 2022). Repetitive, regular patterns result in lower entropy values, while higher entropy estimations can be interpreted as less regular patterns. The family of entropy-derived metrics comprises single-scale and multi-scale descriptors. Single-scale metrics assess the regularity of the signals in the original time scale of the rsEEG. In contrast, multi-scale metrics use downsampling (coarse-graining method) to quantify entropy at different time scales. For practical applications, and given the extensive number of potential variations in estimating entropy in time series, we will focus on the following single-scale entropy-derived metrics: Approximate Entropy, Sample Entropy, Permutation Entropy, and Singular Value Decomposition (SVD) Entropy, which have shown good test-retest reliability in preliminary reports (Gudmundsson et al., 2007).

Approximate Entropy was introduced early in biomedical research to study heart rate variability; it quantifies the regularity by taking a template of signal points (embedding sequence) and comparing it with another template obtained from subsequent points. However, this metric depends on the signal's length (shorter signals will lead to smaller Approximate Entropy). Considering this, modified algorithms originated new entropy descriptors, such as Sample Entropy, to reduce this length dependency. Sample Entropy demonstrated more reliable estimates than Approximate Entropy but might still be biased when very short segments are considered in the embedding sequence. Noise can also conflate estimations of regularity, giving origin to metrics like Permutation Entropy (Lau et al., 2022). SVD Entropy uses matrix orthogonalization methods to determine the minimal number of eigenvectors to estimate the temporal embeddings of the signal, with lower SVD Entropy values indicating more regular signals, see **Figure 13**.

One final approach to signal regularity is the estimation of Hjorth parameters. Hjorth parameters (complexity and mobility) compute statistical properties of the signal in the time domain (Gudmundsson et al., 2007; Hinchliffe et al., 2022). The Hjorth complexity, which indicates the similarity of the signal's shape to a sine wave, is augmented in regular signals, whereas the Hjorth mobility (i.e. the proportion of standard deviation of the power spectrum) is reduced (Hag et al., 2021; Hjorth, 1970).

Besides, signal predictability can be examined by using mathematical descriptors of the fractal dimension (FD) or detrended fluctuation analysis (DFA). Considering the signal in the time domain, FD analysis computes the minimum number of necessary coordinates to locate any signal point (Lau et al., 2022). We will focus on three FD estimates: Higuchi FD, Katz FD, and Petrosian FD (Goh et al., 2005). Katz FD quantifies the predictability using the Euclidean distance between signal points, which implies making assumptions about the stationarity of the time series. Higuchi FD works similarly but is not sensitive to the stationarity of the signals and is also robust against high amplitudes in the signal (often generated by noise). The Petrosian algorithm provides a faster quantification of FD of a dynamic system by converting the signals into binary sequences based on thresholding methods and then determining the difference across time. Although faster, Petrosian FD is sensitive to noise compared to Higuchi and Katz's methods. As a general rule, FD decreases with more predictable signals (less complex); see **Figure 13**.

Statistical approaches to the predictability of rsEEG signals have also been proposed. Thus, DFA describes long-term statistical dependencies in the signals as a measure of self-affinity by approximating the time series fluctuations in short and large time windows. DFA was formulated to analyse genetic sequences and has been adapted to multiple biological research contexts, where

higher DFA values imply more long-range temporal correlations (i.e. more self-affine signals) (Averna et al., 2023).

In NDDs, the complexity of rsEEG has been repeatedly assessed, although the consistency of findings has been reported due to variations in the parameters of the algorithms. Despite inter-lab variability in methods, narrative and systematic reviews have stated a notable trend towards reduced complexity in AD, even from the MCI stages (Al-Nuaimi et al., 2018; Averna et al., 2023; Lau et al., 2022; Ouchani et al., 2021; Sun et al., 2020). Similarly, a reduced rsEEG complexity has been reported in PD, predicting a 3-year cognitive decline in those with low entropy (Keller et al., 2020; Yi et al., 2017). However, one rsEEG study in PD-MCI and cognitively spared PD patients offers contrastive results of increased complexity also observed in local neurophysiological signals of basal ganglia (Averna et al., 2023; Yi et al., 2022). In DLB and FTD, complexity seems to be less explored. Still, results from a large Chinese cohort report significantly reduced complexity (assessed via Hjort Mobility) in DLB compared to healthy controls, amnestic MCI, FTD, and AD subjects. Complexity in FTD patients was comparable to AD subjects, slightly reduced compared to healthy controls, but significantly higher than in DLB cases. Correlations between complexity in the rsEEG and CSF biomarkers of A β and tau pathology, as well as cognitive performance, were reported (Jiao et al., 2023). Overall, reduced complexity seems to characterise NDDs, see **Figure 14**.

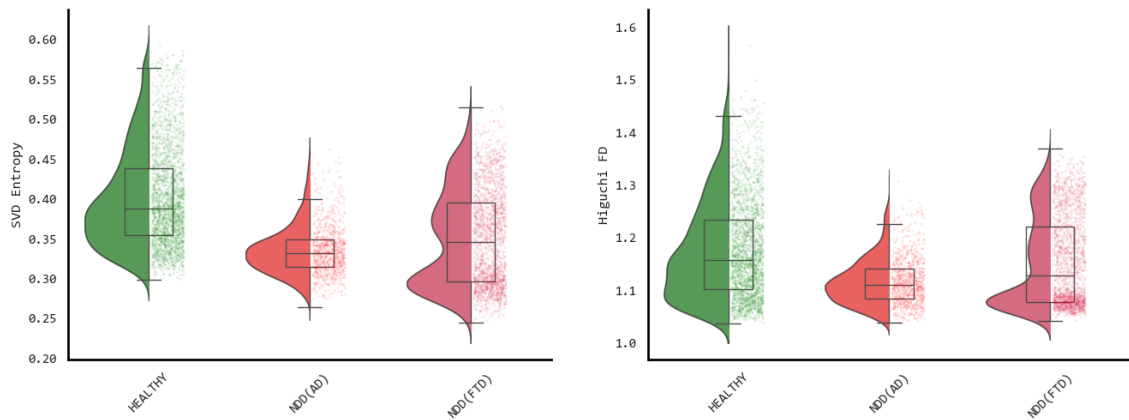


Figure 14. Approximations to global complexity metrics in healthy subjects and neurodegenerative diseases (NDDs), exemplary cases. Raincloud plots show Singular Value Decomposition (SVD) Entropy and Higuchi Fractal Dimension (FD) for all electrodes in healthy controls when compared to two NDDs groups (Alzheimer's Disease -AD- and Frontotemporal Dementia -FTD-). Data from three exemplary cases matched by age (70 years) and Sex (Male). Global cognitive performance assessed with the Mini-Mental State Examination was 30 in the healthy subject, 14 in AD, and 22 in FTD cases; perfect performance results in a test score of 30. Each dot represents the complexity estimations for each of the epochs and channels. Reduced global complexity can be observed in the two NDDs groups. Figure created with signals from (Miltiadous et al., 2023).

Relationships between complexity estimations based on regularity and predictability of the signals support consistency and reliability across methods in rsEEG data (Gudmundsson et al., 2007). As part of a complementary phenomenon, abnormalities in spectral activity (oscillatory and aperiodic) observed in NDDs have been associated with complexity metrics (Dauwels et al., 2011). For an extensive review of the link between complexity features and aperiodic (scale-free, fractal) parameters of the spectrum, we refer the reader to the simulations performed by Donoghue in <https://aperiodicmethods.github.io/docs/index.html>

2.3.3. Abnormal connectivity and synchronisation.

To reflect rsEEG connectivity, synchronization in the signals from two or more channels can be estimated through more than 42 different methods (and other potential slight variations). Based on simulations with synthetic data and real-data confirmations, none of these connectivity descriptors have proved to outperform the others (Mohanty et al., 2020; Prado et al., 2022).

Effective connectivity estimators provide inferences about the causality (directionality) of the interdependences of the examined signals. By contrast, functional connectivity is based on model-free assumptions about causation. Connectivity can be estimated at the sensor space (determining pairwise interdependences across channels) or at the source space (determining interdependencies across inferred sources of rsEEG signals). Source space methods offer an accurate spatial description of the sources but demand much more intensive computational resources than sensor space connectivity analysis. An extensive revision on rsEEG connectivity methods has been recently published; the reader is referred there for more details (Miljevic et al., 2022).

To settle the thesis framework, we will expand on functional connectivity abnormalities in NDDs on sensor space for practical applications. Hypoconnectivity and hyperconnectivity are two main phenomena reported in the rsEEG connectivity and seem to be linked to neurodegeneration and cognitive decline, as depicted in **Figure 15**. Functional connectivity is often assessed in frequency bands to approximate the synchronization of different brain rhythms.

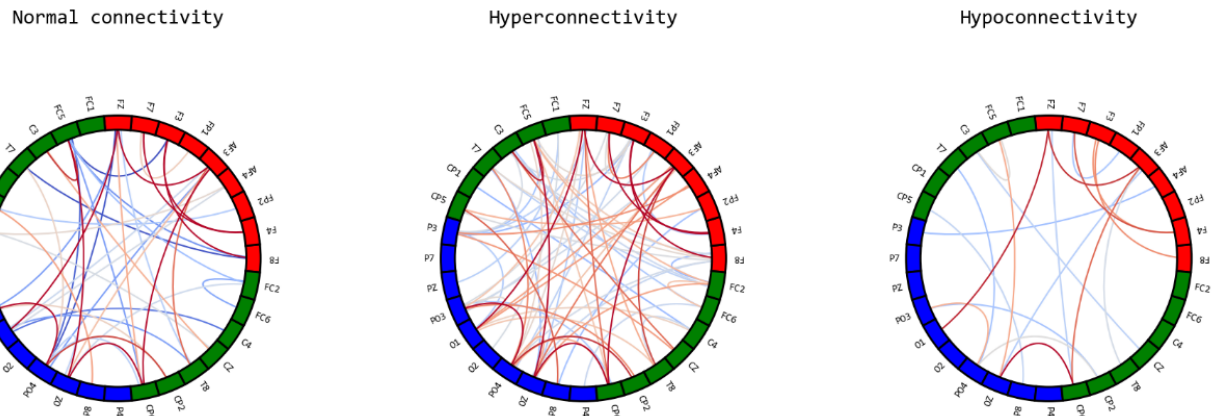


Figure 15. Representation of changes in sensor space connectivity attributed to neurodegenerative diseases (NDDs). Each circle depicts all-to-all sensor functional connectivity (frontal electrodes are represented in red squares, central electrodes in green squares, and posterior electrodes in blue squares). Red lines inside the circles indicate higher estimates of connectivity, and blue lines depict lower values. Compared to normal connectivity, hyperconnectivity states are characterised by increased links between pairs of electrodes. In contrast, hypoconnectivity is illustrated by less intense channel interdependencies and a reduction in the number of links. Adapted from (Badhwar et al., 2017; Koelewijn et al., 2019; Prado et al., 2023).

From functional imaging studies, mainly conducted in the spectrum of AD, the hypothesis of inverted U-shaped connectivity trajectories across the continuum of NDDs has been suggested. Thus, genetic risk factors, protein aggregation/accumulation, and preclinical and prodromal stages lead to hyperconnectivity as a compensatory (adaptive/hormetic) effect, followed by reduced connectivity in the later stages of the disease (Schultz et al., 2017; Ye et al., 2018). Similarly, magnetoencephalographic data support these observations; compared to age-matched

healthy controls, amnestic MCI and carriers of the APOE epsilon 4 allele exhibit resting-state hyperconnectivity in posterior alpha rhythms but subsequent hypoconnectivity in AD (Briels et al., 2020; Gaubert et al., 2019; Koelewijn et al., 2019; Ranasinghe et al., 2020). Also, hyperconnectivity in the delta and theta bands has been observed in AD, showing significant differences in frontal sources strongly associated with A β and tau cortical accumulation (Ranasinghe et al., 2020). In rsEEG, one recent publication employed nine different connectivity metrics and reported temporo-posterior hypoconnectivity in the beta band, with frontal hyperconnectivity in the delta and theta bands as the most consistent finding in AD. The authors also described FTD's more pronounced fronto-temporo-parietal hypoconnectivity (in the alpha and gamma bands), with non-statistically significant findings supporting hyperconnectivity (Prado et al., 2023). The latter study was conducted on source space, allowing for a more precise estimation of the generators of the signal and reducing the effects of volume conduction.

A recent systematic review of connectivity in DLB has shown that reduced frontoparietal connectivity in the alpha band was a distinctive pattern observed across rsEEG studies (Habich et al., 2023). This finding was consistently observed in sensor and source space, was independent of A β co-pathology, present from the MCI stages, and correlated with hallucinations DLB (Babiloni et al., 2019; Mehraram et al., 2020; van der Zande et al., 2018). Similarly, PDD exhibited reduced posterior alpha-band connectivity when compared to healthy subjects. Reduced connectivity in the beta band was more prominent in LBDs versus AD subjects and control individuals (Mehraram et al., 2020).

Altogether, abnormalities in functional connectivity related to NDDs are reminiscent of abnormalities observed in the spectral analysis of the rsEEG. As a matter of fact, changes in spectral power could be associated with abnormalities in frequency-specific estimated connectivity (Briels et al., 2020). Due to the large number of connectivity metrics, assessing the comparability between studies might be troublesome, and it is recommended to conduct consistency/sensitivity analyses with multiple methods to estimate synchronization (Miljevic et al., 2022; Prado et al., 2023). Inferring spatial attributes from functional connectivity calculated at the sensor space is not recommended (Schaworonkow and Nikulin, 2022). Nevertheless, the average connectivity estimates across sensors (i.e. global connectivity) have reproduced most neurodegeneration-related abnormalities observed in source space (Mehraram et al., 2020; Smailovic et al., 2018). Quantifying average sensor space connectivity employing methods such as Phase Lag Index and Amplitude Correlation Envelope–corrected offers high consistency with the average source space estimations (Lai et al., 2018). The latter represents an opportunity for clinical research: Low-density recordings (19-21 channels) are commonly acquired in clinical practice, and subject-specific neuroimaging data is not always available to extract structural aspects necessary for modelling triangulations on surfaces, which might lead to imprecise source localization (Nguyen-Danse et al., 2021). Novel initiatives have recently emerged to overcome volume conduction issues and the high computational demand required for source space analysis (Engemann et al., 2022a; Hebling Vieira et al., 2022). In the subsequent years, implementing these innovative approaches into clinical practice will refine current methods and provide a better understanding of rsEEG connectivity patterns in NDDs.

2.4. Towards integrative multi-feature models in rsEEG research.

Throughout previous sections of **Chapter 2**, a general overview of specific rsEEG patterns in the most frequent NDDs has been presented. After a brief review, we could conclude that rsEEG metrics (i.e. features) extracted from a single conceptual family are not accurate enough to achieve perfect discrimination of subjects with different NDDs leading to dementia. This section will expand on this issue, providing the rationale for combining spectral, complexity and connectivity analysis as a potential solution.

First, we discussed the focus of researchers on rsEEG spectral analysis in NDDs. One potential argument is that a prominent focus on rsEEG spectral analysis would arise from the need for a practical interpretation for clinicians (i.e. changes in the power of a particular brain rhythm) (Al-Qazzaz et al., 2014). Despite its apparent simplicity, the potential bias of interpreting spectral analysis without correction for aperiodic activity has been remarked, as well as the risk of obtaining conflated results when solely using band power ratios. Second, the relative standardization of procedures and the socialization and adoption of international guidelines on rsEEG spectral analysis have facilitated the pre-eminence of these methods against complexity and connectivity methods, which complement the information of spectral analysis and might reflect additional associations with oscillatory and aperiodic parameters as previously stated. Finally, inherent aspects of NDDs, such as the clinical course, symptoms, or neuropathological hallmarks, evince associations with abnormality patterns in the spectrum, complexity and connectivity.

With all the above, and based on the conceptual evolution of NDDs (i.e. integrating other relevant aspects beyond protein accumulation/aggregation), rsEEG research has moved towards multi-feature approaches that can capture various types of information from the signal (Gil Ávila et al., 2023).

In other neurological conditions, such as disorders of consciousness, researchers have emphasised the importance of considering combinations of metrics from various conceptual families to assess synaptic and network dysfunction in the rsEEG. The combined approach supports more integrative conclusions and better predictive/classification performance (Engemann et al., 2018; Sitt et al., 2014). In NDDs, most multi-feature rsEEG analyses have reported significantly better results compared to unitary metrics (Gaubert et al., 2019; Jiao et al., 2023; Moguilner et al., 2022; Prado et al., 2023). On the other hand, the solid applicability of rsEEG multi-feature approaches in clinical practice demands validation on multicentric studies with representative samples (Prado et al., 2022), which poses specific challenges that will be discussed in the subsections of **Chapter 2.5**.

Novel successful results have been achieved in the classification of different NDDs, whether by estimating composite indexes or by obtaining multiple features and subsequently refining them based on their relative importance to the classification of different diagnosis groups (Jiao et al., 2023; Moguilner et al., 2022; Prado et al., 2022; Prado et al., 2023). However, the multi-centric studies from Prado et al. and Moguilner et al. have scopes beyond an expeditious automated and accurate classification of NDDs in clinical practice. These methods focus on disentangling a mechanistic explainability of dementia-related rsEEG patterns, focusing on connectivity metrics and rsEEG integration with structural imaging. As additional limitations, these studies have been restricted to FTD and AD subjects, lacking representativity due to a relatively small sample size ($n = 130$, AD plus FTD) (Moguilner et al., 2022; Prado et al., 2023). Finally, these authors primarily consider source space analysis of high-density rsEEG recordings (not typically acquired in clinical practice). The latter might result in demanding computational resources (unavailable in all hospital infrastructures).

On the other hand, the approximation from Jiao et al. is much more consistent with our proposed approach (i.e. multi-feature integration from low-density rsEEG recordings). These authors achieved a much larger sample size than other works ($n = 644$ individuals with the most common NDDs or vascular dementia). Moreover, their promising results identified features from spectral analysis (particularly posterior theta power) and complexity features (especially posterior Hjorth parameters) as the most relevant rsEEG features for the classification of NDDs. Moderate correlations with global cognitive performance and AD-related neuropathology were also observed, elucidating the meaningfulness of the abovementioned features. Nevertheless, these findings should be taken cautiously as the authors did not correct the $1/f$ aperiodic activity in their spectral estimations. At the same time, the external validity of such promising conclusions should still be determined as the study sample was recruited at a single Neurology Unit (Jiao et al., 2023).

Despite possible limitations of the currently available evidence, multi-feature analysis is emerging in neuroscience and NDDs research to exploit rsEEG data. The following section will expand on overcoming present barriers and discuss essential steps towards broader adoption of rsEEG in diagnosing various diseases leading to neurodegeneration and dementia.

2.5. Current challenges: Why is rsEEG not included in most criteria for NDDs leading to dementia?

Divergent conceptual definitions of NDDs (i.e. biological, phenotypical, clinic-pathological) and slight differences in classification schemes constitute part of the difficulties in adopting rsEEG-based diagnostic biomarkers. In other situations, low sensibility or specificity has hindered their inclusion as indicative disease biomarkers. Yet, methodological limitations and rsEEG-specific challenges the reproducibility and generalizability of evidence-based conclusions.

From the conceptual framework of a biological definition of AD based on amyloid deposition, tau accumulation, and neurodegeneration (ATN scheme), biomarkers were classified as pathophysiological or topographical. The former quantifies protein accumulation/aggregation *in vivo*, while the latter tracks regional neurodegeneration-related structural or functional abnormalities (mainly through neuroimaging methods) (Dubois et al., 2014; Dubois et al., 2021). In the conception of the ATN scheme, it was also stated that rsEEG could add value to the current scheme, representing synaptic dysfunction. Following this, synaptic dysfunction could be subsumed into the "neurodegeneration" category, as the latter might also be defined as a progressive loss of neurons (and functions) (Jack et al., 2016). Despite this, multiple national guidelines do not recommend routine assessment of rsEEG in cognitively spared subjects (Gouw and Stam, 2016; Pippenger, 2021).

The Electrophysiology – Professional Interest Area of the International Society to Advance Alzheimer's Research and Treatment extended on this matter and recently stated expert consensus recommendations. After revising basic and clinical evidence in the pathophysiology of brain hyperexcitability, this panel suggested including EEG methods in the ATN scheme for clinical applications in AD. Among the arguments in favour of the rsEEG inclusion in the ATN scheme, a high classification accuracy of NDDs ($> 80\%$, particularly for AD) has been noted (Babiloni, 2022). In agreement with this, a recent systematic review and methodological analysis of EEG-based biomarkers of Alzheimer's disease have posited similar observations (Modir et al., 2023). Nevertheless, biomarkers should be sensitive and specific rather than accurate (Khoury and Ghossoub, 2019). Also, as emphasised by other authors (Gaubert et al., 2021), a cautious

interpretation of these reported high accuracies should be considered based on methodological and statistical aspects detailed in the following sections.

2.5.1. Challenges to reproducibility and validity of rsEEG findings.

In addition to the abovementioned preeminence of direct biomarkers of protein accumulation/aggregation in the biological definitions of NDDs, specific aspects of rsEEG acquisition, study design, and analysis methods might originate discrepancies in the results and conclusions across samples, ultimately compromising its reproducibility and external validity.

Despite the publication of international guidelines for clinical research on rsEEG, the lack of unified/operationalised procedures limits the comparability across studies (Babiloni et al., 2020a; Miljevic et al., 2022). The latter has also been reported in meta-analytic results from epilepsy (where rsEEG abnormal patterns are often more pronounced than in NDDs), revealing that high inter-rater variability in qualitative visual inspection of the rsEEG ($> 37\%$) could reduce the sensibility and specificity (Gilbert et al., 2003). Similarly, in dementia research, artefact rejection based on visual inspection is not precisely reproducible and might be prone to bias (Cassani et al., 2018).

Beyond possible inter-rater variability, the small sample size in most rsEEG studies has been prominently criticised (Larson and Carbine, 2017; Modir et al., 2023). In neuroimaging, this limitation of underpowered studies was also evinced, and secondary analyses pooling multiple single studies improved methodological rigour and promoted successful open science-based platforms for data centralization and sharing worldwide (Harding et al., 2023; Hayashi et al., 2023). Although data centralization assures access to raw data, common structures for file organization across individual datasets facilitate automatizing analytic procedures and database querying. Consistently, structuralised organization and naming systems have been adopted in rsEEG from neuroimaging, standardising conventions and differences in file structures since channel names, file extensions of the signal, and voltage data units can vary according to the specific configurations of a large number of manufacturers of EEG devices. Also, issues caused by each research centre's idiosyncratic methods/practices for file organization and naming and analysis scripts (not often published) could be tackled by implementing this organization structure (Pernet et al., 2019). However, increasing the sample size by simply pooling multi-centre data acquired with different amplifiers/headsets could cause site-related (batch) effects that should be corrected. Moreover, NDDs are age-related and cross-site biological variability must be considered (and preserved) during this batch effects harmonisation process (Bigdely-Shamlo et al., 2020; Li et al., 2022b; Pomponio et al., 2020; Prado et al., 2022). With all the above, automated multi-feature rsEEG analysis for the classification of different NDDs (rather than binary separation from healthy controls) would provide more robust methods toward identifying relevant features on the signals, examining the generalizability of these potential rsEEG biomarkers across heterogeneous samples.

2.5.2. Small samples draw small conclusions: Harmonising and pooling multicentric data.

Two systematic reviews published in 2017 and 2018 highlighted the low statistical power of human electrophysiology studies and rsEEG publications on AD diagnosis (Cassani et al., 2018; Larson and Carbine, 2017). Unfortunately, according to a 2023 systematic review of AD publications from 2018 – 2022, this panorama has not changed in the last five years. In the latter, the authors reported that only 18 % ($n = 13$) of primary studies included more than 100

individuals (Modir et al., 2023). One of the earlier syntheses of evidence identified that limited resources and participation in multiple low-powered studies, rather than fewer with high statistical power, were listed among the reasons for conducting small samples in rsEEG projects (Larson and Carbine, 2017).

The high classification accuracy of some studies applying machine learning to small datasets has been questioned, and the potential overfitting of the models cannot be ruled out (Gaubert et al., 2021). Multiple efforts in the community of EEG researchers aimed to replicate the experience gained from neuroimaging by pooling individual datasets into large multi-site meta-analysis (i.e., analysis of statistical estimates) and mega-analysis (i.e., analysis of the raw data) (Bigdely-Shamlo et al., 2020; Bonanni et al., 2016; Costafreda, 2009; Engemann et al., 2022a; M. Li et al., 2022).

Due to international collaborations and open science initiatives, the neuroimaging community has supported the aggregation (or pooling) of imaging data from multiple sites to improve statistical power and validity. In a recently published review, correcting batch effects (caused by scanner differences) has been recommended to avoid drawing biased conclusions that can emerge by simply pooling the datasets. In addition, statistical normalization of batch effects by regressing the “site” variable from the extracted features might not be enough to correct cross-site differences (Hu et al., 2023). In the few rsEEG studies gathering multi-site data from NDDs, batch effects are rarely analyzed or reported, and regression methods have been implemented (Babiloni et al., 2004; Babiloni et al., 2022; Bonanni et al., 2016; Chen et al., 2015; Franciotti et al., 2020). Specific studies addressing factors that influence EEG variability have demonstrated that acquisition systems (scanners) can account for at least 9% of the variance when pooling signals from four different EEG scanners (amplifiers/headsets) (Melnik et al., 2017). Fortunately, significant batch effects have been reported in rsEEG in projects creating normative data from healthy controls, mega-analysis, and NDDs. Still, the codes used for analyses were not published along with the manuscript, limiting the exact replicability of these harmonisation procedures (Bigdely-Shamlo et al., 2020; Li et al., 2022b; Prado et al., 2022).

By contrast, open-source harmonisation approaches used in neuroimaging have been freely disposed to researchers to mitigate batch effects while preserving relevant biological information for subsequent analyses. As a case in point, the Combining Batches (ComBat) method and several variations/optimizations have been successfully tested in imaging data based on synthetic and real-life data. The ComBat algorithm was developed in genetics, where batch effects were also problematic for pooling data, advancing research and filling knowledge gaps in microarray expression data (Johnson et al., 2007). ComBat demonstrated good performance in a wide variety of radiomic datasets (Beer et al., 2020; Bell et al., 2022; Pomponio et al., 2020; Shiri et al., 2022; Voß et al., 2022; Xu et al., 2023) as well as in transcriptomics (Ryan et al., 2022). Conversely, there are scarce reports on the specific effects of statistical harmonisation of multisite rsEEG features with ComBat-derived methods in the currently available literature (Kurbatskaya et al., 2023b; Kurbatskaya et al., 2023a; Li et al., 2022b).

The adaptations to the original ComBat method for neuroimaging data allow modelling site-specific scaling factors, resulting in suitable alternatives for exploiting small sample-size datasets given the use of empirical Bayes to estimate the site parameters. Besides, the estimations of most ComBat variants preserve the effect of biological covariates of interest, such as age, gender, or diagnosis (Adamer et al., 2022; Fortin et al., 2018; Horng et al., 2022; Pomponio et al., 2020). At last, pooling multisite datasets while controlling for batch effects might contribute to more generalizable findings in rsEEG studies and the potential discovery of robust biomarkers for neurological and psychiatric conditions that might be influenced by biological factors, including age, gender, and educational level (Jovicich et al., 2019; Li et al., 2022b; Modir et al., 2023; Moguilner et al., 2022; Prado et al., 2022).

2.5.3. Lack of uniform standardised preprocessing of rsEEG signals.

Preprocessing biological signals like rsEEG aims to increase the signal-to-noise ratio, preserving brain-related activity and ameliorating artifactual components. In extensive datasets and long (continuous) signals, manual preprocessing can become time-consuming, tedious, and prone to arbitrary decisions that might vary across experimenters (Pedroni et al., 2019). Issues in the reproducibility of analyses using visual inspection for manual artefact remotion have already been stated in section 2.5.1.

Beyond inter-rater variability, the effects of preprocessing can affect the estimations of derivative metrics such as power spectrum, complexity, and connectivity (Bigdely-Shamlo et al., 2015; Isaza et al., 2023; Jas et al., 2017; Pedroni et al., 2019; Robbins et al., 2020; Suarez-Revelo et al., 2016; Suárez-Revelo et al., 2018). Thus, rigorous comparability of results across studies (e.g. in meta-analysis) might be virtually impossible due to differences in the preprocessing schemes. Custom codes and scripts used for preprocessing are rarely published in rsEEG studies assessing NDDs (Modir et al., 2023). Considering the above, employing a standard and open preprocessing pipeline (common to all signals) is essential to analyse large rsEEG data collections (Bigdely-Shamlo et al., 2015; Pedroni et al., 2019).

In light of this context, multiple initiatives have developed open-source preprocessing pipelines, benchmarking them against other methods in different EEG datasets and making them freely available (Bigdely-Shamlo et al., 2015; Jas et al., 2017; Li et al., 2022a). The Organization for Human Brain Mapping instantiated guidelines for best reproducibility in EEG studies, recommending detailed reporting of preprocessing schemes (Pernet et al., 2020). Given the open-source availability of the state-of-the-art preprocessing algorithms, challenges to reproducibility have been reduced, as observed in age-related rsEEG studies where preprocessing and analysis codes accompany the publications. The latter facilitated exact methodological replication but also allowed the exploitation of anaesthesia monitoring data and sleep EEG recordings from portable devices to assess “brain age” (Banville et al., 2023; Donoghue et al., 2020b; Engemann et al., 2022a; D. Sabbagh et al., 2023). Learning from the experience of rsEEG age-related studies might help researchers in NDDs obtain reproducible results through more replicable methods.

2.5.4. Applicability of rsEEG in clinical settings.

Typically, clinical rsEEG recordings are conducted with low-density montages, which might produce bias estimation on the topography of the sources when using templates instead of subject-specific neuroimaging data (Nguyen-Danse et al., 2021). As a case in point, a single EEG channel has been used to assess event-related attentional changes in a large cohort of patients with schizophrenia (Light et al., 2015). Moreover, some authors have suggested that the test-retest reliability of source space estimations is reduced compared to sensor space analysis (Duan et al., 2021; Moezzi et al., 2018). Therefore, sensor space analysis could be considered to exploit already collected datasets when the specific topography of the sources does not need to be known.

Another advantage of sensor space over source space is the convenience of sensor space analysis in terms of computational demand. Thus, sensor space analysis can be implemented for faster computation of derivative features and identify patterns of abnormality in clinical settings. Thus, exploitation of already collected rsEEG recordings by extracting multiple features in sensor space can provide valuable data for machine learning applications in memory clinics, as observed in recent publications (Jiao et al., 2023).

Furthermore, pooling single datasets and harmonising batch effects has been suggested to identify the best analysis methods, augment the reproducibility of the findings, and yield robust

conclusions regarding detection (classification/diagnosis), prediction, and monitoring of NDDs (Modir et al., 2023). With all the above, pre-training models with extensive collections of rsEEG data and the future deployment of machine learning models for diagnosing and managing NDDs do not seem to be a distant reality.

2.5.5. Overcoming some of the challenges of rsEEG in NDDs diagnosis.

Crucial methodological aspects affecting the robustness and reproducibility of rsEEG signals in age-related and general biomedical research were previously reviewed. However, two crucial determinants for accurately detecting NDDs using rsEEG should be discussed: a) Focus on single-nature features, and b) Focus on binary classification. These inherent issues of rsEEG research in NDDs will be reviewed next.

The analysis of rsEEG features derived from a single-nature conceptual family (i.e., only spectral, complexity, or connectivity) has been prominent in NDDs. However, more recent studies aim to overcome this limitation by combining different types of information from the rsEEG signal (Gaubert et al., 2019; Gaubert et al., 2021; Jiao et al., 2023; Moguilner et al., 2022; Prado et al., 2023). The latter seems a reasonable alternative, considering overlapping characteristics of the rsEEG patterns in NDDs. Spectral analysis has been recommended as a starting point as these features are relatively more standardised (Cassani et al., 2018). Furthermore, this multi-feature approach could provide meaningful information in case of difficulties in classification due to overlap in a single metric between two or more disease phenotypes.

However, computing and modelling multi-feature data pose challenges due to multicollinearity and multiplicity of hypothesis tests; thus, feature selection methods can refine the set of features, keeping the most relevant features for the classification of NDDs (Al-Qazzaz et al., 2014; Modir et al., 2023). With this in mind, multi-feature rsEEG analysis would promote the synthesis of meaningful information rather than a detailed, narrow analysis.

Across the last decade, the preeminence of studies in rsEEG focused on detecting NDDs from signal features has been documented in revisions of the available literature (Cassani et al., 2018; Geraedts et al., 2018; Modir et al., 2023). Briefly, despite the reconceptualization of NDDs under biological definitions, most of the rsEEG datasets use the clinical phenotype and clinical diagnostic criteria (which often do not include biological biomarkers) to categorise patients in different groups and identify those patients with a “similar” phenotype. Thus, the potential clinical heterogeneity in symptoms or differences in disease severity is often left aside and not deeply assessed in detection (classification) studies (Pedroni et al., 2019). In addition, binary classification between healthy individuals and diseased patients is frequently examined but is not a realistic classification scenario, as rsEEG is mainly conducted in clinical practice for the differential diagnosis of NDDs (Garn et al., 2017; Gouw and Stam, 2016; Pippenger, 2021; Stylianou et al., 2018). Lastly, including subjects with more subtle rsEEG changes (i.e., preclinical and prodromal stages of AD, such as amnestic MCI) is essential to translate scientific discoveries into clinical practice routines (Gaubert et al., 2019).

3. Ph.D. Project in context.

In this section, we delve into the fundamental principles that underpin the conceptual framework of this project. As illustrated in **Figure 16**, the project can be summarized in three stages, each addressing a crucial facet of our research: A) Data organization/acquisition and curation, B) Data analysis and model construction, and C) Model test and validation.

Firstly, the organization and formatting of rsEEG data following standard conventions facilitate further collaborative efforts. Given the large number of manufacturers of EEG devices, we should consider the large variability in data formats, differences in the default filenames and channel name conventions, and acquisition parameters, among others. With this in mind, cross-lab sharing of rsEEG results in a tedious and time-consuming effort. Based on imaging and magnetoencephalography developments to organize multicentric datasets, the research community on EEG designed the Brain Imaging Data Structure (BIDS) to achieve a common system of file organization with standard conventions (Pernet et al., 2019). Briefly, the BIDS specification defines rules for naming and storing rsEEG signals and their associated metadata (i.e., dataset description, acquisition parameters, code for data conversion and preprocessing, and subject variables of interest). Thus, the whole dataset from a single centre is organized in a root folder. For each subject, a subfolder inside the root folder will be created. The folder of an individual subject will contain specific subfolders for each of the data modalities acquired (i.e., imaging, EEG, genetic data). The format of the EEG signals is also converted to a list of widely used and computationally efficient file extensions. Within the EEG folder, longitudinal recordings are also organized in a “session” subfolder. Altogether, the EEG BIDS specification has been progressively adopted by the scientific community with a growing number of datasets released to contribute to new developments and, potentially, big-data methods (Engemann et al., 2022a; Hatlestad-Hall et al., 2022a; Miltiadous et al., 2023). Similarly, in this project, we adopted the EEG BIDS standards to organize multicentric datasets that were already collected and ongoing data collections.

In addition to organization, raw rsEEG signals often require extensive curation to be usable for analysis (i.e. rejection of bad segments with artefacts, channels interpolation, etc.). However, most available clinical research studies have performed artefact remotion based on visual inspection, lacking standards for data preparation and increasing the interobserver and inter-lab variability when conducting validation and reproduction of findings. The differences in preprocessing also can affect classification or prediction accuracy in machine-learning methods. Thus, previously validated automatic curation pipelines are crucial for harmonising and comparing rsEEG data from different research centres. In this project, we implemented a fully automated preprocessing with a high test-retest reliability validated in different healthy samples (Isaza et al., 2023; Suárez-Revelo et al., 2016; Suárez-Revelo et al., 2018; Zapata-Saldarriaga et al., 2023). Also, our preprocessing approach has been successfully applied to PD, MCI and AD samples (García-Pretelt et al., 2022; Jaramillo-Jimenez et al., 2021; Jaramillo-Jimenez et al., 2023; Kurbatskaya et al., 2023b; Kurbatskaya et al., 2023a).

Secondly, after preprocessing rsEEG signals, derivative metrics (features) were extracted from the clean data based on mathematical descriptors from three different conceptual families, as follows: A) Spectral analysis, B) Complexity and Regularity analysis, and C) Connectivity Analysis. Spectral features included peak frequencies (dominant frequency and its variability), aperiodic ($1/f$) and $1/f$ corrected oscillatory parameters extracted in the sensor space and computed for three regions of interest (ROI), namely, anterior, central, and posterior. Concordantly, complexity and regularity features were extracted in the time domain using descriptors from information theory, including entropy and fractal dimension estimators, as well as descriptors of the statistical properties of the signal. Additionally, connectivity features in the sensor space were

computed using volume conduction-corrected phase-based metrics to approximate the global connectivity in the whole bandwidth and by frequency bands. Subsequently, potential site-related effects were mitigated using statistical harmonisation of the extracted features. The latter was performed with a variant of the combining batches (ComBat) popularized for genetics and imaging modalities in neuroscience research (Adamer et al., 2022). In this project, site-related differences in rsEEG data were observed, and the mitigation effects of multiple ComBat variants were analysed in multi-site rsEEG collections with a heterogeneous population. The multi-centric harmonised data was used to train multiple machine learning (ML) models to classify each subject according to his/her clinical diagnosis. In order to implement an automated approach for reproducible results, we used automated ML (autoML) methods tested in different types of data and research fields (Angarita-Zapata et al., 2021; Byeon et al., 2022; Conrad et al., 2022; Lin et al., 2023; Raj et al., 2023a). Based only on rsEEG-derived features, the autoML framework fitted several models, implementing optimization, stacking, and ensembling, among other steps, to provide multi-class classification predictions given the presence of multiple clinical phenotypes (Healthy Controls, and patients with PD, AD, MCI, among others).

Finally, unseen data was used to test the results of the pre-trained model in a new sample, as well as individual subjects. Relevant graphical outputs for model performance and interpretability of classification predictions support the results.

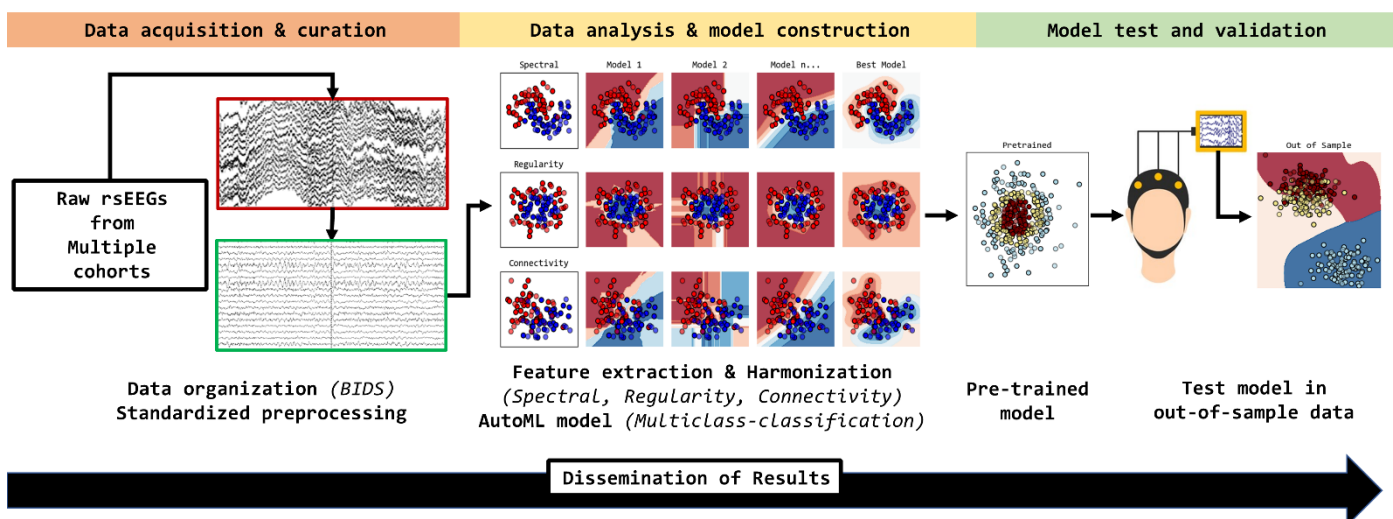


Figure 16. Graphical abstract of the PhD project. The first step (red segment) constituted organization following Brain Imaging Data Structure (BIDS) and data preprocessing. The dark-red box shows a raw resting-state EEG (rsEEG) signal, and the green box shows the results observed in preprocessing the dark-red rsEEG epochs. The second step (yellow segment) was focused on data analysis. Scatterplots represent features from different conceptual families (spectral, regularity, connectivity). These features were harmonised across sites and used to train multiple automated machine learning (autoML) models, selecting the model with the best performance (pre-trained model). The third step (green segment) was model testing and validation. On the diagram, the scatterplot represents the pre-trained model estimating the predictions for new unseen data (out-of-sample testing). Note the presence of multiple classes (clinical diagnoses) in this illustration.

3.1. PhD project Aims.

This thesis aims to provide an integrative approach for the analysis of multicentric rsEEG signals in the study of NDDs leading to dementia. The primary objective was to evaluate how combining multiple features impacts the rsEEG classification accuracy for different diseases leading to dementia.

The specific secondary objectives were as follows:

- To identify specific patterns of multiple NDDs using rsEEG features from different conceptual families.
- To compare the performance of various harmonisation pipelines in multicentric rsEEG datasets.
- To contrast the classification performance for different NDDs between single-nature and multi-feature rsEEG analysis.

4. Methods.

4.1. Datasets description.

To achieve the main objective of this thesis, we included data from ten research centres in eight countries (Colombia, Finland, France, Germany, Greece, Italy, Norway, and the USA) as part of the final analysis. Data from Finland (Railo, 2021), Germany (Babayan et al., 2019), Greece (Miltiadous et al., 2023), Norway (Oslo) (Høstestad-Hall, 2022), and the USA (Narayanan Lab, 2020; Rockhill et al., 2021) were stored in open repositories. Detailed descriptions of these datasets can be obtained in the individual references. Briefly, two of the above datasets consisted only of healthy controls (HC), namely the Leipzig Study for Mind-Body-Emotion Interactions (Lemon dataset – Germany) and the Oslo – Norway dataset. These studies aimed to study age-related physiology by including large samples of healthy young and old subjects. The remaining datasets assessed patients with NDDs: PD versus HC comparisons in the Finland dataset, AD vs. FTD vs. HC comparisons in the Greece dataset, and PD vs. HC in the Iowa and California datasets.

Apart from open sources of rsEEG signals, we gathered data from four other sites conducting ongoing clinical research studies. Thus, PD and PD-MCI patients in Medellín - Colombia were acquired in a cross-sectional study (Carmona Arroyave et al., 2019; Jaramillo-Jimenez et al., 2021; Jaramillo-Jimenez et al., 2023). Whereas data from France, Genova – Italy, and Stavanger – Norway were acquired as part of cohort studies, namely the European DLB consortium (France and Genova) (Bonanni et al., 2015; Bonanni et al., 2016) and the Dementia Disease Initiation (Stavanger) (Fladby et al., 2017). Genova dataset consisted of AD patients only. MCI stages were recruited in France and Stavanger; MCI in the DLB spectrum (MCI-LB) was only acquired in France, whereas MCI-AD (namely, amnestic MCI cases) were available for both datasets.

The diagnosis of PD was made using the United Kingdom Brain Bank criteria (Gibb and Lees, 1988) in the Finland and Iowa datasets, as well as the Movement Disorder Society (MDS) criteria (Postuma et al., 2015) in the Medellín – Colombia dataset. PD-MCI was diagnosed using the MDS task force level I criteria (Litvan et al., 2012). MCI-LB was diagnosed if a patient had two or more core DLB symptoms or one core symptom in addition to a positive dopaminergic abnormality scan in 123-iodine-metido-benzyl-guanidine myocardial scintigraphy or 123I-N-fluoropropyl-2β-carbomethoxy-3β-(4-iodophenyl) single-photon emission computed tomography according to the most recent international research criteria for prodromal DLB (McKeith et al., 2020). MCI-AD and AD were diagnosed using the National Institute of Aging – Alzheimer’s Association criteria (Albert et al., 2011; Babiloni et al., 2021; McKhann et al., 2011).

To identify specific patterns of multiple NDDs based on harmonised multicentric data and multi-feature rsEEG analysis, we included data from patients with different diagnoses of NDDs (including MCI stages) and healthy controls. Unfortunately, a complete analysis of potential demographic confounders, such as years of education, could not be assessed due to the retrospective nature of this study and the lack of availability of this data across all studies. Therefore, we limited the descriptive analysis of the sample characteristics to age and sex variables.

Thus, as an initial exploratory analysis, multi-feature rsEEG data from 752 subjects was harmonised and analysed using traditional statistics. The subgroups of patients with NDDs consisted of AD ($n = 113$), MCI-AD ($n = 76$), PD ($n = 67$), PD-MCI ($n = 16$), MCI-LB ($n = 16$), and FTD ($n = 23$). Data from 441 healthy controls (HC) was also included in this analysis. The HC group was subdivided into two subgroups: young adults (YA, $n = 220$) and older adults (OA, $n = 221$). Subjects in the OA subgroup had an equal or greater age based on the median value in the HC group ($M = 44$, IQR = 27.5 – 66). PD-MCI and MCI-LB subjects were combined into a

single MCI-LBD group according to preliminary reports supporting this methodology (Jellinger and Korczyn, 2018). Age and sex distributions by dataset, in the pooled sample, and by clinical phenotype subgroups are presented in **Figure 17A**.

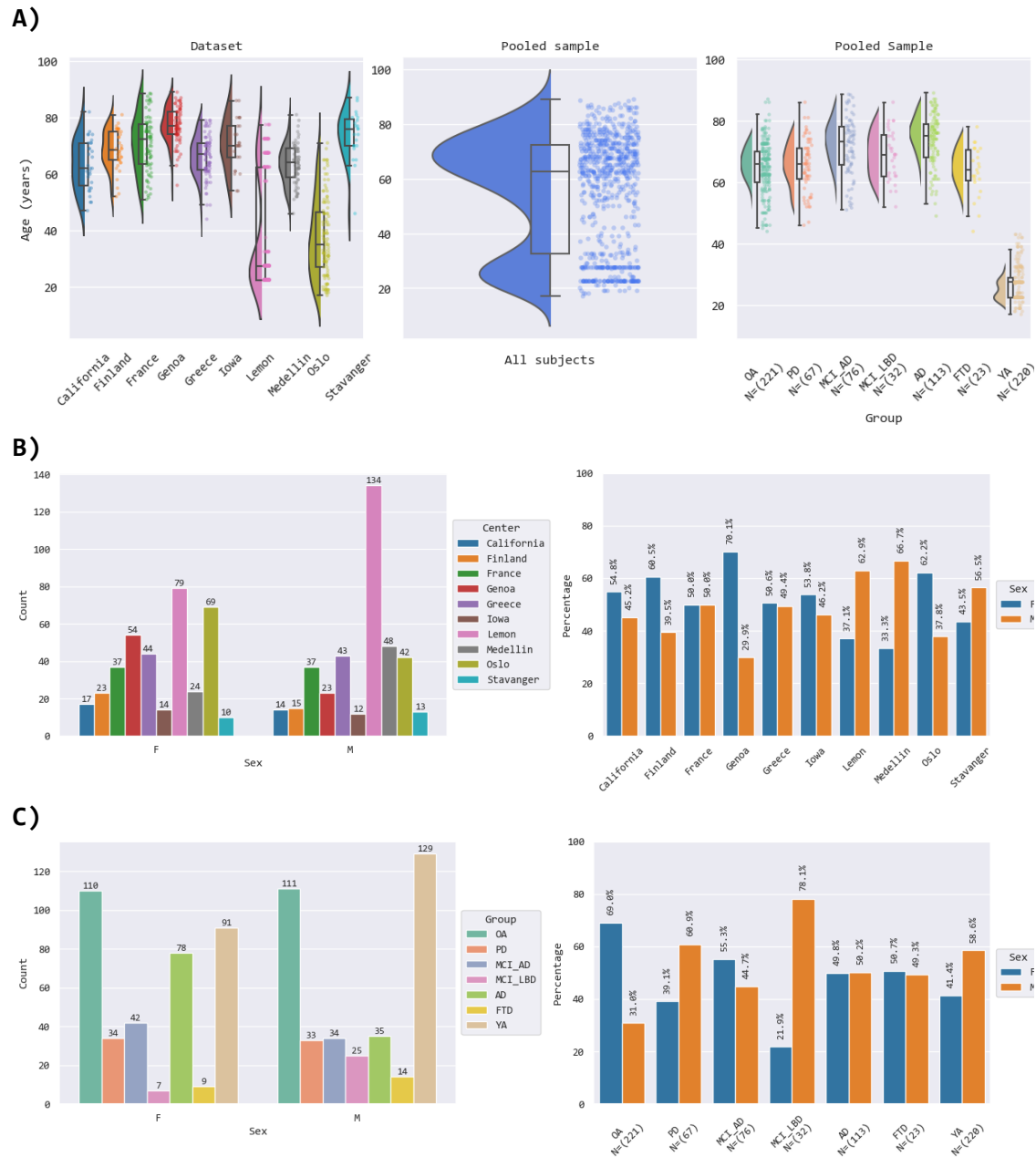


Figure 17. Demographical characteristics of the total sample for exploratory analyses (n = 752). A) Raincloud plots show the age distributions of age by dataset, in the pooled sample, and by diagnosis from left to right. B) Barplots show the absolute and relative frequency of Female (F) and Male (M) participants in each dataset. C) Barplots show the absolute and relative frequency by diagnosis subgroups. **AD:** Alzheimer's Disease; **MCI-AD:** Mild Cognitive Impairment – AD; **FTD:** Frontotemporal Dementia; **PD:** Parkinson's Disease; **MCI-LBD:** Mild Cognitive Impairment – Lewy Body Diseases; **OA:** Older Adults - Healthy Controls; **YA:** Young Adults - Healthy Controls.

The age median (Med) and interquartile range (IQR) for each group were as follows: YA (Med = 27.5 IQR = 22.5 - 29), OA (Med = 66; IQR = 60 – 70), MCI-AD (Med = 73.1; IQR = 65.5 - 78.1), AD (Med = 75; IQR = 68 – 79), PD (Med = 66; IQR = 61 – 71), MCI-LBD (Med = 69; IQR = 62 - 75.3), FTD (Med = 64; IQR = 60.5 - 70.5). Statistical analysis of variance (ANOVA) showed statistically significant differences in age among subgroups ($F = 734.8$; $p < 0.001$). Age-by-group pairwise comparisons are condensed in **Table 1**.

Overall, slightly more men were in the pooled dataset (Male n = 381, Female n = 371). The absolute and relative frequencies of male and female individuals by research centre and group are depicted in **Figures 17B and 17C**, respectively.

Table 1. Post Hoc Age comparisons by Neurodegenerative Diseases (NDDs) in the total sample (n = 752) - Exploratory analysis

| | | Mean Difference | SE | t | Cohen's d | p tukey |
|---------|---------|-----------------|-------|--------|-----------|---------|
| AD | FTD | 10.135 | 1.794 | 5.649 | 1.292 | < .001 |
| | MCI-AD | 2.195 | 1.164 | 1.886 | 0.280 | 0.490 |
| | MCI-LBD | 4.756 | 1.571 | 3.028 | 0.606 | 0.041 |
| | OA | 8.903 | 0.907 | 9.815 | 1.135 | < .001 |
| | PD | 8.295 | 1.209 | 6.859 | 1.058 | < .001 |
| | YA | 46.924 | 0.908 | 51.691 | 5.983 | < .001 |
| FTD | MCI-AD | -7.940 | 1.867 | -4.254 | -1.012 | < .001 |
| | MCI-LBD | -5.379 | 2.144 | -2.509 | -0.686 | 0.158 |
| | OA | -1.232 | 1.718 | -0.717 | -0.157 | 0.992 |
| | PD | -1.840 | 1.896 | -0.971 | -0.235 | 0.960 |
| | YA | 36.789 | 1.719 | 21.403 | 4.690 | < .001 |
| MCI-AD | MCI-LBD | 2.561 | 1.653 | 1.550 | 0.327 | 0.714 |
| | OA | 6.708 | 1.043 | 6.431 | 0.855 | < .001 |
| | PD | 6.100 | 1.314 | 4.641 | 0.778 | < .001 |
| | YA | 44.729 | 1.044 | 42.860 | 5.703 | < .001 |
| MCI-LBD | OA | 4.147 | 1.484 | 2.795 | 0.529 | 0.078 |
| | PD | 3.539 | 1.685 | 2.100 | 0.451 | 0.354 |
| | YA | 42.168 | 1.484 | 28.416 | 5.376 | < .001 |
| OA | PD | -0.608 | 1.094 | -0.556 | -0.078 | 0.998 |
| | YA | 38.021 | 0.747 | 50.898 | 4.847 | < .001 |
| PD | YA | 38.629 | 1.094 | 35.295 | 4.925 | < .001 |

AD: Alzheimer's Disease; **MCI-AD:** Mild Cognitive Impairment – AD; **FTD:** Frontotemporal Dementia; **PD:** Parkinson's Disease; **MCI-LBD:** Mild Cognitive Impairment – Lewy Body Diseases; **OA:** Older Adults - Healthy Controls; **YA:** Young Adults - Healthy Controls; **S.E:** Standard Error.

The exploratory pooled dataset was refined to achieve the main objective of the thesis. Due to the small sample size of the FTD subgroup, it was not included in the subsequent autoML analysis. The latter was justified in order to avoid additional imbalance across groups and favour training based on enough subjects. To mitigate the confounding effects of YA on the predictions, we excluded subjects in the HC class with ages lower than 46 years old (based on the minimum age in the NDDs groups). Therefore, the final dataset for autoML consisted of a moderate to large sample ($n = 507$). According to conventions used in machine learning studies, where very small datasets account for less than 200 samples, small datasets range from 200 to 1000, and large datasets often have more than 1000 (Conrad et al., 2022). This final dataset was subsequently split into train ($n = 354$) and test ($n = 153$) sets based on a 70/30 ratio. The train set was used to conduct cross-validation for optimization and model selection. In contrast, the test set was held out to evaluate the performance of the pre-trained model with unseen data. The group variable stratified the proportion of subjects in the train and test set.

Potential differences in demographics between the train and test subsets were examined. Non-significant differences (parametric and non-parametric independent samples tests, p -values > 0.683) were observed in the overall age distributions in the train (Med = 68; IQR = 62.5 – 75), and test (Med = 68; IQR = 62 – 75.1) subsets. Non-significant differences in the overall proportion of subjects based on gender were evidenced when comparing the train (Female percentage = 52.5) and test (Female proportion = 54.9) subsets (Chi-squared p -value = 0.625).

The absolute and relative frequencies of participants and patients in each subset are presented in **Table 2**.

Table 2. Absolute and relative frequency of Neurodegenerative Diseases (NDDs) in the final set ($n = 507$) for automated machine-learning (autoML)

| Subset | Group | Absolute Frequency | Relative Frequency |
|--------|-----------|--------------------|--------------------|
| Train | AD | 79 | 22.316 |
| | HC | 153 | 43.220 |
| | MCI - AD | 53 | 14.972 |
| | MCI - LBD | 22 | 6.215 |
| | PD | 47 | 13.277 |
| | Total | 354 | 100.000 |
| Test | AD | 34 | 22.222 |
| | HC | 66 | 43.137 |
| | MCI - AD | 23 | 15.033 |
| | MCI - LBD | 10 | 6.536 |
| | PD | 20 | 13.072 |
| | Total | 153 | 100.000 |

AD: Alzheimer's Disease; **MCI-AD:** Mild Cognitive Impairment – AD; **FTD:** Frontotemporal Dementia; **PD:** Parkinson's Disease; **MCI-LBD:** Mild Cognitive Impairment – Lewy Body Diseases; **HC:** Healthy Controls.

4.2. RsEEG acquisition and preprocessing.

Different headsets and amplifiers were used for acquisition as follows:

In the Greece dataset, a Nihon Kohden EEG 2100 clinical device was used with a sampling rate of 500 Hz, and 19 channels were placed according to the international 10-20 system. For the Oslo dataset, a BioSemi ActiveTwo system amplifier with a sampling rate of 1024 Hz was used, and 64 electrodes were placed following the extended international 10-20 system (10-10). The Stavanger dataset was acquired with a SomnoMedics – SOMNO HD eco amplifier with a sampling rate of 512 Hz and 19 channels (10-20 system). The California dataset used a BioSemi ActiveTwo system with a 512 Hz sampling rate and 32 channels placed according to the international 10-10 system. The Finland dataset used a NeurOne Tesla amplifier with 64 channels (10-10 system) and a 500 Hz sampling rate. Data from the Iowa dataset was acquired with a Brain Vision system with 64 channels (10-10 system). Unfortunately, data about the amplifier/headset used in the Genoa (sampling rate 128 Hz, 19 channels, 10-20 system) dataset was unavailable in preliminary publications (Babiloni et al., 2021; Bonanni et al., 2016) or for the France dataset (sampling rate 256 Hz, 19 channels, 10-20 system). Finally, the Medellin – Colombia dataset used a Neuro Scan Labs - Synamps2 with 64 channels placed according to the 10-10 system and a sampling rate of 1024 Hz.

4.2.1. Brain Imaging Data Structure (BIDS) Standardisation.

Given the differences in specific amplifiers/headsets, variations in channel name conventions (e.g. vendors only using uppercase letters in channel names or adding prefixes like “EEG” before channel names), standard organization of the files is required for further preprocessing and automatization of analysis steps. The latter was achieved by applying the Brain Imaging Data Structure (BIDS) organization. We used the EEG-BIDS extension (Pernet et al., 2019), following international recommendations for best practices toward reproducible EEG findings (Pernet et al., 2020). The general organization of rsEEG data under the BIDS structure is depicted in **Figure 18**.

Briefly, a site directory (dataset folder) is created for each of the individual datasets, and information about the acquisition, authors, and reference papers is stored within the dataset folder, as well as general tabular demographic and clinical information about the participants. Individual folders for each subject are generated inside the dataset folder using anonym IDs. The rsEEG signals for each participant and information about the signal (e.g. voltage units), channel names and positions (using standard conventions) are also stored in the subject’s folder. The raw signals are, therefore, always accompanied by side-car information files that are interoperable across datasets.

In addition to the raw signals, BIDS covers the storage of derivative data, such as preprocessed signals or features extracted from the EEG files. Codes used for analysis and preprocessing can be similarly saved in the BIDS structure, as shown in **Figure 19**.

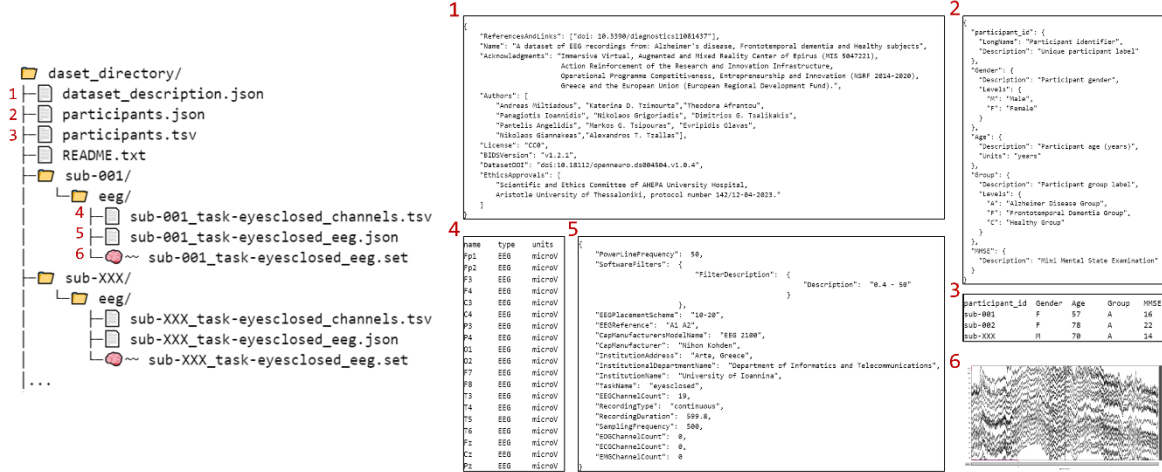


Figure 18. General organisation of the Brain Imaging Data Structure (BIDS). On the left-hand side, a schematic representation of the directory tree of a BIDS dataset and its components (red numbers). On the right-hand side, a preview of core component files in the BIDS standard is presented: 1) Dictionary with the dataset information, authors, and publications (dataset_description.json); 2) Dictionary with the metadata and details about participants' variables (participants.json); 3) Tabular file with information of participants (participants.tsv) including identifier, demographic variables, and other variables of interest; 4) Tabular text file with information about channels and units of the signal amplitude (sub-XXX-task-YYY-channels.tsv); 5) Dictionary with information about acquisition parameters including line noise frequency, placement system, reference electrode, online filters, (sub-XXX-task-YYY_eeg.json); and 6) Raw rsEEG signals (sub-XXX-task-YYY_eeg.set). Adapted from (Pernet et al., 2019).

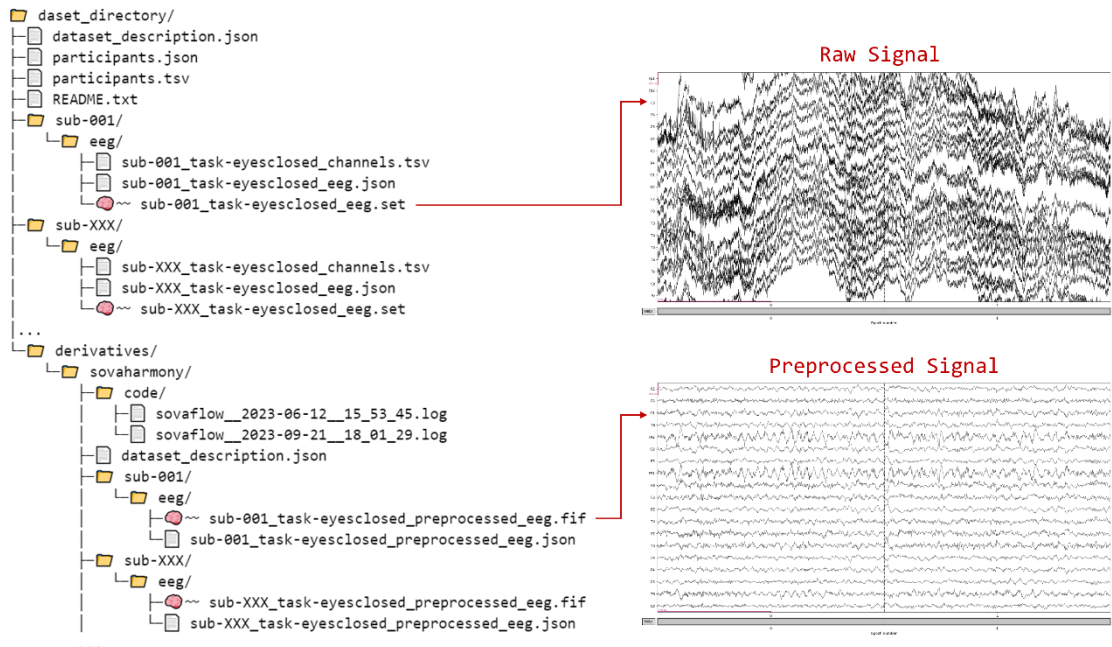


Figure 19. Raw signals and derivatives organised in the Brain Imaging Data Structure (BIDS). On the left-hand side a schematic representation of the directory tree of a BIDS dataset and its components. The first level includes main folders for each subject (sub-XXX). The second level consists of the derivatives folder containing codes, preprocessed signals and other derivative metrics obtained from each subject. On the right-hand side, the top plot shows the raw rsEEG signals without artefact removal, and the bottom plot shows the rsEEG signal after conducting an automatic preprocessing pipeline.

4.2.2. Preprocessing pipeline for rsEEG.

All the included rsEEG signals underwent a common automatic preprocessing pipeline. We selected the common electrodes across all studies, resulting in 18 common channels in the 10-20 system, namely (Fp1, Fp2, F3, F4, Fz, F7, F8, C3, C4, Cz, T7, T8, P3, P4, P7, P8, O1, O2). All signals were downsampled to 128 Hz to set an equal sampling frequency across all datasets.

We used a Python implementation of an already validated workflow previously published elsewhere. This automatic preprocessing method was successfully tested in rsEEG data from HC, AD, and PD samples (Carmona Arroyave et al., 2019; García-Pretelt et al., 2022; Isaza et al., 2023; Jaramillo-Jimenez et al., 2021; Jaramillo-Jimenez et al., 2023; Suárez-Revelo et al., 2016; Suárez-Revelo et al., 2016; Suárez-Revelo et al., 2018).

The pipeline was built by wrapping multiple preprocessing tools. Initially, robust average re-referencing, adaptative line-noise correction, and bad channel interpolation were performed using a Python reimplementation of the MATLAB PREP pipeline (Bigdely-Shamlo et al., 2015) done by the authors of the PyPREP library (Appelhoff et al., 2022). Average re-referencing aims to get a comparable reference scheme across datasets. Nevertheless, the average reference can be affected by noisy channels. Thus, the main goal of the PyPREP pipeline is to estimate a robust average reference by excluding these noisy channels from it.

After PyPREP, a wavelet-enhanced independent component analysis (ICA) artefact smoothing stage was carried out (Castellanos and Makarov, 2006). Thus, a 1 Hz high-pass Finite Impulse Response (FIR) filter was conducted to remove low-frequency drifts that would affect the following ICA stage. Then, the FastICA algorithm, available at the MNE library (Gramfort et al., 2013), was applied to obtain both artifactual and brain components from the EEG signal. Brain and Non-brain components were labelled using the automated MNE-ICA label method, which capitalizes a pre-trained ML model for artefact classification on EEG data (Li et al., 2022a; Pion-Tonachini et al., 2019). These components were then decomposed into wavelets, and wavelet thresholding smoothed out strong artefacts in the data (such as those originating from muscular or eye-blink components). Later, the signal was low pass filtered at 30 Hz to capture frequencies from delta to beta bands. Afterwards, five seconds-length epochs (5 s epochs) were segmented from the rsEEG recordings.

Finally, the automatic rejection of artifactual epochs was conducted as the last step of our pipeline, based on signal parameters such as extreme amplitude, spectral power values and statistical features like linear trends, joint probability, and kurtosis.

The number of available epochs in each dataset variated across sites. Based on preliminary reports showing good test-retest reliability and diagnosis accuracy with more than 40 seconds of rsEEG (Gudmundsson et al., 2007) and considering preliminary findings in DLB and AD (Cassani et al., 2018; Jin et al., 2023), we only included subjects with at least 20 non-overlapping consecutive epochs after preprocessing (i.e., 100 seconds) in the exploratory and autoML analyses.

4.3. RsEEG features.

Features belonging to three conceptual families (Spectral, Complexity, and Connectivity) were extracted in the sensor space.

All rsEEG features were extracted from 100 seconds of the signal. In those subjects with more than 100 seconds, we took the first 20 epochs exclusively to compute all our estimations, guaranteeing a uniform equal signal length for all subjects.

In order to reduce the dimensionality of the data, spectral and connectivity features were subsequently averaged across channels in three ROI, as follows: Anterior (Fp1, Fp2, F3, F4, F7, F8, Fz), Central (T7, T8, C3, C4, Cz), Posterior (P3, P4, P7, P8, O1, O2). In order to approximate global connectivity indexed at each frequency band, we summarized the connectivity of each patient by taking the median value and IQR of the distribution as described in previously reported methods (Lai et al., 2018).

4.3.1. Spectral features.

As an estimation of 1/f uncorrected relative power, power spectral density (PSD) vectors were obtained for each epoch using the `psd_multitaper` function implemented in MNE with full normalisation (length and sampling rate) and a `low_bias` parameter (Gramfort et al., 2013). Then, the median of the PSD vectors of each epoch was computed to obtain channel-wise PSD vectors. Aperiodic uncorrected band powers were obtained using the `bandpower` function from the Yet Another Spindle Algorithm (YASA) library. This function computes the relative power of a given frequency band (i.e. estimated band power/total power within the 1 - 30 Hz bandwidth) by approximating its area under the PSD curve using the composite Simpson's rule (i.e. decomposing the band-indexed area with several parabolas and then sum the area of these parabolas) (Vallat and Walker, 2021). Thus, the relative PSD was expressed as 0 – 1 values in the delta (1 - < 4 Hz), slow-theta (4 - < 5.5 Hz) and pre-alpha (or fast-theta) (5.5 - < 8 Hz), alpha (8 - < 13 Hz), and beta (13 - < 30 Hz) bands, as recommended by international guidelines and based on preliminary findings on the pre-alpha band (Babiloni et al., 2020a; Bonanni et al., 2016, 2015; Jaramillo-Jimenez et al., 2023). Variability of PSD across epochs was assessed using other spectral features, such as the 1/f uncorrected dominant frequency (i.e., peak frequency), dominant frequency variability (i.e., epoch-to-epoch variability in the peak frequency), and frequency prevalence in each band (i.e., percentage of time where the peak frequency lies in a given frequency band).

From the median channel-wise PSD vectors, we parameterized the oscillatory and aperiodic activity of the PSD. Thus, we used the Fitting Oscillations and One Over Frequency (FOOOF) method (Donoghue et al., 2020b). The FOOOF method uses an iterative fitting of Gaussian functions to the PSD vectors to estimate the signal's oscillatory component. Similarly, the aperiodic activity is estimated by fitting a Lorentzian function to the frequencies in the whole bandwidth of the PSD vector. Then, the aperiodic activity is subtracted from the Gaussians, resulting in a flattened oscillatory component, as shown in **Figure 20**. Finally, the aperiodic parameters (exponent and offset) and the oscillatory descriptors (power, bandwidth, and the centre frequency of the peaks) were extracted in the extended alpha band (5 – 14 Hz) and the beta band (13 – 30 Hz).

In the first publication supporting this thesis (**Paper 1**), band power ratios were used to identify rsEEG spectral patterns that could be associated with cognitive performance in PD and PD-MCI (Jaramillo-Jimenez et al., 2021). However, we prescinded band power ratios for the final analysis

in light of current evidence supporting a greater likelihood of conflated results when computing these composite metrics (Donoghue et al., 2020a).

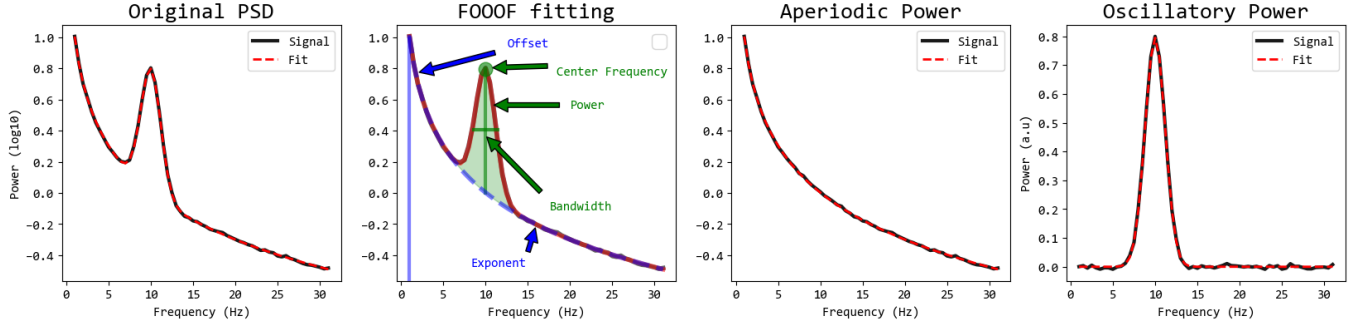


Figure 20. Illustration of the Fitting Oscillations and One-over-frequency (FOOOF) on rsEEG simulated data. The first subplot shows the power spectral density (PSD) vector without 1/f correction (original PSD in black, fitted spectrum in dashed red line). The second subplot depicts the fitting of the aperiodic model (dashed blue line) and aperiodic parameters (in blue); iterative Gaussian fitting represents the 1/f corrected oscillatory activity (green area) and oscillatory parameters (in green). The third and fourth subplots illustrate aperiodic and oscillatory reconstructed signals (black) and FOOOF fittings (dashed red).

4.3.2. Complexity and Regularity Features.

All complexity features were extracted using the AntroPy package. The following definitions are taken from the library's documentation. Unless noted, all parameters were kept as default for reproducibility (Vallat, 2022).

Regularity features included entropy-derived metrics and Hjorth parameters. Besides, the predictability of the signal was assessed via fractal estimators (FD) or detrended fluctuations (DFA).

Approximate entropy quantifies regularity over time series. Smaller values indicate that the data is more regular and predictable. The formula for approximate entropy is as follows:

$$\text{ApEn}(m, r, N) = \phi(m + 1, r, N) - \phi(m, r, N)$$

Where:

- m is the embedding dimension (the length of sequences/data points to be compared).
- r is the tolerance parameter (similarity criterion).
- N is the length of the signal.

The function $\phi(m, r, N)$ is defined as follows:

$$\phi(m, r, N) = \frac{1}{N - m + 1} \sum_{i=1}^{N-m+1} \ln \left(\frac{C_i^m(r)}{C_{i+1}^m(r)} \right)$$

The term $C_i^m(r)$ is the number of data point pairs within a tolerance (r) for which the distance between the points in a m -dimensional space is less than r . For this analysis, the parameter r was set to $0.2 * \text{std}(x)$.

Sample entropy is a modification of approximate entropy to reduce data length dependencies. Large values indicate high complexity, whereas smaller values characterize regular signals.

The sample entropy of a signal (x) is defined as:

$$H(x, m, r) = -\log \frac{C(m+1, r)}{C(m, r)}$$

Where m is the embedding dimension (= order), r is the radius of the neighbourhood with a default value of $0.2 * \text{std}(x)$.

$C(m+1, r)$ is the number of embedded vectors of length $m+1$ having a Chebyshev distance inferior to r , and $C(m, r)$ is the number of embedded vectors of length m having a Chebyshev distance inferior to r .

Permutation entropy is another variation of sample entropy that uses phase information of the signal and provides a more robust estimate of complexity in the presence of outliers (i.e., noise). Permutation entropy is parameter-free as it does not include tolerance parameters. The formula for the permutation entropy of a signal is as follows:

$$H = -\sum p(\pi) \log_2(\pi)$$

Where the summation runs over all the $n!$ permutations (π) of order n , and represents the information contained in comparing n consecutive values of the signal (in bits). This magnitude can be normalized between 0 – 1 values (where lower values represent lower complexity and high regularity).

SVD entropy is another entropy metric with less sensitivity to noise. SVD entropy aims to measure the dimensionality of the time series by identifying the minimal number of eigenvectors needed to explain the signal. Higher values of SVD entropy suggest high complexity. SVD entropy is defined as:

$$H = -\sum_{i=1}^M \bar{\sigma}_i \log_2(\bar{\sigma}_i)$$

Where M denotes the number of singular values of the embedded matrix Y , created from the time series as follows:

$$y(i) = [x_i, x_{i+\text{delay}}, \dots, x_{i+(\text{order}-1)*\text{delay}}]$$

The term $\sigma_1, \sigma_2, \dots, \sigma_M$ represents the normalized singular values of Y .

Hjorth Parameters estimate statistical properties of the signal in the time domain. The parameters comprise activity, mobility, and complexity. The mobility parameter approximates the proportion of the standard deviation of the power spectrum by computing the square root of the variance of the first derivative of the signal divided by the variance of the whole signal, as shown below:

$$Mobility = \sqrt{\frac{\text{var}\left(\frac{dx(t)}{dt}\right)}{\text{var}(x(t))}}$$

The complexity parameter is related to the signal's bandwidth (indicating the shape's similarity to a pure sine wave). For regular sinusoidal activity, the complexity parameter converges to 1. Complexity can be calculated as the mobility of the first derivative of the signal divided by the mobility of the signal.

$$Complexity = \frac{\text{mobility}\left(\frac{dx(t)}{dt}\right)}{\text{mobility}(x(t))}$$

Metrics assessing the fractal characteristics of the signal included Katz, Petrosian and Higuchi FD methods. The following formula defines Katz FD:

$$KatzFD = \frac{\log_{10}(L/a)}{\log_{10}(d/a)} = \frac{\log_{10}(n)}{\log_{10}(d/L) + \log_{10}(n)}$$

The numerator represents the sum and average of the Euclidean distances between the successive points of the signal (L and a , respectively), and the denominator expresses the maximum distance between the first point and any other time series (d).

Petrosian FD is defined as follows:

$$PetrosianFD = \frac{\log_{10}(N)}{\log_{10}(N) + \log_{10}(\frac{N}{N+0.4N_\delta})}$$

Where N represents the length of the signal, and N_δ expresses the number of sign changes in the first derivative of the time series.

The last FD metric extracted was Higuchi FD, which estimates the irregularity of a signal across different scales (k) by estimating changes in patterns. Multiple methods are used to compute Higuchi FD in a multi-step algorithm. In brief, the length of a fitting curve is calculated for each signal segment, and the mean length of the curves for each k is subsequently computed. The fractal dimension is then derived from the scaling behaviour of these segments through a least-squares linear best-fitting approach.

Finally, DFA characterizes the long-term statistical dependencies in a given signal. DFA is based on the concept of self-affine processes. DFA can be estimated utilizing the following formula:

$$DFA = \text{std}(X, L * n) = L^H * \text{std}(X, n)$$

A signal X can be considered self-similar/self-affine if the standard deviation of the signal points within a window of length n changes with the window length factor L in a power law. Higher DFA values are obtained from more regular signals.

4.3.3. Connectivity features.

Phase-based connectivity has gained traction in neuroscience research. Notably, the weighted Phase Lag Index (wPLI) is considered less sensitive to volume conduction effects than many other methods. The wPLI has been shown to have good test-retest reliability in assessing connectivity in AD subjects, i.e., consistently higher theta band connectivity (Briels et al., 2020). Similarly, it has been reported that the global (average) functional connectivity assessed in sensor space could be comparable with the global connectivity in the source space, particularly with the original implementation of wPLI, the Phase Lag Index (PLI), although there is no available evidence for wPLI (Lai et al., 2018).

The wPLI quantifies the asymmetry in the distribution of phase differences between pairs of signals (channels), avoiding zero-lag (immediate) associations. The wPLI can be defined as follows:

$$wPLI = \frac{|E[\mathcal{I}(X_{ij})]|}{E[|\mathcal{I}(X_{ij})|]}$$

Where X_{ij} represents the cross-spectral density between two channel pairs (i, j) , $E\{\}$ expresses the expected value (average over time), and \mathcal{I} denotes the imaginary part of the cross-spectral density (which tends to maximise in the presence of zero-lag phase differences).

On the other hand, imaginary coherence (iCoh) is a frequency-based approach to pairwise signal relationships. The iCoh is not affected by non-stationary processes. Also, compared to classical coherence methods, iCoh is less affected by volume conduction. As a zero-lag metric, iCoh eliminates all unexpected coherence arising from instantaneous coupled activity. The iCoh has been examined particularly in AD subjects, reporting a reduced alpha iCoh compared to control individuals (Fide et al., 2022).

The iCoh can be defined as follows:

$$iCoh(f) = \frac{|E\{e^{i\phi_{XY}(t)}\}|}{E\{|e^{i\phi_{XY}(t)}|\}}$$

Where $\phi_{XY}(t)$ represents the instantaneous phase difference between signals X and Y at a time t , and $E\{\}$ express the expected value (or average across t).

4.4. Feature harmonisation.

The ComBat harmonisation was performed on the unharmonised pooled train and test sets. Due to the absence of evidence using ComBat variants in rsEEG, we compared the performance of multiple ComBat variants in multicentric rsEEG open datasets from HC subjects as part of the secondary objectives of this thesis. Initially, ComBat was not focused on preserving the effects of biological covariates of interest, but later adaptations allowed this functionality.

The ComBat model can be summarised as follows:

$$Y_{ij\nu} = \alpha_\nu + \mathbf{X}_{ij}^T \boldsymbol{\beta}_\nu + \mathbf{Z}_{ij}^T \boldsymbol{\theta}_\nu + \delta_{i\nu} \varepsilon_{ij\nu}$$

Where $Y_{ij\nu}$ represents a 1-dimensional vector in a given site batch i , for a subject j , and a feature value ν . Besides, $\boldsymbol{\beta}$ represents the coefficients of the biological covariates (X), and $\boldsymbol{\theta}_\nu$ represents the coefficients of the batch variable (Z) to be estimated via parametric or nonparametric empirical Bayes, plus the error (ε).

After estimating the coefficients of the batch variable, the harmonised feature can be re-expressed as:

$$Y_{ij\nu}^{\text{ComBat}} = \frac{y_{ij\nu} - \hat{\alpha}_\nu - \mathbf{X}_{ij} \hat{\boldsymbol{\beta}}_\nu - \gamma_{i\nu}^*}{\delta_{i\nu}^*} + \hat{\alpha}_\nu + \mathbf{X}_{ij} \hat{\boldsymbol{\beta}}_\nu$$

Of note, the effects of covariates are reincorporated in the term $\mathbf{X}_{ij}^T \hat{\boldsymbol{\beta}}_\nu$, whereas $\gamma_{i\nu}$ and $\delta_{i\nu}$ represents the estimated additive and multiplicative effects of the batch variable.

The original version of ComBat was adapted to neuroimaging cortical thickness metrics in the neuroCombat library. NeuroCombat retains the linear effect of biological covariates on the harmonised features (Fortin et al., 2018). Later, neuroHarmonize emerged as a variation of neuroCombat, which allows for estimating nonlinear effects of biological covariates (Implemented using Generalized Additive Models) (Pomponio et al., 2020). Furthermore, the Optimized Nested ComBat – Gaussian Mixture Model (OPNComBat-GMM) was developed to handle bimodal distributions while preserving the effects of unknown biological covariates treated as latent variables that will be preserved (Hornig et al., 2022). HarmonizR is a variant of the original ComBat designed to handle datasets with missing values using an iterative splitting of the unharmonised data followed by harmonising non-missing. However, biological variance cannot be retained in HarmonizR (Voß et al., 2022). Recently, the reComBat variant was published by capitalizing on existing advantages of previous versions but achieving appropriate fitting in situations where the covariate matrix is singular (i.e., a site with only one diagnosis for all subjects) by employing elastic-net regularization (Adamer et al., 2022).

In a second publication supporting this thesis (**Paper 2**), we aimed to compare the performance of various harmonisation pipelines (i.e., ComBat variants) in multicentric rsEEG datasets. As this workflow aims to be available for researchers, we capitalized on open-source repositories. Therefore, we selected signals acquired in HC subjects to avoid potential confounding effects of NDDs on the harmonisation. Details of the demographic characteristics of the HC subsample from open repositories ($n = 374$) are presented in **Figure 21** and extended in **Paper 2**.

Identification of existent batch effects was conducted through T-distributed Stochastic Neighbor Embedding (tSNE), which visually represents site-related differences in the unharmonised and

harmonised datasets, as suggested in prior publications on different rsEEG features (Bigdely-Shamlo et al., 2020; Kottlarz et al., 2020; Li et al., 2022b).

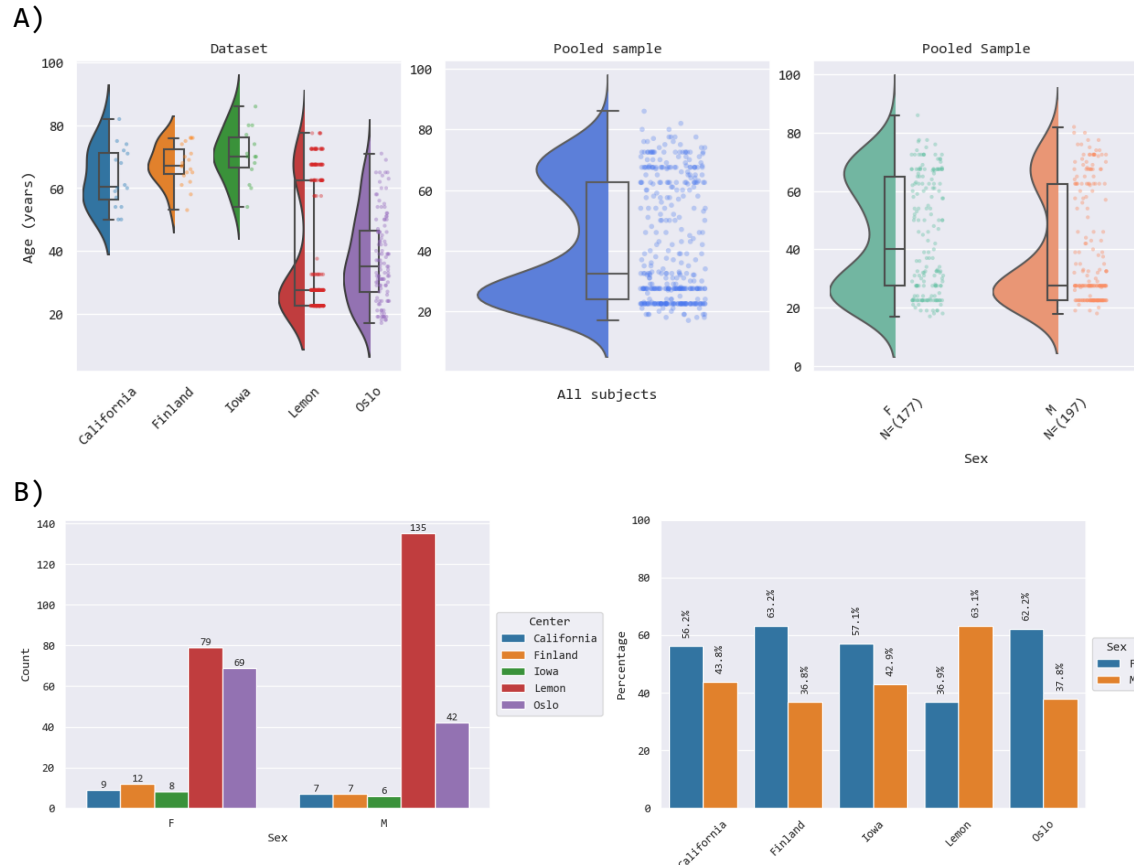


Figure 21. Demographic characteristics of the healthy controls subsample (n = 374) used to evaluate batch harmonisation. **A)** From left to right, each raincloud plot shows the age distributions by dataset, in the pooled sample, and by gender. **B)** Barplots depict the absolute and relative frequency of Female (F) and Male (M) healthy controls in each dataset.

Briefly, tSNE maps high-dimensional data to a lower-dimensional space while preserving local similarities. By visualizing the data in this reduced space, tSNE helps identify patterns, clusters, and trends that may not be apparent in the original feature space. In line with this, individual tSNE models were independently fitted to the unharmonised HC subsample (n = 374) and each harmonised version (generated by each ComBat variant).

Subsequently, site-related batch effects were quantified. Thus, the mean points in tSNE components 1 and 2 were calculated for each site to represent the central tendency of potential batches. The Euclidian distances between sites were calculated and presented in distance matrixes, as well as the average site-related distance representing the overall estimation of batch effects. The abovementioned procedure was conducted in unharmonised datasets, and each harmonised dataset (i.e., neuroCombat, neuroHarmonize, OPNComBat-GMM, HarmonizR, and reComBat), see **Figure 22**.

The assessment of preservation of the biological variability (i.e., age-related effects) after harmonisation with ComBat models was detailed in **Paper 2**.

Overall, reComBat exhibited the best performance in reducing site-related differences in this sample of healthy subjects (see **Figure 22**) and was therefore selected for subsequent analyses as the harmonisation method for the whole dataset.

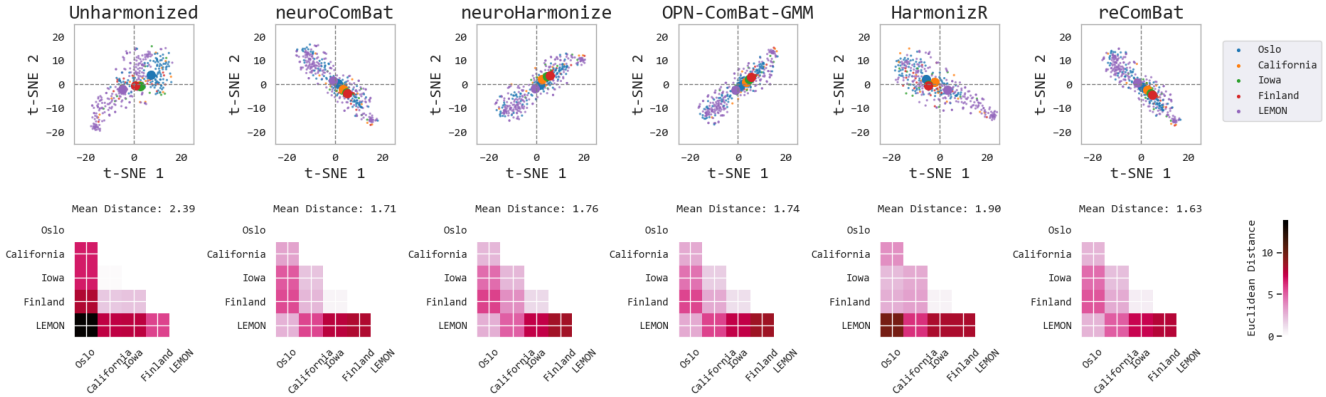


Figure 22. Statistical harmonisation of resting-state electroencephalogram (rsEEG) spectral features extracted from multicentric data in a subsample of healthy subjects ($n = 374$). On the top row, t-distributed stochastic neighbour embedding (t-SNE) of the rsEEG features. The t-SNE reduces the dimensionality of rsEEG features in two components (tSNE1 and t-SNE2); each small dot in the scatterplot represents all rsEEG features from a single subject. Bigger dots represent the mean point of all subjects belonging to a specific research centre (colour-coded in the t-SNE labels). On the bottom row, the distances between the mean values of each centre were quantified using Euclidean distance and represented in a matrix (darker red colours represent a greater distance between centres' data). From left to right, the unharmonised and harmonised data (with neuroComBat, neuroHarmonize, Optimised Nested ComBat – Gaussian Mixture Model, HarmonizR, and reComBat). Compared to the unharmonised data, all harmonisation methods re-scale and centre the site average distributions (big dots), reducing site-related differences as shown in the distance matrixes. The mean distance of the matrix is calculated and presented on top of each matrix.

For the final analysis, reComBat was fitted with multi-feature rsEEG data ($n = 507$) using research centres as the batch variable to be corrected. Also, parametric Empirical Bayes and “elastic-net” regularization ($\alpha = 1e-6$) were set in the reComBat parameters. Age, gender, and group were included as covariates of biological variability to be retained in the harmonisation. The reComBat algorithm also allows transfer learning of the re-scaling parameters resulting from the fitting of the training dataset to harmonise the test set, avoiding covariate shift problems in the subsequent autoML analyses (Adamer et al., 2022).

4.5. Multiclass classification.

Building handcrafted machine-learning models may require time and expert human resources, limiting the application of this technology for a broad range of clinical researchers with less developed coding skills (Conrad et al., 2022; Liu et al., 2023; Musigmann et al., 2022; Ou et al., 2021). In contrast, autoML solutions aim to break down this barrier by offering code-free or one-liner implementations. These solutions enable the simultaneous assessment of multiple model architectures, expediting the exploration and discovery process from a data-driven perspective.

AutoML pipelines have been tested in regression and classification tasks and across multiple data types (including biomedical), often producing models with good to excellent performance, even in small tabular datasets with less than 1000 examples (Conrad et al., 2022; Liu et al., 2023; Musigmann et al., 2022; Ou et al., 2021). Despite the growing interest in autoML in neuroimaging and cancer research, and emerging evidence suggests that autoML approaches could surpass hand-crafted models, its application in rsEEG remains relatively unexplored and keeps the focus on epilepsy (Lenkala et al., 2023; Liu et al., 2022). Following this, we employed autoML to perform multiclass classification of NDDs based on harmonised multi-feature rsEEG data.

Among available autoML models, we have chosen the AutoGluon framework (Erickson et al., 2020). The latter was supported by considering preliminary reports in different biomedical data modalities stating that AutoGluon could have comparable results to hand-crafted models in both prediction and classification tasks (Jaotombo et al., 2023; Kamboj et al., 2023; Lin et al., 2023; Raj et al., 2023b).

The steps of autoML include features pre-processing, model architecture search, and hyperparameter fine-tuning. Pre-processing of derivative features often implies re-scaling the feature values from 0 – 1 for specific models, recoding of categorical variables into numeric indexes, and data imputation of missing values, among others. Next, AutoGluon integrates numerous standard ML models that can handle multiple scenarios (i.e., non-linearity, multicollinearity). These base ML models of AutoGluon comprise logistic regression, K-Nearest Neighbours, Random Forest, Extra-trees model, extreme gradient-boosting (XGBoost), Light gradient-boosted machine (LightGBM), Category boosting (CatBoost), and Neural Networks for tabular data. In addition, AutoGluon implements a multi-layer stacking strategy, outlined in **Figure 23**.

The multi-layer stacking method of AutoGluon is inspired by deep learning architectures (i.e., layer-wise training). Briefly, multi-layer stacking aims to combine predictions from different base models to increase their individual performance. Several base models are trained in the first step of traditional approximation for stacking. Then, another model called "stacker" is created to learn from the predictions of the base models. This stacker model helps improve predictions and captures interactions between the initial models, making the overall prediction more powerful. AutoGluon goes one step further by mimicking deep learning layers. Instead of using different models for each layer, AutoGluon uses the same models at every layer. Besides, each layer consists of the predictions from the previous layer but also concatenates the original data features as input for the stacker models (allowing the higher-layer stackers to consider the original data during training). As a complement to multi-layer stacking, AutoGluon employs “ensembling” methods to combine the predictions from all the stacker models in a weighted manner. This final step ensures a robust and accurate prediction that is less sensitive to overfitting (Erickson et al., 2020).

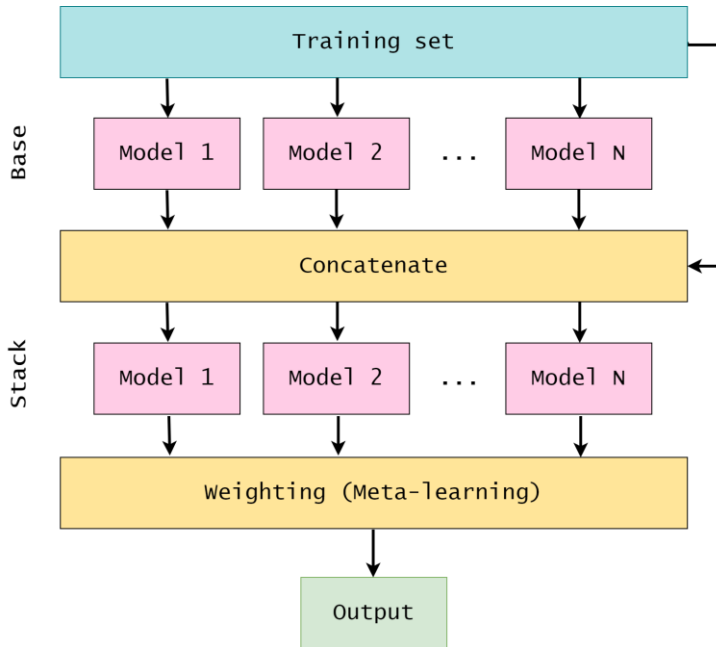


Figure 23. Multilayer stacking implemented in the AutoGluon automated machine learning pipeline.
A simplified schematic overview of multilayer stacking with two layers is presented. The training set (blue) is preprocessed, and N base models with different hyperparameters are trained, creating one layer of models (upper pink boxes). Next, predictions of each base model are concatenated with the original features of the training set (right-hand side arrow). The values of the aggregated layer are used as inputs for a second layer of models (lower pink boxes). Each layer keeps the same N base models (with the same hyperparameters) in an iterative stacking process. After stacking, a meta-learning process called model ensemble weights the predictions of stacker models, weighting them based on a user-defined metric that maximizes model performance. Adapted from (Erickson et al., 2020).

Additionally, AutoGluon enhances its stacking performance by maximizing the use of available data for both training and validation through k -fold ensemble bagging across all models at every layer of the stack. In k -fold bagging, the data is randomly divided into k separate folds, ensuring a balance based on labels (i.e., diagnosis). Subsequently, each model is trained k times, with a distinct data chunk in each iteration, minimizing the aggregated prediction variability. This strategy improves the traditional stacking method (without k -fold bagging), which utilizes only a fraction of the data for each stacker training.

Finally, AutoGluon offers an overview of the classification or prediction performance of all the models based on a user-defined metric (e.g. accuracy, balanced accuracy, F1 score, among others). Thus, a leaderboard displays each model's performance in the training, validation and testing sets and selects the best model.

For a detailed description of AutoGluon methods, we refer the reader to the AutoGluon methods paper (Erickson et al., 2020) and a comprehensive review of AutoML methods (Bezrukavnikov and Linder, 2021).

With all the above, we used the autoML dataset ($n = 507$) to perform the final analyses and accomplish two objectives of this thesis:

- a) To contrast the classification performance for different NDDs between single-nature and multi-feature rsEEG analysis.
- b) To evaluate how combining multiple features impacts the rsEEG classification accuracy for different diseases leading to dementia.

Thus, multiclass classification models were performed using the AutoGluon tabular Python library (v. 0.8.2). Unharmonised pooled data ($n = 507$) was split in a 70/30 stratified manner (based on the group) to obtain the train ($n = 354$) and test ($n = 153$) splits, respectively.

The train and test sets were harmonised as described in **Section 4.5** to assess the effect of reComBat harmonisation in the autoML performance. Thus, unharmonised and harmonised train sets were used as separate inputs in the AutoGluon tabular predictor algorithm with the “best_quality” presets (achieving higher performance), “balanced_accuracy” as the evaluation metric, and “auto_weight” (automatically choosing a weighting strategy based on the data) given the unbalanced number of subjects across groups (classes). Of note, the test sets (unharmonised and harmonised) were held out for subsequent evaluation of the best pre-trained model resulting from AutoGluon.

Subsequently, the rsEEG features of each subject were considered as predictors of the group variable (i.e. HC, MCI-AD, AD, PD, and MCI-LBD). First, the autoML models were fitted using spectral features only, as recommended in a previously published systematic review (Modir et al., 2023), and the performance of the best model selected with AutoGluon was evaluated. We repeated this, adding spectral + complexity features to another AutoGluon predictor (keeping all parameters as in the fitting of spectral features only) and assessed the best model performance. Finally, spectral + complexity + connectivity features fit the last AutoGluon predictor. Following this, we can evaluate the best model performance with single-type and multi-feature approaches, achieving specific and general objectives of this research.

In summary, a set of six “best models” were pre-trained with the AutoGluon pipeline, as follows:

- A) Unharmonised – Spectral only
- B) Unharmonised – Spectral + Complexity
- C) Unharmonised – Spectral + Complexity + Connectivity
- D) Harmonised – Spectral only
- E) Harmonised – Spectral + Complexity
- F) Harmonised – Spectral + Complexity + Connectivity

4.5.1. Interpretability of model estimations.

After obtaining the best pre-trained models, we evaluated the performance in classifying unseen subjects from the respective (held-out) test set. Therefore, balanced accuracy, sensitivity, specificity, and positive and negative predictive values were computed for each of the six best models.

The relevance of meaningful features for the classification was assessed using permutation-based feature importance. Permutation-based feature importance quantifies the reduction in predictive performance when one feature’s values are randomly shuffled across subjects. The contribution of individual features in the predictions for each subject is available from AutoGluon outputs and can be determined with the SHAP (SHapley Additive exPlanations) library (Lundberg and Lee, 2017). An extended description of the autoML methods can be found in **Paper 3**.

5. Summary of main findings.

5.1. RsEEG patterns in specific clinical phenotypes.

Exploratory data analyses of unharmonised and harmonised features were performed on a two-step approach:

First, independent Analysis of Covariance (ANCOVA) models were fitted for each feature with feature values as the dependent variable, group as the factor, and centre, age, and gender as covariates (as well as age*gender + age*center + gender*center interactions). Given the multiplicity of comparisons and taking into account dependencies across rsEEG features, we used the Benjamini-Yekutieli False Discovery Rate (FDR) to correct the p-values of the ANCOVA models for multiple testing (Benjamini and Yekutieli, 2001). Statistical significance was assessed by setting a significance level of alpha = 0.01.

In the second step, we conducted pairwise comparisons by groups with parametric and non-parametric independent sample tests for each significant feature showing group-related differences in the ANCOVAs. The resulting p-values of these pairwise comparisons were also corrected with the same FDR method mentioned above and the same significance level.

The following sections will summarize the results of this exploratory analysis, focusing on NDDs group-related differences in the rsEEG spectral, complexity and connectivity features.

5.1.1. Spectral patterns.

Based on ANCOVA estimates, statistically significant group-related effects were consistently observed in both unharmonised and harmonised data for 30 spectral features. Significant findings are summarised below.

Aperiodic uncorrected powers in the slow-theta, pre-alpha, and alpha bands showed significant group-related differences in the tree ROI (anterior, central, and posterior channels). Similarly, statistically significant differences were observed in the aperiodic uncorrected slow-theta, pre-alpha, and alpha frequency prevalence in all ROI. The dominant frequency in the three ROIs exhibited statistically significant main effects of the group variable.

The FOOOF-derived spectral features (i.e., 1/f corrected) revealed statistically significant group-related findings. Specifically, exploratory analysis supported significant group differences in the aperiodic corrected extended alpha centre frequency in the three ROI, as well as posterior beta and alpha band powers. Anterior and posterior extended alpha bandwidths indicated statistically significant results. Pair-wise group comparisons of the abovementioned spectral features are depicted in **Figure 24**.

The patterns of aperiodic uncorrected power and frequency prevalence in each band were similar in most cases, representing potentially redundant information unless noted. This was also confirmed by statistically significant parametric positive correlations between the uncorrected power and the frequency prevalence in each band (Pearson's $r > 0.8$ in the alpha band and between 0.65 and 0.85 in the slow-theta and pre-alpha bands); results not shown. Therefore, 1/f uncorrected spectral findings will be assessed by frequency band.

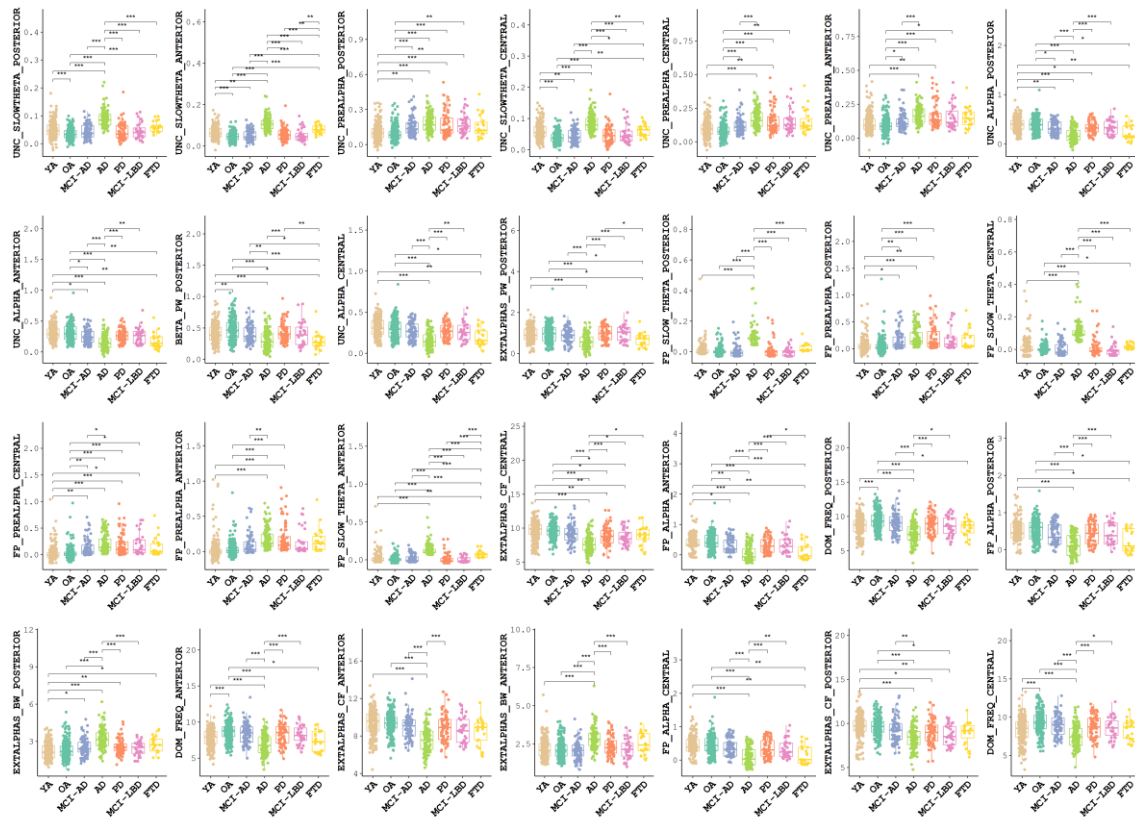


Figure 24. Group-level exploratory analysis of spectral features in the harmonised dataset (n = 752). Boxplots represent the harmonised values for each of the 30 features with significant main effects of the group variable identified in the ANCOVA exploratory models. Only significant group comparisons (parametric independent samples t-tests) are plotted (FDR corrected q-values < 0.01). **AD:** Alzheimer's Disease; **MCI-AD:** Mild Cognitive Impairment – AD; **FTD:** Frontotemporal Dementia; **PD:** Parkinson's Disease; **MCI-LBD:** Mild Cognitive Impairment – Lewy Body Diseases; **OA:** Older Adults - Healthy Controls; **YA:** Young Adults - Healthy Controls. Prefixes and suffixes employed in spectral feature names: **UNC:** Aperiodic Uncorrected. **FP:** Frequency Prevalence. **DOM_FREQ:** Dominant Frequency. **PW:** 1/f oscillatory corrected power. **BW:** 1/f oscillatory corrected bandwidth. **CF:** 1/f oscillatory corrected centre frequency. **EXTALPHA:** Extended alpha band. The Regions of Interest (ROI) names are suffixes (**ANTERIOR**, **CENTRAL** and **POSTERIOR**) in all features.

- **Slow-theta band:** Compared to other NDDs, both 1/f uncorrected power and frequency prevalence in the slow-theta band were greater in AD subjects, followed by FTD individuals. OA were comparable with other NDDs except for AD and FTD. However, given the significant differences between HC subgroups (i.e., anterior and posterior slow-theta power YA > OA), potential age-related effects should be considered.
- **Pre-alpha band:** The aperiodic uncorrected power and the frequency prevalence in this band did not show age-related differences. OA exhibited lower pre-alpha uncorrected power than MCI-AD, AD, PD, and MCI-LBD individuals. Consistent findings were observed for pre-alpha frequency prevalence, although MCI-LBD vs OA significance was not observed. Central and anterior ROI evidenced significantly greater values in AD subjects than in MCI-AD.
- **Alpha band:** Our results did not support significant age-related differences in the uncorrected power and frequency prevalence of this band. Compared to OA, anterior and posterior ROI showed remarkably lower power and frequency prevalence in AD and

FTD subjects. MCI-AD subjects also exhibited lower values than OA (particularly in the anterior ROI). Significantly lower values were observed in AD when compared to MCI-AD. Other NDDs (except FTD) exhibited significantly greater alpha power and frequency prevalence than AD.

- **Beta band:** Significant findings in this band were only achieved with 1/f correction of the power spectrum.

The dominant frequency (estimated from the 1/f uncorrected spectrum) accounted for statistically significant age-related effects in all ROI. Besides, the mean dominant frequency of AD subjects was significantly reduced compared to other NDDs and HC subgroups, especially in the anterior and posterior ROI. However, age-related differences were no longer observed when parameterising the 1/f component of the spectrum and determining the extended alpha centre frequency (aperiodic corrected equivalent of the dominant frequency). Overall, the extended alpha centre frequency was prominently low in AD subjects in all ROI. Notably, the extended alpha centre frequency indicated significant differences between OA versus AD, MCI-LBD, and PD in the central and posterior ROI.

Oscillatory (1/f corrected) power in the posterior extended alpha band did not show age-related differences in the HC subgroups. However, AD and FTD exhibited reduced extended alpha power compared to OA. Extended alpha bandwidth was greater in AD when compared to other NDDs (except by FTD). Reduced oscillatory posterior beta band power in AD (compared to OA) and significant age-related differences were observed (OA > YA).

5.1.2. Complexity patterns.

Both unharmonised and harmonised datasets lead to convergent results regarding 13 complexity features showing significant group-related differences in the ANCOVA exploratory models. In addition to these features, the harmonised dataset showed statistically significant group main effects for the Hjorth mobility in the anterior ROI. Pair-wise group comparisons of the rsEEG complexity features are presented in **Figure 25**.

Higuchi FD, Katz FD, DFA, and Hjorth complexity were identified as candidate variables with significant group differences in the three ROI. Statistically significant findings in Hjorth mobility were also observed in the anterior and posterior ROI.

Briefly, age-related differences in the HC subgroups were observed for the majority of complexity features. Complexity features assessing the predictability of the signal (i.e., fractal dimensions and DFA) exhibited a similar pattern of significant differences in AD vs OA, with AD subjects showing significantly greater DFA and lower fractal dimensions (i.e., more self-affine/predictable signals). Significantly lower complexity in AD was observed when compared to MCI-AD. Anterior Higuchi FD and Katz FD were also reduced in PD compared to OA.

On the other hand, complexity features assessing the regularity of the signal included Hjorth parameters. Compared to OA, the Hjorth complexity was prominently high in AD, followed by FTD subjects. MCI-AD subjects also showed a lower Hjorth complexity than AD individuals. Complementary to this was the Hjorth mobility, which was significantly lower in AD vs OA. Finally, MCI-AD subjects had significantly higher Hjorth mobility compared to AD subjects.

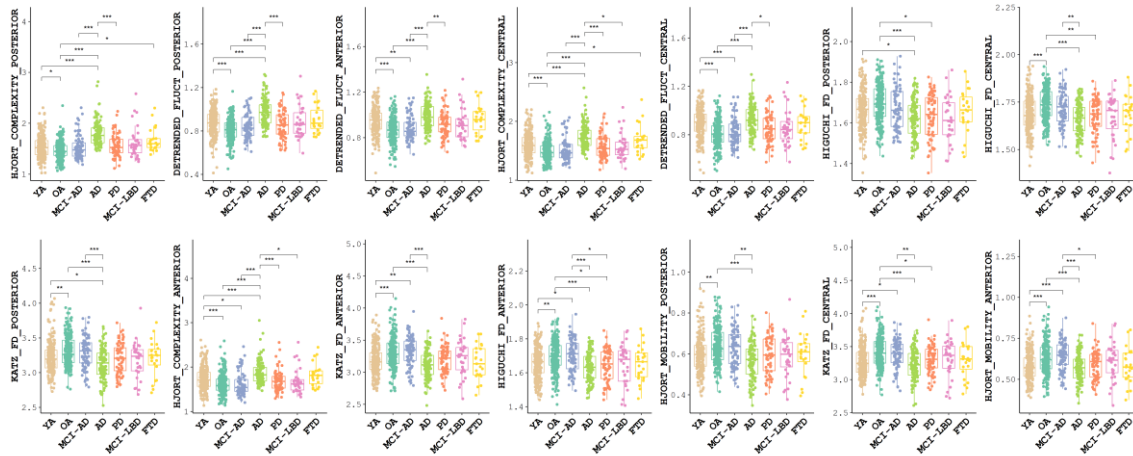


Figure 25. Group-level exploratory analysis of complexity features in the harmonised set ($n = 752$). Boxplots represent the harmonised values for each of the 14 complexity features with significant main-effects of group identified in the ANCOVA exploratory models. Only significant group comparisons (parametric independent samples t-tests) are plotted (FDR corrected q-values < 0.01). **AD:** Alzheimer’s Disease; **MCI-AD:** Mild Cognitive Impairment – AD; **FTD:** Frontotemporal Dementia; **PD:** Parkinson’s Disease; **MCI-LBD:** Mild Cognitive Impairment – Lewy Body Diseases; **OA:** Older Adults - Healthy Controls; **YA:** Young Adults - Healthy Controls. Prefixes and suffixes employed in complexity feature names: **FD:** Fractal Dimension. **DETREND_FLUCT:** Detrended Fluctuation Analysis. The Regions of Interest (ROI) names are suffixes (**ANTERIOR**, **CENTRAL** and **POSTERIOR**) in all features.

5.1.3. Global connectivity patterns.

Two global connectivity metrics were consistently identified in the exploratory analysis of both unharmonised and harmonised datasets: the IQR of the iCoh and wPLI theta band connectivity distributions. No other frequency-specific connectivity estimates were identified as candidate features. Pair-wise group comparisons are presented in **Figure 26**.

Overall, no age-related differences were observed in these connectivity descriptors. The global theta connectivity was higher in AD compared to young and old HC, MCI-AD, PD and MCI-LBD subjects.

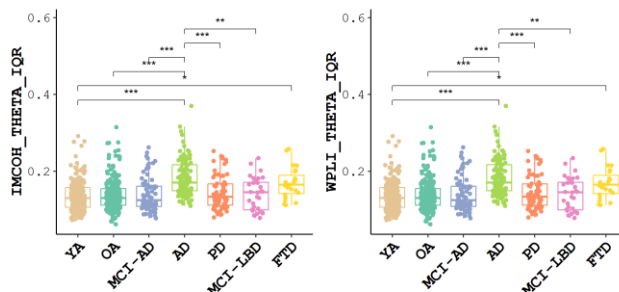


Figure 26. Group-level exploratory analysis of connectivity features in the harmonised set ($n = 752$). Boxplots represent the harmonised values for the two connectivity features with significant main-effects of group identified in the ANCOVA exploratory models. Only significant group comparisons (parametric independent samples t-tests) are plotted (FDR corrected q-values < 0.01). **AD:** Alzheimer’s Disease; **MCI-AD:** Mild Cognitive Impairment – AD; **FTD:** Frontotemporal Dementia; **PD:** Parkinson’s Disease; **MCI-LBD:** Mild Cognitive Impairment – Lewy Body Diseases; **OA:** Older Adults - Healthy Controls; **YA:** Young Adults - Healthy Controls. Prefixes and suffixes employed in complexity feature names: **IMCOH:** Imaginary Coherence. **WPLI:** Weighted Phase Lag Index. **IQR:** Inter Quartile Range.

5.2. Harmonisation of rsEEG features in multicenter data.

As stated in the methods section, statistical harmonisation was performed using the reComBat method, which evidenced better average mitigation of batch effects in pilot results on HC subjects. Also, reComBat adapts to singular matrix issues presented when adjusting for biological covariates in sites (batches) with only one single group (such as only HCs in Lemon and Oslo datasets or only AD subjects in Genoa). Therefore, after the initial exploratory analysis, we conducted a reComBat harmonisation of the dataset selected for the final analysis and autoML models ($n = 507$). The visual outputs of the harmonisation process are presented in **Figure 27**.

Consistently with preliminary observations on HCs, the not-harmonised dataset presented higher distance magnitudes of average batch effects (mean cross-site distance = 2.24). This distance was reduced by 35% (to 1.54) after reComBat harmonisation. The visualizations from tSNE evince compatible results with concentric mean points across sites and reduction of the clusters observed before harmonisation in large datasets such as Lemon or France.

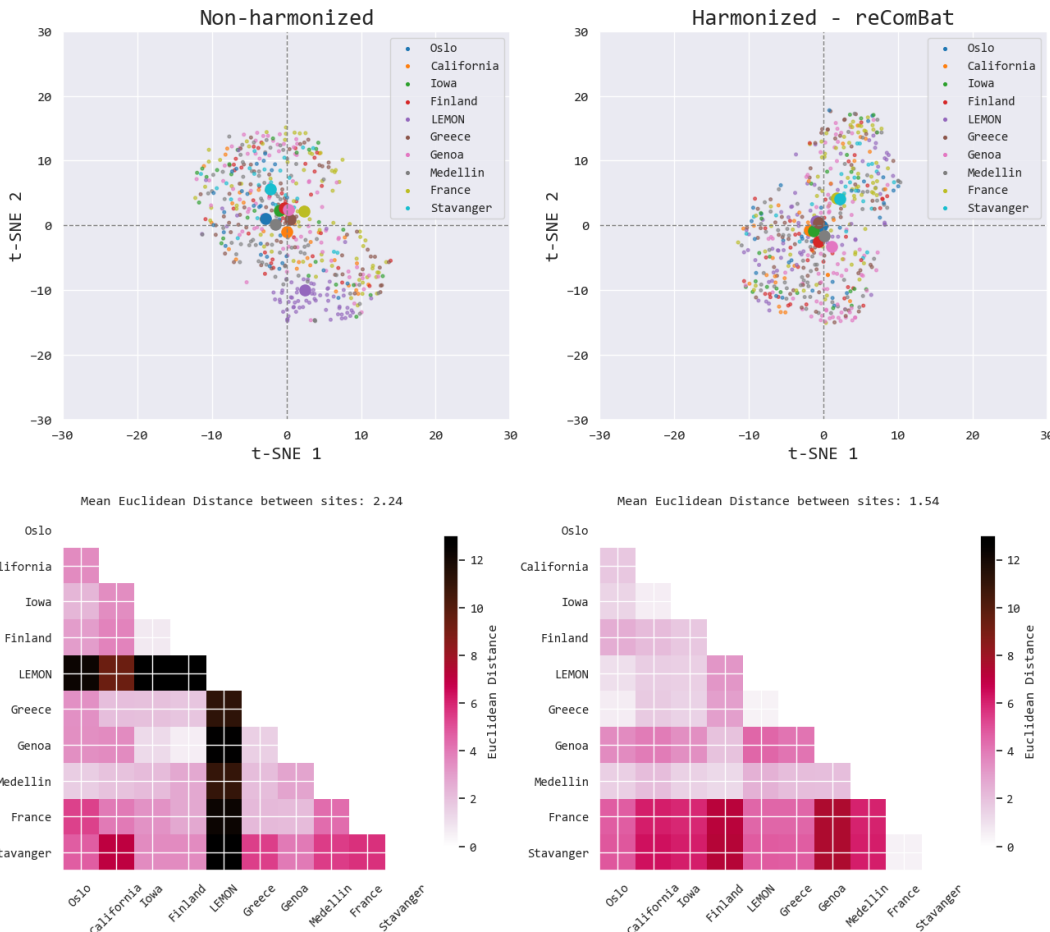


Figure 27. Statistical harmonisation of the final dataset for automated Machine Learning ($n = 507$). On the top row, t-distributed stochastic neighbour embedding (t-SNE) of the rsEEG features. The t-SNE reduces the dimensionality of rsEEG features in two components (tSNE1 and t-SNE2); each small dot in the scatterplot represents all rsEEG features from a single subject. Bigger dots represent the mean point of all subjects belonging to a specific research centre (colour-coded in the t-SNE labels). On the bottom row, the distances between the mean values of each centre were quantified using Euclidean distance and represented in a matrix (darker red colours represent a greater distance between centres' data). The mean distance of the matrix is presented.

5.3. Combined features of the rsEEG for diagnosis of NDDs.

As reported, the exploratory analysis revealed significant group-related differences in spectral, complexity and connectivity features. These exploratory findings are summarized in **Figure 28**.

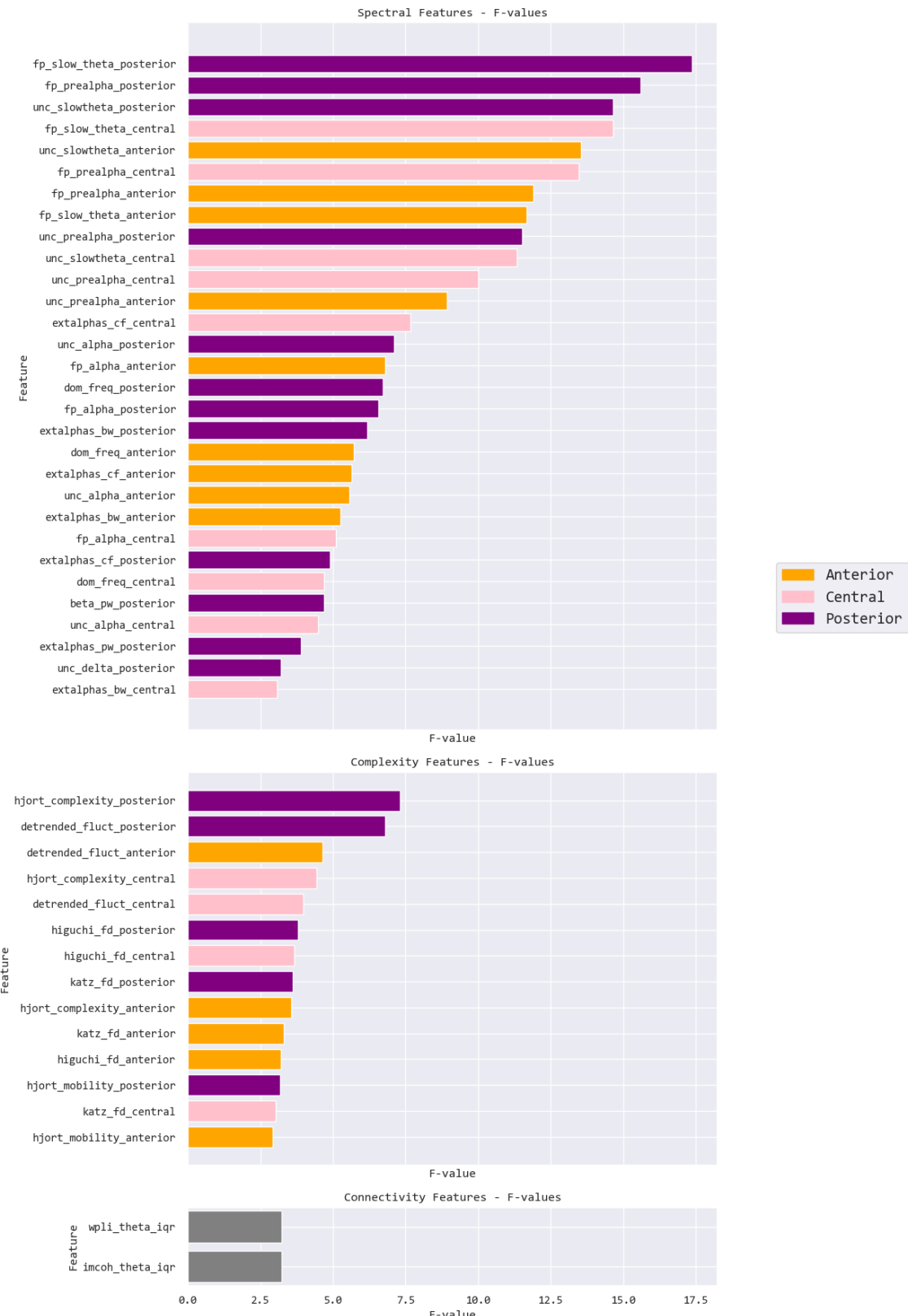


Figure 28. Summary of significant results in the exploratory analysis of harmonised data (n = 752) by feature type. F-values of ANCOVA models assessing group-related differences are presented.

In line with the exploratory findings, 21 of the previously identified features were selected as the most important features in the final multi-feature harmonised autoML model. In addition, 15 other metrics were identified as relevant features; see **Figure 29**.

Among relevant spectral features, we observed the aperiodic uncorrected delta and beta powers in anterior ROI and the posterior dominant frequency variability. Besides, 1/f corrected beta centre frequency (posterior) and beta power (anterior and central), as well as the aperiodic offset (posterior) and aperiodic exponent (central), exhibited significant permutation-based feature importance. Other features selected as important included the Petrosian FD (anterior and posterior), Singular Value Decomposition entropy (posterior), approximate entropy (posterior and central), as well as the IQR of the wPLI in the alpha band.

Overall, the importance of complexity features as a complement of spectral features is observed in spite of the analytical approach.

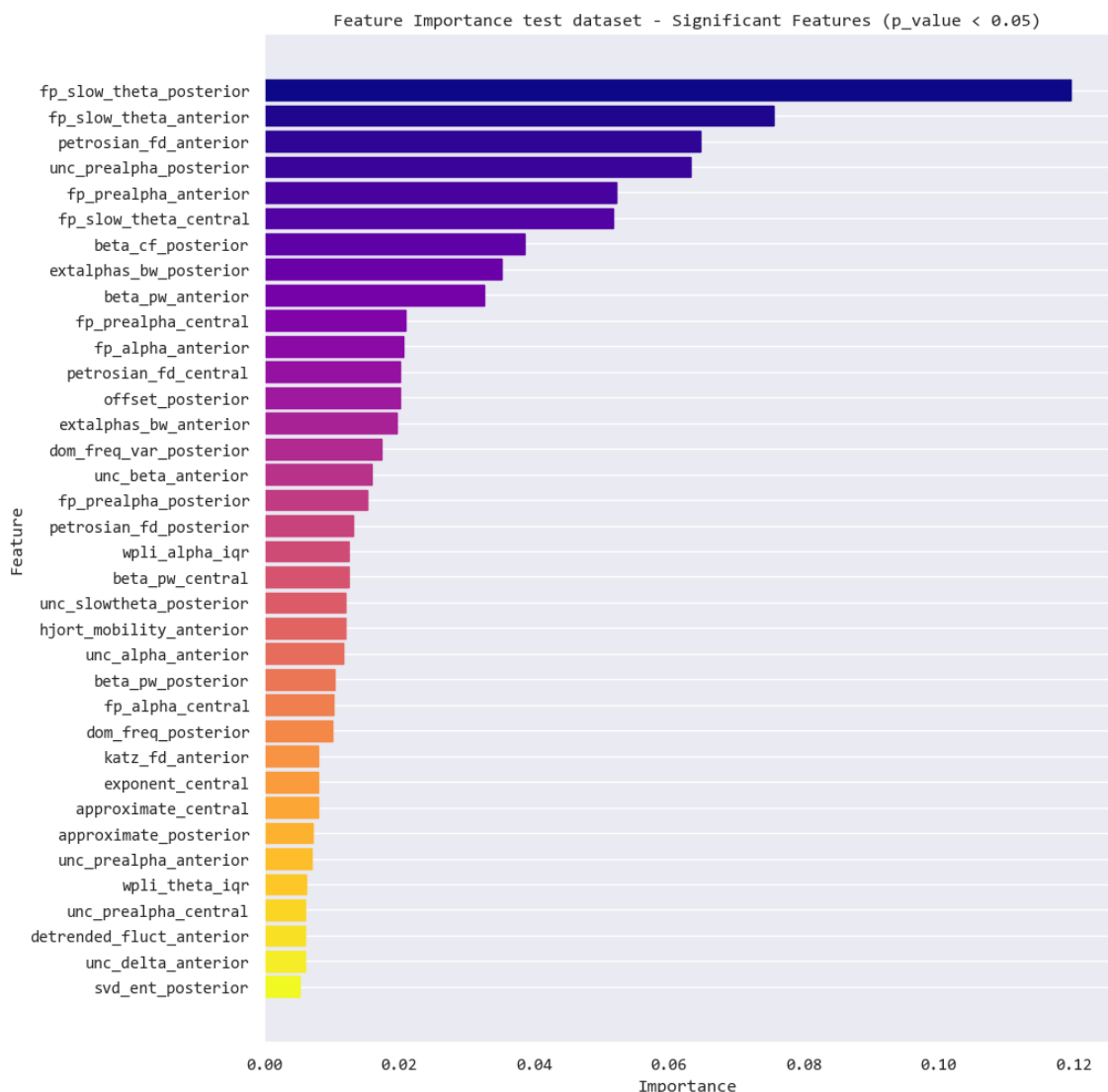


Figure 29. Most relevant rsEEG features for multiclass classification in the harmonised multi-feature final model (spectral + complexity + connectivity; n = 507). Feature importance after permutation-based methods. Significant results permutation p-value < 0.05 are presented.

In order to compare the performance of the harmonisation and multi-feature approaches, confusion matrixes were generated for the six best models detailed in **Chapter 4.5**. These differences are exhibited in **Figure 30**.

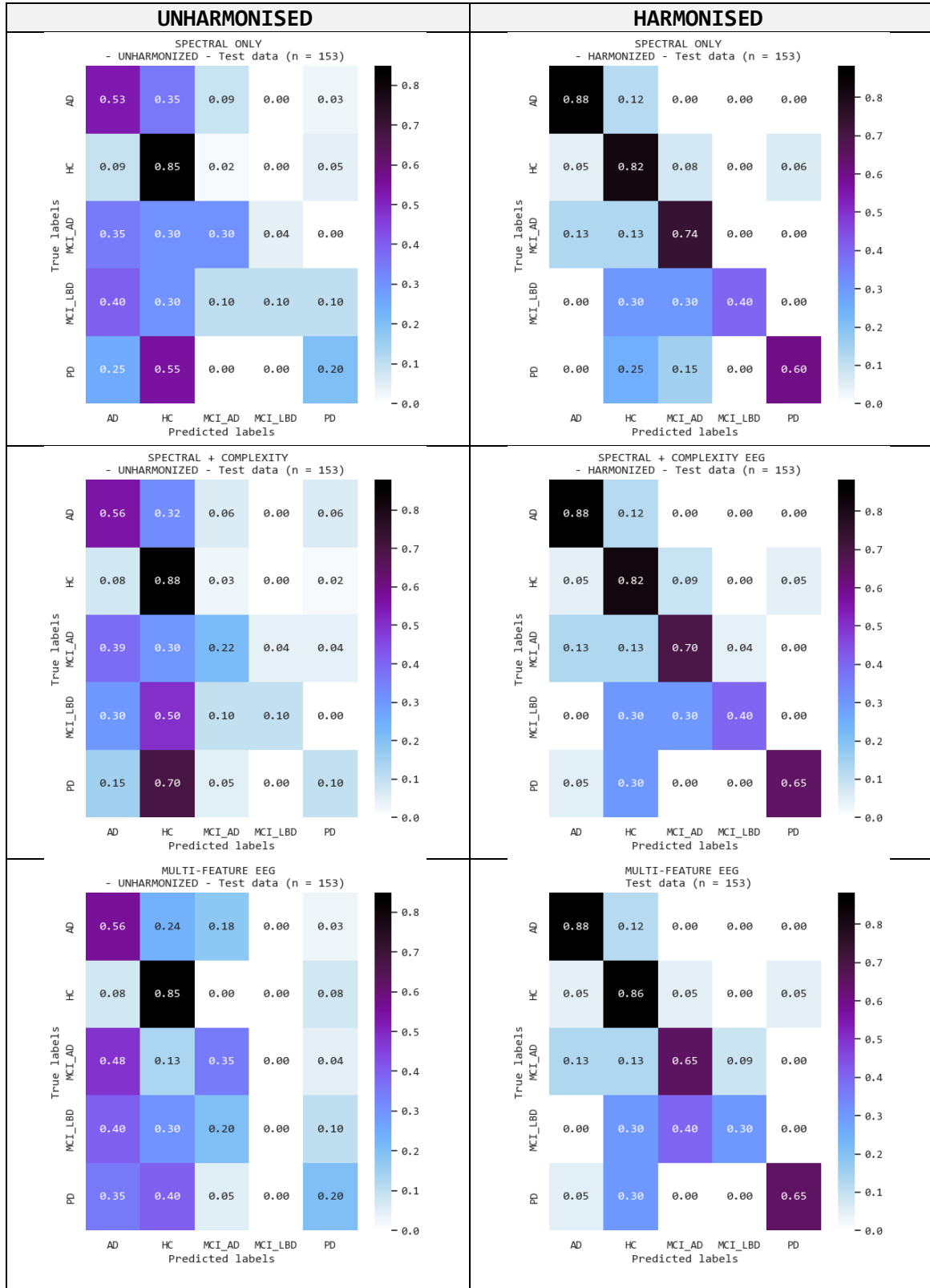


Figure 30. Normalized confusion matrixes (0 to 1) of unharmonised and harmonised spectral features (top) and their combination with complexity (middle row) and connectivity features (bottom row). Diagonal values closer to 1 indicate a 100% correct classification of a given class.

As shown in the diagonals of the confusion matrixes, a greater proportion of subjects correctly classified was achieved with harmonisation. The latter was observed independently of the nature of the features considered for training the autoML models.

Based on the normalised confusion matrixes of the harmonised test datasets, we could have an overview of the model performance when combining single-nature and multi-feature information. Beyond this, we quantified the performance of the models by estimating performance metrics and ROC curves for each of the classes in the out-of-sample test set.

XGBoost with bagged ensemble was selected as the best pre-trained model architecture in all harmonised sets: a) Harmonised – Spectral only, b) Harmonised – Spectral + Complexity, c) Harmonised – Spectral + Complexity + Connectivity. Performance evaluation for each model is presented in **Table 3** and **Figure 31**.

Table 3. Summary of model performance evaluation metrics (harmonised single-nature vs multi-features)

| Spectral Only | | | | |
|--------------------------------------|-------------|-------------|----------|----------|
| Group | Sensitivity | Specificity | PPV | NPV |
| AD | 0.882353 | 0.949580 | 0.833333 | 0.965812 |
| HC | 0.818182 | 0.827586 | 0.782609 | 0.857143 |
| MCI-AD | 0.739130 | 0.915385 | 0.607143 | 0.952000 |
| MCI-LBD | 0.400000 | | 1 | 1 |
| PD | 0.600000 | 0.969925 | 0.750000 | 0.941606 |
| Spectral + Complexity | | | | |
| Group | Sensitivity | Specificity | PPV | NPV |
| AD | 0.882353 | 0.941176 | 0.810811 | 0.965517 |
| HC | 0.818182 | 0.816092 | 0.771429 | 0.855422 |
| MCI-AD | 0.695652 | 0.930769 | 0.640000 | 0.945312 |
| MCI-LBD | 0.400000 | 0.993007 | 0.800000 | 0.959459 |
| PD | 0.650000 | 0.977444 | 0.812500 | 0.948905 |
| Spectral + Complexity + Connectivity | | | | |
| Group | Sensitivity | Specificity | PPV | NPV |
| AD | 0.882353 | 0.941176 | 0.810811 | 0.965517 |
| HC | 0.863636 | 0.816092 | 0.780822 | 0.887500 |
| MCI-AD | 0.652174 | 0.946154 | 0.681818 | 0.938931 |
| MCI-LBD | 0.300000 | 0.986014 | 0.600000 | 0.952703 |
| PD | 0.650000 | 0.977444 | 0.812500 | 0.948905 |

AD: Alzheimer’s Disease; **MCI-AD:** Mild Cognitive Impairment – AD; **PD:** Parkinson’s Disease; **MCI-LBD:** Mild Cognitive Impairment – Lewy Body Diseases; **HC:** Healthy Controls. **PPV:** Positive Predictive Value; **NPV:** Negative Predictive Value.

Minimal effects were observed in these estimators of model performance, nor balanced accuracy (Bacc), after multi-feature combination. The latter was consistently reflected in unharmonised and harmonised data. Unharmonised dataset with Spectral only (Bacc = 0.380) and Spectral + Complexity (Bacc = 0.396) exhibited a better performance than Spectral + Complexity + Connectivity (Bacc = 0.345). Besides, the Bacc in the harmonised multi-feature model was 0.67, whereas the harmonised Spectral Only and Spectral + Complexity had a comparable performance (Bacc of 0.68). Consistent results were observed in ROC curves with subtle variations after multi-feature combinations (best performance with Spectral + Complexity features).

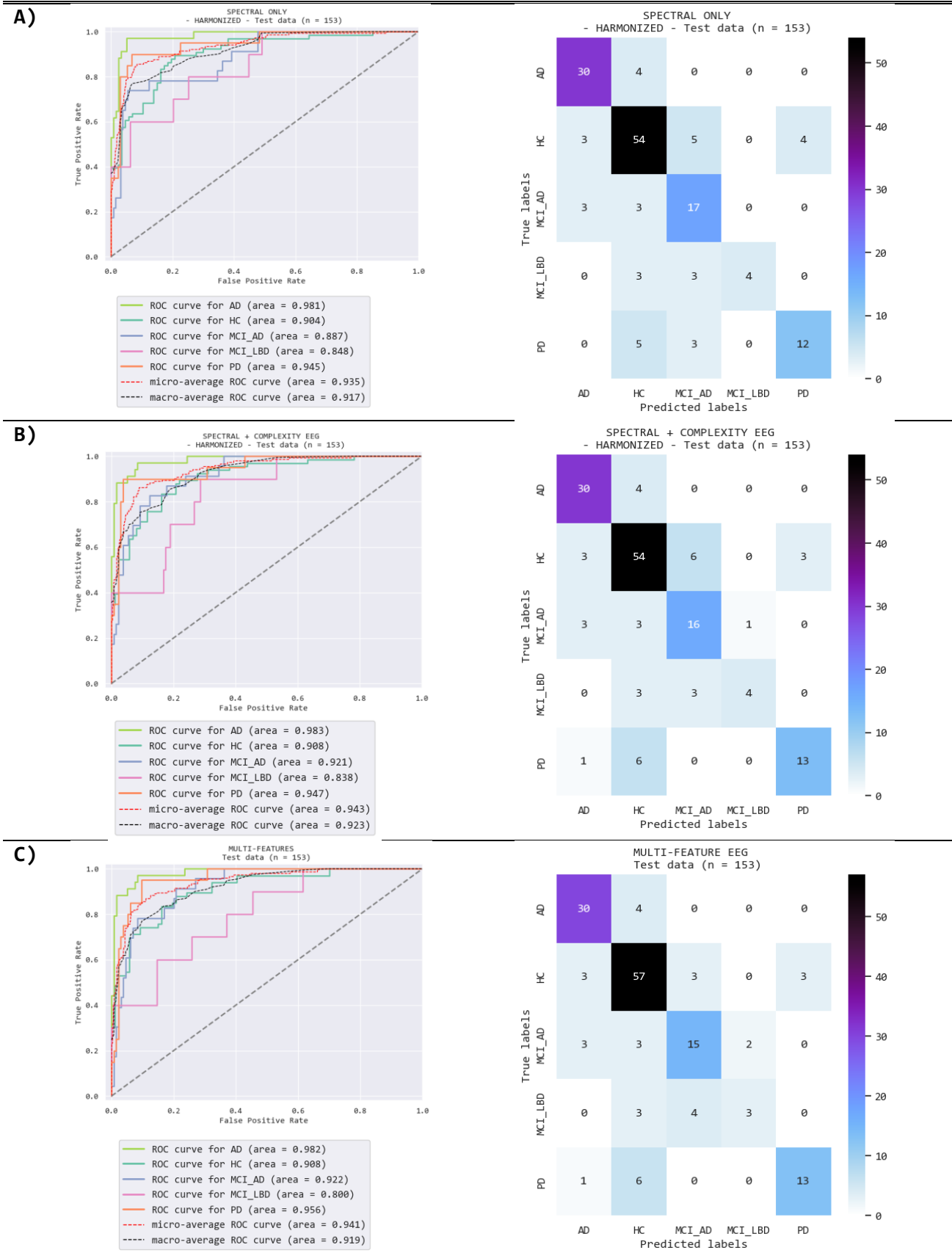


Figure 31. Receiver Operator Characteristics (ROC) curves and confusion matrixes for best models tested with the harmonised spectral-only features (A) and their combination with complexity (B) and connectivity features (C).

A closer examination of these results suggests that including complexity features especially improved PD classification but reduced the performance for MCI-AD separation. Further incorporation of connectivity descriptors increased the correct identification of HC but reduced the classification performance for the MCI-AD and MCI-LBD groups.

With all the above, we can conclude that harmonisation of rsEEG features applying reComBat elevated the average model performance (in terms of Bacc) by improving the correct classification of patients. On the other hand, convergent results from the exploratory analysis and autoML models suggest that spectral features (including descriptors of frequency prevalence, dominant frequency, oscillatory and aperiodic parameters, as well as aperiodic uncorrected band powers) were meaningful contributors to model predictions, followed by complexity features. The global connectivity metrics included in this analysis did not improve classification performance.

6. Discussion.

This thesis introduces an integrative approach for analyzing multicentric rsEEG signals to tackle critical methodological challenges associated with this potential diagnostic biomarker. The primary objective guiding this investigation is to evaluate the impact of combining multiple rsEEG features on the classification accuracy of various NDDs. To achieve our main objective, we first identified patterns of multiple NDDs using rsEEG spectral, complexity and connectivity features extracted at the sensor space. The robustness of these results in the presence of site-related differences was examined, and the mitigation of such batch effects was compared in five harmonisation pipelines. Finally, supervised models for multiclass classification (HC, MCI-AD, AD, PD, and MCI-LBD) were trained utilizing an autoML framework. The performance of the best models trained with A) spectral-only, B) spectral + complexity, and C) spectral + complexity + connectivity features were compared based on model predictions in a hold-out test set. Overall, the harmonisation of rsEEG features applying reComBat elevated the average model performance and the correct classification of patients. Exploratory analysis and autoML models point to spectral features as the most meaningful contributors to model predictions, which may benefit from combining with complexity descriptors.

Our main findings will be unfolded in the subsequent subsections:

6.1. Parameterisation of oscillatory activity and epoch-to-epoch descriptors help to identify spectral abnormalities in NDDs.

In **Paper 1**, we reported an increased theta/alpha ratio in PD subjects, which exhibited modulatory effects over the distribution of visuospatial performance. We linked this finding to potential abnormalities in the theta-to-alpha transition frequency, as reported by (Babiloni et al., 2004; Moretti et al., 2004). However, it was demonstrated in simulated and real-world datasets that different power spectra could lead to equivalent band power ratios (Donoghue et al., 2020a). In a further publication in four independent PD cohorts, we confirmed this lack of consistency in the theta/alpha ratio across epochs (Jaramillo-Jimenez et al., 2023). Therefore, we considered subdividing the theta band into slow-theta and fast-theta (pre-alpha), following successful methods employed in DLB research (Bonanni et al., 2016, 2008; Franciotti et al., 2020; Law et al., 2020; Schumacher et al., 2020a), and classical strategies of subdividing band frequencies to examine spectral theta and alpha abnormalities (Klimesch, 1999). In line with the above, we evinced that increased posterior pre-alpha power characterised PD groups as reflected by

significant differences in an epoch-to-epoch analysis. We have dedicated special attention to the advantages of epoch-to-epoch differences with statistical modelling via functional data analysis elsewhere (Jaramillo-Jimenez et al., 2023).

Unfortunately, harmonisation of batch effects with epoch-to-epoch data structures is not available. Spectral estimators in rsEEG analysis are often calculated for averaged epochs in clinical research, and most autoML pipelines operate with tabular data (rows -subjects- by columns -features-), so we constrained our methods to average epochs to make them more comparable with prior findings. Despite this limitation, we capitalized on frequency prevalence descriptors scarcely applied in dementia research. Frequency prevalences could indicate epoch-to-epoch power (i.e., the percentage of epochs where the peak/dominant frequency lies in each of the frequency bands), potentially mitigating the effects of averaging across epochs (Bonanni et al., 2015, 2008; Gimenez-Aparisi et al., 2023; Stylianou et al., 2018). One last and crucial unsolved challenge that could affect the robustness of our earlier observations in the PD cohorts was the parameterisation of the aperiodic spectrum, which could conflate the estimated power in the pre-alpha band (Donoghue et al., 2020b). Therefore, considering the limitations of our previous work on PD samples, we abandoned band power ratios, incorporated the pre-alpha band, and parameterised oscillatory and aperiodic activity of the spectrum.

Taken together, our exploratory results suggest that spectral features in the slow-theta, pre-alpha, and alpha bands were crucial to separate all NDDs from HCs. Thus, power and frequency descriptors in the slow-theta (increased) and alpha (reduced) bands prominently differentiated FTD and AD. This pattern has been recognized in prior evidence comparing these two diseases with HC (Caso et al., 2012; Chang and Chang, 2023; Yener et al., 1996). In contrast with our findings, the absence of a significant reduction in slow frequencies of the rsEEG was reported in FTD compared to HC (Lindau et al., 2003). This divergence in the results could be attributed to the utilization of a composite band power ratio (alpha + beta /delta + theta), differences in the definition of the theta band (4.0 – 7.5 Hz), and the length of the recording in such study (15 epochs – 2 seconds each).

On the other hand, power changes in pre-alpha (increased) represented MCI-AD, AD, PD, and MCI-LBD, in agreement with preceding studies investigating PD, AD, and MCI groups (MCI-AD & MCI-LBD) separately (Azami et al., 2023; Jaramillo-Jimenez et al., 2023; Kopčanová et al., 2023; Rosenblum et al., 2023; Schumacher et al., 2020a). This discriminatory pattern has been replicated when assessing frequency prevalence in the pre-alpha band, in congruence with (Gimenez-Aparisi et al., 2023; Stylianou et al., 2018). Of note, most of the mentioned studies have not directly discretised the pre-alpha frequency band, reporting the parameterised and full power spectrum in AD and PD samples (Azami et al., 2023; Kopčanová et al., 2023; Rosenblum et al., 2023; Vanneste et al., 2018). Among studies examining discretised pre-alpha power, the conclusions of Schumacher et al. accepted the hypothesis of increased pre-alpha power in MCI-AD and MCI-LBD compared to HC (in agreement with our observation), results presented by Bonanni et al. presented a scarce pre-alpha frequency prevalence (< 11%) in MCI-AD, and AD with comparable relative power compared to HC individuals (Bonanni et al., 2015, 2008). We observed that HC had significantly lower pre-alpha power and frequency prevalence than MCI-AD and MCI-LBD groups, but notably, pre-alpha values in MCI-AD were significantly lower than in AD. Thus, future efforts should assess the robustness and generalisability of pre-alpha power and frequency prevalence as correlates of the progression across the AD continuum.

In addition to frequency prevalence, the dominant frequency was quantified from the full spectrum (1/f uncorrected) and its aperiodic corrected equivalent (i.e., extended alpha centre frequency). While significant group differences in the dominant frequency were only present for HC > AD and HC > FTD comparisons, our findings in the central-posterior extended alpha centre frequency estimated lower group values in AD, MCI-LBD, and PD than those in the HC group.

A reduced dominant frequency in the posterior channels has been included as part of the supportive biomarkers for DLB and MCI-LB (Attems et al., 2021; McKeith et al., 2020). The latter has been replicated in MCI-LBD (Bonanni et al., 2015; Schumacher et al., 2020a). We speculate that combining PD-MCI and MCI-LB, having a relatively small sample size ($n = 32$), and not conducting an explicit age and sex matching for the pairwise group comparisons could explain the lack of consistency with our results. We also consider the potential confounding effect of aperiodic parameters when estimating dominant frequency from the $1/f$ uncorrected spectrum. Our exploratory analysis revealed that extended alpha centre frequency in central and posterior ROI was comparable between MCI-LBD and PD, which exhibited a lower peak frequency than HC. In line with this, prior evidence in PD has pointed out that the reduction of background frequency could indicate cognitive decline, with a tendency towards reduction of the dominant frequency in subjects that progress to PD-MCI and PDD (Caviness et al., 2016b; Geraedts et al., 2018; Yassine et al., 2023). The idea of dominant frequency and extended-alpha centre frequency as a biomarker of the DLB continuum was supported by our findings in the MCI-LBD group, but reduced extended alpha centre frequency was also observed in AD in both harmonised and unharmonized data. Prospective studies with more control of the experimental design should evaluate the reliability of peak frequency markers by controlling for potential confounders such as the balance of the groups, education level, medication and severity of dementia (with dedicated sample selection and matching) and use single-site amplifiers and headsets to avoid batch effects in the recording. By implementing these recommendations, future investigations could evaluate the robustness, specificity of the metric in LBDs, reliability and potential disparities in dominant frequency when estimated in the full spectrum and the parameterised oscillatory power spectrum, among other confounding factors that should be considered when interpreting our results.

The hypothesis of a reduction in the dominant frequency in the rsEEG (from alpha to pre-alpha rhythm) is supported by the model of thalamocortical dysrhythmia, indicated in prior research as a potential mechanistic explanation of this supportive biomarker of DLB (Bonanni et al., 2016, 2015, 2008; Franciotti et al., 2020). Basic and clinical research concludes that this augmented prevalence of pre-alpha rhythm could be led by deprivations on thalamic input, which reduces information processing in thalamocortical columns and subsequently cortico-cortical systems, manifesting as core symptoms of LBD or negative symptoms (e.g. depression) in other neuropsychiatric disorders (Franciotti et al., 2020; Llinás et al., 1999; Llinás and Steriade, 2006; Vanneste et al., 2018). Despite the relative consensus on the “thalamic pacemaker” of cortical rhythms in vigilance and sleep stages, the idea of this bottom-up process has been criticized, as the model arose from results on extracranial recordings (i.e., magnetoencephalographic spectral power without $1/f$ correction) or in-vitro analyses. These limitations have been remarked on in light of contrasting results from resting-state intracranial EEG recordings acquired in epilepsy surgeries. The authors observed that resting-state anterior alpha rhythm propagated to posterior regions (cortico-cortical supragranular feedback) and subsequently modulated thalamic pulvinar oscillations in a top-down manner (quantified with Granger Causality - Directed connectivity) (Halgren et al., 2019). This discrepancy serves as a new field of investigation aimed at reproducing these intracranial observations utilizing magnetoencephalographic recordings with multiple source reconstruction methods or intracranial signals from PD patients during deep-brain stimulation surgery.

6.2. Reduced complexity characterises rsEEG signals of AD patients.

Reduced complexity characterised AD subjects against HC, with significant differences in Higuchi FD, Katz FD, DFA, Hjorth complexity and Hjorth mobility. Two systematic reviews have also recognized these features when summarizing potential biomarkers of rsEEG reduced complexity in AD across the last decade (Cassani et al., 2018; Modir et al., 2023). Our exploratory analyses coincide with the group-level reported trend of reduced complexity in AD and MCI-AD groups (McBride et al., 2014; Poil et al., 2013). It has been hypothesized that neural cell death and synaptic dysfunction in specific cortical columns could cause “simpler” rsEEG activity (Cassani et al., 2018). Consistent with our findings, reports on low-density rsEEG argue that a reduced Higuchi FD across frontal, central, and posterior channels characterises AD subjects. A prominent decrease in the complexity of beta and gamma bands was proposed in the mentioned study to explain the reduced fractality in AD (i.e., more predictable signals), which significantly correlated with cognitive decline (Nobukawa et al., 2019). Reduced Katz FD conveys with the estimations of Higuchi FD in AD subjects (Puri et al., 2023). Reports on reduced Hjorth parameters (mobility) in a large sample of AD subjects are aligned with our examinations (Jiao et al., 2023). Transcranial magnetic stimulation in conjunction with EEG recordings has also indicated an increased Hjorth complexity in AD subjects, with high feature importance when discriminating between AD and HC individuals (Tăuțan et al., 2023).

Despite these promising findings, we emphasize that age-related effects on complexity features (U-shaped) could play a critical confounding when interpreting our complexity results, considering prior reports on FD (Smits et al., 2016) and Hjorth parameters (Gordillo et al., 2023). In line with our results, age-related publications have shown higher DFA values in young HC compared to older individuals (Sleimen-Malkoun et al., 2015). An in-depth analysis of the associations between complexity features in cohorts with the characterisation of protein aggregation/accumulation markers is lacking in current evidence, favouring knowledge gaps of potential mechanisms that explain reduced complexity in AD. Simulations (<https://aperiodicmethods.github.io/>) and magnetoencephalographic clinical data have pointed out potential interdependencies of complexity metrics and aperiodic parameters considering abnormalities in the inhibition/excitation balance, in which AD could reflect inhibition-predominant activity manifested as reduced complexity, with steeper non-oscillatory slopes, and higher offsets. In contrast, MCI-AD might reflect excitatory-predominant activity manifested as increased complexity, with flatter aperiodic slopes and lower intercepts (van Nifterick et al., 2023).

Unfortunately, complexity features alone have not proved to perform better than spectral features and have been proposed as ancillary features in the correct identification of AD via rsEEG (Abásolo et al., 2008; Modir et al., 2023). **Section 6.4.** expands on current evidence favouring the combined utilization of these features in the classification of NDDs.

6.3. Harmonisation of rsEEG features mitigates batch effects in multi-centric studies.

Harmonisation of multi-site batch effects has been suggested as a necessary step when analysing pooled rsEEG datasets (Bigdely-Shamlo et al., 2020; M. Li et al., 2022; Prado et al., 2022). Thus, in **Paper 2**, we contrasted the effects of various methods for statistical batch harmonisation of rsEEG spectral features in a large subsample of HC subjects (in order to avoid potential confounding effects of NDDs). Overall, batch effects reflecting site-related variability on the rsEEG spectral features were identified. Statistical harmonisation based on ComBat variants effectively mitigated the observed batch effects while preserving the direction and significance of early reported age-related effects on oscillatory (reduced alpha centre frequency and increased beta power) and aperiodic parameters (reduced slope and offset) (He et al., 2019; Hill et al., 2022; Merkin et al., 2021). Further, considering the limitations of the four ComBat variants compared in **Paper 2**, a fifth variant (reComBat) was considered, given the nature of our final dataset with NDDs. Thus, singular matrix problems were identified when estimating the biological variability covariance matrix in the final pooled datasets. The latter was explained due to all subjects from a given batch belonging to the same group category (such as HCs in the Lemon and Oslo datasets or AD subjects from the Genoa dataset). The authors of the reComBat variant propose an innovative approach to this issue by solving the biological variability matrix with elastic-net regularisation parameters that specifically tackle this issue (Adamer et al., 2022). In addition, the potential issues of missing data in the estimated ComBat harmonised features were observed in **Paper 2**. This missing data originated when estimating the oscillatory parameters for slow frequency bands such as delta and theta, where the oscillatory curve was flat (with no peaks), and computation of power (i.e., the area under the oscillatory 1/f corrected curve) was not possible (originating missing values). In our final analysis, we accounted for these limitations by computing oscillatory power in the extended alpha and beta bands (where physiological oscillatory peaks are expected) and subsequently computing the ROI average, resulting in no missing values for reComBat harmonisation. Also, the exploratory analysis in the HC subsample (presented in **Figure 22**) illustrated that the best mitigation of average batch effects was achieved with reComBat, which also justified the selection of this harmonisation method among other variants for subsequent analyses.

One last limitation of our prior publications on ComBat harmonisation in PD using machine learning methods (Kurbatskaya et al., 2023b; Kurbatskaya et al., 2023a) was the harmonisation of the pooled dataset as a whole rather than the harmonisation of the test set based on the fitting parameters obtained in the train set harmonisation. In the context of machine learning, normalisation or re-scaling before splitting the dataset into train and test sets could lead to potential data leakage (i.e., re-scaling the test set using the parameters estimated from the distribution of the whole dataset – including the train set) (Tampu et al., 2022). Following this recommendation of fitting and re-scaling the train set and extracting these parameters to re-scale the test set, we run reComBat in all our autoML models. In line with our exploratory observations on spectral features and HC subjects, harmonising the train and test sets with multiple-feature information and multiple NDDs suggested mitigation in the average batch effects, centring the data across sites and making them comparable (**Figure 27**). The effect of reComBat harmonisation successfully increased model performance, as evidenced by a greater balanced accuracy in the spectral-only harmonised data (Bacc = 0.68) compared to the spectral-only unharmonized data (Bacc = 0.38). The multi-feature harmonised models consistently achieved a better classification performance than those trained with the equivalent non-harmonised data (**Figure 30**). The improvement in the classification performance was observed for all the included groups (i.e., HC, MCI-AD, AD, PD, MCI-LB). Therefore, as proven in imaging studies, the evidence we have obtained makes us affirm that reComBat could be a promising strategy for future research capitalising on existing data collections for identifying NDDs and HC subjects.

6.4. Combination of Spectral and Complexity abnormalities in the classification of NDDs.

In line with our findings presented in **Paper 3**, the combination of spectral + complexity features has demonstrated prominent importance in AD and MCI-AD identification, as supported by a recent Chinese study with a large sample size conducted in a single reference site for neurology (Jiao et al., 2023). These authors trained rsEEG binary and three-class classification (HC vs AD vs MCI-AD) supportive vector machine and linear discriminant analysis models by combining 1/f uncorrected spectral powers (absolute and relative), sample entropy, Hjorth parameters, time-frequency statistics (entropy, kurtosis, skewness, standard deviation and mean), and EEG microstates extracted at the sensor level with a 16-channel montage.

The authors recognized spectral and complexity features as the key biomarkers for differentiation of HC, MCI-AD, AD, DLB, FTD and vascular dementia, namely the 1/f uncorrected relative and absolute right occipital theta power, as well as the right parietal and bilateral occipital Hjorth mobility. The most relevant features reported in the mentioned preliminary study are presented in **Table 4**.

Table 4. Previously identified rsEEG features for AD and MCI-AD in a multiclass classification task, results reported by (Jiao et al., 2023)

| Feature | Anterior | Central | Posterior |
|--------------------------|----------------------|---------------------------|---------------------------|
| Absolute power | Delta, Theta, Beta | Delta, Theta, Alpha, Beta | Delta, Theta, Alpha, Beta |
| Relative power | Theta, Beta | Theta, Alpha, Beta | Delta, Theta, Alpha, Beta |
| Hjorth param. | Complexity, Mobility | Complexity, Mobility | Complexity, Mobility |
| Time-Freq. Stats. | | Standard deviation, Mean | |
| Sample entropy | X | X | X |
| Microstates | | X | |

Hjorth param.: Hjorth parameters; **Time-Freq. Stat**: Time-frequency domain. **X**: The feature was selected as relevant for AD vs MCI-AD vs HC classification. Adapted from (Jiao et al., 2023)

Another study with low-density rsEEG recordings found that Hjorth complexity + Entropy metrics + Aperiodic uncorrected spectral band powers were the most relevant features in binary classifications (AD vs HC, and MCI negative for AD pathology vs HC) in a small sample ($n = 21$; AD = 8, MCI non-AD = 5, HC=8) (Perez-Valero et al., 2022). Transcranial magnetic stimulation combined with EEG has also pointed out increased Hjorth complexity in AD, emphasizing the value of combining Hjorth parameters with spectral features (Tăuțan et al., 2023).

Despite concordant features between this earlier work and our results, we did not find significant group differences between MCI-AD and HC with complexity features, as reported by Jiao et al. In the mentioned study, significance was considered with q-values < 0.05 . However, we intentionally undertook a conservative approach in the exploratory analyses (significance level, alpha = 0.001), which could explain this discrepancy. Beyond the well-known issues of a dichotomous accept/reject perspective arising from significance levels (Alger, 2022), methodological aspects of signal processing should be considered. Thus, our features were extracted in 1.7 minutes (5 second-length epochs, sampled at 128 Hz) of signal, while the average length of the signals in the study from Jiao et al. was 6.2 minutes (5 second-length epochs, sampled at 128 Hz). Considering this, each of our epochs included 640 points for calculating complexity-derived metrics, while the study of Jiao et al. had 1000 points per epoch. The length

of the epoch and the number of points have been reported earlier as potential factors affecting the reliability of some complexity features in the rsEEG. A previous report showed good reliability of most complexity descriptors with at least 40 seconds of 5-second length epochs (each with 1280 points) (Gudmundsson et al., 2007).

Nevertheless, it is important to acknowledge that we opted for undersampling due to the nature of the available rsEEG data, where some signals were acquired at a sample rate of 128 Hz. This decision was made to maximize the utility of the data while being mindful of the constraints imposed by varying sample rates across the dataset. The enormous potential of data augmentation in rsEEG signals has been highlighted particularly for deep learning applications with up to 45 % improved accuracy performance (Rommel et al., 2022). Data augmentation methods could potentially overcome some of the limitations we encountered due to the imbalance of classes (where FTD and MCI-LBD were underrepresented). Also, data augmentation techniques could benefit further research to exploit already acquired data with short-length signals and low sampling rates to pre-train generalisable models for diagnostic purposes.

This multi-centric sample did not identify the extensive contributions of connectivity to group differences, where AD subjects exhibited higher variability in the distribution of the iCoh and wPLI theta band connectivity (i.e., greater IQR values) when compared to healthy subjects and other NDDs (except FTD). The necessity of relatively extensive feature extraction (i.e., calculation of several connectivity metrics) has been proposed in earlier research in NDDs (Briels et al., 2020; Dottori et al., 2017; Moguilner et al., 2022; Prado et al., 2022; Prado et al., 2023). Previous evidence supported the observation of a global increase in theta band wPLI and iCoh, especially emphasizing the appropriate reproducibility of wPLI (Briels et al., 2020). These authors also found higher wPLI variability (assessed through standard deviation) in the theta band in AD compared to subjects with subjective cognitive impairment. However, the statistical significance of the wPLI theta band AD-related findings disappeared when correcting for potential confounding effects of relative theta power. The latter supports the reduced F-values in the exploratory analyses, the low scores of connectivity metrics in the importance of permutation-based features, and the lack of improvement in the autoML classifications when adding connectivity features. In addition, we acknowledge that our estimation of global connectivity is a gross evaluation of connectivity that could be refined by the computation of graph-theory connectivity metrics with subsequent potential threshold bias to be assessed and consistency scores, which imply increased computational demands. Despite these potential opportunities, we agree with the observations of an early publication where high-density montages were dedicated to approximate connectivity features of AD and MCI-AD. In contrast, low-density montages offered a better classification when combining spectral + complexity features (Gaubert et al., 2021). Having said that, compared to spectral features only, a slight increase in the sensitivity of MCI-AD, MCI-LBD, and PD classes was achieved when combining spectral and complexity features (although this was not reflected in the Bacc = 0.68). Thus, the best model with spectral and complexity features achieved good discrimination of HC (Accuracy = 76.5%, Bacc = 68.9%, Sensitivity -Sens- = 81.8%, Specificity – Spec- = 81.6% PPV = 77.1%, NPV = 85.5%), MCI-AD (Sens = 69.5%, Spec = 93.1%, PPV = 64%, NPV = 94.5%) and AD (Sens = 88.2%, Spec = 94.1%, PPV = 81.1%, NPV = 96.5%). Our best model (XGBoost with k-fold bagging) performed better than those fitted by Jiao et al., who reported a model accuracy of 70.2% on a three-class classification (HC vs MCI-AD vs AD) in a single-site study with a large sample (Jiao et al., 2023). Despite their large sample size, the groups were not balanced (HC = 246, MCI = 189, AD = 330), and the authors did not account for class imbalance when reporting model performance.

With all the above, we can conclude that specific spectral abnormalities in the full spectrum and 1/f corrected oscillations characterise NDDs from the MCI stages. AD-related differences might

be reflected by complexity features of fractality and Hjorth parameters, but potential age-related differences should be considered. Besides, studies analysing multi-site rsEEG data may benefit from the harmonisation of derivative features in order to control for batch effects. In the context of multi-site pooled data, utilization of AutoML models on tabular rsEEG features achieved accurate multi-class classification of HCs and NDDs, particularly for individuals in the AD continuum. Finally, the combination of rsEEG spectral + complexity harmonised features offers the best performance among all the examined models. Our proposed approach improves the state-of-the-art results of supervised models for multi-class classification of AD continuum trained with low-density rsEEG data extracted at the sensor space.

7. Future perspectives.

Throughout the discussion section, we presented some of this research's limitations and solutions proposed. However, some methodological challenges could not be addressed due to the retrospective nature of this study and should be considered when interpreting our results. In line with this, the observational findings in our study should not be interpreted as causal directions. Also, the lack of a biological characterisation of the underlying neuropathology in our sample makes us rely on clinical phenotypes to classify the included subjects, which might not entirely reflect the protein aggregation/accumulation despite the use of operationalised diagnostic criteria in the individual studies included in our analyses. The latter can be assessed by integrating rsEEG data with other biomarkers such as CSF, imaging or blood-based tests assessing other hallmarks of neurodegeneration or vascular-related pathology from a multi-modal perspective (Iturria-Medina et al., 2016; Moguilner et al., 2022).

Besides, balanced groups could not be achieved as it would imply undersampling subjects and, thus, losing a large sample. This lack of balance is evident across machine learning studies on rsEEG diagnosis of NDDs, opening the gate for data augmentation techniques that could be implemented to train better models based on balanced samples (Lashgari et al., 2020; Rommel et al., 2022).

In addition, our analyses were conducted with features extracted at the sensor space, which might offer potential confounding effects of volume conduction. Although source space represented the state-of-the-art method to reduce the effects of volume conduction and represent the source of rsEEG spectral activity, source solutions from low-density rsEEG recordings might still misrepresent the appropriate spatial patterns of source activity as these estimations are often estimated from forward modelling in anatomical templates that do not correspond to specific-subject anatomy (which might be affected by NDDs with gliosis and cortical atrophy) (Nguyen-Danse et al., 2021). Statistical-based source separation methods such as spatio-spectral decomposition appeared as an emergent solution to assess brain rhythms controlling for volume conduction effects without the necessity of anatomical head models. In brain-age prediction studies, these methods have been implemented by computing the covariance matrixes from rsEEG channels (even from very low-density montages, such as four channels) in a computationally efficient manner (Engemann et al., 2022a; D. Sabbagh et al., 2023). Spatio-spectral decomposition could also mitigate the documented interference created by posterior sources of alpha rhythm over anterior rsEEG channels at the sensor level (Schaworonkow and Nikulin, 2022). In addition, the combination of spatio-spectral decompositions from rsEEG covariance matrixes with Riemannian geometry-based machine learning models has demonstrated notable performance in brain-age prediction, achieving better results than handcrafted features used in our research (e.g. spectral and complexity) (Engemann et al., 2022a).

However, current methods for batch harmonisation available for covariance-based representations of the rsEEG signals (i.e., re-centring and re-scaling via Procrustes analysis) lack specific strategies to control for biological variability (Rodrigues et al., 2019). Future efforts should be taken to address this critical limitation.

Overall, the overseen panorama is plenty of opportunities and new challenges to be faced in rsEEG for NDDs biomarkers discovery. Integrative multi-site, multi-modal, and multi-feature approaches could be formulated to determine redundant and relevant features across biomarkers, determining the optimal minimal set of panel metrics that can be used for early detection of NDDs.

8. References.

- Aarsland D, Batzu L, Halliday GM, Geurtsen GJ, Ballard C, Ray Chaudhuri K, et al. Parkinson disease-associated cognitive impairment. *Nat Rev Dis Primers* 2021;7:1–21. <https://doi.org/10.1038/s41572-021-00280-3>.
- Aarsland D, Creese B, Politis M, Chaudhuri KR, Ffytche DH, Weintraub D, et al. Cognitive decline in Parkinson disease. *Nat Rev Neurol* 2017;13:217–31. <https://doi.org/10.1038/nrneurol.2017.27>.
- Abásolo D, Hornero R, Escudero J, Espino P. A study on the possible usefulness of detrended fluctuation analysis of the electroencephalogram background activity in Alzheimer’s disease. *IEEE Trans Biomed Eng* 2008;55:2171–9. <https://doi.org/10.1109/TBME.2008.923145>.
- Abubakar MB, Sanusi KO, Uguzman A, Mohamed W, Kamal H, Ibrahim NH, et al. Alzheimer’s Disease: An Update and Insights Into Pathophysiology. *Front Aging Neurosci* 2022;14:742408. [https://doi.org/10.3389/FNAGI.2022.742408/BIBTEX](https://doi.org/10.3389/FNAGI.2022.742408).
- Adamer MF, Brüningk SC, Tejada-Arranz A, Estermann F, Basler M, Borgwardt K. reComBat: batch-effect removal in large-scale multi-source gene-expression data integration. *Bioinformatics Advances* 2022;2. <https://doi.org/10.1093/BIOADV/VBAC071>.
- Aisen PS, Cummings J, Jack CR, Morris JC, Sperling R, Frölich L, et al. On the path to 2025: Understanding the Alzheimer’s disease continuum. *Alzheimers Res Ther* 2017;9:60. <https://doi.org/10.1186/s13195-017-0283-5>.
- Albert MS, DeKosky ST, Dickson D, Dubois B, Feldman HH, Fox NC, et al. The diagnosis of mild cognitive impairment due to Alzheimer’s disease: recommendations from the National Institute on Aging-Alzheimer’s Association workgroups on diagnostic guidelines for Alzheimer’s disease. *Alzheimers Dement* 2011;7:270–9. <https://doi.org/10.1016/J.JALZ.2011.03.008>.
- Alger BE. Neuroscience Needs to Test Both Statistical and Scientific Hypotheses. *The Journal of Neuroscience* 2022;42:8432. <https://doi.org/10.1523/JNEUROSCI.1134-22.2022>.
- Allegri RF. Moving from neurodegenerative dementias, to cognitive proteinopathies, replacing “where” by “what”.... *Dementia e Neuropsychologia* 2020;14:237–42. <https://doi.org/10.1590/1980-57642020dn14-030005>.
- Al-Nuaimi AHH, Jammeh E, Sun L, Ifeachor E. Complexity Measures for Quantifying Changes in Electroencephalogram in Alzheimer’s Disease. *Complexity* 2018;2018. <https://doi.org/10.1155/2018/8915079>.
- Al-Qazzaz NK, Ali SHBMD, Ahmad SA, Chellappan K, Islam MdS, Escudero J. Role of EEG as biomarker in the early detection and classification of dementia. *Scientific World Journal* 2014;2014. <https://doi.org/10.1155/2014/906038>.
- Alzheimer A. Über eine eigenartige Erkrankung der Hirnrinde. *Allgemeine Zeitschrift Fur Psychiatrie Und Psychisch-Gerichtliche Medizin* 1907;64:146–8.
- American Psychiatric Association. Diagnostic and Statistical Manual of Mental Disorders, 5th Edition. 2013. <https://doi.org/10.1176/appi.books.9780890425596.893619>.

Angarita-Zapata JS, Maestre-Gongora G, Calderín JF. A Bibliometric Analysis and Benchmark of Machine Learning and AutoML in Crash Severity Prediction: The Case Study of Three Colombian Cities. *Sensors* (Basel) 2021;21. <https://doi.org/10.3390/S21248401>.

Angelakis E, Lubar JF, Stathopoulou S, Kounios J. Peak alpha frequency: an electroencephalographic measure of cognitive preparedness. *Clinical Neurophysiology* 2004;115:887–97. <https://doi.org/10.1016/J.CLINPH.2003.11.034>.

Appelhoff S, Hurst AJ, Lawrence A, Li A, Mantilla Ramos YJ, O'Reilly C, et al. PyPREP: A Python implementation of the preprocessing pipeline (PREP) for EEG data. 2022. <https://doi.org/10.5281/ZENODO.6363576>.

Armstrong MJ. Advances in dementia with Lewy bodies. *Ther Adv Neurol Disord* 2021;14. https://doi.org/10.1177/17562864211057666/ASSET/IMAGES/LARGE/10.1177_17562864211057666-FIG1.jpeg.

Armstrong MJ, MJ A. Lewy Body Dementias 2019;25:128–46. <https://doi.org/10.1212/CON.0000000000000685>.

Attems J, Toledo JB, Walker L, Gelpi E, Gentleman S, Halliday G, et al. Neuropathological consensus criteria for the evaluation of Lewy pathology in post-mortem brains: a multi-centre study. *Acta Neuropathol* 2021;141:159–72. <https://doi.org/10.1007/S00401-020-02255-2/FIGURES/5>.

Averna A, Coelli S, Ferrara R, Cerutti S, Priori A, Bianchi AM. Entropy and fractal analysis of brain-related neurophysiological signals in Alzheimer's and Parkinson's disease. *J Neural Eng* 2023;20. <https://doi.org/10.1088/1741-2552/ACF8FA>.

Azami H, Zrenner C, Brooks H, Zomorrodi R, Blumberger DM, Fischer CE, et al. Beta to theta power ratio in EEG periodic components as a potential biomarker in mild cognitive impairment and Alzheimer's dementia. *Alzheimers Res Ther* 2023;15:1–12. <https://doi.org/10.1186/S13195-023-01280-Z/FIGURES/5>.

Babadi B, Brown EN. A review of multitaper spectral analysis. *IEEE Trans Biomed Eng* 2014;61:1555–64. <https://doi.org/10.1109/TBME.2014.2311996>.

Babayan A, Erbey M, Kumral D, Reinelt JD, Reiter AMF, Röbbig J, et al. A mind-brain-body dataset of MRI, EEG, cognition, emotion, and peripheral physiology in young and old adults. *Scientific Data* 2019 6:1 2019;6:1–21. <https://doi.org/10.1038/sdata.2018.308>.

Babiloni C. The Dark Side of Alzheimer's Disease: Neglected Physiological Biomarkers of Brain Hyperexcitability and Abnormal Consciousness Level. *Journal of Alzheimer's Disease* 2022;88:801–7. <https://doi.org/10.3233/JAD-220582>.

Babiloni C, Barry RJ, Başar E, Blinowska KJ, Cichocki A, Dringenburg WHM, et al. International Federation of Clinical Neurophysiology (IFCN) – EEG research workgroup: Recommendations on frequency and topographic analysis of resting state EEG rhythms. Part 1: Applications in clinical research studies. *Clinical Neurophysiology* 2020;131:285–307. <https://doi.org/10.1016/j.clinph.2019.06.234>.

Babiloni C, Binetti G, Cassetta E, Cerboneschi D, Dal Forno G, Del Percio C, et al. Mapping distributed sources of cortical rhythms in mild Alzheimer's disease. A multicentric EEG study. *Neuroimage* 2004;22:57–67. <https://doi.org/10.1016/j.neuroimage.2003.09.028>.

Babiloni C, Ferri R, Noce G, Lizio R, Lopez S, Lorenzo I, et al. Resting State Alpha Electroencephalographic Rhythms Are Differently Related to Aging in Cognitively Unimpaired Seniors and Patients with Alzheimer's Disease and Amnesic Mild Cognitive Impairment. *J Alzheimers Dis* 2021;82:1085–114. <https://doi.org/10.3233/JAD-201271>.

Babiloni C, Lorenzo I, Lizio R, Lopez S, Tucci F, Ferri R, et al. Reactivity of posterior cortical electroencephalographic alpha rhythms during eyes opening in cognitively intact older adults and patients with dementia due to Alzheimer's and Lewy body diseases. *Neurobiol Aging* 2022;115:88–108. <https://doi.org/10.1016/J.NEUROBIOLAGING.2022.04.001>.

Babiloni C, Del Percio C, Pascarelli MT, Lizio R, Noce G, Lopez S, et al. Abnormalities of functional cortical source connectivity of resting-state electroencephalographic alpha rhythms are similar in patients with mild cognitive impairment due to Alzheimer's and Lewy body diseases. *Neurobiol Aging* 2019;77:112–27. <https://doi.org/10.1016/j.neurobiolaging.2019.01.013>.

Babiloni C, Vecchio F, Lizio R, Ferri R, Rodriguez G, Marzano N, et al. Resting State Cortical Rhythms in Mild Cognitive Impairment and Alzheimer's Disease: Electroencephalographic Evidence. *Journal of Alzheimer's Disease* 2011;26:201–14. <https://doi.org/10.3233/JAD-2011-0051>.

Badhwar AP, Tam A, Dansereau C, Orban P, Hoffstaedter F, Bellec P. Resting-state network dysfunction in Alzheimer's disease: A systematic review and meta-analysis. *Alzheimer's & Dementia: Diagnosis, Assessment & Disease Monitoring* 2017;8:73–85. <https://doi.org/10.1016/J.DADM.2017.03.007>.

Bailey NW, Hoy KE. The promise of artificial neural networks, EEG, and MRI for Alzheimer's disease. *Clinical Neurophysiology* 2021;132:207–9. <https://doi.org/10.1016/J.CLINPH.2020.10.009>.

Banville H, Jaoude MA, Wood SUN, Aimone C, Holst SC, Gramfort A, et al. Do try this at home: Age prediction from sleep and meditation with large-scale low-cost mobile EEG. *BioRxiv* 2023;2023.04.29.538328. <https://doi.org/10.1101/2023.04.29.538328>.

Bastos AM, Schoffelen JM. A tutorial review of functional connectivity analysis methods and their interpretational pitfalls. *Front Syst Neurosci* 2016;9:165147. [https://doi.org/10.3389/FNSYS.2015.00175/BIBTEX](https://doi.org/10.3389/FNSYS.2015.00175).

Beam CR, Kaneshiro C, Jang JY, Reynolds CA, Pedersen NL, Gatz M. Differences Between Women and Men in Incidence Rates of Dementia and Alzheimer's Disease. *J Alzheimers Dis* 2018;64:1077. <https://doi.org/10.3233/JAD-180141>.

Beer JC, Tustison NJ, Cook PA, Davatzikos C, Sheline YI, Shinohara RT, et al. Longitudinal ComBat: A method for harmonizing longitudinal multi-scanner imaging data. *Neuroimage* 2020;220:117129. <https://doi.org/10.1016/j.neuroimage.2020.117129>.

Bell TK, Godfrey KJ, Ware AL, Yeates KO, Harris AD. Harmonization of multi-site MRS data with ComBat. *Neuroimage* 2022;257. <https://doi.org/10.1016/j.neuroimage.2022.119330>.

Benjamini Y, Yekutieli D. The control of the false discovery rate in multiple testing under dependency. <https://doi.org/10.1214/AOS/1013699998> 2001;29:1165–88. <https://doi.org/10.1214/AOS/1013699998>.

Bennys K, Rondouin G, Vergnes C, Touchon J. Diagnostic value of quantitative EEG in Alzheimer's disease. *Neurophysiologie Clinique* 2001;31:153–60. [https://doi.org/10.1016/S0987-7053\(01\)00254-4](https://doi.org/10.1016/S0987-7053(01)00254-4).

Benwell CSY, Davila-Pérez P, Fried PJ, Jones RN, Travison TG, Santarecchi E, et al. EEG spectral power abnormalities and their relationship with cognitive dysfunction in patients with Alzheimer's disease and type 2 diabetes. *Neurobiol Aging* 2020;85:83–95. <https://doi.org/10.1016/J.NEUROBOLAGING.2019.10.004>.

Berger H. Über das Elektrenkephalogramm des Menschen - XI. Mitteilung. *Arch Psychiatr Nervenkr* 1936;104:678–89. [https://doi.org/10.1007/BF01814250/METRICS](https://doi.org/10.1007/BF01814250).

Berger H. Über das Elektrenkephalogramm des Menschen. *Arch Psychiatr Nervenkr* 1929;87:527–70. [https://doi.org/10.1007/BF01797193/METRICS](https://doi.org/10.1007/BF01797193).

Bergeron D, Gorno-Tempini ML, Rabinovici GD, Santos-Santos MA, Seeley W, Miller BL, et al. Prevalence of amyloid- β pathology in distinct variants of primary progressive aphasia. *Ann Neurol* 2018;84:729–40. <https://doi.org/10.1002/ANA.25333>.

Bernasconi F, Pagonabarraga J, Bejr-Kasem H, Martínez-Horta S, Marín-Lahoz J, Horta-Barba A, et al. Theta oscillations and minor hallucinations in Parkinson's disease reveal decrease in frontal lobe functions and later cognitive decline. *Nature Mental Health* 2023;1:7 2023;1:477–88. <https://doi.org/10.1038/s44220-023-00080-6>.

Bezrukavnikov O, Linder R. A Neophyte With AutoML: Evaluating the Promises of Automatic Machine Learning Tools 2021.

Bhattacharya S, Cauchois MBL, Iglesias PA, Chen ZS. The impact of a closed-loop thalamocortical model on the spatiotemporal dynamics of cortical and thalamic traveling waves. *Sci Rep* 2021;11:1–19. <https://doi.org/10.1038/s41598-021-93618-6>.

Bigdely-Shamlo N, Mullen T, Kothe C, Su K-M, Robbins KA. The PREP pipeline: standardized preprocessing for large-scale EEG analysis. *Front Neuroinform* 2015;9. <https://doi.org/10.3389/fninf.2015.00016>.

Bigdely-Shamlo N, Touryan J, Ojeda A, Kothe C, Mullen T, Robbins K. Automated EEG mega-analysis I: Spectral and amplitude characteristics across studies. *Neuroimage* 2020;207:116361. <https://doi.org/10.1016/j.neuroimage.2019.116361>.

Biundo R, Weis L, Antonini A. Cognitive decline in Parkinson's disease: the complex picture. *NPJ Parkinsons Dis* 2016;2:16018. <https://doi.org/10.1038/NPJ PARKD.2016.18>.

Blacker D, Albert MS, Bassett SS, Rodney CP, Harrell LE, Folstein MF. Reliability and Validity of NINCDS-ADRDA Criteria for Alzheimer's Disease: The National Institute of Mental Health Genetics Initiative. *Arch Neurol* 1994;51:1198–204. <https://doi.org/10.1001/ARCHNEUR.1994.00540240042014>.

De Boer EMJ, Orie VK, Williams T, Baker MR, De Oliveira HM, Polvikoski T, et al. TDP-43 proteinopathies: a new wave of neurodegenerative diseases. *J Neurol Neurosurg Psychiatry* 2021;92:86–95. <https://doi.org/10.1136/JNNP-2020-322983>.

Bonanni L, Franciotti R, Nobili F, Kramberger MG, Taylor JP, Garcia-Ptacek S, et al. EEG Markers of Dementia with Lewy Bodies: A Multicenter Cohort Study. *Journal of Alzheimer's Disease* 2016;54:1649–57. <https://doi.org/10.3233/JAD-160435>.

Bonanni L, Perfetti B, Bifolchetti S, Taylor JP, Franciotti R, Parnetti L, et al. Quantitative electroencephalogram utility in predicting conversion of mild cognitive impairment to dementia with Lewy bodies. *Neurobiol Aging* 2015;36:434. <https://doi.org/10.1016/J.NEUROBIOLAGING.2014.07.009>.

Bonanni L, Thomas A, Tiraboschi P, Perfetti B, Varanese S, Onofrj M, et al. EEG comparisons in early Alzheimer's disease, dementia with Lewy bodies and Parkinson's disease with dementia patients with a 2-year follow-up 2008;131:690–705.

Borghammer P, Horsager J, Andersen K, Van Den Berge N, Raunio A, Murayama S, et al. Neuropathological evidence of body-first vs. brain-first Lewy body disease. *Neurobiol Dis* 2021;161:105557. <https://doi.org/10.1016/J.NBD.2021.105557>.

Briels CT, Briels CT, Schoonhoven DN, Schoonhoven DN, Stam CJ, De Waal H, et al. Reproducibility of EEG functional connectivity in Alzheimer's disease. *Alzheimers Res Ther* 2020;12:1–14. <https://doi.org/10.1186/S13195-020-00632-3/TABLES/3>.

Brueggen K, Fiala C, Berger C, Ochmann S, Babiloni C, Teipel SJ. Early changes in alpha band power and DMN BOLD activity in Alzheimer's disease: A simultaneous resting state EEG-fMRI study. *Front Aging Neurosci* 2017;9:319. <https://doi.org/10.3389/fnagi.2017.00319>.

Buzsáki G, Anastassiou CA, Koch C. The origin of extracellular fields and currents — EEG, ECoG, LFP and spikes. *Nature Reviews Neuroscience* 2012 13:6 2012;13:407–20. <https://doi.org/10.1038/nrn3241>.

Byeon SK, Madugundu AK, Garapati K, Ramarajan MG, Saraswat M, Kumar-M P, et al. Development of a multiomics model for identification of predictive biomarkers for COVID-19 severity: a retrospective cohort study. *Lancet Digit Health* 2022;4:e632–45. [https://doi.org/10.1016/S2589-7500\(22\)00112-1](https://doi.org/10.1016/S2589-7500(22)00112-1).

Calabrese EJ. Neuroscience and Hormesis: Overview and General Findings. *Crit Rev Toxicol* 2008;38:249–52. <https://doi.org/10.1080/10408440801981957>.

Calabrese EJ, Mattson MP. How does hormesis impact biology, toxicology, and medicine? *Npj Aging and Mechanisms of Disease* 2017 3:1 2017;3:1–8. <https://doi.org/10.1038/s41514-017-0013-z>.

Carmona Arroyave JA, Tobón Quintero CA, Suárez Revelo JJ, Ochoa Gómez JF, García YB, Gómez LM, et al. Resting functional connectivity and mild cognitive impairment in Parkinson's disease. An electroencephalogram study. *Future Neurol* 2019;14:FNL18. <https://doi.org/10.2217/fnl-2018-0048>.

Caso F, Cursi M, Magnani G, Fanelli G, Falautano M, Comi G, et al. Quantitative EEG and LORETA: valuable tools in discerning FTD from AD? *Neurobiol Aging* 2012;33:2343–56. <https://doi.org/10.1016/J.NEUROBIOLAGING.2011.12.011>.

Cassani R, Estarellas M, San-Martin R, Fraga FJ, Falk TH. Systematic review on resting-state EEG for Alzheimer's disease diagnosis and progression assessment. *Dis Markers* 2018;2018. <https://doi.org/10.1155/2018/5174815>.

Castellanos NP, Makarov VA. Recovering EEG brain signals: artifact suppression with wavelet enhanced independent component analysis. *J Neurosci Methods* 2006;158:300–12. <https://doi.org/10.1016/J.JNEUMETH.2006.05.033>.

Caviness JN, Hentz JG, Evidente VG, Driver-Dunckley E, Samanta J, Mahant P, et al. Both early and late cognitive dysfunction affects the electroencephalogram in Parkinson's disease. *Parkinsonism Relat Disord* 2007;13:348–54. <https://doi.org/10.1016/J.PARKRELDIS.2007.01.003>.

Caviness JN, Utianski RL, Hentz JG, Beach TG, Dugger BN, Shill HA, et al. Differential spectral quantitative electroencephalography patterns between control and Parkinson's disease cohorts. *Eur J Neurol* 2016a;23:387–92. <https://doi.org/10.1111/ene.12878>.

Caviness JN, Utianski RL, Hentz JG, Beach TG, Dugger BN, Shill HA, et al. Differential spectral quantitative electroencephalography patterns between control and Parkinson's disease cohorts. *Eur J Neurol* 2016b;23:387–92. <https://doi.org/10.1111/ENE.12878>.

Chang J, Chang C. Quantitative Electroencephalography Markers for an Accurate Diagnosis of Frontotemporal Dementia: A Spectral Power Ratio Approach. *Medicina* 2023, Vol 59, Page 2155 2023;59:2155. <https://doi.org/10.3390/MEDICINA59122155>.

Chatterjee A, Hirsch-Reinshagen V, Moussavi SA, Ducharme B, Mackenzie IR, Hsiung GYR. Clinico-pathological comparison of patients with autopsy-confirmed Alzheimer's disease, dementia with Lewy bodies, and mixed pathology. *Alzheimer's & Dementia: Diagnosis, Assessment & Disease Monitoring* 2021;13. <https://doi.org/10.1002/DAD2.12189>.

Chatzikonstantinou S, McKenna J, Karantali E, Petridis F, Kazis D, Mavroudis I. Electroencephalogram in dementia with Lewy bodies: a systematic review. *Aging Clin Exp Res* 2021;33:1197–208. <https://doi.org/10.1007/s40520-020-01576-2>.

Chen CC, Hsu CY, Chiu HW, Hu CJ, Lee TC. Frequency power and coherence of electroencephalography are correlated with the severity of Alzheimer's disease: A multicenter analysis in Taiwan. *Journal of the Formosan Medical Association* 2015;114:729–35. <https://doi.org/10.1016/j.jfma.2013.07.008>.

Cheng ST. Dementia Caregiver Burden: a Research Update and Critical Analysis. *Curr Psychiatry Rep* 2017;19. <https://doi.org/10.1007/S11920-017-0818-2>.

Chu KT, Lei WC, Wu MH, Fuh JL, Wang SJ, French IT, et al. A holo-spectral EEG analysis provides an early detection of cognitive decline and predicts the progression to Alzheimer's disease. *Front Aging Neurosci* 2023;15:1195424. <https://doi.org/10.3389/FNAGI.2023.1195424/BIBTEX>.

Collino S, Montoliu I, Martin FPJ, Scherer M, Mari D, Salvioli S, et al. Metabolic Signatures of Extreme Longevity in Northern Italian Centenarians Reveal a Complex Remodeling of Lipids, Amino Acids, and Gut Microbiota Metabolism. *PLoS One* 2013;8:e56564. <https://doi.org/10.1371/JOURNAL.PONE.0056564>.

Collura TF. History and evolution of electroencephalographic instruments and techniques. *J Clin Neurophysiol* 1993;10:476–504. <https://doi.org/10.1097/00004691-199310000-00007>.

Colom-Cadena M, Spires-Jones T, Zetterberg H, Blennow K, Caggiano A, Dekosky ST, et al. The clinical promise of biomarkers of synapse damage or loss in Alzheimer's disease. *Alzheimer's Research & Therapy* 2020 12:1 2020;12:1–12. <https://doi.org/10.1186/S13195-020-00588-4>.

Conrad F, Mälzer M, Schwarzenberger M, Wiemer H, Ihlenfeldt S. Benchmarking AutoML for regression tasks on small tabular data in materials design. *Sci Rep* 2022;12:19350. <https://doi.org/10.1038/S41598-022-23327-1>.

Costafreda SG. Pooling fMRI data: Meta-analysis, mega-analysis and multi-center studies. *Front Neuroinform* 2009;3:639. <https://doi.org/10.3389/NEURO.11.033.2009/BIBTEX>.

Coughlan GT, Betthauser TJ, Boyle R, Koscik RL, Klinger HM, Chibnik LB, et al. Association of Age at Menopause and Hormone Therapy Use With Tau and β-Amyloid Positron Emission Tomography. *JAMA Neurol* 2023;80:462–73. <https://doi.org/10.1001/JAMANEUROL.2023.0455>.

Cozac V V., Gschwandtner U, Hatz F, Hardmeier M, Rüegg S, Fuhr P. Quantitative EEG and cognitive decline in Parkinson's disease. *Parkinsons Dis* 2016;2016. <https://doi.org/10.1155/2016/9060649>.

Dauwels J, Srinivasan K, Ramasubba Reddy M, Musha T, Vialatte FB, Latchoumane C, et al. Slowing and loss of complexity in Alzheimer's EEG: Two sides of the same coin? *Int J Alzheimers Dis* 2011. <https://doi.org/10.4061/2011/539621>.

Donaghay PC, McKeith IG. The clinical characteristics of dementia with Lewy bodies and a consideration of prodromal diagnosis. *Alzheimers Res Ther* 2014;6:46. <https://doi.org/10.1186/alzrt274>.

Donoghue T, Dominguez J, Voytek B. Electrophysiological Frequency Band Ratio Measures Conflate Periodic and Aperiodic Neural Activity. *ENeuro* 2020a;7. <https://doi.org/10.1523/ENEURO.0192-20.2020>.

Donoghue T, Haller M, Peterson EJ, Varma P, Sebastian P, Gao R, et al. Parameterizing neural power spectra into periodic and aperiodic components. *Nature Neuroscience* 2020 23:12 2020b;23:1655–65. <https://doi.org/10.1038/s41593-020-00744-x>.

Dottori M, Sedenõ L, Martorell Caro M, Alifano F, Hesse E, Mikulan E, et al. Towards affordable biomarkers of frontotemporal dementia: A classification study via network's information sharing. *Sci Rep* 2017;7. <https://doi.org/10.1038/s41598-017-04204-8>.

Duan W, Chen X, Wang YJ, Zhao W, Yuan H, Lei X. Reproducibility of power spectrum, functional connectivity and network construction in resting-state EEG. *J Neurosci Methods* 2021;348:108985. <https://doi.org/10.1016/J.JNEUMETH.2020.108985>.

Dubois B, Feldman HH, Jacova C, Hampel H, Molinuevo JL, Blennow K, et al. Advancing research diagnostic criteria for Alzheimer's disease: the IWG-2 criteria. *Lancet Neurol* 2014;13:614–29. [https://doi.org/10.1016/S1474-4422\(14\)70090-0](https://doi.org/10.1016/S1474-4422(14)70090-0).

Dubois B, Villain N, Frisoni GB, Rabinovici GD, Sabbagh M, Cappa S, et al. Clinical diagnosis of Alzheimer's disease: recommendations of the International Working Group. *Lancet Neurol* 2021;20:484–96. [https://doi.org/10.1016/S1474-4422\(21\)00066-1](https://doi.org/10.1016/S1474-4422(21)00066-1).

Duran-Aniotz C, Orellana P, Leon Rodriguez T, Henriquez F, Cabello V, Aguirre-Pinto MF, et al. Systematic Review: Genetic, Neuroimaging, and Fluids Biomarkers for Frontotemporal Dementia Across Latin America Countries. *Front Neurol* 2021;12:663407. <https://doi.org/10.3389/FNEUR.2021.663407/BIBTEX>.

Elahi FM, Miller BL. A clinicopathological approach to the diagnosis of dementia. *Nat Rev Neurol* 2017;13:457. <https://doi.org/10.1038/NRNEUROL.2017.96>.

Engemann DA, Mellot A, Höchenberger R, Banville H, Sabbagh D, Gemein L, et al. A reusable benchmark of brain-age prediction from M/EEG resting-state signals. *Neuroimage* 2022;262. <https://doi.org/10.1016/J.NEUROIMAGE.2022.119521>.

Engemann DA, Raimondo F, King JR, Rohaut B, Louppe G, Faugeras F, et al. Robust EEG-based cross-site and cross-protocol classification of states of consciousness. *Brain* 2018;141:3179–92. <https://doi.org/10.1093/BRAIN/AWY251>.

Erickson N, Mueller J, Shirkov A, Zhang H, Larroy P, Li M, et al. AutoGluon-Tabular: Robust and Accurate AutoML for Structured Data 2020.

Fide E, Hünerli-Gündüz D, Öztura İ, Yener GG. Hyperconnectivity matters in early-onset Alzheimer's disease: a resting-state EEG connectivity study. *Neurophysiologie Clinique* 2022;52:459–71. <https://doi.org/10.1016/J.NEUCLI.2022.10.003>.

Finger EC. Frontotemporal dementias. *CONTINUUM Lifelong Learning in Neurology* 2016;22:464–89. <https://doi.org/10.1212/CON.0000000000000300>.

Fladby T, Palhaugen L, Selnes P, Waterloo K, Brathen G, Hessen E, et al. Detecting At-Risk Alzheimer's Disease Cases. *J Alzheimers Dis* 2017;60:97–105. <https://doi.org/10.3233/JAD-170231>.

Fonseca LC, Tedrus GMAS, Letro GH, Bossoni AS. Dementia, Mild Cognitive Impairment and Quantitative EEG in Patients with Parkinson's Disease. <Https://DoiOrg/101177/155005940904000309> 2009;40:168–72. <https://doi.org/10.1177/155005940904000309>.

Forchetti CM. Treating Patients With Moderate to Severe Alzheimer's Disease: Implications of Recent Pharmacologic Studies. *Prim Care Companion J Clin Psychiatry* 2005;7:155. <https://doi.org/10.4088/PCC.V07N0403>.

Fortin JP, Cullen N, Sheline YI, Taylor WD, Aselcioglu I, Cook PA, et al. Harmonization of cortical thickness measurements across scanners and sites. *Neuroimage* 2018;167:104–20. <https://doi.org/10.1016/j.neuroimage.2017.11.024>.

Frahm-Falkenberg S, Ibsen R, Kjellberg J, Jennum P. Health, social and economic consequences of dementias: a comparative national cohort study. *Eur J Neurol* 2016;23:1400–7. <https://doi.org/10.1111/ENE.13043>.

Franceschi C, Garagnani P, Morsiani C, Conte M, Santoro A, Grignolio A, et al. The continuum of aging and age-related diseases: Common mechanisms but different rates. *Front Med (Lausanne)* 2018a;5:349810. <https://doi.org/10.3389/FMED.2018.00061/BIBTEX>.

Franceschi C, Garagnani P, Parini P, Giuliani C, Santoro A. Inflammaging: a new immune–metabolic viewpoint for age-related diseases. *Nature Reviews Endocrinology* 2018 14:10 2018b;14:576–90. <https://doi.org/10.1038/s41574-018-0059-4>.

Franciotti R, Pilotto A, Moretti D V., Falasca NW, Arnaldi D, Taylor JP, et al. Anterior EEG slowing in dementia with Lewy bodies: a multicenter European cohort study. *Neurobiol Aging* 2020;93:55–60. <https://doi.org/10.1016/j.neurobiolaging.2020.04.023>.

Gao R, Peterson EJ, Voytek B. Inferring synaptic excitation/inhibition balance from field potentials. *Neuroimage* 2017;158:70–8. <https://doi.org/10.1016/J.NEUROIMAGE.2017.06.078>.

García-Pretelt FJ, Suárez-Relevo JX, Aguilera-Niño DF, Lopera-Restrepo FJ, Ochoa-Gómez JF, Tobón-Quintero CA. Automatic Classification of Subjects of the PSEN1-E280A Family at Risk of Developing Alzheimer's Disease Using Machine Learning and Resting State Electroencephalography. *Journal of Alzheimer's Disease* 2022;87:817–32. <https://doi.org/10.3233/JAD-210148>.

Garn H, Coronel C, Waser M, Caravias G, Ransmayr G. Differential diagnosis between patients with probable Alzheimer's disease, Parkinson's disease dementia, or dementia with Lewy bodies and frontotemporal dementia, behavioral variant, using quantitative electroencephalographic features. *J Neural Transm* 2017;124:569. <https://doi.org/10.1007/S00702-017-1699-6>.

Gaubert S, Houot M, Raimondo F, Ansart M, Corsi MC, Naccache L, et al. A machine learning approach to screen for preclinical Alzheimer's disease. *Neurobiol Aging* 2021;105:205–16. <https://doi.org/10.1016/J.NEUBIOLAGING.2021.04.024>.

Gaubert S, Raimondo F, Houot M, Corsi MC, Naccache L, Sitt JD, et al. EEG evidence of compensatory mechanisms in preclinical Alzheimer's disease. *Brain* 2019;142:2096–112. <https://doi.org/10.1093/BRAIN/AWZ150>.

Gauthier S, Zhang H, Ng KP, Pascoal TA, Rosa-Neto P. Impact of the biological definition of Alzheimer's disease using amyloid, tau and neurodegeneration (ATN): what about the role of vascular changes, inflammation, Lewy body pathology? *Transl Neurodegener* 2018;7. <https://doi.org/10.1186/S40035-018-0117-9>.

Geraedts VJ, Boon LI, Marinus J, Gouw AA, Van Hilten JJ, Stam CJ, et al. Clinical correlates of quantitative EEG in Parkinson disease: A systematic review. *Neurology* 2018;91:871–83. <https://doi.org/10.1212/WNL.0000000000006473>.

Gerster M, Waterstraat G, Litvak V, Lehnertz K, Schnitzler A, Florin E, et al. Separating Neural Oscillations from Aperiodic 1/f Activity: Challenges and Recommendations. *Neuroinformatics* 2022;20:991–1012. <https://doi.org/10.1007/S12021-022-09581-8/FIGURES/8>.

Gil Ávila C, Bott FS, Tiemann L, Hohn VD, May ES, Nickel MM, et al. DISCOVER-EEG: an open, fully automated EEG pipeline for biomarker discovery in clinical neuroscience. *Scientific Data* 2023 10:1 2023;10:1–14. <https://doi.org/10.1038/s41597-023-02525-0>.

Gilbert DL, Sethuraman G, Kotagal U, Buncher CR. Meta-analysis of EEG test performance shows wide variation among studies. *Neurology* 2003;60:564–70. <https://doi.org/10.1212/01.WNL.0000044152.79316.27>.

Gimenez-Aparisi G, Guijarro-Estelles E, Chornet-Lurbe A, Ballesta-Martinez S, Pardo-Hernandez M, Ye-Lin Y. Early detection of Parkinson's disease: Systematic analysis of the influence of the eyes on quantitative biomarkers in resting state electroencephalography. *Heliyon* 2023;9:e20625. <https://doi.org/10.1016/J.HELIYON.2023.E20625>.

Goetz CG. The History of Parkinson's Disease: Early Clinical Descriptions and Neurological Therapies. *Cold Spring Harb Perspect Med* 2011;1. <https://doi.org/10.1101/CSHPERSPECT.A008862>.

Goh Cindy, Hamadicharef Brahim, Henderson Goeff T, Ifeachor Emmanuel C, Goh C, Hamadicharef B, et al. Comparison of Fractal Dimension Algorithms for the Computation of EEG Biomarkers for Dementia. 2nd International Conference on Computational Intelligence in Medicine and Healthcare (CIMED2005), Lisbon: 2005.

Gordillo D, Ramos da Cruz J, Moreno D, Garobbio S, Herzog MH. Do we really measure what we think we are measuring? *IScience* 2023;26. <https://doi.org/10.1016/J.ISCI.2023.106017>.

Gouw AA, Stam CJ. Electroencephalography in the Differential Diagnosis of Dementia. *Epileptologie* 2016;33:173–82.

Gramfort A, Luessi M, Larson E, Engemann DA, Strohmeier D, Brodbeck C, et al. MEG and EEG data analysis with MNE-Python. *Front Neurosci* 2013;0:267. <https://doi.org/10.3389/fnins.2013.00267>.

Granatiero V, Manfredi G. Mitochondrial Transport and Turnover in the Pathogenesis of Amyotrophic Lateral Sclerosis. *Biology* 2019, Vol 8, Page 36 2019;8:36. <https://doi.org/10.3390/BIOLOGY8020036>.

Grimbert F, Faugeras O. Analysis of Jansen's model of a single cortical column. vol. 18. 2006.

- Gudmundsson S, Runarsson TP, Sigurdsson S, Eiriksdottir G, Johnsen K. Reliability of quantitative EEG features. *Clinical Neurophysiology* 2007;118:2162–71. <https://doi.org/10.1016/j.clinph.2007.06.018>.
- Gustavsson A, Norton N, Fast T, Frölich L, Georges J, Holzapfel D, et al. Global estimates on the number of persons across the Alzheimer's disease continuum. *Alzheimer's & Dementia* 2023;19:658–70. <https://doi.org/10.1002/ALZ.12694>.
- Haas LF. Hans Berger (1873–1941), Richard Caton (1842–1926), and electroencephalography. *J Neurol Neurosurg Psychiatry* 2003;74:9–9. <https://doi.org/10.1136/JNNP.74.1.9>.
- Habich A, Wahlund LO, Westman E, Dierks T, Ferreira D. (Dis-)Connected Dots in Dementia with Lewy Bodies—A Systematic Review of Connectivity Studies. *Movement Disorders* 2023;38:4–15. <https://doi.org/10.1002/MDS.29248>.
- Hag A, Handayani D, Pillai T, Mantoro T, Kit MH, Al-Shargie F. EEG Mental Stress Assessment Using Hybrid Multi-Domain Feature Sets of Functional Connectivity Network and Time-Frequency Features. *Sensors* 2021, Vol 21, Page 6300 2021;21:6300. <https://doi.org/10.3390/S21186300>.
- Halgren M, Ulbert I, Bastuji H, Fabó D, Eross L, Rey M, et al. The generation and propagation of the human alpha rhythm. *Proc Natl Acad Sci U S A* 2019;116:23772–82. https://doi.org/10.1073/PNAS.1913092116/SUPPL_FILE/PNAS.1913092116.SAPP.PDF.
- Hampel H, Lista S, Neri C, Vergallo A. Time for the systems-level integration of aging: Resilience enhancing strategies to prevent Alzheimer's disease. *Prog Neurobiol* 2019;181. <https://doi.org/10.1016/J.PNEUROBIO.2019.101662>.
- Harada CN, Natelson Love MC, Triebel KL. Normal Cognitive Aging. *Clin Geriatr Med* 2013;29:737. <https://doi.org/10.1016/J.CGER.2013.07.002>.
- Harding RJ, Bermudez P, Bernier A, Beauvais M, Bellec P, Hill S, et al. The Canadian Open Neuroscience Platform—An open science framework for the neuroscience community. *PLoS Comput Biol* 2023;19. <https://doi.org/10.1371/JOURNAL.PCBI.1011230>.
- Hatlestad-Hall C. SRM Resting-state EEG - OpenNeuro. *OpenNeuro* 2022.
- Hatlestad-Hall C, Rygvold TW, Andersson S. BIDS-structured resting-state electroencephalography (EEG) data extracted from an experimental paradigm. *Data Brief* 2022;45. <https://doi.org/10.1016/J.DIB.2022.108647>.
- Hayashi S, Caron BA, Heinsfeld AS, Vinci-Booher S, McPherson B, Bullock DN, et al. brainlife.io: A decentralized and open source cloud platform to support neuroscience research 2023.
- He BJ. Scale-free brain activity: past, present, and future. *Trends Cogn Sci* 2014;18:480–7. <https://doi.org/10.1016/J.TICS.2014.04.003>.
- He W, Donoghue T, Sowman PF, Seymour RA, Brock J, Crain S, et al. Co-Increasing Neuronal Noise and Beta Power in the Developing Brain. *BioRxiv* 2019;839258. <https://doi.org/10.1101/839258>.
- Hebling Vieira B, Liem F, Dadi K, Engemann DA, Gramfort A, Bellec P, et al. Predicting future cognitive decline from non-brain and multimodal brain imaging data in healthy and pathological aging. *Neurobiol Aging* 2022;118:55–65. <https://doi.org/10.1016/J.NEUROBIOLAGING.2022.06.008>.
- Hendriks S, Peetoom K, Bakker C, Van Der Flier WM, Papma JM, Koopmans R, et al. Global Prevalence of Young-Onset Dementia: A Systematic Review and Meta-analysis. *JAMA Neurol* 2021;78:1080–90. <https://doi.org/10.1001/JAMANEUROL.2021.2161>.
- Hill AT, Clark GM, Bigelow FJ, Lum JAG, Enticott PG. Periodic and aperiodic neural activity displays age-dependent changes across early-to-middle childhood. *Dev Cogn Neurosci* 2022;54:101076. <https://doi.org/10.1016/J.DCN.2022.101076>.
- Hinchliffe C, Yogarajah M, Elkommos S, Tang H, Abasolo D. Entropy Measures of Electroencephalograms towards the Diagnosis of Psychogenic Non-Epileptic Seizures. *Entropy* 2022;24. <https://doi.org/10.3390/E24101348/S1>.
- Hjorth B. EEG analysis based on time domain properties. *Electroencephalogr Clin Neurophysiol* 1970;29:306–10. [https://doi.org/10.1016/0013-4694\(70\)90143-4](https://doi.org/10.1016/0013-4694(70)90143-4).
- Hock EM, Polymenidou M. Prion-like propagation as a pathogenic principle in frontotemporal dementia. *J Neurochem* 2016a;138:163–83. <https://doi.org/10.1111/JNC.13668>.
- Hock EM, Polymenidou M. Prion-like propagation as a pathogenic principle in frontotemporal dementia. *J Neurochem* 2016b;138 Suppl 1:163–83. <https://doi.org/10.1111/JNC.13668>.

Hogan DB, Jetté N, Fiest KM, Roberts JI, Pearson D, Smith EE, et al. The Prevalence and Incidence of Frontotemporal Dementia: a Systematic Review. Canadian Journal of Neurological Sciences 2016;43:S96–109. <https://doi.org/10.1017/CJN.2016.25>.

Horng H, Singh A, Yousefi B, Cohen EA, Haghghi B, Katz S, et al. Improved generalized ComBat methods for harmonization of radiomic features. Sci Rep 2022;12. <https://doi.org/10.1038/s41598-022-23328-0>.

Hu F, Chen AA, Horng H, Bashyam V, Davatzikos C, Alexander-Bloch A, et al. Image harmonization: A review of statistical and deep learning methods for removing batch effects and evaluation metrics for effective harmonization. Neuroimage 2023;274:120125. <https://doi.org/10.1016/J.NEUROIMAGE.2023.120125>.

Huang C, Wahlund LO, Dierks T, Julin P, Winblad B, Jelic V. Discrimination of Alzheimer's disease and mild cognitive impairment by equivalent EEG sources: A cross-sectional and longitudinal study. Clinical Neurophysiology 2000;111:1961–7. [https://doi.org/10.1016/S1388-2457\(00\)00454-5](https://doi.org/10.1016/S1388-2457(00)00454-5).

Isaza VH, Castro VC, Saldarriaga LZ, Mantilla-Ramos Y, Quintero CT, Suarez-Revelo J, et al. Tackling EEG test-retest reliability with a pre-processing pipeline based on ICA and wavelet-ICA. Authorea Preprints 2023. <https://doi.org/10.22541/AU.168570191.12788016/V1>.

Iturria-Medina Y, Sotero RC, Toussaint PJ, Mateos-Pérez JM, Evans AC, Weiner MW, et al. Early role of vascular dysregulation on late-onset Alzheimer's disease based on multifactorial data-driven analysis. Nature Communications 2016;7:1 2016;7:1–14. <https://doi.org/10.1038/ncomms11934>.

Jack CR, Bennett DA, Blennow K, Carrillo MC, Feldman HH, Frisoni GB, et al. A/T/N: An unbiased descriptive classification scheme for Alzheimer disease biomarkers. Neurology 2016;87:539–47. <https://doi.org/10.1212/WNL.0000000000002923>.

Jack CR, Knopman DS, Jagust WJ, Petersen RC, Weiner MW, Aisen PS, et al. Tracking pathophysiological processes in Alzheimer's disease: an updated hypothetical model of dynamic biomarkers. Lancet Neurol 2013;12:207–16. [https://doi.org/10.1016/S1474-4422\(12\)70291-0](https://doi.org/10.1016/S1474-4422(12)70291-0).

Jacobs HIL, Radua J, Lückmann HC, Sack AT. Meta-analysis of functional network alterations in Alzheimer's disease: toward a network biomarker. Neurosci Biobehav Rev 2013;37:753–65. <https://doi.org/10.1016/J.NEUBIOREV.2013.03.009>.

Jaotombo F, Adorni L, Ghattas B, Boyer L. Finding the best trade-off between performance and interpretability in predicting hospital length of stay using structured and unstructured data. PLoS One 2023;18:e0289795. <https://doi.org/10.1371/JOURNAL.PONE.0289795>.

Jaramillo-Jimenez A, Suarez-Revelo JX, Ochoa-Gomez JF, Carmona Arroyave JA, Bocanegra Y, Lopera F, et al. Resting-state EEG alpha/theta ratio related to neuropsychological test performance in Parkinson's Disease. Clinical Neurophysiology 2021;132:756–64. <https://doi.org/10.1016/j.clinph.2021.01.001>.

Jaramillo-Jimenez A, Tovar-Rios DA, Ospina JA, Mantilla-Ramos YJ, Loaiza-López D, Henao Isaza V, et al. Spectral features of resting-state EEG in Parkinson's Disease: A multicenter study using functional data analysis. Clin Neurophysiol 2023;151:28–40. <https://doi.org/10.1016/J.CLINPH.2023.03.363>.

Jas M, Engemann DA, Bekhti Y, Raimondo F, Gramfort A. Autoreject: Automated artifact rejection for MEG and EEG data. Neuroimage 2017;159:417–29. <https://doi.org/10.1016/j.neuroimage.2017.06.030>.

Jellinger KA, Attems J. Prevalence and impact of vascular and Alzheimer pathologies in Lewy body disease. Acta Neuropathol 2008;115:427–36. <https://doi.org/10.1007/S00401-008-0347-5/TABLES/3>.

Jellinger KA, Korczyn AD. Are dementia with Lewy bodies and Parkinson's disease dementia the same disease? BMC Med 2018;16. <https://doi.org/10.1186/S12916-018-1016-8>.

Jennekens FGI. A short history of the notion of neurodegenerative disease. J Hist Neurosci 2014;23:85–94. <https://doi.org/10.1080/0964704X.2013.809297>.

Jiao B, Li R, Zhou H, Qing K, Liu H, Pan H, et al. Neural biomarker diagnosis and prediction to mild cognitive impairment and Alzheimer's disease using EEG technology. Alzheimers Res Ther 2023;15:1–14. <https://doi.org/10.1186/S13195-023-01181-1/FIGURES/6>.

Jin L, Nawaz H, Ono K, Nowell J, Haley E, Berman BD, et al. One Minute of EEG Data Provides Sufficient and Reliable Data for Identifying Lewy Body Dementia. Alzheimer Dis Assoc Disord 2023;37:66–72. <https://doi.org/10.1097/WAD.0000000000000536>.

Johnson WE, Li C, Rabinovic A. Adjusting batch effects in microarray expression data using empirical Bayes methods. *Biostatistics* 2007;8:118–27. <https://doi.org/10.1093/biostatistics/kxj037>.

Jovicich J, Barkhof F, Babiloni C, Herholz K, Mulert C, van Berckel BNM, et al. Harmonization of neuroimaging biomarkers for neurodegenerative diseases: A survey in the imaging community of perceived barriers and suggested actions. *Alzheimer's & Dementia: Diagnosis, Assessment & Disease Monitoring* 2019;11:69. <https://doi.org/10.1016/J.DADM.2018.11.005>.

Julin P, Wahlund LO, Basun H, Persson A, Måre K, Rudberg U. Clinical diagnosis of frontal lobe dementia and Alzheimer's disease: relation to cerebral perfusion, brain atrophy and electroencephalography. *Dementia* 1995;6:142–7. <https://doi.org/10.1159/000106937>.

Kamboj N, Metcalfe K, Chu CH, Conway A. Predicting Blood Pressure After Nitroglycerin Infusion Dose Titration in Critical Care Units: A Multicenter Retrospective Study. *Comput Inform Nurs* 2023. <https://doi.org/10.1097/CIN.0000000000001086>.

Keil A, Bernat EM, Cohen MX, Ding M, Fabiani M, Gratton G, et al. Recommendations and publication guidelines for studies using frequency domain and time-frequency domain analyses of neural time series. *Psychophysiology* 2022;59:e14052. <https://doi.org/10.1111/PSYP.14052>.

Keller SM, Gschwandtner U, Meyer A, Chaturvedi M, Roth V, Fuhr P. Cognitive decline in Parkinson's disease is associated with reduced complexity of EEG at baseline. *Brain Commun* 2020;2. <https://doi.org/10.1093/BRAINCOMMS/FCAA207>.

Kertesz A. Pick complex--historical introduction. *Alzheimer Dis Assoc Disord* 2007;21. <https://doi.org/10.1097/WAD.0B013E31815BF65A>.

Khoury R, Ghossoub E. Diagnostic biomarkers of Alzheimer's disease: A state-of-the-art review. *Biomark Neuropsychiatry* 2019;1:100005. <https://doi.org/10.1016/J.BIONPS.2019.100005>.

Kinge JM, Dieleman JL, Karlstad Ø, Knudsen AK, Klitkou ST, Hay SI, et al. Disease-specific health spending by age, sex, and type of care in Norway: a national health registry study. *BMC Med* 2023;21:1–14. <https://doi.org/10.1186/S12916-023-02896-6/FIGURES/3>.

Klietz M. Caregiver Burden in Movement Disorders and Neurodegenerative Diseases: Editorial. *Brain Sci* 2022;12. <https://doi.org/10.3390/BRAINSCI12091184>.

Klimesch W. EEG alpha and theta oscillations reflect cognitive and memory performance: a review and analysis. *Brain Res Brain Res Rev* 1999;29:169–95. [https://doi.org/10.1016/S0165-0173\(98\)00056-3](https://doi.org/10.1016/S0165-0173(98)00056-3).

Klimesch W, Sauseng P, Hanslmayr S. EEG alpha oscillations: The inhibition–timing hypothesis. *Brain Res Rev* 2007;53:63–88. <https://doi.org/10.1016/J.BRAINRESREV.2006.06.003>.

Klonowski W. Everything you wanted to ask about EEG but were afraid to get the right answer. *Nonlinear Biomed Phys* 2009;3:2. <https://doi.org/10.1186/1753-4631-3-2>.

Koelewijn L, Lancaster TM, Linden D, Dima DC, Routley BC, Magazzini L, et al. Oscillatory hyperactivity and hyperconnectivity in young APOE-ε4 carriers and hypoconnectivity in alzheimer's disease. *Elife* 2019;8. <https://doi.org/10.7554/ELIFE.36011>.

Kopčanová M, Tait L, Donoghue T, Stothat G, Smith L, Sandoval AAF, et al. Resting-state EEG signatures of Alzheimer's disease are driven by periodic but not aperiodic changes. *BioRxiv* 2023. <https://doi.org/10.1101/2023.06.11.544491>.

Kosaka K. Lewy body disease and dementia with Lewy bodies. *Proc Jpn Acad Ser B Phys Biol Sci* 2014;90:301. <https://doi.org/10.2183/PJAB.90.301>.

Kottlarz I, Berg S, Toscano-Tejeida D, Steinmann I, Bähr M, Luther S, et al. Extracting Robust Biomarkers From Multichannel EEG Time Series Using Nonlinear Dimensionality Reduction Applied to Ordinal Pattern Statistics and Spectral Quantities. *Front Physiol* 2020;11:614565. <https://doi.org/10.3389/FPHYS.2020.614565>.

Kropotov JD. Alpha Rhythms. *Functional Neuromarkers for Psychiatry* 2016:89–105. <https://doi.org/10.1016/B978-0-12-410513-3.00008-5>.

Kurbatskaya A, Jaramillo-Jimenez A, Fredy Ochoa-Gomez J, Brønnick K, Fernandez-Quilez A. Machine Learning-Based Detection of Parkinson's Disease From Resting-State EEG: A Multi-Center Study. *ArXiv* 2023a.

- Kurbatskaya A, Jaramillo-Jimenez A, Ochoa-Gomez JF, Brønnick K, Fernandez-Quilez A. Assessing gender fairness in EEG-based machine learning detection of Parkinson's disease: A multi-center study 2023b:1020–4. <https://doi.org/10.23919/eusipco58844.2023.10289837>.
- Lai M, Demuru M, Hillebrand A, Fraschini M. A comparison between scalp- and source-reconstructed EEG networks. *Sci Rep* 2018;8. <https://doi.org/10.1038/s41598-018-30869-w>.
- Larson MJ, Carbine KA. Sample size calculations in human electrophysiology (EEG and ERP) studies: A systematic review and recommendations for increased rigor. *International Journal of Psychophysiology* 2017;111:33–41. <https://doi.org/10.1016/j.ijpsycho.2016.06.015>.
- Lashgari E, Liang D, Maoz U. Data augmentation for deep-learning-based electroencephalography. *J Neurosci Methods* 2020;346. <https://doi.org/10.1016/J.JNEUMETH.2020.108885>.
- Lau ZJ, Pham T, Chen SHA, Makowski D. Brain entropy, fractal dimensions and predictability: A review of complexity measures for EEG in healthy and neuropsychiatric populations. *Eur J Neurosci* 2022;56:5047. <https://doi.org/10.1111/EJN.15800>.
- Law ZK, Todd C, Mehraram R, Schumacher J, Baker MR, LeBeau FEN, et al. The role of EEG in the diagnosis, prognosis and clinical correlations of dementia with Lewy bodies—a systematic review. *Diagnostics* 2020;10:616. <https://doi.org/10.3390/diagnostics10090616>.
- Lenkala S, Marry R, Gopovaram SR, Akinci TC, Topsakal O. Comparison of Automated Machine Learning (AutoML) Tools for Epileptic Seizure Detection Using Electroencephalograms (EEG). *Computers* 2023, Vol 12, Page 197 2023;12:197. <https://doi.org/10.3390/COMPUTERS12100197>.
- Li A, Feitelberg J, Saini AP, Höchenberger R, Scheltienne M. MNE-ICALabel: Automatically annotating ICA components with ICLLabel in Python. *J Open Source Softw* 2022;7:4484. <https://doi.org/10.21105/joss.04484>.
- Li M, Wang Y, Lopez-Naranjo C, Hu S, Reyes RCG, Paz-Linares D, et al. Harmonized-Multinational qEEG norms (HarMNqEEG). *Neuroimage* 2022;256:119190. <https://doi.org/10.1016/j.neuroimage.2022.119190>.
- Light GA, Swerdlow NR, Thomas ML, Calkins ME, Green MF, Greenwood TA, et al. Validation of mismatch negativity and P3a for use in multi-site studies of schizophrenia: characterization of demographic, clinical, cognitive, and functional correlates in COGS-2. *Schizophr Res* 2015;163:63–72. <https://doi.org/10.1016/J.SCHRES.2014.09.042>.
- Lin C-Y, Guo S-M, Lien J-JJ, Lin W-T, Liu Y-S, Lai C-H, et al. Combined model integrating deep learning, radiomics, and clinical data to classify lung nodules at chest CT. *Radiol Med* 2023. <https://doi.org/10.1007/S11547-023-01730-6>.
- Lindau M, Jelic V, Johansson SE, Andersen C, Wahlund LO, Almkvist O. Quantitative EEG abnormalities and cognitive dysfunctions in frontotemporal dementia and Alzheimer's disease. *Dement Geriatr Cogn Disord* 2003;15:106–14. <https://doi.org/10.1159/000067973>.
- Litvan I, Goldman JG, Tröster AI, Schmand BA, Weintraub D, Petersen RC, et al. Diagnostic criteria for mild cognitive impairment in Parkinson's disease: Movement Disorder Society Task Force guidelines. *Movement Disorders* 2012;27:349–56. <https://doi.org/10.1002/mds.24893>.
- Liu J, Du Y, Wang X, Yue W, Feng J. Automated Machine Learning for Epileptic Seizure Detection Based on EEG Signals. *Computers, Materials & Continua* 2022;73:1995–2011. <https://doi.org/10.32604/CMC.2022.029073>.
- Liu L, Zhang R, Shi D, Li R, Wang Q, Feng Y, et al. Automated machine learning to predict the difficulty for endoscopic resection of gastric gastrointestinal stromal tumor. *Front Oncol* 2023;13:1190987. <https://doi.org/10.3389/FONC.2023.1190987/FULL>.
- Livingston G, Huntley J, Sommerlad A, Ames D, Ballard C, Banerjee S, et al. Dementia prevention, intervention, and care: 2020 report of the Lancet Commission. *The Lancet* 2020;396:413–46. [https://doi.org/10.1016/S0140-6736\(20\)30367-6/ATTACHMENT/DFC82F21-55AB-4950-8828-93F27077EF6D/MMC1.PDF](https://doi.org/10.1016/S0140-6736(20)30367-6/ATTACHMENT/DFC82F21-55AB-4950-8828-93F27077EF6D/MMC1.PDF).
- Llinás RR, Ribary U, Jeanmonod D, Kronberg E, Mitra PP. Thalamocortical dysrhythmia: A neurological and neuropsychiatric syndrome characterized by magnetoencephalography. *Proc Natl Acad Sci U S A* 1999;96:15222–7. <https://doi.org/10.1073/pnas.96.26.15222>.
- Llinás RR, Steriade M. Bursting of thalamic neurons and states of vigilance. *J Neurophysiol* 2006;95:3297–308. <https://doi.org/10.1152/JN.00166.2006/ASSET/IMAGES/LARGE/Z9K0060674860004.JPG>.

Logroscino G, Piccininni M, Graff C, Hardiman O, Ludolph AC, Moreno F, et al. Incidence of Syndromes Associated With Frontotemporal Lobar Degeneration in 9 European Countries. *JAMA Neurol* 2023;80:279–86. <https://doi.org/10.1001/JAMANEUROL.2022.5128>.

Lopes Da Silva F. EEG: Origin and measurement. EEG - FMRI: Physiological Basis, Technique, and Applications 2010:19–38. https://doi.org/10.1007/978-3-540-87919-0_2/FIGURES/3.

López-Sanz D, Brunà R, Garcés P, Camara C, Serrano N, Rodríguez-Rojo IC, et al. Alpha band disruption in the AD-continuum starts in the Subjective Cognitive Decline stage: a MEG study. *Scientific Reports* 2016;6:1 2016;6:1–11. <https://doi.org/10.1038/srep37685>.

Lundberg SM, Lee SI. A Unified Approach to Interpreting Model Predictions. *Adv Neural Inf Process Syst* 2017;2017-December:4766–75.

Lyketsos CG, Lopez O, Jones B, Fitzpatrick AL, Breitner J, Dekosky S. Prevalence of Neuropsychiatric Symptoms in Dementia and Mild Cognitive Impairment: Results From the Cardiovascular Health Study. *JAMA* 2002;288:1475–83. <https://doi.org/10.1001/JAMA.288.12.1475>.

Maestú F, de Haan W, Busche MA, DeFelipe J. Neuronal excitation/inhibition imbalance: core element of a translational perspective on Alzheimer pathophysiology. *Ageing Res Rev* 2021;69:101372. <https://doi.org/10.1016/J.ARR.2021.101372>.

Maresova P, Hruska J, Klimova B, Barakovic S, Krejcar O. Activities of Daily Living and Associated Costs in the Most Widespread Neurodegenerative Diseases: A Systematic Review. *Clin Interv Aging* 2020;15:1841. <https://doi.org/10.2147/CIA.S264688>.

Maserejian N, Vinikoor-Imler L, Dilley A. Estimation of the 2020 Global Population of Parkinson's Disease (PD) [abstract]. *Mov Disord* 2020;35.

Massa F, Meli R, Grazzini M, Famà F, De Carli F, Filippi L, et al. Utility of quantitative EEG in early Lewy body disease. *Parkinsonism Relat Disord* 2020;75:70–5. <https://doi.org/10.1016/j.parkreldis.2020.05.007>.

McBride JC, Zhao X, Munro NB, Smith CD, Jicha GA, Hively L, et al. Spectral and complexity analysis of scalp EEG characteristics for mild cognitive impairment and early Alzheimer's disease. *Comput Methods Programs Biomed* 2014;114:153–63. <https://doi.org/10.1016/J.CMPB.2014.01.019>.

McDonald WM. Overview of Neurocognitive Disorders. *Focus: Journal of Life Long Learning in Psychiatry* 2017;15:4. <https://doi.org/10.1176/APPI.FOCUS.20160030>.

McKeith IG, Boeve BF, Dickson DW, Halliday G, Taylor JP, Weintraub D, et al. Diagnosis and management of dementia with Lewy bodies. *Neurology* 2017;89:88–100. <https://doi.org/10.1212/WNL.0000000000004058>.

McKeith IG, Ferman TJ, Thomas AJ, Blanc F, Boeve BF, Fujishiro H, et al. Research criteria for the diagnosis of prodromal dementia with Lewy bodies. *Neurology* 2020;94:743–55. <https://doi.org/10.1212/WNL.0000000000009323>.

McKeown DJ, Jones M, Pihl C, Finley A, Kelley N, Baumann O, et al. Medication-invariant resting aperiodic and periodic neural activity in Parkinson's disease. *Psychophysiology* 2023;00:e14478. <https://doi.org/10.1111/PSYP.14478>.

McKhann G, Drachman D, Folstein M, Katzman R, Price D, Stadlan EM. Clinical diagnosis of alzheimer's disease: Report of the NINCDS-ADRDA work group under the auspices of department of health and human services task force on alzheimer's disease. *Neurology* 1984;34:939–44. <https://doi.org/10.1212/wnl.34.7.939>.

McKhann GM, Knopman DS, Chertkow H, Hyman BT, Jack CR, Kawas CH, et al. The diagnosis of dementia due to Alzheimer's disease: Recommendations from the National Institute on Aging-Alzheimer's Association workgroups on diagnostic guidelines for Alzheimer's disease. *Alzheimer's & Dementia* 2011;7:263–9. <https://doi.org/10.1016/J.JALZ.2011.03.005>.

Meeter LH, Kaat LD, Rohrer JD, Van Swieten JC. Imaging and fluid biomarkers in frontotemporal dementia. *Nature Reviews Neurology* 2017;13:7 2017;13:406–19. <https://doi.org/10.1038/nrneurol.2017.75>.

Meghdadi AH, Karic MS, McConnell M, Rupp G, Richard C, Hamilton J, et al. Resting state EEG biomarkers of cognitive decline associated with Alzheimer's disease and mild cognitive impairment. *PLoS One* 2021;16. <https://doi.org/10.1371/JOURNAL.PONE.0244180>.

Mehraram R, Kaiser M, Cromarty R, Graziadio S, O'Brien JT, Killen A, et al. Weighted network measures reveal differences between dementia types: An EEG study. *Hum Brain Mapp* 2020;41:1573. <https://doi.org/10.1002/HBM.24896>.

Melnik A, Legkov P, Izdebski K, Kärcher SM, Hairston WD, Ferris DP, et al. Systems, subjects, sessions: To what extent do these factors influence EEG data? *Front Hum Neurosci* 2017;11:245570. <https://doi.org/10.3389/FNHUM.2017.00150/BIBTEX>.

Menšíková K, Matěj R, Colosimo C, Rosales R, Tučková L, Ehrmann J, et al. Lewy body disease or diseases with Lewy bodies? *Npj Parkinson's Disease* 2022;8:1 2022;8:1–11. <https://doi.org/10.1038/s41531-021-00273-9>.

Merkin A, Sghirripa S, Graetz L, Smith AE, Hordacre B, Harris R, et al. Do age-related differences in aperiodic neural activity explain differences in resting EEG alpha? *Neurobiol Aging* 2023;121:78–87. <https://doi.org/10.1016/J.NEUROBIOLAGING.2022.09.003>.

Merkin A, Sghirripa S, Graetz L, Smith AE, Hordacre B, Harris R, et al. Age differences in aperiodic neural activity measured with resting EEG. *BioRxiv* 2021;2021.08.31.458328. <https://doi.org/10.1101/2021.08.31.458328>.

Mhyre TR, Boyd JT, Hamill RW, Maguire-Zeiss KA. Parkinson's disease. *Subcell Biochem* 2012;65:389–455. https://doi.org/10.1007/978-94-007-5416-4_16.

Miljevic A, Bailey NW, Vila-Rodriguez F, Herring SE, Fitzgerald PB. Electroencephalographic Connectivity: A Fundamental Guide and Checklist for Optimal Study Design and Evaluation. *Biol Psychiatry Cogn Neurosci Neuroimaging* 2022;7:546–54. <https://doi.org/10.1016/J.BPSC.2021.10.017>.

Miltiadous A, Tzimourta KD, Afrantou T, Ioannidis P, Grigoriadis N, Tsalikakis DG, et al. A Dataset of Scalp EEG Recordings of Alzheimer's Disease, Frontotemporal Dementia and Healthy Subjects from Routine EEG. *Data* 2023, Vol 8, Page 95 2023;8:95. <https://doi.org/10.3390/DATA8060095>.

Modir A, Shamekhi S, Ghaderyan P. A systematic review and methodological analysis of EEG-based biomarkers of Alzheimer's disease. *Measurement* 2023;220:113274. <https://doi.org/10.1016/J.MEASUREMENT.2023.113274>.

Moezzi B, Hordacre B, Berryman C, Ridding MC, Goldsworthy MR. Test-retest reliability of functional brain network characteristics using resting-state EEG and graph theory. *BioRxiv* 2018;385302. <https://doi.org/10.1101/385302>.

Moguilner S, Birba A, Fittipaldi S, Gonzalez-Campo C, Tagliazucchi E, Reyes P, et al. Multi-feature computational framework for combined signatures of dementia in underrepresented settings. *J Neural Eng* 2022;19:046048. <https://doi.org/10.1088/1741-2552/ac87d0>.

Mohanty R, Sethares WA, Nair VA, Prabhakaran V. Rethinking Measures of Functional Connectivity via Feature Extraction. *Scientific Reports* 2020;10:1 2020;10:1–17. <https://doi.org/10.1038/s41598-020-57915-w>.

Moretti D V. Theta and alpha EEG frequency interplay in subjects with mild cognitive impairment: evidence from EEG, MRI, and SPECT brain modifications. *Front Aging Neurosci* 2015;7. <https://doi.org/10.3389/FNAGI.2015.00031>.

Moretti D V, Babiloni C, Binetti G, Cassetta E, Dal Forno G, Ferreric F, et al. Individual analysis of EEG frequency and band power in mild Alzheimer's disease. *Clinical Neurophysiology* 2004;115:299–308. [https://doi.org/10.1016/S1388-2457\(03\)00345-6](https://doi.org/10.1016/S1388-2457(03)00345-6).

Moretti D V., Paternicò D, Binetti G, Zanetti O, Frisoni GB. EEG upper/low alpha frequency power ratio relates to temporo-parietal brain atrophy and memory performances in mild cognitive impairment. *Front Aging Neurosci* 2013;5:65285. <https://doi.org/10.3389/FNAGI.2013.00063/BIBTEX>.

Mouton A, Blanc F, Gros A, Manera V, Fabre R, Sauleau E, et al. Sex ratio in dementia with Lewy bodies balanced between Alzheimer's disease and Parkinson's disease dementia: a cross-sectional study. *Alzheimers Res Ther* 2018;10. <https://doi.org/10.1186/S13195-018-0417-4>.

Müller EJ, Munn B, Hearne LJ, Smith JB, Fulcher B, Arnatkevičiūtė A, et al. Core and matrix thalamic sub-populations relate to spatio-temporal cortical connectivity gradients. *Neuroimage* 2020;222:117224. <https://doi.org/10.1016/J.NEUROIMAGE.2020.117224>.

Müller EJ, Munn BR, Redinbaugh MJ, Lizier J, Breakspear M, Saalmann YB, et al. The non-specific matrix thalamus facilitates the cortical information processing modes relevant for conscious awareness. *Cell Rep* 2023;42:112844. <https://doi.org/10.1016/J.CELREP.2023.112844>.

Munn BR, Müller EJ, Medel V, Naismith SL, Lizier JT, Sanders RD, et al. Neuronal connected burst cascades bridge macroscale adaptive signatures across arousal states. *Nature Communications* 2023;14:1 2023;14:1–17. <https://doi.org/10.1038/s41467-023-42465-2>.

Musigmann M, Akkurt BH, Krähling H, Nacul NG, Remonda L, Sartoretti T, et al. Testing the applicability and performance of Auto ML for potential applications in diagnostic neuroradiology. *Sci Rep* 2022;12. <https://doi.org/10.1038/S41598-022-18028-8>.

Nandi A, Counts N, Chen S, Seligman B, Tortorice D, Vigo D, et al. Global and regional projections of the economic burden of Alzheimer's disease and related dementias from 2019 to 2050: A value of statistical life approach. *EClinicalMedicine* 2022;51:101580. <https://doi.org/10.1016/j.eclim.2022.101580>.

Narayanan Lab. Datasets 2020. <https://narayanan.lab.uiowa.edu/article/datasets> (accessed August 10, 2022).

Nardone R, Sebastianelli L, Versace V, Saltuari L, Lochner P, Frey V, et al. Usefulness of EEG Techniques in Distinguishing Frontotemporal Dementia from Alzheimer's Disease and Other Dementias. *Dis Markers* 2018;2018. <https://doi.org/10.1155/2018/6581490>.

Nedelska Z, Schwarz CG, Lesnick TG, Boeve BF, Przybelski SA, Lowe VJ, et al. Association of Longitudinal β-Amyloid Accumulation Determined by Positron Emission Tomography With Clinical and Cognitive Decline in Adults With Probable Lewy Body Dementia. *JAMA Netw Open* 2019;2:e1916439–e1916439. <https://doi.org/10.1001/JAMANETWORKOPEN.2019.16439>.

Neto E, Allen EA, Aurlien H, Nordby H, Eichele T. EEG spectral features discriminate between Alzheimer's and vascular dementia. *Front Neurol* 2015;6:108906. <https://doi.org/10.3389/FNEUR.2015.00025/ABSTRACT>.

Newson JJ, Thiagarajan TC. EEG Frequency Bands in Psychiatric Disorders: A Review of Resting State Studies. *Front Hum Neurosci* 2019;12. <https://doi.org/10.3389/fnhum.2018.00521>.

Nguyen-Danse DA, Singaravelu S, Chauvigné LAS, Mottaz A, Allaman L, Guggisberg AG. Feasibility of Reconstructing Source Functional Connectivity with Low-Density EEG. *Brain Topogr* 2021;34:709. <https://doi.org/10.1007/S10548-021-00866-W>.

Nichols E, Abd-Allah F, Abdoli A, Abosetugn AE, Abrha WA, Abualhasan A, et al. Global mortality from dementia: Application of a new method and results from the Global Burden of Disease Study 2019. *Alzheimer's & Dementia: Translational Research & Clinical Interventions* 2021;7:e12200. <https://doi.org/10.1002/TRC2.12200>.

Nichols E, Steinmetz JD, Vollset SE, Fukutaki K, Chalek J, Abd-Allah F, et al. Estimation of the global prevalence of dementia in 2019 and forecasted prevalence in 2050: an analysis for the Global Burden of Disease Study 2019. *Lancet Public Health* 2022;7:e105–25. [https://doi.org/10.1016/S2468-2667\(21\)00249-8](https://doi.org/10.1016/S2468-2667(21)00249-8).

Nichols E, Vos T. The estimation of the global prevalence of dementia from 1990–2019 and forecasted prevalence through 2050: An analysis for the Global Burden of Disease (GBD) study 2019. *Alzheimer's & Dementia* 2021;17:e051496. <https://doi.org/10.1002/alz.051496>.

van Nifterick AM, Mulder D, Duineveld DJ, Diachenko M, Scheltens P, Stam CJ, et al. Resting-state oscillations reveal disturbed excitation–inhibition ratio in Alzheimer's disease patients. *Scientific Reports* 2023;13:1 2023;13:1–13. <https://doi.org/10.1038/s41598-023-33973-8>.

Nishida K, Yoshimura M, Isotani T, Yoshida T, Kitaura Y, Saito A, et al. Differences in quantitative EEG between frontotemporal dementia and Alzheimer's disease as revealed by LORETA. *Clin Neurophysiol* 2011;122:1718–25. <https://doi.org/10.1016/J.CLINPH.2011.02.011>.

Nobukawa S, Yamanishi T, Nishimura H, Wada Y, Kikuchi M, Takahashi T. Atypical temporal-scale-specific fractal changes in Alzheimer's disease EEG and their relevance to cognitive decline. *Cogn Neurodyn* 2019;13:1–11. <https://doi.org/10.1007/S11571-018-9509-X/FIGURES/8>.

Nowrangi MA, Lyketsos CG, Rosenberg PB. Principles and management of neuropsychiatric symptoms in Alzheimer's dementia. *Alzheimers Res Ther* 2015;7:1–10. <https://doi.org/10.1186/S13195-015-0096-3/TABLES/2>.

Ou C, Liu J, Qian Y, Chong W, Liu D, He X, et al. Automated Machine Learning Model Development for Intracranial Aneurysm Treatment Outcome Prediction: A Feasibility Study. *Front Neurol* 2021;12:735142. <https://doi.org/10.3389/FNEUR.2021.735142/FULL>.

Ouchani M, Gharibzadeh S, Jamshidi M, Amini M. A Review of Methods of Diagnosis and Complexity Analysis of Alzheimer's Disease Using EEG Signals. *Biomed Res Int* 2021;2021. <https://doi.org/10.1155/2021/5425569>.

- Özbek Y, Fide E, Yener GG. Resting-state EEG alpha/theta power ratio discriminates early-onset Alzheimer's disease from healthy controls. *Clinical Neurophysiology* 2021;132:2019–31. <https://doi.org/10.1016/j.clinph.2021.05.012>.
- Palmqvist S, Schöll M, Strandberg O, Mattsson N, Stomrud E, Zetterberg H, et al. Earliest accumulation of β -amyloid occurs within the default-mode network and concurrently affects brain connectivity. *Nature Communications* 2017 8:1 2017;8:1–13. <https://doi.org/10.1038/s41467-017-01150-x>.
- Pappalettera C, Cacciotti A, Nucci L, Miraglia F, Rossini PM, Vecchio F. Approximate entropy analysis across electroencephalographic rhythmic frequency bands during physiological aging of human brain. *Geroscience* 2023;45:1131. <https://doi.org/10.1007/S11357-022-00710-4>.
- Parkinson J. An essay on the shaking palsy. 1817. *J Neuropsychiatry Clin Neurosci* 2002;14. <https://doi.org/10.1176/JNP.14.2.223>.
- Pavlov YG, Adamian N, Appelhoff S, Arvaneh M, Benwell CSY, Beste C, et al. #EEGManyLabs: Investigating the replicability of influential EEG experiments. *Cortex* 2021;144:213–29. <https://doi.org/10.1016/J.CORTEX.2021.03.013>.
- Pedroni A, Bahreini A, Langer N. Automagic: Standardized preprocessing of big EEG data. *Neuroimage* 2019;200:460–73. <https://doi.org/10.1016/J.NEUROIMAGE.2019.06.046>.
- Peraza LR, Cromarty R, Kobeleva X, Firbank MJ, Killen A, Graziadio S, et al. Electroencephalographic derived network differences in Lewy body dementia compared to Alzheimer's disease patients. *Scientific Reports* 2018 8:1 2018;8:1–13. <https://doi.org/10.1038/s41598-018-22984-5>.
- Perez-Valero E, Morillas C, Lopez-Gordo MA, Carrera-Muñoz I, López-Alcalde S, Vilchez-Carrillo RM. An Automated Approach for the Detection of Alzheimer's Disease From Resting State Electroencephalography. *Front Neuroinform* 2022;16:924547. <https://doi.org/10.3389/FNINF.2022.924547/BIBTEX>.
- Pernet C, Garrido MI, Gramfort A, Maurits N, Michel CM, Pang E, et al. Issues and recommendations from the OHBM COBIDAS MEG committee for reproducible EEG and MEG research. *Nature Neuroscience* 2020 23:12 2020;23:1473–83. <https://doi.org/10.1038/s41593-020-00709-0>.
- Pernet CR, Appelhoff S, Gorgolewski KJ, Flandin G, Phillips C, Delorme A, et al. EEG-BIDS, an extension to the brain imaging data structure for electroencephalography. *Sci Data* 2019;6:1–5. <https://doi.org/10.1038/s41597-019-0104-8>.
- Perry DC, Brown JA, Possin KL, Datta S, Trujillo A, Radke A, et al. Clinicopathological correlations in behavioural variant frontotemporal dementia. *Brain* 2017;140:3329–45. <https://doi.org/10.1093/BRAIN/AWX254>.
- Petersen RC, Aisen P, Boeve BF, Geda YE, Ivnik RJ, Knopman DS, et al. Criteria for Mild Cognitive Impairment Due to Alzheimer's Disease in the Community. *Ann Neurol* 2013;74:199. <https://doi.org/10.1002/ANA.23931>.
- Peterson EK. Associations Between EEG and Cognition in Parkinson's Disease. Christchurch, New Zealand: 2020.
- Pion-Tonachini L, Kreutz-Delgado K, Makeig S. ICLLabel: An automated electroencephalographic independent component classifier, dataset, and website. *Neuroimage* 2019;198:181. <https://doi.org/10.1016/J.NEUROIMAGE.2019.05.026>.
- Pippenger MA. How often is EEG used as part of routine dementia evaluation in community practice? *Alzheimer's & Dementia* 2021;17:e056638. <https://doi.org/10.1002/ALZ.056638>.
- Poil SS, de Haan W, van der Flier WM, Mansvelder HD, Scheltens P, Linkenaer-Hansen K. Integrative EEG biomarkers predict progression to Alzheimer's disease at the MCI stage. *Front Aging Neurosci* 2013;5. <https://doi.org/10.3389/FNAGI.2013.00058>.
- Pomponio R, Erus G, Habes M, Doshi J, Srinivasan D, Mamourian E, et al. Harmonization of large MRI datasets for the analysis of brain imaging patterns throughout the lifespan. *Neuroimage* 2020;208. <https://doi.org/10.1016/j.neuroimage.2019.116450>.
- Porsteinsson AP, Isaacson RS, Knox S, Sabbagh MN, Rubino I. Diagnosis of Early Alzheimer's Disease: Clinical Practice in 2021. *The Journal of Prevention of Alzheimer's Disease* 2021 8:3 2021;8:371–86. <https://doi.org/10.14283/JPAD.2021.23>.
- Portillo-Lara R, Tahirbegi B, Chapman CAR, Goding JA, Green RA. Mind the gap: State-of-the-art technologies and applications for EEG-based brain-computer interfaces. *APL Bioeng* 2021;5:31507. <https://doi.org/10.1063/5.0047237/149807>.

Postuma RB, Berg D, Stern M, Poewe W, Olanow CW, Oertel W, et al. MDS clinical diagnostic criteria for Parkinson's disease. *Movement Disorders* 2015;30:1591–601. <https://doi.org/10.1002/mds.26424>.

Prado P, Birba A, Cruzat J, Santamaría-García H, Parra M, Moguilner S, et al. Dementia ConnEEGtome: Towards multicentric harmonization of EEG connectivity in neurodegeneration. *International Journal of Psychophysiology* 2022;172:24–38. <https://doi.org/10.1016/j.ijpsycho.2021.12.008>.

Prado P, Moguilner S, Mejía JA, Sainz-Ballesteros A, Otero M, Birba A, et al. Source space connectomics of neurodegeneration: One-metric approach does not fit all. *Neurobiol Dis* 2023;179:106047. <https://doi.org/10.1016/J.NBD.2023.106047>.

Przedborski S, Vila M, Jackson-Lewis V. Series Introduction: Neurodegeneration: What is it and where are we? *Journal of Clinical Investigation* 2003;111:3–10. <https://doi.org/10.1172/jci17522>.

Puri D V., Nalbalwar SL, Nandgaonkar AB, Gawande JP, Wagh A. Automatic detection of Alzheimer's disease from EEG signals using low-complexity orthogonal wavelet filter banks. *Biomed Signal Process Control* 2023;81:104439. <https://doi.org/10.1016/J.BSPC.2022.104439>.

Querfurth HW, LaFerla FM. Alzheimer's Disease. *New England Journal of Medicine* 2010;362:329–44. <https://doi.org/10.1056/NEJMra0909142>.

Railo H. Parkinson's disease: Resting state EEG. *OSF* 2021. <https://osf.io/pehj9/> (accessed August 9, 2022).

Raj R, Kannath SK, Mathew J, Sylaja PN. AutoML accurately predicts endovascular mechanical thrombectomy in acute large vessel ischemic stroke. *Front Neurol* 2023a;14. <https://doi.org/10.3389/FNEUR.2023.1259958>.

Raj R, Kannath SK, Mathew J, Sylaja PN. AutoML accurately predicts endovascular mechanical thrombectomy in acute large vessel ischemic stroke. *Front Neurol* 2023b;14. <https://doi.org/10.3389/FNEUR.2023.1259958/FULL>.

Ranasinghe KG, Cha J, Iaccarino L, Hinkley LB, Beagle AJ, Pham J, et al. Neurophysiological signatures in Alzheimer's disease are distinctly associated with TAU, amyloid- β accumulation, and cognitive decline. *Sci Transl Med* 2020;12:4069. https://doi.org/10.1126/SCITRANSLMED.AAZ4069/SUPPL_FILE/AAZ4069_SM.PDF.

Ranasinghe KG, Verma P, Cai C, Xie X, Kudo K, Gao X, et al. Altered excitatory and inhibitory neuronal subpopulation parameters are distinctly associated with tau and amyloid in Alzheimer's disease. *Elife* 2022;11. <https://doi.org/10.7554/ELIFE.77850>.

Rasmussen KL, Tybjarg-Hansen A, Nordestgaard BG, Frikke-Schmidt R. Absolute 10-year risk of dementia by age, sex and APOE genotype: A population-based cohort study. *CMAJ* 2018;190:E1033–41. <https://doi.org/10.1503/CMAJ.180066/-DC1>.

Rea RC, Berlot R, Martin SL, Craig CE, Holmes PS, Wright DJ, et al. Quantitative EEG and cholinergic basal forebrain atrophy in Parkinson's disease and mild cognitive impairment. *Neurobiol Aging* 2021;106:37–44. <https://doi.org/10.1016/j.neurobiolaging.2021.05.023>.

Reisberg B. Diagnostic criteria in dementia: A comparison of current criteria, research challenges, and implications for DSM-V. *J Geriatr Psychiatry Neurol* 2006;19:137–46. <https://doi.org/10.1177/0891988706291083>.

Reynolds EH. Todd, Faraday, and the electrical basis of brain activity. *Lancet Neurology* 2004;3:557–63. [https://doi.org/10.1016/S1474-4422\(04\)00842-7](https://doi.org/10.1016/S1474-4422(04)00842-7).

Robbins KA, Touryan J, Mullen T, Kothe C, Bigdely-Shamlo N. How Sensitive Are EEG Results to Preprocessing Methods: A Benchmarking Study. *IEEE Trans Neural Syst Rehabil Eng* 2020;28:1081–90. <https://doi.org/10.1109/TNSRE.2020.2980223>.

Rockhill AP, Jackson N, George J, Aron A, Swann NC. UC San Diego Resting State EEG Data from Patients with Parkinson's Disease 2021. <https://doi.org/10.18112/openneuro.ds002778.v1.0.5>.

Rodrigues PLC, Jutten C, Congedo M. Riemannian Procrustes Analysis: Transfer Learning for Brain-Computer Interfaces. *IEEE Trans Biomed Eng* 2019;66:2390–401. <https://doi.org/10.1109/TBME.2018.2889705>.

Rommel C, Paillard J, Moreau T, Gramfort A. Data augmentation for learning predictive models on EEG: a systematic comparison. *J Neural Eng* 2022;19:066020. <https://doi.org/10.1088/1741-2552/ACA220>.

Rosenblum Y, Shiner T, Bregman N, Giladi N, Maidan I, Fahoum F, et al. Decreased aperiodic neural activity in Parkinson's disease and dementia with Lewy bodies. *J Neurol* 2023;270:3958–69. <https://doi.org/10.1007/S00415-023-11728-9/FIGURES/2>.

Rujeedawa T, Félez EC, Clare ICH, Fortea J, Strydom A, Rebillat AS, et al. The Clinical and Neuropathological Features of Sporadic (Late-Onset) and Genetic Forms of Alzheimer's Disease. *J Clin Med* 2021;10:4582. <https://doi.org/10.3390/JCM10194582>.

Ryan FJ, Ma Y, Ashander LM, Kvopka M, Appukuttan B, Lynn DJ, et al. Transcriptomic Responses of Human Retinal Vascular Endothelial Cells to Inflammatory Cytokines. *Transl Vis Sci Technol* 2022;11. <https://doi.org/10.1167/tvst.11.8.27>.

Sabbagh D, Cartailler J, Touchard C, Joachim J, Mebazaa A, Vallée F, et al. Repurposing electroencephalogram monitoring of general anaesthesia for building biomarkers of brain ageing: an exploratory study. *BJA Open* 2023;7:100145. <https://doi.org/10.1016/J.BJAO.2023.100145>.

Sabbagh MN, Taylor A, Galasko D, Galvin JE, Goldman JG, Leverenz JB, et al. Listening session with the US Food and Drug Administration, Lewy Body Dementia Association, and an expert panel. *Alzh & Dem: Trans Res & Clin Intervent* 2023;9. <https://doi.org/10.1002/TRC2.12375>.

Sachdev PS, Blacker D, Blazer DG, Ganguli M, Jeste D V., Paulsen JS, et al. Classifying neurocognitive disorders: the DSM-5 approach. *Nat Rev Neurol* 2014;10:634–42. <https://doi.org/10.1038/NRNEUROL.2014.181>.

Sakata N, Okumura Y. Job Loss After Diagnosis of Early-Onset Dementia: A Matched Cohort Study. *Journal of Alzheimer's Disease* 2017;60:1231. <https://doi.org/10.3233/JAD-170478>.

Santoro A, Martucci M, Conte M, Capri M, Franceschi C, Salvioli S. Inflammaging, hormesis and the rationale for anti-aging strategies. *Ageing Res Rev* 2020;64:101142. <https://doi.org/10.1016/J.ARR.2020.101142>.

Schaworonkow N, Nikulin V V. Is sensor space analysis good enough? Spatial patterns as a tool for assessing spatial mixing of EEG/MEG rhythms. *Neuroimage* 2022;253:119093. <https://doi.org/10.1016/j.neuroimage.2022.119093>.

Scheijbeler EP, de Haan W, Stam CJ, Twisk JWR, Gouw AA. Longitudinal resting-state EEG in amyloid-positive patients along the Alzheimer's disease continuum: considerations for clinical trials. *Alzheimers Res Ther* 2023;15:1–19. <https://doi.org/10.1186/S13195-023-01327-1/TABLES/10>.

Schmidt F, Danböck SK, Trinka E, Demarchi G, Weisz N. Age-related changes in “cortical” 1/f dynamics are linked to cardiac activity. *BioRxiv* 2023:2022.11.07.515423. <https://doi.org/10.1101/2022.11.07.515423>.

Schmidt MT, Kanda PAM, Basile LFH, da Silva Lopes HF, Baratho R, Demario JLC, et al. Index of alpha/theta ratio of the electroencephalogram: A new marker for Alzheimer's disease. *Front Aging Neurosci* 2013;5:60. <https://doi.org/10.3389/fnagi.2013.00060>.

Schultz AP, Chhatwal JP, Hedden T, Mormino EC, Hanseeuw BJ, Sepulcre J, et al. Phases of Hyperconnectivity and Hypoconnectivity in the Default Mode and Salience Networks Track with Amyloid and Tau in Clinically Normal Individuals. *The Journal of Neuroscience* 2017;37:4323. <https://doi.org/10.1523/JNEUROSCI.3263-16.2017>.

Schumacher J, Taylor JP, Hamilton CA, Firbank M, Cromarty RA, Donaghy PC, et al. Quantitative EEG as a biomarker in mild cognitive impairment with Lewy bodies. *Alzheimers Res Ther* 2020a;12. <https://doi.org/10.1186/s13195-020-00650-1>.

Schumacher J, Thomas AJ, Peraza LR, Firbank M, Cromarty R, Hamilton CA, et al. EEG alpha reactivity and cholinergic system integrity in Lewy body dementia and Alzheimer's disease. *Alzheimers Res Ther* 2020b;12. <https://doi.org/10.1186/s13195-020-00613-6>.

Seeck M, Koessler L, Bast T, Leijten F, Michel C, Baumgartner C, et al. The standardized EEG electrode array of the IFCN. *Clin Neurophysiol* 2017;128:2070–7. <https://doi.org/10.1016/J.CLINPH.2017.06.254>.

Shiri I, Amini M, Nazari M, Hajianfar G, Haddadi Avval A, Abdollahi H, et al. Impact of feature harmonization on radiogenomics analysis: Prediction of EGFR and KRAS mutations from non-small cell lung cancer PET/CT images. *Comput Biol Med* 2022;142. <https://doi.org/10.1016/J.COMPBIOMED.2022.105230>.

Simuni T, Chahine LM, Poston K, Brumm M, Buracchio T, Campbell M, et al. A biological definition of neuronal α-synuclein disease: towards an integrated staging system for research. *Lancet Neurol* 2024;23:178–90. [https://doi.org/10.1016/S1474-4422\(23\)00405-2](https://doi.org/10.1016/S1474-4422(23)00405-2).

Sitt JD, King JR, El Karoui I, Rohaut B, Faugeras F, Gramfort A, et al. Large scale screening of neural signatures of consciousness in patients in a vegetative or minimally conscious state. *Brain* 2014;137:2258–70. <https://doi.org/10.1093/BRAIN/AWU141>.

- Skouras S, Falcon C, Tucholka A, Rami L, Sanchez-Valle R, Lladó A, et al. Mechanisms of functional compensation, delineated by eigenvector centrality mapping, across the pathophysiological continuum of Alzheimer's disease. *Neuroimage Clin* 2019;22:101777. <https://doi.org/10.1016/J.NICL.2019.101777>.
- Sleimen-Malkoun R, Perdikis D, Müller V, Blanc JL, Huys R, Temprado JJ, et al. Brain Dynamics of Aging: Multiscale Variability of EEG Signals at Rest and during an Auditory Oddball Task. *ENeuro* 2015;2. <https://doi.org/10.1523/ENEURO.0067-14.2015>.
- Smailovic U, Jelic V. Neurophysiological Markers of Alzheimer's Disease: Quantitative EEG Approach. *Neurol Ther* 2019;8:37–55. <https://doi.org/10.1007/s40120-019-00169-0>.
- Smailovic U, Koenig T, Kåreholt I, Andersson T, Kramberger MG, Winblad B, et al. Quantitative EEG power and synchronization correlate with Alzheimer's disease CSF biomarkers. *Neurobiol Aging* 2018;63:88–95. <https://doi.org/10.1016/j.neurobiolaging.2017.11.005>.
- Smits FM, Porcaro C, Cottone C, Cancelli A, Rossini PM, Tecchio F. Electroencephalographic Fractal Dimension in Healthy Ageing and Alzheimer's Disease. *PLoS One* 2016;11:e0149587. <https://doi.org/10.1371/JOURNAL.PONE.0149587>.
- Sperling RA, Aisen PS, Beckett LA, Bennett DA, Craft S, Fagan AM, et al. Toward defining the preclinical stages of Alzheimer's disease: recommendations from the National Institute on Aging-Alzheimer's Association workgroups on diagnostic guidelines for Alzheimer's disease. *Alzheimers Dement* 2011;7:280–92. <https://doi.org/10.1016/J.JALZ.2011.03.003>.
- Srinivasan R, Nunez PL. Electroencephalography. *Encyclopedia of Human Behavior: Second Edition* 2012:15–23. <https://doi.org/10.1016/B978-0-12-375000-6.00395-5>.
- Stelzmann RA, Norman Schnitzlein H, Reed Murtagh F. An english translation of alzheimer's 1907 paper, "über eine eigenartige erkankung der hirnrinde." *Clinical Anatomy* 1995;8:429–31. <https://doi.org/10.1002/CA.980080612>.
- Stoddart WHBAB. Presbyophrenia (Alzheimer's Disease). *Proc R Soc Med* 1913;6:13.
- Stylianou M, Murphy N, Peraza LR, Graziadio S, Cromarty R, Killen A, et al. Quantitative electroencephalography as a marker of cognitive fluctuations in dementia with Lewy bodies and an aid to differential diagnosis. *Clinical Neurophysiology* 2018;129:1209–20. <https://doi.org/10.1016/j.clinph.2018.03.013>.
- Suarez-Revelo J, Ochoa-Gomez J, Duque-Grajales J. Improving test-retest reliability of quantitative electroencephalography using different preprocessing approaches. 38th Annual International Conference of the IEEE Engineering in Medicine and Biology Society (EMBC) 2016:961–4. <https://doi.org/10.1109/EMBC.2016.7590861>.
- Suárez-Revelo JX, Ochoa-Gómez JF, Duque-Grajales JE, Tobón-Quintero CA. Biomarkers identification in Alzheimer's disease using effective connectivity analysis from electroencephalography recordings. *Ingeniería e Investigación* 2016;36:50–7. <https://doi.org/10.15444/ing.investig.v36n3.54037>.
- Suárez-Revelo JX, Ochoa-Gómez JF, Tobón-Quintero CA. Validation of EEG Pre-processing Pipeline by Test-Retest Reliability. *Communications in Computer and Information Science*, vol. 916, Springer Verlag; 2018, p. 290–9. https://doi.org/10.1007/978-3-030-00353-1_26.
- Sun J, Wang B, Niu Y, Tan Y, Fan C, Zhang N, et al. Complexity Analysis of EEG, MEG, and fMRI in Mild Cognitive Impairment and Alzheimer's Disease: A Review. *Entropy* 2020, Vol 22, Page 239 2020;22:239. <https://doi.org/10.3390/E22020239>.
- Sun Y, Islam S, Gao Y, Nakamura T, Zou K, Michikawa M. Apolipoprotein E4 inhibits γ -secretase activity via binding to the γ -secretase complex. *J Neurochem* 2023;164:858–74. <https://doi.org/10.1111/JNC.15750>.
- Swardfager W, Lanctt K, Rothenburg L, Wong A, Cappell J, Herrmann N. A meta-analysis of cytokines in Alzheimer's disease. *Biol Psychiatry* 2010;68:930–41. <https://doi.org/10.1016/J.BIOPSYCH.2010.06.012>.
- Tampu IE, Eklund A, Haj-Hosseini N. Inflation of test accuracy due to data leakage in deep learning-based classification of OCT images. *Scientific Data* 2022 9:1 2022;9:1–8. <https://doi.org/10.1038/s41597-022-01618-6>.
- Tăuțan AM, Casula EP, Pellicciari MC, Borghi I, Maiella M, Bonni S, et al. TMS-EEG perturbation biomarkers for Alzheimer's disease patients classification. *Scientific Reports* 2023 13:1 2023;13:1–13. <https://doi.org/10.1038/s41598-022-22978-4>.
- Thal DR, Rüb U, Orantes M, Braak H. Phases of A beta-deposition in the human brain and its relevance for the development of AD. *Neurology* 2002;58:1791–800. <https://doi.org/10.1212/WNL.58.12.1791>.

Toledo JB, Gopal P, Raible K, Irwin DJ, Brettschneider J, Sedor S, et al. Pathological α -synuclein distribution in subjects with coincident Alzheimer's and Lewy body pathology. *Acta Neuropathol* 2016;131:393–409. [https://doi.org/10.1007/S00401-015-1526-9/FIGURES/6](https://doi.org/10.1007/S00401-015-1526-9).

Tönnies E, Trushina E. Oxidative Stress, Synaptic Dysfunction, and Alzheimer's Disease. *Journal of Alzheimer's Disease* 2017;57:1105. <https://doi.org/10.3233/JAD-161088>.

Turner RS, Stubbs T, Davies DA, Albensi BC. Potential New Approaches for Diagnosis of Alzheimer's Disease and Related Dementias. *Front Neurol* 2020;11:496. <https://doi.org/10.3389/FNEUR.2020.00496>.

Tyebji S, Hannan AJ. Synaptopathic mechanisms of neurodegeneration and dementia: Insights from Huntington's disease. *Prog Neurobiol* 2017;153:18–45. <https://doi.org/10.1016/J.PNEUROBIO.2017.03.008>.

Vallat R. Antropy: entropy and complexity of (EEG) time-series in Python 2022. <https://github.com/raphaelvallat/antropy> (accessed February 19, 2023).

Vallat R, Walker MP. An open-source, high-performance tool for automated sleep staging. *Elife* 2021;10. <https://doi.org/10.7554/eLife.70092>.

Vanneste S, Song JJ, De Ridder D. Thalamocortical dysrhythmia detected by machine learning. *Nature Communications* 2018 9:1 2018;9:1–13. <https://doi.org/10.1038/s41467-018-02820-0>.

Vermeiren Y, Hirschberg Y, Mertens I, De Deyn PP. Biofluid Markers for Prodromal Parkinson's Disease: Evidence From a Catecholaminergic Perspective. *Front Neurol* 2020;11:521285. [https://doi.org/10.3389/FNEUR.2020.00595/BIBTEX](https://doi.org/10.3389/FNEUR.2020.00595).

Vik-Mo AO, Giil LM, Ballard C, Aarsland D. Course of neuropsychiatric symptoms in dementia: 5-year longitudinal study. *Int J Geriatr Psychiatry* 2018;33:1361–9. <https://doi.org/10.1002/GPS.4933>.

Vogel JW, Young AL, Oxtoby NP, Smith R, Ossenkoppele R, Strandberg OT, et al. Four distinct trajectories of tau deposition identified in Alzheimer's disease. *Nat Med* 2021;27:871. <https://doi.org/10.1038/S41591-021-01309-6>.

Voß H, Schlumbohm S, Barwikowski P, Wurlitzer M, Dottermusch M, Neumann P, et al. HarmonizR enables data harmonization across independent proteomic datasets with appropriate handling of missing values. *Nat Commun* 2022;13. <https://doi.org/10.1038/S41467-022-31007-X>.

Voytek B, Knight RT. Dynamic Network Communication as a Unifying Neural Basis for Cognition, Development, Aging, and Disease. *Biol Psychiatry* 2015;77:1089–97. <https://doi.org/10.1016/J.BIOPSYCH.2015.04.016>.

Wan L, Huang H, Schwab N, Tanner J, Rajan A, Lam NB, et al. From eyes-closed to eyes-open: Role of cholinergic projections in EC-to-EO alpha reactivity revealed by combining EEG and MRI. *Hum Brain Mapp* 2019;40:566–77. <https://doi.org/10.1002/HBM.24395>.

Wang Z, Liu A, Yu J, Wang P, Bi Y, Xue S, et al. The effect of aperiodic components in distinguishing Alzheimer's disease from frontotemporal dementia. *Research Square [Preprint]* 2023. <https://doi.org/10.21203/RS.3.RS-2915225/V1>.

Waschke L, Donoghue T, Fiedler L, Smith S, Garrett DD, Voytek B, et al. Modality-specific tracking of attention and sensory statistics in the human electrophysiological spectral exponent. *Elife* 2021;10. <https://doi.org/10.7554/ELIFE.70068>.

Wen H, Liu Z. Separating Fractal and Oscillatory Components in the Power Spectrum of Neurophysiological Signal. *Brain Topogr* 2016;29:13. <https://doi.org/10.1007/S10548-015-0448-0>.

Wilson DM, Cookson MR, Van Den Bosch L, Zetterberg H, Holtzman DM, Dewachter I. Hallmarks of neurodegenerative diseases. *Cell* 2023;186:693–714. <https://doi.org/10.1016/J.CELL.2022.12.032>.

Xu H, Abdallah N, Marion JM, Chauvet P, Tauber C, Carlier T, et al. Radiomics prognostic analysis of PET/CT images in a multicenter head and neck cancer cohort: investigating ComBat strategies, sub-volume characterization, and automatic segmentation. *Eur J Nucl Med Mol Imaging* 2023;50. <https://doi.org/10.1007/s00259-023-06118-2>.

Xu Y, Yang J, Shang H. Meta-analysis of risk factors for Parkinson's disease dementia. *Transl Neurodegener* 2016;5. <https://doi.org/10.1186/S40035-016-0058-0>.

Yassine S, Gschwandtner U, Auffret M, Duprez J, Verin M, Fuhr P, et al. Identification of Parkinson's Disease Subtypes from Resting-State Electroencephalography. *Movement Disorders* 2023;38:1451–60. <https://doi.org/10.1002/MDS.29451>.

Ye Q, Chen H, Su F, Shu H, Gong L, Xie C, et al. An Inverse U-Shaped Curve of Resting-State Networks in Individuals at High Risk of Alzheimer's Disease. *J Clin Psychiatry* 2018;79. <https://doi.org/10.4088/JCP.17M11583>.

Yener GG, Leuchter AF, Jenden D, Read SL, Cummings JL, Miller BL. Quantitative EEG in frontotemporal dementia. *Clin Electroencephalogr* 1996;27:61–8. <https://doi.org/10.1177/155005949602700204>.

Yi G, Wang L, Chu C, Liu C, Zhu X, Shen X, et al. Analysis of complexity and dynamic functional connectivity based on resting-state EEG in early Parkinson's disease patients with mild cognitive impairment. *Cogn Neurodyn* 2022;16:309–23. <https://doi.org/10.1007/S11571-021-09722-W/FIGURES/11>.

Yi GS, Wang J, Deng B, Wei X Le. Complexity of resting-state EEG activity in the patients with early-stage Parkinson's disease. *Cogn Neurodyn* 2017;11:147. <https://doi.org/10.1007/S11571-016-9415-Z>.

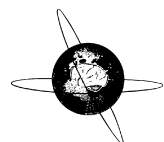
van der Zande JJ, Gouw AA, Steenoven I van, Scheltens P, Stam CJ, Lemstra AW. EEG Characteristics of Dementia With Lewy Bodies, Alzheimer's Disease and Mixed Pathology. *Front Aging Neurosci* 2018;10. <https://doi.org/10.3389/FNAGI.2018.00190>.

Zapata-Saldaña L-M, Vargas-Serna A-D, Gil-Gutiérrez J, Mantilla-Ramos Y-J, Ochoa-Gómez J-F. Evaluation of Strategies Based on Wavelet-ICA and ICLabel for Artifact Correction in EEG Recordings. *Revista Científica* 2023;46:61–76. <https://doi.org/10.14483/23448350.19068>.

Zimmermann R, Gschwandtner U, Hatz F, Schindler C, Bousleiman H, Ahmed S, et al. Correlation of EEG slowing with cognitive domains in nondemented patients with Parkinson's disease. *Dement Geriatr Cogn Disord* 2015;39:207–14. <https://doi.org/10.1159/000370110>.

Appendices

Paper I



Resting-state EEG alpha/theta ratio related to neuropsychological test performance in Parkinson's Disease



Alberto Jaramillo-Jimenez ^{a,b,c,d,e,f,*}, Jazmin Ximena Suarez-Revelo ^{c,d}, John Fredy Ochoa-Gomez ^{c,d}, Jairo Alexander Carmona Arroyave ^{c,d}, Yamile Bocanegra ^{c,d}, Francisco Lopera ^c, Omar Buriticá ^c, David Antonio Pineda-Salazar ^{c,d}, Leonardo Moreno Gómez ^g, Carlos Andrés Tobón Quintero ^{c,d,h}, Miguel Germán Borda ^{a,b,i}, Laura Bonanni ^j, Dominic H. Ffytche ^{k,l}, Kolbjørn Brønnick ^{a,b}, Dag Aarsland ^{a,l}

^a Centre for Age-Related Medicine (SESAM), Stavanger University Hospital, Stavanger, Norway

^b Faculty of Health Sciences, University of Stavanger, Stavanger, Norway

^c Grupo de Neurociencias de Antioquia, Universidad de Antioquia, School of Medicine, Medellín, Colombia

^d Grupo Neuropsicología y Conducta, Universidad de Antioquia, School of Medicine, Medellín, Colombia

^e Semillero de Investigación SINAPSIS, Universidad de Antioquia, School of Medicine, Medellín, Colombia

^f Semillero de Investigación NeuroCo, Universidad de Antioquia, School of Medicine & School of Engineering, Medellín, Colombia

^g Neurology Unit, Pablo Tobón Uribe Hospital, Medellín, Colombia

^h Área Investigación e Innovación, Institución Prestadora de Servicios de Salud "IPS Universitaria", Medellín, Colombia

ⁱ Semillero de Neurociencias y Envejecimiento, Ageing Institute, Medical School, Pontificia Universidad Javeriana, Bogotá, Colombia

^j Department of Neuroscience, Imaging and Clinical Science, and Aging Research Centre, G. d'Annunzio University, Chieti, Italy

^k Department of Old Age Psychiatry, Institute of Psychiatry, Psychology, and Neuroscience, King's College London, London, UK

^l KCL-PARCOG Group, Institute of Psychiatry, Psychology, and Neuroscience, King's College London, London, UK

ARTICLE INFO

Article history:

Accepted 6 January 2021

Available online 13 January 2021

Keywords:

Electroencephalography

Parkinson's Disease

Alpha rhythm

Theta rhythm

Neuropsychological tests

HIGHLIGHTS

- Parkinson's related performance in the Judgment of Line Orientation Test is influenced by the right occipital α/θ .
- A hemispheric approach of occipital α/θ must be considered for further research.
- The right occipital α/θ is a promising marker for evaluating Parkinson's Disease patients with visuospatial impairment.

ABSTRACT

Objective: To determine possible associations of hemispheric-regional alpha/theta ratio (α/θ) with neuropsychological test performance in Parkinson's Disease (PD) non-demented patients.

Methods: 36 PD were matched to 36 Healthy Controls (HC). The α/θ in eight hemispheric regions was computed from the relative power spectral density of the resting-state quantitative electroencephalogram (qEEG). Correlations between α/θ and performance in several neuropsychological tests were conducted, significant findings were included in a moderation analysis.

Results: The α/θ in all regions was lower in PD than in HC, with larger effect sizes in the posterior regions. Right parietal, and right and left occipital α/θ had significant positive correlations with performance in Judgement of Line Orientation Test (JLOT) in PD. Adjusted moderation analysis indicated that right, but not left, occipital α/θ influenced the JLOT performance related to PD.

Conclusions: Reduction of the occipital α/θ , in particular on the right side, was associated with visuospatial performance impairment in PD.

Significance: Visuospatial impairment in PD, which is highly correlated with the subsequent development of dementia, is reflected in α/θ in the right posterior regions. The right occipital α/θ may represent a useful qEEG marker for evaluating the presence of early signs of cognitive decline in PD and the subsequent risk of dementia.

© 2021 International Federation of Clinical Neurophysiology. Published by Elsevier B.V. All rights reserved.

* Corresponding author at: Centre for Age-Related Medicine (SESAM), Stavanger University Hospital, PB 8100, N-4068 Stavanger, Norway.

E-mail address: alberto.jaramilloj@udea.edu.co (A. Jaramillo-Jimenez).

1. Introduction

Parkinson's Disease (PD) is defined primarily as a movement disorder pathologically characterized by the loss of nigrostriatal dopaminergic neurons and Lewy bodies in the remaining neurons. In addition to dopamine-related motor symptoms, serotonin, norepinephrine, and acetylcholine may play a key role in the genesis of nonmotor symptoms including cognitive decline. Cognitive decline is among the most common and important nonmotor symptoms in PD, increasing the risk of PD dementia (PDD), although the rate of cognitive decline and time to dementia varies (Armstrong, 2019). Around 36% of PD patients have Mild Cognitive Impairment (MCI) at diagnosis compromising executive function, attention, memory, or visuospatial domains (Aarsland et al., 2017). In PD, early dysexecutive and attentional impairments depend on dopaminergic frontostriatal circuit lesions (Kehagia et al., 2012). Besides, cortical and striatal cholinergic pathways become affected, contributing to frontostriatal dysfunction (Ballinger et al., 2016). Worsening of visual memory, visuospatial abilities, and semantic fluency have been associated with posterior cortical and temporal lobe dysfunction which, to some extent, can improve with cholinergic treatments (Kehagia et al., 2012). Although the cognitive profile in PD is heterogeneous, mild visuospatial impairment represents a higher risk of PDD compared to attentional/executive impairment (Williams-Gray et al., 2007). Synaptic and network dysfunction models have been proposed for explaining different electrophysiological patterns of cognitive decline. For instance, aggregation and accumulation of misfolded proteins cause an imbalance between excitatory and inhibitory neurotransmitter activity (Roberts and Breakspear, 2018). Hence, identifying biomarkers that can reliably measure synaptic and neuronal network disruptions is important for diagnosis and prognosis in neurodegenerative diseases, and may serve as predictors for cognitive decline in PD.

The quantitative electroencephalogram (qEEG) may reflect cholinergic dysfunction (Massa et al., 2020; van der Zande et al., 2018), and some qEEG features seem to be promising biomarkers for PD and other neurodegenerative dementias (Babiloni et al., 2020; Bonanni et al., 2016, 2008; Geraedts et al., 2018). As a case in point, our group has shown that frontal coherence is related to executive function in MCI due to PD (Carmona Arroyave et al., 2019). However, Power Spectral Density (PSD) is one of the most widely used qEEG features, and the progression of cognitive decline in PD patients is associated with increased PSD in delta and theta bands, as well as decreased alpha PSD (Bousleiman et al., 2014; Caviness et al., 2016). Those findings have been interpreted as "slowing-down" in posterior regions (Al-Qazzaz et al., 2014; Schmidt et al., 2013), but synoptic PSD indexes such as the ratio between alpha and theta PSD may enhance the differences between patients and healthy controls (Massa et al., 2020; Schmidt et al., 2013). However, few studies have calculated those indexes in PD, and if so, have computed an average of alpha/theta ratio (α/θ) rather than regional ratios in the right and left hemisphere (Eichelberger et al., 2017; Massa et al., 2020) despite known asymmetries in PSD (Bousleiman et al., 2014). Other works have examined the correlation of qEEG features with global scores of cognition rather than domain-specific neuropsychological impairments (Cozac et al., 2016; Geraedts et al., 2018). With the present study, we aim to determine possible associations of hemispheric-regional α/θ changes with impairment in specific neuropsychological tests in PD patients without dementia. Based on previous preliminary findings, we hypothesize that visuospatial and semantic fluency impairments of PD are associated with a reduction of the α/θ in posterior hemispheric-regions.

2. Methods:

2.1. Participants

We analyzed a non-randomized sample of PD patients from the outpatient service of the Grupo de Neurociencias de Antioquia (Neuroscience group of Antioquia) (Carmona Arroyave et al., 2019). Detailed inclusion criteria were stated in Section 2.2. We excluded participants with parkinsonian syndromes other than PD, other major neurological or psychiatric disorders, and dementia (based on impairment in cognition and function) (Emre et al., 2007), intracranial devices, and current use of other drugs than antiparkinsonian that could alter the qEEG rhythms. PD patients were under stable antiparkinsonian treatment for at least 4 weeks before evaluations and recordings. We included PD patients without MCI (PD-nMCI, n = 22) if Montreal Cognitive Assessment (MoCA) (see below) was 23 or above - according to validation in Colombian population- (Gil et al., 2015), and had no significant cognitive complaints or cognition-related functional decline. Besides, PD patients with MCI (PD-MCI, n = 14), defined following level one task force criteria - Movement Disorders Society (MDS) (Litvan et al., 2012), i.e. subjective cognitive complaints, MoCA < 23, and no significant cognition-related functional decline, were also included. Finally, from an open call for volunteers, we selected 36 participants with normal cognition and no relevant neurologic or psychiatric disorders as Healthy Controls (HC). HC were manually matched to the PD groups based on gender, age, and years of education. The study had the approval of the Ethical Research Committee of the Universidad de Antioquia (Certificate No. 15-10-569). All participants signed informed consent before enrollment in the study. All assessments, including qEEG acquisition, were completed in phase 'On' of levodopa treatment.

2.2. Clinical and neuropsychological assessment

For determining PD diagnosis, all participants were assessed by a team of two neurologists and one trained physician following the MDS Clinical Diagnostic Criteria for Parkinson's Disease (Postuma et al., 2015). The Hoehn & Yahr scale (Hoehn and Yahr, 1967) and the Unified Parkinson's Disease Rating Scale part III (UPDRS-III) (Goetz, 2003) were used for evaluating the severity of the disease stage and motor symptoms. The two neurologists ruled out alternative diagnoses of parkinsonism and verified pharmacological regimens and the presence of intracranial devices, as per exclusion criteria.

Neuropsychological examinations of PD and HC subjects were performed by a team of four trained psychologists who evaluated MCI and excluded dementia. The cognitive screening was performed using the MoCA test with validated cut-offs for the Colombian population (Gil et al., 2015). The functional level was evaluated through the Barthel Index (Mahoney and Barthel, 1965) and Lawton & Brody scale (Lawton and Brody, 1969). To test executive functions and attention, we administered the Stroop test – Golden version (Stroop) (Golden and Freshwater, 1978), and INECO Frontal Screening battery (IFS) (Torralva et al., 2009) composed of: Luria motor series, conflicting instructions, go-no-go, modified Hayling test, backward months, backward digit span, modified Corsi tapping test and proverb interpretation. Language domain tests included the semantic fluency of animals test (SF) and FAS phonemic fluency test (FAS) (Casals-Coll et al., 2013). Memory was assessed using the delayed free recall of the Memory Capacity Test (MCT-DFR) (Rentz et al., 2010). Visuospatial abilities were evaluated using the Judgment of Line Orientation Test (JLOT) (Benton et al., 1978) and the free-drawn of the clock drawing test

(Clock) (Agrell and Dehlin, 1998). We included the raw scores of each test in the analysis.

3. qEEG recordings and preprocessing

A qEEG was recorded for five minutes in resting-state (i.e. quiet wakefulness with eyes closed) in a Faraday cage. A cap of tin electrodes and 58 scalp leads was placed according to the international 10–10 system with the reference electrode on the right earlobe with subsequent re-reference to average in the preprocessing. Another electrode between Cz and Fz was used as ground. Impedances were kept below 10 kOhm. The sampling frequency was fixed at 1000 Hz. Signals were filtered online with a band-pass (0.05 to 200 Hz) and a notch filter (60 Hz). A semi-automated pipeline was implemented for pre-processing using two MATLAB toolboxes: EEGLAB (Delorme and Makeig, 2004), and a standardized qEEG preprocessing pipeline (PREP) (Bigdely-Shamlo et al., 2015) validated in our group (Suarez-Revelo et al., 2018) with proved test-retest reliability (Suarez-Revelo et al., 2016) (See Supplementary Material for details regarding preprocessing method). For each recording, 50 randomly automatically selected epochs of 2 seconds length and free-of-artifacts, were used to compute relative PSD. We used the multi-taper method available in the MATLAB toolbox Chronux (<http://chronux.org>) (Mitra and Bokil, 2007) to have less variance, bias, and better frequency resolution on PSD (Babadi and Brown, 2014; Prerau et al., 2017). The magnitude of relative PSD in the selected epochs was averaged for each electrode. Then, relative PSD in each electrode was calculated in four frequency bands: delta (1–4 Hz), theta (4–8 Hz), alpha (8–13 Hz), beta (13–30 Hz), and eight Regions of Interest (ROI), as follows: left frontal (AF3, F1, F3, FC1, FC3), right frontal (AF4, F2, F4, FC2, FC4), left temporal (FC5, C5, CP5, T7, TP7), right temporal (FC6, C6, CP6, T8, TP8), left parietal (CP1, CP3, P1, P3), right parietal (CP2, CP4, P2, P4), left occipital (PO3, PO5, PO7, O1), and right occipital (PO4, PO6, PO8, O2). Finally, we computed the α/θ from the alpha relative PSD/theta relative PSD and calculated its logarithmic transformation (i.e. natural log) following previously published methods (Massa et al., 2020; Moretti et al., 2004; Schmidt et al., 2013). Delta and frequencies higher than alpha were excluded from the current analysis.

3.1. Statistical analysis

Statistical analyses were performed using the Statistical Package for the Social Sciences (SPSS) version 25. Statistical significance was set at $p < 0.05$. Since α/θ in most of the posterior regions was different when comparing HC and the two PD groups, but not when PD-MCI and PD-nMCI were compared (Supplementary Tables S1–S3), we merged PD-MCI and PD-nMCI in a single PD group to increase our statistical power with greater sample size, and evaluate a wider spectrum of PD. Group comparisons were conducted using independent samples t-test or Mann-Whitney's U for continuous variables, and the Chi-square test for categorical variables. Multiple testing correction of the p-values obtained in the group comparisons of neuropsychological and qEEG data was conducted using the False Discovery Rate (FDR) method, defining a threshold of 0.05. Effect sizes were calculated with Cohen's d. In addition, Receiver Operator Characteristic (ROC) curves for the neuropsychological test and α/θ with the largest effect size were obtained. The cut-off value for the α/θ with the largest effect size was calculated with Youden's J statistic.

To determine any possible confounder effect of dopaminergic treatment over qEEG variables, Pearson correlations between the Levodopa Equivalent Daily Dose (LEDD) and the α/θ in each ROI were conducted. Given no significant results in the latter correla-

tions (Supplementary Table S4), we did not adjust for LEDD the subsequent analyses. Besides, Pearson correlations were used to explore the effect of age on α/θ in HC (Supplementary Table S5), but no significant results were found in most of the posterior regions (i.e. right and left occipital, and right parietal). Therefore, we performed age-unadjusted bivariate correlations to explore the relationship between α/θ in the eight ROI and the scores of the eight neuropsychological tests. However, the results of these exploratory correlations were also confirmed using partial non-parametric correlations controlling for the effect of age (Supplementary Table S6). As JLOT, Clock, and MoCA were non-normally distributed, we performed non-parametric correlations with these variables and Pearson correlations with the remaining. FDR correction was not conducted in these correlations due to the exploratory nature of this step but was made in the subsequent analyses after selecting target ROI and neuropsychological tests.

Finally, to test our hypothesis that PD performance in some neuropsychological tests was influenced by the α/θ , those ROI that were significantly correlated with neuropsychological tests in the exploratory correlations were included independently as a moderator variable through a conditional process analysis (moderation analysis) using the SPSS macro "PROCESS" (Preacher and Hayes, 2004). These moderation analyses were conducted using 10,000 Bootstrap sampling. The p-values of the three resulting moderation models were corrected for multiple testing with the FDR method.

4. Results

72 participants were included (HC = 36; PD = 36). Given the matched design of our study, non-significant differences among the groups were found in the demographic characteristics of the sample, Table 1.

The neuropsychological test scores of the PD group were worse in all the neuropsychological tests compared to HC as shown in Fig. 1 and Table 2. In the PD group, the α/θ exhibited statistically significant lower values in all the ROI, Table 2.

When comparing regional α/θ values in PD and HC, large effect sizes were seen, particularly in the occipital regions: right occipital ($t = 4.33$; FDR < 0.001; Cohen's d = 1.00), and left occipital ($t = 3.89$; FDR < 0.001; d = 0.92). Differences in other ROI also reflected a large effect size in right temporal ($t = 3.82$; FDR < 0.001; d = 0.90), left temporal ($t = 3.88$; FDR < 0.001; d = 0.91), right parietal ($t = 3.64$; FDR < 0.001; d = 0.86), and left frontal ($t = 3.10$; FDR = 0.004; d = 0.75). Right frontal ($t = 2.99$; FDR = 0.004; d = 0.70) and left parietal ($t = 2.99$; FDR = 0.004; d = 0.71) showed moderate effect size. Fig. 2A depicts the mean value of α/θ in each ROI in PD and HC.

The ROC curves for right occipital α/θ and MCT-DFR (the test which exhibit the largest effect size; $t = 6.96$; $p < 0.001$; d = 1.64) were presented in Fig. 2B. To separate PD patients from HC, the cut-off value obtained in ROC analysis for α/θ right occipital

Table 1
Demographic and clinical characteristics of the sample.

| | HC (n = 36) | PD (n = 36) |
|------------------------------|-------------|-------------|
| Age (years) | 63 (6) | 63 (8) |
| Gender (F/M) | 12/24 | 12/24 |
| Education (years) | 12(5) | 12 (5) |
| Years from diagnosis | - | 5.2 (3.1) |
| Hoehn & Yahr ^a | - | 2 (0) |
| UPDRS-III score ^a | - | 28 (17) |

HC: Healthy Controls; PD: Parkinson's Disease; F: Female; M: Male; UPDRS-III: Unified Parkinson's Disease Rating Scale part III.

Values presented in the table are means with Standard Deviation (S.D.).

^a The marked situations show median (interquartile range).

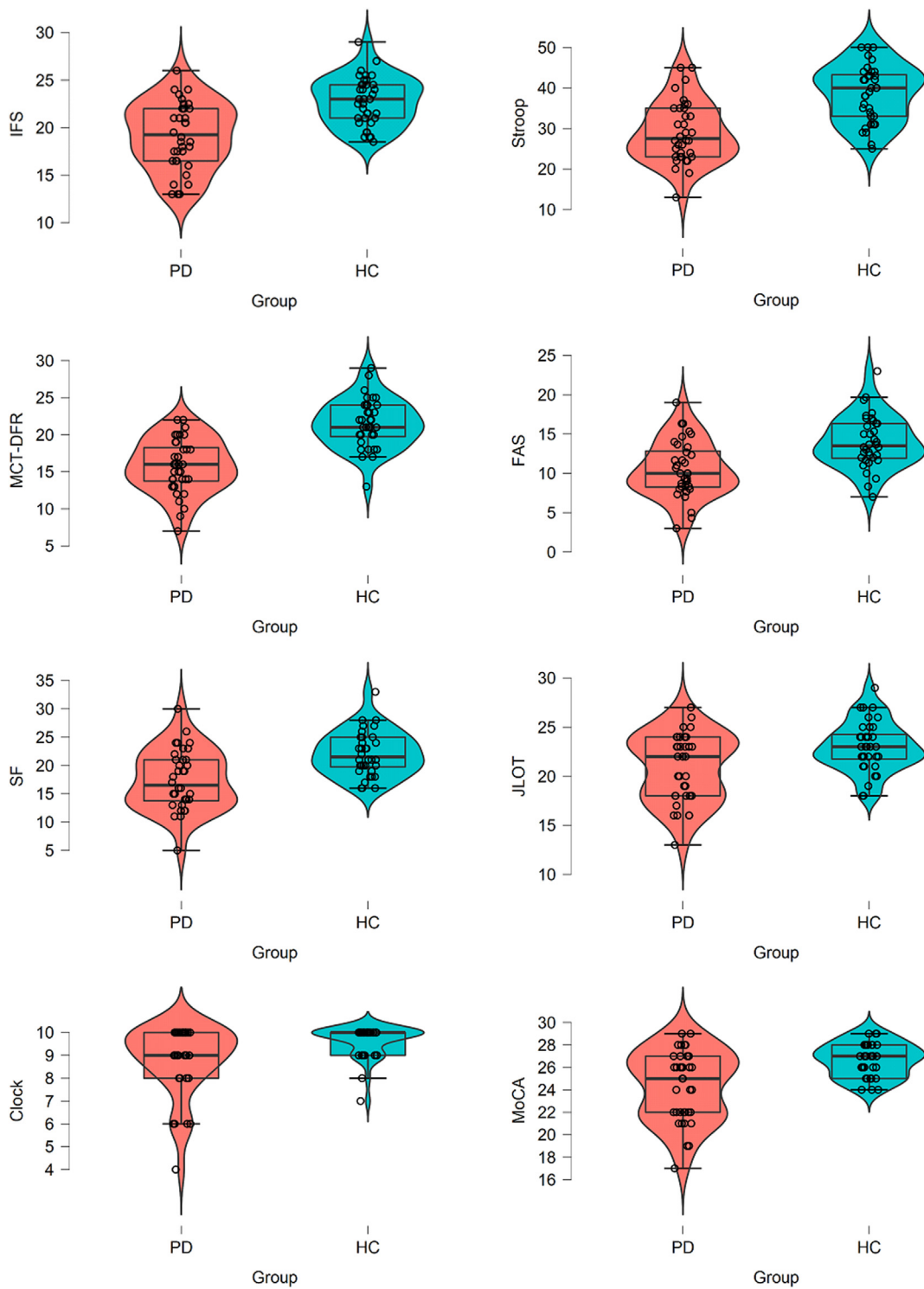


Fig. 1. Performance of PD patients and HC in neuropsychological tests. PD: Parkinson's Disease; HC: Healthy Controls; IFS: INECO Frontal Screening battery; Stroop: Stroop test – Golden version; MCT-DFT: Delayed free recall of the Memory Capacity Test; FAS: FAS phonemic fluency test; SF: Semantic fluency of animals; Clock: Free-drawn of the clock drawing test; JLOT: Judgment of Line Orientation Test; MoCA: Montreal Cognitive Assessment.

was 0.832, providing a sensitivity of 89% (95% CI: 74 – 97%), specificity of 56 % (95% CI: 38 – 72%), positive predictive value of 67% (95% CI: 58 – 75%), negative predictive value of 83% (95% CI: 65–93%), and accuracy of 72% (95% CI: 60–82%).

We then conducted exploratory correlations between hemispheric-regional α/θ and neuropsychological test scores in the PD group. Significant positive correlations between performance in JLOT and α/θ were found in right parietal

($\rho = 0.362$; $p = 0.030$), right occipital ($\rho = 0.407$; $p = 0.014$), and left occipital regions ($\rho = 0.382$; $p = 0.022$), see Fig. 3. We did not find any other significant correlations in these exploratory analyses, see Table 3. We confirmed these results controlling for the effect of age and obtained significant findings in the same ROI (Supplementary Table S6). All these p-values were not corrected given the exploratory nature of these correlations.

Table 2

Neuropsychological and qEEG characteristics of the sample.

| | HC (n = 36) | PD (n = 36) | FDR |
|---|-------------|-------------|------------------|
| Neuropsychological Characteristics | | | |
| Executive/attention | | | |
| IFS ^b | 22.8 (2.5) | 19.2 (3.5) | <0.001 |
| Stroop ^b | 38.7 (6.9) | 29 (7.4) | <0.001 |
| Memory | | | |
| MCT – DFR ^b | 21.4 (3.3) | 15.8 (3.6) | <0.001 |
| Language | | | |
| FAS ^b | 14 (3.3) | 10.5 (3.6) | <0.001 |
| SF ^b | 22.1 (3.9) | 17.4 (5.3) | <0.001 |
| Visuospatial abilities | | | |
| Clock ^{a,c} | 10 (1) | 9 (2) | 0.005 |
| JLOT ^{a,c} | 23 (4) | 22 (6) | 0.023 |
| Global cognition | | | |
| MoCA ^{a,c} | 27 (3) | 25 (5) | 0.002 |
| qEEG – $\alpha/0$ | | | |
| $\alpha/0$ right frontal ^b | 0.40 (0.49) | 0.05 (0.51) | 0.004 |
| $\alpha/0$ left frontal ^b | 0.41 (0.51) | 0.03 (0.51) | 0.004 |
| $\alpha/0$ right temporal ^b | 0.54 (0.38) | 0.15 (0.48) | <0.001 |
| $\alpha/0$ left temporal ^b | 0.57 (0.37) | 0.18 (0.48) | <0.001 |
| $\alpha/0$ right parietal ^b | 0.69 (0.47) | 0.26 (0.53) | <0.001 |
| $\alpha/0$ left parietal ^b | 0.63 (0.50) | 0.27 (0.52) | 0.004 |
| $\alpha/0$ right occipital ^b | 0.81 (0.58) | 0.22 (0.60) | <0.001 |
| $\alpha/0$ left occipital ^b | 0.74 (0.56) | 0.20 (0.61) | <0.001 |

HC: Healthy Controls; PD: Parkinson's Disease; FDR: False discovery ratio; IFS: INECO Frontal Screening battery; Stroop: Stroop test – Golden version; MCT-DFT: Delayed free recall of the Memory Capacity Test; FAS: FAS phonemic fluency test; SF: Semantic fluency of animals; Clock: Free-drawn of the clock drawing test; JLOT: Judgment of Line Orientation Test; MoCA: Montreal Cognitive Assessment; qEEG: Quantitative electroencephalogram.

p-values were FDR corrected. FDR values < 0.05 are printed in bold.

Values presented in the table are means with Standard Deviation (S.D.).

^a The marked situations shown median (interquartile range).

^b Independent samples t-test ^c Mann-Whitney U test.

Further, we tested the moderation effect of each region significantly correlated with the JLOT performance of PD patients using three independent moderation analyses (i.e. one moderation model per each ROI). Among the three moderation models, we only found significant effects after the FDR correction in the model that included the $\alpha/0$ in the right occipital region as a moderator of the JLOT performance related to PD diagnosis ($p < 0.005$; FDR = 0.014).

Fig. 4 shows the moderation model including the $\alpha/0$ in the right occipital region. Three different pathways in this model were examined: a direct pathway from the group (HC vs. PD) to JLOT performance (X to Y) ($b = -3.3$; $p = 0.002$); a direct pathway from $\alpha/0$ in right occipital in both groups (W) to JLOT performance (Y) ($b = 0.32$; $p = 0.594$); the conditional effect of $\alpha/0$ in right occipital (W) on the relation between PD diagnosis (X) and JLOT performance (Y) ($b = -2.6$; $p = 0.034$). Therefore, the $\alpha/0$ in the right occipital region influenced significantly the effect of PD diagnosis in JLOT performance.

Conversely, no significant moderation effects were found in the two remaining models that included the right parietal ($p = 0.115$) and the left occipital ($p = 0.066$) ROI as moderators (Figure S3 – Supplementary Material). Finally, we explored the conditional effect of different values of the $\alpha/0$ – right occipital on the relationship between PD diagnosis and JLOT performance. Natural Log transformed $\alpha/0$ - right occipital values below 0.633 significantly modulate the JLOT performance related to PD (Supplementary Figures S1 and S2). Thus, low $\alpha/0$ (i.e. slowing-down) in the right occipital region, influenced the JLOT impairment related to PD diagnosis.

5. Discussion

In this study, we investigated the associations between hemispheric-regional $\alpha/0$ (i.e. slowing-down of the qEEG) and neu-

ropsychological performance in non-demented PD patients. We observed, in most of the posterior regions, significant correlations between $\alpha/0$ and performance in JLOT, which tested visuospatial abilities. The lower the $\alpha/0$ in right and left occipital, and right parietal regions, the worse the performance in the JLOT test. However, after examining how posterior $\alpha/0$ influences the JLOT performance related to PD diagnosis, only the slowing-down in the right occipital region showed significant effects. The latter suggests a hemispheric asymmetric effect that has to be considered in further research since hemispheric asymmetry in theta, alpha, and beta PSD have been reported previously in PD (Bousleiman et al., 2014; Yuvaraj et al., 2014).

PSD has been one of the most widely explored qEEG features (Al-Qazzaz et al., 2014; Geraedts et al., 2018; van der Zande et al., 2018), and also is an easily obtainable marker that can reflect cholinergic pathways damage (Moretti et al., 2004). Both dopaminergic and cholinergic dysfunctions explain the cognitive symptoms in PD as indicated in a dual syndrome hypothesis: Early dysexecutive syndrome and attentional impairments have been related to frontostriatal dopaminergic dysfunction secondary to caudate denervation (Kehagia et al., 2012). On the other hand, deficits in visual memory, visuospatial abilities, and semantic fluency that improve with cholinergic treatments have been associated with posterior cortical and temporal lobe dysfunction (Kehagia et al., 2012). Additionally, cholinergic impairment appears to be greater in PD than in Alzheimer's Disease, seems to trigger the global cognitive decline and progression to dementia, and precedes further basal forebrain cell loss (Ballinger et al., 2016; Bohnen et al., 2015). Apart from functional mechanisms, structural changes such as reduced cortical thickness in the right hemisphere (including right occipital) have been identified in PD patients with formed hallucinations and low performance in JLOT, supporting the link between visuospatial impairment, complex visual hallucinations, and progression to PDD (Fyfche et al., 2017).

In line with those findings, both PSD and frequency features may also exhibit impairments in non-dopaminergic ascending systems (Massa et al., 2020), but the alpha frequency is relatively independent of cholinergic dysfunction (Moretti et al., 2004). Cholinergic deficits lead to cortico-cortical and cortico-thalamocortical dysfunction resulting in slowing-down of the qEEG rhythms (Franciotti et al., 2020). This slowing-down can be observed with increasing PSD in low-frequency bands (i.e. delta and theta) while reducing in high-frequencies (i.e. alpha and beta) (Eichelberger et al., 2017; Geraedts et al., 2018). In consequence, the full integrity of cholinergic systems, and cortico-cortical dynamics are reflected by alpha PSD (Moretti et al., 2004). Besides, global deafferentation due to pathophysiological processes (i.e. functional or anatomic injuries on cholinergic systems) and non-specific thalamic systems may be involved in the augment of delta and theta PSD (Llinás et al., 1999; Schmidt et al., 2013). Therefore, combining alpha and theta PSD in a synoptic index of the alpha-to-theta transition frequency may be useful for indicating the cholinergic dysfunction, and enhancing the differences between HC and patients with neurodegenerative diseases such as Alzheimer's Disease (Moretti et al., 2004; Schmidt et al., 2013), dementia with Lewy bodies (Bonanni et al., 2016, 2008) and PD (Massa et al., 2020). Nevertheless, further research is needed to determine the patterns of $\alpha/0$ related to MCI, but a recent publication has shown similar $\alpha/0$ in PD-MCI and PD-nMCI in concordance with our results (Massa et al., 2020).

To evaluate the resting-state qEEG correlates of cognitive decline in PD, we suggest to use specific neuropsychological tests for cognitive domains, rather than screening tests for global cognition due to the heterogeneity of cognitive symptoms in PD (Kehagia et al., 2012; Williams-Gray et al., 2007). In our study, an $\alpha/0$ association with MoCA was not observed. Similarly, PSD and

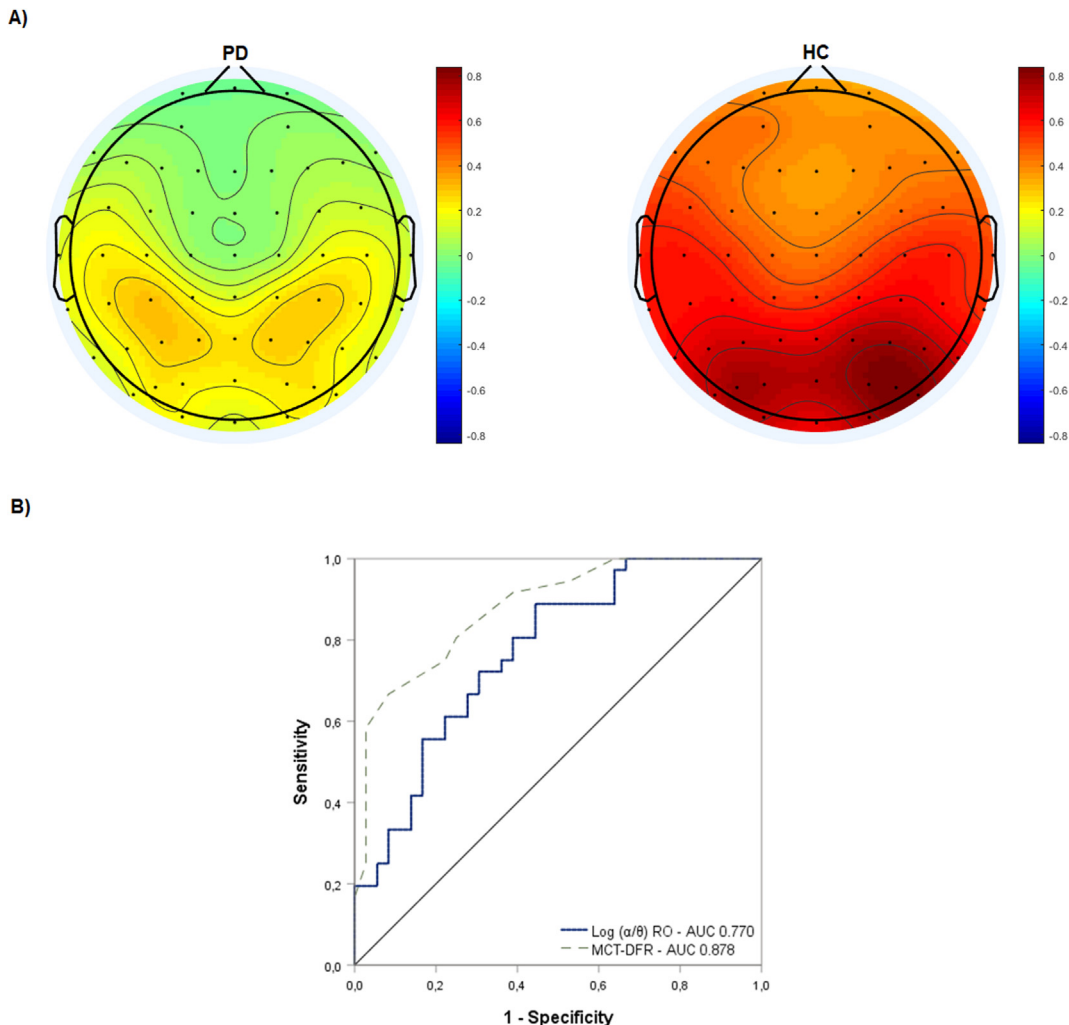


Fig. 2. Log (α/θ) values and its accuracy to separate PD patients from HC. A. Topographic plot of the Log (α/θ) in the PD and HC groups. The color bars indicate the mean values of the Log (α/θ) in each group, a high value indicates less slowing down of the qEEG rhythms. B. ROC curves for the right occipital α/θ and MCT-DFR. The blue line represents the ROC curve for the right occipital α/θ , the green dotted (dashed) line represents the ROC curve for the MCT-DFR. R: Right; L: Left; CI: Confidence Interval; RO: Right occipital; AUC: Area Under Curve. For interpretation of the colors in this figure, the reader is referred to the web version of this article.

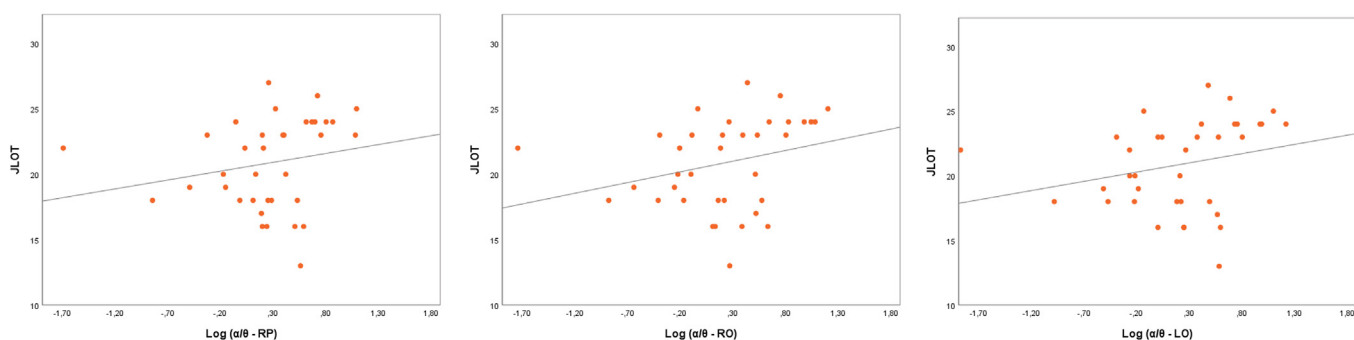


Fig. 3. Correlation plots between JLOT performance and the Log (α/θ) in the right parietal, and the right and left occipital regions in the PD group. RP: right parietal; RO: right occipital; LO: left occipital; JLOT: Judgement of Line Orientation Test.

tests of global-cognition (e.g. Mini-Mental State Examination) have not always shown significant correlations, but specific neuropsychological tests have exhibited consistent results (van der Hiele et al., 2007). One previous work has associated visuospatial impairments with occipital and parietal α/θ in non-demented PD patients (Eichelberger et al., 2017), yet PD-MCI patients were not included and those results cannot be extrapolated to PD-MCI. In our study,

a reduced right occipital α/θ ratio was associated with an impairment in visuospatial functions measured by JLOT, but not with performance on the clock drawing test. The clock drawing test presented a ceiling effect (i.e. scores of 10 ± 1 in HC, and 9 ± 2 in PD), thus, bivariate correlations could be affected by the minimal variation in this variable. Another possible explanation for the different associations is that the JLOT test is considered a “pure”

Table 3Exploratory correlations between α/θ and neuropsychological performance in PD patients.

| Log (α/θ) | IFS ^a | Stroop ^a | MCT-DFR ^a | FAS ^a | SF ^a | Clock ^b | JLOT ^b | MoCA ^b |
|-------------------------|------------------|---------------------|----------------------|------------------|-----------------|--------------------|-------------------|-------------------|
| R. Frontal | -0.182 | 0.093 | -0.072 | -0.202 | 0.032 | -0.064 | 0.315 | -0.174 |
| L. Frontal | -0.135 | 0.135 | -0.070 | -0.194 | 0.047 | -0.092 | 0.321 | -0.177 |
| R. Temporal | -0.122 | 0.027 | 0.052 | -0.118 | 0.034 | -0.014 | 0.254 | -0.044 |
| L. Temporal | -0.163 | 0.011 | -0.061 | -0.111 | 0.059 | -0.044 | 0.324 | -0.163 |
| R. Parietal | -0.200 | 0.024 | -0.098 | -0.162 | 0.044 | -0.133 | 0.362 | -0.205 |
| L. Parietal | -0.120 | 0.067 | 0.022 | -0.151 | 0.079 | -0.079 | 0.237 | -0.165 |
| R. Occipital | -0.077 | 0.128 | 0.026 | -0.194 | 0.112 | -0.092 | 0.407 | -0.081 |
| L. Occipital | -0.066 | 0.101 | 0.036 | -0.191 | 0.072 | -0.057 | 0.382 | -0.086 |

IFS: INECO Frontal Screening battery; Stroop: Stroop test – Golden version; MCT-DFT: Delayed free recall of the Memory Capacity Test; FAS: FAS phonemic fluency test; SF: Semantic fluency of animals; Clock: Free-drawn of the clock drawing test; JLOT: Judgment of Line Orientation Test; MoCA: Montreal Cognitive Assessment; R: Right; L: Left. Coefficients with unadjusted $p < 0.05$ are printed in bold.

^a Pearson correlation.

^b Spearman correlation.

Model summary

$p = 0,005$; FDR = 0,014

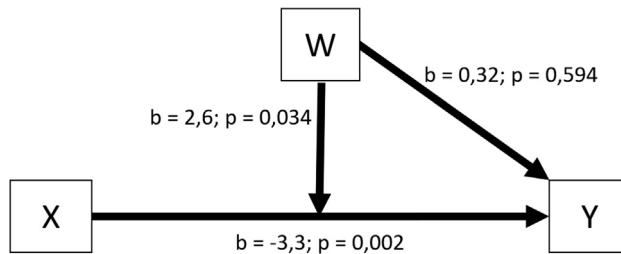


Fig. 4. Moderation effect of the α/θ - right occipital on JLOT performance related to PD. JLOT was used as the dependent variable (Y) while group (HC vs. PD) was the independent variable (X). The effect of α/θ - right occipital independently of PD diagnosis (W) over JLOT performance was examined. The moderation effect of W (α/θ - right occipital) on the PD-related JLOT performance (X to Y) was also considered. PD: Parkinson's Disease; HC: Healthy Control; JLOT: Judgement of Line Orientation Test; FDR: False Discovery Ratio.

visual-perceptual task, without major involvement of the motor component, whereas the clock drawing test assesses both visuospatial, visuoconstructive, and executive functions (Watson et al., 2013). Thus, in line with our findings, injuries in the right lateral superior occipital gyri and other areas of the visual dorsal stream such as the supramarginal gyri have been proposed as the neuropathological substrate related to decreased performance in the JLOT. Therefore, JLOT seems to represent a good clinical test for the right occipitoparietal functioning (Tranel et al., 2009), whereas the clock drawing test depends more on the right parietal and left inferior frontoparietal opercular lesions and it is not a very specific test for the right posterior functioning in chronic injuries (Tranel et al., 2008). Further research is necessary to elucidate the role of Lewy pathology in neurophysiological and neuropsychological impairment of different Lewy body diseases.

With all the above, our findings seem to support that slowing-down in the right occipital region is related to visuospatial performance patterns in non-demented PD patients. We suggest that the right occipital α/θ may be a promising marker of dementia risk in PD since patients with mild visuospatial impairment had more rapid progression PDD (Kehagia et al., 2012; Williams-Gray et al., 2007).

6. Limitations

There are some limitations to this study. The cross-sectional design and non-randomized sample may affect the statistical power and the external validity of our results in other populations. Also, the lack of follow-up did not make us able to determine the

progression to PD-MCI or PDD in PD subjects. In addition, the effect of dopamine agonists on cortical excitability (i.e. widespread variations in delta and alpha sources) (Babiloni et al., 2019) has to be considered. However, little effect of dopaminergic treatments has been related to PSD changes (George et al., 2013) as reported in our results (Table S6 – Supplementary Material), also it is unlikely that medication effects would only apply to specific brain regions (i.e. left but not right occipital). Also, the lack of correction for multiple testing in some of our analyses should be considered when interpreting our results. This important limitation of our exploratory study encourages future investigations to replicate our results and provide external validation to our findings.

Moreover, our work has several strengths. Even if there are more sophisticated features on qEEG than relative PSD (Al-Qazzaz et al., 2014), highly refined techniques may apart us from the usefulness in a clinical setting (van der Hiele et al., 2007). Thus, we aimed to improve PSD extraction with our proposed signal processing methods. Therefore, we implemented a standardized, validated, and reliable method for qEEG preprocessing (Bigdely-Shamlo et al., 2015; Suarez-Revelo et al., 2018; 2016). PREP pipeline is a semi-automatic algorithm that enhances a more uniform statistical behavior of qEEG data, even between different paradigms, headsets, or collections of data (Bigdely-Shamlo et al., 2015). Also, we used a highly accurate method for obtaining PSD features based on multi-tapers. The multi-taper method has been widely recommended due to its better tradeoff among variance, bias, frequency resolution for PSD, and for assessing attenuation estimations when compared with the single-tapers and Welch method (Babadi and Brown, 2014; Prerau et al., 2017). Besides, assessing our participants with an extensive neuropsychological battery allowed us to evaluate neuropsychological patterns in several cognitive domains which are highly heterogeneous in PD patients (Aarsland et al., 2017; Kehagia et al., 2012; Williams-Gray et al., 2007), and most of the statistical methods we used to test our hypothesis has been also implemented previously, supporting our analysis (van der Hiele et al., 2007).

7. Conclusion

Slowing-down in the right occipital α/θ seems to be associated with, and influences, the visuospatial performance impairments related to PD diagnosis. Single averaged measures of occipital α/θ must be avoided due to possible hemispheric asymmetry, but further research is needed to confirm this hypothesis. The right occipital α/θ may represent a promising qEEG feature for evaluating PD patients with mild visuospatial impairments, who have a higher risk of progression to PDD (Kehagia et al., 2012; Williams-Gray et al., 2007).

Declaration of Competing Interest

The authors declare that they have no known competing financial interests or personal relationships that could have appeared to influence the work reported in this paper.

Acknowledgments

We want to thank all the participants, researchers that collaborated (Ana Baena, Paula Andrea Ospina Lopera, Diana Paola Alzate), the Research Development Committee (CODI) at Universidad de Antioquia (University of Antioquia), as well as the staff and facilities provided by Grupo de Neurociencias de Antioquia (GNA), Grupo Neuropsicología y Conducta (GRUNECO), Semillero SINAPSIS and NeuroCo (research incubator programs) and the School of Medicine at the Universidad de Antioquia in Colombia, as well to the Centre for age-related medicine (SESAM) in Norway.

Funding

This work was supported by the Research Development Committee (CODI) - Universidad de Antioquia (University of Antioquia), Colombia, under the research project: "Procesamiento del lenguaje de acción en pacientes con enfermedad ganglio-basal desde una perspectiva neuropsicológica y neurofisiológica" (grant reference PRG-2014-768). In addition, this paper represents independent research supported by the Norwegian government, through hospital owner Helse Vest (Western Norway Regional Health Authority).

Appendix A. Supplementary material

Supplementary data to this article can be found online at <https://doi.org/10.1016/j.clinph.2021.01.001>.

References

- Aarsland D, Creese B, Politis M, Chaudhuri KR, Fytche DH, Weintraub D, et al. Cognitive decline in Parkinson disease. *Nat Rev Neurol* 2017;13:217–31. <https://doi.org/10.1038/nrneurol.2017.27>
- Agrell B, Dehlin O. The clock-drawing test. *Age Ageing* 1998;27:399–403.
- Ali-Qazzaz NK, Ali SHBM, Ahmad SA, Chellappan K, Islam MS, Escudero J. Role of EEG as Biomarker in the Early Detection and Classification of Dementia. *Sci World J* 2014. <https://doi.org/10.1155/2014/906038>.
- Armstrong MJ. Lewy Body Dementias. *Contin Lifelong Learn Neurol* 2019;25:128–46. <https://doi.org/10.1212/CON.0000000000000685>.
- Babadi B, Brown EN. A review of multitaper spectral analysis. *IEEE Trans Biomed Eng* 2014;61:1555–64. <https://doi.org/10.1109/TBME.2014.2311996>.
- Babiloni C, Blinowska K, Bonanni L, Cichocki A, De Haan W, Del Percio C, et al. What electrophysiology tells us about Alzheimer's disease: a window into the synchronization and connectivity of brain neurons. *Neurobiol Aging* 2020;85:58–73. <https://doi.org/10.1016/j.neurobiolaging.2019.09.008>.
- Babiloni C, Del Percio C, Lizio R, Noce G, Lopez S, Soricelli A, et al. Levodopa may affect cortical excitability in Parkinson's disease patients with cognitive deficits as revealed by reduced activity of cortical sources of resting state electroencephalographic rhythms. *Neurobiol Aging* 2019;73:9–20. <https://doi.org/10.1016/j.neurobiolaging.2018.08.010>.
- Ballinger EC, Ananth M, Talmage DA, Role LW. Basal Forebrain Cholinergic Circuits and Signaling in Cognition and Cognitive Decline. *Neuron* 2016;91:1199–218. <https://doi.org/10.1016/j.neuron.2016.09.006>.
- Benton AL, Varney NR, Hamsher K Des. Visuospatial Judgment: A Clinical Test. *Arch Neurol* 1978;35:364–7. <https://doi.org/10.1001/archneur.1978.00500300038006>.
- Bigdely-Shamlo N, Mullen T, Kothe C, Su K-M, Robbins KA. The PREP pipeline: standardized preprocessing for large-scale EEG analysis. *Front Neuroinform* 2015;9. <https://doi.org/10.3389/fninf.2015.00016>.
- Bohnen NI, Albin RL, Müller MLTM, Petrou M, Kotagal V, Koeppen RA, et al. Frequency of cholinergic and caudate nucleus dopaminergic deficits across the premented cognitive spectrum of parkinson disease and evidence of interaction effects. *JAMA Neurol* 2015;72:194–200. <https://doi.org/10.1001/jamaneurol.2014.2757>.
- Bonanni L, Franciotti R, Nobili F, Kramerberger MG, Taylor J-P, Garcia-Ptacek S, et al. EEG Markers of Dementia with Lewy Bodies: A Multicenter Cohort Study. *J Alzheimer's Dis* 2016;54:1649–57. <https://doi.org/10.3233/JAD-160435>.
- Bonanni L, Thomas A, Tiraboschi P, Perfetti B, Varanese S, Onofrj M. EEG comparisons in early Alzheimer's disease, dementia with Lewy bodies and Parkinson's disease with dementia patients with a 2-year follow-up. *Brain* 2008;131:690–705. <https://doi.org/10.1093/brain/awm322>.
- Bousleiman H, Zimmermann R, Ahmed S, Hardmeier M, Hatz F, Schindler C, et al. Power spectra for screening parkinsonian patients for mild cognitive impairment. *Ann Clin Transl Neurol* 2014;1:884–90. <https://doi.org/10.1002/acn3.129>.
- Carmona Arroyave JA, Tobón Quintero CA, Suárez Revelo JJ, Ochoa Gómez JF, García YB, Gómez LM, et al. Resting functional connectivity and mild cognitive impairment in Parkinson's disease. An electroencephalogram study. *Future Neurol* 2019;14. <https://doi.org/10.2217/fnl-2018-0048>. FNL18.
- Casals-Coll M, Sánchez-Benavides G, Quintana M, Manero RM, Rognoni T, Calvo L, et al. Spanish normative studies in young adults (NEURONORMA young adults project): Norms for verbal fluency tests. *Neurología* 2013;28:33–40. <https://doi.org/10.1016/j.nrleng.2012.02.003>.
- Caviness JN, Utianski RL, Hentz JG, Beach TG, Dugger BN, Shill HA, et al. Differential spectral quantitative electroencephalography patterns between control and Parkinson's disease cohorts. *Eur J Neurol* 2016;23:387–92. <https://doi.org/10.1111/ene.12878>.
- Cozac VV, Gschwandtner U, Hatz F, Hardmeier M, Rüegg S, Fuhr P. Quantitative EEG and cognitive decline in Parkinson's disease. *Parkinsons Dis* 2016. <https://doi.org/10.1155/2016/9060649>.
- Delorme A, Makeig S. EEGLAB: an open source toolbox for analysis of single-trial EEG dynamics including independent component analysis. *J Neurosci Meth* 2004;134:9–21.
- Eichelberger D, Calabrese P, Meyer A, Chaturvedi M, Hatz F, Fuhr P, et al. Correlation of Visuospatial Ability and EEG Slowing in Patients with Parkinson's Disease. *Parkinsons Dis* 2017;2017:3659784. <https://doi.org/10.1155/2017/3659784>.
- Emre M, Aarsland D, Brown R, Burn DJ, Duyckaerts C, Mizuno Y, et al. Clinical diagnostic criteria for dementia associated with Parkinson's disease. *Mov Disord* 2007;22:1689–707. <https://doi.org/10.1002/mds.21507>.
- Fytche DH, Pereira JB, Ballard C, Chaudhuri KR, Weintraub D, Aarsland D. Risk factors for early psychosis in PD: Insights from the Parkinson's Progression markers initiative. *J Neurol Neurosurg Psychiatry* 2017;88:325–31. <https://doi.org/10.1136/jnnp-2016-314832>.
- Franciotti R, Pilotto A, Moretti DV, Falasca NW, Arnaldi D, Taylor J-P, et al. Anterior EEG slowing in dementia with Lewy bodies: a multicenter European cohort study. *Neurobiol Aging* 2020;93:55–60. <https://doi.org/10.1016/j.neurobiolaging.2020.04.023>.
- George JS, Strunk J, Mak-Mccully R, Houser M, Poizner H, Aron AR. Dopaminergic therapy in Parkinson's disease decreases cortical beta band coherence in the resting state and increases cortical beta band power during executive control. *NeuroImage Clin* 2013;3:261–70. <https://doi.org/10.1016/j.nicl.2013.07.013>.
- Geraedts VJ, Boon LI, Marinus J, Gouw AA, van Hilten JJ, Stam CJ, et al. Clinical correlates of quantitative EEG in Parkinson disease. *Neurology* 2018;91:871–83. <https://doi.org/10.1212/WNL.0000000000006473>.
- Gil L, Ruiz De Sánchez C, Gil F, Romero SJ, Pretel Burgos F. Validation of the Montreal Cognitive Assessment (MoCA) in Spanish as a screening tool for mild cognitive impairment and mild dementia in patients over 65 years old in Bogotá, Colombia. *Int J Geriatr Psychiatry* 2015;30:655–62. <https://doi.org/10.1002/gps.4199>.
- Goetz CC. The Unified Parkinson's Disease Rating Scale (UPDRS): Status and recommendations. *Mov Disord* 2003;18:738–50. <https://doi.org/10.1002/mds.10473>.
- Golden C, Freshwater S. Stroop Color and Word Test: A Manual for Clinical and Experimental Use. Chicago, IL: Stoelting Co; 1978.
- van der Hiele K, Vein AA, Reijntjes RHAM, Westendorp RGJ, Bollen ELEM, van Buchem MA, et al. EEG correlates in the spectrum of cognitive decline. *Clin Neurophysiol* 2007;118:1931–9. <https://doi.org/10.1016/j.clinph.2007.05.070>.
- Hoehn MM, Yahr MD. Parkinsonism: Onset, progression, and mortality. *Neurology* 1967;17:427–42. <https://doi.org/10.1212/wnl.17.5.427>.
- Kehagia AA, Barker RA, Robbins TW. Cognitive impairment in Parkinson's disease: The dual syndrome hypothesis. *Neurodegener Dis* 2012;11:79–92. <https://doi.org/10.1159/000341998>.
- Lawton MP, Brody EM. Assessment of Older People: Self-Maintaining and Instrumental Activities of Daily Living1. *Gerontologist* 1969;9:179–86. https://doi.org/10.1093/geront/9.3_Part_1.179.
- Litvan I, Goldman JC, Tröster AI, Schmand BA, Weintraub D, Petersen RC, et al. Diagnostic criteria for mild cognitive impairment in Parkinson's disease: Movement Disorder Society Task Force guidelines. *Mov Disord* 2012;27:349–56. <https://doi.org/10.1002/mds.24893>.
- Llinás RR, Ribary U, Jeanmonod D, Kronberg E, Mitra PP. Thalamocortical dysrhythmia: A neurological and neuropsychiatric syndrome characterized by magnetoencephalography. *Proc Natl Acad Sci U S A* 1999;96:15222–7. <https://doi.org/10.1073/pnas.96.26.15222>.
- Mahoney FI, Barthel DW. Functional Evaluation: The Barthel Index. *Md State Med J* 1965;14:61–5.
- Massa F, Meli R, Grazzini M, Famà F, De Carli F, Filippi L, et al. Utility of quantitative EEG in early Lewy body disease. *Park Relat Disord* 2020;75:70–5. <https://doi.org/10.1016/j.parkreldis.2020.05.007>.
- Mitra PP, Bokil H. Observed Brain Dynamics. New York: Oxford University Press; 2007. <https://doi.org/10.1093/acprof:oso/9780195178081.003.0012>.
- Moretti DV, Babiloni C, Binetti G, Cassetta E, Dal Forno G, Ferreric F, et al. Individual analysis of EEG frequency and band power in mild Alzheimer's disease. *Clin Neurophysiol* 2004;115:299–308.

- Postuma RB, Berg D, Stern M, Poewe W, Olanow CW, Oertel W, et al. MDS clinical diagnostic criteria for Parkinson's disease. *Mov Disord* 2015;30:1591–601. <https://doi.org/10.1002/mds.26424>.
- Preacher KJ, Hayes AF. SPSS and SAS procedures for estimating indirect effects in simple mediation models. *Behav Res Meth Instruments Comput* 2004;36:717–31. <https://doi.org/10.3758/BF03206553>.
- Prerau MJ, Brown RE, Bianchi MT, Ellenbogen JM, Purdon PL. Sleep neurophysiological dynamics through the lens of multitaper spectral analysis. *Physiology* 2017;32:60–92. <https://doi.org/10.1152/physiol.00062.2015>.
- Rentz DM, Locascio JJ, Becker JA, Moran EK, Eng E, Buckner RL, et al. Cognition, reserve, and amyloid deposition in normal aging. *Ann Neurol* 2010;67:353–64. <https://doi.org/10.1002/ana.21904>.
- Roberts JA, Breakspear M. Synaptic assays: using biophysical models to infer neuronal dysfunction from non-invasive EEG. *Brain* 2018;141:1583. <https://doi.org/10.1093/brain/awy136>.
- Schmidt MT, Kanda PAM, Basile LFH, da Silva Lopes HF, Baratho R, Demario JLC, et al. Index of alpha/theta ratio of the electroencephalogram: a new marker for Alzheimer's disease. *Front Aging Neurosci* 2013;5:60. <https://doi.org/10.3389/fnagi.2013.00060>.
- Suarez-Revelo J, Ochoa-Gómez J, Duque-Grajales J. Improving test-retest reliability of quantitative electroencephalography using different preprocessing approaches. 38th Annu Int Conf IEEE Eng Med Biol Soc 2016:961–4. <https://doi.org/10.1109/EMBC.2016.7590861>.
- Suarez-Revelo J, Ochoa-Gómez J, Tobón-Quintero C. Validation of EEG Pre-processing Pipeline by Test-Retest Reliability. *Commun Comput Inf Sci* 2018;916:290–9. https://doi.org/10.1007/978-3-030-00353-1_26.
- Torralva T, Roca M, Gleichgerrcht E, López P, Manes F. INECO Frontal Screening (IFS): A brief, sensitive, and specific tool to assess executive functions in dementia. *J Int Neuropsychol Soc* 2009;15:777–86. <https://doi.org/10.1017/S1355617709990415>.
- Tranel D, Rudrauf D, Vianna EPM, Damasio H. Does the Clock Drawing Test Have Focal Neuroanatomical Correlates. *Neuropsychology* 2008;22:553–62. <https://doi.org/10.1037/0894-4105.22.5.553>.
- Tranel D, Vianna E, Manzel K, Damasio H, Grabowski T. Neuroanatomical correlates of the Benton Facial Recognition Test and Judgment of Line Orientation Test. *J Clin Exp Neuropsychol* 2009;31:219–33. <https://doi.org/10.1080/13803390802317542>.
- Watson G Stennis, Cholerton Brenna A, Gross Rachel G, Weintraub Daniel, Zabetian Cyrus P, Trojanowski John Q, et al. Neuropsychologic assessment in collaborative Parkinson's disease research: A proposal from the National Institute of Neurological Disorders and Stroke Morris K. Udall Centers of Excellence for Parkinson's Disease Research at the University of Pennsylvania and the University of Washington. *Alzheimer's and Dementia* 2013;9 (5):609–14. <https://doi.org/10.1016/j.jalz.2012.07.006>.
- Williams-Gray CH, Foltyne T, Brayne CEG, Robbins TW, Barker RA. Evolution of cognitive dysfunction in an incident Parkinson's disease cohort. *Brain* 2007;130:1787–98. <https://doi.org/10.1093/brain/awm111>.
- Yuvraj R, Murugappan M, Mohamed Ibrahim N, Iqbal Omar M, Sundaraj K, Mohamad K, et al. On the analysis of EEG power, frequency and asymmetry in Parkinson's disease during emotion processing. *Behav Brain Funct* 2014;10. <https://doi.org/10.1186/1744-9081-10-12>.
- van der Zande JJ, Gouw AA, van Steenoven I, Scheltens P, Stam CJ, Lemstra AW. EEG characteristics of dementia with Lewy Bodies, Alzheimer's Disease and mixed pathology. *Front Aging Neurosci* 2018;10. <https://doi.org/10.3389/fnagi.2018.00190>.

Paper II

ComBat models for harmonization of resting-state EEG features in multi-site studies

Alberto Jaramillo-Jimenez ^{1,2,3,4,5 *}, Diego A Tovar-Rios ^{1,2,6,7}, Yorguin-Jose Mantilla-Ramos ^{4,5}, John-Fredy Ochoa-Gomez ⁴, Dag Aarsland ^{1,2,8}, Laura Bonanni ⁹ and Kolbjørn Brønnick ^{1,2}

1. Centre for Age-Related Medicine (SESAM), Stavanger University Hospital. Stavanger, Norway
2. Faculty of Health Sciences, University of Stavanger. Stavanger, Norway
3. Grupo de Neurociencias de Antioquia, Universidad de Antioquia. Medellín, Colombia
4. Grupo Neuropsicología y Conducta, Universidad de Antioquia. Medellín, Colombia
5. Semillero de Investigación NeuroCo, Universidad de Antioquia, Medellín, Colombia
6. Grupo de Investigación en Estadística Aplicada - INFERIR, Universidad del Valle, Cali, Colombia
7. Prevención y Control de la Enfermedad Crónica - PRECEC, Universidad del Valle, Colombia
8. Department of Old Age Psychiatry, King's College London - Institute of Psychiatry, Psychology, and Neuroscience, London, UK
9. Department of Medicine and Aging Sciences, G. d'Annunzio University, Chieti, Italy

* Corresponding author: Alberto Jaramillo-Jimenez. Centre for Age-Related Medicine (SESAM), Stavanger University Hospital, PB 8100, N-4068. Stavanger, Norway. Email: alberto.jaramilloj@udea.edu.co

Short running title: ComBat harmonization of EEG features

Abstract

Pooling multi-site resting-state electroencephalography (rsEEG) datasets may introduce type I errors due to site-specific "batch" effects. The Combining Batches (ComBat) models can control for batch effects while preserving the variability of biological covariates. We aim to evaluate four ComBat harmonization pipelines in a pooled sample from five independent rsEEG datasets of young and old adults. RsEEG signals ($n = 374$) were automatically preprocessed. Aperiodic features and 1/f adjusted band powers in canonical frequency bands were extracted in sensor space. Features were harmonized using neuroCombat, neuroHarmonize, OPNested-GMM Combat, and HarmonizR. Batch effects across centers were identified in spectral features. All ComBat methods reduced batch effects and sparsity of rsEEG features. HarmonizR and OPNested-GMM ComBat achieved the greatest reduction in features' average distances and average differences between datasets. Harmonized Beta power, individual Alpha peak frequency, Aperiodic exponent, and offset in posterior electrodes showed significant relations with age. All ComBat models maintained the direction of observed relationships while increasing the effect size. ComBat models, particularly HarmonizeR and OPNested-GMM ComBat, effectively control for site-specific batch effects in rsEEG spectral features. This workflow can be used in multi-site studies to harmonize sensor-space rsEEG spectral features, achieving greater statistical power while controlling for batch effects.

Keywords: Electroencephalography, Spectral Parameterization, Harmonization, Ageing.

1. Introduction

Resting-state Electroencephalogram (rsEEG) signals have been used to represent brain-related electrical correlates of development, aging, and diseases (Babiloni et al., 2020a). In recent decades, the corpus of clinical research using rsEEG has significantly grown (Colom-Cadena et al., 2020b; Yao et al., 2022), and the open-science philosophy adopted by several researchers and institutions granted full accessibility to software and datasets (Niso et al., 2022). However, the sample size of numerous datasets is often small, limiting the statistical power, generalizability, and external validity of the findings of single-site studies (Newson and Thiagarajan, 2019).

Pooling multi-site rsEEG data into a larger single dataset can introduce the effects of site-specific variability ("batch" effects) affecting the statistical inference by introducing potential type I errors. Variability across centers could be attributed to headset/hardware differences, non-identical experimental setup, biological variability across site samples, and particular parameters for acquisition and processing (Bigdely-Shamlo et al., 2020; M. Li et al., 2022). In genetics, proteomics, and neuroimaging, various attempts have been made to mitigate batch effects, including statistical harmonization of derivative features by re-scaling unharmonized features based on regression residuals (i.e., adjusted for the site variable and potential biological covariates) and estimating specific site parameters using generalized additive models with Bayesian optimization as implemented in the combining batches (ComBat) method (Fortin et al., 2018; Voß et al., 2022). The ComBat approach was initially applied in genomics (Johnson et al., 2007), also showing good performance in a wide variety of radiomic datasets (Beer et al., 2020; Bell et al., 2022; Pomponio et al., 2020; Shiri et al., 2022; Voß et al., 2022; Xu et al., 2023) \cite{Fortin2018, Pomponio2020, Beer2020, Xu2023, Bell2022, Shiri2022}, as well as transcriptomics (Ryan et al., 2022). Conversely, there are scarce reports on the specific effects of statistical harmonization of multi-site rsEEG features with ComBat-derived methods in the currently available literature (Kurbatskaya et al., 2023a).

Adaptations to the original ComBat method for neuroimaging data allow modeling site-specific scaling factors, resulting in suitable alternatives for small sample-size datasets given the use of empirical Bayes to estimate the site parameters. Besides, the estimations of most ComBat variants preserve the effect of biological covariates of interest, such as age, gender, or diagnosis (Fortin et al., 2018; Horng et al., 2022; Pomponio et al., 2020). Thus, standard processing workflows and pooling multi-site datasets while controlling for "batch" effects might contribute to more generalizable findings in rsEEG studies.

With all the above, we aim to evaluate four ComBat harmonization pipelines in a pooled sample from five independent rsEEG datasets of young and old adults. As a practical tool for clinical

researchers, this openly available harmonization workflow is conducted on robust features (Babiloni et al., 2020a), namely, oscillatory and non-oscillatory spectral parameterization features extracted in sensor space from rsEEG signals (Donoghue et al., 2020b).

2. Methods

2.1 Study Design and Participants

This secondary analysis capitalizes on five primary cross-sectional studies conducted in four countries (USA, Finland, Norway, and Germany) with openly available datasets. Three of these datasets were acquired in healthy controls to explore rsEEG differences with Parkinson's disease patients (Anjum et al., 2020; Railo et al., 2020; Rockhill et al., 2021), while the remaining studies aimed to study the effect of aging over rsEEG features (Babayan et al., 2019; Hatlestad-Hall et al., 2022a). The presence of neurological or psychiatric conditions was considered an exclusion criterion in most primary studies.

Details on each primary study are listed below for each primary study:

2.1.1. California dataset: Data was acquired in 2013. Cognitively normal older adults ($n = 16$) were recruited at Scripps Clinic in La Jolla, California, USA. Participants were recruited from the community (or were spouses of the Parkinson's Disease patients assessed in this primary study). All subjects signed a written informed consent approved by the University of California, San Diego. An extended description is provided elsewhere (George et al., 2013; Jackson et al., 2019).

2.1.2. Finland dataset: Data was acquired in 2018. Cognitively normal older adults ($n = 20$) were recruited as a control group at the University of Turku, and Turku University Hospital, Turku, Finland. Participants signed written informed consent with ethical approval from the local committee. An extended description is provided elsewhere (Railo et al., 2020).

2.1.3. Iowa dataset: Data was acquired from 2017 to 2019. Cognitively normal older adults ($n = 14$) were recruited as a control group at the University of Iowa, Narayanan Lab, Iowa, USA. All participants provided written informed consent, approved by the Office of Institutional Review Board. An extended description is provided elsewhere (Anjum et al., 2020; Singh et al., 2020).

2.1.4. Oslo dataset: Data was acquired in 2017. Cognitively normal young and old adults (n = 111) were recruited from the local community at the University of Oslo, Oslo, Norway. The primary study explored visual and auditory stimulus-specific response modulation and the effects of aging; in addition to the event-related data, rsEEG recordings were acquired. Participants signed a written informed consent approved by the regional ethics committee. An extended description is provided elsewhere (Hatlestad-Hall et al., 2022b; Rygvold et al., 2021).

2.1.5. LEMON dataset: Data was acquired between 2013 and 2015. Participants (n = 216) were included in the "Leipzig Study for Mind-Body-Emotion Interactions" (LEMON) study to explore mind-brain-body-emotion interactions across aging. The sample consisted of healthy young (20-35 years) and old adults (59-77 years) recruited at the Day Clinic for Cognitive Neurology of the University Clinic Leipzig and the Max Planck Institute for Human and Cognitive and Brain Sciences, Leipzig, Germany. Participants signed a written informed consent approved by the ethics committee at the University of Leipzig - medical faculty. An extended description is provided elsewhere (Babayan et al., 2019).

2.2. RsEEG recordings and Signal preprocessing:

All raw rsEEG data is available in open repositories as follows California (Rockhill et al., 2021), Finland (Railo, 2021), Iowa (Narayanan Lab, 2020), Oslo (Hatlestad-Hall, 2022), and LEMON (Babayan et al., 2019). The LEMON dataset was downloaded using a Python script present in the GitHub repository of a previous report (Engemann et al., 2022b).

RsEEG signals were acquired with electrode caps with monopolar montages. Headsets and amplifiers used for acquisition were the BioSemi ActiveTwo system (32 channels in the California dataset and 64 channels in the Oslo dataset), NeurOne Tesla (64 channels in the Finland dataset), Brain Vision system (64 channels in the Iowa dataset), and BrainAmp MR plus (62 channels in the LEMON dataset). Twenty-nine common channels across all recordings were considered for this analysis (i.e., AF3, AF4, Fp1, Fp2, F7, F8, F3, Fz, F4, FC1, FC2, FC5, FC6, C3, Cz, C4, CP1, CP2, CP5, CP6, T7, T8, P7, P8, P3, P4, O1, Oz, and O2). See supplementary Figure 1.

Rs-EEG signals from Iowa were recorded during the eyes open condition, while recordings from the remaining research sites were under eyes closed. An extended description of the acquisition parameters of these datasets can be found in the abovementioned primary publications and repositories.

In order to automatize the preprocessing and feature extraction steps, all datasets were standardized following the Brain Image Data Structure (BIDS) specification (Pernet et al., 2019) using the sovaBIDS package (Mantilla-Ramos, 2023).

For preprocessing of all rs-EEG signals, we used a Python implementation of an already validated workflow previously published by our group (Isaza et al., 2023; Jaramillo-Jimenez et al., 2023; Suárez-Revelo et al., 2018). This fully automated pipeline wrapped multiple preprocessing tools. First, robust average re-referencing, adaptative line-noise correction, and bad channel interpolation were performed using the PyPREP library (Appelhoff et al., 2022), a Python reimplemention of the MATLAB PREP pipeline (Bigdely-Shamlo et al., 2015). PyPREP pipeline aims to estimate a robust average reference by excluding noisy channels, ensuring a comparable reference scheme across datasets. Following PyPREP, a stage of wavelet-enhanced Independent Component Analysis (ICA) was performed to smooth strong artifacts in the data (such as those originating from muscular or eye-blink components) (Castellanos and Makarov, 2006). Therefore, a 1Hz high-pass Finite Impulse Response (FIR) filter was applied to remove low-frequency drifts that would affect the following ICA stage. The MNE library's FastICA algorithm was subsequently employed to extract artifactual and brain components from the signal (Gramfort et al., 2013). These components were decomposed into wavelets, and artifacts were smoothed through wavelet thresholding. The signal was then low-pass filtered at 30 Hz. From the rsEEG recordings, epochs of 5 seconds were obtained. Finally, artifactual epochs were automatically rejected based on signal parameters, including extreme amplitude and spectral power values, as well as statistical features such as linear trends, joint probability, and kurtosis. A detailed description of the preprocessing flow and its test-retest reliability can be found elsewhere (Isaza et al., 2023).

The number of available epochs in each dataset varied depending on each center's protocols. We used all available artifact-free epochs from each participant to leverage as much data as possible. The number of clean epochs in Oslo (Mean = 39.12; S.D = 1.48), California (Mean = 32.31; S.D = 1.40), Iowa (Mean = 32.21; S.D = 10.11), Finland (Mean = 25.53; S.D = 2.12), and LEMON (Mean = 179.99; S.D = 16.97) is depicted in Supplementary Figure 2.

2.3. Features extraction: Spectral parameterization

The preprocessed signals were down-sampled to a uniform sampling rate of 500 Hz. For each of the 5-second epochs included in the analysis, Power Spectral Density (PSD) vectors were computed at the sensor level using the `psd_array_multitaper` function implemented in MNE, with default parameters (Gramfort et al., 2013). Next, the median of the PSD vectors was computed across epochs. Given the potential confounder effect of aperiodic activity in the PSD vectors, spectral parameterization was conducted using the Fitting Oscillations & One Over

Frequency algorithm (FOOOF) (Donoghue et al., 2020b). FOOOF models aperiodic (1/f) and oscillatory activity in the PSD vectors, providing the following descriptors: Oscillatory parameters (Power – P.W., Bandwidth – B.W., Center Frequency – C.F.), Aperiodic parameters (Exponent, Offset), Fitting parameters (error, and R-squared). FOOOF Oscillatory band powers were computed in fixed bands: delta (1 – 4 Hz), theta (4 – 8 Hz), alpha (8 – 13 Hz), and beta (13 – 30 Hz) (Babiloni et al., 2020a). The FOOOF center frequency and bandwidth were computed in the extended alpha (5 – 14 Hz) to represent the individual alpha peak frequency [Moretti et al., 2013]. Besides, the aperiodic exponent represents the slope of the 1/f activity, while the aperiodic offset represents the y-axis intercept of the 1/f activity in the PSD vector of each channel.

The current analysis only used spectral parameters from channels with a good fitting, defined here as a FOOOF fitting R-squared equal to or greater than 0.8 for further analyses (83,51 % of all channel fittings were included). A complete description of FOOOF fitting estimations is presented in Supplementary Figure 2 and Supplementary Table 1. Despite the multiple benefits of FOOOF, we noticed that oscillatory parameters might produce missing values if the band power is equal to 0 (as the area under the curve cannot be computed) or where the center frequency (peak frequency) is not within a given frequency band. Thus, in the final dataset containing all spectral features from all subjects ($n = 374$) by channel (channels = 29), the missing values achieved 19.83% of all spectral parameters. The percentage of missing values across features was: Delta power (74.98%), theta power (69.93%), alpha power (18.49%), beta power (4.85%), extended alpha center frequency & bandwidth (15.03%), aperiodic parameters (0 %).

2.4. Harmonization of rsEEG spectral parameters

The pooled dataset (i.e., unharmonized) was harmonized across batches (i.e., research centers) using four ComBat variants: neuroCombat (Fortin et al., 2018), neuroHarmonize (Pomponio et al., 2020), and Optimized Nested ComBat – Gaussian Mixture Model (Horng et al., 2022) were implemented in Python, while HarmonizR (Voß et al., 2022) was implemented in R. For all ComBat variants, we used the default parameters.

Briefly, the neuroCombat model incorporates site-specific scaling factors (i.e., location and scale factors, accounting for mean and variance site-related differences in a given feature) and uses empirical Bayes for improved estimation of these site parameters in studies with small sample sizes. Thus, neuroCombat re-scales the feature values to make them comparable across batches. In addition, neuroCombat retains the linear effect of biological covariates on the harmonized features (Fortin et al., 2018). NeuroHarmonize emerged as a variation of

neuroCombat that lets the user specify covariates with generic nonlinear effects (Implemented using Generalized Additive Models) (Pomponio et al., 2020). Furthermore, the Optimized Nested ComBat – Gaussian Mixture Model (OPNComBat-GMM) was developed to handle bimodal distributions while preserving the effect of unknown biological covariates treated as latent variables that will be preserved in the harmonization (Horng et al., 2022). Finally, HarmonizR is a variant of the original ComBat (Johnson et al., 2007) designed to handle datasets with missing values using an iterative splitting process while preserving the maximum amount of data during the harmonization (Voß et al., 2022).

As none of the Python-based ComBat variants could operate with missing values, we replaced them with zeros. Considering that HarmonizR can harmonize features with missing values, the replacement with zeros was not conducted for that harmonization method. To retain the variability of biological covariates, all the Python-based harmonization models allow the introduction of biological covariates (sex and age), whereas HarmonizR does not. Thus, age and sex variability were controlled only in the Python-based harmonization variants.

2.5 Statistical analysis

All statistical analyses were performed in Python version 3.9.13 and R version 4.3.

T-distributed Stochastic Neighbor Embedding (tSNE) models were used to explore site-related differences in the unharmonized and harmonized datasets. As a dimensionality reduction algorithm, tSNE maps high-dimensional data to a lower-dimensional space while preserving local similarities. By visualizing the data in this reduced space, tSNE helps identify patterns, clusters, and trends that may not be apparent in the original feature space. Thus, tSNE models were fitted for each dataset (i.e., unharmonized and ComBat harmonized datasets) to identify potential batch effects across all available rsEEG features. The perplexity parameter was set to 30 in all tSNE models. Further, euclidean distances were calculated for each site's average tSNE components 1 and 2; distances between sites were also calculated and presented in distance matrixes and the average site-related distance for a given dataset. The abovementioned procedure was conducted in unharmonized datasets (with and without the replacement of missing values with zero) and each of the harmonized datasets (i.e., neuroCombat, neuroHarmonize, OPNComBat-GMM, and HarmonizR).

As tSNE models provide a broader perspective on the overall site-related patterns in the unharmonized and harmonized datasets, probability plots offer a more detailed examination of the feature-wise variations across sites. Probability plots depict the cumulative probability distribution for each rsEEG feature (i.e., the likelihood of observing a specific value). For the current analysis, probability plots contrast the cumulative probability distribution of a given

feature across site datasets. Probability plots were also computed for unharmonized and harmonized datasets.

Kruskal-Wallis models provided an estimated magnitude to quantify the harmonization process features-wise. For each Kruskal-Wallis model, a given dataset (unharmonized or harmonized) was used, and the site-related differences (independent variable) were estimated for each of the rsEEG features (dependent variable). Given the distribution of the datasets, violation of assumptions for parametric methods, and considering that some of the harmonization methods could not handle biological covariates, we did not perform covariate adjustment or other parametric tests.

Finally, as prior reports with the FOOOF method have shown age-related differences in some spectral parameters (i.e., older adults exhibit higher power in delta, low-alpha, beta, and gamma bands with reduced aperiodic parameters, as well as decreased alpha peak frequency and bandwidth) (He et al., 2019; Karekal et al., 2023; Merkin et al., 2021), we used ordinary least squares fitting to examine the effect of harmonization methods on the direction, magnitude, and statistical significance of potential relationships between rsEEG features and age. Therefore, for each subject and rsEEG feature, we computed the average value in the posterior Region Of Interest (ROI) sensors, namely, P7, P8, P3, P4, O1, Oz, and O2. Pearson R coefficients were included to represent the direction and effect size of the relationship between age and each feature in the posterior ROI. Given the exploratory nature of this analysis and to explore the effect of harmonization on the estimated uncorrected p-values, statistical significance was not corrected for multiple testing.

This manuscript adheres to the STROBE statement guidelines, which ensure clear reporting in observational studies (Vandenbroucke et al., 2007). Additionally, in line with the principles of open science, we have included the raw data sources and shared the codes used for feature extraction, harmonization, and analysis. Also, the datasets with unharmonized and harmonized features are available for reproducibility of the analyses of this manuscript. These files can be found on the following GitHub repository (https://github.com/alberto-jj/combat_eeg).

3. Results

3.1. Demographic characteristics of the sample

The current study includes data from healthy adults (n = 374). There were significant differences in age across the site datasets (Kruskal-Wallis $p < 0.001$, H statistic = 73.04, df = 4), with significantly younger participants in the LEMON and Oslo datasets ($p < 0.001$). Overall,

there were significant differences in the proportion of male and female participants across centers ($X^2 = 22.07$, $p < 0.001$, $df = 4$).

The pooled sample had 177 females (47.33 %) and 197 males (52.67 %). Also, in the pooled dataset, age varied from 17 to 86 years (Mean = 42.36, S.D = 19.83, Median = 32.5, IQR = 24 - 62.5). Also, males were significantly younger than female participants (Welch test = 2.15, $p = 0.32$, Mann-Whitney test = 19561, $p = 0.040$). Descriptive statistics for the demographic characteristics of the sample are presented in Figure 1.

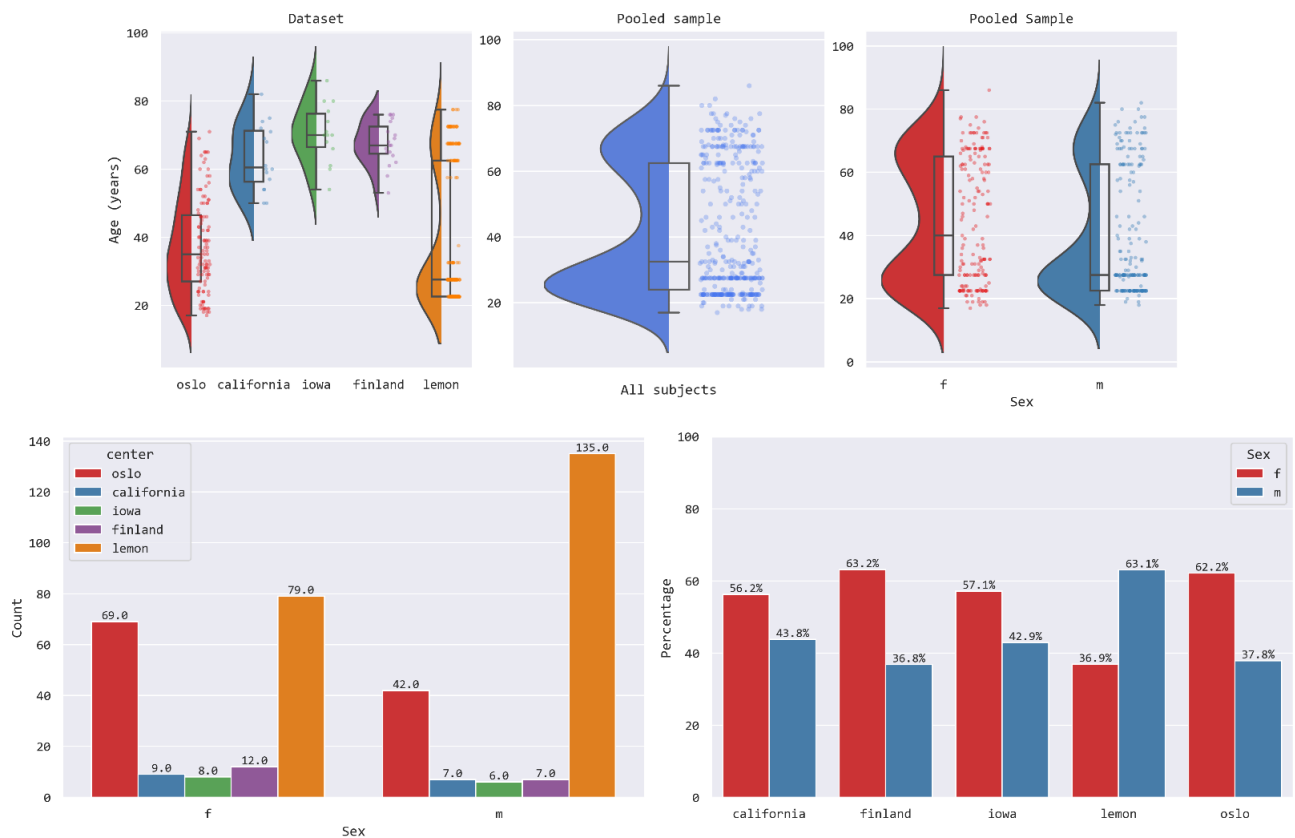


Figure 1. Demographic characteristics of the sample. Raincloud plots show age distributions across centers and in the pooled sample. Bar plots show the sex proportion (in absolute counts and relative frequency) for each dataset.

3.2. Rs-EEG spectral parameterization

Figure 2 shows the resulting FOOOF estimations for unharmonized PSD, oscillatory, and aperiodic fitting vectors across all datasets and in the pooled data. This initial inspection showed potential batch effects across centers, as evidenced by the differences in the scales of the vectors for each center. In the Iowa dataset (eyes open), older adults showed higher mean uncorrected power, aperiodic fit, and oscillatory fit.

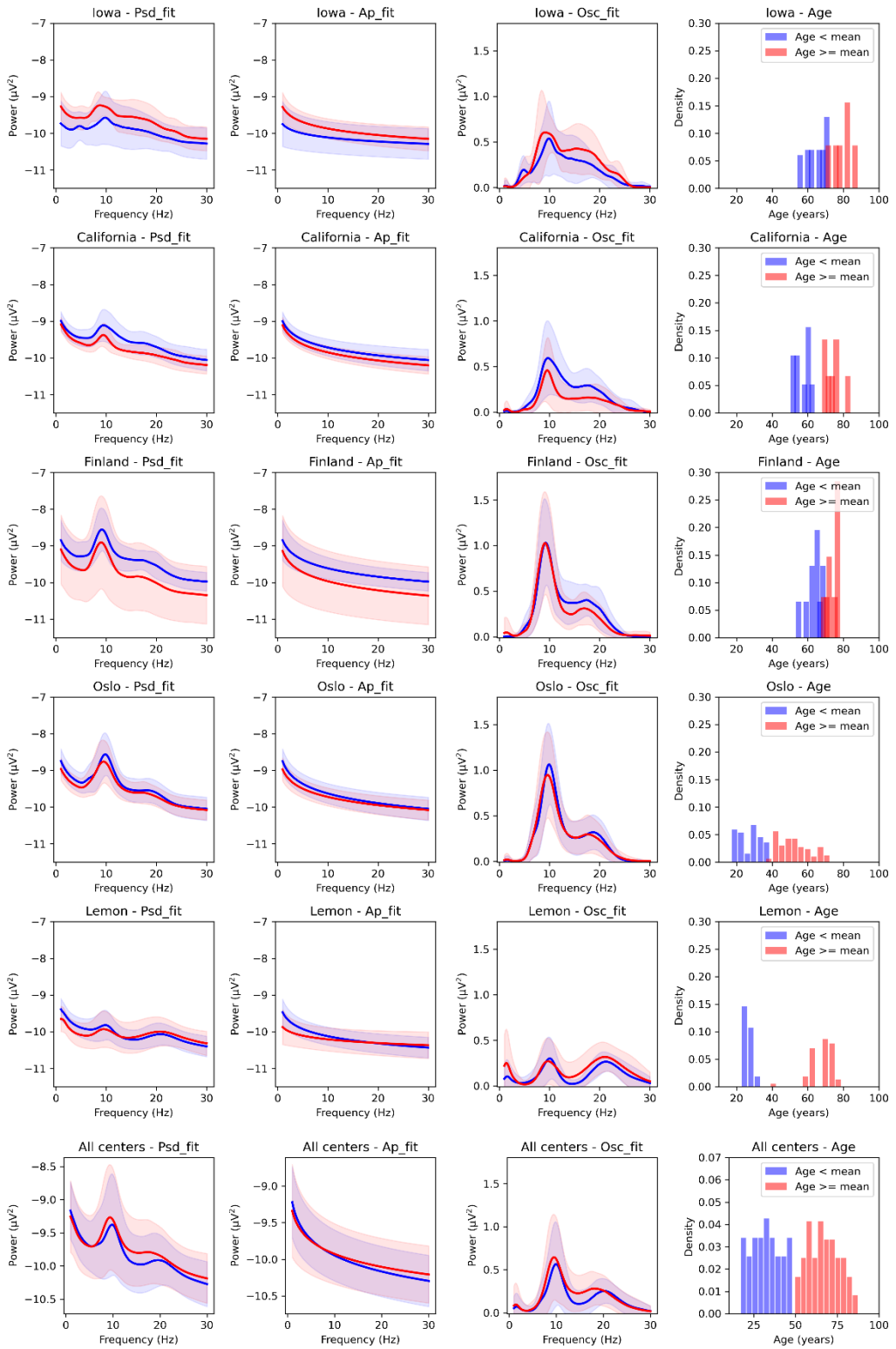


Figure 2. Spectral parameterization of rsEEG signals. Mean uncorrected power, aperiodic fit, and oscillatory fit (columns) in each dataset and the total sample (rows). Colors are based on the mean age of the sample. Shadow areas indicate standard deviation.

3.3. Rs-EEG features harmonization

All ComBat harmonization models reduced dispersion and centered the average tSNE values for each site/research center. Also, the average distance between datasets' average tSNE values was reduced by all ComBat variants compared to the unharmonized dataset (with the replacement of missing values with zeros). OPNComBat-GMM, followed by HarmonizR, achieved the lowest average site-related distance. However, pair-wise site distances for the LEMON dataset were better controlled by OPNComBat-GMM.

The average performance of neuroCombat and neuroHarmonize was comparable, as reflected by tSNE-based distance estimates. Harmonization effects over all the rsEEG features are presented in Figure 3.

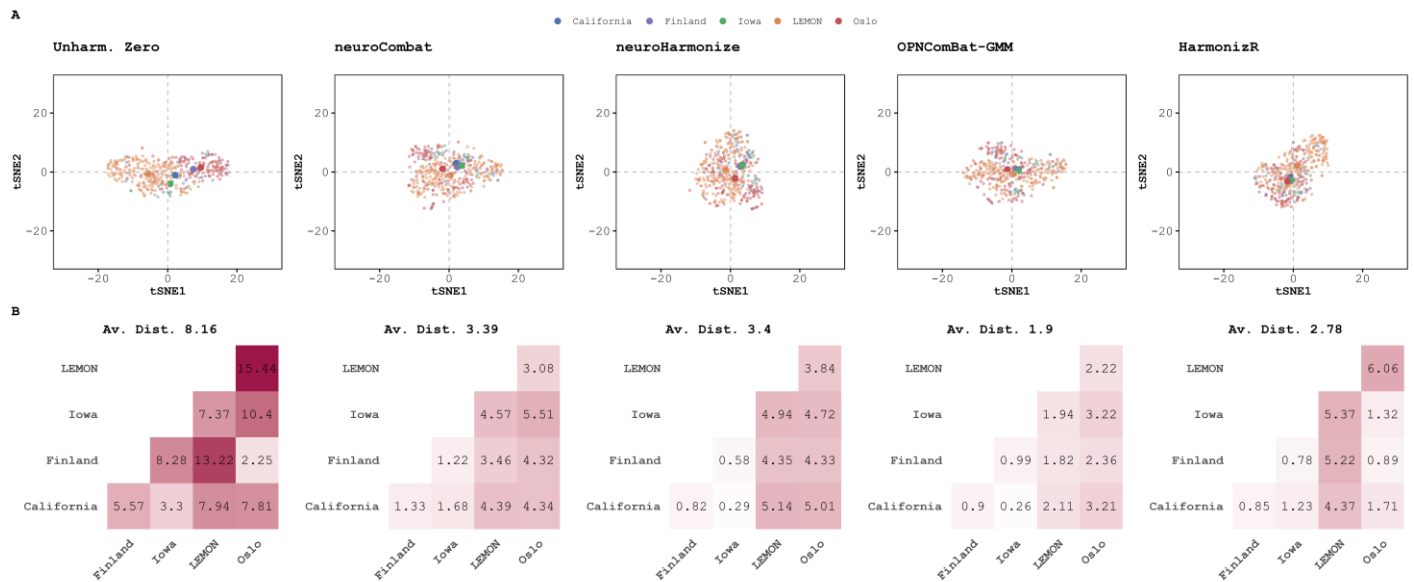


Figure 3. Harmonization effects across all rsEEG spectral features. A) T-distributed stochastic neighbor embedding (tSNE) components, perplexity = 30. Each plot shows the tSNE fit for the unharmonized (with zeros instead of missing) and harmonized datasets with different ComBat variants. Dots depict a given subject (all rsEEG features reduced), color-coded by the site/research center. Bold dots represent the average of the tSNE components for each site/research center. **B)** Distance matrixes show the Euclidean distance between site-average values (obtained from tSNE models). The average distance in unharmonized and harmonized datasets is computed from each matrix.

A detailed description of the distribution of each rsEEG feature is presented in Table 1 and Figure 4, as well as in Supplementary Figures 4 - 9.

| <i>Harmonization</i> | | <i>Delta_pw</i> | <i>Theta_pw</i> | <i>Alpha_pw</i> | <i>Beta_pw</i> | <i>Ext. alpha_cf</i> | <i>Ext. alpha_bw</i> | <i>Offset</i> | <i>Exponent</i> |
|--|---------------|-----------------|-----------------|-----------------|----------------|----------------------|----------------------|---------------|-----------------|
| <i>Unharmonized</i> | <i>Median</i> | 0,00 | 0,00 | 0,39 | 0,34 | 9,56 | 1,97 | -9,41 | 0,65 |
| | <i>IQR</i> | 0,01 | 0,15 | 0,64 | 0,22 | 2,07 | 1,23 | 0,75 | 0,48 |
| | <i>Mean</i> | 0,09 | 0,10 | 0,52 | 0,35 | 8,23 | 1,93 | -9,45 | 0,60 |
| | <i>Std</i> | 0,22 | 0,19 | 0,47 | 0,18 | 3,67 | 1,15 | 0,57 | 0,38 |
| <i>neuroCombat</i> | <i>Median</i> | 0,02 | 0,03 | 0,50 | 0,34 | 9,13 | 1,97 | -9,43 | 0,63 |
| | <i>IQR</i> | 0,12 | 0,13 | 0,54 | 0,22 | 3,73 | 1,33 | 0,57 | 0,46 |
| | <i>Mean</i> | 0,09 | 0,10 | 0,52 | 0,35 | 8,23 | 1,94 | -9,45 | 0,60 |
| | <i>Std</i> | 0,20 | 0,17 | 0,34 | 0,17 | 3,31 | 1,06 | 0,46 | 0,35 |
| <i>neuroHarmonize</i> | <i>Median</i> | 0,01 | 0,03 | 0,50 | 0,34 | 9,14 | 1,96 | -9,42 | 0,63 |
| | <i>IQR</i> | 0,12 | 0,13 | 0,54 | 0,22 | 3,73 | 1,32 | 0,57 | 0,46 |
| | <i>Mean</i> | 0,09 | 0,10 | 0,52 | 0,35 | 8,23 | 1,94 | -9,45 | 0,60 |
| | <i>Std</i> | 0,20 | 0,17 | 0,34 | 0,17 | 3,31 | 1,06 | 0,46 | 0,35 |
| <i>OPNested-GMM</i> | <i>Median</i> | 0,02 | 0,03 | 0,50 | 0,34 | 9,14 | 1,96 | -9,42 | 0,63 |
| | <i>IQR</i> | 0,11 | 0,14 | 0,55 | 0,22 | 3,73 | 1,28 | 0,56 | 0,45 |
| | <i>Mean</i> | 0,09 | 0,10 | 0,52 | 0,35 | 8,24 | 1,94 | -9,45 | 0,60 |
| | <i>Std</i> | 0,20 | 0,17 | 0,34 | 0,17 | 3,31 | 1,06 | 0,45 | 0,35 |
| <i>Unharmonized</i> <i>(with NaN)</i> | <i>Median</i> | 0,25 | 0,26 | 0,50 | 0,35 | 9,78 | 2,14 | -9,41 | 0,65 |
| | <i>IQR</i> | 0,37 | 0,22 | 0,64 | 0,21 | 1,43 | 1,03 | 0,75 | 0,48 |
| | <i>Mean</i> | 0,37 | 0,32 | 0,64 | 0,37 | 9,68 | 2,28 | -9,45 | 0,60 |
| | <i>Std</i> | 0,31 | 0,22 | 0,44 | 0,16 | 1,33 | 0,89 | 0,57 | 0,38 |
| <i>HarmonizR</i> | <i>Median</i> | 0,25 | 0,25 | 0,56 | 0,35 | 9,77 | 2,13 | -9,41 | 0,63 |
| | <i>IQR</i> | 0,36 | 0,20 | 0,47 | 0,21 | 1,45 | 1,01 | 0,55 | 0,43 |
| | <i>Mean</i> | 0,33 | 0,29 | 0,60 | 0,37 | 9,67 | 2,26 | -9,45 | 0,60 |
| | <i>Std</i> | 0,29 | 0,19 | 0,33 | 0,16 | 1,29 | 0,85 | 0,45 | 0,34 |

Table 1. Descriptive statistics by rsEEG features; results on unharmonized and harmonized datasets. Central tendency metrics, as well as dispersion (interquartile range – IQR, and standard deviation – Std) for each rsEEG feature (i.e., Delta power, theta power, alpha power, beta power, extended alpha center frequency, extended alpha bandwidth, aperiodic offset, aperiodic exponent) in the pooled sample.

The largest site-related differences were observed for alpha power and aperiodic offset. Replacing missing values with zeros increased the average site-related differences in the unharmonized data while introducing bimodal distributions and skewness in most rsEEG features, see Figure 4 and Supplementary Figures 4 – 9. This feature-wise approach showed the lowest average site-related differences for HarmonizR, followed by OPNComBat-GMM, see Figure 4. Site-related differences were not fully controlled, particularly in the distribution tails of multiple rsEEG features. Also, site-related differences in distributions (and extreme values skewness) were more prominent in the extended alpha center frequency and bandwidth when replacing missing values for zeros versus maintaining missing values and using the HarmonizR method. Supplementary Figures 8 – 9.

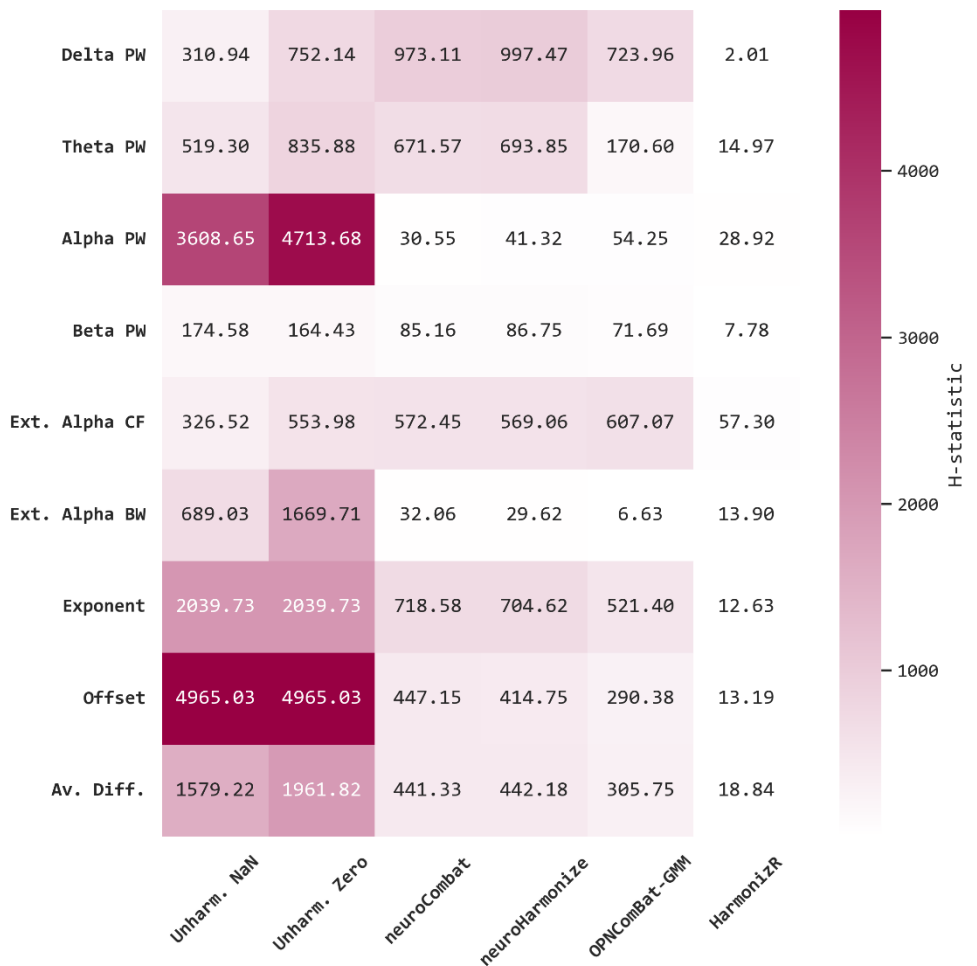


Figure 4. Estimated site-related differences, results for each rsEEG feature. Heatmap represents the Kruskal-Wallis H statistic for site-related differences in the values of each rsEEG feature (in rows) and unharmonized (with missing values or zeros) or harmonized data (in columns). The last row includes the average site-related difference, defined as the average H statistic for all features for a given dataset. Darker colors indicate higher H-statistic estimates for site-related nonparametric differences in a given rsEEG feature.

3.4. Relation between rs-EEG features in the posterior region and age

The median values of Delta and Beta power in the posterior ROI exhibited significant positive relationships with age in the unharmonized data (both with zeros and missing values). Comparable direction, magnitude, and significance of the relationship were observed across all ComBat variants, see Figure 5. Besides, the median values of the extended alpha center frequency (i.e., individual alpha peak frequency), aperiodic offset, and aperiodic exponent exhibited significant negative relationships with age in the unharmonized data (with zeros and

missing values). The relationship's direction, magnitude, and significance were slightly increased in the harmonized datasets and comparable across ComBat variants, see Figure 6.

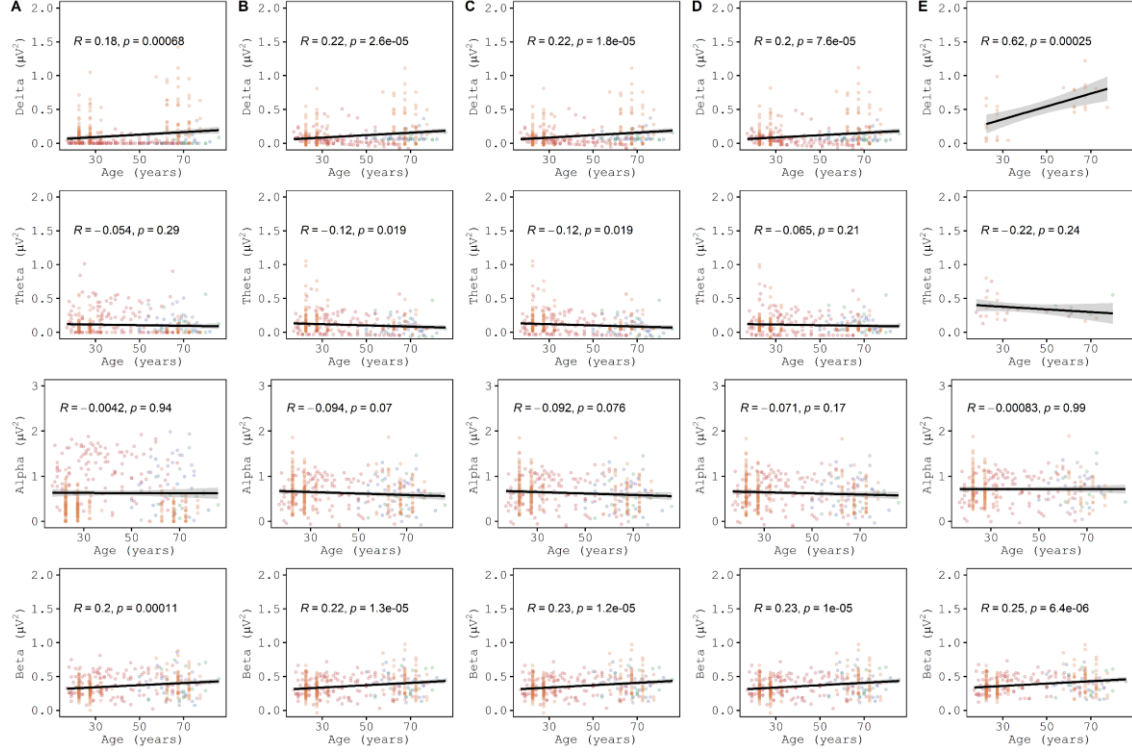


Figure 5. Relationship between power features and age, results by dataset. Each column represents one dataset (unharmonized or harmonized). From left to right columns (A-E): Unharmonized dataset (with zeros), neuroCombat dataset, neuroHarmonize dataset, OPNComBat-GMM dataset, and HarmonizR dataset. Dots indicate each subject's median value in the posterior Region Of Interest (ROI), color-coded by site/research center. Ordinary Least Squares fit was conducted on the full sample. Each frequency band is represented in one different row.

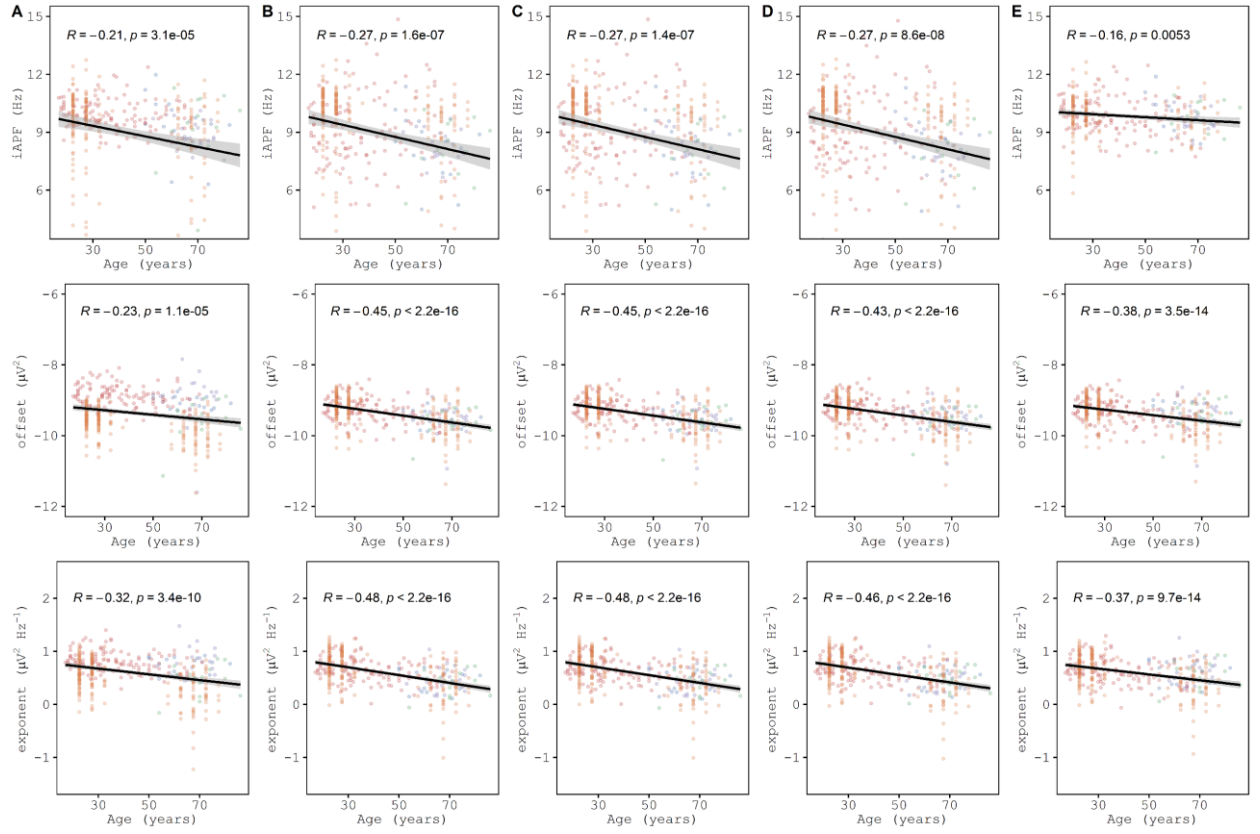


Figure 6. Relationship between center frequency, aperiodic features, and age, results by dataset. Each column represents one dataset (unharmonized or harmonized). From left to right columns (A-E): Unharmonized dataset (with zeros), neuroCombat dataset, neuroHarmonize dataset, OPNComBat-GMM dataset, and HarmonizR dataset. Dots indicate each subject's median value in the posterior Region Of Interest (ROI), color-coded by site/research center. Ordinary Least Squares fit was conducted on the full sample. Each rsEEG feature is represented in one different row.

4. Discussion

For the first time in rsEEG data, this study evaluated the impact of various ComBat pipelines on harmonizing site-related differences. Batch effects were detected in rsEEG-parameterized power-derived features. Our results indicate that all the examined ComBat variants successfully mitigated site-related batch effects in rsEEG spectral features, with OPNComBat and HarmonizR outperforming the others. Finally, our age-related findings in the harmonized datasets are consistent with preliminary works on different neurophysiological modalities reporting increased beta power, lower individual alpha peak frequency, and reduced aperiodic parameters in older individuals when compared to younger subjects, supporting the hypothesis

that ComBat harmonization methods preserve the biological variability while controlling for batch effects.

As a practical tool for clinical researchers, this openly available harmonization workflow is conducted on robust features (Babiloni et al., 2020a), namely, oscillatory and non-oscillatory spectral parameterization features extracted in sensor space from rsEEG signals (Donoghue et al., 2020b). We benchmarked multiple ComBat harmonization pipelines using a large dataset of rsEEG-derived features. ComBat models effectively reduced batch effects from the unharmonized data. However, inappropriate outliers (i.e., negative peak frequencies) have been introduced in the distribution tails for features with larger variance, such as center frequency (ranging from 0 – for models with missing extended alpha peaks - to 15 Hz). The re-scaling to inappropriate values was particularly observed in the Python-based ComBat versions that cannot handle missing values in the unharmonized dataset. By contrast, HarmonizR did not introduce outliers in the extended alpha center frequency (i.e., individual alpha peak frequency) but preserved potential batch-related differences in the extreme values of most features' distributions, as shown in Supplementary Figures 8 and 9. These inconsistencies in re-scaling were also evident in power features, generating negative estimations of power that should be positive by definition. Further development in ComBat models could consider introducing constraints to the re-scaling parameters or providing the harmonized features in a standardized manner to avoid unplausible harmonized estimates and facilitate the interpretability of results. Another potential explanation for the harmonization inconsistencies in the tails has been proposed by simulation studies assessing the presence of outliers in the dataset, which can affect the harmonization and even introduce larger site-related differences if the outliers are not balanced and significantly differ in proportion across the site datasets (Han et al., 2023). Our study aimed to control the quality of the unharmonized data by excluding features derived from FOOOF fittings with an R-squared below 0.8. Also, we examined the center differences using a nonparametric approach, showing a reduction in the estimated site-related difference in all the ComBat harmonized results. Finally, given our data-driven approach and considering this work as an automatic and reproducible solution intended to leverage as much data as possible from heterogeneous datasets, we did not perform any manual data selection that might introduce interobserver variability or contribute to the reduction of the amount of available data for further analysis.

As suggested by prior reports, OPNComBat-GMM outperformed traditional ComBat variants unsuitable for non-normal distribution in the unharmonized features (Horng et al., 2022). In the case of rsEEG features, bimodal distributions were observed when replacing the missing values

in the FOOOF power estimations for zeros (as the area under the PSD curve is assumed to be null). Consistently, the introduction of zeros did not affect the performance of OPNComBat-GMM compared to neuroCombat and neuroHarmonize. However, the better performance of HarmonizR over OPNComBat-GMM might be explained as unimodal distributions (with large skewness) were observed in the unharmonized data with missing values. Of note, even if the replacement of missing values with zeros may be naturally conceived given the rationale for generating missing values in the FOOOF estimates (i.e., a null area under the PSD curve for a given band power), it affected the overall structure of the distribution of most features and potentially affected ComBat models which assume normality of the data such as neuroCombat and neuroHarmonize. Future improvements on the existing ComBat versions should consider handling missing values and including biological covariates (in the case of HarmonizR).

Our results of increased beta power, with decreased individual alpha peak frequency (but not power), as age-related phenomena extend a large corpus of evidence in smaller individual datasets. RsEEG beta power (modeled with FOOOF at sensor level) has been reported as reduced in healthy young adults compared to older individuals (Karekal et al., 2023; Merkin et al., 2021). The age-related increase in beta power has also been replicated in magnetoencephalographic (MEG) studies assessing neurodevelopment from childhood to adulthood in source-reconstructed power (He et al., 2019). This large corpus of evidence in multiple M/EEG datasets highlights the important role of beta band maturation as an age-dependent process. However, non-consistent results in the beta band have been reported in early-to-middle childhood (Hill et al., 2022). The latter might be explained due to the role of beta and higher frequency oscillations in cognitive control (which improves through adolescence) (Crone and Steinbeis, 2017; He et al., 2019).

In addition to our findings in oscillatory power, the age-related changes on aperiodic parameters (offset and exponent) have been extensively and robustly reproduced in smaller individual datasets across different neurophysiological modalities (including rsEEG, visual and auditory event-related potentials, MEG, and electrocorticography - ECoG) (He et al., 2019; Hill et al., 2022; Merkin et al., 2021). Thus, healthy older adults exhibit a flattened aperiodic 1/f signal compared to young adults or children. Similarly, the offset of the aperiodic component has been shown to decline as an age-dependent process. The observations of a flattened aperiodic spectrum (i.e., increase in "neural noise") in resting-state modalities have been considered a correlate of a large number of asynchronous neuronal spiking, which reflects a decoupling in the oscillatory behavior of cortical columns due to the increased ratio between excitation/inhibition (mainly associated with the activity of GABAergic interneurons and pyramidal neurons,

respectively). Complementarily, the age-related decrease observed in the aperiodic offset has been considered a surrogate of a reduced broadband power, and computational insights point out the loss of grey matter and slower spiking rate due to pruning and ageing as a potential explanation (He et al., 2019)

As potential limitations that might affect the results and interpretation of the findings, we consider the lack of longitudinal rsEEG data to assess the test-retest reliability of the abovementioned findings. There are few studies assessing the test-retest reliability in sensor space rsEEG, but this evidence suggests fair-to-excellent reliability in the posterior alpha and beta FOOOF-derived features as well as the aperiodic parameters (Pathania et al., 2021; Popov et al., 2023; Tröndle et al., 2022). Larger evidence with longitudinal assessments can contribute to determining the reproducibility and reliability of our cross-sectional findings. Also, using fully automated workflows might introduce bias in the analysis. The robustness of automated preprocessing workflows in event-related potential features estimated in sensor space has recently been questioned and suggested to be equal to using a high-pass filter only (Delorme, 2023). Despite this, an increased signal-to-noise ratio has been demonstrated in rsEEG data preprocessed using our automated pipeline in multiple datasets, showing high test-retest reliability [Isaza et al., 2023; Suárez-Revelo et al., 2018]. In addition, obtaining features in the sensor space might be insufficient to examine the contribution of adjacent sources of a given brain rhythm due to the volume conduction mixing across sensors. Nevertheless, occipital generators seem to be the most important contributing sources for the power spectrum estimated in parietal and occipital sensors, as demonstrated in M/EEG datasets and simulations on source-space data estimated using spatio-spectral decomposition (Schaworonkow and Nikulin, 2022). Also, source-space reconstruction was not considered in this approach as it implies a higher computational load than sensor-space analysis, which can complicate the local analysis of large data collections. Finally, HarmonizR results did not include modelling of biological covariates, which can explain the outperformance of this model in the harmonization process.

Notwithstanding, our exploratory findings across all harmonization methods showed consistent direction and size of the relationship between age and most analyzed features.

4.1. Conclusions

In conclusion, batch effects were found in rsEEG sensor-level spectral parameters across multiple centers. All ComBat methods reduced batch effects and overall sparsity of rsEEG features. HarmonizR and OPNested-GMM ComBat had the greatest impact on reducing feature differences between datasets. Harmonized Beta power, individual Alpha peak frequency,

Aperiodic exponent, and offset in posterior electrodes showed significant relations with age. All ComBat models preserved the observed relationships and increased their effect size. This openly available workflow can be useful for harmonizing sensor-space rsEEG spectral features in multi-site studies, enhancing statistical power while addressing batch effects.

Acknowledgments: We thank all the participants who contributed to this research with their data. Also, we want to thank all researchers and staff at the University of California – San Diego, the University of Turku and Turku University Hospital, the University of Iowa, the University of Oslo, and the University of Leipzig. We especially express our gratitude to the investigators in the primary studies. They believed in open science principles and made these datasets publicly available. Finally, we thank all institutions and organizations who have supported the research efforts of many of the authors in this paper, including funding institutions such as Helse Vest and the Centre for Age-Related Medicine (SESAM) in Norway, as well as research incubator programs like Semillero NeuroCo, and Semillero SINAPSIS at the School of Medicine of the University de Antioquia, Colombia.

Declaration of Competing Interest: The authors have no conflicts of interest to declare. The sponsor has no role in collecting, analyzing, interpreting the data, and writing the final manuscript.

Funding: This paper represents independent research funded by the Norwegian government through hospital owner Helse Vest (Western Norway Regional Health Authority), project number F-12155. Kind support is also received from the National Institute for Health Research (NIHR) Biomedical Research Centre in South London, the Maudsley NHS Foundation Trust, King's College London in the U.K., and the Center for Innovative Medicine (CIMED) in Sweden. The views expressed are those of the author(s) and not necessarily those of the abovementioned institutions.

Author contributions:

A: conception and design; **B:** data curation; **C:** data analysis; **D:** interpretation of results; **E:** writing the manuscript draft; **F:** review and approval of the final manuscript.

Alberto, Jaramillo-Jimenez: A, B, C, D, E, F.

Diego A., Tovar-Rios: A, C, D, E, F.

Yorguin-Jose, Mantilla-Ramos: A, B, C, E, F.

John Fredy, Ochoa-Gomez: B, D, E, F.

Laura, Bonanni: D, E, F.

Dag, Aarsland: D, E, F.

Kolbjørn, Brønnick: D, E, F.

References

- Aarsland D, Batzu L, Halliday GM, Geurtsen GJ, Ballard C, Ray Chaudhuri K, Weintraub D (2021): Parkinson disease-associated cognitive impairment. *Nat Rev Dis Primers* 7:1–21. <https://www.nature.com/articles/s41572-021-00280-3>.
- Aarsland D, Creese B, Politis M, Chaudhuri KR, Ffytche DH, Weintraub D, Ballard C (2017): Cognitive decline in Parkinson disease. *Nature Reviews Neurology*. Nature Publishing Group.
- Abásolo D, Hornero R, Escudero J, Espino P (2008): A study on the possible usefulness of detrended fluctuation analysis of the electroencephalogram background activity in Alzheimer's disease. *IEEE Trans Biomed Eng* 55:2171–2179. <https://pubmed.ncbi.nlm.nih.gov/18713686/>.
- Abubakar MB, Sanusi KO, Uguzman A, Mohamed W, Kamal H, Ibrahim NH, Khoo CS, Kumar J (2022): Alzheimer's Disease: An Update and Insights Into Pathophysiology. *Front Aging Neurosci* 14:742408.
- Adamer MF, Brüningk SC, Tejada-Arranz A, Estermann F, Basler M, Borgwardt K (2022): reComBat: batch-effect removal in large-scale multi-source gene-expression data integration. *Bioinformatics Advances* 2. <https://dx.doi.org/10.1093/bioadv/vbac071>.
- Aisen PS, Cummings J, Jack CR, Morris JC, Sperling R, Frölich L, Jones RW, Dowsett SA, Matthews BR, Raskin J, Scheltens P, Dubois B (2017): On the path to 2025: Understanding the Alzheimer's disease continuum. *Alzheimer's Research and Therapy*. BioMed Central Ltd. <https://alzres.biomedcentral.com/articles/10.1186/s13195-017-0283-5>.
- Albert MS, DeKosky ST, Dickson D, Dubois B, Feldman HH, Fox NC, Gamst A, Holtzman DM, Jagust WJ, Petersen RC, Snyder PJ, Carrillo MC, Thies B, Phelps CH (2011): The diagnosis of mild cognitive impairment due to Alzheimer's disease: recommendations from the National Institute on Aging-Alzheimer's Association workgroups on diagnostic guidelines for Alzheimer's disease. *Alzheimers Dement* 7:270–279. <https://pubmed.ncbi.nlm.nih.gov/21514249/>.
- Alger BE (2022): Neuroscience Needs to Test Both Statistical and Scientific Hypotheses. *The Journal of Neuroscience* 42:8432. [/pmc/articles/PMC9665931/](https://PMC9665931/).
- Allegri RF (2020): Moving from neurodegenerative dementias, to cognitive proteinopathies, replacing “where” by “what”.... *Dementia e Neuropsychologia* 14:237–242. <http://www.scielo.br/j/dn/a/ftRYYctPTnkfb9yL7cD6nXK/?lang=en>.
- Al-Nuaimi AHH, Jammeh E, Sun L, Ifeachor E (2018): Complexity Measures for Quantifying Changes in Electroencephalogram in Alzheimer's Disease. *Complexity* 2018.
- Al-Qazzaz NK, Ali SHBMD, Ahmad SA, Chellappan K, Islam MdS, Escudero J (2014): Role of EEG as biomarker in the early detection and classification of dementia. *Scientific World Journal*. Hindawi Limited. [/pmc/articles/PMC4100295/?report=abstract](https://PMC4100295/?report=abstract).
- Alzheimer A (1907): Über eine eigenartige Erkrankung der Hirnrinde. *Allgemeine Zeitschrift für Psychiatrie und Psychisch-gerichtliche Medizin* 64:146–148.
- American Psychiatric Association (2013): Diagnostic and Statistical Manual of Mental Disorders, 5th Edition. *Diagnostic and Statistical Manual of Mental Disorders*, 5th Edition.

Angarita-Zapata JS, Maestre-Gongora G, Calderín JF (2021): A Bibliometric Analysis and Benchmark of Machine Learning and AutoML in Crash Severity Prediction: The Case Study of Three Colombian Cities. *Sensors* (Basel) 21. <https://pubmed.ncbi.nlm.nih.gov/34960494/>.

Angelakis E, Lubar JF, Stathopoulou S, Kounios J (2004): Peak alpha frequency: an electroencephalographic measure of cognitive preparedness. *Clinical Neurophysiology* 115:887–897.

Anjum MF, Dasgupta S, Mudumbai R, Singh A, Cavanagh JF, Narayanan NS (2020): Linear predictive coding distinguishes spectral EEG features of Parkinson's disease. *Parkinsonism Relat Disord* 79:79–85.

Appelhoff S, Hurst AJ, Lawrence A, Li A, Mantilla Ramos YJ, O'Reilly C, Xiang L, Dancker J (2022): PyPREP: A Python implementation of the preprocessing pipeline (PREP) for EEG data. <https://zenodo.org/record/6363576>.

Armstrong MJ (2021): Advances in dementia with Lewy bodies. *Ther Adv Neurol Disord* 14. <https://journals.sagepub.com/doi/10.1177/17562864211057666>.

Armstrong MJ, MJ A (2019): Lewy Body Dementias 25:128–146. <https://pubmed.ncbi.nlm.nih.gov/30707190/>.

Attems J, Toledo JB, Walker L, Gelpi E, Gentleman S, Halliday G, Hortobagyi T, Jellinger K, Kovacs GG, Lee EB, Love S, McAleese KE, Nelson PT, Neumann M, Parkkinen L, Polvikoski T, Sikorska B, Smith C, Grinberg LT, Thal DR, Trojanowski JQ, McKeith IG (2021): Neuropathological consensus criteria for the evaluation of Lewy pathology in post-mortem brains: a multi-centre study. *Acta Neuropathol* 141:159–172. <https://link.springer.com/article/10.1007/s00401-020-02255-2>.

Averna A, Coelli S, Ferrara R, Cerutti S, Priori A, Bianchi AM (2023): Entropy and fractal analysis of brain-related neurophysiological signals in Alzheimer's and Parkinson's disease. *J Neural Eng* 20. <https://pubmed.ncbi.nlm.nih.gov/37746822/>.

Azami H, Zrenner C, Brooks H, Zomorrodi R, Blumberger DM, Fischer CE, Flint A, Herrmann N, Kumar S, Lanctôt K, Mah L, Mulsant BH, Pollock BG, Rajji TK (2023): Beta to theta power ratio in EEG periodic components as a potential biomarker in mild cognitive impairment and Alzheimer's dementia. *Alzheimers Res Ther* 15:1–12. <https://alzres.biomedcentral.com/articles/10.1186/s13195-023-01280-z>.

Babadi B, Brown EN (2014): A review of multitaper spectral analysis. *IEEE Transactions on Biomedical Engineering*. IEEE Computer Society. <https://pubmed.ncbi.nlm.nih.gov/24759284/>.

Babayan A, Erbey M, Kumral D, Reinelt JD, Reiter AMF, Röbbig J, Lina Schaare H, Uhlig M, Anwander A, Bazin PL, Horstmann A, Lampe L, Nikulin V V., Okon-Singer H, Preusser S, Pampel A, Rohr CS, Sacher J, Thöne-Otto A, Trapp S, Nierhaus T, Altmann D, Arelin K, Blöchl M, Bongartz E, Breig P, Cesnate E, Chen S, Cozatl R, Czerwonatis S, Dambrauskaite G, Dreyer M, Enders J, Engelhardt M, Fischer MM, Forschack N, Golchert J, Golz L, Guran CA, Hedrich S, Hentschel N, Hoffmann DI, Huntenburg JM, Jost R, Kosatschek A, Kunzendorf S, Lammers H, Lauckner ME, Mahjoory K, Kanaan AS, Mendes N, Menger R, Morino E, Näthe K, Neubauer J, Noyan H, Oligschläger S, Panczyszyn-Trzewik P, Poehlchen D, Putzke N, Roski S, Schaller MC, Schieferbein A, Schlaak B, Schmidt R, Gorgolewski KJ, Schmidt HM, Schrimpf A, Stasch S, Voss M, Wiedemann A, Margulies DS, Gaebler M, Villringer A (2019): A mind-brain-body dataset of MRI, EEG,

cognition, emotion, and peripheral physiology in young and old adults. *Scientific Data* 2019 6:1 6:1–21. <https://www.nature.com/articles/sdata2018308>.

Babiloni C (2022): The Dark Side of Alzheimer's Disease: Neglected Physiological Biomarkers of Brain Hyperexcitability and Abnormal Consciousness Level. *Journal of Alzheimer's Disease* 88:801–807. <http://www.alz.org>.

Babiloni C, Barry RJ, Başar E, Blinowska KJ, Cichocki A, Dringenburg WHIM, Klimesch W, Knight RT, Lopes da Silva F, Nunez P, Oostenveld R, Jeong J, Pascual-Marqui R, Valdes-Sosa P, Hallett M (2020a): International Federation of Clinical Neurophysiology (IFCN) – EEG research workgroup: Recommendations on frequency and topographic analysis of resting state EEG rhythms. Part 1: Applications in clinical research studies. *Clinical Neurophysiology*. Elsevier Ireland Ltd. <http://www.ncbi.nlm.nih.gov/pubmed/31501011>.

Babiloni C, Binetti G, Cassetta E, Cerboneschi D, Dal Forno G, Del Percio C, Ferreri F, Ferri R, Lanuzza B, Miniussi C, Moretti D V., Nobili F, Pascual-Marqui RD, Rodriguez G, Romani GL, Salinari S, Tecchio F, Vitali P, Zanetti O, Zappasodi F, Rossini PM (2004): Mapping distributed sources of cortical rhythms in mild Alzheimer's disease. A multicentric EEG study. *Neuroimage* 22:57–67. <https://pubmed.ncbi.nlm.nih.gov/15109997/>.

Babiloni C, Blinowska K, Bonanni L, Cichocki A, De Haan W, Del Percio C, Dubois B, Escudero J, Fernández A, Frisoni G, Güntekin B, Hajos M, Hampel H, Ifeachor E, Kilborn K, Kumar S, Johnsen K, Johannsson M, Jeong J, LeBeau F, Lizio R, Lopes da Silva F, Maestú F, McGeown WJ, McKeith I, Moretti DV, Nobili F, Olichney J, Onofrj M, Palop JJ, Rowan M, Stocchi F, Struzik ZM, Tanila H, Teipel S, Taylor JP, Weiergräber M, Yener G, Young-Pearse T, Dringenburg WH, Randall F (2020b): What electrophysiology tells us about Alzheimer's disease: a window into the synchronization and connectivity of brain neurons. *Neurobiology of Aging*. Elsevier Inc. <http://www.ncbi.nlm.nih.gov/pubmed/31739167>.

Babiloni C, Ferri R, Noce G, Lizio R, Lopez S, Lorenzo I, Tucci F, Soricelli A, Nobili F, Arnaldi D, Famà F, Orzi F, Buttinelli C, Giubilei F, Cipollini V, Marizzoni M, Güntekin B, Aktürk T, Hanoğlu L, Yener G, Özbeğ Y, Stocchi F, Vacca L, Frisoni GB, Del Percio C (2021): Resting State Alpha Electroencephalographic Rhythms Are Differently Related to Aging in Cognitively Unimpaired Seniors and Patients with Alzheimer's Disease and Amnesic Mild Cognitive Impairment. *J Alzheimers Dis* 82:1085–1114. <https://pubmed.ncbi.nlm.nih.gov/34151788/>.

Babiloni C, Lorenzo I, Lizio R, Lopez S, Tucci F, Ferri R, Soricelli A, Nobili F, Arnaldi D, Famà F, Buttinelli C, Giubilei F, Cipollini V, Onofrj M, Stocchi F, Vacca L, Fuhr P, Gschwandtner U, Ransmayr G, Aarsland D, Parnetti L, Marizzoni M, D'Antonio F, De Lena C, Güntekin B, Yıldırım E, Hanoğlu L, Yener G, Gündüz DH, Taylor JP, Schumacher J, McKeith I, Frisoni GB, De Pandis MF, Bonanni L, Percio C Del, Noce G (2022): Reactivity of posterior cortical electroencephalographic alpha rhythms during eyes opening in cognitively intact older adults and patients with dementia due to Alzheimer's and Lewy body diseases. *Neurobiol Aging* 115:88–108.

Babiloni C, Del Percio C, Pasquarelli MT, Lizio R, Noce G, Lopez S, Rizzo M, Ferri R, Soricelli A, Nobili F, Arnaldi D, Famà F, Orzi F, Buttinelli C, Giubilei F, Salvetti M, Cipollini V, Franciotti R, Onofrj M, Stirpe P, Fuhr P, Gschwandtner U, Ransmayr G, Aarsland D, Parnetti L, Farotti L, Marizzoni M, D'Antonio F, De Lena C, Güntekin B, Hanoğlu L, Yener G, Emek-Savaş DD, Triggiani AI, Taylor JP, McKeith I, Stocchi F, Vacca L, Hampel H, Frisoni GB, De Pandis MF, Bonanni L (2019): Abnormalities of functional cortical source connectivity of resting-state

electroencephalographic alpha rhythms are similar in patients with mild cognitive impairment due to Alzheimer's and Lewy body diseases. *Neurobiol Aging* 77:112–127.

Babiloni C, Vecchio F, Lizio R, Ferri R, Rodriguez G, Marzano N, Frisoni GB, Rossini PM (2011): Resting State Cortical Rhythms in Mild Cognitive Impairment and Alzheimer's Disease: Electroencephalographic Evidence. *Journal of Alzheimer's Disease* 26:201–214.

Badhwar AP, Tam A, Dansereau C, Orban P, Hoffstaedter F, Bellec P (2017): Resting-state network dysfunction in Alzheimer's disease: A systematic review and meta-analysis. *Alzheimer's & Dementia: Diagnosis, Assessment & Disease Monitoring* 8:73–85.
<https://onlinelibrary.wiley.com/doi/full/10.1016/j.dadm.2017.03.007>.

Bailey NW, Hoy KE (2021): The promise of artificial neural networks, EEG, and MRI for Alzheimer's disease. *Clinical Neurophysiology* 132:207–209.

Banville H, Jaoude MA, Wood SUN, Aimone C, Holst SC, Gramfort A, Engemann D-A (2023): Do try this at home: Age prediction from sleep and meditation with large-scale low-cost mobile EEG. *bioRxiv*:2023.04.29.538328. <https://www.biorxiv.org/content/10.1101/2023.04.29.538328v1>.

Bastos AM, Schoffelen JM (2016): A tutorial review of functional connectivity analysis methods and their interpretational pitfalls. *Front Syst Neurosci* 9:165147.

Beam CR, Kaneshiro C, Jang JY, Reynolds CA, Pedersen NL, Gatz M (2018): Differences Between Women and Men in Incidence Rates of Dementia and Alzheimer's Disease. *J Alzheimers Dis* 64:1077. [./pmc/articles/PMC6226313/](https://pmc/articles/PMC6226313/).

Beer JC, Tustison NJ, Cook PA, Davatzikos C, Sheline YI, Shinohara RT, Linn KA (2020): Longitudinal ComBat: A method for harmonizing longitudinal multi-scanner imaging data. *Neuroimage* 220:117129.

Bell TK, Godfrey KJ, Ware AL, Yeates KO, Harris AD (2022): Harmonization of multi-site MRS data with ComBat. *Neuroimage* 257. <https://pubmed.ncbi.nlm.nih.gov/35618196/>.

Benjamini Y, Yekutieli D (2001): The control of the false discovery rate in multiple testing under dependency. <https://doi.org/10.1214/aos/1013699998> 29:1165–1188.
<https://projecteuclid.org/journals/annals-of-statistics/volume-29/issue-4/The-control-of-the-false-discovery-rate-in-multiple-testing/10.1214/aos/1013699998.full>.

Bennys K, Rondouin G, Vergnes C, Touchon J (2001): Diagnostic value of quantitative EEG in Alzheimer's disease. *Neurophysiologie Clinique* 31:153–160.
<https://pubmed.ncbi.nlm.nih.gov/11488226/>.

Benwell CSY, Davila-Pérez P, Fried PJ, Jones RN, Travison TG, Santarecchi E, Pascual-Leone A, Shafi MM (2020): EEG spectral power abnormalities and their relationship with cognitive dysfunction in patients with Alzheimer's disease and type 2 diabetes. *Neurobiol Aging* 85:83–95. <https://pubmed.ncbi.nlm.nih.gov/31727363/>.

Berger H (1929): Über das Elektrenkephalogramm des Menschen. *Arch Psychiatr Nervenkr* 87:527–570. <https://link.springer.com/article/10.1007/BF01797193>.

Berger H (1936): Über das Elektrenkephalogramm des Menschen - XI. Mitteilung. *Arch Psychiatr Nervenkr* 104:678–689. <https://link.springer.com/article/10.1007/BF01814250>.

Bergeron D, Gorno-Tempini ML, Rabinovici GD, Santos-Santos MA, Seeley W, Miller BL, Pijnenburg Y, Keulen MA, Groot C, van Berckel BNM, van der Flier WM, Scheltens P, Rohrer JD, Warren JD, Schott JM, Fox NC, Sanchez-Valle R, Grau-Rivera O, Gelpi E, Seelaar H, Papma JM, van Swieten JC, Hodges JR, Leyton CE, Piguet O, Rogalski EJ, Mesulam MM, Koric L, Nora K, Pariente J, Dickerson B, Mackenzie IR, Hsiung GYR, Belliard S, Irwin DJ, Wolk DA, Grossman M, Jones M, Harris J, Mann D, Snowden JS, Chrem-Mendez P, Calandri IL, Amengual AA, Miguet-Alfonsi C, Magnin E, Magnani G, Santangelo R, Deramecourt V, Pasquier F, Mattsson N, Nilsson C, Hansson O, Keith J, Masellis M, Black SE, Matías-Guiu JA, Cabrera-Martin MN, Paquet C, Dumurgier J, Teichmann M, Sarazin M, Bottlaender M, Dubois B, Rowe CC, Villemagne VL, Vandenberghe R, Granadillo E, Teng E, Mendez M, Meyer PT, Frings L, Lleó A, Blesa R, Fortea J, Seo SW, Diehl-Schmid J, Grimmer T, Frederiksen KS, Sánchez-Juan P, Chételat G, Jansen W, Bouchard RW, Laforce RJ, Visser PJ, Ossenkoppele R (2018): Prevalence of amyloid- β pathology in distinct variants of primary progressive aphasia. Ann Neurol 84:729–740.
<https://pubmed.ncbi.nlm.nih.gov/30255971/>.

Bernasconi F, Pagonabarraga J, Bejr-Kasem H, Martinez-Horta S, Marín-Lahoz J, Horta-Barba A, Kulisevsky J, Blanke O (2023): Theta oscillations and minor hallucinations in Parkinson's disease reveal decrease in frontal lobe functions and later cognitive decline. Nature Mental Health 2023 1:7 1:477–488. <https://www.nature.com/articles/s44220-023-00080-6>.

Bezrukavnikov O, Linder R (2021): A Neophyte With AutoML: Evaluating the Promises of Automatic Machine Learning Tools. <https://arxiv.org/abs/2101.05840v1>.

Bhattacharya S, Cauchois MBL, Iglesias PA, Chen ZS (2021): The impact of a closed-loop thalamocortical model on the spatiotemporal dynamics of cortical and thalamic traveling waves. Sci Rep 11:1–19. <https://www.nature.com/articles/s41598-021-93618-6>.

Bigdely-Shamlo N, Mullen T, Kothe C, Su K-M, Robbins KA (2015): The PREP pipeline: standardized preprocessing for large-scale EEG analysis. Front Neuroinform 9.
<http://journal.frontiersin.org/Article/10.3389/fninf.2015.00016/abstract>.

Bigdely-Shamlo N, Touryan J, Ojeda A, Kothe C, Mullen T, Robbins K (2020): Automated EEG mega-analysis I: Spectral and amplitude characteristics across studies. Neuroimage 207:116361.

Biundo R, Weis L, Antonini A (2016): Cognitive decline in Parkinson's disease: the complex picture. NPJ Parkinsons Dis 2:16018. [/pmc/articles/PMC5516581/](https://PMC5516581/).

Blacker D, Albert MS, Bassett SS, Rodney CP, Harrell LE, Folstein MF (1994): Reliability and Validity of NINCDS-ADRDA Criteria for Alzheimer's Disease: The National Institute of Mental Health Genetics Initiative. Arch Neurol 51:1198–1204.
<https://jamanetwork.com/journals/jamaneurology/fullarticle/593178>.

De Boer EMJ, Orie VK, Williams T, Baker MR, De Oliveira HM, Polvikoski T, Silsby M, Menon P, Van Den Bos M, Halliday GM, Van Den Berg LH, Van Den Bosch L, Van Damme P, Kiernan M, Van Es MA, Vucic S (2021): TDP-43 proteinopathies: a new wave of neurodegenerative diseases. J Neurol Neurosurg Psychiatry 92:86–95. <https://jnnp.bmjjournals.org/content/92/1/86>.

Bonanni L, Franciotti R, Nobili F, Kramberger MG, Taylor JP, Garcia-Ptacek S, Falasca NW, Famá F, Cromarty R, Onofrj M, Aarsland D (2016): EEG Markers of Dementia with Lewy Bodies: A Multicenter Cohort Study. Journal of Alzheimer's Disease 54:1649–1657.
<http://www.ncbi.nlm.nih.gov/pubmed/27589528>.

Bonanni L, Perfetti B, Bifolchetti S, Taylor JP, Franciotti R, Parnetti L, Thomas A, Onofrj M (2015): Quantitative electroencephalogram utility in predicting conversion of mild cognitive impairment to dementia with Lewy bodies. *Neurobiol Aging* 36:434. [/pmc/articles/PMC4270449/](https://www.ncbi.nlm.nih.gov/pmc/articles/PMC4270449/).

Bonanni L, Thomas A, Tiraboschi P, Perfetti B, Varanese S, Onofrj M, L B, A T, P T, B P, S V, M O (2008): EEG comparisons in early Alzheimer's disease, dementia with Lewy bodies and Parkinson's disease with dementia patients with a 2-year follow-up 131:690–705. <https://pubmed.ncbi.nlm.nih.gov/18202105/>.

Borghammer P, Horsager J, Andersen K, Van Den Berge N, Raunio A, Murayama S, Parkkinen L, Myllykangas L (2021): Neuropathological evidence of body-first vs. brain-first Lewy body disease. *Neurobiol Dis* 161:105557.

Briels CT, Briels CT, Schoonhoven DN, Schoonhoven DN, Stam CJ, De Waal H, Scheltens P, Gouw AA (2020): Reproducibility of EEG functional connectivity in Alzheimer's disease. *Alzheimers Res Ther* 12:1–14. <https://alzres.biomedcentral.com/articles/10.1186/s13195-020-00632-3>.

Brueggen K, Fiala C, Berger C, Ochmann S, Babiloni C, Teipel SJ (2017): Early changes in alpha band power and DMN BOLD activity in Alzheimer's disease: A simultaneous resting state EEG-fMRI study. *Front Aging Neurosci* 9:319.

Buzsáki G, Anastassiou CA, Koch C (2012): The origin of extracellular fields and currents — EEG, ECoG, LFP and spikes. *Nature Reviews Neuroscience* 2012 13:6 13:407–420. <https://www.nature.com/articles/nrn3241>.

Byeon SK, Madugundu AK, Garapati K, Ramarajan MG, Saraswat M, Kumar-M P, Hughes T, Shah R, Patnaik MM, Chia N, Ashrafzadeh-Kian S, Yao JD, Pritt BS, Cattaneo R, Salama ME, Zenka RM, Kipp BR, Grebe SKG, Singh RJ, Sadighi Akha AA, Algeciras-Schimnich A, Dasari S, Olson JE, Walsh JR, Venkatakrishnan AJ, Jenkinson G, O'Horo JC, Badley AD, Pandey A (2022): Development of a multiomics model for identification of predictive biomarkers for COVID-19 severity: a retrospective cohort study. *Lancet Digit Health* 4:e632–e645. <http://www.thelancet.com/article/S2589750022001121/fulltext>.

Calabrese EJ (2008): Neuroscience and Hormesis: Overview and General Findings. *Crit Rev Toxicol* 38:249–252. <https://www.tandfonline.com/doi/abs/10.1080/10408440801981957>.

Calabrese EJ, Mattson MP (2017): How does hormesis impact biology, toxicology, and medicine? *npj Aging and Mechanisms of Disease* 2017 3:1 3:1–8. <https://www.nature.com/articles/s41514-017-0013-z>.

Carmona Arroyave JA, Tobón Quintero CA, Suárez Revelo JJ, Ochoa Gómez JF, García YB, Gómez LM, Pineda Salazar DA (2019): Resting functional connectivity and mild cognitive impairment in Parkinson's disease. An electroencephalogram study. *Future Neurol* 14:FNL18. <https://www.futuremedicine.com/doi/10.2217/fnl-2018-0048>.

Caso F, Cursi M, Magnani G, Fanelli G, Falautano M, Comi G, Leocani L, Minicucci F (2012): Quantitative EEG and LORETA: valuable tools in discerning FTD from AD? *Neurobiol Aging* 33:2343–2356.

Cassani R, Estarellas M, San-Martin R, Fraga FJ, Falk TH (2018): Systematic review on resting-state EEG for Alzheimer's disease diagnosis and progression assessment. *Dis Markers* 2018.

- Castellanos NP, Makarov VA (2006): Recovering EEG brain signals: artifact suppression with wavelet enhanced independent component analysis. *J Neurosci Methods* 158:300–312.
[https://pubmed.ncbi.nlm.nih.gov/16828877/.](https://pubmed.ncbi.nlm.nih.gov/16828877/)
- Caviness JN, Hentz JG, Evidente VG, Driver-Dunckley E, Samanta J, Mahant P, Connor DJ, Sabbagh MN, Shill HA, Adler CH (2007): Both early and late cognitive dysfunction affects the electroencephalogram in Parkinson's disease. *Parkinsonism Relat Disord* 13:348–354.
- Caviness JN, Utianski RL, Hentz JG, Beach TG, Dugger BN, Shill HA, Driver-Dunckley ED, Sabbagh MN, Mehta S, Adler CH (2016a): Differential spectral quantitative electroencephalography patterns between control and Parkinson's disease cohorts. *Eur J Neurol* 23:387–392.
[http://www.ncbi.nlm.nih.gov/pubmed/26518336.](http://www.ncbi.nlm.nih.gov/pubmed/26518336)
- Caviness JN, Utianski RL, Hentz JG, Beach TG, Dugger BN, Shill HA, Driver-Dunckley ED, Sabbagh MN, Mehta S, Adler CH (2016b): Differential spectral quantitative electroencephalography patterns between control and Parkinson's disease cohorts. *Eur J Neurol* 23:387–392.
[https://onlinelibrary.wiley.com/doi/full/10.1111/ene.12878.](https://onlinelibrary.wiley.com/doi/full/10.1111/ene.12878)
- Chang J, Chang C (2023): Quantitative Electroencephalography Markers for an Accurate Diagnosis of Frontotemporal Dementia: A Spectral Power Ratio Approach. *Medicina* 2023, Vol 59, Page 2155 59:2155. [https://www.mdpi.com/1648-9144/59/12/2155/htm.](https://www.mdpi.com/1648-9144/59/12/2155/htm)
- Chatterjee A, Hirsch-Reinshagen V, Moussavi SA, Ducharme B, Mackenzie IR, Hsiung GYR (2021): Clinico-pathological comparison of patients with autopsy-confirmed Alzheimer's disease, dementia with Lewy bodies, and mixed pathology. *Alzheimer's & Dementia : Diagnosis, Assessment & Disease Monitoring* 13. [/pmc/articles/PMC8129858/](https://pmc/articles/PMC8129858/).
- Chatzikonstantinou S, McKenna J, Karantali E, Petridis F, Kazis D, Mavroudis I (2021): Electroencephalogram in dementia with Lewy bodies: a systematic review. *Aging Clinical and Experimental Research*. Springer. [https://link.springer.com/article/10.1007/s40520-020-01576-2.](https://link.springer.com/article/10.1007/s40520-020-01576-2)
- Chen CC, Hsu CY, Chiu HW, Hu CJ, Lee TC (2015): Frequency power and coherence of electroencephalography are correlated with the severity of Alzheimer's disease: A multicenter analysis in Taiwan. *Journal of the Formosan Medical Association* 114:729–735.
[http://www.ncbi.nlm.nih.gov/pubmed/23969043.](http://www.ncbi.nlm.nih.gov/pubmed/23969043)
- Cheng ST (2017): Dementia Caregiver Burden: a Research Update and Critical Analysis. *Curr Psychiatry Rep* 19. [/pmc/articles/PMC5550537/](https://pmc/articles/PMC5550537/).
- Chu KT, Lei WC, Wu MH, Fuh JL, Wang SJ, French IT, Chang WS, Chang CF, Huang NE, Liang WK, Juan CH (2023): A holo-spectral EEG analysis provides an early detection of cognitive decline and predicts the progression to Alzheimer's disease. *Front Aging Neurosci* 15:1195424.
- Collino S, Montoliu I, Martin FPJ, Scherer M, Mari D, Salvioli S, Bucci L, Ostan R, Monti D, Biagi E, Brigidi P, Franceschi C, Rezzi S (2013): Metabolic Signatures of Extreme Longevity in Northern Italian Centenarians Reveal a Complex Remodeling of Lipids, Amino Acids, and Gut Microbiota Metabolism. *PLoS One* 8:e56564.
[https://journals.plos.org/plosone/article?id=10.1371/journal.pone.0056564.](https://journals.plos.org/plosone/article?id=10.1371/journal.pone.0056564)
- Collura TF (1993): History and evolution of electroencephalographic instruments and techniques. *J Clin Neurophysiol* 10:476–504. <https://pubmed.ncbi.nlm.nih.gov/8308144/>.

Colom-Cadena M, Spires-Jones T, Zetterberg H, Blennow K, Caggiano A, Dekosky ST, Fillit H, Harrison JE, Schneider LS, Scheltens P, De Haan W, Grundman M, Van Dyck CH, Izzo NJ, Catalano SM (2020a): The clinical promise of biomarkers of synapse damage or loss in Alzheimer's disease. *Alzheimer's Research & Therapy* 2020 12:1 12:1–12.
<https://alzres.biomedcentral.com/articles/10.1186/s13195-020-00588-4>.

Colom-Cadena M, Spires-Jones T, Zetterberg H, Blennow K, Caggiano A, Dekosky ST, Fillit H, Harrison JE, Schneider LS, Scheltens P, De Haan W, Grundman M, Van Dyck CH, Izzo NJ, Catalano SM (2020b): The clinical promise of biomarkers of synapse damage or loss in Alzheimer's disease. *Alzheimer's Research and Therapy*. BioMed Central Ltd.

Conrad F, Mälzer M, Schwarzenberger M, Wiemer H, Ihlenfeldt S (2022): Benchmarking AutoML for regression tasks on small tabular data in materials design. *Sci Rep* 12:19350. /pmc/articles/PMC9652348/.

Costafreda SG (2009): Pooling fMRI data: Meta-analysis, mega-analysis and multi-center studies. *Front Neuroinform* 3:639.

Coughlan GT, Betthauser TJ, Boyle R, Koscik RL, Klinger HM, Chibnik LB, Jonaitis EM, Yau WYW, Wenzel A, Christian BT, Gleason CE, Saelzler UG, Properzi MJ, Schultz AP, Hanseeuw BJ, Manson JAE, Rentz DM, Johnson KA, Sperling R, Johnson SC, Buckley RF (2023): Association of Age at Menopause and Hormone Therapy Use With Tau and β -Amyloid Positron Emission Tomography. *JAMA Neurol* 80:462–473.
<https://jamanetwork.com/journals/jamaneurology/fullarticle/2802791>.

Cozac V V., Gschwandtner U, Hatz F, Hardmeier M, Rüegg S, Fuhr P (2016): Quantitative EEG and cognitive decline in Parkinson's disease. *Parkinsons Dis* 2016.

Crone EA, Steinbeis N (2017): Neural Perspectives on Cognitive Control Development during Childhood and Adolescence. *Trends Cogn Sci* 21:205–215.

Da-ano R, Masson I, Lucia F, Doré M, Robin P, Alfieri J, Rousseau C, Mervoyer A, Reinhold C, Castelli J, De Crevoisier R, Rameé JF, Pradier O, Schick U, Visvikis D, Hatt M (2020): Performance comparison of modified ComBat for harmonization of radiomic features for multicenter studies. *Sci Rep* 10:10. /pmc/articles/PMC7314795/.

Dauwels J, Srinivasan K, Ramasubba Reddy M, Musha T, Vialatte FB, Latchoumane C, Jeong J, Cichocki A (2011): Slowing and loss of complexity in Alzheimer's EEG: Two sides of the same coin? *Int J Alzheimers Dis*.

Delorme A (2023): EEG is better left alone. *Scientific Reports* 2023 13:1 13:1–12.
<https://www.nature.com/articles/s41598-023-27528-0>.

Donaghay PC, McKeith IG (2014): The clinical characteristics of dementia with Lewy bodies and a consideration of prodromal diagnosis. *Alzheimer's Research and Therapy*. BioMed Central. /pmc/articles/PMC4255387/.

Donoghue T, Dominguez J, Voytek B (2020a): Electrophysiological Frequency Band Ratio Measures Conflate Periodic and Aperiodic Neural Activity. *eNeuro* 7.
<https://www.eneuro.org/content/7/6/ENEURO.0192-20.2020>.

Donoghue T, Haller M, Peterson EJ, Varma P, Sebastian P, Gao R, Noto T, Lara AH, Wallis JD, Knight RT, Shestyuk A, Voytek B (2020b): Parameterizing neural power spectra into periodic and

aperiodic components. *Nature Neuroscience* 2020; 23:1655–1665.
<https://www.nature.com/articles/s41593-020-00744-x>.

Dottori M, Sedenõ L, Martorell Caro M, Alifano F, Hesse E, Mikulan E, Garcíá AM, Ruiz-Tagle A, Lillo P, Slachevsky A, Serrano C, Fraiman D, Ibanez A (2017): Towards affordable biomarkers of frontotemporal dementia: A classification study via network's information sharing. *Sci Rep* 7.

Duan W, Chen X, Wang YJ, Zhao W, Yuan H, Lei X (2021): Reproducibility of power spectrum, functional connectivity and network construction in resting-state EEG. *J Neurosci Methods* 348:108985.

Dubois B, Feldman HH, Jacova C, Hampel H, Molinuevo JL, Blennow K, Dekosky ST, Gauthier S, Selkoe D, Bateman R, Cappa S, Crutch S, Engelborghs S, Frisoni GB, Fox NC, Galasko D, Habert MO, Jicha GA, Nordberg A, Pasquier F, Rabinovici G, Robert P, Rowe C, Salloway S, Sarazin M, Epelbaum S, de Souza LC, Vellas B, Visser PJ, Schneider L, Stern Y, Scheltens P, Cummings JL (2014): Advancing research diagnostic criteria for Alzheimer's disease: the IWG-2 criteria. *Lancet Neurol* 13:614–629. <https://pubmed.ncbi.nlm.nih.gov/24849862/>.

Dubois B, Villain N, Frisoni GB, Rabinovici GD, Sabbagh M, Cappa S, Bejanin A, Bombois S, Epelbaum S, Teichmann M, Habert MO, Nordberg A, Blennow K, Galasko D, Stern Y, Rowe CC, Salloway S, Schneider LS, Cummings JL, Feldman HH (2021): Clinical diagnosis of Alzheimer's disease: recommendations of the International Working Group. *Lancet Neurol* 20:484–496.

Duran-Aniotz C, Orellana P, Leon Rodriguez T, Henriquez F, Cabello V, Aguirre-Pinto MF, Escobedo T, Takada LT, Pina-Escudero SD, Lopez O, Yokoyama JS, Ibanez A, Parra MA, Slachevsky A (2021): Systematic Review: Genetic, Neuroimaging, and Fluids Biomarkers for Frontotemporal Dementia Across Latin America Countries. *Front Neurol* 12:663407.

Elahi FM, Miller BL (2017): A clinicopathological approach to the diagnosis of dementia. *Nat Rev Neurol* 13:457. [/pmc/articles/PMC5771416/](https://pmc/articles/PMC5771416/).

Engemann DA, Mellot A, Höchenberger R, Banville H, Sabbagh D, Gemein L, Ball T, Gramfort A (2022a): A reusable benchmark of brain-age prediction from M/EEG resting-state signals. *Neuroimage* 262. <https://pubmed.ncbi.nlm.nih.gov/35905809/>.

Engemann DA, Mellot A, Höchenberger R, Banville H, Sabbagh D, Gemein L, Ball T, Gramfort A (2022b): A reusable benchmark of brain-age prediction from M/EEG resting-state signals. *Neuroimage* 262:119521.

Engemann DA, Raimondo F, King JR, Rohaut B, Louppe G, Faugeras F, Annen J, Cassol H, Gosseries O, Fernandez-Slezak D, Laureys S, Naccache L, Dehaene S, Sitt JD (2018): Robust EEG-based cross-site and cross-protocol classification of states of consciousness. *Brain* 141:3179–3192. <https://dx.doi.org/10.1093/brain/awy251>.

Erickson N, Mueller J, Shirkov A, Zhang H, Larroy P, Li M, Smola A (2020): AutoGluon-Tabular: Robust and Accurate AutoML for Structured Data. <https://arxiv.org/abs/2003.06505v1>.

Fide E, Hünerli-Gündüz D, Öztura İ, Yener GG (2022): Hyperconnectivity matters in early-onset Alzheimer's disease: a resting-state EEG connectivity study. *Neurophysiologie Clinique* 52:459–471.

Finger EC (2016): Frontotemporal dementias. *CONTINUUM Lifelong Learning in Neurology*. Lippincott Williams and Wilkins.

Fladby T, Palhaugen L, Selnes P, Waterloo K, Brathen G, Hessen E, Almdahl IS, Arntzen KA, Auning E, Eliassen CF, Espenes R, Grambaite R, Grøntvedt GR, Johansen KK, Johnsen SH, Kalheim LF, Kirsebom BE, Muller KI, Nakling AE, Rongven A, Sando SB, Siafarikas N, Stav AL, Tecelao S, Timon S, Bekkelund SI, Aarsland D (2017): Detecting At-Risk Alzheimer's Disease Cases. *J Alzheimers Dis* 60:97–105. <https://pubmed.ncbi.nlm.nih.gov/28826181/>.

Fonseca LC, Tedrus GMAS, Letro GH, Bossoni AS (2009): Dementia, Mild Cognitive Impairment and Quantitative EEG in Patients with Parkinson's Disease. <https://doi.org/10.1177/155005940904000309> 40:168–172. <https://journals.sagepub.com/doi/10.1177/155005940904000309>.

Forchetti CM (2005): Treating Patients With Moderate to Severe Alzheimer's Disease: Implications of Recent Pharmacologic Studies. *Prim Care Companion J Clin Psychiatry* 7:155. /pmc/articles/PMC1192433/.

Fortin JP, Cullen N, Sheline YI, Taylor WD, Aselcioglu I, Cook PA, Adams P, Cooper C, Fava M, McGrath PJ, McInnis M, Phillips ML, Trivedi MH, Weissman MM, Shinohara RT (2018): Harmonization of cortical thickness measurements across scanners and sites. *Neuroimage* 167:104–120. <https://pubmed.ncbi.nlm.nih.gov/29155184/>.

Frahm-Falkenberg S, Ibsen R, Kjellberg J, Jennum P (2016): Health, social and economic consequences of dementias: a comparative national cohort study. *Eur J Neurol* 23:1400–1407. <https://pubmed.ncbi.nlm.nih.gov/27297659/>.

Franceschi C, Garagnani P, Morsiani C, Conte M, Santoro A, Grignolio A, Monti D, Capri M, Salvioli S (2018a): The continuum of aging and age-related diseases: Common mechanisms but different rates. *Front Med (Lausanne)* 5:349810.

Franceschi C, Garagnani P, Parini P, Giuliani C, Santoro A (2018b): Inflammaging: a new immune–metabolic viewpoint for age-related diseases. *Nature Reviews Endocrinology* 2018 14:10 14:576–590. <https://www.nature.com/articles/s41574-018-0059-4>.

Franciotti R, Pilotto A, Moretti D V., Falasca NW, Arnaldi D, Taylor JP, Nobili F, Kramberger M, Ptacek SG, Padovani A, Aarlsand D, Onofrj M, Bonanni L (2020): Anterior EEG slowing in dementia with Lewy bodies: a multicenter European cohort study. *Neurobiol Aging* 93:55–60. <https://linkinghub.elsevier.com/retrieve/pii/S0197458020301433>.

Gao R, Peterson EJ, Voytek B (2017): Inferring synaptic excitation/inhibition balance from field potentials. *Neuroimage* 158:70–78. <https://pubmed.ncbi.nlm.nih.gov/28676297/>.

García-Prete FJ, Suárez-Relevo JX, Aguilón-Niño DF, Lopera-Restrepo FJ, Ochoa-Gómez JF, Tobón-Quintero CA (2022): Automatic Classification of Subjects of the PSEN1-E280A Family at Risk of Developing Alzheimer's Disease Using Machine Learning and Resting State Electroencephalography. *Journal of Alzheimer's Disease* 87:817–832.

Garn H, Coronel C, Waser M, Caravias G, Ransmayr G (2017): Differential diagnosis between patients with probable Alzheimer's disease, Parkinson's disease dementia, or dementia with Lewy bodies and frontotemporal dementia, behavioral variant, using quantitative electroencephalographic features. *J Neural Transm* 124:569. /pmc/articles/PMC5399050/.

Gaubert S, Houot M, Raimondo F, Ansart M, Corsi MC, Naccache L, Sitt JD, Habert MO, Dubois B, De Vico Fallani F, Durrleman S, Epelbaum S (2021): A machine learning approach to screen for preclinical Alzheimer's disease. *Neurobiol Aging* 105:205–216.

Gaubert S, Raimondo F, Houot M, Corsi MC, Naccache L, Sitt JD, Hermann B, Oudiette D, Gagliardi G, Habert MO, Dubois B, De Vico Fallani F, Bakardjian H, Epelbaum S (2019): EEG evidence of compensatory mechanisms in preclinical Alzheimer's disease. *Brain* 142:2096–2112. <https://pubmed.ncbi.nlm.nih.gov/31211359/>.

Gauthier S, Zhang H, Ng KP, Pascoal TA, Rosa-Neto P (2018): Impact of the biological definition of Alzheimer's disease using amyloid, tau and neurodegeneration (ATN): what about the role of vascular changes, inflammation, Lewy body pathology? *Transl Neurodegener* 7. /pmc/articles/PMC5977549/.

George JS, Strunk J, Mak-Mccully R, Houser M, Poizner H, Aron AR (2013): Dopaminergic therapy in Parkinson's disease decreases cortical beta band coherence in the resting state and increases cortical beta band power during executive control. *Neuroimage Clin* 3:261–270. /pmc/articles/PMC3814961/.

Geraedts VJ, Boon LI, Marinus J, Gouw AA, Van Hilten JJ, Stam CJ, Tannemaat MR, Contarino MF (2018): Clinical correlates of quantitative EEG in Parkinson disease: A systematic review. *Neurology*. <http://www.ncbi.nlm.nih.gov/pubmed/30291182>.

Gerster M, Waterstraat G, Litvak V, Lehnertz K, Schnitzler A, Florin E, Curio G, Nikulin V (2022): Separating Neural Oscillations from Aperiodic 1/f Activity: Challenges and Recommendations. *Neuroinformatics* 20:991–1012. <https://link.springer.com/article/10.1007/s12021-022-09581-8>.

Gil Ávila C, Bott FS, Tiemann L, Hohn VD, May ES, Nickel MM, Zebhauser PT, Gross J, Ploner M (2023): DISCOVER-EEG: an open, fully automated EEG pipeline for biomarker discovery in clinical neuroscience. *Scientific Data* 2023 10:1 10:1–14. <https://www.nature.com/articles/s41597-023-02525-0>.

Gilbert DL, Sethuraman G, Kotagal U, Buncher CR (2003): Meta-analysis of EEG test performance shows wide variation among studies. *Neurology* 60:564–570.

Gimenez-Aparisi G, Guijarro-Estelles E, Chornet-Lurbe A, Ballesta-Martinez S, Pardo-Hernandez M, Ye-Lin Y (2023): Early detection of Parkinson's disease: Systematic analysis of the influence of the eyes on quantitative biomarkers in resting state electroencephalography. *Heliyon* 9:e20625.

Goetz CG (2011): The History of Parkinson's Disease: Early Clinical Descriptions and Neurological Therapies. *Cold Spring Harb Perspect Med* 1. /pmc/articles/PMC3234454/.

Goh C, Hamadicharef B, Henderson GT, Ifeachor EC, Goh C, Hamadicharef B, Henderson GT, Ifeachor EC (2005): Comparison of Fractal Dimension Algorithms for the Computation of EEG Biomarkers for Dementia. In: . 2nd International Conference on Computational Intelligence in Medicine and Healthcare (CIMED2005). Lisbon. <https://inria.hal.science/inria-00442374>.

Gordillo D, Ramos da Cruz J, Moreno D, Garobbio S, Herzog MH (2023): Do we really measure what we think we are measuring? *iScience* 26. /pmc/articles/PMC9947309/.

Gouw AA, Stam CJ (2016): Electroencephalography in the Differential Diagnosis of Dementia. *Epileptologie* 33:173–182. https://www.epi.ch/wp-content/uploads/Artikel-Gouw_E_3_16.pdf.

- Gramfort A, Luessi M, Larson E, Engemann DA, Strohmeier D, Brodbeck C, Goj R, Jas M, Brooks T, Parkkonen L, Hämäläinen M (2013): MEG and EEG data analysis with MNE-Python. *Front Neurosci* 0:267.
- Granatiero V, Manfredi G (2019): Mitochondrial Transport and Turnover in the Pathogenesis of Amyotrophic Lateral Sclerosis. *Biology* 2019, Vol 8, Page 36 8:36. <https://www.mdpi.com/2079-7737/8/2/36/htm>.
- Grimbert F, Faugeras O (2006): Analysis of Jansen's model of a single cortical column. *Neural Comput.* Vol. 18. <https://inria.hal.science/file/index/docid/70410/filename/RR-5597.pdf>.
- Gudmundsson S, Runarsson TP, Sigurdsson S, Eiriksdottir G, Johnsen K (2007): Reliability of quantitative EEG features. *Clinical Neurophysiology* 118:2162–2171. <https://linkinghub.elsevier.com/retrieve/pii/S1388245707002994>.
- Gustavsson A, Norton N, Fast T, Frölich L, Georges J, Holzapfel D, Kirabali T, Krolak-Salmon P, Rossini PM, Ferretti MT, Lanman L, Chadha AS, van der Flier WM (2023): Global estimates on the number of persons across the Alzheimer's disease continuum. *Alzheimer's & Dementia* 19:658–670. <https://onlinelibrary.wiley.com/doi/full/10.1002/alz.12694>.
- Haas LF (2003): Hans Berger (1873–1941), Richard Caton (1842–1926), and electroencephalography. *J Neurol Neurosurg Psychiatry* 74:9–9. <https://jnnp.bmjjournals.org/content/74/1/9>.
- Habich A, Wahlund LO, Westman E, Dierks T, Ferreira D (2023): (Dis-)Connected Dots in Dementia with Lewy Bodies—A Systematic Review of Connectivity Studies. *Movement Disorders* 38:4–15. <https://onlinelibrary.wiley.com/doi/full/10.1002/mds.29248>.
- Hag A, Handayani D, Pillai T, Mantoro T, Kit MH, Al-Shargie F (2021): EEG Mental Stress Assessment Using Hybrid Multi-Domain Feature Sets of Functional Connectivity Network and Time-Frequency Features. *Sensors* 2021, Vol 21, Page 6300 21:6300. <https://www.mdpi.com/1424-8220/21/18/6300/htm>.
- Halgren M, Ulbert I, Bastuji H, Fabó D, Eross L, Rey M, Devinsky O, Doyle WK, Mak-McCully R, Halgren E, Wittner L, Chauvel P, Heit G, Eskandar E, Mandell A, Cash SS (2019): The generation and propagation of the human alpha rhythm. *Proc Natl Acad Sci U S A* 116:23772–23782. <https://www.pnas.org/doi/abs/10.1073/pnas.1913092116>.
- Hampel H, Lista S, Neri C, Vergallo A (2019): Time for the systems-level integration of aging: Resilience enhancing strategies to prevent Alzheimer's disease. *Prog Neurobiol* 181. <https://pubmed.ncbi.nlm.nih.gov/31351912/>.
- Han Q, Xiao X, Wang S, Qin W, Yu C, Liang M (2023): Characterization of the effects of outliers on ComBat harmonization for removing inter-site data heterogeneity in multisite neuroimaging studies. *Front Neurosci* 17:1146175. <https://www.frontiersin.org/articles/10.3389/fnins.2023.1146175/full>.
- Harada CN, Natelson Love MC, Triebel KL (2013): Normal Cognitive Aging. *Clin Geriatr Med* 29:737. [/pmc/articles/PMC4015335/](https://pmc.ncbi.nlm.nih.gov/PMC4015335/).
- Harding RJ, Bermudez P, Bernier A, Beauvais M, Bellec P, Hill S, Karakuzu A, Knoppers BM, Pavlidis P, Poline JB, Roskams J, Stikov N, Stone J, Strother S, Evans AC (2023): The Canadian Open Neuroscience Platform—An open science framework for the neuroscience community. *PLoS Comput Biol* 19. [/pmc/articles/PMC10374086/](https://pmc.ncbi.nlm.nih.gov/PMC10374086/).

Hatlestad-Hall C (2022): SRM Resting-state EEG - OpenNeuro. OpenNeuro.

<https://openneuro.org/datasets/ds003775/versions/1.2.1>.

Hatlestad-Hall C, Rygvold TW, Andersson S (2022a): BIDS-structured resting-state electroencephalography (EEG) data extracted from an experimental paradigm. Data Brief 45.

Hatlestad-Hall C, Rygvold TW, Andersson S (2022b): BIDS-structured resting-state electroencephalography (EEG) data extracted from an experimental paradigm. Data Brief 45:108647.

Hayashi S, Caron BA, Heinsfeld AS, Vinci-Booher S, McPherson B, Bullock DN, Bertò G, Niso G, Hanekamp S, Levitas D, Ray K, MacKenzie A, Kitchell L, Leong JK, Nascimento-Silva F, Koudoro S, Willis H, Jolly JK, Pisner D, Zuidema TR, Kurzawski JW, Mikellidou K, Bussalb A, Rorden C, Victory C, Bhatia D, Aydogan DB, Yeh F-CF, Delogu F, Guaje J, Veraart J, Bollman S, Stewart A, Fischer J, Faskowitz J, Chaumon M, Fabrega R, Hunt D, McKee S, Brown ST, Heyman S, Iacobella V, Mejia AF, Marinazzo D, Craddock RC, Olivetti E, Hanson JL, Avesani P, Garyfallidis E, Stanzione D, Carson J, Henschel R, Hancock DY, Stewart CA, Schnyer D, Eke DO, Poldrack RA, George N, Bridge H, Sani I, Freiwald WA, Puce A, Port NL, Pestilli F (2023): brainlife.io: A decentralized and open source cloud platform to support neuroscience research.
<http://arxiv.org/abs/2306.02183>.

He BJ (2014): Scale-free brain activity: past, present, and future. Trends Cogn Sci 18:480–487.
<https://pubmed.ncbi.nlm.nih.gov/24788139/>.

He W, Donoghue T, Sowman PF, Seymour RA, Brock J, Crain S, Voytek B, Hillebrand A (2019): Co-Increasing Neuronal Noise and Beta Power in the Developing Brain. bioRxiv:839258.
<https://www.biorxiv.org/content/10.1101/839258v1>.

Hebling Vieira B, Liem F, Dadi K, Engemann DA, Gramfort A, Bellec P, Craddock RC, Damoiseaux JS, Steele CJ, Yarkoni T, Langer N, Margulies DS, Varoquaux G (2022): Predicting future cognitive decline from non-brain and multimodal brain imaging data in healthy and pathological aging. Neurobiol Aging 118:55–65. <https://pubmed.ncbi.nlm.nih.gov/35878565/>.

Hendriks S, Peetoom K, Bakker C, Van Der Flier WM, Papma JM, Koopmans R, Verhey FRJ, De Vugt M, Köhler S, Withall A, Parlevliet JL, Uysal-Bozkir Ö, Gibson RC, Neita SM, Nielsen TR, Salem LC, Nyberg J, Lopes MA, Dominguez JC, De Guzman MF, Egeberg A, Radford K, Broe T, Subramaniam M, Abdin E, Bruni AC, Di Lorenzo R, Smith K, Flicker L, Mol MO, Basta M, Yu D, Masika G, Petersen MS, Ruano L (2021): Global Prevalence of Young-Onset Dementia: A Systematic Review and Meta-analysis. JAMA Neurol 78:1080–1090.
<https://jamanetwork.com/journals/jamaneurology/fullarticle/2781919>.

Hill AT, Clark GM, Bigelow FJ, Lum JAG, Enticott PG (2022): Periodic and aperiodic neural activity displays age-dependent changes across early-to-middle childhood. Dev Cogn Neurosci 54:101076.

Hinchliffe C, Yogarajah M, Elkommos S, Tang H, Abasolo D (2022): Entropy Measures of Electroencephalograms towards the Diagnosis of Psychogenic Non-Epileptic Seizures. Entropy 24. [/pmc/articles/PMC9601450/](https://pmc/articles/PMC9601450/).

Hjorth B (1970): EEG analysis based on time domain properties. Electroencephalogr Clin Neurophysiol 29:306–310.

Hock EM, Polymenidou M (2016a): Prion-like propagation as a pathogenic principle in frontotemporal dementia. *J Neurochem* 138:163–183.
<https://onlinelibrary.wiley.com/doi/full/10.1111/jnc.13668>.

Hock EM, Polymenidou M (2016b): Prion-like propagation as a pathogenic principle in frontotemporal dementia. *J Neurochem* 138 Suppl 1:163–183.
<https://pubmed.ncbi.nlm.nih.gov/27502124/>.

Hogan DB, Jetté N, Fiest KM, Roberts JI, Pearson D, Smith EE, Roach P, Kirk A, Pringsheim T, Maxwell CJ (2016): The Prevalence and Incidence of Frontotemporal Dementia: a Systematic Review. *Canadian Journal of Neurological Sciences* 43:S96–S109.
<https://www.cambridge.org/core/journals/canadian-journal-of-neurological-sciences/article/prevalence-and-incidence-of-frontotemporal-dementia-a-systematic-review/F9B6DDFC2310DB4E02A500DD0A3A9263>.

Horng H, Singh A, Yousefi B, Cohen EA, Haghghi B, Katz S, Noël PB, Kontos D, Shinohara RT (2022): Improved generalized ComBat methods for harmonization of radiomic features. *Sci Rep* 12.
<https://pubmed.ncbi.nlm.nih.gov/36348002/>.

Hu F, Chen AA, Horng H, Bashyam V, Davatzikos C, Alexander-Bloch A, Li M, Shou H, Satterthwaite TD, Yu M, Shinohara RT (2023): Image harmonization: A review of statistical and deep learning methods for removing batch effects and evaluation metrics for effective harmonization. *Neuroimage* 274:120125.

Huang C, Wahlund LO, Dierks T, Julin P, Winblad B, Jelic V (2000): Discrimination of Alzheimer's disease and mild cognitive impairment by equivalent EEG sources: A cross-sectional and longitudinal study. *Clinical Neurophysiology* 111:1961–1967.
<https://pubmed.ncbi.nlm.nih.gov/11068230/>.

Isaza VH, Castro VC, Saldarriaga LZ, Mantilla-Ramos Y, Quintero CT, Suarez-Revelo J, Gómez JO (2023): Tackling EEG test-retest reliability with a pre-processing pipeline based on ICA and wavelet-ICA. *Authorea Preprints*. <https://www.authorea.com/users/624863/articles/647023-tackling-eeg-test-retest-reliability-with-a-pre-processing-pipeline-based-on-ica-and-wavelet-ica>.

Iturria-Medina Y, Sotero RC, Toussaint PJ, Mateos-Pérez JM, Evans AC, Weiner MW, Aisen P, Petersen R, Jack CR, Jagust W, Trojanowski JQ, Toga AW, Beckett L, Green RC, Saykin AJ, Morris J, Shaw LM, Khachaturian Z, Sorensen G, Kuller L, Raichle M, Paul S, Davies P, Fillit H, Hefti F, Holtzman D, Mesulam MM, Potter W, Snyder P, Schwartz A, Montine T, Thomas RG, Donohue M, Walter S, Gessert D, Sather T, Jiminez G, Harvey D, Bernstein M, Fox N, Thompson P, Schuff N, Borowski B, Gunter J, Senjem M, Vemuri P, Jones D, Kantarci K, Ward C, Koeppen RA, Foster N, Reiman EM, Chen K, Mathis C, Landau S, Cairns NJ, Householder E, Taylor-Reinwald L, Lee V, Korecka M, Figurski M, Crawford K, Neu S, Foroud TM, Potkin S, Shen L, Faber K, Kim S, Nho K, Thal L, Buckholtz N, Albert M, Frank R, Hsiao J, Kaye J, Quinn J, Lind B, Carter R, Dolen S, Schneider LS, Pawluczyk S, Beccera M, Teodoro L, Spann BM, Brewer J, Vanderswag H, Fleisher A, Heidebrink JL, Lord JL, Mason SS, Albers CS, Knopman D, Johnson K, Doody RS, Villanueva-Meyer J, Chowdhury M, Rountree S, Dang M, Stern Y, Honig LS, Bell KL, Ances B, Carroll M, Leon S, Mintun MA, Schneider S, Oliver A, Marson D, Griffith R, Clark D, Geldmacher D, Brockington J, Roberson E, Grossman H, Mitsis E, De Toledo-Morrell L, Shah RC, Duara R, Varon D, Greig MT, Roberts P, Albert M, Onyike C, D'Agostino D, Kielb S, Galvin JE, Cerbone B, Michel CA, Rusinek H, De Leon MJ, Glodzik L, De Santi S, Doraiswamy PM, Petrella JR, Wong TZ, Arnold

SE, Karlawish JH, Wolk D, Smith CD, Jicha G, Hardy P, Sinha P, Oates E, Conrad G, Lopez OL, Oakley M, Simpson DM, Porsteinsson AP, Goldstein BS, Martin K, Makino KM, Ismail MS, Brand C, Mulnard RA, Thai G, Mc-Adams-Ortiz C, Womack K, Mathews D, Quiceno M, Diaz-Arrastia R, King R, Weiner M, Martin-Cook K, DeVous M, Levey AI, Lah JJ, Cellar JS, Burns JM, Anderson HS, Swerdlow RH, Apostolova L, Tingus K, Woo E, Silverman DHS, Lu PH, Bartzokis G, Graff-Radford NR, Parfitt F, Kendall T, Johnson H, Farlow MR, Hake A, Matthews BR, Herring S, Hunt C, Van Dyck CH, Carson RE, MacAvoy MG, Chertkow H, Bergman H, Hosein C, Black S, Stefanovic B, Caldwell C, Hsiung GYR, Feldman H, Mudge B, Assaly M, Kertesz A, Rogers J, Bernick C, Munic D, Kerwin D, Mesulam MM, Lipowski K, Wu CK, Johnson N, Sadowsky C, Martinez W, Villena T, Turner RS, Johnson K, Reynolds B, Sperling RA, Johnson KA, Marshall G, Frey M, Lane B, Rosen A, Tinklenberg J, Sabbagh MN, Belden CM, Jacobson SA, Sirrel SA, Kowall N, Killiany R, Budson AE, Norbash A, Johnson PL, Allard J, Lerner A, Ogrocki P, Hudson L, Fletcher E, Carmichael O, Olichney J, DeCarli C, Kittur S, Borrie M, Lee TY, Bartha R, Johnson S, Asthana S, Carlsson CM, Potkin SG, Preda A, Nguyen D, Tariot P, Reeder S, Bates V, Capote H, Rainka M, Scharre DW, Kataki M, Adeli A, Zimmerman EA, Celmins D, Brown AD, Pearlson GD, Blank K, Anderson K, Santulli RB, Kitzmiller TJ, Schwartz ES, Sink KM, Williamson JD, Garg P, Watkins F, Ott BR, Querfurth H, Tremont G, Salloway S, Malloy P, Correia S, Rosen HJ, Miller BL, Mintzer J, Spicer K, Bachman D, Finger E, Pasternak S, Rachinsky I, Drost D, Pomara N, Hernando R, Sarrael A, Schultz SK, Ponto LLB, Shim H, Smith KE, Relkin N, Chaing G, Raudin L, Smith A, Fargher K, Raj BA, Neylan T, Grafman J, Davis M, Morrison R, Hayes J, Finley S, Friedl K, Fleischman D, Arfanakis K, James O, Massoglia D, Fruehling JJ, Harding S, Peskind ER, Petrie EC, Li G, Yesavage JA, Taylor JL, Furst AJ (2016): Early role of vascular dysregulation on late-onset Alzheimer's disease based on multifactorial data-driven analysis. *Nature Communications* 2016 7:1 7:1–14. <https://www.nature.com/articles/ncomms11934>.

Jack CR, Bennett DA, Blennow K, Carrillo MC, Feldman HH, Frisoni GB, Hampel H, Jagust WJ, Johnson KA, Knopman DS, Petersen RC, Scheltens P, Sperling RA, Dubois B (2016): A/T/N: An unbiased descriptive classification scheme for Alzheimer disease biomarkers. *Neurology*. Lippincott Williams and Wilkins. [/pmc/articles/PMC4970664/?report=abstract](https://pmc/articles/PMC4970664/?report=abstract).

Jack CR, Knopman DS, Jagust WJ, Petersen RC, Weiner MW, Aisen PS, Shaw LM, Vemuri P, Wiste HJ, Weigand SD, Lesnick TG, Pankratz VS, Donohue MC, Trojanowski JQ (2013): Tracking pathophysiological processes in Alzheimer's disease: an updated hypothetical model of dynamic biomarkers. *Lancet Neurol* 12:207–216. <https://pubmed.ncbi.nlm.nih.gov/23332364/>.

Jackson N, Cole SR, Voytek B, Swann NC (2019): Characteristics of waveform shape in Parkinson's disease detected with scalp electroencephalography. *eNeuro* 6. <https://www.eneuro.org/content/6/3/ENEURO.0151-19.2019>.

Jacobs HIL, Radua J, Lückmann HC, Sack AT (2013): Meta-analysis of functional network alterations in Alzheimer's disease: toward a network biomarker. *Neurosci Biobehav Rev* 37:753–765. <https://pubmed.ncbi.nlm.nih.gov/23523750/>.

Jaotombo F, Adorni L, Ghattas B, Boyer L (2023): Finding the best trade-off between performance and interpretability in predicting hospital length of stay using structured and unstructured data. *PLoS One* 18:e0289795. <https://pubmed.ncbi.nlm.nih.gov/38032876/>.

Jaramillo-Jimenez A, Suarez-Revelo JX, Ochoa-Gomez JF, Carmona Arroyave JA, Bocanegra Y, Lopera F, Buriticá O, Pineda-Salazar DA, Moreno Gómez L, Tobón Quintero CA, Borda MG, Bonanni L, Fytche DH, Brønnick K, Aarsland D (2021): Resting-state EEG alpha/theta ratio related to

- neuropsychological test performance in Parkinson's Disease. *Clinical Neurophysiology* 132:756–764. <https://pubmed.ncbi.nlm.nih.gov/33571883/>.
- Jaramillo-Jimenez A, Tovar-Rios DA, Ospina JA, Mantilla-Ramos YJ, Loaiza-López D, Henao Isaza V, Zapata Saldarriaga LM, Cadavid Castro V, Suarez-Revelo JX, Bocanegra Y, Lopera F, Pineda-Salazar DA, Tobón Quintero CA, Ochoa-Gomez JF, Borda MG, Aarsland D, Bonanni L, Brønnick K (2023): Spectral features of resting-state EEG in Parkinson's Disease: A multicenter study using functional data analysis. *Clin Neurophysiol* 151:28–40. <https://pubmed.ncbi.nlm.nih.gov/37146531/>.
- Jas M, Engemann DA, Bekhti Y, Raimondo F, Gramfort A (2017): Autoreject: Automated artifact rejection for MEG and EEG data. *Neuroimage* 159:417–429.
- Jellinger KA, Attems J (2008): Prevalence and impact of vascular and Alzheimer pathologies in Lewy body disease. *Acta Neuropathol* 115:427–436. <https://link.springer.com/article/10.1007/s00401-008-0347-5>.
- Jellinger KA, Korczyn AD (2018): Are dementia with Lewy bodies and Parkinson's disease dementia the same disease? *BMC Med* 16. <https://pubmed.ncbi.nlm.nih.gov/29510692/>.
- Jennekens FGI (2014): A short history of the notion of neurodegenerative disease. *J Hist Neurosci* 23:85–94. <https://pubmed.ncbi.nlm.nih.gov/24512132/>.
- Jiao B, Li R, Zhou H, Qing K, Liu H, Pan H, Lei Y, Fu W, Wang X, Xiao X, Liu X, Yang Q, Liao X, Zhou Y, Fang L, Dong Y, Yang Y, Jiang H, Huang S, Shen L (2023): Neural biomarker diagnosis and prediction to mild cognitive impairment and Alzheimer's disease using EEG technology. *Alzheimers Res Ther* 15:1–14. <https://alzres.biomedcentral.com/articles/10.1186/s13195-023-01181-1>.
- Jin L, Nawaz H, Ono K, Nowell J, Haley E, Berman BD, Mukhopadhyay ND, Barrett MJ (2023): One Minute of EEG Data Provides Sufficient and Reliable Data for Identifying Lewy Body Dementia. *Alzheimer Dis Assoc Disord* 37:66–72. <https://pubmed.ncbi.nlm.nih.gov/36413637/>.
- Johnson WE, Li C, Rabinovic A (2007): Adjusting batch effects in microarray expression data using empirical Bayes methods. *Biostatistics* 8:118–127. <https://pubmed.ncbi.nlm.nih.gov/16632515/>.
- Jovicich J, Barkhof F, Babiloni C, Herholz K, Mulert C, van Berckel BNM, Frisoni GB (2019): Harmonization of neuroimaging biomarkers for neurodegenerative diseases: A survey in the imaging community of perceived barriers and suggested actions. *Alzheimer's & Dementia : Diagnosis, Assessment & Disease Monitoring* 11:69. [/pmc/articles/PMC6816469/](https://pmc/articles/PMC6816469/).
- Julin P, Wahlund LO, Basun H, Persson A, Måre K, Rudberg U (1995): Clinical diagnosis of frontal lobe dementia and Alzheimer's disease: relation to cerebral perfusion, brain atrophy and electroencephalography. *Dementia* 6:142–147. <https://pubmed.ncbi.nlm.nih.gov/7620526/>.
- Kamboj N, Metcalfe K, Chu CH, Conway A (2023): Predicting Blood Pressure After Nitroglycerin Infusion Dose Titration in Critical Care Units: A Multicenter Retrospective Study. *Comput Inform Nurs*. <https://pubmed.ncbi.nlm.nih.gov/38112619/>.
- Karekal A, Stuart S, Mancini M, Swann NC (2023): Elevated Gaussian-modeled beta power in the cortex characterizes aging, but not Parkinson's disease. *J Neurophysiol* 129:1086–1093. <https://journals.physiology.org/doi/10.1152/jn.00480.2022>.

- Keil A, Bernat EM, Cohen MX, Ding M, Fabiani M, Gratton G, Kappenman ES, Maris E, Mathewson KE, Ward RT, Weisz N (2022): Recommendations and publication guidelines for studies using frequency domain and time-frequency domain analyses of neural time series. *Psychophysiology* 59:e14052. [/pmc/articles/PMC9717489/](https://PMC9717489/).
- Keller SM, Gschwandtner U, Meyer A, Chaturvedi M, Roth V, Fuhr P (2020): Cognitive decline in Parkinson's disease is associated with reduced complexity of EEG at baseline. *Brain Commun* 2. [/pmc/articles/PMC7749793/](https://PMC7749793/).
- Kertesz A (2007): Pick complex--historical introduction. *Alzheimer Dis Assoc Disord* 21. <https://pubmed.ncbi.nlm.nih.gov/18090424/>.
- Khoury R, Ghossoub E (2019): Diagnostic biomarkers of Alzheimer's disease: A state-of-the-art review. *Biomark Neuropsychiatry* 1:100005.
- Kinge JM, Dieleman JL, Karlstad Ø, Knudsen AK, Klitkou ST, Hay SI, Vos T, Murray CJL, Vollset SE (2023): Disease-specific health spending by age, sex, and type of care in Norway: a national health registry study. *BMC Med* 21:1–14. <https://bmcmedicine.biomedcentral.com/articles/10.1186/s12916-023-02896-6>.
- Klietz M (2022): Caregiver Burden in Movement Disorders and Neurodegenerative Diseases: Editorial. *Brain Sci* 12. [/pmc/articles/PMC9497330/](https://PMC9497330/).
- Klimesch W (1999): EEG alpha and theta oscillations reflect cognitive and memory performance: a review and analysis. *Brain Res Brain Res Rev* 29:169–195. <https://pubmed.ncbi.nlm.nih.gov/10209231/>.
- Klimesch W, Sauseng P, Hanslmayr S (2007): EEG alpha oscillations: The inhibition-timing hypothesis. *Brain Res Rev* 53:63–88.
- Klonowski W (2009): Everything you wanted to ask about EEG but were afraid to get the right answer. *Nonlinear Biomed Phys* 3:2. [/pmc/articles/PMC2698918/](https://PMC2698918/).
- Koelewijn L, Lancaster TM, Linden D, Dima DC, Routley BC, Magazzini L, Barawi K, Brindley L, Adams R, Tansey KE, Bompas A, Tales A, Bayer A, Singh K (2019): Oscillatory hyperactivity and hyperconnectivity in young APOE-ε4 carriers and hypoconnectivity in alzheimer's disease. *Elife* 8.
- Kopčanová M, Tait L, Donoghue T, Stothart G, Smith L, Sandoval AAF, Davila-Perez P, Buss S, Shafi MM, Pascual-Leone A, Fried PJ, Benwell CSY (2023): Resting-state EEG signatures of Alzheimer's disease are driven by periodic but not aperiodic changes. *bioRxiv*. [/pmc/articles/PMC10312609/](https://PMC10312609/).
- Kosaka K (2014): Lewy body disease and dementia with Lewy bodies. *Proc Jpn Acad Ser B Phys Biol Sci* 90:301. [/pmc/articles/PMC4275567/](https://PMC4275567/).
- Kottlarz I, Berg S, Toscano-Tejeida D, Steinmann I, Bähr M, Luther S, Wilke M, Parlitz U, Schlemmer A (2020): Extracting Robust Biomarkers From Multichannel EEG Time Series Using Nonlinear Dimensionality Reduction Applied to Ordinal Pattern Statistics and Spectral Quantities. *Front Physiol* 11:614565. [/pmc/articles/PMC7882607/](https://PMC7882607/).
- Kropotov JD (2016): Alpha Rhythms. *Functional Neuromarkers for Psychiatry*:89–105.

Kurbatskaya A, Jaramillo-Jimenez A, Fredy Ochoa-Gomez J, Brønnick K, Fernandez-Quilez A (2023a): Machine Learning-Based Detection of Parkinson's Disease From Resting-State EEG: A Multi-Center Study. ArXiv.

Kurbatskaya A, Jaramillo-Jimenez A, Ochoa-Gomez JF, Brønnick K, Fernandez-Quilez A (2023b): Assessing gender fairness in EEG-based machine learning detection of Parkinson's disease: A multi-center study:1020–1024. <https://arxiv.org/abs/2303.06376v1>.

Lai M, Demuru M, Hillebrand A, Fraschini M (2018): A comparison between scalp- and source-reconstructed EEG networks. *Sci Rep* 8. [/pmc/articles/PMC6095906/](https://pmc/articles/PMC6095906/).

Lantero-Rodriguez J, Vrillon A, Fernández-Lebrero A, Ortiz-Romero P, Snellman A, Montoliu-Gaya L, Brum WS, Cognat E, Dumurgier J, Puig-Pijoan A, Navalpotro-Gómez I, García-Escobar G, Karikari TK, Vanmechelen E, Ashton NJ, Zetterberg H, Suárez-Calvet M, Paquet C, Blennow K (2023): Clinical performance and head-to-head comparison of CSF p-tau235 with p-tau181, p-tau217 and p-tau231 in two memory clinic cohorts. *Alzheimers Res Ther* 15:1–15. <https://alzres.biomedcentral.com/articles/10.1186/s13195-023-01201-0>.

Larson MJ, Carbine KA (2017): Sample size calculations in human electrophysiology (EEG and ERP) studies: A systematic review and recommendations for increased rigor. *International Journal of Psychophysiology* 111:33–41. <https://linkinghub.elsevier.com/retrieve/pii/S0167876016301180>.

Lashgari E, Liang D, Maoz U (2020): Data augmentation for deep-learning-based electroencephalography. *J Neurosci Methods* 346. <https://pubmed.ncbi.nlm.nih.gov/32745492/>.

Lau ZJ, Pham T, Chen SHA, Makowski D (2022): Brain entropy, fractal dimensions and predictability: A review of complexity measures for EEG in healthy and neuropsychiatric populations. *Eur J Neurosci* 56:5047. [/pmc/articles/PMC9826422/](https://pmc/articles/PMC9826422/).

Law ZK, Todd C, Mehraram R, Schumacher J, Baker MR, LeBeau FEN, Yarnall A, Onofrj M, Bonanni L, Thomas A, Taylor JP (2020): The role of EEG in the diagnosis, prognosis and clinical correlations of dementia with Lewy bodies—a systematic review. *Diagnostics. Multidisciplinary Digital Publishing Institute (MDPI)*. [/pmc/articles/PMC7555753/](https://pmc/articles/PMC7555753/).

Leithner D, Schöder H, Haug A, Vargas HA, Gibbs P, Häggström I, Rausch I, Weber M, Becker AS, Schwartz J, Mayerhoefer ME (2022): Impact of ComBat Harmonization on PET Radiomics-Based Tissue Classification: A Dual-Center PET/MRI and PET/CT Study. *J Nucl Med* 63:1611–1616. <https://pubmed.ncbi.nlm.nih.gov/35210300/>.

Lenkala S, Marry R, Gopovaram SR, Akinci TC, Topsakal O (2023): Comparison of Automated Machine Learning (AutoML) Tools for Epileptic Seizure Detection Using Electroencephalograms (EEG). *Computers 2023, Vol 12, Page 197* 12:197. <https://www.mdpi.com/2073-431X/12/10/197/htm>.

Li A, Feitelberg J, Saini AP, Höchenberger R, Scheltienne M (2022a): MNE-ICALabel: Automatically annotating ICA components with ICLLabel in Python. *J Open Source Softw* 7:4484. <https://joss.theoj.org/papers/10.21105/joss.04484>.

Li M, Wang Y, Lopez-Naranjo C, Hu S, Reyes RCG, Paz-Linares D, Areces-Gonzalez A, Hamid AIA, Evans AC, Savostyanov AN, Calzada-Reyes A, Villringer A, Tobon-Quintero CA, Garcia-Agustin D, Yao D, Dong L, Aubert-Vazquez E, Reza F, Razzaq FA, Omar H, Abdullah JM, Galler JR, Ochoa-

Gomez JF, Prichep LS, Galan-Garcia L, Morales-Chacon L, Valdes-Sosa MJ, Tröndle M, Zulkifly MFM, Abdul Rahman MR Bin, Milakhina NS, Langer N, Rudych P, Koenig T, Virues-Alba TA, Lei X, Bringas-Vega ML, Bosch-Bayard JF, Valdes-Sosa PA (2022b): Harmonized-Multinational qEEG norms (HarMNqEEG). *Neuroimage* 256:119190.

Light GA, Swerdlow NR, Thomas ML, Calkins ME, Green MF, Greenwood TA, Gur RE, Gur RC, Lazzeroni LC, Nuechterlein KH, Pela M, Radant AD, Seidman LJ, Sharp RF, Siever LJ, Silverman JM, Srock J, Stone WS, Sugar CA, Tsuang DW, Tsuang MT, Braff DL, Turetsky BI (2015): Validation of mismatch negativity and P3a for use in multi-site studies of schizophrenia: characterization of demographic, clinical, cognitive, and functional correlates in COGS-2. *Schizophr Res* 163:63–72. <https://pubmed.ncbi.nlm.nih.gov/25449710/>.

Lin C-Y, Guo S-M, Lien J-JJ, Lin W-T, Liu Y-S, Lai C-H, Hsu I-L, Chang C-C, Tseng Y-L (2023): Combined model integrating deep learning, radiomics, and clinical data to classify lung nodules at chest CT. *Radiol Med.* <https://pubmed.ncbi.nlm.nih.gov/37971691/>.

Lindau M, Jelic V, Johansson SE, Andersen C, Wahlund LO, Almkvist O (2003): Quantitative EEG abnormalities and cognitive dysfunctions in frontotemporal dementia and Alzheimer's disease. *Dement Geriatr Cogn Disord* 15:106–114.

Litvan I, Goldman JG, Tröster AI, Schmand BA, Weintraub D, Petersen RC, Mollenhauer B, Adler CH, Marder K, Williams-Gray CH, Aarsland D, Kulisevsky J, Rodriguez-Oroz MC, Burn DJ, Barker RA, Emre M (2012): Diagnostic criteria for mild cognitive impairment in Parkinson's disease: Movement Disorder Society Task Force guidelines. *Movement Disorders* 27:349–356. [/pmc/articles/PMC3641655/?report=abstract](https://pmc/articles/PMC3641655/?report=abstract).

Liu J, Du Y, Wang X, Yue W, Feng J (2022): Automated Machine Learning for Epileptic Seizure Detection Based on EEG Signals. *Computers, Materials & Continua* 73:1995–2011. <https://www.techscience.com/cmc/v73n1/47863/html>.

Liu L, Zhang R, Shi D, Li R, Wang Q, Feng Y, Lu F, Zong Y, Xu X (2023): Automated machine learning to predict the difficulty for endoscopic resection of gastric gastrointestinal stromal tumor. *Front Oncol* 13:1190987. [/pmc/articles/PMC10206233/](https://pmc/articles/PMC10206233/).

Livingston G, Huntley J, Sommerlad A, Ames D, Ballard C, Banerjee S, Brayne C, Burns A, Cohen-Mansfield J, Cooper C, Costafreda SG, Dias A, Fox N, Gitlin LN, Howard R, Kales HC, Kivimäki M, Larson EB, Oggunniyi A, Orgeta V, Ritchie K, Rockwood K, Sampson EL, Samus Q, Schneider LS, Selbæk G, Teri L, Mukadam N (2020): Dementia prevention, intervention, and care: 2020 report of the Lancet Commission. *The Lancet* 396:413–446. <http://www.thelancet.com/article/S0140673620303676/fulltext>.

Llinás RR, Ribary U, Jeanmonod D, Kronberg E, Mitra PP (1999): Thalamocortical dysrhythmia: A neurological and neuropsychiatric syndrome characterized by magnetoencephalography. *Proc Natl Acad Sci U S A* 96:15222–15227. www.pnas.org.

Llinás RR, Steriade M (2006): Bursting of thalamic neurons and states of vigilance. *J Neurophysiol* 95:3297–3308. <https://journals.physiology.org/doi/10.1152/jn.00166.2006>.

Logroscino G, Piccininni M, Graff C, Hardiman O, Ludolph AC, Moreno F, Otto M, Remes AM, Rowe JB, Seelaar H, Solje E, Stefanova E, Traykov L, Jelic V, Rydell MT, Pender N, Anderl-Straub S, Barandiaran M, Gabilondo A, Krüger J, Murley AG, Rittman T, Ende EL van der, Swieten JC van, Hartikainen P, Stojmenović GM, Mehrabian S, Benussi L, Alberici A, Dell'Abate MT, Zecca C,

Borroni B, group F, Belezhanska D, Bianchetti A, Binetti G, Cotelli M, Cotelli MS, Dreherova I, Filardi M, Fostinelli S, Ghidoni R, Gnoni V, Nacheva G, Novaković I, Padovani A, Popivanov I, Raycheva M, Stockton K, Stoyanova K, Suhonen N-M, Tainta M, Toncheva D, Urso D, Zlatareva D, Zulaica M (2023): Incidence of Syndromes Associated With Frontotemporal Lobar Degeneration in 9 European Countries. *JAMA Neurol* 80:279–286.
<https://jamanetwork.com/journals/jamaneurology/fullarticle/2800415>.

Lopes Da Silva F (2010): EEG: Origin and measurement. *EEG - fMRI: Physiological Basis, Technique, and Applications*:19–38. https://link.springer.com/chapter/10.1007/978-3-540-87919-0_2.

López-Sanz D, Brunã R, Garcés P, Camara C, Serrano N, Rodríguez-Rojo IC, Delgado ML, Montenegro M, López-Higes R, Yus M, Maestú F (2016): Alpha band disruption in the AD-continuum starts in the Subjective Cognitive Decline stage: a MEG study. *Scientific Reports* 2016 6:1 6:1–11.
<https://www.nature.com/articles/srep37685>.

Lundberg SM, Lee SI (2017): A Unified Approach to Interpreting Model Predictions. *Adv Neural Inf Process Syst* 2017–December:4766–4775. <https://arxiv.org/abs/1705.07874v2>.

Lyketsos CG, Lopez O, Jones B, Fitzpatrick AL, Breitner J, Dekosky S (2002): Prevalence of Neuropsychiatric Symptoms in Dementia and Mild Cognitive Impairment: Results From the Cardiovascular Health Study. *JAMA* 288:1475–1483.
<https://jamanetwork.com/journals/jama/fullarticle/195320>.

Maestú F, de Haan W, Busche MA, DeFelipe J (2021): Neuronal excitation/inhibition imbalance: core element of a translational perspective on Alzheimer pathophysiology. *Ageing Res Rev* 69:101372.

Mantilla-Ramos Y-J (2023): sovabids: A python package for the automatic conversion of EEG datasets to the BIDS standard, with a focus on making the most out of metadata.
<https://github.com/yjmantilla/sovabids>.

Maresova P, Hruska J, Klimova B, Barakovic S, Krejcar O (2020): Activities of Daily Living and Associated Costs in the Most Widespread Neurodegenerative Diseases: A Systematic Review. *Clin Interv Aging* 15:1841. [/pmc/articles/PMC7538005/](https://pmc/articles/PMC7538005/).

Maserejian N, Vinikoor-Imler L, Dilley A (2020): Estimation of the 2020 Global Population of Parkinson's Disease (PD) [abstract]. *Mov Disord*.
<https://www.mdsabstracts.org/abstract/estimation-of-the-2020-global-population-of-parkinsons-disease-pd/>.

Massa F, Meli R, Grazzini M, Famà F, De Carli F, Filippi L, Arnaldi D, Pardini M, Morbelli S, Nobili F (2020): Utility of quantitative EEG in early Lewy body disease. *Parkinsonism Relat Disord* 75:70–75. <https://pubmed.ncbi.nlm.nih.gov/32480310/>.

McBride JC, Zhao X, Munro NB, Smith CD, Jicha GA, Hively L, Broster LS, Schmitt FA, Kryscio RJ, Jiang Y (2014): Spectral and complexity analysis of scalp EEG characteristics for mild cognitive impairment and early Alzheimer's disease. *Comput Methods Programs Biomed* 114:153–163.

McDonald WM (2017): Overview of Neurocognitive Disorders. *Focus: Journal of Life Long Learning in Psychiatry* 15:4. [/pmc/articles/PMC6519631/](https://pmc/articles/PMC6519631/).

McKeith IG, Boeve BF, Dickson DW, Halliday G, Taylor JP, Weintraub D, Aarsland D, Galvin J, Attems J, Ballard CG, Bayston A, Beach TG, Blanc F, Bohnen N, Bonanni L, Bras J, Brundin P, Burn D,

Chen-Plotkin A, Duda JE, El-Agnaf O, Feldman H, Ferman TJ, Ffytche D, Fujishiro H, Galasko D, Goldman JG, Gomperts SN, Graff-Radford NR, Honig LS, Iranzo A, Kantarci K, Kaufer D, Kukull W, Lee VMY, Leverenz JB, Lewis S, Lippa C, Lunde A, Masellis M, Masliah E, McLean P, Mollenhauer B, Montine TJ, Moreno E, Mori E, Murray M, O'Brien JT, Orimo S, Postuma RB, Ramaswamy S, Ross OA, Salmon DP, Singleton A, Taylor A, Thomas A, Tiraboschi P, Toledo JB, Trojanowski JQ, Tsuang D, Walker Z, Yamada M, Kosaka K (2017): Diagnosis and management of dementia with Lewy bodies. *Neurology*. *Neurology*. <https://pubmed.ncbi.nlm.nih.gov/28592453/>.

McKeith IG, Ferman TJ, Thomas AJ, Blanc F, Boeve BF, Fujishiro H, Kantarci K, Muscio C, O'Brien JT, Postuma RB, Aarsland D, Ballard C, Bonanni L, Donaghy P, Emre M, Galvin JE, Galasko D, Goldman JG, Gomperts SN, Honig LS, Ikeda M, Leverenz JB, Lewis SJG, Marder KS, Masellis M, Salmon DP, Taylor JP, Tsuang DW, Walker Z, Tiraboschi P (2020): Research criteria for the diagnosis of prodromal dementia with Lewy bodies. *Neurology*. *Neurology*. <https://pubmed.ncbi.nlm.nih.gov/32241955/>.

McKeown DJ, Jones M, Pihl C, Finley A, Kelley N, Baumann O, Schinazi VR, Moustafa AA, Cavanagh JF, Angus DJ (2023): Medication-invariant resting aperiodic and periodic neural activity in Parkinson's disease. *Psychophysiology* 00:e14478. <https://onlinelibrary.wiley.com/doi/full/10.1111/psyp.14478>.

McKhann G, Drachman D, Folstein M, Katzman R, Price D, Stadlan EM (1984): Clinical diagnosis of alzheimer's disease: Report of the NINCDS-ADRDA work group* under the auspices of department of health and human services task force on alzheimer's disease. *Neurology* 34:939–944.

McKhann GM, Knopman DS, Chertkow H, Hyman BT, Jack CR, Kawas CH, Klunk WE, Koroshetz WJ, Manly JJ, Mayeux R, Mohs RC, Morris JC, Rossor MN, Scheltens P, Carrillo MC, Thies B, Weintraub S, Phelps CH (2011): The diagnosis of dementia due to Alzheimer's disease: Recommendations from the National Institute on Aging-Alzheimer's Association workgroups on diagnostic guidelines for Alzheimer's disease. *Alzheimer's & Dementia* 7:263–269. <https://onlinelibrary.wiley.com/doi/full/10.1016/j.jalz.2011.03.005>.

Meeter LH, Kaat LD, Rohrer JD, Van Swieten JC (2017): Imaging and fluid biomarkers in frontotemporal dementia. *Nature Reviews Neurology* 2017 13:7 13:406–419. <https://www.nature.com/articles/nrneurol.2017.75>.

Meghdadi AH, Karic MS, McConnell M, Rupp G, Richard C, Hamilton J, Salat D, Berka C (2021): Resting state EEG biomarkers of cognitive decline associated with Alzheimer's disease and mild cognitive impairment. *PLoS One* 16. <https://pubmed.ncbi.nlm.nih.gov/33544703/>.

Mehraram R, Kaiser M, Cromarty R, Graziadio S, O'Brien JT, Killen A, Taylor JP, Peraza LR (2020): Weighted network measures reveal differences between dementia types: An EEG study. *Hum Brain Mapp* 41:1573. [/pmc/articles/PMC7267959/](https://pmc/articles/PMC7267959/).

Melnik A, Legkov P, Izdebski K, Kärcher SM, Hairston WD, Ferris DP, König P (2017): Systems, subjects, sessions: To what extent do these factors influence EEG data? *Front Hum Neurosci* 11:245570.

Menšíková K, Matěj R, Colosimo C, Rosales R, Tučková L, Ehrmann J, Hraboš D, Kolaříková K, Vodička R, Vrtěl R, Procházka M, Nevrly M, Kaiserová M, Kurčová S, Otruba P, Kaňovský P (2022): Lewy

body disease or diseases with Lewy bodies? *npj Parkinson's Disease* 2022 8:1 8:1–11.
<https://www.nature.com/articles/s41531-021-00273-9>.

Merkin A, Sghirripa S, Graetz L, Smith AE, Hordacre B, Harris R, Pitcher J, Semmler J, Rogasch NC, Goldsworthy M (2021): Age differences in aperiodic neural activity measured with resting EEG. *bioRxiv*:2021.08.31.458328. <https://www.biorxiv.org/content/10.1101/2021.08.31.458328v1>.

Merkin A, Sghirripa S, Graetz L, Smith AE, Hordacre B, Harris R, Pitcher J, Semmler J, Rogasch NC, Goldsworthy M (2023): Do age-related differences in aperiodic neural activity explain differences in resting EEG alpha? *Neurobiol Aging* 121:78–87.

Mhyre TR, Boyd JT, Hamill RW, Maguire-Zeiss KA (2012): Parkinson's disease. *Subcell Biochem* 65:389–455. [/pmc/articles/PMC4372387/?report=abstract](https://PMC4372387/?report=abstract).

Miljevic A, Bailey NW, Vila-Rodriguez F, Herring SE, Fitzgerald PB (2022): Electroencephalographic Connectivity: A Fundamental Guide and Checklist for Optimal Study Design and Evaluation. *Biol Psychiatry Cogn Neurosci Neuroimaging* 7:546–554.

Miltiadous A, Tzimourta KD, Afrantou T, Ioannidis P, Grigoriadis N, Tsaklikakis DG, Angelidis P, Tsipouras MG, Glavas E, Giannakeas N, Tzallas AT (2023): A Dataset of Scalp EEG Recordings of Alzheimer's Disease, Frontotemporal Dementia and Healthy Subjects from Routine EEG. *Data* 2023, Vol 8, Page 95 8:95. <https://www.mdpi.com/2306-5729/8/6/95/htm>.

Modir A, Shamekhi S, Ghaderyan P (2023): A systematic review and methodological analysis of EEG-based biomarkers of Alzheimer's disease. *Measurement* 220:113274.

Moezzi B, Hordacre B, Berryman C, Riddin MC, Goldsworthy MR (2018): Test-retest reliability of functional brain network characteristics using resting-state EEG and graph theory. *bioRxiv*:385302. <https://www.biorxiv.org/content/10.1101/385302v1>.

Moguilner S, Birba A, Fittipaldi S, Gonzalez-Campo C, Tagliazucchi E, Reyes P, Matallana D, Parra MA, Slachevsky A, Farías G, Cruzat J, García A, Eyre HA, La Joie R, Rabinovici G, Whelan R, Ibáñez A (2022): Multi-feature computational framework for combined signatures of dementia in underrepresented settings. *J Neural Eng* 19:046048.
<https://iopscience.iop.org/article/10.1088/1741-2552/ac87d0>.

Mohanty R, Sethares WA, Nair VA, Prabhakaran V (2020): Rethinking Measures of Functional Connectivity via Feature Extraction. *Scientific Reports* 2020 10:1 10:1–17.
<https://www.nature.com/articles/s41598-020-57915-w>.

Moretti D V. (2015): Theta and alpha EEG frequency interplay in subjects with mild cognitive impairment: evidence from EEG, MRI, and SPECT brain modifications. *Front Aging Neurosci* 7. [/pmc/articles/PMC4396516/](https://PMC4396516/).

Moretti D V, Babiloni C, Binetti G, Cassetta E, Dal Forno G, Ferreric F, Ferri R, Lanuzza B, Miniussi C, Nobili F, Rodriguez G, Salinari S, Rossini PM (2004): Individual analysis of EEG frequency and band power in mild Alzheimer's disease. *Clinical Neurophysiology* 115:299–308.
<http://www.ncbi.nlm.nih.gov/pubmed/14744569>.

Moretti D V., Paternicò D, Binetti G, Zanetti O, Frisoni GB (2013): EEG upper/low alpha frequency power ratio relates to temporo-parietal brain atrophy and memory performances in mild cognitive impairment. *Front Aging Neurosci* 5:65285.

- Mouton A, Blanc F, Gros A, Manera V, Fabre R, Sauleau E, Gomez-Luporsi I, Tifratene K, Friedman L, Thümmler S, Pradier C, Robert PH, David R (2018): Sex ratio in dementia with Lewy bodies balanced between Alzheimer's disease and Parkinson's disease dementia: a cross-sectional study. *Alzheimers Res Ther* 10. /pmc/articles/PMC6136211/.
- Müller EJ, Munn B, Hearne LJ, Smith JB, Fulcher B, Arnatkevičiūtė A, Lurie DJ, Cocchi L, Shine JM (2020): Core and matrix thalamic sub-populations relate to spatio-temporal cortical connectivity gradients. *Neuroimage* 222:117224.
- Müller EJ, Munn BR, Redinbaugh MJ, Lizier J, Breakspear M, Saalmann YB, Shine JM (2023): The non-specific matrix thalamus facilitates the cortical information processing modes relevant for conscious awareness. *Cell Rep* 42:112844.
- Munn BR, Müller EJ, Medel V, Naismith SL, Lizier JT, Sanders RD, Shine JM (2023): Neuronal connected burst cascades bridge macroscale adaptive signatures across arousal states. *Nature Communications* 2023 14:1 14:1–17. <https://www.nature.com/articles/s41467-023-42465-2>.
- Musigmann M, Akkurt BH, Krähling H, Nacul NG, Remonda L, Sartoretti T, Henssen D, Brokinkel B, Stummer W, Heindel W, Mannil M (2022): Testing the applicability and performance of Auto ML for potential applications in diagnostic neuroradiology. *Sci Rep* 12. <https://pubmed.ncbi.nlm.nih.gov/35953588/>.
- Nandi A, Counts N, Chen S, Seligman B, Tortorice D, Vigo D, Bloom DE (2022): Global and regional projections of the economic burden of Alzheimer's disease and related dementias from 2019 to 2050: A value of statistical life approach. *EClinicalMedicine* 51:101580. <http://www.thelancet.com/article/S2589537022003108/fulltext>.
- Narayanan Lab (2020): Datasets. <https://narayanan.lab.uiowa.edu/article/datasets>.
- Nardone R, Sebastianelli L, Versace V, Saltuari L, Lochner P, Frey V, Golaszewski S, Brigo F, Trinka E, Höller Y (2018): Usefulness of EEG Techniques in Distinguishing Frontotemporal Dementia from Alzheimer's Disease and Other Dementias. *Dis Markers* 2018. /pmc/articles/PMC6140274/.
- Nedelska Z, Schwarz CG, Lesnick TG, Boeve BF, Przybelski SA, Lowe VJ, Kremers WK, Gunter JL, Senjem ML, Graff-Radford J, Ferman TJ, Fields JA, Knopman DS, Petersen RC, Jack CR, Kantarci K (2019): Association of Longitudinal β -Amyloid Accumulation Determined by Positron Emission Tomography With Clinical and Cognitive Decline in Adults With Probable Lewy Body Dementia. *JAMA Netw Open* 2:e1916439–e1916439. <https://jamanetwork.com/journals/jamanetworkopen/fullarticle/2756108>.
- Neto E, Allen EA, Auriel H, Nordby H, Eichele T (2015): EEG spectral features discriminate between Alzheimer's and vascular dementia. *Front Neurol* 6:108906.
- Newson JJ, Thiagarajan TC (2019): EEG Frequency Bands in Psychiatric Disorders: A Review of Resting State Studies. *Frontiers in Human Neuroscience*. Frontiers Media S.A. /pmc/articles/PMC6333694/.
- Nguyen-Danse DA, Singaravelu S, Chauvigné LAS, Mottaz A, Allaman L, Guggisberg AG (2021): Feasibility of Reconstructing Source Functional Connectivity with Low-Density EEG. *Brain Topogr* 34:709. /pmc/articles/PMC8556201/.

Nichols E, Abd-Allah F, Abdoli A, Abosetugn AE, Abrha WA, Abualhasan A, Abu-Gharbieh E, Akinyemi RO, Alahdab F, Alanezi FM, Alipour V, Ansari I, Arabloo J, Ashraf-Ganjouei A, Avan A, Ayano G, Babar ZUD, Baig AA, Banach M, Barboza MA, Barker-Collo SL, Baune BT, Srikanth Bhagavathula A, Bhattacharyya K, Bijani A, Biondi A, Birhan TA, Biswas A, Bolla SR, Boloor A, Brayne C, Brenner H, Burkart K, Burns RA, Nagaraja SB, Carvalho F, Castro-De-araujo LFS, Catalá-López F, Cerin E, Cernigliaro A, Cherbuin N, Jasmine Choi JY, Chu DT, Dagnew B, Dai X, Dandona L, Dandona R, Diaz D, Dibaji Forooshani ZS, Douiri A, Duncan BB, Edvardsson D, El-Jaafary SI, Eskandari K, Eskandarieh S, Feigin VL, Fereshtehnejad SM, Fernandes E, Ferrara P, Filip I, Fischer F, Gaidhane S, Gebregzabiher KZ, Ghashghaei A, Gholamian A, Gnedovskaya E V., Golechha M, Gupta R, Hachinski V, Hamidi S, Hankey GJ, Haro JM, Hassan A, Hay SI, Heidari G, Heidari-Soureshjani R, Househ M, Hussain R, Hwang BF, Ilic IM, Ilic MD, Naghibi Irvani SS, Iso H, Iwagami M, Jha RP, Kalani R, Kandel H, Karch A, Kasa AS, Kengne AP, Kim YE, Kim YJ, Kisa S, Kisa A, Kivimäki M, Komaki H, Aikoyanagi, Kukull WA, Kumar GA, Kumar M, Landires I, Leonardi M, Lim SS, Liu X, Logroscino G, Lopez AD, Lorkowski S, Loy CT, Amin HIM, Manafi N, Manjunatha N, Mehndiratta MM, Menezes RG, Meretoja A, Merkin A, Metekiya WM, Misganaw AT, Mohajer B, Ibrahim NM, Mohammad Y, Mohapatra A, Mohebi F, Mokdad AH, Mondello S, Mossie TB, Mulugeta A, Nagel G, Naveed M, Nayak VC, Kandel SN, Nguyen SH, Nguyen HLT, Nuñez-Samudio V, Ogbo FA, Olagunju AT, Orru H, Ostojic SM, Ostroff SM, Otstavnov N, Otstavnov SS, Owolabi MO, Pathak M, Toroudi HP, Peterson CB, Pham HQ, Phillips MR, Piradov MA, Pottoo FH, Prada SI, Angga Pribadi DR, Radfar A, Raggi A, Rahim F, Ram P, Rana J, Rashedi V, Rawaf S, Rawaf DL, Reinig N, Rezaei N, Robinson SR, Romoli M, Sachdev PS, Sahathevan R, Sahebkar A, Sahraian MA, Sattin D, Saylan M, Sayyah M, Schiavolin S, Schmidt MI, Shahid I, Shaikh MA, Shigematsu M, Shin J II, Shiri R, Siddiqi TJ, Silva JP, Singh JA, Soheili A, Spurlock EE, Szoke CEI, Tabarés-Seisdedos R, Taddele BW, Thakur B, Thekke Purakkal AS, Tovani-Palone MR, Tran BX, Travillian RS, Tripathi M, Tsegaye GW, Usman MS, Vacante M, Velazquez DZ, Venketasubramanian N, Vidale S, Vlassov V, Wang YP, Wei J, Weiss J, Weldomariam AH, Wimo A, Wu C, Yadollahpour A, Yamagishi K, Yesilita YG, Yonemoto N, Zadey S, Zhang ZJ, Murray CJL, Vos T (2021): Global mortality from dementia: Application of a new method and results from the Global Burden of Disease Study 2019. *Alzheimer's & Dementia: Translational Research & Clinical Interventions* 7:e12200.

<https://onlinelibrary.wiley.com/doi/full/10.1002/trc2.12200>.

Nichols E, Steinmetz JD, Vollset SE, Fukutaki K, Chalek J, Abd-Allah F, Abdoli A, Abualhasan A, Abu-Gharbieh E, Akram TT, Al Hamad H, Alahdab F, Alanezi FM, Alipour V, Almustanyir S, Amu H, Ansari I, Arabloo J, Ashraf T, Astell-Burt T, Ayano G, Ayuso-Mateos JL, Baig AA, Barnett A, Barrow A, Baune BT, Béjot Y, Bezabhe WMM, Bezabih YM, Bhagavathula AS, Bhaskar S, Bhattacharyya K, Bijani A, Biswas A, Bolla SR, Boloor A, Brayne C, Brenner H, Burkart K, Burns RA, Cámera LA, Cao C, Carvalho F, Castro-de-Araujo LFS, Catalá-López F, Cerin E, Chavan PP, Cherbuin N, Chu DT, Costa VM, Couto RAS, Dadras O, Dai X, Dandona L, Dandona R, De la Cruz-Góngora V, Dhamnetiya D, Dias da Silva D, Diaz D, Douiri A, Edvardsson D, Ekholuenetale M, El Sayed I, El-Jaafary SI, Eskandari K, Eskandarieh S, Esmaeilnejad S, Fares J, Faro A, Farooque U, Feigin VL, Feng X, Fereshtehnejad SM, Fernandes E, Ferrara P, Filip I, Fillit H, Fischer F, Gaidhane S, Galluzzo L, Ghashghaei A, Ghith N, Gianni A, Gilani SA, Glavan IR, Gnedovskaya E V., Golechha M, Gupta R, Gupta VB, Gupta VK, Haider MR, Hall BJ, Hamidi S, Hanif A, Hankey GJ, Haque S, Hartono RK, Hasaballah AI, Hasan MT, Hassan A, Hay SI, Hayat K, Hegazy MI, Heidari G, Heidari-Soureshjani R, Herteliu C, Househ M, Hussain R, Hwang BF, Iacoviello L, Iavicoli I, Ilesanmi OS, Ilic IM, Ilic MD, Irvani SSN, Iso H, Iwagami M, Jabbarinejad R, Jacob L, Jain V, Jayapal SK, Jayawardena R, Jha RP, Jonas JB, Joseph N, Kalani R, Kandel A, Kandel H, Karch A,

Kasa AS, Kassie GM, Keshavarz P, Khan MA, Khatib MN, Khoja TAM, Khubchandani J, Kim MS, Kim YJ, Kisa A, Kisa S, Kivimäki M, Koroshetz WJ, Koyanagi A, Kumar GA, Kumar M, Lak HM, Leonardi M, Li B, Lim SS, Liu X, Liu Y, Logroscino G, Lorkowski S, Lucchetti G, Lutzky Saute R, Magnani FG, Malik AA, Massano J, Mehndiratta MM, Menezes RG, Meretoja A, Mohajer B, Mohamed Ibrahim N, Mohammad Y, Mohammed A, Mokdad AH, Mondello S, Moni MAA, Moniruzzaman M, Mossie TB, Nagel G, Naveed M, Nayak VC, Neupane Kandel S, Nguyen TH, Oancea B, Otstavnov N, Otstavnov SS, Owolabi MO, Panda-Jonas S, Pashazadeh Kan F, Pasovic M, Patel UK, Pathak M, Peres MFP, Perianayagam A, Peterson CB, Phillips MR, Pinheiro M, Piradov MA, Pond CD, Potashman MH, Pottor FH, Prada SI, Radfar A, Raggi A, Rahim F, Rahman M, Ram P, Ranasinghe P, Rawaf DL, Rawaf S, Rezaei N, Rezapour A, Robinson SR, Romoli M, Roshandel G, Sahathevan R, Sahebkar A, Sahraian MA, Sathian B, Sattin D, Sawhney M, Saylan M, Schiavolin S, Seylani A, Sha F, Shaikh MA, Shaji KS, Shannawaz M, Shetty JK, Shigematsu M, Shin J II, Shiri R, Silva DAS, Silva JP, Silva R, Singh JA, Skryabin VY, Skryabina AA, Smith AE, Soshnikov S, Spurlock EE, Stein DJ, Sun J, Tabarés-Seisdedos R, Thakur B, Timalsina B, Tovani-Palone MR, Tran BX, Tsegaye GW, Valadan Tahbaz S, Valdez PR, Venketasubramanian N, Vlassov V, Vu GT, Vu LG, Wang YP, Wimo A, Winkler AS, Yadav L, Yahyazadeh Jabbari SH, Yamagishi K, Yang L, Yano Y, Yonemoto N, Yu C, Yunusa I, Zadey S, Zastrozhin MS, Zastrozhina A, Zhang ZJ, Murray CJL, Vos T (2022): Estimation of the global prevalence of dementia in 2019 and forecasted prevalence in 2050: an analysis for the Global Burden of Disease Study 2019. *Lancet Public Health* 7:e105–e125.
<http://www.thelancet.com/article/S2468266721002498/fulltext>.

Nichols E, Vos T (2021): The estimation of the global prevalence of dementia from 1990-2019 and forecasted prevalence through 2050: An analysis for the Global Burden of Disease (GBD) study 2019. *Alzheimer's & Dementia* 17:e051496.
<https://onlinelibrary.wiley.com/doi/full/10.1002/alz.051496>.

van Nifterick AM, Mulder D, Duineveld DJ, Diachenko M, Scheltens P, Stam CJ, van Kesteren RE, Linkenkaer-Hansen K, Hillebrand A, Gouw AA (2023): Resting-state oscillations reveal disturbed excitation-inhibition ratio in Alzheimer's disease patients. *Scientific Reports* 2023 13:1 13:1–13. <https://www.nature.com/articles/s41598-023-33973-8>.

Nishida K, Yoshimura M, Isotani T, Yoshida T, Kitaura Y, Saito A, Mii H, Kato M, Takekita Y, Suwa A, Morita S, Kinoshita T (2011): Differences in quantitative EEG between frontotemporal dementia and Alzheimer's disease as revealed by LORETA. *Clin Neurophysiol* 122:1718–1725.
<https://pubmed.ncbi.nlm.nih.gov/21396882/>.

Niso G, Botvinik-Nezer R, Appelhoff S, De La Vega A, Esteban O, Etzel JA, Finc K, Ganz M, Gau R, Halchenko YO, Herholz P, Karakuza A, Keator DB, Markiewicz CJ, Maumet C, Pernet CR, Pestilli F, Queder N, Schmitt T, Sójka W, Wagner AS, Whitaker KJ, Rieger JW (2022): Open and reproducible neuroimaging: From study inception to publication. *Neuroimage* 263:119623. [/pmc/articles/PMC10008521/](https://pmc/articles/PMC10008521/).

Nobukawa S, Yamanishi T, Nishimura H, Wada Y, Kikuchi M, Takahashi T (2019): Atypical temporal-scale-specific fractal changes in Alzheimer's disease EEG and their relevance to cognitive decline. *Cogn Neurodyn* 13:1–11. <https://link.springer.com/article/10.1007/s11571-018-9509-x>.

Nowrangi MA, Lyketsos CG, Rosenberg PB (2015): Principles and management of neuropsychiatric symptoms in Alzheimer's dementia. *Alzheimers Res Ther* 7:1–10.
<https://alzres.biomedcentral.com/articles/10.1186/s13195-015-0096-3>.

- Ou C, Liu J, Qian Y, Chong W, Liu D, He X, Zhang X, Duan CZ (2021): Automated Machine Learning Model Development for Intracranial Aneurysm Treatment Outcome Prediction: A Feasibility Study. *Front Neurol* 12:735142. [/pmc/articles/PMC8666475/](https://www.ncbi.nlm.nih.gov/pmc/articles/PMC8666475/).
- Ouchani M, Gharibzadeh S, Jamshidi M, Amini M (2021): A Review of Methods of Diagnosis and Complexity Analysis of Alzheimer's Disease Using EEG Signals. *Biomed Res Int* 2021.
- Özbek Y, Fide E, Yener GG (2021): Resting-state EEG alpha/theta power ratio discriminates early-onset Alzheimer's disease from healthy controls. *Clinical Neurophysiology* 132:2019–2031.
- Palmqvist S, Schöll M, Strandberg O, Mattsson N, Stomrud E, Zetterberg H, Blennow K, Landau S, Jagust W, Hansson O (2017): Earliest accumulation of β -amyloid occurs within the default-mode network and concurrently affects brain connectivity. *Nature Communications* 2017 8:1 8:1–13. <https://www.nature.com/articles/s41467-017-01150-x>.
- Pappalettera C, Cacciotti A, Nucci L, Miraglia F, Rossini PM, Vecchio F (2023): Approximate entropy analysis across electroencephalographic rhythmic frequency bands during physiological aging of human brain. *Geroscience* 45:1131. [/pmc/articles/PMC9886767/](https://www.ncbi.nlm.nih.gov/pmc/articles/PMC9886767/).
- Parkinson J (2002): An essay on the shaking palsy. 1817. *J Neuropsychiatry Clin Neurosci* 14.
- Pathania A, Schreiber M, Miller MW, Euler MJ, Lohse KR (2021): Exploring the reliability and sensitivity of the EEG power spectrum as a biomarker. *International Journal of Psychophysiology* 160:18–27.
- Pavlov YG, Adamian N, Appelhoff S, Arvaneh M, Benwell CSY, Beste C, Bland AR, Bradford DE, Bublitzky F, Busch NA, Clayson PE, Cruse D, Czeszumski A, Dreber A, Dumas G, Ehinger B, Ganis G, He X, Hinojosa JA, Huber-Huber C, Inzlicht M, Jack BN, Johannesson M, Jones R, Kalenkovich E, Kaltwasser L, Karimi-Rouzbahani H, Keil A, König P, Kouara L, Kulke L, Ladouceur CD, Langer N, Liesefeld HR, Luque D, MacNamara A, Mudrik L, Muthuraman M, Neal LB, Nilsonne G, Niso G, Ocklenburg S, Oostenveld R, Pernet CR, Pourtois G, Ruzzoli M, Sass SM, Schaefer A, Senderecka M, Snyder JS, Tamnes CK, Tognoli E, van Vugt MK, Verona E, Vloeberghs R, Welke D, Wessel JR, Zakharov I, Mushtaq F (2021): #EEGManyLabs: Investigating the replicability of influential EEG experiments. *Cortex* 144:213–229.
- Pedroni A, Bahreini A, Langer N (2019): Automagic: Standardized preprocessing of big EEG data. *Neuroimage* 200:460–473.
- Peraza LR, Cromarty R, Kobeleva X, Firbank MJ, Killen A, Graziadio S, Thomas AJ, O'Brien JT, Taylor JP (2018): Electroencephalographic derived network differences in Lewy body dementia compared to Alzheimer's disease patients. *Scientific Reports* 2018 8:1 8:1–13. <https://www.nature.com/articles/s41598-018-22984-5>.
- Perez-Valero E, Morillas C, Lopez-Gordo MA, Carrera-Muñoz I, López-Alcalde S, Vílchez-Carrillo RM (2022): An Automated Approach for the Detection of Alzheimer's Disease From Resting State Electroencephalography. *Front Neuroinform* 16:924547.
- Pernet C, Garrido MI, Gramfort A, Maurits N, Michel CM, Pang E, Salmelin R, Schoffelen JM, Valdes-Sosa PA, Puce A (2020): Issues and recommendations from the OHBM COBIDAS MEEG committee for reproducible EEG and MEG research. *Nature Neuroscience* 2020 23:12 23:1473–1483. <https://www.nature.com/articles/s41593-020-00709-0>.

Pernet CR, Appelhoff S, Gorgolewski KJ, Flandin G, Phillips C, Delorme A, Oostenveld R (2019): EEG-BIDS, an extension to the brain imaging data structure for electroencephalography. *Scientific Data*. Nature Publishing Group. <https://www.nature.com/articles/s41597-019-0104-8>.

Perry DC, Brown JA, Possin KL, Datta S, Trujillo A, Radke A, Karydas A, Kornak J, Sias AC, Rabinovici GD, Gorno-Tempini ML, Boxer AL, De May M, Rankin KP, Sturm VE, Lee SE, Matthews BR, Kao AW, Vossel KA, Tartaglia MC, Miller ZA, Seo SW, Sidhu M, Gaus SE, Nana AL, Vargas JNS, Hwang JHL, Ossenkoppele R, Brown AB, Huang EJ, Coppola G, Rosen HJ, Geschwind D, Trojanowski JQ, Grinberg LT, Kramer JH, Miller BL, Seeley WW (2017): Clinicopathological correlations in behavioural variant frontotemporal dementia. *Brain* 140:3329–3345.
<https://pubmed.ncbi.nlm.nih.gov/29053860/>.

Petersen RC, Aisen P, Boeve BF, Geda YE, Ivnik RJ, Knopman DS, Mielke M, Pankratz VS, Roberts R, Rocca WA, Weigand S, Weiner M, Wiste H, Jack CR (2013): Criteria for Mild Cognitive Impairment Due to Alzheimer's Disease in the Community. *Ann Neurol* 74:199. /pmc/articles/PMC3804562/.

Peterson EK (2020): Associations Between EEG and Cognition in Parkinson's Disease. Ed. University of Canterbury. Christchurch, New Zealand.
<https://ir.canterbury.ac.nz/server/api/core/bitstreams/b575d676-14ed-4de4-815cf3e30c35fad4/content>.

Pion-Tonachini L, Kreutz-Delgado K, Makeig S (2019): ICLLabel: An automated electroencephalographic independent component classifier, dataset, and website. *Neuroimage* 198:181. /pmc/articles/PMC6592775/.

Pippenger MA (2021): How often is EEG used as part of routine dementia evaluation in community practice? *Alzheimer's & Dementia* 17:e056638.
<https://onlinelibrary.wiley.com/doi/full/10.1002/alz.056638>.

Poil SS, de Haan W, van der Flier WM, Mansvelder HD, Scheltens P, Linkenkaer-Hansen K (2013): Integrative EEG biomarkers predict progression to Alzheimer's disease at the MCI stage. *Front Aging Neurosci* 5. /pmc/articles/PMC3789214/.

Pomponio R, Erus G, Habes M, Doshi J, Srinivasan D, Mamourian E, Bashyam V, Nasrallah IM, Satterthwaite TD, Fan Y, Launer LJ, Masters CL, Maruff P, Zhuo C, Völzke H, Johnson SC, Fripp J, Koutsouleris N, Wolf DH, Gur R, Gur R, Morris J, Albert MS, Grabe HJ, Resnick SM, Bryan RN, Wolk DA, Shinohara RT, Shou H, Davatzikos C (2020): Harmonization of large MRI datasets for the analysis of brain imaging patterns throughout the lifespan. *Neuroimage* 208.
<https://pubmed.ncbi.nlm.nih.gov/31821869/>.

Popov T, Tröndle M, Baranczuk-Turska Z, Pfeiffer C, Haufe S, Langer N, Tzvetan Popov C (2023): Test-retest reliability of resting-state EEG in young and older adults. *Psychophysiology* 60:e14268. <https://onlinelibrary.wiley.com/doi/full/10.1111/psyp.14268>.

Porsteinsson AP, Isaacson RS, Knox S, Sabbagh MN, Rubino I (2021): Diagnosis of Early Alzheimer's Disease: Clinical Practice in 2021. *The Journal of Prevention of Alzheimer's Disease* 2021 8:3 8:371–386. <https://link.springer.com/article/10.14283/jpad.2021.23>.

Postuma RB, Berg D, Stern M, Poewe W, Olanow CW, Oertel W, Obeso J, Marek K, Litvan I, Lang AE, Halliday G, Goetz CG, Gasser T, Dubois B, Chan P, Bloem BR, Adler CH, Deuschl G (2015): MDS

clinical diagnostic criteria for Parkinson's disease. *Movement Disorders*. John Wiley and Sons Inc. <http://doi.wiley.com/10.1002/mds.26424>.

Prado P, Birba A, Cruzat J, Santamaría-García H, Parra M, Moguilner S, Tagliazucchi E, Ibáñez A (2022): Dementia ConnEEGtome: Towards multicentric harmonization of EEG connectivity in neurodegeneration. *International Journal of Psychophysiology* 172:24–38.

Prado P, Moguilner S, Mejía JA, Sainz-Ballesteros A, Otero M, Birba A, Santamaría-García H, Legaz A, Fittipaldi S, Cruzat J, Tagliazucchi E, Parra M, Herzog R, Ibáñez A (2023): Source space connectomics of neurodegeneration: One-metric approach does not fit all. *Neurobiol Dis* 179:106047.

Przedborski S, Vila M, Jackson-Lewis V (2003): Series Introduction: Neurodegeneration: What is it and where are we? *Journal of Clinical Investigation* 111:3–10. [/pmc/articles/PMC151843/](https://www.ncbi.nlm.nih.gov/pmc/articles/PMC151843/).

Puri D V., Nalbalwar SL, Nandgaonkar AB, Gawande JP, Wagh A (2023): Automatic detection of Alzheimer's disease from EEG signals using low-complexity orthogonal wavelet filter banks. *Biomed Signal Process Control* 81:104439.

Querfurth HW, LaFerla FM (2010): Alzheimer's Disease. *New England Journal of Medicine* 362:329–344. <http://www.nejm.org/doi/abs/10.1056/NEJMra0909142>.

Railo H (2021): Parkinson's disease: Resting state EEG. OSF. <https://osf.io/pehj9/>.

Railo H, Suuronen I, Kaasinen V, Murtojärvi M, Pahikkala T, Airola A (2020): Resting state EEG as a biomarker of Parkinson's disease: Influence of measurement conditions. [bioRxiv:2020.05.08.084343](https://www.ncbi.nlm.nih.gov/pmc/articles/PMC7207000/). [http://biorxiv.org/content/early/2020/05/10/2020.05.08.084343.abstract](https://www.ncbi.nlm.nih.gov/pmc/articles/PMC7207000/).

Raj R, Kannath SK, Mathew J, Sylaja PN (2023a): AutoML accurately predicts endovascular mechanical thrombectomy in acute large vessel ischemic stroke. *Front Neurol* 14. <https://pubmed.ncbi.nlm.nih.gov/37840939/>.

Raj R, Kannath SK, Mathew J, Sylaja PN (2023b): AutoML accurately predicts endovascular mechanical thrombectomy in acute large vessel ischemic stroke. *Front Neurol* 14. [/pmc/articles/PMC10569475/](https://www.ncbi.nlm.nih.gov/pmc/articles/PMC10569475/).

Ranasinghe KG, Cha J, Iaccarino L, Hinkley LB, Beagle AJ, Pham J, Jagust WJ, Miller BL, Rankin KP, Rabinovici GD, Vossel KA, Nagarajan SS (2020): Neurophysiological signatures in Alzheimer's disease are distinctly associated with TAU, amyloid-β accumulation, and cognitive decline. *Sci Transl Med* 12:4069. <https://www.science.org/doi/10.1126/scitranslmed.aaz4069>.

Ranasinghe KG, Verma P, Cai C, Xie X, Kudo K, Gao X, Lerner H, Mizuiri D, Strom A, Iaccarino L, Joie R La, Miller BL, Gorno-Tempini ML, Rankin KP, Jagust WJ, Vossel K, Rabinovici GD, Raj A, Nagarajan SS (2022): Altered excitatory and inhibitory neuronal subpopulation parameters are distinctly associated with tau and amyloid in Alzheimer's disease. *Elife* 11.

Rasmussen KL, Tybjarg-Hansen A, Nordestgaard BG, Frikke-Schmidt R (2018): Absolute 10-year risk of dementia by age, sex and APOE genotype: A population-based cohort study. *CMAJ* 190:E1033–E1041. [/pmc/articles/PMC6148649/](https://www.ncbi.nlm.nih.gov/pmc/articles/PMC6148649/).

Rea RC, Berlot R, Martin SL, Craig CE, Holmes PS, Wright DJ, Bon J, Pirtošek Z, Ray NJ (2021): Quantitative EEG and cholinergic basal forebrain atrophy in Parkinson's disease and mild cognitive impairment. *Neurobiol Aging* 106:37–44.

- Reisberg B (2006): Diagnostic criteria in dementia: A comparison of current criteria, research challenges, and implications for DSM-V. *Journal of Geriatric Psychiatry and Neurology*. <http://www.ncbi.nlm.nih.gov/pubmed/16880355>.
- Reynolds EH (2004): Todd, Faraday, and the electrical basis of brain activity. *Lancet Neurology* 3:557–563. <https://pubmed.ncbi.nlm.nih.gov/15324724/>.
- Robbins KA, Touryan J, Mullen T, Kothe C, Bigdely-Shamlo N (2020): How Sensitive Are EEG Results to Preprocessing Methods: A Benchmarking Study. *IEEE Trans Neural Syst Rehabil Eng* 28:1081–1090. <https://pubmed.ncbi.nlm.nih.gov/32217478/>.
- Rockhill AP, Jackson N, George J, Aron A, Swann NC (2021): UC San Diego Resting State EEG Data from Patients with Parkinson’s Disease. <https://openneuro.org/datasets/ds002778/versions/1.0.5>.
- Rodrigues PLC, Jutten C, Congedo M (2019): Riemannian Procrustes Analysis: Transfer Learning for Brain-Computer Interfaces. *IEEE Trans Biomed Eng* 66:2390–2401.
- Rommel C, Paillard J, Moreau T, Gramfort A (2022): Data augmentation for learning predictive models on EEG: a systematic comparison. *J Neural Eng* 19:066020. <https://iopscience.iop.org/article/10.1088/1741-2552/aca220>.
- Rosenblum Y, Shiner T, Bregman N, Giladi N, Maidan I, Fahoum F, Mirelman A (2023): Decreased aperiodic neural activity in Parkinson’s disease and dementia with Lewy bodies. *J Neurol* 270:3958–3969. <https://link.springer.com/article/10.1007/s00415-023-11728-9>.
- Rujeedawa T, Félez EC, Clare ICH, Fortea J, Strydom A, Rebillat AS, Coppus A, Levin J, Zaman SH (2021): The Clinical and Neuropathological Features of Sporadic (Late-Onset) and Genetic Forms of Alzheimer’s Disease. *J Clin Med* 10:4582. [/pmc/articles/PMC8509365/](https://pmc/articles/PMC8509365/).
- Ryan FJ, Ma Y, Ashander LM, Kvopka M, Appukuttan B, Lynn DJ, Smith JR (2022): Transcriptomic Responses of Human Retinal Vascular Endothelial Cells to Inflammatory Cytokines. *Transl Vis Sci Technol* 11. <https://pubmed.ncbi.nlm.nih.gov/36018584/>.
- Rygvold TW, Hatlestad-Hall C, Elvsåshagen T, Moberget T, Andersson S (2021): Do visual and auditory stimulus-specific response modulation reflect different mechanisms of neocortical plasticity? *European Journal of Neuroscience* 53:1072–1085. <https://onlinelibrary.wiley.com/doi/full/10.1111/ejn.14964>.
- Sabbagh D, Cartailler J, Touchard C, Joachim J, Mebazaa A, Vallée F, Gayat É, Gramfort A, Engemann DA (2023a): Repurposing electroencephalogram monitoring of general anaesthesia for building biomarkers of brain ageing: an exploratory study. *BJA open* 7:100145. <https://pubmed.ncbi.nlm.nih.gov/37638087/>.
- Sabbagh MN, Taylor A, Galasko D, Galvin JE, Goldman JG, Leverenz JB, Poston KL, Boeve BF, Irwin DJ, Quinn JF (2023b): Listening session with the US Food and Drug Administration, Lewy Body Dementia Association, and an expert panel. *Alzh & Dem: Trans Res & Clin Intervent* 9. [/pmc/articles/PMC9983146/](https://pmc/articles/PMC9983146/).
- Sachdev PS, Blacker D, Blazer DG, Ganguli M, Jeste D V., Paulsen JS, Petersen RC (2014): Classifying neurocognitive disorders: the DSM-5 approach. *Nat Rev Neurol* 10:634–642. <https://pubmed.ncbi.nlm.nih.gov/25266297/>.

Sakata N, Okumura Y (2017): Job Loss After Diagnosis of Early-Onset Dementia: A Matched Cohort Study. *Journal of Alzheimer's Disease* 60:1231. [/pmc/articles/PMC5676857/](https://www.ncbi.nlm.nih.gov/pmc/articles/PMC5676857/).

Santoro A, Martucci M, Conte M, Capri M, Franceschi C, Salvioli S (2020): Inflammaging, hormesis and the rationale for anti-aging strategies. *Ageing Res Rev* 64:101142.

Schaworonkow N, Nikulin V V. (2022): Is sensor space analysis good enough? Spatial patterns as a tool for assessing spatial mixing of EEG/MEG rhythms. *Neuroimage* 253:119093.

Scheijbeler EP, de Haan W, Stam CJ, Twisk JWR, Gouw AA (2023): Longitudinal resting-state EEG in amyloid-positive patients along the Alzheimer's disease continuum: considerations for clinical trials. *Alzheimers Res Ther* 15:1–19.
<https://alzres.biomedcentral.com/articles/10.1186/s13195-023-01327-1>.

Schmidt F, Danböck SK, Trinka E, Demarchi G, Weisz N (2023): Age-related changes in “cortical” 1/f dynamics are linked to cardiac activity. *bioRxiv*:2022.11.07.515423.
<https://www.biorxiv.org/content/10.1101/2022.11.07.515423v2>.

Schmidt MT, Kanda PAM, Basile LFH, da Silva Lopes HF, Baratho R, Demario JLC, Jorge MS, Nardi AE, Machado S, Ianof JN, Nitrini R, Anghinah R (2013): Index of alpha/theta ratio of the electroencephalogram: A new marker for Alzheimer's disease. *Front Aging Neurosci* 5:60.
<http://www.ncbi.nlm.nih.gov/pubmed/24130529>.

Schultz AP, Chhatwal JP, Hedden T, Mormino EC, Hanseeuw BJ, Sepulcre J, Huijbers W, LaPoint M, Buckley RF, Johnson KA, Sperling RA (2017): Phases of Hyperconnectivity and Hypoconnectivity in the Default Mode and Salience Networks Track with Amyloid and Tau in Clinically Normal Individuals. *The Journal of Neuroscience* 37:4323. [/pmc/articles/PMC5413178/](https://www.ncbi.nlm.nih.gov/pmc/articles/PMC5413178/).

Schumacher J, Taylor JP, Hamilton CA, Firbank M, Cromarty RA, Donaghy PC, Roberts G, Allan L, Lloyd J, Durcan R, Barnett N, O'Brien JT, Thomas AJ (2020a): Quantitative EEG as a biomarker in mild cognitive impairment with Lewy bodies. *Alzheimers Res Ther* 12.
<https://pubmed.ncbi.nlm.nih.gov/32641111/>.

Schumacher J, Thomas AJ, Peraza LR, Firbank M, Cromarty R, Hamilton CA, Donaghy PC, O'Brien JT, Taylor JP (2020b): EEG alpha reactivity and cholinergic system integrity in Lewy body dementia and Alzheimer's disease. *Alzheimers Res Ther* 12. [/pmc/articles/PMC7178985/](https://www.ncbi.nlm.nih.gov/pmc/articles/PMC7178985/).

Seeck M, Koessler L, Bast T, Leijten F, Michel C, Baumgartner C, He B, Beniczky S (2017): The standardized EEG electrode array of the IFCN. *Clin Neurophysiol* 128:2070–2077.
<https://pubmed.ncbi.nlm.nih.gov/28778476/>.

Shiri I, Amini M, Nazari M, Hajianfar G, Haddadi Avval A, Abdollahi H, Oveisí M, Arabi H, Rahmim A, Zaidi H (2022): Impact of feature harmonization on radiogenomics analysis: Prediction of EGFR and KRAS mutations from non-small cell lung cancer PET/CT images. *Comput Biol Med* 142.
<https://pubmed.ncbi.nlm.nih.gov/35051856/>.

Simuni T, Chahine LM, Poston K, Brumm M, Buracchio T, Campbell M, Chowdhury S, Coffey C, Concha-Marambio L, Dam T, DiBiaso P, Foroud T, Frasier M, Gochanour C, Jennings D, Kieburtz K, Kopil CM, Merchant K, Mollenhauer B, Montine T, Nudelman K, Pagano G, Seibyl J, Sherer T, Singleton A, Stephenson D, Stern M, Soto C, Tanner CM, Tolosa E, Weintraub D, Xiao Y, Siderowf A, Dunn B, Marek K (2024): A biological definition of neuronal α -synuclein disease: towards an integrated staging system for research. *Lancet Neurol* 23:178–190.
<http://www.thelancet.com/article/S1474442223004052/fulltext>.

- Singh A, Cole RC, Espinoza AI, Brown D, Cavanagh JF, Narayanan NS (2020): Frontal theta and beta oscillations during lower-limb movement in Parkinson's disease. *Clinical Neurophysiology* 131:694–702. [/pmc/articles/PMC8112379/](https://www.ncbi.nlm.nih.gov/pmc/articles/PMC8112379/).
- Sitt JD, King JR, El Karoui I, Rohaut B, Faugeras F, Gramfort A, Cohen L, Sigman M, Dehaene S, Naccache L (2014): Large scale screening of neural signatures of consciousness in patients in a vegetative or minimally conscious state. *Brain* 137:2258–2270. <https://pubmed.ncbi.nlm.nih.gov/24919971/>.
- Skouras S, Falcon C, Tucholka A, Rami L, Sanchez-Valle R, Lladó A, Gispert JD, Molinuevo JL (2019): Mechanisms of functional compensation, delineated by eigenvector centrality mapping, across the pathophysiological continuum of Alzheimer's disease. *Neuroimage Clin* 22:101777. [/pmc/articles/PMC6434094/](https://www.ncbi.nlm.nih.gov/pmc/articles/PMC6434094/).
- Sleimen-Malkoun R, Perdikis D, Müller V, Blanc JL, Huys R, Temprado JJ, Jirsa VK (2015): Brain Dynamics of Aging: Multiscale Variability of EEG Signals at Rest and during an Auditory Oddball Task. *eNeuro* 2. <https://www.eneuro.org/content/2/3/ENEURO.0067-14.2015>.
- Smailovic U, Jelic V (2019): Neurophysiological Markers of Alzheimer's Disease: Quantitative EEG Approach. *Neurology and Therapy*. Adis. <http://www.ncbi.nlm.nih.gov/pubmed/31833023>.
- Smailovic U, Koenig T, Kåreholt I, Andersson T, Kramberger MG, Winblad B, Jelic V (2018): Quantitative EEG power and synchronization correlate with Alzheimer's disease CSF biomarkers. *Neurobiol Aging* 63:88–95.
- Smits FM, Porcaro C, Cottone C, Cancelli A, Rossini PM, Tecchio F (2016): Electroencephalographic Fractal Dimension in Healthy Ageing and Alzheimer's Disease. *PLoS One* 11:e0149587. <https://journals.plos.org/plosone/article?id=10.1371/journal.pone.0149587>.
- Sperling RA, Aisen PS, Beckett LA, Bennett DA, Craft S, Fagan AM, Iwatsubo T, Jack CR, Kaye J, Montine TJ, Park DC, Reiman EM, Rowe CC, Siemers E, Stern Y, Yaffe K, Carrillo MC, Thies B, Morrison-Bogorad M, Wagster M V., Phelps CH (2011): Toward defining the preclinical stages of Alzheimer's disease: recommendations from the National Institute on Aging-Alzheimer's Association workgroups on diagnostic guidelines for Alzheimer's disease. *Alzheimers Dement* 7:280–292. <https://pubmed.ncbi.nlm.nih.gov/21514248/>.
- Srinivasan R, Nunez PL (2012): Electroencephalography. *Encyclopedia of Human Behavior*: Second Edition:15–23.
- Stelzmann RA, Norman Schnitzlein H, Reed Murtagh F (1995): An english translation of alzheimer's 1907 paper, "über eine eigenartige erkankung der hirnrinde." *Clinical Anatomy* 8:429–431. <https://onlinelibrary.wiley.com/doi/full/10.1002/ca.980080612>.
- Stoddart WHBAB (1913): Presbyophrenia (Alzheimer's Disease). *Proc R Soc Med* 6:13. <https://www.ncbi.nlm.nih.gov/pmc/articles/PMC2005437/>.
- Stylianou M, Murphy N, Peraza LR, Graziadio S, Cromarty R, Killen A, O' Brien JT, Thomas AJ, LeBeau FEN, Taylor JP (2018): Quantitative electroencephalography as a marker of cognitive fluctuations in dementia with Lewy bodies and an aid to differential diagnosis. *Clinical Neurophysiology* 129:1209–1220.
- Suarez-Revelo J, Ochoa-Gomez J, Duque-Grajales J (2016): Improving test-retest reliability of quantitative electroencephalography using different preprocessing approaches. *38th Annual*

International Conference of the IEEE Engineering in Medicine and Biology Society (EMBC):961–964.

Suárez-Revelo JX, Ochoa-Gómez JF, Duque-Grajales JE, Tobón-Quintero CA (2016): Biomarkers identification in Alzheimer's disease using effective connectivity analysis from electroencephalography recordings. *Ingenieria e Investigacion* 36:50–57.
<http://www.revistas.unal.edu.co/index.php/ingeinv/article/view/54037>.

Suárez-Revelo JX, Ochoa-Gómez JF, Tobón-Quintero CA (2018): Validation of EEG Pre-processing Pipeline by Test-Retest Reliability. In: . Communications in Computer and Information Science. Springer Verlag. Vol. 916, pp 290–299. https://doi.org/10.1007/978-3-030-00353-1_26.

Sun J, Wang B, Niu Y, Tan Y, Fan C, Zhang N, Xue J, Wei J, Xiang J (2020): Complexity Analysis of EEG, MEG, and fMRI in Mild Cognitive Impairment and Alzheimer's Disease: A Review. *Entropy* 2020, Vol 22, Page 239 22:239. <https://www.mdpi.com/1099-4300/22/2/239/htm>.

Sun Y, Islam S, Gao Y, Nakamura T, Zou K, Michikawa M (2023): Apolipoprotein E4 inhibits γ -secretase activity via binding to the γ -secretase complex. *J Neurochem* 164:858–874.
<https://onlinelibrary.wiley.com/doi/full/10.1111/jnc.15750>.

Swardfager W, Lanctt K, Rothenburg L, Wong A, Cappell J, Herrmann N (2010): A meta-analysis of cytokines in Alzheimer's disease. *Biol Psychiatry* 68:930–941.
<https://pubmed.ncbi.nlm.nih.gov/20692646/>.

Tampu IE, Eklund A, Haj-Hosseini N (2022): Inflation of test accuracy due to data leakage in deep learning-based classification of OCT images. *Scientific Data* 2022 9:1 9:1–8.
<https://www.nature.com/articles/s41597-022-01618-6>.

Tăutăan AM, Casula EP, Pellicciari MC, Borghi I, Maiella M, Bonni S, Minei M, Assogna M, Palmisano A, Smeralda C, Romanella SM, Ionescu B, Koch G, Santaracchi E (2023): TMS-EEG perturbation biomarkers for Alzheimer's disease patients classification. *Scientific Reports* 2023 13:1 13:1–13. <https://www.nature.com/articles/s41598-022-22978-4>.

Thal DR, Rüb U, Orantes M, Braak H (2002): Phases of A beta-deposition in the human brain and its relevance for the development of AD. *Neurology* 58:1791–1800.
<https://pubmed.ncbi.nlm.nih.gov/12084879/>.

Thölke P, Mantilla-Ramos YJ, Abdelhedi H, Maschke C, Dehgan A, Harel Y, Kemtur A, Mekki Berrada L, Sahraoui M, Young T, Bellemare Pépin A, El Khantour C, Landry M, Pasquarella A, Hadid V, Combrisson E, O'Byrne J, Jerbi K (2023): Class imbalance should not throw you off balance: Choosing the right classifiers and performance metrics for brain decoding with imbalanced data. *Neuroimage* 277. <https://pubmed.ncbi.nlm.nih.gov/37385392/>.

Toledo JB, Gopal P, Raible K, Irwin DJ, Brettschneider J, Sedor S, Waits K, Boluda S, Grossman M, Van Deerlin VM, Lee EB, Arnold SE, Duda JE, Hurtig H, Lee VMY, Adler CH, Beach TG, Trojanowski JQ (2016): Pathological α -synuclein distribution in subjects with coincident Alzheimer's and Lewy body pathology. *Acta Neuropathol* 131:393–409.
<https://link.springer.com/article/10.1007/s00401-015-1526-9>.

Tönnies E, Trushina E (2017): Oxidative Stress, Synaptic Dysfunction, and Alzheimer's Disease. *Journal of Alzheimer's Disease* 57:1105. [/pmc/articles/PMC5409043/](https://pmc/articles/PMC5409043/).

Tröndle M, Popov T, Dziedzic S, Langer N (2022): Decomposing the role of alpha oscillations during brain maturation. *Elife* 11.

Turner RS, Stubbs T, Davies DA, Albensi BC (2020): Potential New Approaches for Diagnosis of Alzheimer's Disease and Related Dementias. *Front Neurol* 11:496.
[/pmc/articles/PMC7290039/](https://PMC7290039/).

Tyebji S, Hannan AJ (2017): Synaptopathic mechanisms of neurodegeneration and dementia: Insights from Huntington's disease. *Prog Neurobiol* 153:18–45.

Tzimourta KD, Christou V, Tzallas AT, Giannakeas N, Astrakas LG, Angelidis P, Tsalikakis D, Tsipouras MG (2021): Machine Learning Algorithms and Statistical Approaches for Alzheimer's Disease Analysis Based on Resting-State EEG Recordings: A Systematic Review.
<https://doi.org/101142/S0129065721300023> 31.

Vallat R (2022): AntroPy: entropy and complexity of (EEG) time-series in Python.
<https://github.com/raphaelvallat/antropy>.

Vallat R, Walker MP (2021): An open-source, high-performance tool for automated sleep staging. *Elife* 10.

Vandenbroucke JP, Von Elm E, Altman DG, Gøtzsche PC, Mulrow CD, Pocock SJ, Poole C, Schlesselman JJ, Egger M (2007): Strengthening the Reporting of Observational Studies in Epidemiology (STROBE): Explanation and elaboration. *PLoS Med* 4:1628–1654.
[/pmc/articles/PMC2020496/?report=abstract](https://PMC2020496/?report=abstract).

Vanneste S, Song JJ, De Ridder D (2018): Thalamocortical dysrhythmia detected by machine learning. *Nature Communications* 2018 9:1 9:1–13. <https://www.nature.com/articles/s41467-018-02820-0>.

Vermeiren Y, Hirschberg Y, Mertens I, De Deyn PP (2020): Biofluid Markers for Prodromal Parkinson's Disease: Evidence From a Catecholaminergic Perspective. *Front Neurol* 11:521285.

Vik-Mo AO, Gil LM, Ballard C, Aarsland D (2018): Course of neuropsychiatric symptoms in dementia: 5-year longitudinal study. *Int J Geriatr Psychiatry* 33:1361–1369.
<https://pubmed.ncbi.nlm.nih.gov/29979473/>.

Vogel JW, Young AL, Oxtoby NP, Smith R, Ossenkoppele R, Strandberg OT, La Joie R, Aksman LM, Grothe MJ, Iturria-Medina Y, Weiner M, Aisen P, Petersen R, Jack CR, Jagust W, Trojanowski JQ, Toga AW, Beckett L, Green RC, Saykin AJ, Morris JC, Shaw LM, Liu E, Montine T, Thomas RG, Donohue M, Walter S, Gessert D, Sather T, Jiminez G, Harvey D, Bernstein M, Fox N, Thompson P, Schuff N, DeCarli C, Borowski B, Gunter J, Senjem M, Vemuri P, Jones D, Kantarci K, Ward C, Koeppe RA, Foster N, Reiman EM, Chen K, Mathis C, Landau S, Cairns NJ, Householder E, Reinwald LT, Lee V, Korecka M, Figurski M, Crawford K, Neu S, Foroud TM, Potkin S, Shen L, Kelley F, Kim S, Nho K, Kachaturian Z, Frank R, Snyder PJ, Molchan S, Kaye J, Quinn J, Lind B, Carter R, Dolen S, Schneider LS, Pawluczyk S, Beccera M, Teodoro L, Spann BM, Brewer J, Vanderswag H, Fleisher A, Heidebrink JL, Lord JL, Mason SS, Albers CS, Knopman D, Johnson K, Doody RS, Meyer JV, Chowdhury M, Rountree S, Dang M, Stern Y, Honig LS, Bell KL, Ances B, Carroll M, Leon S, Mintun MA, Schneider S, Oliver A, Griffith R, Clark D, Geldmacher D, Brockington J, Roberson E, Grossman H, Mitsis E, deToledo-Morrell L, Shah RC, Duara R, Varon D, Greig MT, Roberts P, Albert M, Onyike C, D'Agostino D, Kielb S, Galvin JE, Pogorelec DM, Cerbone B, Michel CA, Rusinek H, de Leon MJ, Glodzik L, De Santi S, Doraiswamy PM, Petrella

JR, Wong TZ, Arnold SE, Karlawish JH, Wolk D, Smith CD, Jicha G, Hardy P, Sinha P, Oates E, Conrad G, Lopez OL, Oakley MA, Simpson DM, Porsteinsson AP, Goldstein BS, Martin K, Makino KM, Ismail MS, Brand C, Mulnard RA, Thai G, McAdams Ortiz C, Womack K, Mathews D, Quiceno M, Arrastia RD, King R, Weiner M, Cook KM, DeVos M, Levey AI, Lah JJ, Cellar JS, Burns JM, Anderson HS, Swerdlow RH, Apostolova L, Tingus K, Woo E, Silverman DHS, Lu PH, Bartzokis G, Radford NRG, Parfitt F, Kendall T, Johnson H, Farlow MR, Hake AM, Matthews BR, Herring S, Hunt C, van Dyck CH, Carson RE, MacAvoy MG, Chertkow H, Bergman H, Hosein C, Black S, Stefanovic B, Caldwell C, Hsiung GYR, Feldman H, Mudge B, Past MA, Kertesz A, Rogers J, Trost D, Bernick C, Munic D, Kerwin D, Mesulam MM, Lipowski K, Wu CK, Johnson N, Sadowsky C, Martinez W, Villena T, Turner RS, Johnson K, Reynolds B, Sperling RA, Johnson KA, Marshall G, Frey M, Yesavage J, Taylor JL, Lane B, Rosen A, Tinklenberg J, Sabbagh MN, Belden CM, Jacobson SA, Sirrel SA, Kowall N, Killiany R, Budson AE, Norbush A, Johnson PL, Obisesan TO, Wolday S, Allard J, Lerner A, Ogracki P, Hudson L, Fletcher E, Carmichael O, Olichney J, DeCarli C, Kittur S, Borrie M, Lee TY, Bartha R, Johnson S, Asthana S, Carlsson CM, Potkin SG, Preda A, Nguyen D, Tariot P, Reeder S, Bates V, Capote H, Rainka M, Scharre DW, Kataki M, Adeli A, Zimmerman EA, Celmins D, Brown AD, Pearson GD, Blank K, Anderson K, Santulli RB, Kitzmiller TJ, Schwartz ES, Sink KM, Williamson JD, Garg P, Watkins F, Ott BR, Querfurth H, Tremont G, Salloway S, Malloy P, Correia S, Rosen HJ, Miller BL, Mintzer J, Spicer K, Bachman D, Finger E, Pasternak S, Rachinsky I, Drost D, Pomara N, Hernando R, Sarrael A, Schultz SK, Ponto LLB, Shim H, Smith KE, Relkin N, Chaing G, Raudin L, Smith A, Fargher K, Raj BA, Pontecorvo MJ, Devous MD, Rabinovici GD, Alexander DC, Lyoo CH, Evans AC, Hansson O (2021): Four distinct trajectories of tau deposition identified in Alzheimer's disease. *Nat Med* 27:871. [/pmc/articles/PMC8686688/](https://pmc/articles/PMC8686688/).

Voß H, Schlumbohm S, Barwikowski P, Wurlitzer M, Dottermusch M, Neumann P, Schlueter H, Neumann JE, Krisp C (2022): HarmonizR enables data harmonization across independent proteomic datasets with appropriate handling of missing values. *Nat Commun* 13. <https://pubmed.ncbi.nlm.nih.gov/35725563/>.

Voytek B, Knight RT (2015): Dynamic Network Communication as a Unifying Neural Basis for Cognition, Development, Aging, and Disease. *Biol Psychiatry* 77:1089–1097.

Wan L, Huang H, Schwab N, Tanner J, Rajan A, Lam NB, Zaborszky L, Li C shan R, Price CC, Ding M (2019): From eyes-closed to eyes-open: Role of cholinergic projections in EC-to-EO alpha reactivity revealed by combining EEG and MRI. *Hum Brain Mapp* 40:566–577.

Wang Z, Liu A, Yu J, Wang P, Bi Y, Xue S, J Z, H G, W Z (2023): The effect of aperiodic components in distinguishing Alzheimer's disease from frontotemporal dementia. Research Square [preprint]. <https://europepmc.org/article/ppr/ppr660352>.

Waschke L, Donoghue T, Fiedler L, Smith S, Garrett DD, Voytek B, Obleser J (2021): Modality-specific tracking of attention and sensory statistics in the human electrophysiological spectral exponent. *Elife* 10.

Wen H, Liu Z (2016): Separating Fractal and Oscillatory Components in the Power Spectrum of Neurophysiological Signal. *Brain Topogr* 29:13. [/pmc/articles/PMC4706469/](https://pmc/articles/PMC4706469/).

Wilson DM, Cookson MR, Van Den Bosch L, Zetterberg H, Holtzman DM, Dewachter I (2023): Hallmarks of neurodegenerative diseases. *Cell* 186:693–714. <https://pubmed.ncbi.nlm.nih.gov/36803602/>.

- Xu H, Abdallah N, Marion JM, Chauvet P, Tauber C, Carlier T, Lu L, Hatt M (2023): Radiomics prognostic analysis of PET/CT images in a multicenter head and neck cancer cohort: investigating ComBat strategies, sub-volume characterization, and automatic segmentation. *Eur J Nucl Med Mol Imaging* 50. <https://pubmed.ncbi.nlm.nih.gov/36690882/>.
- Xu Y, Yang J, Shang H (2016): Meta-analysis of risk factors for Parkinson's disease dementia. *Transl Neurodegener* 5. [/pmc/articles/PMC4890279/](https://pmc/articles/PMC4890279/).
- Yao S, Zhu J, Li S, Zhang R, Zhao J, Yang X, Wang Y (2022): Bibliometric Analysis of Quantitative Electroencephalogram Research in Neuropsychiatric Disorders From 2000 to 2021. *Front Psychiatry* 13:830819. [/pmc/articles/PMC9167960/](https://pmc/articles/PMC9167960/).
- Yassine S, Gschwandtner U, Auffret M, Duprez J, Verin M, Fuhr P, Hassan M (2023): Identification of Parkinson's Disease Subtypes from Resting-State Electroencephalography. *Movement Disorders* 38:1451–1460. <https://onlinelibrary.wiley.com/doi/full/10.1002/mds.29451>.
- Ye Q, Chen H, Su F, Shu H, Gong L, Xie C, Zhou H, Bai F (2018): An Inverse U-Shaped Curve of Resting-State Networks in Individuals at High Risk of Alzheimer's Disease. *J Clin Psychiatry* 79. <https://pubmed.ncbi.nlm.nih.gov/29474008/>.
- Yener GG, Leuchter AF, Jenden D, Read SL, Cummings JL, Miller BL (1996): Quantitative EEG in frontotemporal dementia. *Clin Electroencephalogr* 27:61–68. <https://pubmed.ncbi.nlm.nih.gov/8681464/>.
- Yi GS, Wang J, Deng B, Wei X Le (2017): Complexity of resting-state EEG activity in the patients with early-stage Parkinson's disease. *Cogn Neurodyn* 11:147. [/pmc/articles/PMC5350085/](https://pmc/articles/PMC5350085/).
- Yi G, Wang L, Chu C, Liu C, Zhu X, Shen X, Li Z, Wang F, Yang M, Wang J (2022): Analysis of complexity and dynamic functional connectivity based on resting-state EEG in early Parkinson's disease patients with mild cognitive impairment. *Cogn Neurodyn* 16:309–323. <https://link.springer.com/article/10.1007/s11571-021-09722-w>.
- van der Zande JJ, Gouw AA, Steenoven I van, Scheltens P, Stam CJ, Lemstra AW (2018): EEG Characteristics of Dementia With Lewy Bodies, Alzheimer's Disease and Mixed Pathology. *Front Aging Neurosci* 10. [/pmc/articles/PMC6037893/](https://pmc/articles/PMC6037893/).
- Zapata-Saldarriaga L-M, Vargas-Serna A-D, Gil-Gutiérrez J, Mantilla-Ramos Y-J, Ochoa-Gómez J-F (2023): Evaluation of Strategies Based on Wavelet-ICA and ICLabel for Artifact Correction in EEG Recordings. *Revista Científica* 46:61–76.
- Zimmermann R, Gschwandtner U, Hatz F, Schindler C, Bousleiman H, Ahmed S, Hardmeier M, Meyer A, Calabrese P, Fuhr P (2015): Correlation of EEG slowing with cognitive domains in nondemented patients with Parkinson's disease. *Dement Geriatr Cogn Disord* 39:207–214. <https://pubmed.ncbi.nlm.nih.gov/25591733/>.

Paper III

Classifying Neurodegenerative Diseases from Resting-State EEG Signals Using Automated Machine Learning: A Multicenter Study

Alberto Jaramillo-Jimenez ^{1,2,3,4,5 *}, Diego A Tovar-Rios ^{1,2,6,7}, Yorguin-Jose Mantilla-Ramos ^{4,5}, John-Fredy Ochoa-Gomez ⁴, Ketil Oppedal ^{6,7}, Dag Aarsland ^{1,8}, Kolbjørn Brønnick ^{1,2}, and Laura Bonanni ⁹

1. Centre for Age-Related Medicine (SESAM), Stavanger University Hospital. Stavanger, Norway.
2. Faculty of Health Sciences, University of Stavanger. Stavanger, Norway.
3. Grupo de Neurociencias de Antioquia, Universidad de Antioquia. Medellín, Colombia.
4. Grupo Neuropsicología y Conducta, Universidad de Antioquia. Medellín, Colombia.
5. Semillero de Investigación NeuroCo, Universidad de Antioquia. Medellín, Colombia.
6. Stavanger Medical Imaging Laboratory, Department of Radiology, Stavanger University Hospital. Stavanger, Norway.
7. Department of Electrical Engineering and Computer Science, University of Stavanger. Stavanger, Norway.
8. Department of Psychological Medicine, Institute of Psychiatry, Psychology & Neuroscience, King's College London. London, UK.
9. Department of Medicine and Aging Sciences University Gd'Annunzio of Chieti-Pescara. Chieti, Italy.

Abstract

Background: Site-specific "batch" effects are reported when pooling multisite resting-state electroencephalography (rsEEG) datasets. The Combining Batches (ComBat) models can control for batch effects, preserving biological covariates' variability. Automatic machine learning (autoML) methods have demonstrated comparable performance to hand-crafted models but have not been tested on rsEEG-derived features for classifying neurodegenerative diseases (NDDs).

Objective: This study aims to evaluate the effect of ComBat harmonisation of multiple features extracted from the rsEEG over the performance of autoML models for multi-class classification of NDDs leading to dementia.

Methods: RsEEG signals ($n = 507$) from healthy controls (HC, $n = 219$), Alzheimer's Disease (AD, $n = 113$), Mild Cognitive Impairment in AD (MCI-AD, $n = 76$), Parkinson's Disease (PD, $n = 67$), and MCI in Lewy body diseases (MCI-LBD, $n = 32$) were automatically pre-processed. Multiple rsEEG features (spectral, complexity and connectivity) were extracted in sensor space. Features were harmonised across sites ($n = 10$) using the reComBat model. The AutoGluon autoML pipeline was used to run and fit multiple supervised models on the training set ($n = 354$). The best pre-trained models were evaluated in a hold-out test set ($n = 153$).

Results: Batch effects were mitigated with reComBat harmonisation. When evaluated in the unharmonised test set, the best model trained with unharmonised features achieved a balanced accuracy (Bacc) of 38 %. Besides, the best model trained with harmonised spectral + complexity features achieved a Bacc of 68.9 % in the test set (XGBoost with repeated k-fold bagging). Training on spectral features resulted in Bacc = 68.8%, and integrating all features reduced performance (Bacc = 66.9 %).

Conclusions: Harmonisation of rsEEG features improves the performance of AutoML in the multi-class classification of NDDs, especially in the AD continuum.

Keywords: Electroencephalography, Automated Machine Learning, Harmonisation, Neurodegenerative Diseases

1. Introduction

Resting-state Electroencephalogram (rsEEG) signals have been used to represent brain-related electrical correlates of development, ageing, and diseases (Babiloni et al., 2020a). In recent decades, the corpus of clinical research using rsEEG has significantly grown (Colom-Cadena et al., 2020b; Yao et al., 2022), and the open-science philosophy adopted by several researchers and institutions granted full accessibility to software and datasets (Niso et al., 2022). However, the sample size of numerous datasets is often small, limiting the statistical power, generalizability, and external validity of the findings of single-site studies (Newson and Thiagarajan, 2019). Pooling multisite rsEEG data into a larger dataset can introduce the effects of site-specific variability ("batch" effects) affecting the statistical inference by potentially introducing type I errors. Variability across centres could be attributed to headset/hardware differences, non-identical experimental setup, biological variability across site samples, and particular parameters for acquisition and processing (Bigdely-Shamlo et al., 2020; M. Li et al., 2022).

Among methods to mitigate batch effects, the combining batches (ComBat) method (Fortin et al., 2018; Voß et al., 2022), initially applied in genomics (Johnson et al., 2007), has shown good performance in a wide variety of radiomic datasets (Beer et al., 2020; Bell et al., 2022; Pomponio et al., 2020; Shiri et al., 2022; Voß et al., 2022; Xu et al., 2023), as well as transcriptomics [Ryan et al., 2022]. Conversely, there are scarce reports on the specific effects of statistical harmonisation of multisite rsEEG features with ComBat-derived methods in the currently available literature (Kurbatskaya et al., 2023b, 2023a; M. Li et al., 2022).

Besides, group-level analysis has contributed to discovering rsEEG patterns in subjects with certain conditions (like ageing) or diseases (such as neurodegenerative diseases - NDDs) (Bonanni et al., 2016; Donoghue et al., 2020b), and results from machine learning analysis have become promising in the rsEEG research field (Babiloni et al., 2020b; Tzimourta et al., 2021). However, building hand-crafted machine-learning models may require time and expert human resources, limiting the application of this technology for a broad range of clinical researchers with less developed coding skills [Conrad et al., 2022; Liu et al., 2023; Musigmann et al., 2022; Ou et al., 2021]. Conversely, automated machine-learning (autoML) frameworks have been developed to ease this barrier by providing code-free (or one-liner) implementations to train and test multiple model architectures simultaneously, boosting the exploration and discovery process from a data-driven perspective. Multiple openly available AutoML toolboxes also implement early stopping, regularisation, hyperparameter optimisation, and validation techniques, facilitating the fitting of more precise models developed and evaluated in a shorter time frame. AutoML pipelines have been tested in regression and classification tasks and across multiple data types, often producing models with good to excellent performance, even in small tabular datasets with less than 1000 samples (Conrad et al., 2022; Liu et al., 2023; Musigmann et al., 2022; Ou et al., 2021). Despite the recent interest of biomedical researchers in autoML and emergent evidence supporting that autoML approaches might outperform manually designed models, the potential use of autoML in neuroscientific research has been less extensively tested. As a case in point, there is limited evidence on indexed databases (PUBMED, ScienceDirect) about the utilisation of autoML in rsEEG-derived features for the classification of NDD, such as Alzheimer's Disease (AD) or Parkinson's Disease (PD).

With all the above, we aim to evaluate the effect of ComBat harmonisation of multiple features extracted from the rsEEG over the performance of autoML models for multi-class classification of NDDs leading to dementia. Thus, this openly available workflow for rsEEG multi-site harmonisation and automated multi-class classification is intended to be a practical tool for clinical researchers.

2. Methods

2.1 Study Design and Participants

This secondary analysis capitalises on ten primary cross-sectional datasets collected in eight countries (Colombia, Finland, France, Germany, Greece, Italy, Norway, and the USA). Most of these datasets were acquired to explore rsEEG differences between NDD patients and HC (Anjum et al., 2020; Bonanni et al., 2016; Jaramillo-Jimenez et al., 2021; Miltiadous et al., 2023; Railo et al., 2020; Rockhill et al., 2021), while two research centres (Oslo, and Leipzig) aimed to study the effects of healthy ageing over rsEEG (Babayan et al., 2019; Hatlestad-Hall et al., 2022a). Neurological or psychiatric conditions were considered an exclusion criterion in all primary studies. Samples on each primary study setting are listed below:

2.1.1. California dataset: Data was acquired in 2013. PD patients ($n = 15$) and cognitively normal healthy controls (HC, $n = 16$) were recruited at Scripps Clinic in La Jolla, California, USA. HC group was recruited from the community (or were the patients' spouses) (George et al., 2013; Jackson et al., 2019).

2.1.2. Finland dataset: Data was acquired in 2018. PD patients ($n = 19$) and cognitively normal HC ($n = 19$) were recruited at the Turku University Hospital, Turku, Finland. (Railo et al., 2020).

2.1.3. Iowa dataset: Data was acquired from 2017 to 2019. PD patients ($n = 14$) and cognitively normal HC ($n = 14$) were recruited at the University of Iowa, Narayanan Lab, Iowa, USA (Anjum et al., 2020; Singh et al., 2020). Two ($n = 2$) PD patients presented abnormal global cognitive performance and were labelled as Mild Cognitive Impairment (MCI) in PD.

2.1.4. Oslo dataset: Data was acquired in 2017. Cognitively normal young and old HC ($n = 111$) were recruited from the local community at the University of Oslo, Oslo, Norway (Hatlestad-Hall et al., 2022b; Rygvold et al., 2021).

2.1.5. LEMON dataset: Data was acquired between 2013 and 2015. HC participants ($n = 216$) were included in the "Leipzig Study for Mind-Body-Emotion Interactions" (LEMON) study. The original sample consisted of healthy young (20-35 years) and old adults (59-77 years) recruited at the Day Clinic for Cognitive Neurology of the University Clinic Leipzig and the Max Planck Institute for Human and Cognitive and Brain Sciences, Leipzig, Germany (Babayan et al., 2019). In order to limit potential confounders of age in our current analysis, only subjects with age greater or equal to 46 (i.e., minimum age value in NDDs groups) were included ($n = 69$).

2.1.6. Medellin dataset: The dataset was acquired in 2016 in Medellin, Colombia. PD subjects ($n = 36$) were recruited from the outpatient neurology service of the Group of Neurosciences of Antioquia and the Group of Neuropsychology and Behavior, School of Medicine – University of Antioquia. A subgroup of PD patients fulfilled the criteria for MCI-PD ($n = 14$). The HC group ($n = 36$) was recruited from local community volunteers and the patient's spouse [Jaramillo-Jimenez et al., 2021].

2.1.7. Genoa dataset: AD patients ($n = 80$) were recruited at the Clinical Neurology, Department of Neuroscience (DINOOGMI), University of Genoa, and IRCCS AOU San Martino-IST, Genoa, Italy, as part of the European – Dementia with Lewy Bodies Consortium [Bonanni et al., 2016].

2.1.8. Greece dataset: No information about the data collection timeframe. HC participants ($n = 28$) and AD patients ($n = 36$) were recruited at the 2nd Department of Neurology of AHEPA General Hospital of Thessaloniki, Arta, Greece. An extended description is provided elsewhere [Miltiadous et al., 2023].

2.1.9. France dataset: From 2005 to 2022, patients with MCI due to AD (MCI-AD, $n = 58$) and MCI with Lewy Bodies (MCI-LB, $n = 16$) were recruited at the Centre de Neurologie

Cognitive, Groupe Hospital Universitaire Assistance Publique Hôpitaux de Paris Nord Hôpital Lariboisière Fernand-Widal, Paris, France, as part of the European – Dementia with Lewy Bodies Consortium (Lantero-Rodriguez et al., 2023).

2.1.10. Stavanger dataset: Data was collected from 2021 to 2023 in HC participants ($n = 5$) and MCI-AD patients ($n = 18$) recruited at the Centre for Age-related Medicine (SESAM), Psychiatry division, Stavanger University Hospital - Stavanger, Norway, as part of the European – Dementia with Lewy Bodies Consortium.

The PD-MCI and MCI-LB subjects were combined in a single group (MCI-LBD, $n = 32$) to reduce class imbalance. Our decision was supported by preliminary methods combining Lewy body diseases (LBD) (Jellinger and Korczyn, 2018).

2.2. RsEEG recordings and Signal pre-processing:

RsEEG signals were acquired with monopolar montages. Headsets and amplifiers used for acquisition were the BioSemi ActiveTwo system (32 channels in the California dataset and 64 channels in the Oslo dataset), NeurOne Tesla (64 channels in the Finland dataset), Nihon Kohden EEG 2100 (in the Greece dataset), Brain Vision system (64 channels in the Iowa dataset), NeuroScan – Synamps II (58 channels in the Medellin dataset), BrainAmp MR plus (62 channels in the LEMON dataset), Somno-Medics SOMNO HD eco (19 channels in the Stavanger dataset). Unfortunately, the amplifier manufacturer for the Genoa (19 channels) and the France (19 channels) datasets were not previously reported. Sampling rates varied from 128 – 1024 Hz.

Rs-EEG signals from Iowa were recorded during the eyes open condition, while recordings from the remaining research sites were under eyes closed. An extended description of the acquisition parameters of these datasets can be found in the mentioned original publications.

Eighteen common channels across all recordings were considered for this analysis (i.e., Fp1, Fp2, F7, F8, F3, Fz, F4, C3, Cz, C4, T7, T8, P7, P8, P3, P4, O1, and O2). These channels were subsequently used to create three Regions of Interest (ROI) in anterior, central and posterior topographies. See **Figure 1A** for details on channels belonging to each ROI.

In order to automatise the pre-processing and feature extraction steps, all datasets were standardised following the Brain Image Data Structure (BIDS) specification (Pernet et al., 2019) using the sovaBIDS package (Mantilla-Ramos, 2023). For the pre-processing of all rs-EEG signals, we utilised a Python implementation of an already validated workflow previously published by our group (Isaza et al., 2023; Jaramillo-Jimenez et al., 2023; Suárez-Revelo et al., 2018). This fully automated pipeline wrapped multiple pre-processing tools. First, robust average re-referencing, adaptative line-noise correction, and bad channel interpolation were performed using the PyPREP library (Appelhoff et al., 2022), a Python reimplemention of the MATLAB PREP pipeline (Bigdely-Shamlo et al., 2015). PyPREP pipeline aims to estimate a robust average reference by excluding noisy channels, ensuring a comparable reference scheme across datasets. Following PyPREP, wavelet-enhanced Independent Component Analysis (ICA) was performed to smooth strong artefacts in the data (such as those originating from muscular or eye-blink components) (Castellanos and Makarov, 2006). Therefore, a 1Hz high-pass Finite Impulse Response (FIR) filter was applied to remove low-frequency drifts that would affect the following ICA stage. The MNE library's FastICA algorithm was subsequently employed to extract artifactual and brain components from the signal (Gramfort et al., 2013). These components were decomposed into wavelets, and artefacts were smoothed through wavelet thresholding, preserving "brain" activity annotated with automated ICA labelling (MNE-ICA label) (A. Li et al., 2022). From the rsEEG recordings, epochs of 5 seconds were obtained. Finally, artifactual epochs were automatically rejected based on signal parameters, including

extreme amplitude and spectral power values, as well as statistical features such as linear trends, joint probability, and kurtosis. A detailed description of the pre-processing flow and its test-retest reliability can be found elsewhere (Isaza et al., 2023).

The number of clean epochs in each dataset varied depending on each centre's protocols. We analysed 20 consecutive artefact-free epochs (100 seconds of signal) to retain as many subjects as possible. The mean number of clean epochs was as follows: California (Mean = 32.7; Standard Deviation – SD = 3.2), Finland (Mean = 25.3; SD = 1.9), France (Mean = 162.6; SD = 63.7), Genoa (Mean = 192.5; SD = 44.6), Greece (Mean = 129.1; SD = 21.1), Iowa (Mean = 32.7; SD = 11), LEMON (Mean = 181; SD = 9.7), Medellin (Mean = 58.7; SD = 9.7), Oslo (Mean = 39.5; SD = 1.7), Stavanger (Mean = 49.3; SD = 7.9). See **Figure 1B** for details.

2.3. Feature extraction

The pre-processed signals were downsampled to a uniform sampling rate of 128 Hz and low-pass filtered at 30 Hz for feature extraction.

2.3.1. Spectral band powers, frequency prevalence, and oscillatory/aperiodic parameterisation

For each of the 5-second epochs included in the analysis, Power Spectral Density (PSD) vectors were computed at the sensor level using the `psd_array_multitaper` function implemented in MNE, with default parameters (Gramfort et al., 2013). Next, the channel-wise median of the PSD vectors was computed across all available epochs. Aperiodic (1/f) uncorrected band powers were computed in the following frequency bands: delta (1 – 4 Hz), slow theta (4 – 5.5 Hz), fast theta or "pre-alpha" (5.5 – 8 Hz), (alpha (8 – 13 Hz), and beta (13 – 30 Hz) as supported by early findings in NDDs (Babiloni et al., 2020a; Bonanni et al., 2008; Jaramillo-Jimenez et al., 2023). Thus, 1/f uncorrected relative band powers (expressed as 0 – 1 values) were computed for each of the above frequency bands through the `bandpower` function from the Yet Another Spindle Algorithm (YASA) library. This function computes the relative power of a given frequency band (i.e. estimated band power/total power within the 1 - 30 Hz bandwidth) by approximating its area under the PSD curve using the composite Simpson's rule (i.e. decomposing the band-indexed area with several parabolas and then sum the area of these parabolas) (Vallat and Walker, 2021).

We computed the dominant frequency (DF), dominant frequency variability (DFV), and frequency prevalence (FP) features to assess epoch-to-epoch variability in line with preliminary published approaches (Bonanni et al., 2016, 2015, 2008; Schumacher et al., 2020a) Thus, the maximum peak within the extended alpha band (5 – 14 Hz) was identified for each epoch, and the mean value across the 20 epochs was computed, representing the DF. At the same time, the standard deviation of the DF across epochs corresponded to the DFV. The values of FP (from 0 – 1) estimated the percentage of epochs where the maximum peak lies in a particular frequency band.

Given the potential confounder effect of aperiodic activity (1/f) in the PSD vectors, spectral parameterisation was conducted using the Fitting Oscillations and One Over-Frequency algorithm (FOOOF) (Donoghue et al., 2020b). FOOOF models aperiodic (1/f) and oscillatory activity in the PSD vectors, providing the following descriptors: Oscillatory parameters (Power – PW, Bandwidth – BW, Center Frequency – CF), Aperiodic parameters (Exponent, Offset), and Fitting parameters (error, and R-squared). FOOOF Oscillatory band powers were computed for target frequency bands where peaks are expected, namely, the extended alpha (5 – 14 Hz) representing the individual alpha peak frequency [Moretti et al., 2013] and the beta band (13 – 30 Hz).

The current analysis only used spectral parameters from channels with a good fitting, defined here as a FOOOF fitting R-squared equal to or greater than 0.8 for further analyses (90.62 % of all channel fittings were included). A complete description of FOOOF fitting estimations is presented in **Figures 1C and 1D**.

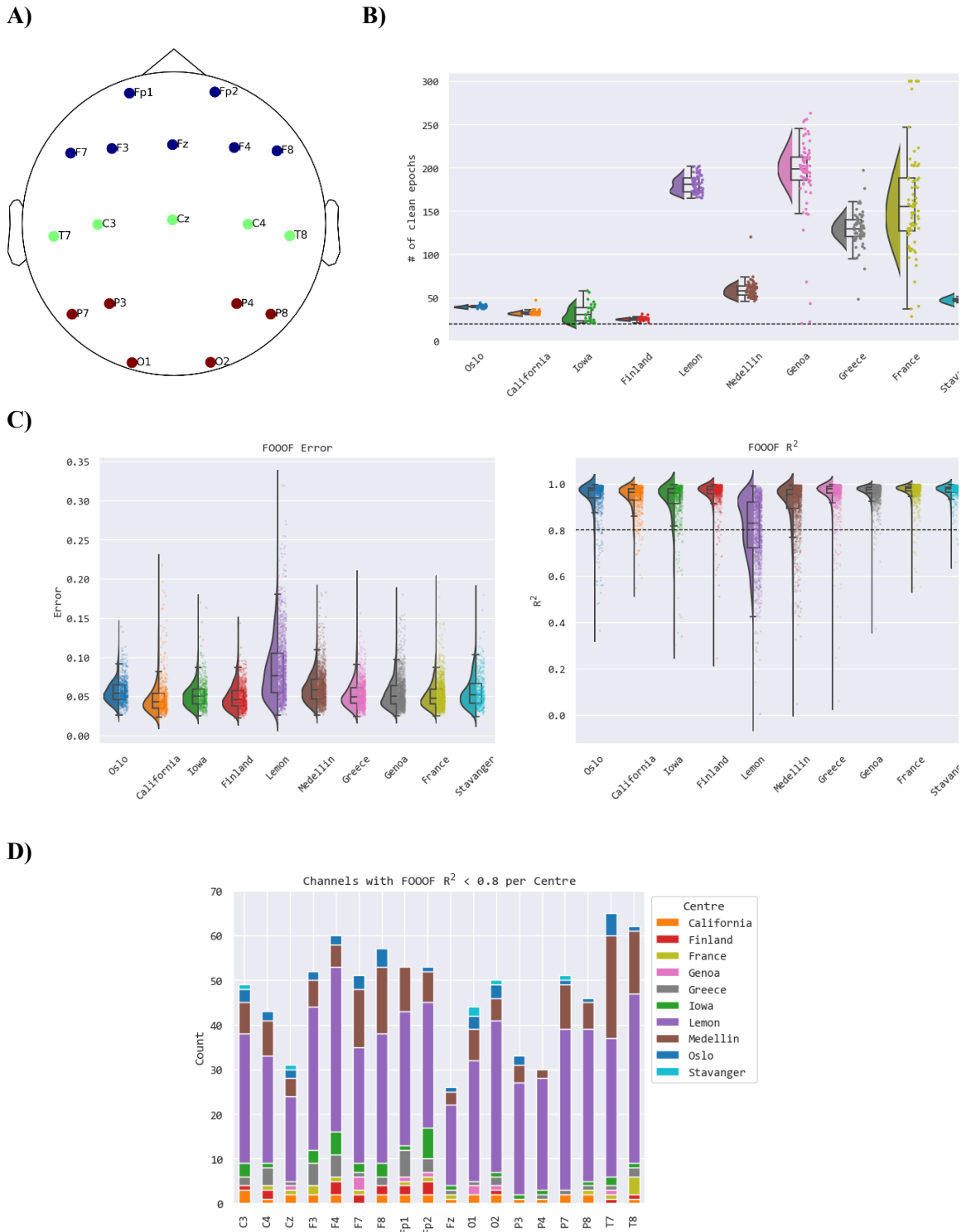


Figure 1. Description of rsEEG data and spectral parameterisation fittings across centres. **A)** Shows the topography of common sensors across datasets (in the international 10-05 system positions) selected for analysis. Three Regions of Interest (ROI) were created, namely Anterior (Blue), Central (Green), and Posterior (Dark red). **B)** Raincloud plots with the number of artefact-free rsEEG epochs for each participant after pre-processing. Each raincloud plot represents data from a single centre (colour-coded). The horizontal dashed line represents the chosen cutoff at 20 epochs (100 seconds of signal). **C)** Raincloud plots with each research centre's error and R-squared FOOOF fitting parameters. Each dot represents the corresponding value per channel and participant (colour-coded by centre). The horizontal dashed line represents the chosen cutoff at R-squared < 0.8 for a "good" fitting. **D)** Absolute counts of bad fitting (R-squared < 0.8) for spectral parameterisation per channel (bars) and centre (colours).

Despite the potential advantages of FOOOF parameters over uncorrected band powers, we noticed that oscillatory parameters might produce missing values if the band power is equal to 0

(as the area under the curve cannot be computed) or where the centre frequency (peak frequency) is not within a given frequency band. Thus, from the oscillatory parameters in the beta and extended alpha bands (# of spectral parameters = 54756; 3 parameters per band PW, BW, and CF * 18 channels * 507 subjects), 4425 (8.08%) were estimated as missing values. The channel-wise percentage of missing values across oscillatory features was more pronounced in the beta band due to lack of peak (missing = 10.02%) than in the extended alpha band (missing = 6.15%). These missing values were addressed for all subjects by averaging the feature values across channels in the anterior, central, and posterior ROI.

2.3.2. Complexity features

Regularity features included entropy-derived metrics and Hjorth parameters. Besides, the predictability of the signal was assessed via fractal estimators (FD) or detrended fluctuations (DFA).

All complexity features were extracted using the AntroPy package. Unless noted, all parameters were kept as default for reproducibility (Vallat, 2022). The following definitions are taken from the library's documentation.

Approximate entropy quantifies regularity over time series. Smaller values indicate that the data is more regular and predictable. The formula for approximate entropy is as follows:

$$\text{ApEn}(m, r, N) = \phi(m + 1, r, N) - \phi(m, r, N)$$

Where:

- m is the embedding dimension (the length of sequences/data points to be compared).
- r is the tolerance parameter (similarity criterion).
- N is the length of the signal.

The function $\phi(m, r, N)$ is defined as follows:

$$\phi(m, r, N) = \frac{1}{N - m + 1} \sum_{i=1}^{N-m+1} \ln \left(\frac{C_i^m(r)}{C_{i+1}^m(r)} \right)$$

The term $C_i^m(r)$ is the number of data point pairs within a tolerance (r) for which the distance between the points in a m -dimensional space is less than r . For this analysis, the parameter r was set to $0.2 * \text{std}(x)$.

Sample entropy is a modification of approximate entropy to reduce data length dependencies. Large values indicate high complexity, whereas smaller values characterise regular signals.

The sample entropy of a signal (x) is defined as:

$$H(x, m, r) = -\log \frac{C(m + 1, r)}{C(m, r)}$$

Where m is the embedding dimension (= order), r is the radius of the neighbourhood with a default value of $0.2 * \text{std}(x)$.

$C(m + 1, r)$ is the number of embedded vectors of length $m + 1$ having a Chebyshev distance inferior to r , and $C(m, r)$ is the number of embedded vectors of length m having a Chebyshev distance inferior to r .

Permutation entropy is another variation of sample entropy that uses phase information of the signal and provides a more robust estimate of complexity in the presence of outliers (i.e., noise). Permutation entropy is parameter-free as it does not include tolerance parameters. The formula for the permutation entropy of a signal is as follows:

$$H = - \sum p(\pi) \log_2(\pi)$$

Where the summation runs over all the $n!$ permutations (π) of order n , and represents the information contained in comparing n consecutive values of the signal (in bits). This magnitude can be normalised between 0 – 1 values (where lower values represent lower complexity and high regularity).

SVD entropy is another entropy metric with less sensitivity to noise. SVD entropy aims to measure the dimensionality of the time series by identifying the minimal number of eigenvectors needed to explain the signal. Higher values of SVD entropy suggest high complexity. SVD entropy is defined as:

$$H = - \sum_{i=1}^M \bar{\sigma}_i \log_2(\bar{\sigma}_i)$$

Where M denotes the number of singular values of the embedded matrix Y , created from the time series as follows:

$$y(i) = [x_i, x_{i+\text{delay}}, \dots, x_{i+(\text{order}-1)*\text{delay}}]$$

The term $\sigma_1, \sigma_2, \dots, \sigma_M$ represents the normalised singular values of Y .

Hjorth Parameters estimate statistical properties of the signal in the time domain. The parameters comprise activity, mobility, and complexity. The mobility parameter approximates the proportion of the standard deviation of the power spectrum by computing the square root of the variance of the first derivative of the signal divided by the variance of the whole signal, as shown below:

$$\text{Mobility} = \sqrt{\frac{\text{var}\left(\frac{dx(t)}{dt}\right)}{\text{var}(x(t))}}$$

The complexity parameter is related to the signal's bandwidth (indicating the shape's similarity to a pure sine wave). For regular sinusoidal activity, the complexity parameter converges to 1. Complexity can be calculated as the mobility of the first derivative of the signal divided by the mobility of the signal.

$$Complexity = \frac{\text{mobility} \left(\frac{dx(t)}{dt} \right)}{\text{mobility}(x(t))}$$

Metrics assessing the fractal characteristics of the signal included Katz, Petrosian and Higuchi FD methods. The following formula defines Katz FD:

$$KatzFD = \frac{\log_{10}(L/a)}{\log_{10}(d/a)} = \frac{\log_{10}(n)}{\log_{10}(d/L) + \log_{10}(n)}$$

The numerator represents the sum and average of the Euclidean distances between the successive points of the signal (L and a , respectively) and the denominator expresses the maximum distance between the first point and any other time series (d).

Petrosian FD is defined as follows:

$$PetrosianFD = \frac{\log_{10}(N)}{\log_{10}(N) + \log_{10}(\frac{N}{N+0.4N_\delta})}$$

Where N represents the length of the signal, and N_δ expresses the number of sign changes in the first derivative of the time series.

The last FD metric extracted was Higuchi FD, which estimates the irregularity of a signal across different scales (k) by estimating changes in patterns. Multiple methods are used to compute Higuchi FD in a multi-step algorithm. In brief, the length of a fitting curve is calculated for each signal segment, and the mean length of the curves for each k is subsequently computed. The fractal dimension is then derived from the scaling behaviour of these segments through a least-squares linear best-fitting approach.

Finally, DFA characterises the long-term statistical dependencies in a given signal. DFA is based on the concept of self-affine processes. DFA can be estimated utilising the following formula:

$$DFA = \text{std}(X, L * n) = L^H * \text{std}(X, n)$$

A signal X can be considered self-similar/self-affine if the standard deviation of the signal points within a window of length n changes with the window length factor L in a power law. Higher DFA values are obtained from more regular signals.

2.3.3. Functional connectivity features

The weighted phase lag index (wPLI) was considered due to the potential lower sensitivity to volume conduction effects than many other methods. The wPLI has been shown to have good test-retest reliability in assessing connectivity in AD subjects, i.e., consistently higher theta band connectivity (Briels et al., 2020). Similarly, it has been reported that the global (average) functional connectivity assessed in sensor space could be comparable with the global connectivity in the source space, particularly with the original implementation of wPLI, the Phase Lag Index (PLI), although there is no available evidence for wPLI (Lai et al., 2018).

The wPLI quantifies the asymmetry in the distribution of phase differences between pairs of signals (channels), avoiding zero-lag (immediate) associations. The wPLI can be defined as follows:

$$wPLI = \frac{|E[\mathcal{I}(X_{ij})]|}{E[|\mathcal{I}(X_{ij})|]}$$

Where X_{ij} represents the cross-spectral density between two channel pairs (i, j) , $E\{\}$ expresses the expected value (average over time), and \mathcal{I} denotes the imaginary part of the cross-spectral density (which tends to maximise in the presence of zero-lag phase differences).

On the other hand, imaginary coherence (iCoh) is a frequency-based approach to pair-wise signal relationships. The iCoh is not affected by non-stationary processes. Also, compared to classical coherence methods, iCoh is less affected by volume conduction. As a zero-lag metric, iCoh eliminates all unexpected coherence arising from instantaneous coupled activity. The iCoh has been examined particularly in AD subjects, reporting a reduced alpha iCoh compared to control individuals (Fide et al., 2022).

The iCoh can be defined as follows:

$$iCoh(f) = \frac{|E\{e^{i\phi_{XY}(t)}\}|}{E\{|e^{i\phi_{XY}(t)}|\}}$$

Where $\phi_{XY}(t)$ represents the instantaneous phase difference between signals X and Y at a time t , and $E\{\}$ express the expected value (or average across t).

2.4. Harmonisation of rsEEG spectral parameters

The statistical harmonisation of rsEEG features (spectral, complexity, connectivity) was performed on the unharmonised pooled train and test sets. Initial versions of ComBat were not focused on preserving the effects of biological covariates of interest, but later adaptations allowed this functionality.

The general ComBat model can be summarised as follows:

$$Y_{ij\nu} = \alpha_\nu + \mathbf{X}_{ij}^T \boldsymbol{\beta}_\nu + \mathbf{Z}_{ij}^T \boldsymbol{\theta}_\nu + \delta_{i\nu} \varepsilon_{ij\nu}$$

Where $Y_{ij\nu}$ represents a 1-dimensional vector in a given site batch i , for a subject j , and a feature value v . Besides, $\boldsymbol{\beta}$ represents the coefficients of the biological covariates (X), and $\boldsymbol{\theta}_v$ represents the coefficients of the batch variable (Z) to be estimated via parametric or nonparametric empirical Bayes, plus the error (ε).

After estimating the coefficients of the batch variable, the harmonised feature can be re-expressed as:

$$Y_{ij\nu}^{\text{ComBat}} = \frac{y_{ij\nu} - \hat{\alpha}_\nu - \mathbf{X}_{ij} \hat{\boldsymbol{\beta}}_\nu - \gamma_{i\nu}^*}{\delta_{i\nu}^*} + \hat{\alpha}_\nu + \mathbf{X}_{ij} \hat{\boldsymbol{\beta}}_\nu$$

Of note, the effects of covariates are reincorporated in the term $\mathbf{X}_{ij}^T \boldsymbol{\beta}_\nu$, whereas $\gamma_{i\nu}$ and $\delta_{i\nu}$ represents the estimated additive and multiplicative effects of the batch variable.

With these notions in mind, the pooled train and test sets were harmonised across batches using the reComBat method, which capitalising on some advantages of previous ComBat versions but achieving appropriate fitting in situations where the covariate matrix is singular (i.e., a site with only one diagnosis for all subjects) by employing elastic-net regularisation (Adamer et al., 2022). The biological variability of group, age and sex was modelled to be retained after harmonisation. The demographic characteristics of the sample are summarised in **Figure 2**.

To avoid data leakage issues (Tampu et al., 2022), reComBat implements a `fit_transform` function suitable for machine learning applications. The latter allows users to harmonise the test dataset based on the estimates of the training set harmonisation.

Identification of existent batch effects was conducted through T-distributed Stochastic Neighbor Embedding (tSNE), which visually represents site-related differences in the unharmonised and harmonised datasets, as suggested in prior publications on different rsEEG features (Bigdely-Shamlo et al., 2020; Kotlacz et al., 2020; M. Li et al., 2022). Briefly, tSNE maps high-dimensional data to a lower-dimensional space while preserving local similarities. By visualising the data in this reduced space, tSNE helps identify patterns, clusters, and trends that may not be apparent in the original feature space. The tSNE perplexity parameter was set to 50.

Subsequently, the mean points in tSNE components 1 and 2 were calculated for each site to represent the average estimation of batch effects across sites. Thus, the Euclidian distances between sites and the overall batch effects were calculated and presented in distance matrixes, see **Figure 3**.

2.5 AutoML

AutoML was conducted using the AutoGluon Python package. Among available autoML frameworks, we have chosen the AutoGluon framework (Erickson et al., 2020), considering preliminary reports in different biomedical data modalities supporting that AutoGluon could have comparable results to hand-crafted models in both prediction and classification tasks (Jaotombo et al., 2023; Kamboj et al., 2023; Lin et al., 2023; Raj et al., 2023b). A detailed description of AutoGluon methods can be found elsewhere [Erickson et al., 2020], along with a comprehensive review of AutoML strategies (Bezrukavnikov and Linder, 2021).

The steps of autoML include features pre-processing, model architecture search, and hyperparameter fine-tuning. Pre-processing steps might include re-scaling the feature values from 0 – 1 for specific models and encoding categorical variables into numeric indexes. Next, AutoGluon integrates numerous standard ML models that can handle multiple scenarios (i.e., non-linearity, multi-collinearity). These base ML models of AutoGluon comprise logistic regression, K-Nearest Neighbours, Random Forest, Extra-trees model, extreme gradient-boosting (XGBoost), Light gradient-boosted machine (LightGBM), Category boosting (CatBoost), and Neural Networks for tabular data. In addition, AutoGluon implements a multi-layer stacking strategy. The multi-layer stacking method of AutoGluon aims to combine predictions from different base models to obtain a better performance. Several base models are trained in the first step of traditional approximation for stacking.

Then, another model called "stacker" is created to learn from the predictions of the base models. This stacker model helps improve predictions and captures interactions between the initial models, making the overall prediction more powerful. AutoGluon goes one step further by mimicking deep learning layers. Instead of using different models for each layer, AutoGluon uses the same models at every layer. Besides, each layer consists of the predictions from the previous layer but also concatenates the original data features as input for the stacker models (allowing the higher-layer stackers to consider the original data during training). As a complement to multi-layer stacking, AutoGluon employs "ensembling" methods to combine the predictions from all the stacker models in a weighted manner. This final step ensures a robust and accurate prediction that is less sensitive to overfitting. AutoGluon enhances its stacking

performance by maximising the use of available data for training and validation through k-fold ensemble bagging across all models at every stack layer. In k -fold bagging, the data is randomly divided into k separate folds, ensuring a balance based on labels (i.e., group/diagnosis).

Subsequently, each model is trained k times, with a distinct data chunk in each iteration, minimising the aggregated prediction variability. This strategy improves the traditional stacking method (without k -fold bagging), which utilises only a fraction of the data for each stacker training. Finally, AutoGluon offers an overview of the classification performance of all the models based on a user-defined metric (e.g. accuracy, balanced accuracy, F1 score, among others). Thus, a leaderboard displays each model's performance in the training, validation and testing sets and selects the best model based on these metrics (Erickson et al., 2020).

For our analyses, multi-class classification models were performed in AutoGluon tabular (v. 0.8.2) (Erickson et al., 2020). Unharmonised pooled data ($n = 507$) was split in a 70/30 stratified manner (based on the group) to obtain the train ($n = 354$) and test ($n = 153$) splits, respectively.

The train and test sets were harmonised as described in **Section 2.4** to assess the effect of reComBat harmonisation in the autoML performance. Thus, unharmonised and harmonised train sets were used as separate inputs in the AutoGluon tabular predictor algorithm with the "best_quality" presets (achieving higher performance), "balanced_accuracy" as the evaluation metric, and "auto_weight" (automatically choosing a weighting strategy based on the data) given the unbalanced number of subjects across groups (classes). Of note, the test sets (unharmonised and harmonised) were held out for subsequent evaluation of the best pre-trained model resulting from AutoGluon.

Subsequently, the rsEEG features of each subject were considered as predictors of the group variable (i.e. HC, MCI-AD, AD, PD, and MCI-LBD). First, the autoML models were fitted using spectral features only, as recommended in a previously published systematic review (Modir et al., 2023), and the performance of the best model selected with AutoGluon was evaluated. We repeated this, adding spectral + complexity features to another AutoGluon predictor (keeping all parameters as in the fitting of spectral features only) and assessed the best model performance. Finally, spectral + complexity + connectivity features fit the last AutoGluon predictor. Following this, we can evaluate the best model performance with single-type and multi-feature approaches, achieving specific and general objectives of this research.

In summary, a set of six "best models" were pre-trained with the AutoGluon pipeline, as follows:

- A) Unharmonised – Spectral only
- B) Unharmonised – Spectral + Complexity
- C) Unharmonised – Spectral + Complexity + Connectivity
- D) Harmonised – Spectral only
- E) Harmonised – Spectral + Complexity
- F) Harmonised – Spectral + Complexity + Connectivity

After obtaining the best pre-trained models, we evaluated the performance in classifying unseen subjects from the respective (held-out) test set. Therefore, balanced accuracy, sensitivity, specificity, and positive and negative predictive values were computed for the six best models. The relevance of meaningful features for the classification was assessed using permutation-based feature importance. Permutation-based feature importance quantifies the reduction in predictive performance when one feature's values are randomly shuffled across subjects.

In line with the principles of open science, we have included the raw data sources and shared the codes used for feature extraction, harmonisation, and autoML analysis. The notebook with the end-to-end process can be found on the following GitHub repository (https://github.com/alberto-jj/eeg_automl).

3. Results

3.1. Demographic characteristics of the sample

The pooled sample included subjects from California (n = 31), Finland (n = 38), France (n = 74), Genoa (n = 77), Greece (n = 64), Iowa (n = 26), Lemon (n = 69), Medellin (n = 72), Oslo (n = 33), and Stavanger (n = 23). The demographic characteristics of the pooled sample (n = 507) are depicted in **Figure 2**.

Age-related differences were observed across sites (ANOVA F = 30.36; p < 0.001). Pair-wise site comparisons supported statistically significant age differences, as presented in **Supplementary Table 1**. Besides, group-related age differences were evidenced (ANOVA F = 24.14; p < 0.001). Pair-wise post hoc tests showed that AD had greater mean age than HC (Mean Difference – Mean diff = 8.71; Standard Error – SE = 0.99; t-value = 8.80; p Tukey < 0.001). Similarly, mean age was higher in AD than PD (Mean diff = 8.30; SE = 1.32; t-value = 6.29; p Tukey < 0.001), and MCI-LBD (Mean diff = 4.76; SE = 1.71; t-value = 2.78; p Tukey = 0.045). Similarly, age was significantly higher in the MCI-AD compared to HC (Mean diff = 6.52; SE = 1.14; t-value = 5.73; p Tukey < 0.001), and PD (Mean diff = 6.10; SE = 1.43; t-value = 4.26; p Tukey < 0.001). No other significant findings were evinced in the pair-wise group comparisons (details are presented in **Supplementary Table 2**).

In the pooled sample, age differences related to gender were not observed (Mean diff = 0.56; SE = 0.83; t-value = 0.67; p Tukey = 0.501). Following the above, age-related differences between the train and test sets were not observed (Mean diff = 0.37; SE = 0.90; t-value = 0.41; p Tukey = 0.68).

On the other hand, sex-related statistically significant differences were observed across sites (χ^2 = 23.99; degrees of freedom – df = 9; p = 0.004) and by group (χ^2 = 25.31; df = 4; p < 0.001). Significant differences in the sex proportion were not observed when comparing the train and test sets (χ^2 = 0.24; df = 1; p = 0.625).

Supplementary Table 3 includes groups' relative and absolute frequency in the train and test sets.

3.2. Rs-EEG features harmonisation

The tSNE 1 and tSNE 2 components approximated the average site-related distributions in the rsEEG features. Site-related batch effects were evidenced through tSNE visualisations, as observed in **Figure 3**. It can be noticed that the differences in the average site-related Euclidean distances were larger in the unharmonised data, mainly due to the prominent batch effects of the Lemon dataset.

After reComBat harmonisation, the pair-wise distance across sites was reduced. Mitigation of the cross-site data dispersion and centroid re-centring were observed in the distance matrixes after harmonisation. In line with the above observation, a lower mean Euclidean distance between sites was observed with reComBat harmonisation; see **Figure 3**.

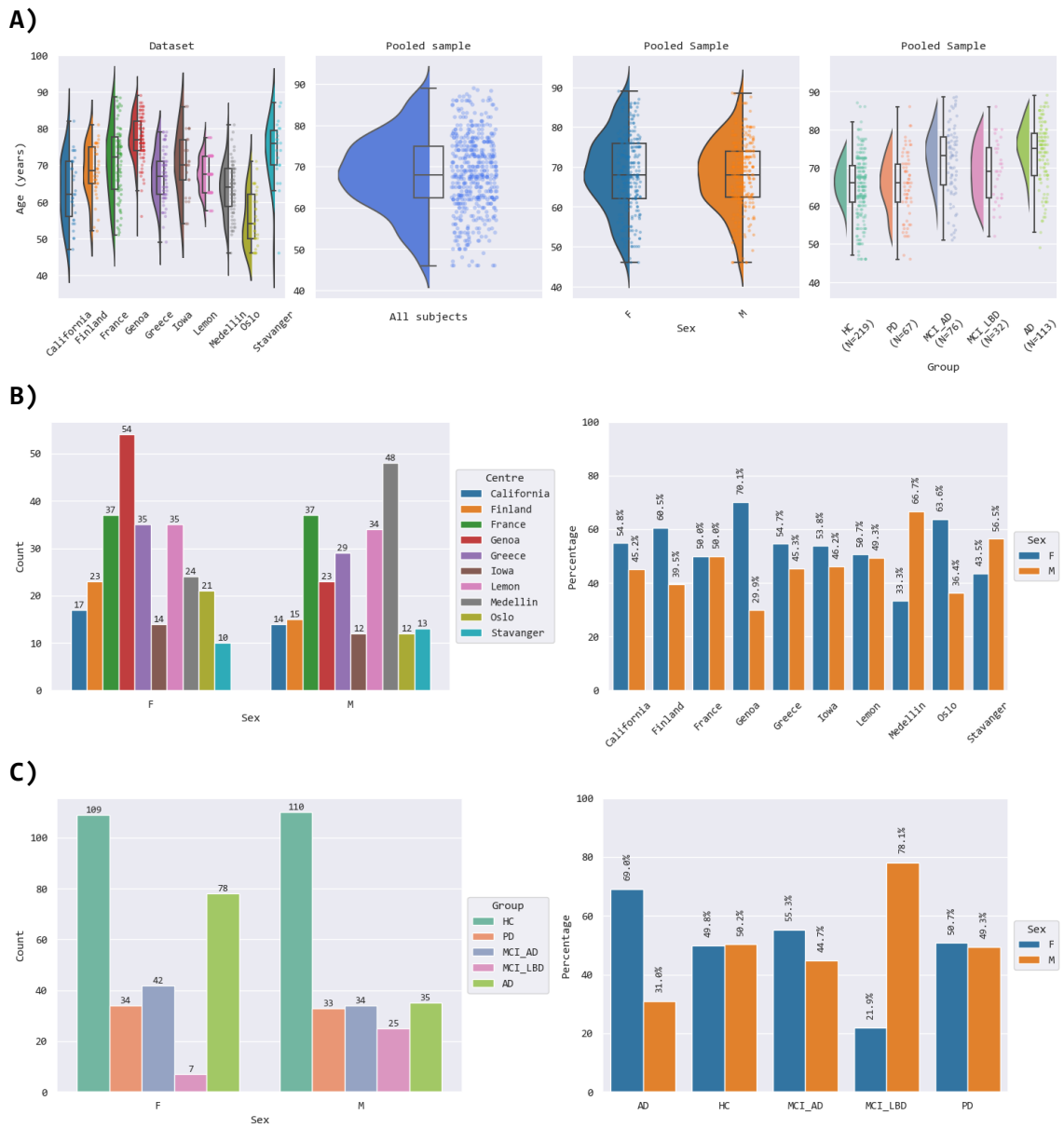


Figure 2. Demographical characteristics of the pooled sample (n = 507). **A)** From the left to the right-hand side, raincloud plots show the age distributions of age by individual dataset, in the pooled sample, by sex, and by diagnosis. **B)** Barplots show the absolute and relative frequency of Female (F) and Male (M) participants in each dataset. **C)** Barplots show the absolute and relative frequency by diagnosis subgroups. **AD:** Alzheimer's Disease; **MCI-AD:** Mild Cognitive Impairment – AD; **PD:** Parkinson's Disease; **MCI-LBD:** Mild Cognitive Impairment – Lewy Body Diseases; **HC:** Healthy Controls.

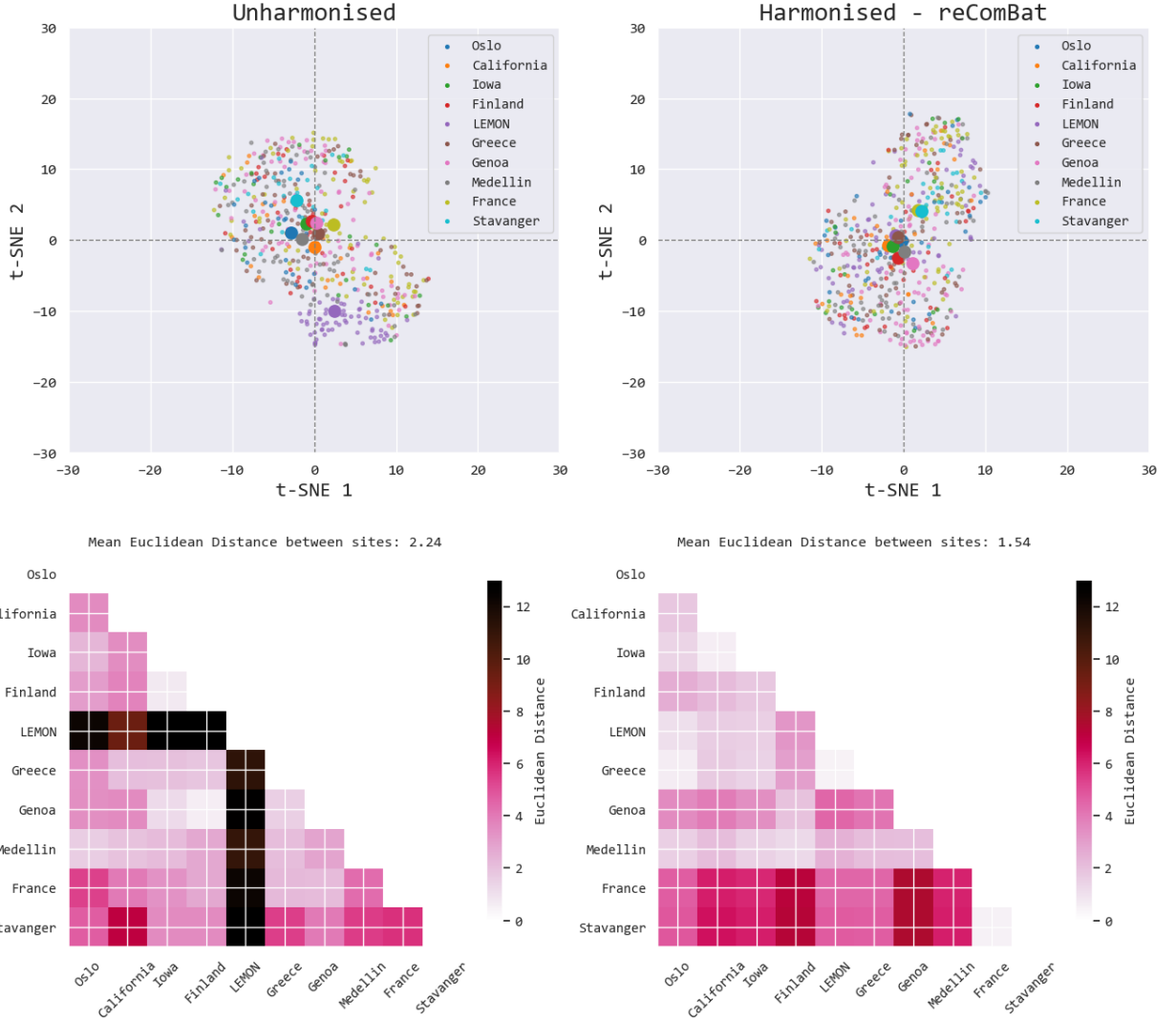


Figure 3. Harmonisation effects across all rsEEG spectral features. The top figures show t-distributed stochastic neighbour embedding (tSNE) components, perplexity = 50. Each plot shows the tSNE fit for the unharmonised and reComBat harmonised datasets ($n = 507$ for each). Dots depict a given subject (all rsEEG features reduced in dimensionality), colour-coded by the site/research centre. Bigger dots represent the average of the tSNE components for each site/research centre (i.e., mean site-related distribution). The bottom figures show the unharmonised and harmonised distance matrixes with the Euclidean distance between site-average values (obtained from tSNE models). The cross-site average distance in unharmonised and harmonised datasets is computed from each matrix.

3.3. Multi-class classification of NDDs using autoML

In order to compare the performance of the harmonisation and multi-feature approaches over NDDs classification, confusion matrixes were generated for the six best models selected with the AutoGluon framework (see details on each model in **Section 2.5**). The performance of these models is presented in **Figures 4 and 5**.

XGBoost was consistently selected as the best-performing model for harmonised data. Further details on the models' architecture and performance metrics are available in **Table 1**.

Table 1. Effects of harmonisation and multi-feature approach on best models' overall performance

| Spectral Only | | | |
|--------------------------------------|-----------------|----------|----------|
| Dataset | Best model | Bacc | Accuracy |
| Unharmonised | Random Forest | 0.396448 | 0.562092 |
| Harmonised | XGBoost | 0.687933 | 0.764706 |
| Spectral + Complexity | | | |
| Unharmonised | Extra Trees | 0.371001 | 0.555556 |
| Harmonised | XGBoost | 0.689237 | 0.764706 |
| Spectral + Complexity + Connectivity | | | |
| Unharmonised | NeuralNet Torch | 0.391027 | 0.568627 |
| Harmonised | XGBoost | 0.669633 | 0.771242 |

Bacc: Balanced accuracy for the whole model; **XGBoost:** Extreme gradient-boosting model. **NeuralNet Torch:** Pytorch Neural Network for multi-class classification. The best model was selected with AutoGluon based on the highest Bacc (assessed on the hold-out test set). All the models selected as "best" by the autoGluon pipeline were trained and validated using k-fold bagging.

The average model performance estimated through Bacc was lower when training the autoML models with unharmonised data (Bacc ranging between 37.1 – 39.6 %). On the contrary, models trained with harmonised data resulted in a higher performance (Bacc ranging between 66.9 – 68.9 %).

Compared to unharmonised datasets, the proportion of correctly classified subjects was higher in all datasets harmonised with reComBat. This increase in classification performance was consistently observed across all groups. Similarly, false positives were lower in the models trained using harmonised data. As shown in the diagonals of the confusion matrixes, The latter was observed independently of the nature of the features considered for training the autoML models; see **Figure 4** and **Table 1**.

On the other hand, multi-feature combinations elicited subtle variations in the classification performance of the harmonised models. Analyses based only on Spectral features yielded a Bacc = 68.79%, whereas Spectral + Complexity + Connectivity features did not improve the model performance (Bacc = 66.96%). The best classification performance was achieved with Spectral + Complexity features (Bacc = 68.92 %); see **Figure 5** and **Table 2**. The estimated values of the most important features in the Spectral + Complexity model used for classification in the test set are presented in **Figure 6**.

The XGBoost models better predicted the AD, HC, and MCI-AD classes independently of the rsEEG features utilised for model training. In addition, specificity was consistently higher than sensitivity in these groups. The complete group-wise estimations of harmonised models' performance are presented in **Table 2** and **Figure 5**.

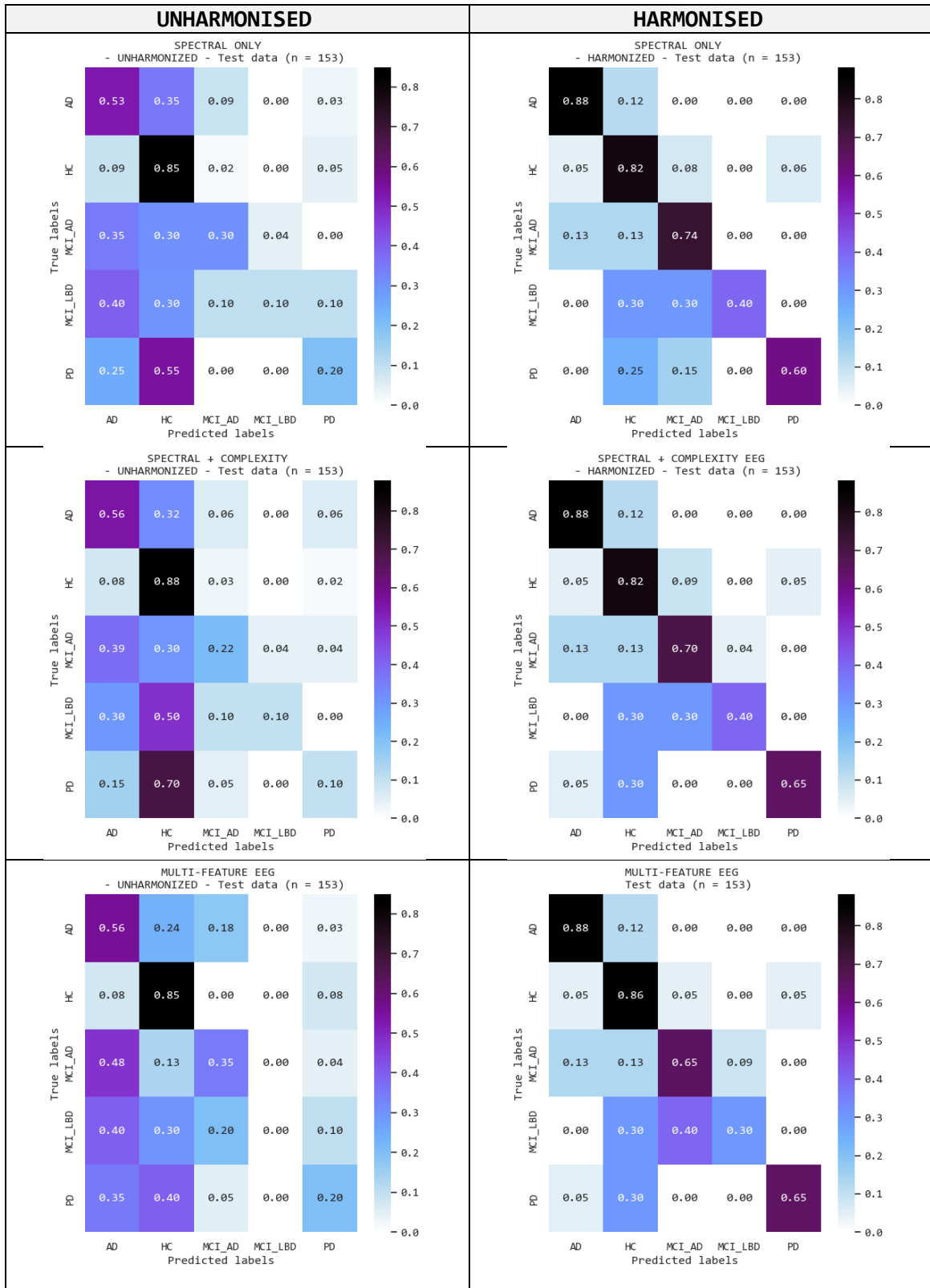
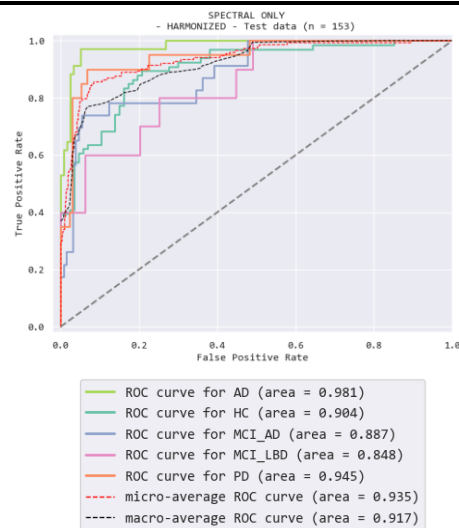


Figure 4. Normalised confusion matrixes (0 to 1) of unharmonised and harmonised spectral features (top) and their combination with complexity (middle row) and connectivity features (bottom row). Diagonal values closer to 1 indicate a 100% correct classification of the subjects belonging to a given class.

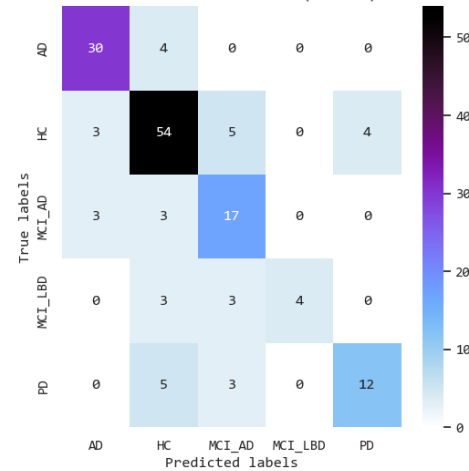
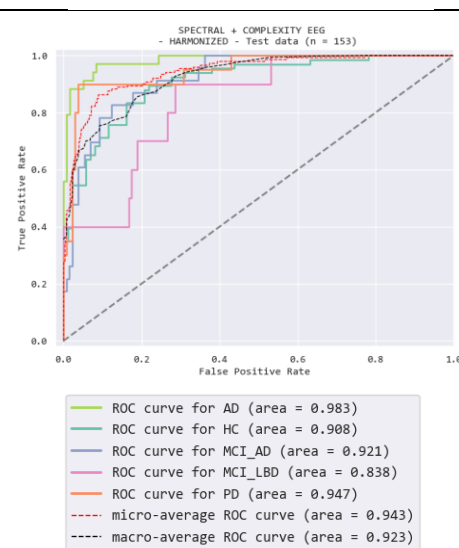
Table 2. Model performance evaluation metrics (harmonised dataset, single-nature vs multi-features)

| Spectral Only | | | | |
|--------------------------------------|-------------|-------------|----------|----------|
| Group | Sensitivity | Specificity | PPV | NPV |
| AD | 0.882353 | 0.949580 | 0.833333 | 0.965812 |
| HC | 0.818182 | 0.827586 | 0.782609 | 0.857143 |
| MCI-AD | 0.739130 | 0.915385 | 0.607143 | 0.952000 |
| MCI-LBD | 0.400000 | | 1 | 1 |
| PD | 0.600000 | 0.969925 | 0.750000 | 0.941606 |
| Spectral + Complexity | | | | |
| Group | Sensitivity | Specificity | PPV | NPV |
| AD | 0.882353 | 0.941176 | 0.810811 | 0.965517 |
| HC | 0.818182 | 0.816092 | 0.771429 | 0.855422 |
| MCI-AD | 0.695652 | 0.930769 | 0.640000 | 0.945312 |
| MCI-LBD | 0.400000 | 0.993007 | 0.800000 | 0.959459 |
| PD | 0.650000 | 0.977444 | 0.812500 | 0.948905 |
| Spectral + Complexity + Connectivity | | | | |
| Group | Sensitivity | Specificity | PPV | NPV |
| AD | 0.882353 | 0.941176 | 0.810811 | 0.965517 |
| HC | 0.863636 | 0.816092 | 0.780822 | 0.887500 |
| MCI-AD | 0.652174 | 0.946154 | 0.681818 | 0.938931 |
| MCI-LBD | 0.300000 | 0.986014 | 0.600000 | 0.952703 |
| PD | 0.650000 | 0.977444 | 0.812500 | 0.948905 |

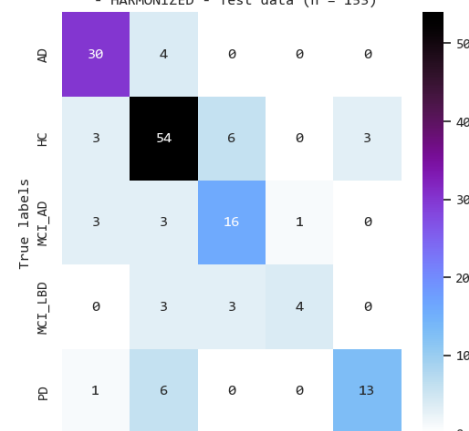
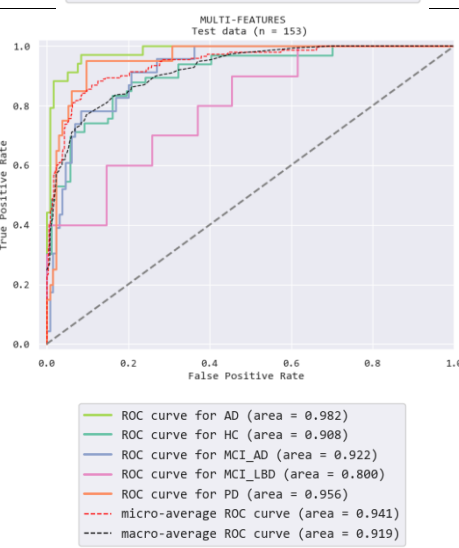
AD: Alzheimer's Disease; **MCI-AD:** Mild Cognitive Impairment – AD; **PD:** Parkinson's Disease; **MCI-LBD:** Mild Cognitive Impairment – Lewy Body Diseases; **HC:** Healthy Controls. **PPV:** Positive Predictive Value; **NPV:** Negative Predictive Value.

A)

SPECTRAL ONLY
- HARMONIZED - Test data (n = 153)

**B)**

SPECTRAL + COMPLEXITY EEG
- HARMONIZED - Test data (n = 153)

**C)**

MULTI-FEATURE EEG
Test data (n = 153)

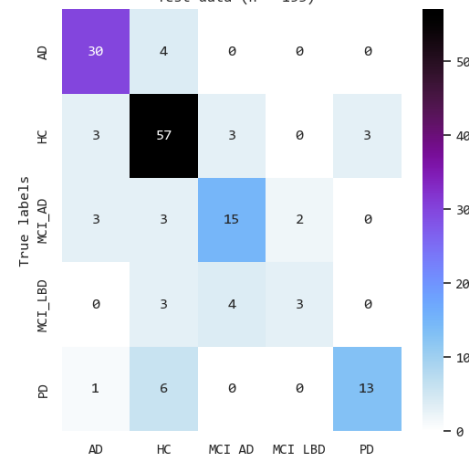


Figure 5. Receiver Operator Characteristics (ROC) curve and confusion matrixes for best models tested with the harmonised spectral-only features (A) and their combination with complexity (B) and connectivity features (C).

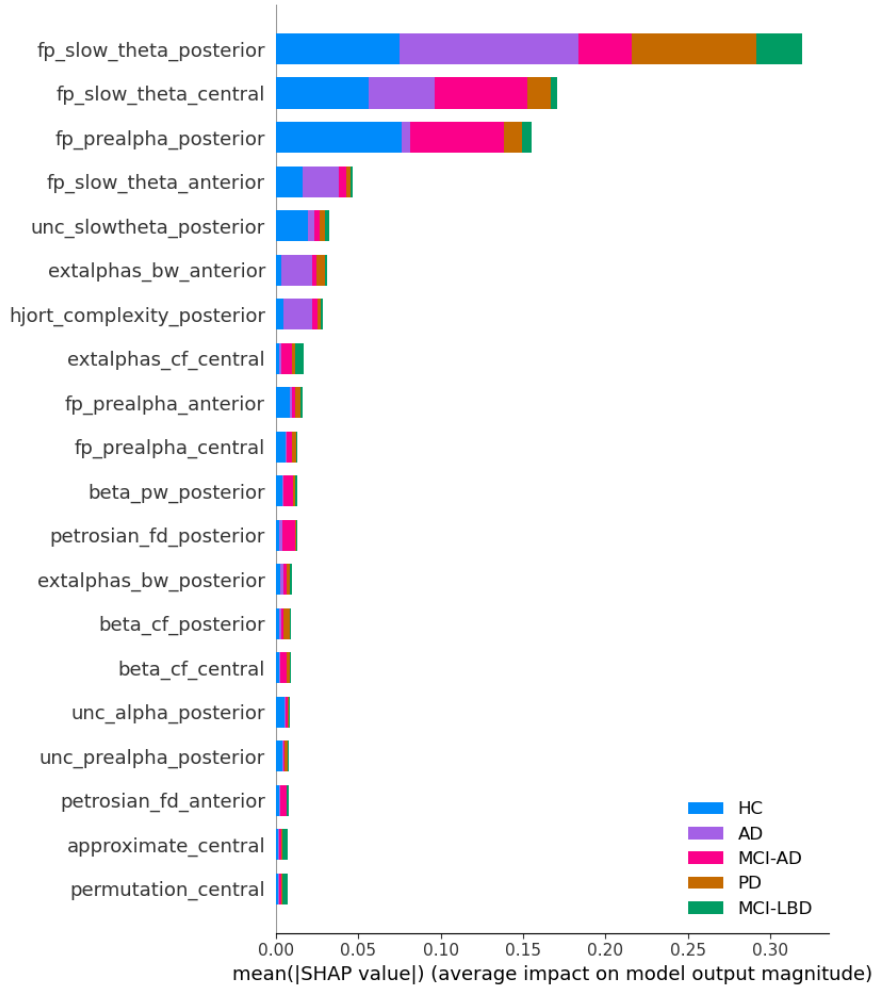


Figure 6. Feature importance for the NDDs classification in the hold-out test set (results from the harmonised Spectral + Complexity model). Shapley Additive exPlanations (SHAP) values reflect the importance of the top twenty rsEEG features. **AD:** Alzheimer's Disease; **MCI-AD:** Mild Cognitive Impairment – AD; **PD:** Parkinson's Disease; **MCI-LBD:** Mild Cognitive Impairment – Lewy Body Diseases; **HC:** Healthy Controls. Prefixes and suffixes employed in spectral feature names: **UNC:** Aperiodic Uncorrected. **FP:** Frequency Prevalence. **PW:** 1/f oscillatory corrected power. **BW:** 1/f oscillatory corrected bandwidth. **CF:** 1/f oscillatory corrected centre frequency. **EXTALPHA:** Extended alpha band. **FD:** Fractal Dimension. **Approximate:** Approximate entropy. **Permutation:** Permutation entropy. The Regions of Interest (ROI) names are suffixes (**anterior**, **central**, and **posterior**) in all features.

4. Discussion

This study evaluated the performance of an autoML framework for multi-class classification of NDD (i.e., HC, MCI-AD, AD, PD, MCI-LBD) from batch-harmonised features extracted from rsEEG signals through different conceptual families of analysis (i.e., Spectral, Complexity, Connectivity). The observed site-related batch effects in rsEEG features might be mitigated through statistical harmonisation (based on the reComBat algorithm). Thus, harmonisation with reComBat reduced the estimated cross-site mean distance in rsEEG features, which resulted in a consistent improvement in the overall classification performance of the autoML models, independently of the conceptual family of features. The XGBoost model architecture with k-fold bagging was consistently selected as the best-performing model, no matter the conceptual families used for training. The XGBoost trained with a combination of harmonised Spectral + Complexity features superseded the performance of other models, with a Bacc of 68.9 % for all

classes. The classification of individuals in the HC (Sensitivity = 81.8%; Specificity = 81.6%; PPV = 77.1%; NPV = 85.5 %), MCI-AD (Sensitivity = 69.6 %; Specificity = 93.1 %; PPV = 64.0 %; NPV = 94.5 %), and AD (Sensitivity = 88.2 %; Specificity = 94.1 %; PPV = 81.1 %; NPV = 96.6 %) was the highest observed among all classes. Altogether, our results suggest the successful application of statistical harmonisation of potential batch effects in conjunction with autoML frameworks on tabular features extracted from rsEEG signals for multi-class classification of NDDs. Our data-driven approach supports the utilisation of automated end-to-end pipelines for rsEEG analysis that could be applied to multi-centric studies in NDDs and dementia research. Finally, autoML facilitates future re-training of an existing pre-trained model (suitable for prospective studies) and allows further evaluation of the generalisability of the results in external datasets (when validating the findings in clinical settings).

4.1. Harmonisation of rsEEG features mitigates batch effects in multi-centric studies

Harmonisation of multi-site batch effects has been suggested as a necessary step when analysing pooled rsEEG datasets [Bigdely-Shamlo et al., 2020; M. Li et al., 2022; Prado et al., 2022]. In a previous study by our group (Jaramillo-Jimenez et al., 2024 – Under review), we contrasted the effects of various ComBat-based algorithms for statistical batch harmonisation of rsEEG spectral features in a moderate-to-large subsample of HC subjects. Overall, batch effects reflecting site-related variability on the rsEEG spectral features were identified. These batch effects have been attributed to potential cross-site differences in the headset/amplifiers (Bigdely-Shamlo et al., 2020) and biological sources of variability present when pooling different samples that could increase type-I errors if not corrected for (Bigdely-Shamlo et al., 2020; M. Li et al., 2022; Prado et al., 2022).

Preserving the biological variability of factors like age, gender, or diagnosis is crucial for the internal validity of the methods in age-related conditions such as NDDs (Adamer et al., 2022; Pomponio et al., 2020). Nonetheless, a flaw of most ComBat-derived models is the estimation of singular biological covariance matrixes (i.e., pooling data from one site with all samples belonging to the same group or gender). Given the nature of the dataset, singular matrix problems were identified in cases such as all individuals labelled as HC in the Lemon and Oslo datasets and AD-only subjects in the Genoa set. By utilising reComBat, the singular biological variability matrix could be solved with elastic-net regularisation parameters that specifically tackle the abovementioned limitation (Adamer et al., 2022).

Our results in a pooled dataset from ten different centres suggested mitigation of overall batch effects as reflected by a reduction in the Mean cross-site Euclidean Distance (unharmonised = 2.24 versus harmonised = 1.54). The latter was observed in tSNE components as a slight recentering, rotation and re-scaling of the reduced representation of multiple features. The effect of reComBat harmonisation successfully increased the overall model performance, as evidenced by a greater balanced accuracy in the harmonised models. The improvement in the classification performance was observed for all the classes (HC, MCI-AD, AD, PD, MCI-LB), with notably better performance for those classes with a higher proportion of participants (i.e., HC, AD, and MCI-AD). Our results were consistent with earlier biomedical studies harmonising other data modalities for further subject classification (Adamer et al., 2022; Bell et al., 2022; Da-an o et al., 2020; Fortin et al., 2018; Horng et al., 2022; Hu et al., 2023; Jovicich et al., 2019; Leithner et al., 2022; Pomponio et al., 2020; Prado et al., 2022; Shiri et al., 2022; Voß et al., 2022). The converging evidence makes us conclude that statistical harmonisation of tabular data could be a promising strategy for future research capitalising on existing data collections in clinical rsEEG research.

4.2. Combination of Spectral and Complexity abnormalities in the classification of NDDs

The combination of Spectral + Complexity features in AD and MCI-AD identification is supported by a recent Chinese study with a large sample size conducted in a single reference site for neurology (Jiao et al., 2023). These authors trained rsEEG binary and three-class classification (HC vs AD vs MCI-AD) supportive vector machine and linear discriminant analysis models by combining 1/f uncorrected spectral powers (absolute and relative), sample entropy, Hjorth parameters, time-frequency statistics (entropy, kurtosis, skewness, standard deviation and mean), and EEG microstates extracted at the sensor level with a low-density montage. In addition, these authors recognized spectral and complexity features as the key biomarkers for differentiation of HC, MCI-AD, AD, DLB, FTD and vascular dementia, namely the 1/f uncorrected relative and absolute right occipital theta power, as well as the right parietal and bilateral occipital Hjorth mobility. In agreement with this single-site study, our observations in this harmonised multi-site dataset support that Hjorth parameters in posterior leads, combined with Spectral features, comprise essential information for classifying HCs and individuals in the AD-continuum.

Two systematic reviews summarising the last ten years' evidence have also recognized these features when summarizing potential biomarkers of rsEEG reduced complexity in AD. Thus, a reduced complexity could characterise AD subjects, with differences captured by fractal and entropy estimators as well as Hjorth parameters (Cassani et al., 2018; Modir et al., 2023). Similarly, another study with low-density rsEEG recordings found that Hjorth complexity + Entropy metrics + Aperiodic uncorrected spectral band powers were the most relevant features in binary classifications (AD vs HC, and MCI negative for AD pathology vs HC) in a small sample ($n = 21$; AD = 8, MCI non-AD = 5, HC=8) (Perez-Valero et al., 2022). Transcranial magnetic stimulation combined with EEG has also pointed out increased Hjorth complexity in AD, emphasizing the value of combining Hjorth parameters with spectral features (Tăuțan et al., 2023).

Compared to spectral features only, a slight increase in the sensitivity of MCI-AD, MCI-LBD, and PD classes was achieved when combining spectral and complexity features (although this was not minimal in terms of average Bacc). Thus, the best model with Spectral and Complexity features achieved good discrimination of HC (Accuracy = 76.5%, Bacc = 68.9%, Sensitivity - Sens- = 81.8%, Specificity – Spec- = 81.6% PPV = 77.1%, NPV = 85.5%), MCI-AD (Sens = 69.5%, Spec = 93.1%, PPV = 64%, NPV = 94.5%) and AD (Sens = 88.2%, Spec = 94.1%, PPV = 81.1%, NPV = 96.5%). Our XGBoost with k-fold bagging model paramounted those fitted by Jiao et al., who reported a model accuracy of 70.2% on a three-class classification (HC vs MCI-AD vs AD) in a single-site study with a large sample (Jiao et al., 2023). Despite their large sample size, the groups were not balanced (HC = 246, MCI = 189, AD = 330), and the authors did not account for class imbalance when reporting model performance. In unbalanced scenarios for rsEEG-based classification tasks, using Bacc for model selection, optimisation, and performance evaluation has been recommended due to its robustness to class imbalance (Thölke et al., 2023). Similarly, a prior large study using supervised models for the binary classification of neurodegeneration found that spectral band powers, mean frequency, algorithmic complexity, and entropy extracted in sensor space (with low montages) were the best predicting features of AD-related neurodegeneration (defined as region-specific glucose hypometabolism in functional neuroimaging), with a Bacc = 61 % (Gaubert et al., 2021).

Frequency prevalence descriptors could indicate epoch-to-epoch power (i.e., the percentage of epochs where the peak/dominant frequency lies in each of the frequency bands), potentially capturing power spectrum variability loss after averaging (or getting the median) of power spectrum estimations across epochs (Bonanni et al., 2015, 2008; Gimenez-Aparisi et al., 2023;

Stylianou et al., 2018). Increased pre-alpha power in MCI-AD, AD, PD, and MCI-LBD has been identified in preceding studies (Azami et al., 2023; Jaramillo-Jimenez et al., 2023; Kopčanová et al., 2023; Rosenblum et al., 2023; Schumacher et al., 2020a). This discriminatory pattern has been replicated when assessing frequency prevalence in the theta band (which includes slow-theta and pre-alpha), in congruence with (Gimenez-Aparisi et al., 2023; Stylianou et al., 2018). Of note, most of the mentioned studies have not directly discretised the theta band into slow-theta and pre-alpha subbands (Azami et al., 2023; Kopčanová et al., 2023; Rosenblum et al., 2023; Vanneste et al., 2018). Among studies assessing pre-alpha power, the findings of Schumacher et al. (Schumacher et al., 2020a) supported the hypothesis of increased pre-alpha power in MCI-AD and MCI-LBD compared to HC but the presented by Bonanni et al. presented a scarce pre-alpha frequency prevalence (< 11%) in MCI-AD, and AD with comparable relative power compared to HC individuals (Bonanni et al., 2015, 2008). We observed that HC had significantly lower pre-alpha power and frequency prevalence than MCI-AD and MCI-LBD groups, but notably, pre-alpha values in MCI-AD were significantly lower than in AD. Thus, future efforts should assess the robustness and generalisability of pre-alpha power and frequency prevalence as correlates of the progression across the AD continuum.

This multi-centric sample did not identify contributions of connectivity features to model performance. The necessity of relatively extensive feature extraction (i.e., calculation of several connectivity metrics) for appropriate characterisation of NDDs has been stated in earlier research (Briels et al., 2020; Dottori et al., 2017; Moguilner et al., 2022; Prado et al., 2023, 2022). Previous evidence supported the observation of a global increase in theta band wPLI, but AD-related differences were no longer observed when accounting for theta power increase (Briels et al., 2020). In addition, we acknowledge that our estimation of global connectivity is a gross evaluation of connectivity that could be refined by the computation of graph-theory connectivity metrics with subsequent potential threshold bias to be assessed and consistency scores, which imply increased computational demands. Despite these potential opportunities, we agree with the observations of an early publication where high-density montages were dedicated to approximate connectivity features of AD and MCI-AD. In contrast to a computationally demanding source space connectivity estimation, sensor space low-density montages offered a better classification of AD-related neurodegeneration when combining Spectral + Complexity features (Gaubert et al., 2021).

4.3 Fitting AutoML from rsEEG tabular features

AutoML frameworks have been tested in regression and classification tasks and across multiple data types (including biomedical), often producing models with good to excellent performance, even in small tabular datasets with less than 1000 examples (Conrad et al., 2022; Liu et al., 2023; Musigmann et al., 2022; Ou et al., 2021). Despite the growing interest in autoML in neuroimaging and cancer research, and emerging evidence suggests that autoML approaches could surpass hand-crafted models, its application in rsEEG remains relatively unexplored and keeps the focus on epilepsy (Lenkala et al., 2023; Liu et al., 2022). We successfully evaluated the AutoGluon autoML framework in the NDDs multi-class classification task. Among available autoML models, we have chosen the AutoGluon framework (Erickson et al., 2020). The latter was supported by considering preliminary reports in different biomedical data modalities stating that AutoGluon could have comparable results to hand-crafted models in both prediction and classification tasks (Jaotombo et al., 2023; Kamboj et al., 2023; Lin et al., 2023; Raj et al., 2023b). The XGBoost architecture has been consistently selected as the best-performing model in harmonised datasets. The remarkable performance of tree-based models (including XGBoost and random forests) has been reported in NDDs classification from rsEEG features (Gaubert et al., 2021; Moguilner et al., 2022). AutoML frameworks also account for

model reproducibility by storing model hyperparameters, validation splits, and predictions for all the trained models . For clinical neurophysiology research, using autoML could ease the implementation of machine learning models trained from tabular data.

Some limitations should be considered when interpreting our results. Thus, due to the retrospective nature of this study, a biological characterisation of the underlying neuropathology in our sample makes us rely on clinical phenotypes to classify the included subjects, which might not entirely reflect the underlying protein aggregation/accumulation despite the use of operationalised diagnostic criteria in the individual studies included in our analyses. As previously suggested, future studies integrating rsEEG data with other biomarkers of NDDs (CSF, imaging or blood-based tests) could shed light on their potential interrelatedness (Iturria-Medina et al., 2016; Moguilner et al., 2022). On the other hand, balanced groups could not be achieved in our final sample. Class imbalance is often presented in machine learning studies using rsEEG for the classification of NDDs, opening the gate for data augmentation techniques that could be implemented to train better models based on balanced groups (Lashgari et al., 2020; Rommel et al., 2022). In addition, our analyses were conducted with features extracted at the sensor space, which might offer potential confounding effects of volume conduction. Although source space represented the state-of-the-art method to reduce the effects of volume conduction and represent the source of rsEEG spectral activity, source solutions from low-density rsEEG recordings might still misrepresent the appropriate spatial patterns of source activity as these estimations are often estimated from forward modelling in anatomical templates that do not correspond to specific-subject anatomy (which might be affected by NDDs with gliosis and cortical atrophy) (Nguyen-Danse et al., 2021). Statistical-based source separation methods such as spatio-spectral decomposition appeared as an emergent solution to assess brain rhythms controlling for volume conduction effects without the necessity of anatomical head models. In brain-age prediction studies, these methods have been implemented by computing the covariance matrixes from rsEEG channels (even from very low-density montages, such as four channels) in a computationally efficient manner (Engemann et al., 2022a; D. Sabbagh et al., 2023). Spatio-spectral decomposition could also mitigate the documented interference created by posterior sources of alpha rhythm over anterior rsEEG channels at the sensor level (Schaworonkow and Nikulin, 2022). In addition, the combination of spatio-spectral decompositions from rsEEG covariance matrixes with Riemannian geometry-based machine learning models has demonstrated notable performance in brain-age prediction, achieving better results than handcrafted features used in our research (e.g. spectral and complexity) (Engemann et al., 2022a). However, current methods for batch harmonisation available for covariance-based representations of the rsEEG signals (i.e., re-centring and re-scaling via Procrustes analysis) lack specific strategies to control biological variability (Rodrigues et al., 2019). Future efforts should be taken to address this critical limitation.

With all the above, we conclude that harmonising rsEEG features improves model performance, and the combination of rsEEG spectral + complexity harmonised features achieved the best performance for multiclass classification of NDDs, particularly in the AD-continuum. Our proposed approach presents a reproducible pipeline for analysing rsEEG signals, suitable for multi-site studies and classification or regression tasks.

5. References

- Aarsland D, Batzu L, Halliday GM, Geurtsen GJ, Ballard C, Ray Chaudhuri K, Weintraub D (2021): Parkinson disease-associated cognitive impairment. *Nat Rev Dis Primers* 7:1–21. <https://www.nature.com/articles/s41572-021-00280-3>.
- Aarsland D, Creese B, Politis M, Chaudhuri KR, Ffytche DH, Weintraub D, Ballard C (2017): Cognitive decline in Parkinson disease. *Nature Reviews Neurology*. Nature Publishing Group.
- Abásolo D, Hornero R, Escudero J, Espino P (2008): A study on the possible usefulness of detrended fluctuation analysis of the electroencephalogram background activity in Alzheimer's disease. *IEEE Trans Biomed Eng* 55:2171–2179. <https://pubmed.ncbi.nlm.nih.gov/18713686/>.
- Abubakar MB, Sanusi KO, Uguzman A, Mohamed W, Kamal H, Ibrahim NH, Khoo CS, Kumar J (2022): Alzheimer's Disease: An Update and Insights Into Pathophysiology. *Front Aging Neurosci* 14:742408.
- Adamer MF, Brüningk SC, Tejada-Arranz A, Estermann F, Basler M, Borgwardt K (2022): reComBat: batch-effect removal in large-scale multi-source gene-expression data integration. *Bioinformatics Advances* 2. <https://dx.doi.org/10.1093/bioadv/vbac071>.
- Aisen PS, Cummings J, Jack CR, Morris JC, Sperling R, Frölich L, Jones RW, Dowsett SA, Matthews BR, Raskin J, Scheltens P, Dubois B (2017): On the path to 2025: Understanding the Alzheimer's disease continuum. *Alzheimer's Research and Therapy*. BioMed Central Ltd. <https://alzres.biomedcentral.com/articles/10.1186/s13195-017-0283-5>.
- Albert MS, DeKosky ST, Dickson D, Dubois B, Feldman HH, Fox NC, Gamst A, Holtzman DM, Jagust WJ, Petersen RC, Snyder PJ, Carrillo MC, Thies B, Phelps CH (2011): The diagnosis of mild cognitive impairment due to Alzheimer's disease: recommendations from the National Institute on Aging-Alzheimer's Association workgroups on diagnostic guidelines for Alzheimer's disease. *Alzheimers Dement* 7:270–279. <https://pubmed.ncbi.nlm.nih.gov/21514249/>.
- Alger BE (2022): Neuroscience Needs to Test Both Statistical and Scientific Hypotheses. *The Journal of Neuroscience* 42:8432. [/pmc/articles/PMC9665931/](https://PMC9665931/).
- Allegri RF (2020): Moving from neurodegenerative dementias, to cognitive proteinopathies, replacing “where” by “what” *Dementia e Neuropsychologia* 14:237–242. <http://www.scielo.br/j/dn/a/ftRYYctPTnkfb9yL7cD6nXK/?lang=en>.
- Al-Nuaimi AHH, Jammeh E, Sun L, Ifeachor E (2018): Complexity Measures for Quantifying Changes in Electroencephalogram in Alzheimer's Disease. *Complexity* 2018.
- Al-Qazzaz NK, Ali SHBMD, Ahmad SA, Chellappan K, Islam MdS, Escudero J (2014): Role of EEG as biomarker in the early detection and classification of dementia. *Scientific World Journal*. Hindawi Limited. [/pmc/articles/PMC4100295/?report=abstract](https://PMC4100295/?report=abstract).
- Alzheimer A (1907): Über eine eigenartige Erkrankung der Hirnrinde. *Allgemeine Zeitschrift für Psychiatrie und Psychisch-gerichtliche Medizin* 64:146–148.
- American Psychiatric Association (2013): *Diagnostic and Statistical Manual of Mental Disorders*, 5th Edition. *Diagnostic and Statistical Manual of Mental Disorders*, 5th Edition.

Angarita-Zapata JS, Maestre-Gongora G, Calderín JF (2021): A Bibliometric Analysis and Benchmark of Machine Learning and AutoML in Crash Severity Prediction: The Case Study of Three Colombian Cities. *Sensors* (Basel) 21. <https://pubmed.ncbi.nlm.nih.gov/34960494/>.

Angelakis E, Lubar JF, Stathopoulou S, Kounios J (2004): Peak alpha frequency: an electroencephalographic measure of cognitive preparedness. *Clinical Neurophysiology* 115:887–897.

Anjum MF, Dasgupta S, Mudumbai R, Singh A, Cavanagh JF, Narayanan NS (2020): Linear predictive coding distinguishes spectral EEG features of Parkinson's disease. *Parkinsonism Relat Disord* 79:79–85.

Appelhoff S, Hurst AJ, Lawrence A, Li A, Mantilla Ramos YJ, O'Reilly C, Xiang L, Dancker J (2022): PyPREP: A Python implementation of the preprocessing pipeline (PREP) for EEG data. <https://zenodo.org/record/6363576>.

Armstrong MJ (2021): Advances in dementia with Lewy bodies. *Ther Adv Neurol Disord* 14. <https://journals.sagepub.com/doi/10.1177/17562864211057666>.

Armstrong MJ, MJ A (2019): Lewy Body Dementias 25:128–146. <https://pubmed.ncbi.nlm.nih.gov/30707190/>.

Attems J, Toledo JB, Walker L, Gelpi E, Gentleman S, Halliday G, Hortobagyi T, Jellinger K, Kovacs GG, Lee EB, Love S, McAleese KE, Nelson PT, Neumann M, Parkkinen L, Polvikoski T, Sikorska B, Smith C, Grinberg LT, Thal DR, Trojanowski JQ, McKeith IG (2021): Neuropathological consensus criteria for the evaluation of Lewy pathology in post-mortem brains: a multi-centre study. *Acta Neuropathol* 141:159–172. <https://link.springer.com/article/10.1007/s00401-020-02255-2>.

Averna A, Coelli S, Ferrara R, Cerutti S, Priori A, Bianchi AM (2023): Entropy and fractal analysis of brain-related neurophysiological signals in Alzheimer's and Parkinson's disease. *J Neural Eng* 20. <https://pubmed.ncbi.nlm.nih.gov/37746822/>.

Azami H, Zrenner C, Brooks H, Zomorrodi R, Blumberger DM, Fischer CE, Flint A, Herrmann N, Kumar S, Lanctôt K, Mah L, Mulsant BH, Pollock BG, Rajji TK (2023): Beta to theta power ratio in EEG periodic components as a potential biomarker in mild cognitive impairment and Alzheimer's dementia. *Alzheimers Res Ther* 15:1–12. <https://alzres.biomedcentral.com/articles/10.1186/s13195-023-01280-z>.

Babadi B, Brown EN (2014): A review of multitaper spectral analysis. *IEEE Transactions on Biomedical Engineering*. IEEE Computer Society. <https://pubmed.ncbi.nlm.nih.gov/24759284/>.

Babayan A, Erbey M, Kumral D, Reinelt JD, Reiter AMF, Röbbig J, Lina Schaare H, Uhlig M, Anwander A, Bazin PL, Horstmann A, Lampe L, Nikulin V V., Okon-Singer H, Preusser S, Pampel A, Rohr CS, Sacher J, Thöne-Otto A, Trapp S, Nierhaus T, Altmann D, Arelin K, Blöchl M, Bongartz E, Breig P, Cesnate E, Chen S, Cozatl R, Czerwonatis S, Dambrauskaite G, Dreyer M, Enders J, Engelhardt M, Fischer MM, Forschack N, Golchert J, Golz L, Guran CA, Hedrich S, Hentschel N, Hoffmann DI, Huntenburg JM, Jost R, Kosatschek A, Kunzendorf S, Lammers H, Lauckner ME, Mahjoory K, Kanaan AS, Mendes N, Menger R, Morino E, Näthe K, Neubauer J, Noyan H, Oligschläger S, Panczyszyn-Trzewik P, Poehlchen D, Putzke N, Roski S, Schaller MC, Schieferbein A, Schlaak B, Schmidt R, Gorgolewski KJ, Schmidt HM, Schrimpf A, Stasch S, Voss M, Wiedemann A, Margulies DS, Gaebler M, Villringer A (2019): A mind-brain-body dataset of MRI, EEG,

cognition, emotion, and peripheral physiology in young and old adults. *Scientific Data* 2019 6:1 6:1–21. <https://www.nature.com/articles/sdata2018308>.

Babiloni C (2022): The Dark Side of Alzheimer's Disease: Neglected Physiological Biomarkers of Brain Hyperexcitability and Abnormal Consciousness Level. *Journal of Alzheimer's Disease* 88:801–807. <http://www.alz.org>.

Babiloni C, Barry RJ, Başar E, Blinowska KJ, Cichocki A, Dringenburg WHIM, Klimesch W, Knight RT, Lopes da Silva F, Nunez P, Oostenveld R, Jeong J, Pascual-Marqui R, Valdes-Sosa P, Hallett M (2020a): International Federation of Clinical Neurophysiology (IFCN) – EEG research workgroup: Recommendations on frequency and topographic analysis of resting state EEG rhythms. Part 1: Applications in clinical research studies. *Clinical Neurophysiology*. Elsevier Ireland Ltd. <http://www.ncbi.nlm.nih.gov/pubmed/31501011>.

Babiloni C, Binetti G, Cassetta E, Cerboneschi D, Dal Forno G, Del Percio C, Ferreri F, Ferri R, Lanuzza B, Miniussi C, Moretti D V., Nobili F, Pascual-Marqui RD, Rodriguez G, Romani GL, Salinari S, Tecchio F, Vitali P, Zanetti O, Zappasodi F, Rossini PM (2004): Mapping distributed sources of cortical rhythms in mild Alzheimer's disease. A multicentric EEG study. *Neuroimage* 22:57–67. <https://pubmed.ncbi.nlm.nih.gov/15109997/>.

Babiloni C, Blinowska K, Bonanni L, Cichocki A, De Haan W, Del Percio C, Dubois B, Escudero J, Fernández A, Frisoni G, Güntekin B, Hajos M, Hampel H, Ifeachor E, Kilborn K, Kumar S, Johnsen K, Johannsson M, Jeong J, LeBeau F, Lizio R, Lopes da Silva F, Maestú F, McGeown WJ, McKeith I, Moretti DV, Nobili F, Olichney J, Onofrj M, Palop JJ, Rowan M, Stocchi F, Struzik ZM, Tanila H, Teipel S, Taylor JP, Weiergräber M, Yener G, Young-Pearse T, Dringenburg WH, Randall F (2020b): What electrophysiology tells us about Alzheimer's disease: a window into the synchronization and connectivity of brain neurons. *Neurobiology of Aging*. Elsevier Inc. <http://www.ncbi.nlm.nih.gov/pubmed/31739167>.

Babiloni C, Ferri R, Noce G, Lizio R, Lopez S, Lorenzo I, Tucci F, Soricelli A, Nobili F, Arnaldi D, Famà F, Orzi F, Buttinelli C, Giubilei F, Cipollini V, Marizzoni M, Güntekin B, Aktürk T, Hanoğlu L, Yener G, Özbeğ Y, Stocchi F, Vacca L, Frisoni GB, Del Percio C (2021): Resting State Alpha Electroencephalographic Rhythms Are Differently Related to Aging in Cognitively Unimpaired Seniors and Patients with Alzheimer's Disease and Amnesic Mild Cognitive Impairment. *J Alzheimers Dis* 82:1085–1114. <https://pubmed.ncbi.nlm.nih.gov/34151788/>.

Babiloni C, Lorenzo I, Lizio R, Lopez S, Tucci F, Ferri R, Soricelli A, Nobili F, Arnaldi D, Famà F, Buttinelli C, Giubilei F, Cipollini V, Onofrj M, Stocchi F, Vacca L, Fuhr P, Gschwandtner U, Ransmayr G, Aarsland D, Parnetti L, Marizzoni M, D'Antonio F, De Lena C, Güntekin B, Yıldırım E, Hanoğlu L, Yener G, Gündüz DH, Taylor JP, Schumacher J, McKeith I, Frisoni GB, De Pandis MF, Bonanni L, Percio C Del, Noce G (2022): Reactivity of posterior cortical electroencephalographic alpha rhythms during eyes opening in cognitively intact older adults and patients with dementia due to Alzheimer's and Lewy body diseases. *Neurobiol Aging* 115:88–108.

Babiloni C, Del Percio C, Pasquarelli MT, Lizio R, Noce G, Lopez S, Rizzo M, Ferri R, Soricelli A, Nobili F, Arnaldi D, Famà F, Orzi F, Buttinelli C, Giubilei F, Salvetti M, Cipollini V, Franciotti R, Onofrj M, Stirpe P, Fuhr P, Gschwandtner U, Ransmayr G, Aarsland D, Parnetti L, Farotti L, Marizzoni M, D'Antonio F, De Lena C, Güntekin B, Hanoğlu L, Yener G, Emek-Savaş DD, Triggiani AI, Taylor JP, McKeith I, Stocchi F, Vacca L, Hampel H, Frisoni GB, De Pandis MF, Bonanni L (2019): Abnormalities of functional cortical source connectivity of resting-state

electroencephalographic alpha rhythms are similar in patients with mild cognitive impairment due to Alzheimer's and Lewy body diseases. *Neurobiol Aging* 77:112–127.

Babiloni C, Vecchio F, Lizio R, Ferri R, Rodriguez G, Marzano N, Frisoni GB, Rossini PM (2011): Resting State Cortical Rhythms in Mild Cognitive Impairment and Alzheimer's Disease: Electroencephalographic Evidence. *Journal of Alzheimer's Disease* 26:201–214.

Badhwar AP, Tam A, Dansereau C, Orban P, Hoffstaedter F, Bellec P (2017): Resting-state network dysfunction in Alzheimer's disease: A systematic review and meta-analysis. *Alzheimer's & Dementia: Diagnosis, Assessment & Disease Monitoring* 8:73–85.
<https://onlinelibrary.wiley.com/doi/full/10.1016/j.dadm.2017.03.007>.

Bailey NW, Hoy KE (2021): The promise of artificial neural networks, EEG, and MRI for Alzheimer's disease. *Clinical Neurophysiology* 132:207–209.

Banville H, Jaoude MA, Wood SUN, Aimone C, Holst SC, Gramfort A, Engemann D-A (2023): Do try this at home: Age prediction from sleep and meditation with large-scale low-cost mobile EEG. *bioRxiv*:2023.04.29.538328. <https://www.biorxiv.org/content/10.1101/2023.04.29.538328v1>.

Bastos AM, Schoffelen JM (2016): A tutorial review of functional connectivity analysis methods and their interpretational pitfalls. *Front Syst Neurosci* 9:165147.

Beam CR, Kaneshiro C, Jang JY, Reynolds CA, Pedersen NL, Gatz M (2018): Differences Between Women and Men in Incidence Rates of Dementia and Alzheimer's Disease. *J Alzheimers Dis* 64:1077. [./pmc/articles/PMC6226313/](https://pmc/articles/PMC6226313/).

Beer JC, Tustison NJ, Cook PA, Davatzikos C, Sheline YI, Shinohara RT, Linn KA (2020): Longitudinal ComBat: A method for harmonizing longitudinal multi-scanner imaging data. *Neuroimage* 220:117129.

Bell TK, Godfrey KJ, Ware AL, Yeates KO, Harris AD (2022): Harmonization of multi-site MRS data with ComBat. *Neuroimage* 257. <https://pubmed.ncbi.nlm.nih.gov/35618196/>.

Benjamini Y, Yekutieli D (2001): The control of the false discovery rate in multiple testing under dependency. <https://doi.org/10.1214/aos/1013699998> 29:1165–1188.
<https://projecteuclid.org/journals/annals-of-statistics/volume-29/issue-4/The-control-of-the-false-discovery-rate-in-multiple-testing/10.1214/aos/1013699998.full>.

Bennys K, Rondouin G, Vergnes C, Touchon J (2001): Diagnostic value of quantitative EEG in Alzheimer's disease. *Neurophysiologie Clinique* 31:153–160.
<https://pubmed.ncbi.nlm.nih.gov/11488226/>.

Benwell CSY, Davila-Pérez P, Fried PJ, Jones RN, Travison TG, Santarecchi E, Pascual-Leone A, Shafi MM (2020): EEG spectral power abnormalities and their relationship with cognitive dysfunction in patients with Alzheimer's disease and type 2 diabetes. *Neurobiol Aging* 85:83–95. <https://pubmed.ncbi.nlm.nih.gov/31727363/>.

Berger H (1929): Über das Elektrenkephalogramm des Menschen. *Arch Psychiatr Nervenkr* 87:527–570. <https://link.springer.com/article/10.1007/BF01797193>.

Berger H (1936): Über das Elektrenkephalogramm des Menschen - XI. Mitteilung. *Arch Psychiatr Nervenkr* 104:678–689. <https://link.springer.com/article/10.1007/BF01814250>.

Bergeron D, Gorno-Tempini ML, Rabinovici GD, Santos-Santos MA, Seeley W, Miller BL, Pijnenburg Y, Keulen MA, Groot C, van Berckel BNM, van der Flier WM, Scheltens P, Rohrer JD, Warren JD, Schott JM, Fox NC, Sanchez-Valle R, Grau-Rivera O, Gelpi E, Seelaar H, Papma JM, van Swieten JC, Hodges JR, Leyton CE, Piguet O, Rogalski EJ, Mesulam MM, Koric L, Nora K, Pariente J, Dickerson B, Mackenzie IR, Hsiung GYR, Belliard S, Irwin DJ, Wolk DA, Grossman M, Jones M, Harris J, Mann D, Snowden JS, Chrem-Mendez P, Calandri IL, Amengual AA, Miguet-Alfonsi C, Magnin E, Magnani G, Santangelo R, Deramecourt V, Pasquier F, Mattsson N, Nilsson C, Hansson O, Keith J, Masellis M, Black SE, Matías-Guiu JA, Cabrera-Martin MN, Paquet C, Dumurgier J, Teichmann M, Sarazin M, Bottlaender M, Dubois B, Rowe CC, Villemagne VL, Vandenberghe R, Granadillo E, Teng E, Mendez M, Meyer PT, Frings L, Lleó A, Blesa R, Fortea J, Seo SW, Diehl-Schmid J, Grimmer T, Frederiksen KS, Sánchez-Juan P, Chételat G, Jansen W, Bouchard RW, Laforce RJ, Visser PJ, Ossenkoppele R (2018): Prevalence of amyloid- β pathology in distinct variants of primary progressive aphasia. Ann Neurol 84:729–740.
<https://pubmed.ncbi.nlm.nih.gov/30255971/>.

Bernasconi F, Pagonabarraga J, Bejr-Kasem H, Martinez-Horta S, Marín-Lahoz J, Horta-Barba A, Kulisevsky J, Blanke O (2023): Theta oscillations and minor hallucinations in Parkinson's disease reveal decrease in frontal lobe functions and later cognitive decline. Nature Mental Health 2023 1:7 1:477–488. <https://www.nature.com/articles/s44220-023-00080-6>.

Bezrukavnikov O, Linder R (2021): A Neophyte With AutoML: Evaluating the Promises of Automatic Machine Learning Tools. <https://arxiv.org/abs/2101.05840v1>.

Bhattacharya S, Cauchois MBL, Iglesias PA, Chen ZS (2021): The impact of a closed-loop thalamocortical model on the spatiotemporal dynamics of cortical and thalamic traveling waves. Sci Rep 11:1–19. <https://www.nature.com/articles/s41598-021-93618-6>.

Bigdely-Shamlo N, Mullen T, Kothe C, Su K-M, Robbins KA (2015): The PREP pipeline: standardized preprocessing for large-scale EEG analysis. Front Neuroinform 9.
<http://journal.frontiersin.org/Article/10.3389/fninf.2015.00016/abstract>.

Bigdely-Shamlo N, Touryan J, Ojeda A, Kothe C, Mullen T, Robbins K (2020): Automated EEG mega-analysis I: Spectral and amplitude characteristics across studies. Neuroimage 207:116361.

Biundo R, Weis L, Antonini A (2016): Cognitive decline in Parkinson's disease: the complex picture. NPJ Parkinsons Dis 2:16018. [/pmc/articles/PMC5516581/](https://PMC5516581/).

Blacker D, Albert MS, Bassett SS, Rodney CP, Harrell LE, Folstein MF (1994): Reliability and Validity of NINCDS-ADRDA Criteria for Alzheimer's Disease: The National Institute of Mental Health Genetics Initiative. Arch Neurol 51:1198–1204.
<https://jamanetwork.com/journals/jamaneurology/fullarticle/593178>.

De Boer EMJ, Orie VK, Williams T, Baker MR, De Oliveira HM, Polvikoski T, Silsby M, Menon P, Van Den Bos M, Halliday GM, Van Den Berg LH, Van Den Bosch L, Van Damme P, Kiernan M, Van Es MA, Vucic S (2021): TDP-43 proteinopathies: a new wave of neurodegenerative diseases. J Neurol Neurosurg Psychiatry 92:86–95. <https://jnnp.bmjjournals.org/content/92/1/86>.

Bonanni L, Franciotti R, Nobili F, Kramberger MG, Taylor JP, Garcia-Ptacek S, Falasca NW, Famá F, Cromarty R, Onofrij M, Aarsland D (2016): EEG Markers of Dementia with Lewy Bodies: A Multicenter Cohort Study. Journal of Alzheimer's Disease 54:1649–1657.
<http://www.ncbi.nlm.nih.gov/pubmed/27589528>.

Bonanni L, Perfetti B, Bifolchetti S, Taylor JP, Franciotti R, Parnetti L, Thomas A, Onofrj M (2015): Quantitative electroencephalogram utility in predicting conversion of mild cognitive impairment to dementia with Lewy bodies. *Neurobiol Aging* 36:434. [/pmc/articles/PMC4270449/](https://www.ncbi.nlm.nih.gov/pmc/articles/PMC4270449/).

Bonanni L, Thomas A, Tiraboschi P, Perfetti B, Varanese S, Onofrj M, L B, A T, P T, B P, S V, M O (2008): EEG comparisons in early Alzheimer's disease, dementia with Lewy bodies and Parkinson's disease with dementia patients with a 2-year follow-up 131:690–705. <https://pubmed.ncbi.nlm.nih.gov/18202105/>.

Borghammer P, Horsager J, Andersen K, Van Den Berge N, Raunio A, Murayama S, Parkkinen L, Myllykangas L (2021): Neuropathological evidence of body-first vs. brain-first Lewy body disease. *Neurobiol Dis* 161:105557.

Briels CT, Briels CT, Schoonhoven DN, Schoonhoven DN, Stam CJ, De Waal H, Scheltens P, Gouw AA (2020): Reproducibility of EEG functional connectivity in Alzheimer's disease. *Alzheimers Res Ther* 12:1–14. <https://alzres.biomedcentral.com/articles/10.1186/s13195-020-00632-3>.

Brueggen K, Fiala C, Berger C, Ochmann S, Babiloni C, Teipel SJ (2017): Early changes in alpha band power and DMN BOLD activity in Alzheimer's disease: A simultaneous resting state EEG-fMRI study. *Front Aging Neurosci* 9:319.

Buzsáki G, Anastassiou CA, Koch C (2012): The origin of extracellular fields and currents — EEG, ECoG, LFP and spikes. *Nature Reviews Neuroscience* 2012 13:6 13:407–420. <https://www.nature.com/articles/nrn3241>.

Byeon SK, Madugundu AK, Garapati K, Ramarajan MG, Saraswat M, Kumar-M P, Hughes T, Shah R, Patnaik MM, Chia N, Ashrafzadeh-Kian S, Yao JD, Pritt BS, Cattaneo R, Salama ME, Zenka RM, Kipp BR, Grebe SKG, Singh RJ, Sadighi Akha AA, Algeciras-Schimnich A, Dasari S, Olson JE, Walsh JR, Venkatakrishnan AJ, Jenkinson G, O'Horo JC, Badley AD, Pandey A (2022): Development of a multiomics model for identification of predictive biomarkers for COVID-19 severity: a retrospective cohort study. *Lancet Digit Health* 4:e632–e645. <http://www.thelancet.com/article/S2589750022001121/fulltext>.

Calabrese EJ (2008): Neuroscience and Hormesis: Overview and General Findings. *Crit Rev Toxicol* 38:249–252. <https://www.tandfonline.com/doi/abs/10.1080/10408440801981957>.

Calabrese EJ, Mattson MP (2017): How does hormesis impact biology, toxicology, and medicine? *npj Aging and Mechanisms of Disease* 2017 3:1 3:1–8. <https://www.nature.com/articles/s41514-017-0013-z>.

Carmona Arroyave JA, Tobón Quintero CA, Suárez Revelo JJ, Ochoa Gómez JF, García YB, Gómez LM, Pineda Salazar DA (2019): Resting functional connectivity and mild cognitive impairment in Parkinson's disease. An electroencephalogram study. *Future Neurol* 14:FNL18. <https://www.futuremedicine.com/doi/10.2217/fnl-2018-0048>.

Caso F, Cursi M, Magnani G, Fanelli G, Falautano M, Comi G, Leocani L, Minicucci F (2012): Quantitative EEG and LORETA: valuable tools in discerning FTD from AD? *Neurobiol Aging* 33:2343–2356.

Cassani R, Estarellas M, San-Martin R, Fraga FJ, Falk TH (2018): Systematic review on resting-state EEG for Alzheimer's disease diagnosis and progression assessment. *Dis Markers* 2018.

- Castellanos NP, Makarov VA (2006): Recovering EEG brain signals: artifact suppression with wavelet enhanced independent component analysis. *J Neurosci Methods* 158:300–312.
[https://pubmed.ncbi.nlm.nih.gov/16828877/.](https://pubmed.ncbi.nlm.nih.gov/16828877/)
- Caviness JN, Hentz JG, Evidente VG, Driver-Dunckley E, Samanta J, Mahant P, Connor DJ, Sabbagh MN, Shill HA, Adler CH (2007): Both early and late cognitive dysfunction affects the electroencephalogram in Parkinson's disease. *Parkinsonism Relat Disord* 13:348–354.
- Caviness JN, Utianski RL, Hentz JG, Beach TG, Dugger BN, Shill HA, Driver-Dunckley ED, Sabbagh MN, Mehta S, Adler CH (2016a): Differential spectral quantitative electroencephalography patterns between control and Parkinson's disease cohorts. *Eur J Neurol* 23:387–392.
[http://www.ncbi.nlm.nih.gov/pubmed/26518336.](http://www.ncbi.nlm.nih.gov/pubmed/26518336)
- Caviness JN, Utianski RL, Hentz JG, Beach TG, Dugger BN, Shill HA, Driver-Dunckley ED, Sabbagh MN, Mehta S, Adler CH (2016b): Differential spectral quantitative electroencephalography patterns between control and Parkinson's disease cohorts. *Eur J Neurol* 23:387–392.
[https://onlinelibrary.wiley.com/doi/full/10.1111/ene.12878.](https://onlinelibrary.wiley.com/doi/full/10.1111/ene.12878)
- Chang J, Chang C (2023): Quantitative Electroencephalography Markers for an Accurate Diagnosis of Frontotemporal Dementia: A Spectral Power Ratio Approach. *Medicina* 2023, Vol 59, Page 2155 59:2155. [https://www.mdpi.com/1648-9144/59/12/2155/htm.](https://www.mdpi.com/1648-9144/59/12/2155/htm)
- Chatterjee A, Hirsch-Reinshagen V, Moussavi SA, Ducharme B, Mackenzie IR, Hsiung GYR (2021): Clinico-pathological comparison of patients with autopsy-confirmed Alzheimer's disease, dementia with Lewy bodies, and mixed pathology. *Alzheimer's & Dementia : Diagnosis, Assessment & Disease Monitoring* 13. [/pmc/articles/PMC8129858/](https://pmc/articles/PMC8129858/).
- Chatzikonstantinou S, McKenna J, Karantali E, Petridis F, Kazis D, Mavroudis I (2021): Electroencephalogram in dementia with Lewy bodies: a systematic review. *Aging Clinical and Experimental Research*. Springer. [https://link.springer.com/article/10.1007/s40520-020-01576-2.](https://link.springer.com/article/10.1007/s40520-020-01576-2)
- Chen CC, Hsu CY, Chiu HW, Hu CJ, Lee TC (2015): Frequency power and coherence of electroencephalography are correlated with the severity of Alzheimer's disease: A multicenter analysis in Taiwan. *Journal of the Formosan Medical Association* 114:729–735.
[http://www.ncbi.nlm.nih.gov/pubmed/23969043.](http://www.ncbi.nlm.nih.gov/pubmed/23969043)
- Cheng ST (2017): Dementia Caregiver Burden: a Research Update and Critical Analysis. *Curr Psychiatry Rep* 19. [/pmc/articles/PMC5550537/](https://pmc/articles/PMC5550537/).
- Chu KT, Lei WC, Wu MH, Fuh JL, Wang SJ, French IT, Chang WS, Chang CF, Huang NE, Liang WK, Juan CH (2023): A holo-spectral EEG analysis provides an early detection of cognitive decline and predicts the progression to Alzheimer's disease. *Front Aging Neurosci* 15:1195424.
- Collino S, Montoliu I, Martin FPJ, Scherer M, Mari D, Salvioli S, Bucci L, Ostan R, Monti D, Biagi E, Brigidi P, Franceschi C, Rezzi S (2013): Metabolic Signatures of Extreme Longevity in Northern Italian Centenarians Reveal a Complex Remodeling of Lipids, Amino Acids, and Gut Microbiota Metabolism. *PLoS One* 8:e56564.
[https://journals.plos.org/plosone/article?id=10.1371/journal.pone.0056564.](https://journals.plos.org/plosone/article?id=10.1371/journal.pone.0056564)
- Collura TF (1993): History and evolution of electroencephalographic instruments and techniques. *J Clin Neurophysiol* 10:476–504. <https://pubmed.ncbi.nlm.nih.gov/8308144/>.

Colom-Cadena M, Spires-Jones T, Zetterberg H, Blennow K, Caggiano A, Dekosky ST, Fillit H, Harrison JE, Schneider LS, Scheltens P, De Haan W, Grundman M, Van Dyck CH, Izzo NJ, Catalano SM (2020a): The clinical promise of biomarkers of synapse damage or loss in Alzheimer's disease. *Alzheimer's Research & Therapy* 2020 12:1 12:1–12.
<https://alzres.biomedcentral.com/articles/10.1186/s13195-020-00588-4>.

Colom-Cadena M, Spires-Jones T, Zetterberg H, Blennow K, Caggiano A, Dekosky ST, Fillit H, Harrison JE, Schneider LS, Scheltens P, De Haan W, Grundman M, Van Dyck CH, Izzo NJ, Catalano SM (2020b): The clinical promise of biomarkers of synapse damage or loss in Alzheimer's disease. *Alzheimer's Research and Therapy*. BioMed Central Ltd.

Conrad F, Mälzer M, Schwarzenberger M, Wiemer H, Ihlenfeldt S (2022): Benchmarking AutoML for regression tasks on small tabular data in materials design. *Sci Rep* 12:19350. /pmc/articles/PMC9652348/.

Costafreda SG (2009): Pooling fMRI data: Meta-analysis, mega-analysis and multi-center studies. *Front Neuroinform* 3:639.

Coughlan GT, Betthauser TJ, Boyle R, Koscik RL, Klinger HM, Chibnik LB, Jonaitis EM, Yau WYW, Wenzel A, Christian BT, Gleason CE, Saelzler UG, Properzi MJ, Schultz AP, Hanseeuw BJ, Manson JAE, Rentz DM, Johnson KA, Sperling R, Johnson SC, Buckley RF (2023): Association of Age at Menopause and Hormone Therapy Use With Tau and β -Amyloid Positron Emission Tomography. *JAMA Neurol* 80:462–473.
<https://jamanetwork.com/journals/jamaneurology/fullarticle/2802791>.

Cozac V V., Gschwandtner U, Hatz F, Hardmeier M, Rüegg S, Fuhr P (2016): Quantitative EEG and cognitive decline in Parkinson's disease. *Parkinsons Dis* 2016.

Crone EA, Steinbeis N (2017): Neural Perspectives on Cognitive Control Development during Childhood and Adolescence. *Trends Cogn Sci* 21:205–215.

Da-ano R, Masson I, Lucia F, Doré M, Robin P, Alfieri J, Rousseau C, Mervoyer A, Reinhold C, Castelli J, De Crevoisier R, Rameé JF, Pradier O, Schick U, Visvikis D, Hatt M (2020): Performance comparison of modified ComBat for harmonization of radiomic features for multicenter studies. *Sci Rep* 10:10. /pmc/articles/PMC7314795/.

Dauwels J, Srinivasan K, Ramasubba Reddy M, Musha T, Vialatte FB, Latchoumane C, Jeong J, Cichocki A (2011): Slowing and loss of complexity in Alzheimer's EEG: Two sides of the same coin? *Int J Alzheimers Dis*.

Delorme A (2023): EEG is better left alone. *Scientific Reports* 2023 13:1 13:1–12.
<https://www.nature.com/articles/s41598-023-27528-0>.

Donaghay PC, McKeith IG (2014): The clinical characteristics of dementia with Lewy bodies and a consideration of prodromal diagnosis. *Alzheimer's Research and Therapy*. BioMed Central. /pmc/articles/PMC4255387/.

Donoghue T, Dominguez J, Voytek B (2020a): Electrophysiological Frequency Band Ratio Measures Conflate Periodic and Aperiodic Neural Activity. *eNeuro* 7.
<https://www.eneuro.org/content/7/6/ENEURO.0192-20.2020>.

Donoghue T, Haller M, Peterson EJ, Varma P, Sebastian P, Gao R, Noto T, Lara AH, Wallis JD, Knight RT, Shestyuk A, Voytek B (2020b): Parameterizing neural power spectra into periodic and

aperiodic components. *Nature Neuroscience* 2020;23:1655–1665.
<https://www.nature.com/articles/s41593-020-00744-x>.

Dottori M, Sedenõ L, Martorell Caro M, Alifano F, Hesse E, Mikulan E, Garcíá AM, Ruiz-Tagle A, Lillo P, Slachevsky A, Serrano C, Fraiman D, Ibanez A (2017): Towards affordable biomarkers of frontotemporal dementia: A classification study via network's information sharing. *Sci Rep* 7.

Duan W, Chen X, Wang YJ, Zhao W, Yuan H, Lei X (2021): Reproducibility of power spectrum, functional connectivity and network construction in resting-state EEG. *J Neurosci Methods* 348:108985.

Dubois B, Feldman HH, Jacova C, Hampel H, Molinuevo JL, Blennow K, Dekosky ST, Gauthier S, Selkoe D, Bateman R, Cappa S, Crutch S, Engelborghs S, Frisoni GB, Fox NC, Galasko D, Habert MO, Jicha GA, Nordberg A, Pasquier F, Rabinovici G, Robert P, Rowe C, Salloway S, Sarazin M, Epelbaum S, de Souza LC, Vellas B, Visser PJ, Schneider L, Stern Y, Scheltens P, Cummings JL (2014): Advancing research diagnostic criteria for Alzheimer's disease: the IWG-2 criteria. *Lancet Neurol* 13:614–629. <https://pubmed.ncbi.nlm.nih.gov/24849862/>.

Dubois B, Villain N, Frisoni GB, Rabinovici GD, Sabbagh M, Cappa S, Bejanin A, Bombois S, Epelbaum S, Teichmann M, Habert MO, Nordberg A, Blennow K, Galasko D, Stern Y, Rowe CC, Salloway S, Schneider LS, Cummings JL, Feldman HH (2021): Clinical diagnosis of Alzheimer's disease: recommendations of the International Working Group. *Lancet Neurol* 20:484–496.

Duran-Aniotz C, Orellana P, Leon Rodriguez T, Henriquez F, Cabello V, Aguirre-Pinto MF, Escobedo T, Takada LT, Pina-Escudero SD, Lopez O, Yokoyama JS, Ibanez A, Parra MA, Slachevsky A (2021): Systematic Review: Genetic, Neuroimaging, and Fluids Biomarkers for Frontotemporal Dementia Across Latin America Countries. *Front Neurol* 12:663407.

Elahi FM, Miller BL (2017): A clinicopathological approach to the diagnosis of dementia. *Nat Rev Neurol* 13:457. [/pmc/articles/PMC5771416/](https://pmc/articles/PMC5771416/).

Engemann DA, Mellot A, Höchenberger R, Banville H, Sabbagh D, Gemein L, Ball T, Gramfort A (2022a): A reusable benchmark of brain-age prediction from M/EEG resting-state signals. *Neuroimage* 262. <https://pubmed.ncbi.nlm.nih.gov/35905809/>.

Engemann DA, Mellot A, Höchenberger R, Banville H, Sabbagh D, Gemein L, Ball T, Gramfort A (2022b): A reusable benchmark of brain-age prediction from M/EEG resting-state signals. *Neuroimage* 262:119521.

Engemann DA, Raimondo F, King JR, Rohaut B, Louppe G, Faugeras F, Annen J, Cassol H, Gosseries O, Fernandez-Slezak D, Laureys S, Naccache L, Dehaene S, Sitt JD (2018): Robust EEG-based cross-site and cross-protocol classification of states of consciousness. *Brain* 141:3179–3192. <https://dx.doi.org/10.1093/brain/awy251>.

Erickson N, Mueller J, Shirkov A, Zhang H, Larroy P, Li M, Smola A (2020): AutoGluon-Tabular: Robust and Accurate AutoML for Structured Data. <https://arxiv.org/abs/2003.06505v1>.

Fide E, Hünerli-Gündüz D, Öztura İ, Yener GG (2022): Hyperconnectivity matters in early-onset Alzheimer's disease: a resting-state EEG connectivity study. *Neurophysiologie Clinique* 52:459–471.

Finger EC (2016): Frontotemporal dementias. *CONTINUUM Lifelong Learning in Neurology*. Lippincott Williams and Wilkins.

Fladby T, Palhaugen L, Selnes P, Waterloo K, Brathen G, Hessen E, Almdahl IS, Arntzen KA, Auning E, Eliassen CF, Espenes R, Grambaite R, Grøntvedt GR, Johansen KK, Johnsen SH, Kalheim LF, Kirsebom BE, Muller KI, Nakling AE, Rongven A, Sando SB, Siafarikas N, Stav AL, Tecelao S, Timon S, Bekkelund SI, Aarsland D (2017): Detecting At-Risk Alzheimer's Disease Cases. *J Alzheimers Dis* 60:97–105. <https://pubmed.ncbi.nlm.nih.gov/28826181/>.

Fonseca LC, Tedrus GMAS, Letro GH, Bossoni AS (2009): Dementia, Mild Cognitive Impairment and Quantitative EEG in Patients with Parkinson's Disease. <https://doi.org/10.1177/155005940904000309> 40:168–172. <https://journals.sagepub.com/doi/10.1177/155005940904000309>.

Forchetti CM (2005): Treating Patients With Moderate to Severe Alzheimer's Disease: Implications of Recent Pharmacologic Studies. *Prim Care Companion J Clin Psychiatry* 7:155. /pmc/articles/PMC1192433/.

Fortin JP, Cullen N, Sheline YI, Taylor WD, Aselcioglu I, Cook PA, Adams P, Cooper C, Fava M, McGrath PJ, McInnis M, Phillips ML, Trivedi MH, Weissman MM, Shinohara RT (2018): Harmonization of cortical thickness measurements across scanners and sites. *Neuroimage* 167:104–120. <https://pubmed.ncbi.nlm.nih.gov/29155184/>.

Frahm-Falkenberg S, Ibsen R, Kjellberg J, Jennum P (2016): Health, social and economic consequences of dementias: a comparative national cohort study. *Eur J Neurol* 23:1400–1407. <https://pubmed.ncbi.nlm.nih.gov/27297659/>.

Franceschi C, Garagnani P, Morsiani C, Conte M, Santoro A, Grignolio A, Monti D, Capri M, Salvioli S (2018a): The continuum of aging and age-related diseases: Common mechanisms but different rates. *Front Med (Lausanne)* 5:349810.

Franceschi C, Garagnani P, Parini P, Giuliani C, Santoro A (2018b): Inflammaging: a new immune–metabolic viewpoint for age-related diseases. *Nature Reviews Endocrinology* 2018 14:10 14:576–590. <https://www.nature.com/articles/s41574-018-0059-4>.

Franciotti R, Pilotto A, Moretti D V., Falasca NW, Arnaldi D, Taylor JP, Nobili F, Kramberger M, Ptacek SG, Padovani A, Aarlsand D, Onofrj M, Bonanni L (2020): Anterior EEG slowing in dementia with Lewy bodies: a multicenter European cohort study. *Neurobiol Aging* 93:55–60. <https://linkinghub.elsevier.com/retrieve/pii/S0197458020301433>.

Gao R, Peterson EJ, Voytek B (2017): Inferring synaptic excitation/inhibition balance from field potentials. *Neuroimage* 158:70–78. <https://pubmed.ncbi.nlm.nih.gov/28676297/>.

García-Prete FJ, Suárez-Relevo JX, Aguilón-Niño DF, Lopera-Restrepo FJ, Ochoa-Gómez JF, Tobón-Quintero CA (2022): Automatic Classification of Subjects of the PSEN1-E280A Family at Risk of Developing Alzheimer's Disease Using Machine Learning and Resting State Electroencephalography. *Journal of Alzheimer's Disease* 87:817–832.

Garn H, Coronel C, Waser M, Caravias G, Ransmayr G (2017): Differential diagnosis between patients with probable Alzheimer's disease, Parkinson's disease dementia, or dementia with Lewy bodies and frontotemporal dementia, behavioral variant, using quantitative electroencephalographic features. *J Neural Transm* 124:569. /pmc/articles/PMC5399050/.

Gaubert S, Houot M, Raimondo F, Ansart M, Corsi MC, Naccache L, Sitt JD, Habert MO, Dubois B, De Vico Fallani F, Durrleman S, Epelbaum S (2021): A machine learning approach to screen for preclinical Alzheimer's disease. *Neurobiol Aging* 105:205–216.

Gaubert S, Raimondo F, Houot M, Corsi MC, Naccache L, Sitt JD, Hermann B, Oudiette D, Gagliardi G, Habert MO, Dubois B, De Vico Fallani F, Bakardjian H, Epelbaum S (2019): EEG evidence of compensatory mechanisms in preclinical Alzheimer's disease. *Brain* 142:2096–2112. <https://pubmed.ncbi.nlm.nih.gov/31211359/>.

Gauthier S, Zhang H, Ng KP, Pascoal TA, Rosa-Neto P (2018): Impact of the biological definition of Alzheimer's disease using amyloid, tau and neurodegeneration (ATN): what about the role of vascular changes, inflammation, Lewy body pathology? *Transl Neurodegener* 7. /pmc/articles/PMC5977549/.

George JS, Strunk J, Mak-Mccully R, Houser M, Poizner H, Aron AR (2013): Dopaminergic therapy in Parkinson's disease decreases cortical beta band coherence in the resting state and increases cortical beta band power during executive control. *Neuroimage Clin* 3:261–270. /pmc/articles/PMC3814961/.

Geraedts VJ, Boon LI, Marinus J, Gouw AA, Van Hilten JJ, Stam CJ, Tannemaat MR, Contarino MF (2018): Clinical correlates of quantitative EEG in Parkinson disease: A systematic review. *Neurology*. <http://www.ncbi.nlm.nih.gov/pubmed/30291182>.

Gerster M, Waterstraat G, Litvak V, Lehnertz K, Schnitzler A, Florin E, Curio G, Nikulin V (2022): Separating Neural Oscillations from Aperiodic 1/f Activity: Challenges and Recommendations. *Neuroinformatics* 20:991–1012. <https://link.springer.com/article/10.1007/s12021-022-09581-8>.

Gil Ávila C, Bott FS, Tiemann L, Hohn VD, May ES, Nickel MM, Zebhauser PT, Gross J, Ploner M (2023): DISCOVER-EEG: an open, fully automated EEG pipeline for biomarker discovery in clinical neuroscience. *Scientific Data* 2023 10:1 10:1–14. <https://www.nature.com/articles/s41597-023-02525-0>.

Gilbert DL, Sethuraman G, Kotagal U, Buncher CR (2003): Meta-analysis of EEG test performance shows wide variation among studies. *Neurology* 60:564–570.

Gimenez-Aparisi G, Guijarro-Estelles E, Chornet-Lurbe A, Ballesta-Martinez S, Pardo-Hernandez M, Ye-Lin Y (2023): Early detection of Parkinson's disease: Systematic analysis of the influence of the eyes on quantitative biomarkers in resting state electroencephalography. *Heliyon* 9:e20625.

Goetz CG (2011): The History of Parkinson's Disease: Early Clinical Descriptions and Neurological Therapies. *Cold Spring Harb Perspect Med* 1. /pmc/articles/PMC3234454/.

Goh C, Hamadicharef B, Henderson GT, Ifeachor EC, Goh C, Hamadicharef B, Henderson GT, Ifeachor EC (2005): Comparison of Fractal Dimension Algorithms for the Computation of EEG Biomarkers for Dementia. In: . 2nd International Conference on Computational Intelligence in Medicine and Healthcare (CIMED2005). Lisbon. <https://inria.hal.science/inria-00442374>.

Gordillo D, Ramos da Cruz J, Moreno D, Garobbio S, Herzog MH (2023): Do we really measure what we think we are measuring? *iScience* 26. /pmc/articles/PMC9947309/.

Gouw AA, Stam CJ (2016): Electroencephalography in the Differential Diagnosis of Dementia. *Epileptologie* 33:173–182. https://www.epi.ch/wp-content/uploads/Artikel-Gouw_E_3_16.pdf.

- Gramfort A, Luessi M, Larson E, Engemann DA, Strohmeier D, Brodbeck C, Goj R, Jas M, Brooks T, Parkkonen L, Hämäläinen M (2013): MEG and EEG data analysis with MNE-Python. *Front Neurosci* 0:267.
- Granatiero V, Manfredi G (2019): Mitochondrial Transport and Turnover in the Pathogenesis of Amyotrophic Lateral Sclerosis. *Biology* 2019, Vol 8, Page 36 8:36. <https://www.mdpi.com/2079-7737/8/2/36/htm>.
- Grimbert F, Faugeras O (2006): Analysis of Jansen's model of a single cortical column. *Neural Comput.* Vol. 18. <https://inria.hal.science/file/index/docid/70410/filename/RR-5597.pdf>.
- Gudmundsson S, Runarsson TP, Sigurdsson S, Eiriksdottir G, Johnsen K (2007): Reliability of quantitative EEG features. *Clinical Neurophysiology* 118:2162–2171. <https://linkinghub.elsevier.com/retrieve/pii/S1388245707002994>.
- Gustavsson A, Norton N, Fast T, Frölich L, Georges J, Holzapfel D, Kirabali T, Krolak-Salmon P, Rossini PM, Ferretti MT, Lanman L, Chadha AS, van der Flier WM (2023): Global estimates on the number of persons across the Alzheimer's disease continuum. *Alzheimer's & Dementia* 19:658–670. <https://onlinelibrary.wiley.com/doi/full/10.1002/alz.12694>.
- Haas LF (2003): Hans Berger (1873–1941), Richard Caton (1842–1926), and electroencephalography. *J Neurol Neurosurg Psychiatry* 74:9–9. <https://jnnp.bmjjournals.org/content/74/1/9>.
- Habich A, Wahlund LO, Westman E, Dierks T, Ferreira D (2023): (Dis-)Connected Dots in Dementia with Lewy Bodies—A Systematic Review of Connectivity Studies. *Movement Disorders* 38:4–15. <https://onlinelibrary.wiley.com/doi/full/10.1002/mds.29248>.
- Hag A, Handayani D, Pillai T, Mantoro T, Kit MH, Al-Shargie F (2021): EEG Mental Stress Assessment Using Hybrid Multi-Domain Feature Sets of Functional Connectivity Network and Time-Frequency Features. *Sensors* 2021, Vol 21, Page 6300 21:6300. <https://www.mdpi.com/1424-8220/21/18/6300/htm>.
- Halgren M, Ulbert I, Bastuji H, Fabó D, Eross L, Rey M, Devinsky O, Doyle WK, Mak-McCully R, Halgren E, Wittner L, Chauvel P, Heit G, Eskandar E, Mandell A, Cash SS (2019): The generation and propagation of the human alpha rhythm. *Proc Natl Acad Sci U S A* 116:23772–23782. <https://www.pnas.org/doi/abs/10.1073/pnas.1913092116>.
- Hampel H, Lista S, Neri C, Vergallo A (2019): Time for the systems-level integration of aging: Resilience enhancing strategies to prevent Alzheimer's disease. *Prog Neurobiol* 181. <https://pubmed.ncbi.nlm.nih.gov/31351912/>.
- Han Q, Xiao X, Wang S, Qin W, Yu C, Liang M (2023): Characterization of the effects of outliers on ComBat harmonization for removing inter-site data heterogeneity in multisite neuroimaging studies. *Front Neurosci* 17:1146175. <https://www.frontiersin.org/articles/10.3389/fnins.2023.1146175/full>.
- Harada CN, Natelson Love MC, Triebel KL (2013): Normal Cognitive Aging. *Clin Geriatr Med* 29:737. [/pmc/articles/PMC4015335/](https://pmc.ncbi.nlm.nih.gov/PMC4015335/).
- Harding RJ, Bermudez P, Bernier A, Beauvais M, Bellec P, Hill S, Karakuzu A, Knoppers BM, Pavlidis P, Poline JB, Roskams J, Stikov N, Stone J, Strother S, Evans AC (2023): The Canadian Open Neuroscience Platform—An open science framework for the neuroscience community. *PLoS Comput Biol* 19. [/pmc/articles/PMC10374086/](https://pmc.ncbi.nlm.nih.gov/PMC10374086/).

Hatlestad-Hall C (2022): SRM Resting-state EEG - OpenNeuro. OpenNeuro.

<https://openneuro.org/datasets/ds003775/versions/1.2.1>.

Hatlestad-Hall C, Rygvold TW, Andersson S (2022a): BIDS-structured resting-state electroencephalography (EEG) data extracted from an experimental paradigm. Data Brief 45.

Hatlestad-Hall C, Rygvold TW, Andersson S (2022b): BIDS-structured resting-state electroencephalography (EEG) data extracted from an experimental paradigm. Data Brief 45:108647.

Hayashi S, Caron BA, Heinsfeld AS, Vinci-Booher S, McPherson B, Bullock DN, Bertò G, Niso G, Hanekamp S, Levitas D, Ray K, MacKenzie A, Kitchell L, Leong JK, Nascimento-Silva F, Koudoro S, Willis H, Jolly JK, Pisner D, Zuidema TR, Kurzawski JW, Mikellidou K, Bussalb A, Rorden C, Victory C, Bhatia D, Aydogan DB, Yeh F-CF, Delogu F, Guaje J, Veraart J, Bollman S, Stewart A, Fischer J, Faskowitz J, Chaumon M, Fabrega R, Hunt D, McKee S, Brown ST, Heyman S, Iacobella V, Mejia AF, Marinazzo D, Craddock RC, Olivetti E, Hanson JL, Avesani P, Garyfallidis E, Stanzione D, Carson J, Henschel R, Hancock DY, Stewart CA, Schnyer D, Eke DO, Poldrack RA, George N, Bridge H, Sani I, Freiwald WA, Puce A, Port NL, Pestilli F (2023): brainlife.io: A decentralized and open source cloud platform to support neuroscience research.
<http://arxiv.org/abs/2306.02183>.

He BJ (2014): Scale-free brain activity: past, present, and future. Trends Cogn Sci 18:480–487.
<https://pubmed.ncbi.nlm.nih.gov/24788139/>.

He W, Donoghue T, Sowman PF, Seymour RA, Brock J, Crain S, Voytek B, Hillebrand A (2019): Co-Increasing Neuronal Noise and Beta Power in the Developing Brain. bioRxiv:839258.
<https://www.biorxiv.org/content/10.1101/839258v1>.

Hebling Vieira B, Liem F, Dadi K, Engemann DA, Gramfort A, Bellec P, Craddock RC, Damoiseaux JS, Steele CJ, Yarkoni T, Langer N, Margulies DS, Varoquaux G (2022): Predicting future cognitive decline from non-brain and multimodal brain imaging data in healthy and pathological aging. Neurobiol Aging 118:55–65. <https://pubmed.ncbi.nlm.nih.gov/35878565/>.

Hendriks S, Peetoom K, Bakker C, Van Der Flier WM, Papma JM, Koopmans R, Verhey FRJ, De Vugt M, Köhler S, Withall A, Parlevliet JL, Uysal-Bozkir Ö, Gibson RC, Neita SM, Nielsen TR, Salem LC, Nyberg J, Lopes MA, Dominguez JC, De Guzman MF, Egeberg A, Radford K, Broe T, Subramaniam M, Abdin E, Bruni AC, Di Lorenzo R, Smith K, Flicker L, Mol MO, Basta M, Yu D, Masika G, Petersen MS, Ruano L (2021): Global Prevalence of Young-Onset Dementia: A Systematic Review and Meta-analysis. JAMA Neurol 78:1080–1090.
<https://jamanetwork.com/journals/jamaneurology/fullarticle/2781919>.

Hill AT, Clark GM, Bigelow FJ, Lum JAG, Enticott PG (2022): Periodic and aperiodic neural activity displays age-dependent changes across early-to-middle childhood. Dev Cogn Neurosci 54:101076.

Hinchliffe C, Yogarajah M, Elkommos S, Tang H, Abasolo D (2022): Entropy Measures of Electroencephalograms towards the Diagnosis of Psychogenic Non-Epileptic Seizures. Entropy 24. [/pmc/articles/PMC9601450/](https://pmc/articles/PMC9601450/).

Hjorth B (1970): EEG analysis based on time domain properties. Electroencephalogr Clin Neurophysiol 29:306–310.

Hock EM, Polymenidou M (2016a): Prion-like propagation as a pathogenic principle in frontotemporal dementia. *J Neurochem* 138:163–183.
<https://onlinelibrary.wiley.com/doi/full/10.1111/jnc.13668>.

Hock EM, Polymenidou M (2016b): Prion-like propagation as a pathogenic principle in frontotemporal dementia. *J Neurochem* 138 Suppl 1:163–183.
<https://pubmed.ncbi.nlm.nih.gov/27502124/>.

Hogan DB, Jetté N, Fiest KM, Roberts JI, Pearson D, Smith EE, Roach P, Kirk A, Pringsheim T, Maxwell CJ (2016): The Prevalence and Incidence of Frontotemporal Dementia: a Systematic Review. *Canadian Journal of Neurological Sciences* 43:S96–S109.
<https://www.cambridge.org/core/journals/canadian-journal-of-neurological-sciences/article/prevalence-and-incidence-of-frontotemporal-dementia-a-systematic-review/F9B6DDFC2310DB4E02A500DD0A3A9263>.

Horng H, Singh A, Yousefi B, Cohen EA, Haghghi B, Katz S, Noël PB, Kontos D, Shinohara RT (2022): Improved generalized ComBat methods for harmonization of radiomic features. *Sci Rep* 12.
<https://pubmed.ncbi.nlm.nih.gov/36348002/>.

Hu F, Chen AA, Horng H, Bashyam V, Davatzikos C, Alexander-Bloch A, Li M, Shou H, Satterthwaite TD, Yu M, Shinohara RT (2023): Image harmonization: A review of statistical and deep learning methods for removing batch effects and evaluation metrics for effective harmonization. *Neuroimage* 274:120125.

Huang C, Wahlund LO, Dierks T, Julin P, Winblad B, Jelic V (2000): Discrimination of Alzheimer's disease and mild cognitive impairment by equivalent EEG sources: A cross-sectional and longitudinal study. *Clinical Neurophysiology* 111:1961–1967.
<https://pubmed.ncbi.nlm.nih.gov/11068230/>.

Isaza VH, Castro VC, Saldarriaga LZ, Mantilla-Ramos Y, Quintero CT, Suarez-Revelo J, Gómez JO (2023): Tackling EEG test-retest reliability with a pre-processing pipeline based on ICA and wavelet-ICA. *Authorea Preprints*. <https://www.authorea.com/users/624863/articles/647023-tackling-eeg-test-retest-reliability-with-a-pre-processing-pipeline-based-on-ica-and-wavelet-ica>.

Iturria-Medina Y, Sotero RC, Toussaint PJ, Mateos-Pérez JM, Evans AC, Weiner MW, Aisen P, Petersen R, Jack CR, Jagust W, Trojanowski JQ, Toga AW, Beckett L, Green RC, Saykin AJ, Morris J, Shaw LM, Khachaturian Z, Sorensen G, Kuller L, Raichle M, Paul S, Davies P, Fillit H, Hefti F, Holtzman D, Mesulam MM, Potter W, Snyder P, Schwartz A, Montine T, Thomas RG, Donohue M, Walter S, Gessert D, Sather T, Jiminez G, Harvey D, Bernstein M, Fox N, Thompson P, Schuff N, Borowski B, Gunter J, Senjem M, Vemuri P, Jones D, Kantarci K, Ward C, Koeppen RA, Foster N, Reiman EM, Chen K, Mathis C, Landau S, Cairns NJ, Householder E, Taylor-Reinwald L, Lee V, Korecka M, Figurski M, Crawford K, Neu S, Foroud TM, Potkin S, Shen L, Faber K, Kim S, Nho K, Thal L, Buckholtz N, Albert M, Frank R, Hsiao J, Kaye J, Quinn J, Lind B, Carter R, Dolen S, Schneider LS, Pawluczyk S, Beccera M, Teodoro L, Spann BM, Brewer J, Vanderswag H, Fleisher A, Heidebrink JL, Lord JL, Mason SS, Albers CS, Knopman D, Johnson K, Doody RS, Villanueva-Meyer J, Chowdhury M, Rountree S, Dang M, Stern Y, Honig LS, Bell KL, Ances B, Carroll M, Leon S, Mintun MA, Schneider S, Oliver A, Marson D, Griffith R, Clark D, Geldmacher D, Brockington J, Roberson E, Grossman H, Mitsis E, De Toledo-Morrell L, Shah RC, Duara R, Varon D, Greig MT, Roberts P, Albert M, Onyike C, D'Agostino D, Kielb S, Galvin JE, Cerbone B, Michel CA, Rusinek H, De Leon MJ, Glodzik L, De Santi S, Doraiswamy PM, Petrella JR, Wong TZ, Arnold

SE, Karlawish JH, Wolk D, Smith CD, Jicha G, Hardy P, Sinha P, Oates E, Conrad G, Lopez OL, Oakley M, Simpson DM, Porsteinsson AP, Goldstein BS, Martin K, Makino KM, Ismail MS, Brand C, Mulnard RA, Thai G, Mc-Adams-Ortiz C, Womack K, Mathews D, Quiceno M, Diaz-Arrastia R, King R, Weiner M, Martin-Cook K, DeVous M, Levey AI, Lah JJ, Cellar JS, Burns JM, Anderson HS, Swerdlow RH, Apostolova L, Tingus K, Woo E, Silverman DHS, Lu PH, Bartzokis G, Graff-Radford NR, Parfitt F, Kendall T, Johnson H, Farlow MR, Hake A, Matthews BR, Herring S, Hunt C, Van Dyck CH, Carson RE, MacAvoy MG, Chertkow H, Bergman H, Hosein C, Black S, Stefanovic B, Caldwell C, Hsiung GYR, Feldman H, Mudge B, Assaly M, Kertesz A, Rogers J, Bernick C, Munic D, Kerwin D, Mesulam MM, Lipowski K, Wu CK, Johnson N, Sadowsky C, Martinez W, Villena T, Turner RS, Johnson K, Reynolds B, Sperling RA, Johnson KA, Marshall G, Frey M, Lane B, Rosen A, Tinklenberg J, Sabbagh MN, Belden CM, Jacobson SA, Sirrel SA, Kowall N, Killiany R, Budson AE, Norbash A, Johnson PL, Allard J, Lerner A, Ogrocki P, Hudson L, Fletcher E, Carmichael O, Olichney J, DeCarli C, Kittur S, Borrie M, Lee TY, Bartha R, Johnson S, Asthana S, Carlsson CM, Potkin SG, Preda A, Nguyen D, Tariot P, Reeder S, Bates V, Capote H, Rainka M, Scharre DW, Kataki M, Adeli A, Zimmerman EA, Celmins D, Brown AD, Pearlson GD, Blank K, Anderson K, Santulli RB, Kitzmiller TJ, Schwartz ES, Sink KM, Williamson JD, Garg P, Watkins F, Ott BR, Querfurth H, Tremont G, Salloway S, Malloy P, Correia S, Rosen HJ, Miller BL, Mintzer J, Spicer K, Bachman D, Finger E, Pasternak S, Rachinsky I, Drost D, Pomara N, Hernando R, Sarrael A, Schultz SK, Ponto LLB, Shim H, Smith KE, Relkin N, Chaing G, Raudin L, Smith A, Fargher K, Raj BA, Neylan T, Grafman J, Davis M, Morrison R, Hayes J, Finley S, Friedl K, Fleischman D, Arfanakis K, James O, Massoglia D, Fruehling JJ, Harding S, Peskind ER, Petrie EC, Li G, Yesavage JA, Taylor JL, Furst AJ (2016): Early role of vascular dysregulation on late-onset Alzheimer's disease based on multifactorial data-driven analysis. *Nature Communications* 2016 7:1 7:1–14. <https://www.nature.com/articles/ncomms11934>.

Jack CR, Bennett DA, Blennow K, Carrillo MC, Feldman HH, Frisoni GB, Hampel H, Jagust WJ, Johnson KA, Knopman DS, Petersen RC, Scheltens P, Sperling RA, Dubois B (2016): A/T/N: An unbiased descriptive classification scheme for Alzheimer disease biomarkers. *Neurology*. Lippincott Williams and Wilkins. [/pmc/articles/PMC4970664/?report=abstract](https://pmc/articles/PMC4970664/?report=abstract).

Jack CR, Knopman DS, Jagust WJ, Petersen RC, Weiner MW, Aisen PS, Shaw LM, Vemuri P, Wiste HJ, Weigand SD, Lesnick TG, Pankratz VS, Donohue MC, Trojanowski JQ (2013): Tracking pathophysiological processes in Alzheimer's disease: an updated hypothetical model of dynamic biomarkers. *Lancet Neurol* 12:207–216. <https://pubmed.ncbi.nlm.nih.gov/23332364/>.

Jackson N, Cole SR, Voytek B, Swann NC (2019): Characteristics of waveform shape in Parkinson's disease detected with scalp electroencephalography. *eNeuro* 6. <https://www.eneuro.org/content/6/3/ENEURO.0151-19.2019>.

Jacobs HIL, Radua J, Lückmann HC, Sack AT (2013): Meta-analysis of functional network alterations in Alzheimer's disease: toward a network biomarker. *Neurosci Biobehav Rev* 37:753–765. <https://pubmed.ncbi.nlm.nih.gov/23523750/>.

Jaotombo F, Adorni L, Ghattas B, Boyer L (2023): Finding the best trade-off between performance and interpretability in predicting hospital length of stay using structured and unstructured data. *PLoS One* 18:e0289795. <https://pubmed.ncbi.nlm.nih.gov/38032876/>.

Jaramillo-Jimenez A, Suarez-Revelo JX, Ochoa-Gomez JF, Carmona Arroyave JA, Bocanegra Y, Lopera F, Buriticá O, Pineda-Salazar DA, Moreno Gómez L, Tobón Quintero CA, Borda MG, Bonanni L, Fytche DH, Brønnick K, Aarsland D (2021): Resting-state EEG alpha/theta ratio related to

- neuropsychological test performance in Parkinson's Disease. *Clinical Neurophysiology* 132:756–764. <https://pubmed.ncbi.nlm.nih.gov/33571883/>.
- Jaramillo-Jimenez A, Tovar-Rios DA, Ospina JA, Mantilla-Ramos YJ, Loaiza-López D, Henao Isaza V, Zapata Saldarriaga LM, Cadavid Castro V, Suarez-Revelo JX, Bocanegra Y, Lopera F, Pineda-Salazar DA, Tobón Quintero CA, Ochoa-Gomez JF, Borda MG, Aarsland D, Bonanni L, Brønnick K (2023): Spectral features of resting-state EEG in Parkinson's Disease: A multicenter study using functional data analysis. *Clin Neurophysiol* 151:28–40. <https://pubmed.ncbi.nlm.nih.gov/37146531/>.
- Jas M, Engemann DA, Bekhti Y, Raimondo F, Gramfort A (2017): Autoreject: Automated artifact rejection for MEG and EEG data. *Neuroimage* 159:417–429.
- Jellinger KA, Attems J (2008): Prevalence and impact of vascular and Alzheimer pathologies in Lewy body disease. *Acta Neuropathol* 115:427–436. <https://link.springer.com/article/10.1007/s00401-008-0347-5>.
- Jellinger KA, Korczyn AD (2018): Are dementia with Lewy bodies and Parkinson's disease dementia the same disease? *BMC Med* 16. <https://pubmed.ncbi.nlm.nih.gov/29510692/>.
- Jennekens FGI (2014): A short history of the notion of neurodegenerative disease. *J Hist Neurosci* 23:85–94. <https://pubmed.ncbi.nlm.nih.gov/24512132/>.
- Jiao B, Li R, Zhou H, Qing K, Liu H, Pan H, Lei Y, Fu W, Wang X, Xiao X, Liu X, Yang Q, Liao X, Zhou Y, Fang L, Dong Y, Yang Y, Jiang H, Huang S, Shen L (2023): Neural biomarker diagnosis and prediction to mild cognitive impairment and Alzheimer's disease using EEG technology. *Alzheimers Res Ther* 15:1–14. <https://alzres.biomedcentral.com/articles/10.1186/s13195-023-01181-1>.
- Jin L, Nawaz H, Ono K, Nowell J, Haley E, Berman BD, Mukhopadhyay ND, Barrett MJ (2023): One Minute of EEG Data Provides Sufficient and Reliable Data for Identifying Lewy Body Dementia. *Alzheimer Dis Assoc Disord* 37:66–72. <https://pubmed.ncbi.nlm.nih.gov/36413637/>.
- Johnson WE, Li C, Rabinovic A (2007): Adjusting batch effects in microarray expression data using empirical Bayes methods. *Biostatistics* 8:118–127. <https://pubmed.ncbi.nlm.nih.gov/16632515/>.
- Jovicich J, Barkhof F, Babiloni C, Herholz K, Mulert C, van Berckel BNM, Frisoni GB (2019): Harmonization of neuroimaging biomarkers for neurodegenerative diseases: A survey in the imaging community of perceived barriers and suggested actions. *Alzheimer's & Dementia : Diagnosis, Assessment & Disease Monitoring* 11:69. [/pmc/articles/PMC6816469/](https://pmc/articles/PMC6816469/).
- Julin P, Wahlund LO, Basun H, Persson A, Måre K, Rudberg U (1995): Clinical diagnosis of frontal lobe dementia and Alzheimer's disease: relation to cerebral perfusion, brain atrophy and electroencephalography. *Dementia* 6:142–147. <https://pubmed.ncbi.nlm.nih.gov/7620526/>.
- Kamboj N, Metcalfe K, Chu CH, Conway A (2023): Predicting Blood Pressure After Nitroglycerin Infusion Dose Titration in Critical Care Units: A Multicenter Retrospective Study. *Comput Inform Nurs*. <https://pubmed.ncbi.nlm.nih.gov/38112619/>.
- Karekal A, Stuart S, Mancini M, Swann NC (2023): Elevated Gaussian-modeled beta power in the cortex characterizes aging, but not Parkinson's disease. *J Neurophysiol* 129:1086–1093. <https://journals.physiology.org/doi/10.1152/jn.00480.2022>.

- Keil A, Bernat EM, Cohen MX, Ding M, Fabiani M, Gratton G, Kappenman ES, Maris E, Mathewson KE, Ward RT, Weisz N (2022): Recommendations and publication guidelines for studies using frequency domain and time-frequency domain analyses of neural time series. *Psychophysiology* 59:e14052. [/pmc/articles/PMC9717489/](https://PMC9717489/).
- Keller SM, Gschwandtner U, Meyer A, Chaturvedi M, Roth V, Fuhr P (2020): Cognitive decline in Parkinson's disease is associated with reduced complexity of EEG at baseline. *Brain Commun* 2. [/pmc/articles/PMC7749793/](https://PMC7749793/).
- Kertesz A (2007): Pick complex--historical introduction. *Alzheimer Dis Assoc Disord* 21. <https://pubmed.ncbi.nlm.nih.gov/18090424/>.
- Khoury R, Ghossoub E (2019): Diagnostic biomarkers of Alzheimer's disease: A state-of-the-art review. *Biomark Neuropsychiatry* 1:100005.
- Kinge JM, Dieleman JL, Karlstad Ø, Knudsen AK, Klitkou ST, Hay SI, Vos T, Murray CJL, Vollset SE (2023): Disease-specific health spending by age, sex, and type of care in Norway: a national health registry study. *BMC Med* 21:1–14. <https://bmcmedicine.biomedcentral.com/articles/10.1186/s12916-023-02896-6>.
- Klietz M (2022): Caregiver Burden in Movement Disorders and Neurodegenerative Diseases: Editorial. *Brain Sci* 12. [/pmc/articles/PMC9497330/](https://PMC9497330/).
- Klimesch W (1999): EEG alpha and theta oscillations reflect cognitive and memory performance: a review and analysis. *Brain Res Brain Res Rev* 29:169–195. <https://pubmed.ncbi.nlm.nih.gov/10209231/>.
- Klimesch W, Sauseng P, Hanslmayr S (2007): EEG alpha oscillations: The inhibition-timing hypothesis. *Brain Res Rev* 53:63–88.
- Klonowski W (2009): Everything you wanted to ask about EEG but were afraid to get the right answer. *Nonlinear Biomed Phys* 3:2. [/pmc/articles/PMC2698918/](https://PMC2698918/).
- Koelewijn L, Lancaster TM, Linden D, Dima DC, Routley BC, Magazzini L, Barawi K, Brindley L, Adams R, Tansey KE, Bompas A, Tales A, Bayer A, Singh K (2019): Oscillatory hyperactivity and hyperconnectivity in young APOE-ε4 carriers and hypoconnectivity in alzheimer's disease. *Elife* 8.
- Kopčanová M, Tait L, Donoghue T, Stothart G, Smith L, Sandoval AAF, Davila-Perez P, Buss S, Shafi MM, Pascual-Leone A, Fried PJ, Benwell CSY (2023): Resting-state EEG signatures of Alzheimer's disease are driven by periodic but not aperiodic changes. *bioRxiv*. [/pmc/articles/PMC10312609/](https://PMC10312609/).
- Kosaka K (2014): Lewy body disease and dementia with Lewy bodies. *Proc Jpn Acad Ser B Phys Biol Sci* 90:301. [/pmc/articles/PMC4275567/](https://PMC4275567/).
- Kottlarz I, Berg S, Toscano-Tejeida D, Steinmann I, Bähr M, Luther S, Wilke M, Parlitz U, Schlemmer A (2020): Extracting Robust Biomarkers From Multichannel EEG Time Series Using Nonlinear Dimensionality Reduction Applied to Ordinal Pattern Statistics and Spectral Quantities. *Front Physiol* 11:614565. [/pmc/articles/PMC7882607/](https://PMC7882607/).
- Kropotov JD (2016): Alpha Rhythms. *Functional Neuromarkers for Psychiatry*:89–105.

Kurbatskaya A, Jaramillo-Jimenez A, Fredy Ochoa-Gomez J, Brønnick K, Fernandez-Quilez A (2023a): Machine Learning-Based Detection of Parkinson's Disease From Resting-State EEG: A Multi-Center Study. ArXiv.

Kurbatskaya A, Jaramillo-Jimenez A, Ochoa-Gomez JF, Brønnick K, Fernandez-Quilez A (2023b): Assessing gender fairness in EEG-based machine learning detection of Parkinson's disease: A multi-center study:1020–1024. <https://arxiv.org/abs/2303.06376v1>.

Lai M, Demuru M, Hillebrand A, Fraschini M (2018): A comparison between scalp- and source-reconstructed EEG networks. *Sci Rep* 8. [/pmc/articles/PMC6095906/](https://pmc/articles/PMC6095906/).

Lantero-Rodriguez J, Vrillon A, Fernández-Lebrero A, Ortiz-Romero P, Snellman A, Montoliu-Gaya L, Brum WS, Cognat E, Dumurgier J, Puig-Pijoan A, Navalpotro-Gómez I, García-Escobar G, Karikari TK, Vanmechelen E, Ashton NJ, Zetterberg H, Suárez-Calvet M, Paquet C, Blennow K (2023): Clinical performance and head-to-head comparison of CSF p-tau235 with p-tau181, p-tau217 and p-tau231 in two memory clinic cohorts. *Alzheimers Res Ther* 15:1–15. <https://alzres.biomedcentral.com/articles/10.1186/s13195-023-01201-0>.

Larson MJ, Carbine KA (2017): Sample size calculations in human electrophysiology (EEG and ERP) studies: A systematic review and recommendations for increased rigor. *International Journal of Psychophysiology* 111:33–41. <https://linkinghub.elsevier.com/retrieve/pii/S0167876016301180>.

Lashgari E, Liang D, Maoz U (2020): Data augmentation for deep-learning-based electroencephalography. *J Neurosci Methods* 346. <https://pubmed.ncbi.nlm.nih.gov/32745492/>.

Lau ZJ, Pham T, Chen SHA, Makowski D (2022): Brain entropy, fractal dimensions and predictability: A review of complexity measures for EEG in healthy and neuropsychiatric populations. *Eur J Neurosci* 56:5047. [/pmc/articles/PMC9826422/](https://pmc/articles/PMC9826422/).

Law ZK, Todd C, Mehraram R, Schumacher J, Baker MR, LeBeau FEN, Yarnall A, Onofrj M, Bonanni L, Thomas A, Taylor JP (2020): The role of EEG in the diagnosis, prognosis and clinical correlations of dementia with Lewy bodies—a systematic review. *Diagnostics. Multidisciplinary Digital Publishing Institute (MDPI)*. [/pmc/articles/PMC7555753/](https://pmc/articles/PMC7555753/).

Leithner D, Schöder H, Haug A, Vargas HA, Gibbs P, Häggström I, Rausch I, Weber M, Becker AS, Schwartz J, Mayerhoefer ME (2022): Impact of ComBat Harmonization on PET Radiomics-Based Tissue Classification: A Dual-Center PET/MRI and PET/CT Study. *J Nucl Med* 63:1611–1616. <https://pubmed.ncbi.nlm.nih.gov/35210300/>.

Lenkala S, Marry R, Gopovaram SR, Akinci TC, Topsakal O (2023): Comparison of Automated Machine Learning (AutoML) Tools for Epileptic Seizure Detection Using Electroencephalograms (EEG). *Computers 2023, Vol 12, Page 197* 12:197. <https://www.mdpi.com/2073-431X/12/10/197/htm>.

Li A, Feitelberg J, Saini AP, Höchenberger R, Scheltienne M (2022a): MNE-ICALabel: Automatically annotating ICA components with ICLLabel in Python. *J Open Source Softw* 7:4484. <https://joss.theoj.org/papers/10.21105/joss.04484>.

Li M, Wang Y, Lopez-Naranjo C, Hu S, Reyes RCG, Paz-Linares D, Areces-Gonzalez A, Hamid AIA, Evans AC, Savostyanov AN, Calzada-Reyes A, Villringer A, Tobon-Quintero CA, Garcia-Agustin D, Yao D, Dong L, Aubert-Vazquez E, Reza F, Razzaq FA, Omar H, Abdullah JM, Galler JR, Ochoa-

Gomez JF, Prichep LS, Galan-Garcia L, Morales-Chacon L, Valdes-Sosa MJ, Tröndle M, Zulkifly MFM, Abdul Rahman MR Bin, Milakhina NS, Langer N, Rudych P, Koenig T, Virues-Alba TA, Lei X, Bringas-Vega ML, Bosch-Bayard JF, Valdes-Sosa PA (2022b): Harmonized-Multinational qEEG norms (HarMNqEEG). *Neuroimage* 256:119190.

Light GA, Swerdlow NR, Thomas ML, Calkins ME, Green MF, Greenwood TA, Gur RE, Gur RC, Lazzeroni LC, Nuechterlein KH, Pela M, Radant AD, Seidman LJ, Sharp RF, Siever LJ, Silverman JM, Srock J, Stone WS, Sugar CA, Tsuang DW, Tsuang MT, Braff DL, Turetsky BI (2015): Validation of mismatch negativity and P3a for use in multi-site studies of schizophrenia: characterization of demographic, clinical, cognitive, and functional correlates in COGS-2. *Schizophr Res* 163:63–72. <https://pubmed.ncbi.nlm.nih.gov/25449710/>.

Lin C-Y, Guo S-M, Lien J-JJ, Lin W-T, Liu Y-S, Lai C-H, Hsu I-L, Chang C-C, Tseng Y-L (2023): Combined model integrating deep learning, radiomics, and clinical data to classify lung nodules at chest CT. *Radiol Med.* <https://pubmed.ncbi.nlm.nih.gov/37971691/>.

Lindau M, Jelic V, Johansson SE, Andersen C, Wahlund LO, Almkvist O (2003): Quantitative EEG abnormalities and cognitive dysfunctions in frontotemporal dementia and Alzheimer's disease. *Dement Geriatr Cogn Disord* 15:106–114.

Litvan I, Goldman JG, Tröster AI, Schmand BA, Weintraub D, Petersen RC, Mollenhauer B, Adler CH, Marder K, Williams-Gray CH, Aarsland D, Kulisevsky J, Rodriguez-Oroz MC, Burn DJ, Barker RA, Emre M (2012): Diagnostic criteria for mild cognitive impairment in Parkinson's disease: Movement Disorder Society Task Force guidelines. *Movement Disorders* 27:349–356. [/pmc/articles/PMC3641655/?report=abstract](https://pmc/articles/PMC3641655/?report=abstract).

Liu J, Du Y, Wang X, Yue W, Feng J (2022): Automated Machine Learning for Epileptic Seizure Detection Based on EEG Signals. *Computers, Materials & Continua* 73:1995–2011. <https://www.techscience.com/cmc/v73n1/47863/html>.

Liu L, Zhang R, Shi D, Li R, Wang Q, Feng Y, Lu F, Zong Y, Xu X (2023): Automated machine learning to predict the difficulty for endoscopic resection of gastric gastrointestinal stromal tumor. *Front Oncol* 13:1190987. [/pmc/articles/PMC10206233/](https://pmc/articles/PMC10206233/).

Livingston G, Huntley J, Sommerlad A, Ames D, Ballard C, Banerjee S, Brayne C, Burns A, Cohen-Mansfield J, Cooper C, Costafreda SG, Dias A, Fox N, Gitlin LN, Howard R, Kales HC, Kivimäki M, Larson EB, Oggunniyi A, Orgeta V, Ritchie K, Rockwood K, Sampson EL, Samus Q, Schneider LS, Selbæk G, Teri L, Mukadam N (2020): Dementia prevention, intervention, and care: 2020 report of the Lancet Commission. *The Lancet* 396:413–446. <http://www.thelancet.com/article/S0140673620303676/fulltext>.

Llinás RR, Ribary U, Jeanmonod D, Kronberg E, Mitra PP (1999): Thalamocortical dysrhythmia: A neurological and neuropsychiatric syndrome characterized by magnetoencephalography. *Proc Natl Acad Sci U S A* 96:15222–15227. www.pnas.org.

Llinás RR, Steriade M (2006): Bursting of thalamic neurons and states of vigilance. *J Neurophysiol* 95:3297–3308. <https://journals.physiology.org/doi/10.1152/jn.00166.2006>.

Logroscino G, Piccininni M, Graff C, Hardiman O, Ludolph AC, Moreno F, Otto M, Remes AM, Rowe JB, Seelaar H, Solje E, Stefanova E, Traykov L, Jelic V, Rydell MT, Pender N, Anderl-Straub S, Barandiaran M, Gabilondo A, Krüger J, Murley AG, Rittman T, Ende EL van der, Swieten JC van, Hartikainen P, Stojmenović GM, Mehrabian S, Benussi L, Alberici A, Dell'Abate MT, Zecca C,

Borroni B, group F, Belezhanska D, Bianchetti A, Binetti G, Cotelli M, Cotelli MS, Dreherova I, Filardi M, Fostinelli S, Ghidoni R, Gnoni V, Nacheva G, Novaković I, Padovani A, Popivanov I, Raycheva M, Stockton K, Stoyanova K, Suhonen N-M, Tainta M, Toncheva D, Urso D, Zlatareva D, Zulaica M (2023): Incidence of Syndromes Associated With Frontotemporal Lobar Degeneration in 9 European Countries. *JAMA Neurol* 80:279–286.
<https://jamanetwork.com/journals/jamaneurology/fullarticle/2800415>.

Lopes Da Silva F (2010): EEG: Origin and measurement. *EEG - fMRI: Physiological Basis, Technique, and Applications*:19–38. https://link.springer.com/chapter/10.1007/978-3-540-87919-0_2.

López-Sanz D, Brunã R, Garcés P, Camara C, Serrano N, Rodríguez-Rojo IC, Delgado ML, Montenegro M, López-Higes R, Yus M, Maestú F (2016): Alpha band disruption in the AD-continuum starts in the Subjective Cognitive Decline stage: a MEG study. *Scientific Reports* 2016 6:1 6:1–11.
<https://www.nature.com/articles/srep37685>.

Lundberg SM, Lee SI (2017): A Unified Approach to Interpreting Model Predictions. *Adv Neural Inf Process Syst* 2017–December:4766–4775. <https://arxiv.org/abs/1705.07874v2>.

Lyketsos CG, Lopez O, Jones B, Fitzpatrick AL, Breitner J, Dekosky S (2002): Prevalence of Neuropsychiatric Symptoms in Dementia and Mild Cognitive Impairment: Results From the Cardiovascular Health Study. *JAMA* 288:1475–1483.
<https://jamanetwork.com/journals/jama/fullarticle/195320>.

Maestú F, de Haan W, Busche MA, DeFelipe J (2021): Neuronal excitation/inhibition imbalance: core element of a translational perspective on Alzheimer pathophysiology. *Ageing Res Rev* 69:101372.

Mantilla-Ramos Y-J (2023): sovabids: A python package for the automatic conversion of EEG datasets to the BIDS standard, with a focus on making the most out of metadata.
<https://github.com/yjmantilla/sovabids>.

Maresova P, Hruska J, Klimova B, Barakovic S, Krejcar O (2020): Activities of Daily Living and Associated Costs in the Most Widespread Neurodegenerative Diseases: A Systematic Review. *Clin Interv Aging* 15:1841. [/pmc/articles/PMC7538005/](https://pmc/articles/PMC7538005/).

Maserejian N, Vinikoor-Imler L, Dilley A (2020): Estimation of the 2020 Global Population of Parkinson's Disease (PD) [abstract]. *Mov Disord*.
<https://www.mdsabstracts.org/abstract/estimation-of-the-2020-global-population-of-parkinsons-disease-pd/>.

Massa F, Meli R, Grazzini M, Famà F, De Carli F, Filippi L, Arnaldi D, Pardini M, Morbelli S, Nobili F (2020): Utility of quantitative EEG in early Lewy body disease. *Parkinsonism Relat Disord* 75:70–75. <https://pubmed.ncbi.nlm.nih.gov/32480310/>.

McBride JC, Zhao X, Munro NB, Smith CD, Jicha GA, Hively L, Broster LS, Schmitt FA, Kryscio RJ, Jiang Y (2014): Spectral and complexity analysis of scalp EEG characteristics for mild cognitive impairment and early Alzheimer's disease. *Comput Methods Programs Biomed* 114:153–163.

McDonald WM (2017): Overview of Neurocognitive Disorders. *Focus: Journal of Life Long Learning in Psychiatry* 15:4. [/pmc/articles/PMC6519631/](https://pmc/articles/PMC6519631/).

McKeith IG, Boeve BF, Dickson DW, Halliday G, Taylor JP, Weintraub D, Aarsland D, Galvin J, Attems J, Ballard CG, Bayston A, Beach TG, Blanc F, Bohnen N, Bonanni L, Bras J, Brundin P, Burn D,

Chen-Plotkin A, Duda JE, El-Agnaf O, Feldman H, Ferman TJ, Ffytche D, Fujishiro H, Galasko D, Goldman JG, Gomperts SN, Graff-Radford NR, Honig LS, Iranzo A, Kantarci K, Kaufer D, Kukull W, Lee VMY, Leverenz JB, Lewis S, Lippa C, Lunde A, Masellis M, Masliah E, McLean P, Mollenhauer B, Montine TJ, Moreno E, Mori E, Murray M, O'Brien JT, Orimo S, Postuma RB, Ramaswamy S, Ross OA, Salmon DP, Singleton A, Taylor A, Thomas A, Tiraboschi P, Toledo JB, Trojanowski JQ, Tsuang D, Walker Z, Yamada M, Kosaka K (2017): Diagnosis and management of dementia with Lewy bodies. *Neurology*. *Neurology*. <https://pubmed.ncbi.nlm.nih.gov/28592453/>.

McKeith IG, Ferman TJ, Thomas AJ, Blanc F, Boeve BF, Fujishiro H, Kantarci K, Muscio C, O'Brien JT, Postuma RB, Aarsland D, Ballard C, Bonanni L, Donaghy P, Emre M, Galvin JE, Galasko D, Goldman JG, Gomperts SN, Honig LS, Ikeda M, Leverenz JB, Lewis SJG, Marder KS, Masellis M, Salmon DP, Taylor JP, Tsuang DW, Walker Z, Tiraboschi P (2020): Research criteria for the diagnosis of prodromal dementia with Lewy bodies. *Neurology*. *Neurology*. <https://pubmed.ncbi.nlm.nih.gov/32241955/>.

McKeown DJ, Jones M, Pihl C, Finley A, Kelley N, Baumann O, Schinazi VR, Moustafa AA, Cavanagh JF, Angus DJ (2023): Medication-invariant resting aperiodic and periodic neural activity in Parkinson's disease. *Psychophysiology* 00:e14478. <https://onlinelibrary.wiley.com/doi/full/10.1111/psyp.14478>.

McKhann G, Drachman D, Folstein M, Katzman R, Price D, Stadlan EM (1984): Clinical diagnosis of alzheimer's disease: Report of the NINCDS-ADRDA work group* under the auspices of department of health and human services task force on alzheimer's disease. *Neurology* 34:939–944.

McKhann GM, Knopman DS, Chertkow H, Hyman BT, Jack CR, Kawas CH, Klunk WE, Koroshetz WJ, Manly JJ, Mayeux R, Mohs RC, Morris JC, Rossor MN, Scheltens P, Carrillo MC, Thies B, Weintraub S, Phelps CH (2011): The diagnosis of dementia due to Alzheimer's disease: Recommendations from the National Institute on Aging-Alzheimer's Association workgroups on diagnostic guidelines for Alzheimer's disease. *Alzheimer's & Dementia* 7:263–269. <https://onlinelibrary.wiley.com/doi/full/10.1016/j.jalz.2011.03.005>.

Meeter LH, Kaat LD, Rohrer JD, Van Swieten JC (2017): Imaging and fluid biomarkers in frontotemporal dementia. *Nature Reviews Neurology* 2017 13:7 13:406–419. <https://www.nature.com/articles/nrneurol.2017.75>.

Meghdadi AH, Karic MS, McConnell M, Rupp G, Richard C, Hamilton J, Salat D, Berka C (2021): Resting state EEG biomarkers of cognitive decline associated with Alzheimer's disease and mild cognitive impairment. *PLoS One* 16. <https://pubmed.ncbi.nlm.nih.gov/33544703/>.

Mehraram R, Kaiser M, Cromarty R, Graziadio S, O'Brien JT, Killen A, Taylor JP, Peraza LR (2020): Weighted network measures reveal differences between dementia types: An EEG study. *Hum Brain Mapp* 41:1573. [/pmc/articles/PMC7267959/](https://pmc/articles/PMC7267959/).

Melnik A, Legkov P, Izdebski K, Kärcher SM, Hairston WD, Ferris DP, König P (2017): Systems, subjects, sessions: To what extent do these factors influence EEG data? *Front Hum Neurosci* 11:245570.

Menšíková K, Matěj R, Colosimo C, Rosales R, Tučková L, Ehrmann J, Hraboš D, Kolaříková K, Vodička R, Vrtěl R, Procházka M, Nevrly M, Kaiserová M, Kurčová S, Otruba P, Kaňovský P (2022): Lewy

body disease or diseases with Lewy bodies? *npj Parkinson's Disease* 2022 8:1 8:1–11.
<https://www.nature.com/articles/s41531-021-00273-9>.

Merkin A, Sghirripa S, Graetz L, Smith AE, Hordacre B, Harris R, Pitcher J, Semmler J, Rogasch NC, Goldsworthy M (2021): Age differences in aperiodic neural activity measured with resting EEG. *bioRxiv*:2021.08.31.458328. <https://www.biorxiv.org/content/10.1101/2021.08.31.458328v1>.

Merkin A, Sghirripa S, Graetz L, Smith AE, Hordacre B, Harris R, Pitcher J, Semmler J, Rogasch NC, Goldsworthy M (2023): Do age-related differences in aperiodic neural activity explain differences in resting EEG alpha? *Neurobiol Aging* 121:78–87.

Mhyre TR, Boyd JT, Hamill RW, Maguire-Zeiss KA (2012): Parkinson's disease. *Subcell Biochem* 65:389–455. [/pmc/articles/PMC4372387/?report=abstract](https://PMC4372387/?report=abstract).

Miljevic A, Bailey NW, Vila-Rodriguez F, Herring SE, Fitzgerald PB (2022): Electroencephalographic Connectivity: A Fundamental Guide and Checklist for Optimal Study Design and Evaluation. *Biol Psychiatry Cogn Neurosci Neuroimaging* 7:546–554.

Miltiadous A, Tzimourta KD, Afrantou T, Ioannidis P, Grigoriadis N, Tsaliakakis DG, Angelidis P, Tsipouras MG, Glavas E, Giannakeas N, Tzallas AT (2023): A Dataset of Scalp EEG Recordings of Alzheimer's Disease, Frontotemporal Dementia and Healthy Subjects from Routine EEG. *Data* 2023, Vol 8, Page 95 8:95. <https://www.mdpi.com/2306-5729/8/6/95/htm>.

Modir A, Shamekhi S, Ghaderyan P (2023): A systematic review and methodological analysis of EEG-based biomarkers of Alzheimer's disease. *Measurement* 220:113274.

Moezzi B, Hordacre B, Berryman C, Ridding MC, Goldsworthy MR (2018): Test-retest reliability of functional brain network characteristics using resting-state EEG and graph theory. *bioRxiv*:385302. <https://www.biorxiv.org/content/10.1101/385302v1>.

Moguilner S, Birba A, Fittipaldi S, Gonzalez-Campo C, Tagliazucchi E, Reyes P, Matallana D, Parra MA, Slachevsky A, Farías G, Cruzat J, García A, Eyre HA, La Joie R, Rabinovici G, Whelan R, Ibáñez A (2022): Multi-feature computational framework for combined signatures of dementia in underrepresented settings. *J Neural Eng* 19:046048.
<https://iopscience.iop.org/article/10.1088/1741-2552/ac87d0>.

Mohanty R, Sethares WA, Nair VA, Prabhakaran V (2020): Rethinking Measures of Functional Connectivity via Feature Extraction. *Scientific Reports* 2020 10:1 10:1–17.
<https://www.nature.com/articles/s41598-020-57915-w>.

Moretti D V. (2015): Theta and alpha EEG frequency interplay in subjects with mild cognitive impairment: evidence from EEG, MRI, and SPECT brain modifications. *Front Aging Neurosci* 7. [/pmc/articles/PMC4396516/](https://PMC4396516/).

Moretti D V, Babiloni C, Binetti G, Cassetta E, Dal Forno G, Ferreric F, Ferri R, Lanuzza B, Miniussi C, Nobili F, Rodriguez G, Salinari S, Rossini PM (2004): Individual analysis of EEG frequency and band power in mild Alzheimer's disease. *Clinical Neurophysiology* 115:299–308.
<http://www.ncbi.nlm.nih.gov/pubmed/14744569>.

Moretti D V., Paternicò D, Binetti G, Zanetti O, Frisoni GB (2013): EEG upper/low alpha frequency power ratio relates to temporo-parietal brain atrophy and memory performances in mild cognitive impairment. *Front Aging Neurosci* 5:65285.

- Mouton A, Blanc F, Gros A, Manera V, Fabre R, Sauleau E, Gomez-Luporsi I, Tifratene K, Friedman L, Thümmler S, Pradier C, Robert PH, David R (2018): Sex ratio in dementia with Lewy bodies balanced between Alzheimer's disease and Parkinson's disease dementia: a cross-sectional study. *Alzheimers Res Ther* 10. /pmc/articles/PMC6136211/.
- Müller EJ, Munn B, Hearne LJ, Smith JB, Fulcher B, Arnatkevičiūtė A, Lurie DJ, Cocchi L, Shine JM (2020): Core and matrix thalamic sub-populations relate to spatio-temporal cortical connectivity gradients. *Neuroimage* 222:117224.
- Müller EJ, Munn BR, Redinbaugh MJ, Lizier J, Breakspear M, Saalmann YB, Shine JM (2023): The non-specific matrix thalamus facilitates the cortical information processing modes relevant for conscious awareness. *Cell Rep* 42:112844.
- Munn BR, Müller EJ, Medel V, Naismith SL, Lizier JT, Sanders RD, Shine JM (2023): Neuronal connected burst cascades bridge macroscale adaptive signatures across arousal states. *Nature Communications* 2023 14:1 14:1–17. <https://www.nature.com/articles/s41467-023-42465-2>.
- Musigmann M, Akkurt BH, Krähling H, Nacul NG, Remonda L, Sartoretti T, Henssen D, Brokinkel B, Stummer W, Heindel W, Mannil M (2022): Testing the applicability and performance of Auto ML for potential applications in diagnostic neuroradiology. *Sci Rep* 12. <https://pubmed.ncbi.nlm.nih.gov/35953588/>.
- Nandi A, Counts N, Chen S, Seligman B, Tortorice D, Vigo D, Bloom DE (2022): Global and regional projections of the economic burden of Alzheimer's disease and related dementias from 2019 to 2050: A value of statistical life approach. *EClinicalMedicine* 51:101580. <http://www.thelancet.com/article/S2589537022003108/fulltext>.
- Narayanan Lab (2020): Datasets. <https://narayanan.lab.uiowa.edu/article/datasets>.
- Nardone R, Sebastianelli L, Versace V, Saltuari L, Lochner P, Frey V, Golaszewski S, Brigo F, Trinka E, Höller Y (2018): Usefulness of EEG Techniques in Distinguishing Frontotemporal Dementia from Alzheimer's Disease and Other Dementias. *Dis Markers* 2018. /pmc/articles/PMC6140274/.
- Nedelska Z, Schwarz CG, Lesnick TG, Boeve BF, Przybelski SA, Lowe VJ, Kremers WK, Gunter JL, Senjem ML, Graff-Radford J, Ferman TJ, Fields JA, Knopman DS, Petersen RC, Jack CR, Kantarci K (2019): Association of Longitudinal β -Amyloid Accumulation Determined by Positron Emission Tomography With Clinical and Cognitive Decline in Adults With Probable Lewy Body Dementia. *JAMA Netw Open* 2:e1916439–e1916439. <https://jamanetwork.com/journals/jamanetworkopen/fullarticle/2756108>.
- Neto E, Allen EA, Auriel H, Nordby H, Eichele T (2015): EEG spectral features discriminate between Alzheimer's and vascular dementia. *Front Neurol* 6:108906.
- Newson JJ, Thiagarajan TC (2019): EEG Frequency Bands in Psychiatric Disorders: A Review of Resting State Studies. *Frontiers in Human Neuroscience*. Frontiers Media S.A. /pmc/articles/PMC6333694/.
- Nguyen-Danse DA, Singaravelu S, Chauvigné LAS, Mottaz A, Allaman L, Guggisberg AG (2021): Feasibility of Reconstructing Source Functional Connectivity with Low-Density EEG. *Brain Topogr* 34:709. /pmc/articles/PMC8556201/.

Nichols E, Abd-Allah F, Abdoli A, Abosetugn AE, Abrha WA, Abualhasan A, Abu-Gharbieh E, Akinyemi RO, Alahdab F, Alanezi FM, Alipour V, Ansari I, Arabloo J, Ashraf-Ganjouei A, Avan A, Ayano G, Babar ZUD, Baig AA, Banach M, Barboza MA, Barker-Collo SL, Baune BT, Srikanth Bhagavathula A, Bhattacharyya K, Bijani A, Biondi A, Birhan TA, Biswas A, Bolla SR, Boloor A, Brayne C, Brenner H, Burkart K, Burns RA, Nagaraja SB, Carvalho F, Castro-De-araujo LFS, Catalá-López F, Cerin E, Cernigliaro A, Cherbuin N, Jasmine Choi JY, Chu DT, Dagnew B, Dai X, Dandona L, Dandona R, Diaz D, Dibaji Forooshani ZS, Douiri A, Duncan BB, Edvardsson D, El-Jaafary SI, Eskandari K, Eskandarieh S, Feigin VL, Fereshtehnejad SM, Fernandes E, Ferrara P, Filip I, Fischer F, Gaidhane S, Gebregzabiher KZ, Ghashghaei A, Gholamian A, Gnedovskaya E V., Golechha M, Gupta R, Hachinski V, Hamidi S, Hankey GJ, Haro JM, Hassan A, Hay SI, Heidari G, Heidari-Soureshjani R, Househ M, Hussain R, Hwang BF, Ilic IM, Ilic MD, Naghibi Irvani SS, Iso H, Iwagami M, Jha RP, Kalani R, Kandel H, Karch A, Kasa AS, Kengne AP, Kim YE, Kim YJ, Kisa S, Kisa A, Kivimäki M, Komaki H, Aikoyanagi, Kukull WA, Kumar GA, Kumar M, Landires I, Leonardi M, Lim SS, Liu X, Logroscino G, Lopez AD, Lorkowski S, Loy CT, Amin HIM, Manafi N, Manjunatha N, Mehndiratta MM, Menezes RG, Meretoja A, Merkin A, Metekiya WM, Misganaw AT, Mohajer B, Ibrahim NM, Mohammad Y, Mohapatra A, Mohebi F, Mokdad AH, Mondello S, Mossie TB, Mulugeta A, Nagel G, Naveed M, Nayak VC, Kandel SN, Nguyen SH, Nguyen HLT, Nuñez-Samudio V, Ogbo FA, Olagunju AT, Orru H, Ostojic SM, Ostroff SM, Otstavnov N, Otstavnov SS, Owolabi MO, Pathak M, Toroudi HP, Peterson CB, Pham HQ, Phillips MR, Piradov MA, Pottoo FH, Prada SI, Angga Pribadi DR, Radfar A, Raggi A, Rahim F, Ram P, Rana J, Rashedi V, Rawaf S, Rawaf DL, Reinig N, Rezaei N, Robinson SR, Romoli M, Sachdev PS, Sahathevan R, Sahebkar A, Sahraian MA, Sattin D, Saylan M, Sayyah M, Schiavolin S, Schmidt MI, Shahid I, Shaikh MA, Shigematsu M, Shin J II, Shiri R, Siddiqi TJ, Silva JP, Singh JA, Soheili A, Spurlock EE, Szoke CEI, Tabarés-Seisdedos R, Taddele BW, Thakur B, Thekke Purakkal AS, Tovani-Palone MR, Tran BX, Travillian RS, Tripathi M, Tsegaye GW, Usman MS, Vacante M, Velazquez DZ, Venketasubramanian N, Vidale S, Vlassov V, Wang YP, Wei J, Weiss J, Weldenariam AH, Wimo A, Wu C, Yadollahpour A, Yamagishi K, Yesilita YG, Yonemoto N, Zadey S, Zhang ZJ, Murray CJL, Vos T (2021): Global mortality from dementia: Application of a new method and results from the Global Burden of Disease Study 2019. *Alzheimer's & Dementia: Translational Research & Clinical Interventions* 7:e12200.

<https://onlinelibrary.wiley.com/doi/full/10.1002/trc2.12200>.

Nichols E, Steinmetz JD, Vollset SE, Fukutaki K, Chalek J, Abd-Allah F, Abdoli A, Abualhasan A, Abu-Gharbieh E, Akram TT, Al Hamad H, Alahdab F, Alanezi FM, Alipour V, Almustanyir S, Amu H, Ansari I, Arabloo J, Ashraf T, Astell-Burt T, Ayano G, Ayuso-Mateos JL, Baig AA, Barnett A, Barrow A, Baune BT, Béjot Y, Bezabhe WMM, Bezabih YM, Bhagavathula AS, Bhaskar S, Bhattacharyya K, Bijani A, Biswas A, Bolla SR, Boloor A, Brayne C, Brenner H, Burkart K, Burns RA, Cámera LA, Cao C, Carvalho F, Castro-de-Araujo LFS, Catalá-López F, Cerin E, Chavan PP, Cherbuin N, Chu DT, Costa VM, Couto RAS, Dadras O, Dai X, Dandona L, Dandona R, De la Cruz-Góngora V, Dhamnetiya D, Dias da Silva D, Diaz D, Douiri A, Edvardsson D, Ekholuenetale M, El Sayed I, El-Jaafary SI, Eskandari K, Eskandarieh S, Esmaeilnejad S, Fares J, Faro A, Farooque U, Feigin VL, Feng X, Fereshtehnejad SM, Fernandes E, Ferrara P, Filip I, Fillit H, Fischer F, Gaidhane S, Galluzzo L, Ghashghaei A, Ghith N, Gianni A, Gilani SA, Glavan IR, Gnedovskaya E V., Golechha M, Gupta R, Gupta VB, Gupta VK, Haider MR, Hall BJ, Hamidi S, Hanif A, Hankey GJ, Haque S, Hartono RK, Hasaballah AI, Hasan MT, Hassan A, Hay SI, Hayat K, Hegazy MI, Heidari G, Heidari-Soureshjani R, Herteliu C, Househ M, Hussain R, Hwang BF, Iacoviello L, Iavicoli I, Ilesanmi OS, Ilic IM, Ilic MD, Irvani SSN, Iso H, Iwagami M, Jabbarinejad R, Jacob L, Jain V, Jayapal SK, Jayawardena R, Jha RP, Jonas JB, Joseph N, Kalani R, Kandel A, Kandel H, Karch A,

Kasa AS, Kassie GM, Keshavarz P, Khan MA, Khatib MN, Khoja TAM, Khubchandani J, Kim MS, Kim YJ, Kisa A, Kisa S, Kivimäki M, Koroshetz WJ, Koyanagi A, Kumar GA, Kumar M, Lak HM, Leonardi M, Li B, Lim SS, Liu X, Liu Y, Logroscino G, Lorkowski S, Lucchetti G, Lutzky Saute R, Magnani FG, Malik AA, Massano J, Mehndiratta MM, Menezes RG, Meretoja A, Mohajer B, Mohamed Ibrahim N, Mohammad Y, Mohammed A, Mokdad AH, Mondello S, Moni MAA, Moniruzzaman M, Mossie TB, Nagel G, Naveed M, Nayak VC, Neupane Kandel S, Nguyen TH, Oancea B, Otstavnov N, Otstavnov SS, Owolabi MO, Panda-Jonas S, Pashazadeh Kan F, Pasovic M, Patel UK, Pathak M, Peres MFP, Perianayagam A, Peterson CB, Phillips MR, Pinheiro M, Piradov MA, Pond CD, Potashman MH, Pottor FH, Prada SI, Radfar A, Raggi A, Rahim F, Rahman M, Ram P, Ranasinghe P, Rawaf DL, Rawaf S, Rezaei N, Rezapour A, Robinson SR, Romoli M, Roshandel G, Sahathevan R, Sahebkar A, Sahraian MA, Sathian B, Sattin D, Sawhney M, Saylan M, Schiavolin S, Seylani A, Sha F, Shaikh MA, Shaji KS, Shannawaz M, Shetty JK, Shigematsu M, Shin J II, Shiri R, Silva DAS, Silva JP, Silva R, Singh JA, Skryabin VY, Skryabina AA, Smith AE, Soshnikov S, Spurlock EE, Stein DJ, Sun J, Tabarés-Seisdedos R, Thakur B, Timalsina B, Tovani-Palone MR, Tran BX, Tsegaye GW, Valadan Tahbaz S, Valdez PR, Venketasubramanian N, Vlassov V, Vu GT, Vu LG, Wang YP, Wimo A, Winkler AS, Yadav L, Yahyazadeh Jabbari SH, Yamagishi K, Yang L, Yano Y, Yonemoto N, Yu C, Yunusa I, Zadey S, Zastrozhin MS, Zastrozhina A, Zhang ZJ, Murray CJL, Vos T (2022): Estimation of the global prevalence of dementia in 2019 and forecasted prevalence in 2050: an analysis for the Global Burden of Disease Study 2019. *Lancet Public Health* 7:e105–e125.
<http://www.thelancet.com/article/S2468266721002498/fulltext>.

Nichols E, Vos T (2021): The estimation of the global prevalence of dementia from 1990-2019 and forecasted prevalence through 2050: An analysis for the Global Burden of Disease (GBD) study 2019. *Alzheimer's & Dementia* 17:e051496.
<https://onlinelibrary.wiley.com/doi/full/10.1002/alz.051496>.

van Nifterick AM, Mulder D, Duineveld DJ, Diachenko M, Scheltens P, Stam CJ, van Kesteren RE, Linkenkaer-Hansen K, Hillebrand A, Gouw AA (2023): Resting-state oscillations reveal disturbed excitation–inhibition ratio in Alzheimer's disease patients. *Scientific Reports* 2023 13:1 13:1–13. <https://www.nature.com/articles/s41598-023-33973-8>.

Nishida K, Yoshimura M, Isotani T, Yoshida T, Kitaura Y, Saito A, Mii H, Kato M, Takekita Y, Suwa A, Morita S, Kinoshita T (2011): Differences in quantitative EEG between frontotemporal dementia and Alzheimer's disease as revealed by LORETA. *Clin Neurophysiol* 122:1718–1725.
<https://pubmed.ncbi.nlm.nih.gov/21396882/>.

Niso G, Botvinik-Nezer R, Appelhoff S, De La Vega A, Esteban O, Etzel JA, Finc K, Ganz M, Gau R, Halchenko YO, Herholz P, Karakuza A, Keator DB, Markiewicz CJ, Maumet C, Pernet CR, Pestilli F, Queder N, Schmitt T, Sójka W, Wagner AS, Whitaker KJ, Rieger JW (2022): Open and reproducible neuroimaging: From study inception to publication. *Neuroimage* 263:119623. [/pmc/articles/PMC10008521/](https://pmc/articles/PMC10008521/).

Nobukawa S, Yamanishi T, Nishimura H, Wada Y, Kikuchi M, Takahashi T (2019): Atypical temporal-scale-specific fractal changes in Alzheimer's disease EEG and their relevance to cognitive decline. *Cogn Neurodyn* 13:1–11. <https://link.springer.com/article/10.1007/s11571-018-9509-x>.

Nowrangi MA, Lyketsos CG, Rosenberg PB (2015): Principles and management of neuropsychiatric symptoms in Alzheimer's dementia. *Alzheimers Res Ther* 7:1–10.
<https://alzres.biomedcentral.com/articles/10.1186/s13195-015-0096-3>.

- Ou C, Liu J, Qian Y, Chong W, Liu D, He X, Zhang X, Duan CZ (2021): Automated Machine Learning Model Development for Intracranial Aneurysm Treatment Outcome Prediction: A Feasibility Study. *Front Neurol* 12:735142. [/pmc/articles/PMC8666475/](https://www.ncbi.nlm.nih.gov/pmc/articles/PMC8666475/).
- Ouchani M, Gharibzadeh S, Jamshidi M, Amini M (2021): A Review of Methods of Diagnosis and Complexity Analysis of Alzheimer's Disease Using EEG Signals. *Biomed Res Int* 2021.
- Özbek Y, Fide E, Yener GG (2021): Resting-state EEG alpha/theta power ratio discriminates early-onset Alzheimer's disease from healthy controls. *Clinical Neurophysiology* 132:2019–2031.
- Palmqvist S, Schöll M, Strandberg O, Mattsson N, Stomrud E, Zetterberg H, Blennow K, Landau S, Jagust W, Hansson O (2017): Earliest accumulation of β -amyloid occurs within the default-mode network and concurrently affects brain connectivity. *Nature Communications* 2017 8:1 8:1–13. <https://www.nature.com/articles/s41467-017-01150-x>.
- Pappalettera C, Cacciotti A, Nucci L, Miraglia F, Rossini PM, Vecchio F (2023): Approximate entropy analysis across electroencephalographic rhythmic frequency bands during physiological aging of human brain. *Geroscience* 45:1131. [/pmc/articles/PMC9886767/](https://www.ncbi.nlm.nih.gov/pmc/articles/PMC9886767/).
- Parkinson J (2002): An essay on the shaking palsy. 1817. *J Neuropsychiatry Clin Neurosci* 14.
- Pathania A, Schreiber M, Miller MW, Euler MJ, Lohse KR (2021): Exploring the reliability and sensitivity of the EEG power spectrum as a biomarker. *International Journal of Psychophysiology* 160:18–27.
- Pavlov YG, Adamian N, Appelhoff S, Arvaneh M, Benwell CSY, Beste C, Bland AR, Bradford DE, Bublitzky F, Busch NA, Clayson PE, Cruse D, Czeszumski A, Dreber A, Dumas G, Ehinger B, Ganis G, He X, Hinojosa JA, Huber-Huber C, Inzlicht M, Jack BN, Johannesson M, Jones R, Kalenkovich E, Kaltwasser L, Karimi-Rouzbahani H, Keil A, König P, Kouara L, Kulke L, Ladouceur CD, Langer N, Liesefeld HR, Luque D, MacNamara A, Mudrik L, Muthuraman M, Neal LB, Nilsonne G, Niso G, Ocklenburg S, Oostenveld R, Pernet CR, Pourtois G, Ruzzoli M, Sass SM, Schaefer A, Senderecka M, Snyder JS, Tamnes CK, Tognoli E, van Vugt MK, Verona E, Vloeberghs R, Welke D, Wessel JR, Zakharov I, Mushtaq F (2021): #EEGManyLabs: Investigating the replicability of influential EEG experiments. *Cortex* 144:213–229.
- Pedroni A, Bahreini A, Langer N (2019): Automagic: Standardized preprocessing of big EEG data. *Neuroimage* 200:460–473.
- Peraza LR, Cromarty R, Kobeleva X, Firbank MJ, Killen A, Graziadio S, Thomas AJ, O'Brien JT, Taylor JP (2018): Electroencephalographic derived network differences in Lewy body dementia compared to Alzheimer's disease patients. *Scientific Reports* 2018 8:1 8:1–13. <https://www.nature.com/articles/s41598-018-22984-5>.
- Perez-Valero E, Morillas C, Lopez-Gordo MA, Carrera-Muñoz I, López-Alcalde S, Vílchez-Carrillo RM (2022): An Automated Approach for the Detection of Alzheimer's Disease From Resting State Electroencephalography. *Front Neuroinform* 16:924547.
- Pernet C, Garrido MI, Gramfort A, Maurits N, Michel CM, Pang E, Salmelin R, Schoffelen JM, Valdes-Sosa PA, Puce A (2020): Issues and recommendations from the OHBM COBIDAS MEEG committee for reproducible EEG and MEG research. *Nature Neuroscience* 2020 23:12 23:1473–1483. <https://www.nature.com/articles/s41593-020-00709-0>.

Pernet CR, Appelhoff S, Gorgolewski KJ, Flandin G, Phillips C, Delorme A, Oostenveld R (2019): EEG-BIDS, an extension to the brain imaging data structure for electroencephalography. *Scientific Data*. Nature Publishing Group. <https://www.nature.com/articles/s41597-019-0104-8>.

Perry DC, Brown JA, Possin KL, Datta S, Trujillo A, Radke A, Karydas A, Kornak J, Sias AC, Rabinovici GD, Gorno-Tempini ML, Boxer AL, De May M, Rankin KP, Sturm VE, Lee SE, Matthews BR, Kao AW, Vossel KA, Tartaglia MC, Miller ZA, Seo SW, Sidhu M, Gaus SE, Nana AL, Vargas JNS, Hwang JHL, Ossenkoppele R, Brown AB, Huang EJ, Coppola G, Rosen HJ, Geschwind D, Trojanowski JQ, Grinberg LT, Kramer JH, Miller BL, Seeley WW (2017): Clinicopathological correlations in behavioural variant frontotemporal dementia. *Brain* 140:3329–3345.
<https://pubmed.ncbi.nlm.nih.gov/29053860/>.

Petersen RC, Aisen P, Boeve BF, Geda YE, Ivnik RJ, Knopman DS, Mielke M, Pankratz VS, Roberts R, Rocca WA, Weigand S, Weiner M, Wiste H, Jack CR (2013): Criteria for Mild Cognitive Impairment Due to Alzheimer's Disease in the Community. *Ann Neurol* 74:199. /pmc/articles/PMC3804562/.

Peterson EK (2020): Associations Between EEG and Cognition in Parkinson's Disease. Ed. University of Canterbury. Christchurch, New Zealand.
<https://ir.canterbury.ac.nz/server/api/core/bitstreams/b575d676-14ed-4de4-815cf3e30c35fad4/content>.

Pion-Tonachini L, Kreutz-Delgado K, Makeig S (2019): ICLLabel: An automated electroencephalographic independent component classifier, dataset, and website. *Neuroimage* 198:181. /pmc/articles/PMC6592775/.

Pippenger MA (2021): How often is EEG used as part of routine dementia evaluation in community practice? *Alzheimer's & Dementia* 17:e056638.
<https://onlinelibrary.wiley.com/doi/full/10.1002/alz.056638>.

Poil SS, de Haan W, van der Flier WM, Mansvelder HD, Scheltens P, Linkenkaer-Hansen K (2013): Integrative EEG biomarkers predict progression to Alzheimer's disease at the MCI stage. *Front Aging Neurosci* 5. /pmc/articles/PMC3789214/.

Pomponio R, Erus G, Habes M, Doshi J, Srinivasan D, Mamourian E, Bashyam V, Nasrallah IM, Satterthwaite TD, Fan Y, Launer LJ, Masters CL, Maruff P, Zhuo C, Völzke H, Johnson SC, Fripp J, Koutsouleris N, Wolf DH, Gur R, Gur R, Morris J, Albert MS, Grabe HJ, Resnick SM, Bryan RN, Wolk DA, Shinohara RT, Shou H, Davatzikos C (2020): Harmonization of large MRI datasets for the analysis of brain imaging patterns throughout the lifespan. *Neuroimage* 208.
<https://pubmed.ncbi.nlm.nih.gov/31821869/>.

Popov T, Tröndle M, Baranczuk-Turska Z, Pfeiffer C, Haufe S, Langer N, Tzvetan Popov C (2023): Test-retest reliability of resting-state EEG in young and older adults. *Psychophysiology* 60:e14268. <https://onlinelibrary.wiley.com/doi/full/10.1111/psyp.14268>.

Porsteinsson AP, Isaacson RS, Knox S, Sabbagh MN, Rubino I (2021): Diagnosis of Early Alzheimer's Disease: Clinical Practice in 2021. *The Journal of Prevention of Alzheimer's Disease* 2021 8:3 8:371–386. <https://link.springer.com/article/10.14283/jpad.2021.23>.

Postuma RB, Berg D, Stern M, Poewe W, Olanow CW, Oertel W, Obeso J, Marek K, Litvan I, Lang AE, Halliday G, Goetz CG, Gasser T, Dubois B, Chan P, Bloem BR, Adler CH, Deuschl G (2015): MDS

clinical diagnostic criteria for Parkinson's disease. *Movement Disorders*. John Wiley and Sons Inc. <http://doi.wiley.com/10.1002/mds.26424>.

Prado P, Birba A, Cruzat J, Santamaría-García H, Parra M, Moguilner S, Tagliazucchi E, Ibáñez A (2022): Dementia ConnEEGtome: Towards multicentric harmonization of EEG connectivity in neurodegeneration. *International Journal of Psychophysiology* 172:24–38.

Prado P, Moguilner S, Mejía JA, Sainz-Ballesteros A, Otero M, Birba A, Santamaría-García H, Legaz A, Fittipaldi S, Cruzat J, Tagliazucchi E, Parra M, Herzog R, Ibáñez A (2023): Source space connectomics of neurodegeneration: One-metric approach does not fit all. *Neurobiol Dis* 179:106047.

Przedborski S, Vila M, Jackson-Lewis V (2003): Series Introduction: Neurodegeneration: What is it and where are we? *Journal of Clinical Investigation* 111:3–10. [/pmc/articles/PMC151843/](https://www.ncbi.nlm.nih.gov/pmc/articles/PMC151843/).

Puri D V., Nalbalwar SL, Nandgaonkar AB, Gawande JP, Wagh A (2023): Automatic detection of Alzheimer's disease from EEG signals using low-complexity orthogonal wavelet filter banks. *Biomed Signal Process Control* 81:104439.

Querfurth HW, LaFerla FM (2010): Alzheimer's Disease. *New England Journal of Medicine* 362:329–344. <http://www.nejm.org/doi/abs/10.1056/NEJMra0909142>.

Railo H (2021): Parkinson's disease: Resting state EEG. OSF. <https://osf.io/pehj9/>.

Railo H, Suuronen I, Kaasinen V, Murtojärvi M, Pahikkala T, Airola A (2020): Resting state EEG as a biomarker of Parkinson's disease: Influence of measurement conditions. [bioRxiv:2020.05.08.084343](https://www.ncbi.nlm.nih.gov/pmc/articles/PMC7207000/). [http://biorxiv.org/content/early/2020/05/10/2020.05.08.084343.abstract](https://www.ncbi.nlm.nih.gov/pmc/articles/PMC7207000/).

Raj R, Kannath SK, Mathew J, Sylaja PN (2023a): AutoML accurately predicts endovascular mechanical thrombectomy in acute large vessel ischemic stroke. *Front Neurol* 14. <https://pubmed.ncbi.nlm.nih.gov/37840939/>.

Raj R, Kannath SK, Mathew J, Sylaja PN (2023b): AutoML accurately predicts endovascular mechanical thrombectomy in acute large vessel ischemic stroke. *Front Neurol* 14. [/pmc/articles/PMC10569475/](https://www.ncbi.nlm.nih.gov/pmc/articles/PMC10569475/).

Ranasinghe KG, Cha J, Iaccarino L, Hinkley LB, Beagle AJ, Pham J, Jagust WJ, Miller BL, Rankin KP, Rabinovici GD, Vossel KA, Nagarajan SS (2020): Neurophysiological signatures in Alzheimer's disease are distinctly associated with TAU, amyloid-β accumulation, and cognitive decline. *Sci Transl Med* 12:4069. <https://www.science.org/doi/10.1126/scitranslmed.aaz4069>.

Ranasinghe KG, Verma P, Cai C, Xie X, Kudo K, Gao X, Lerner H, Mizuiri D, Strom A, Iaccarino L, Joie R La, Miller BL, Gorno-Tempini ML, Rankin KP, Jagust WJ, Vossel K, Rabinovici GD, Raj A, Nagarajan SS (2022): Altered excitatory and inhibitory neuronal subpopulation parameters are distinctly associated with tau and amyloid in Alzheimer's disease. *Elife* 11.

Rasmussen KL, Tybjarg-Hansen A, Nordestgaard BG, Frikke-Schmidt R (2018): Absolute 10-year risk of dementia by age, sex and APOE genotype: A population-based cohort study. *CMAJ* 190:E1033–E1041. [/pmc/articles/PMC6148649/](https://www.ncbi.nlm.nih.gov/pmc/articles/PMC6148649/).

Rea RC, Berlot R, Martin SL, Craig CE, Holmes PS, Wright DJ, Bon J, Pirtošek Z, Ray NJ (2021): Quantitative EEG and cholinergic basal forebrain atrophy in Parkinson's disease and mild cognitive impairment. *Neurobiol Aging* 106:37–44.

- Reisberg B (2006): Diagnostic criteria in dementia: A comparison of current criteria, research challenges, and implications for DSM-V. *Journal of Geriatric Psychiatry and Neurology*. <http://www.ncbi.nlm.nih.gov/pubmed/16880355>.
- Reynolds EH (2004): Todd, Faraday, and the electrical basis of brain activity. *Lancet Neurology* 3:557–563. <https://pubmed.ncbi.nlm.nih.gov/15324724/>.
- Robbins KA, Touryan J, Mullen T, Kothe C, Bigdely-Shamlo N (2020): How Sensitive Are EEG Results to Preprocessing Methods: A Benchmarking Study. *IEEE Trans Neural Syst Rehabil Eng* 28:1081–1090. <https://pubmed.ncbi.nlm.nih.gov/32217478/>.
- Rockhill AP, Jackson N, George J, Aron A, Swann NC (2021): UC San Diego Resting State EEG Data from Patients with Parkinson’s Disease. <https://openneuro.org/datasets/ds002778/versions/1.0.5>.
- Rodrigues PLC, Jutten C, Congedo M (2019): Riemannian Procrustes Analysis: Transfer Learning for Brain-Computer Interfaces. *IEEE Trans Biomed Eng* 66:2390–2401.
- Rommel C, Paillard J, Moreau T, Gramfort A (2022): Data augmentation for learning predictive models on EEG: a systematic comparison. *J Neural Eng* 19:066020. <https://iopscience.iop.org/article/10.1088/1741-2552/aca220>.
- Rosenblum Y, Shiner T, Bregman N, Giladi N, Maidan I, Fahoum F, Mirelman A (2023): Decreased aperiodic neural activity in Parkinson’s disease and dementia with Lewy bodies. *J Neurol* 270:3958–3969. <https://link.springer.com/article/10.1007/s00415-023-11728-9>.
- Rujeedawa T, Félez EC, Clare ICH, Fortea J, Strydom A, Rebillat AS, Coppus A, Levin J, Zaman SH (2021): The Clinical and Neuropathological Features of Sporadic (Late-Onset) and Genetic Forms of Alzheimer’s Disease. *J Clin Med* 10:4582. [/pmc/articles/PMC8509365/](https://pmc/articles/PMC8509365/).
- Ryan FJ, Ma Y, Ashander LM, Kvopka M, Appukuttan B, Lynn DJ, Smith JR (2022): Transcriptomic Responses of Human Retinal Vascular Endothelial Cells to Inflammatory Cytokines. *Transl Vis Sci Technol* 11. <https://pubmed.ncbi.nlm.nih.gov/36018584/>.
- Rygvold TW, Hatlestad-Hall C, Elvsåshagen T, Moberget T, Andersson S (2021): Do visual and auditory stimulus-specific response modulation reflect different mechanisms of neocortical plasticity? *European Journal of Neuroscience* 53:1072–1085. <https://onlinelibrary.wiley.com/doi/full/10.1111/ejn.14964>.
- Sabbagh D, Cartailler J, Touchard C, Joachim J, Mebazaa A, Vallée F, Gayat É, Gramfort A, Engemann DA (2023a): Repurposing electroencephalogram monitoring of general anaesthesia for building biomarkers of brain ageing: an exploratory study. *BJA open* 7:100145. <https://pubmed.ncbi.nlm.nih.gov/37638087/>.
- Sabbagh MN, Taylor A, Galasko D, Galvin JE, Goldman JG, Leverenz JB, Poston KL, Boeve BF, Irwin DJ, Quinn JF (2023b): Listening session with the US Food and Drug Administration, Lewy Body Dementia Association, and an expert panel. *Alzh & Dem: Trans Res & Clin Intervent* 9. [/pmc/articles/PMC9983146/](https://pmc/articles/PMC9983146/).
- Sachdev PS, Blacker D, Blazer DG, Ganguli M, Jeste D V., Paulsen JS, Petersen RC (2014): Classifying neurocognitive disorders: the DSM-5 approach. *Nat Rev Neurol* 10:634–642. <https://pubmed.ncbi.nlm.nih.gov/25266297/>.

Sakata N, Okumura Y (2017): Job Loss After Diagnosis of Early-Onset Dementia: A Matched Cohort Study. *Journal of Alzheimer's Disease* 60:1231. [/pmc/articles/PMC5676857/](https://www.ncbi.nlm.nih.gov/pmc/articles/PMC5676857/).

Santoro A, Martucci M, Conte M, Capri M, Franceschi C, Salvioli S (2020): Inflammaging, hormesis and the rationale for anti-aging strategies. *Ageing Res Rev* 64:101142.

Schaworonkow N, Nikulin V V. (2022): Is sensor space analysis good enough? Spatial patterns as a tool for assessing spatial mixing of EEG/MEG rhythms. *Neuroimage* 253:119093.

Scheijbeler EP, de Haan W, Stam CJ, Twisk JWR, Gouw AA (2023): Longitudinal resting-state EEG in amyloid-positive patients along the Alzheimer's disease continuum: considerations for clinical trials. *Alzheimers Res Ther* 15:1–19.
<https://alzres.biomedcentral.com/articles/10.1186/s13195-023-01327-1>.

Schmidt F, Danböck SK, Trinka E, Demarchi G, Weisz N (2023): Age-related changes in “cortical” 1/f dynamics are linked to cardiac activity. *bioRxiv*:2022.11.07.515423.
<https://www.biorxiv.org/content/10.1101/2022.11.07.515423v2>.

Schmidt MT, Kanda PAM, Basile LFH, da Silva Lopes HF, Baratho R, Demario JLC, Jorge MS, Nardi AE, Machado S, Ianof JN, Nitrini R, Anghinah R (2013): Index of alpha/theta ratio of the electroencephalogram: A new marker for Alzheimer's disease. *Front Aging Neurosci* 5:60.
<http://www.ncbi.nlm.nih.gov/pubmed/24130529>.

Schultz AP, Chhatwal JP, Hedden T, Mormino EC, Hanseeuw BJ, Sepulcre J, Huijbers W, LaPoint M, Buckley RF, Johnson KA, Sperling RA (2017): Phases of Hyperconnectivity and Hypoconnectivity in the Default Mode and Salience Networks Track with Amyloid and Tau in Clinically Normal Individuals. *The Journal of Neuroscience* 37:4323. [/pmc/articles/PMC5413178/](https://www.ncbi.nlm.nih.gov/pmc/articles/PMC5413178/).

Schumacher J, Taylor JP, Hamilton CA, Firbank M, Cromarty RA, Donaghy PC, Roberts G, Allan L, Lloyd J, Durcan R, Barnett N, O'Brien JT, Thomas AJ (2020a): Quantitative EEG as a biomarker in mild cognitive impairment with Lewy bodies. *Alzheimers Res Ther* 12.
<https://pubmed.ncbi.nlm.nih.gov/32641111/>.

Schumacher J, Thomas AJ, Peraza LR, Firbank M, Cromarty R, Hamilton CA, Donaghy PC, O'Brien JT, Taylor JP (2020b): EEG alpha reactivity and cholinergic system integrity in Lewy body dementia and Alzheimer's disease. *Alzheimers Res Ther* 12. [/pmc/articles/PMC7178985/](https://www.ncbi.nlm.nih.gov/pmc/articles/PMC7178985/).

Seeck M, Koessler L, Bast T, Leijten F, Michel C, Baumgartner C, He B, Beniczky S (2017): The standardized EEG electrode array of the IFCN. *Clin Neurophysiol* 128:2070–2077.
<https://pubmed.ncbi.nlm.nih.gov/28778476/>.

Shiri I, Amini M, Nazari M, Hajianfar G, Haddadi Avval A, Abdollahi H, Oveisí M, Arabi H, Rahmim A, Zaidi H (2022): Impact of feature harmonization on radiogenomics analysis: Prediction of EGFR and KRAS mutations from non-small cell lung cancer PET/CT images. *Comput Biol Med* 142.
<https://pubmed.ncbi.nlm.nih.gov/35051856/>.

Simuni T, Chahine LM, Poston K, Brumm M, Buracchio T, Campbell M, Chowdhury S, Coffey C, Concha-Marambio L, Dam T, DiBiaso P, Foroud T, Frasier M, Gochanour C, Jennings D, Kieburtz K, Kopil CM, Merchant K, Mollenhauer B, Montine T, Nudelman K, Pagano G, Seibyl J, Sherer T, Singleton A, Stephenson D, Stern M, Soto C, Tanner CM, Tolosa E, Weintraub D, Xiao Y, Siderowf A, Dunn B, Marek K (2024): A biological definition of neuronal α -synuclein disease: towards an integrated staging system for research. *Lancet Neurol* 23:178–190.
<http://www.thelancet.com/article/S1474442223004052/fulltext>.

- Singh A, Cole RC, Espinoza AI, Brown D, Cavanagh JF, Narayanan NS (2020): Frontal theta and beta oscillations during lower-limb movement in Parkinson's disease. *Clinical Neurophysiology* 131:694–702. [/pmc/articles/PMC8112379/](https://www.ncbi.nlm.nih.gov/pmc/articles/PMC8112379/).
- Sitt JD, King JR, El Karoui I, Rohaut B, Faugeras F, Gramfort A, Cohen L, Sigman M, Dehaene S, Naccache L (2014): Large scale screening of neural signatures of consciousness in patients in a vegetative or minimally conscious state. *Brain* 137:2258–2270. <https://pubmed.ncbi.nlm.nih.gov/24919971/>.
- Skouras S, Falcon C, Tucholka A, Rami L, Sanchez-Valle R, Lladó A, Gispert JD, Molinuevo JL (2019): Mechanisms of functional compensation, delineated by eigenvector centrality mapping, across the pathophysiological continuum of Alzheimer's disease. *Neuroimage Clin* 22:101777. [/pmc/articles/PMC6434094/](https://www.ncbi.nlm.nih.gov/pmc/articles/PMC6434094/).
- Sleimen-Malkoun R, Perdikis D, Müller V, Blanc JL, Huys R, Temprado JJ, Jirsa VK (2015): Brain Dynamics of Aging: Multiscale Variability of EEG Signals at Rest and during an Auditory Oddball Task. *eNeuro* 2. <https://www.eneuro.org/content/2/3/ENEURO.0067-14.2015>.
- Smailovic U, Jelic V (2019): Neurophysiological Markers of Alzheimer's Disease: Quantitative EEG Approach. *Neurology and Therapy*. Adis. <http://www.ncbi.nlm.nih.gov/pubmed/31833023>.
- Smailovic U, Koenig T, Kåreholt I, Andersson T, Kramberger MG, Winblad B, Jelic V (2018): Quantitative EEG power and synchronization correlate with Alzheimer's disease CSF biomarkers. *Neurobiol Aging* 63:88–95.
- Smits FM, Porcaro C, Cottone C, Cancelli A, Rossini PM, Tecchio F (2016): Electroencephalographic Fractal Dimension in Healthy Ageing and Alzheimer's Disease. *PLoS One* 11:e0149587. <https://journals.plos.org/plosone/article?id=10.1371/journal.pone.0149587>.
- Sperling RA, Aisen PS, Beckett LA, Bennett DA, Craft S, Fagan AM, Iwatsubo T, Jack CR, Kaye J, Montine TJ, Park DC, Reiman EM, Rowe CC, Siemers E, Stern Y, Yaffe K, Carrillo MC, Thies B, Morrison-Bogorad M, Wagster M V., Phelps CH (2011): Toward defining the preclinical stages of Alzheimer's disease: recommendations from the National Institute on Aging-Alzheimer's Association workgroups on diagnostic guidelines for Alzheimer's disease. *Alzheimers Dement* 7:280–292. <https://pubmed.ncbi.nlm.nih.gov/21514248/>.
- Srinivasan R, Nunez PL (2012): Electroencephalography. *Encyclopedia of Human Behavior*: Second Edition:15–23.
- Stelzmann RA, Norman Schnitzlein H, Reed Murtagh F (1995): An english translation of alzheimer's 1907 paper, "über eine eigenartige erkankung der hirnrinde." *Clinical Anatomy* 8:429–431. <https://onlinelibrary.wiley.com/doi/full/10.1002/ca.980080612>.
- Stoddart WHBAB (1913): Presbyophrenia (Alzheimer's Disease). *Proc R Soc Med* 6:13. <https://www.ncbi.nlm.nih.gov/pmc/articles/PMC2005437/>.
- Stylianou M, Murphy N, Peraza LR, Graziadio S, Cromarty R, Killen A, O' Brien JT, Thomas AJ, LeBeau FEN, Taylor JP (2018): Quantitative electroencephalography as a marker of cognitive fluctuations in dementia with Lewy bodies and an aid to differential diagnosis. *Clinical Neurophysiology* 129:1209–1220.
- Suarez-Revelo J, Ochoa-Gomez J, Duque-Grajales J (2016): Improving test-retest reliability of quantitative electroencephalography using different preprocessing approaches. *38th Annual*

International Conference of the IEEE Engineering in Medicine and Biology Society (EMBC):961–964.

Suárez-Revelo JX, Ochoa-Gómez JF, Duque-Grajales JE, Tobón-Quintero CA (2016): Biomarkers identification in Alzheimer's disease using effective connectivity analysis from electroencephalography recordings. *Ingenieria e Investigacion* 36:50–57.
<http://www.revistas.unal.edu.co/index.php/ingeinv/article/view/54037>.

Suárez-Revelo JX, Ochoa-Gómez JF, Tobón-Quintero CA (2018): Validation of EEG Pre-processing Pipeline by Test-Retest Reliability. In: . Communications in Computer and Information Science. Springer Verlag. Vol. 916, pp 290–299. https://doi.org/10.1007/978-3-030-00353-1_26.

Sun J, Wang B, Niu Y, Tan Y, Fan C, Zhang N, Xue J, Wei J, Xiang J (2020): Complexity Analysis of EEG, MEG, and fMRI in Mild Cognitive Impairment and Alzheimer's Disease: A Review. *Entropy* 2020, Vol 22, Page 239 22:239. <https://www.mdpi.com/1099-4300/22/2/239/htm>.

Sun Y, Islam S, Gao Y, Nakamura T, Zou K, Michikawa M (2023): Apolipoprotein E4 inhibits γ -secretase activity via binding to the γ -secretase complex. *J Neurochem* 164:858–874.
<https://onlinelibrary.wiley.com/doi/full/10.1111/jnc.15750>.

Swardfager W, Lanctt K, Rothenburg L, Wong A, Cappell J, Herrmann N (2010): A meta-analysis of cytokines in Alzheimer's disease. *Biol Psychiatry* 68:930–941.
<https://pubmed.ncbi.nlm.nih.gov/20692646/>.

Tampu IE, Eklund A, Haj-Hosseini N (2022): Inflation of test accuracy due to data leakage in deep learning-based classification of OCT images. *Scientific Data* 2022 9:1 9:1–8.
<https://www.nature.com/articles/s41597-022-01618-6>.

Tăutăan AM, Casula EP, Pellicciari MC, Borghi I, Maiella M, Bonni S, Minei M, Assogna M, Palmisano A, Smeralda C, Romanella SM, Ionescu B, Koch G, Santaracchi E (2023): TMS-EEG perturbation biomarkers for Alzheimer's disease patients classification. *Scientific Reports* 2023 13:1 13:1–13. <https://www.nature.com/articles/s41598-022-22978-4>.

Thal DR, Rüb U, Orantes M, Braak H (2002): Phases of A beta-deposition in the human brain and its relevance for the development of AD. *Neurology* 58:1791–1800.
<https://pubmed.ncbi.nlm.nih.gov/12084879/>.

Thölke P, Mantilla-Ramos YJ, Abdelhedi H, Maschke C, Dehgan A, Harel Y, Kemtur A, Mekki Berrada L, Sahraoui M, Young T, Bellemare Pépin A, El Khantour C, Landry M, Pasquarella A, Hadid V, Combrisson E, O'Byrne J, Jerbi K (2023): Class imbalance should not throw you off balance: Choosing the right classifiers and performance metrics for brain decoding with imbalanced data. *Neuroimage* 277. <https://pubmed.ncbi.nlm.nih.gov/37385392/>.

Toledo JB, Gopal P, Raible K, Irwin DJ, Brettschneider J, Sedor S, Waits K, Boluda S, Grossman M, Van Deerlin VM, Lee EB, Arnold SE, Duda JE, Hurtig H, Lee VMY, Adler CH, Beach TG, Trojanowski JQ (2016): Pathological α -synuclein distribution in subjects with coincident Alzheimer's and Lewy body pathology. *Acta Neuropathol* 131:393–409.
<https://link.springer.com/article/10.1007/s00401-015-1526-9>.

Tönnies E, Trushina E (2017): Oxidative Stress, Synaptic Dysfunction, and Alzheimer's Disease. *Journal of Alzheimer's Disease* 57:1105. [/pmc/articles/PMC5409043/](https://pmc/articles/PMC5409043/).

Tröndle M, Popov T, Dziedzic S, Langer N (2022): Decomposing the role of alpha oscillations during brain maturation. *Elife* 11.

Turner RS, Stubbs T, Davies DA, Albensi BC (2020): Potential New Approaches for Diagnosis of Alzheimer's Disease and Related Dementias. *Front Neurol* 11:496.
[/pmc/articles/PMC7290039/](https://PMC7290039/).

Tyebji S, Hannan AJ (2017): Synaptopathic mechanisms of neurodegeneration and dementia: Insights from Huntington's disease. *Prog Neurobiol* 153:18–45.

Tzimourta KD, Christou V, Tzallas AT, Giannakeas N, Astrakas LG, Angelidis P, Tsalikakis D, Tsipouras MG (2021): Machine Learning Algorithms and Statistical Approaches for Alzheimer's Disease Analysis Based on Resting-State EEG Recordings: A Systematic Review.
<https://doi.org/101142/S0129065721300023> 31.

Vallat R (2022): AntroPy: entropy and complexity of (EEG) time-series in Python.
<https://github.com/raphaelvallat/antropy>.

Vallat R, Walker MP (2021): An open-source, high-performance tool for automated sleep staging. *Elife* 10.

Vandenbroucke JP, Von Elm E, Altman DG, Gøtzsche PC, Mulrow CD, Pocock SJ, Poole C, Schlesselman JJ, Egger M (2007): Strengthening the Reporting of Observational Studies in Epidemiology (STROBE): Explanation and elaboration. *PLoS Med* 4:1628–1654.
[/pmc/articles/PMC2020496/?report=abstract](https://PMC2020496/?report=abstract).

Vanneste S, Song JJ, De Ridder D (2018): Thalamocortical dysrhythmia detected by machine learning. *Nature Communications* 2018 9:1 9:1–13. <https://www.nature.com/articles/s41467-018-02820-0>.

Vermeiren Y, Hirschberg Y, Mertens I, De Deyn PP (2020): Biofluid Markers for Prodromal Parkinson's Disease: Evidence From a Catecholaminergic Perspective. *Front Neurol* 11:521285.

Vik-Mo AO, Gil LM, Ballard C, Aarsland D (2018): Course of neuropsychiatric symptoms in dementia: 5-year longitudinal study. *Int J Geriatr Psychiatry* 33:1361–1369.
<https://pubmed.ncbi.nlm.nih.gov/29979473/>.

Vogel JW, Young AL, Oxtoby NP, Smith R, Ossenkoppele R, Strandberg OT, La Joie R, Aksman LM, Grothe MJ, Iturria-Medina Y, Weiner M, Aisen P, Petersen R, Jack CR, Jagust W, Trojanowski JQ, Toga AW, Beckett L, Green RC, Saykin AJ, Morris JC, Shaw LM, Liu E, Montine T, Thomas RG, Donohue M, Walter S, Gessert D, Sather T, Jiminez G, Harvey D, Bernstein M, Fox N, Thompson P, Schuff N, DeCarli C, Borowski B, Gunter J, Senjem M, Vemuri P, Jones D, Kantarci K, Ward C, Koeppe RA, Foster N, Reiman EM, Chen K, Mathis C, Landau S, Cairns NJ, Householder E, Reinwald LT, Lee V, Korecka M, Figurski M, Crawford K, Neu S, Foroud TM, Potkin S, Shen L, Kelley F, Kim S, Nho K, Kachaturian Z, Frank R, Snyder PJ, Molchan S, Kaye J, Quinn J, Lind B, Carter R, Dolen S, Schneider LS, Pawluczyk S, Beccera M, Teodoro L, Spann BM, Brewer J, Vanderswag H, Fleisher A, Heidebrink JL, Lord JL, Mason SS, Albers CS, Knopman D, Johnson K, Doody RS, Meyer JV, Chowdhury M, Rountree S, Dang M, Stern Y, Honig LS, Bell KL, Ances B, Carroll M, Leon S, Mintun MA, Schneider S, Oliver A, Griffith R, Clark D, Geldmacher D, Brockington J, Roberson E, Grossman H, Mitsis E, deToledo-Morrell L, Shah RC, Duara R, Varon D, Greig MT, Roberts P, Albert M, Onyike C, D'Agostino D, Kielb S, Galvin JE, Pogorelec DM, Cerbone B, Michel CA, Rusinek H, de Leon MJ, Glodzik L, De Santi S, Doraiswamy PM, Petrella

JR, Wong TZ, Arnold SE, Karlawish JH, Wolk D, Smith CD, Jicha G, Hardy P, Sinha P, Oates E, Conrad G, Lopez OL, Oakley MA, Simpson DM, Porsteinsson AP, Goldstein BS, Martin K, Makino KM, Ismail MS, Brand C, Mulnard RA, Thai G, McAdams Ortiz C, Womack K, Mathews D, Quiceno M, Arrastia RD, King R, Weiner M, Cook KM, DeVos M, Levey AI, Lah JJ, Cellar JS, Burns JM, Anderson HS, Swerdlow RH, Apostolova L, Tingus K, Woo E, Silverman DHS, Lu PH, Bartzokis G, Radford NRG, Parfitt F, Kendall T, Johnson H, Farlow MR, Hake AM, Matthews BR, Herring S, Hunt C, van Dyck CH, Carson RE, MacAvoy MG, Chertkow H, Bergman H, Hosein C, Black S, Stefanovic B, Caldwell C, Hsiung GYR, Feldman H, Mudge B, Past MA, Kertesz A, Rogers J, Trost D, Bernick C, Munic D, Kerwin D, Mesulam MM, Lipowski K, Wu CK, Johnson N, Sadowsky C, Martinez W, Villena T, Turner RS, Johnson K, Reynolds B, Sperling RA, Johnson KA, Marshall G, Frey M, Yesavage J, Taylor JL, Lane B, Rosen A, Tinklenberg J, Sabbagh MN, Belden CM, Jacobson SA, Sirrel SA, Kowall N, Killiany R, Budson AE, Norbush A, Johnson PL, Obisesan TO, Wolday S, Allard J, Lerner A, Ogracki P, Hudson L, Fletcher E, Carmichael O, Olichney J, DeCarli C, Kittur S, Borrie M, Lee TY, Bartha R, Johnson S, Asthana S, Carlsson CM, Potkin SG, Preda A, Nguyen D, Tariot P, Reeder S, Bates V, Capote H, Rainka M, Scharre DW, Kataki M, Adeli A, Zimmerman EA, Celmins D, Brown AD, Pearson GD, Blank K, Anderson K, Santulli RB, Kitzmiller TJ, Schwartz ES, Sink KM, Williamson JD, Garg P, Watkins F, Ott BR, Querfurth H, Tremont G, Salloway S, Malloy P, Correia S, Rosen HJ, Miller BL, Mintzer J, Spicer K, Bachman D, Finger E, Pasternak S, Rachinsky I, Drost D, Pomara N, Hernando R, Sarrael A, Schultz SK, Ponto LLB, Shim H, Smith KE, Relkin N, Chaing G, Raudin L, Smith A, Fargher K, Raj BA, Pontecorvo MJ, Devous MD, Rabinovici GD, Alexander DC, Lyoo CH, Evans AC, Hansson O (2021): Four distinct trajectories of tau deposition identified in Alzheimer's disease. *Nat Med* 27:871. [/pmc/articles/PMC8686688/](https://pmc/articles/PMC8686688/).

Voß H, Schlumbohm S, Barwikowski P, Wurlitzer M, Dottermusch M, Neumann P, Schlueter H, Neumann JE, Krisp C (2022): HarmonizR enables data harmonization across independent proteomic datasets with appropriate handling of missing values. *Nat Commun* 13. <https://pubmed.ncbi.nlm.nih.gov/35725563/>.

Voytek B, Knight RT (2015): Dynamic Network Communication as a Unifying Neural Basis for Cognition, Development, Aging, and Disease. *Biol Psychiatry* 77:1089–1097.

Wan L, Huang H, Schwab N, Tanner J, Rajan A, Lam NB, Zaborszky L, Li C shan R, Price CC, Ding M (2019): From eyes-closed to eyes-open: Role of cholinergic projections in EC-to-EO alpha reactivity revealed by combining EEG and MRI. *Hum Brain Mapp* 40:566–577.

Wang Z, Liu A, Yu J, Wang P, Bi Y, Xue S, J Z, H G, W Z (2023): The effect of aperiodic components in distinguishing Alzheimer's disease from frontotemporal dementia. Research Square [preprint]. <https://europepmc.org/article/ppr/ppr660352>.

Waschke L, Donoghue T, Fiedler L, Smith S, Garrett DD, Voytek B, Obleser J (2021): Modality-specific tracking of attention and sensory statistics in the human electrophysiological spectral exponent. *Elife* 10.

Wen H, Liu Z (2016): Separating Fractal and Oscillatory Components in the Power Spectrum of Neurophysiological Signal. *Brain Topogr* 29:13. [/pmc/articles/PMC4706469/](https://pmc/articles/PMC4706469/).

Wilson DM, Cookson MR, Van Den Bosch L, Zetterberg H, Holtzman DM, Dewachter I (2023): Hallmarks of neurodegenerative diseases. *Cell* 186:693–714. <https://pubmed.ncbi.nlm.nih.gov/36803602/>.

- Xu H, Abdallah N, Marion JM, Chauvet P, Tauber C, Carlier T, Lu L, Hatt M (2023): Radiomics prognostic analysis of PET/CT images in a multicenter head and neck cancer cohort: investigating ComBat strategies, sub-volume characterization, and automatic segmentation. *Eur J Nucl Med Mol Imaging* 50. <https://pubmed.ncbi.nlm.nih.gov/36690882/>.
- Xu Y, Yang J, Shang H (2016): Meta-analysis of risk factors for Parkinson's disease dementia. *Transl Neurodegener* 5. [/pmc/articles/PMC4890279/](https://pmc/articles/PMC4890279/).
- Yao S, Zhu J, Li S, Zhang R, Zhao J, Yang X, Wang Y (2022): Bibliometric Analysis of Quantitative Electroencephalogram Research in Neuropsychiatric Disorders From 2000 to 2021. *Front Psychiatry* 13:830819. [/pmc/articles/PMC9167960/](https://pmc/articles/PMC9167960/).
- Yassine S, Gschwandtner U, Auffret M, Duprez J, Verin M, Fuhr P, Hassan M (2023): Identification of Parkinson's Disease Subtypes from Resting-State Electroencephalography. *Movement Disorders* 38:1451–1460. <https://onlinelibrary.wiley.com/doi/full/10.1002/mds.29451>.
- Ye Q, Chen H, Su F, Shu H, Gong L, Xie C, Zhou H, Bai F (2018): An Inverse U-Shaped Curve of Resting-State Networks in Individuals at High Risk of Alzheimer's Disease. *J Clin Psychiatry* 79. <https://pubmed.ncbi.nlm.nih.gov/29474008/>.
- Yener GG, Leuchter AF, Jenden D, Read SL, Cummings JL, Miller BL (1996): Quantitative EEG in frontotemporal dementia. *Clin Electroencephalogr* 27:61–68. <https://pubmed.ncbi.nlm.nih.gov/8681464/>.
- Yi GS, Wang J, Deng B, Wei X Le (2017): Complexity of resting-state EEG activity in the patients with early-stage Parkinson's disease. *Cogn Neurodyn* 11:147. [/pmc/articles/PMC5350085/](https://pmc/articles/PMC5350085/).
- Yi G, Wang L, Chu C, Liu C, Zhu X, Shen X, Li Z, Wang F, Yang M, Wang J (2022): Analysis of complexity and dynamic functional connectivity based on resting-state EEG in early Parkinson's disease patients with mild cognitive impairment. *Cogn Neurodyn* 16:309–323. <https://link.springer.com/article/10.1007/s11571-021-09722-w>.
- van der Zande JJ, Gouw AA, Steenoven I van, Scheltens P, Stam CJ, Lemstra AW (2018): EEG Characteristics of Dementia With Lewy Bodies, Alzheimer's Disease and Mixed Pathology. *Front Aging Neurosci* 10. [/pmc/articles/PMC6037893/](https://pmc/articles/PMC6037893/).
- Zapata-Saldarriaga L-M, Vargas-Serna A-D, Gil-Gutiérrez J, Mantilla-Ramos Y-J, Ochoa-Gómez J-F (2023): Evaluation of Strategies Based on Wavelet-ICA and ICLabel for Artifact Correction in EEG Recordings. *Revista Científica* 46:61–76.
- Zimmermann R, Gschwandtner U, Hatz F, Schindler C, Bousleiman H, Ahmed S, Hardmeier M, Meyer A, Calabrese P, Fuhr P (2015): Correlation of EEG slowing with cognitive domains in nondemented patients with Parkinson's disease. *Dement Geriatr Cogn Disord* 39:207–214. <https://pubmed.ncbi.nlm.nih.gov/25591733/>.

Supplementary Materials

Supplementary Table 1. Pair-wise age-related differences across research centres

| Reference | Comparator | Mean Difference | SE | t-value | p _{tukey} |
|------------|------------|-----------------|-------|---------|--------------------|
| California | Finland | -5.166 | 1.824 | -2.832 | 0.129 |
| | France | -7.318 | 1.612 | -4.539 | < .001 *** |
| | Genoa | -13.860 | 1.603 | -8.646 | < .001 *** |
| | Greece | -3.597 | 1.649 | -2.181 | 0.471 |
| | Iowa | -7.228 | 2.004 | -3.607 | 0.013 * |
| | Lemon | -4.185 | 1.629 | -2.569 | 0.235 |
| | Medellin | -0.016 | 1.619 | -0.010 | 1.000 |
| | Oslo | 7.963 | 1.885 | 4.225 | 0.001 ** |
| | Stavanger | -10.396 | 2.074 | -5.013 | < .001 *** |
| Finland | France | -2.153 | 1.504 | -1.431 | 0.917 |
| | Genoa | -8.694 | 1.494 | -5.819 | < .001 *** |
| | Greece | 1.568 | 1.543 | 1.016 | 0.991 |
| | Iowa | -2.063 | 1.918 | -1.075 | 0.987 |
| | Lemon | 0.980 | 1.522 | 0.644 | 1.000 |
| | Medellin | 5.150 | 1.511 | 3.408 | 0.024 * |
| | Oslo | 13.128 | 1.793 | 7.321 | < .001 *** |
| | Stavanger | -5.230 | 1.991 | -2.627 | 0.208 |
| France | Genoa | -6.541 | 1.227 | -5.332 | < .001 *** |
| | Greece | 3.721 | 1.286 | 2.893 | 0.110 |
| | Iowa | 0.090 | 1.718 | 0.052 | 1.000 |
| | Lemon | 3.133 | 1.261 | 2.484 | 0.280 |
| | Medellin | 7.303 | 1.247 | 5.854 | < .001 *** |
| | Oslo | 15.281 | 1.577 | 9.687 | < .001 *** |
| | Stavanger | -3.077 | 1.799 | -1.710 | 0.789 |
| Genoa | Greece | 10.262 | 1.275 | 8.051 | < .001 *** |
| | Iowa | 6.631 | 1.709 | 3.880 | 0.005 ** |
| | Lemon | 9.674 | 1.249 | 7.744 | < .001 *** |
| | Medellin | 13.844 | 1.235 | 11.206 | < .001 *** |
| | Oslo | 21.823 | 1.568 | 13.918 | < .001 *** |
| | Stavanger | 3.464 | 1.791 | 1.935 | 0.645 |
| Greece | Iowa | -3.631 | 1.753 | -2.072 | 0.548 |
| | Lemon | -0.588 | 1.308 | -0.450 | 1.000 |
| | Medellin | 3.582 | 1.295 | 2.766 | 0.151 |
| | Oslo | 11.560 | 1.615 | 7.158 | < .001 *** |
| | Stavanger | -6.798 | 1.832 | -3.711 | 0.009 ** |
| Iowa | Lemon | 3.043 | 1.734 | 1.755 | 0.763 |
| | Medellin | 7.213 | 1.724 | 4.183 | 0.001 ** |
| | Oslo | 15.191 | 1.976 | 7.687 | < .001 *** |
| | Stavanger | -3.167 | 2.157 | -1.468 | 0.904 |
| Lemon | Medellin | 4.170 | 1.270 | 3.284 | 0.036 * |
| | Oslo | 12.148 | 1.595 | 7.617 | < .001 *** |
| | Stavanger | -6.210 | 1.814 | -3.423 | 0.023 * |
| Medellin | Oslo | 7.979 | 1.584 | 5.036 | < .001 *** |
| | Stavanger | -10.380 | 1.805 | -5.751 | < .001 *** |
| Oslo | Stavanger | -18.358 | 2.047 | -8.969 | < .001 *** |

Note. P-values were adjusted to compare a family of 10 tests through post-hoc Tukey. SE: Standard Error.

* p < .05, ** p < .01, *** p < .001

Supplementary Table 2. Pair-wise age-related differences across groups

| Reference | Comparator | Mean Difference | SE | t-value | p _{tukey} |
|-----------|------------|-----------------|-------|---------|--------------------|
| AD | HC | 8.717 | 0.990 | 8.803 | < .001 *** |
| | MCI-AD | 2.193 | 1.268 | 1.729 | 0.417 |
| | MCI-LBD | 4.756 | 1.712 | 2.778 | 0.045 * |
| | PD | 8.295 | 1.318 | 6.293 | < .001 *** |
| HC | MCI-AD | -6.524 | 1.138 | -5.732 | < .001 *** |
| | MCI-LBD | -3.960 | 1.618 | -2.448 | 0.105 |
| | PD | -0.422 | 1.193 | -0.353 | 0.997 |
| MCI-AD | MCI-LBD | 2.563 | 1.801 | 1.423 | 0.613 |
| | PD | 6.102 | 1.433 | 4.260 | < .001 *** |
| MCI-LBD | PD | 3.539 | 1.837 | 1.926 | 0.305 |

Note. P-values were adjusted to compare a family of 5 tests through post-hoc Tukey. SE: Standard Error. **AD:** Alzheimer's Disease; **MCI-AD:** Mild Cognitive Impairment – AD; **PD:** Parkinson's Disease; **MCI-LBD:** Mild Cognitive Impairment – Lewy Body Diseases; **HC:** Healthy Controls.

* p < .05, ** p < .01, *** p < .001

Supplementary Table 3. Absolute and relative frequency by group in the train and test subsets

| Subset | Group | Absolute Frequency | Relative Frequency |
|--------|-----------|--------------------|--------------------|
| Train | AD | 79 | 22.316 |
| | HC | 153 | 43.220 |
| | MCI - AD | 53 | 14.972 |
| | MCI - LBD | 22 | 6.215 |
| | PD | 47 | 13.277 |
| | Total | 354 | 100.000 |
| Test | AD | 34 | 22.222 |
| | HC | 66 | 43.137 |
| | MCI - AD | 23 | 15.033 |
| | MCI - LBD | 10 | 6.536 |
| | PD | 20 | 13.072 |
| | Total | 153 | 100.000 |

AD: Alzheimer's Disease; **MCI-AD:** Mild Cognitive Impairment – AD; **PD:** Parkinson's Disease; **MCI-LBD:** Mild Cognitive Impairment – Lewy Body Diseases; **HC:** Healthy Controls.